

A new *Boulenophrys* species (Anura, Megophryidae) from the coastal hills of eastern Fujian Province, China

Shi-Shi Lin¹, Hong-Hui Chen¹, Yuan-Hang Li¹, Zhao-Ning Peng¹, Zhao-Chi Zeng¹, Jian Wang¹

¹ Guangdong Polytechnic of Environmental Protection Engineering, Foshan 528216, China

Corresponding authors: Jian Wang (wangj-1994@outlook.com); Zhao-Chi Zeng (zhaochizeng@outlook.com)

Abstract

A new species of the genus *Boulenophrys* is described from the coastal hills of eastern Fujian Province, China. The new taxon can be distinguished from all recognized congeners by a combination of discrete morphological character state differences and genetic divergences in the combined mitochondrial 16S + CO1 genes. We also provide a map showing the distribution pattern of *Boulenophrys* species in Fujian and a provincial-specific key, which will aid their conservation by helping the local authorities accurately identify species during field identifications and data collection efforts.

Key words: *Boulenophrys lichun* sp. nov., conservation actions, distribution pattern, diversity, Horned Toads, identification, new species, provincial key, taxonomy



Academic editor: Anthony Herrel

Received: 19 June 2024

Accepted: 12 September 2024

Published: 18 October 2024

ZooBank: <https://zoobank.org/A6D95900-0A19-4778-9AA5-6D87622B419F>

Citation: Lin S-S, Chen H-H, Li Y-H, Peng Z-N, Zeng Z-C, Wang J (2024) A new *Boulenophrys* species (Anura, Megophryidae) from the coastal hills of eastern Fujian Province, China. ZooKeys 1216: 1–15. <https://doi.org/10.3897/zookeys.1216.130017>

Copyright: © Shi-Shi Lin et al.

This is an open access article distributed under terms of the Creative Commons Attribution License (Attribution 4.0 International – CC BY 4.0).

Introduction

The Chinese Horned Toads (*Boulenophrys* Fei, Ye & Jiang, 2016) comprise 68 recognized species which are classified within the subfamily Megophryinae (Bonaparte, 1850) (Lyu et al. 2023; Zeng et al. 2024; Wang et al. 2024). They are widespread in the subtropical and tropical areas of mainland East Asia, mostly in southern China and southwards into northernmost Indochina, including Vietnam, Laos, Myanmar, and Thailand (Fei and Ye 2016; Lyu et al. 2023; Frost 2024). Located in southeastern China, Fujian Province possesses a complex mountain system. Its *Boulenophrys* diversity is still underestimated with three of the five species known from the area only described in recent years (Messenger et al. 2019; Lyu et al. 2021). Inger and Romer (1961) included a paratype of *B. brachykolos* (Inger & Romer, 1961) from Fujian, which may be a misidentification of *B. ombrophila* (Messenger & Dahn, 2019) due to morphological similarity (Lyu et al. 2023). Lyu et al. (2023) also restricted *B. brachykolos* to Hong Kong and Shenzhen in the east of the Pearl River Estuary based on voucher specimens and molecular data. Thus, only five recognized species occur in Fujian, namely *B. boettgeri* (Boulenger, 1899), *B. daiyunensis* (Lyu, Wang & Wang, 2021), *B. kuantunensis* (Pope, 1929), *B. ombrophila*, and *B. sanmingensis* (Lyu & Wang, 2021).

During recent field surveys in eastern Fujian, we collected a series of *Boulenophrys* specimens (Fig. 1). Preliminary morphological examination indicated that they could be distinguished from recognized congeners by a series of discrete

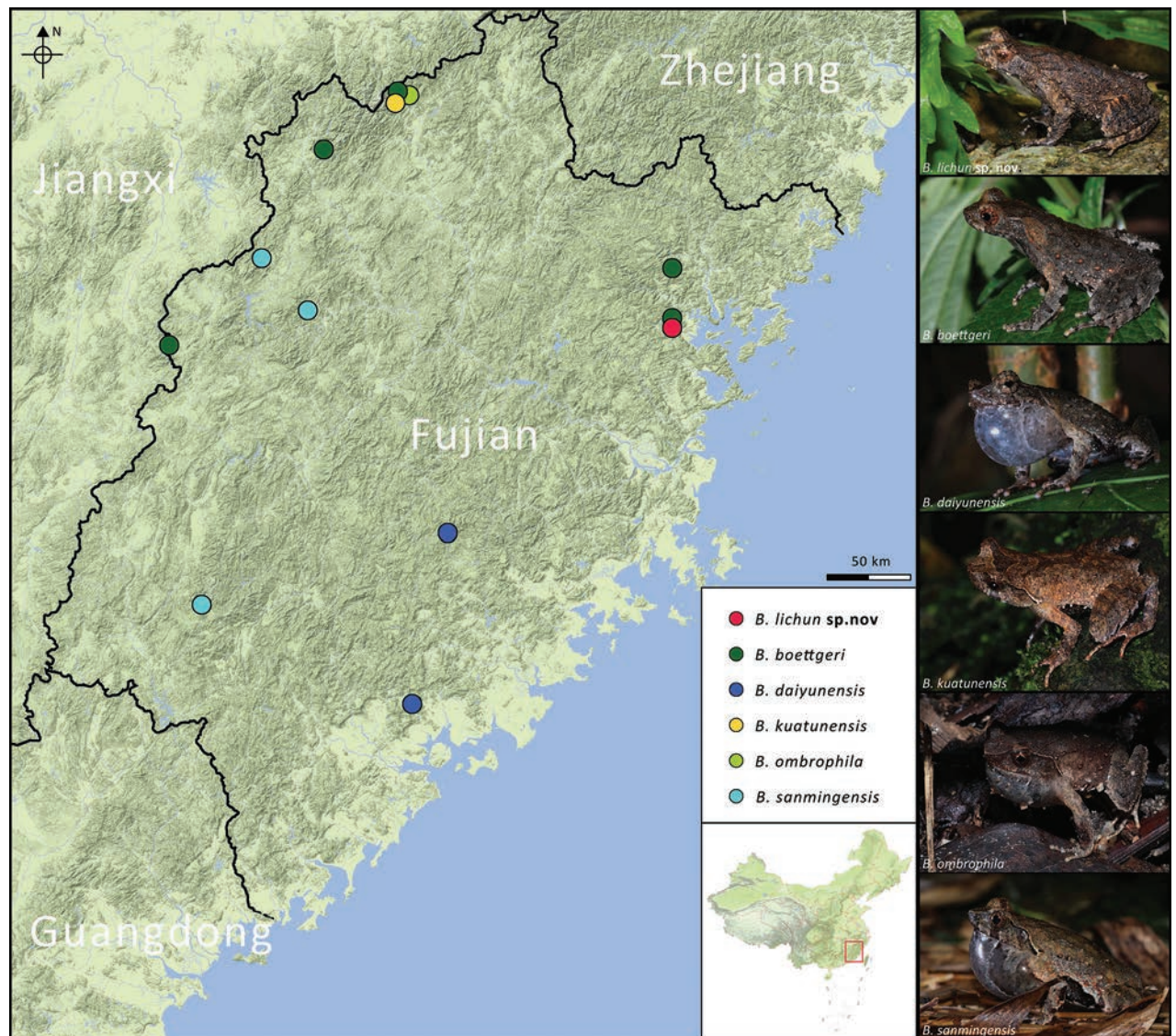


Figure 1. Map showing the distribution pattern of *Boulenophrys* species in Fujian Province, China. Distribution sites accessed from Lyu et al. (2023).

characters. Subsequent molecular analysis further revealed that these specimens represent a separate evolutionary lineage, displaying significant divergence from known congeners. Thus, we describe them as a new species below.

Materials and methods

Morphology

All examined specimens were fixed in 10% buffered formalin and later transferred to 70% ethanol. All studied specimens have been deposited at the Guangdong Polytechnic of Environmental Protection Engineering (GEP), Foshan City, Guangdong, and the Herpetological Museum, Chengdu Institute of Biology, the Chinese Academy of Sciences (CIB), Chengdu City, China.

External measurements were recorded with a digital caliper (Neiko 01407A stainless steel 6-inch digital caliper) to the nearest 0.1 mm. These measurements are as follows: SVL (snout–vent length, from tip of snout to posterior mar-

gin of vent); HDL (head length, from tip of snout to the articulation of the jaw); HDW (head width, head width at the commissure of the jaws); SNT (snout length, from tip of snout to the anterior corner of the eye); IND (internasal distance, distance between nares); IOD (interorbital distance, minimum distance between upper eyelids); ED (eye diameter, from the anterior corner of the eye to posterior corner of the eye); TD (tympanum diameter, horizontal diameter of tympanum); TED (tympanum–eye distance, from anterior edge of tympanum to posterior corner of the eye); HND (hand length, from the proximal border of the outer palmar tubercle to the tip of digit III); RAD (forearm or radiulna length, from the flexed elbow to the proximal border of the outer palmar tubercle); FTL (foot length, from distal end of shank to the tip of digit IV); TIB (crus or tibiofibula length, from the outer surface of the flexed knee to the heel). Sex was determined by external secondary sexual characters, such as the presence of vocal sacs, nuptial pads, or spines in males and their absence in females (Fei et al. 2009).

Morphological characters of all 68 recognized species of the genus *Boulenophrys* used for comparisons were based on information available in the literature (Table 1).

Table 1. Literature for morphological characters of 68 recognized species of *Boulenophrys*.

<i>Boulenophrys</i> species	References
<i>B. acuta</i> (Wang, Li & Jin, 2014)	Li et al. 2014; Lyu et al. 2023
<i>B. angka</i> (Wu, Suwannapoom, Poyarkov, Pawangkhanant, Xu, Jin, Murphy & Che, 2019)	Wu et al. 2019
<i>B. anlongensis</i> (Li, Lu, Liu & Wang, 2020)	Li et al. 2020; Lyu et al. 2023
<i>B. baishanzuensis</i> (Wu, Li, Liu, Wang & Wu, 2020)	Wu et al. 2020
<i>B. baolongensis</i> (Ye, Fei & Xie, 2007)	Ye et al. 2007; Fei and Ye 2016
<i>B. binchuanensis</i> (Ye & Fei, 1995)	Lyu et al. 2023
<i>B. binlingensis</i> (Jiang, Fei & Ye, 2009)	Fei et al. 2009; Lyu et al. 2023
<i>B. boettgeri</i> (Boulenger, 1899)	Lyu et al. 2023
<i>B. brachykolos</i> (Inger & Romer, 1961)	Lyu et al. 2023
<i>B. caobangensis</i> (Nguyen, Pham, Nguyen, Luong & Ziegler, 2020)	Nguyen et al. 2020
<i>B. caudoprocta</i> (Shen, 1994)	Shen 1994; Lyu et al. 2023
<i>B. congjiangensis</i> (Luo, Wang, Wang, Lu, Wang, Deng & Zhou, 2021)	Luo et al. 2021; Lyu et al. 2023
<i>B. cheni</i> (Wang & Liu, 2014)	Wang et al. 2014; Lyu et al. 2023
<i>B. chishuiensis</i> (Xu, Li, Liu, Wei & Wang, 2020)	Lyu et al. 2023
<i>B. daiyunensis</i> (Lyu, Wang & Wang, 2021)	Lyu et al. 2021; Lyu et al. 2023
<i>B. daoji</i> (Lyu, Zeng, Wang & Wang, 2021)	Lyu et al. 2021; Lyu et al. 2023
<i>B. daweimontis</i> (Rao & Yang, 1997)	Rao and Yang 1997
<i>B. dongguanensis</i> (Wang & Wang, 2019)	Lyu et al. 2023
<i>B. elongata</i> Zeng, Wang, Chen, Xiao, Zhan, Li & Lin, 2024	Zeng et al. 2024
<i>B. fengshunensi</i> Wang, Zeng, Lyu & Wang, 2022	Lyu et al. 2023
<i>B. fanjingmontis</i> (Zhang, Liang, Ran & Shen, 2012)	Lyu et al. 2023
<i>B. fansipanensis</i> (Tapley, Cutajar, Mahony, Nguyen, Dau, Luong, Le, Nguyen, Nguyen, Portway, Luong & Rowley, 2018)	Tapley et al. 2018a
<i>B. frigida</i> (Tapley, Cutaja, Nguyen, Portway, Mahony, Nguyen, Harding, Luong & Rowley, 2021)	Tapley et al. 2021
<i>B. hoanglienensis</i> (Tapley, Cutajar, Mahony, Nguyen, Dau, Luong, Le, Nguyen, Nguyen, Portway, Luong & Rowley, 2018)	Tapley et al. 2018a

<i>Boulenophrys</i> species	References
<i>B. hungtai</i> Wang, Zeng, Lyu, Xiao & Wang, 2022	Lyu et al. 2023
<i>B. hengshanensis</i> Qian, Hu, Mo, Gao, Zhang & Yang, 2023	Qian et al. 2023
<i>B. insularis</i> (Wang, Liu, Lyu, Zeng & Wang, 2017)	Wang et al. 2017a; Lyu et al. 2023
<i>B. jiangi</i> (Liu, Li, Wei, Xu, Cheng, Wang & Wu, 2020)	Lyu et al. 2023
<i>B. jingdongensis</i> (Fei & Ye, 1983)	Fei et al. 1983; Lyu et al. 2023
<i>B. jinggangensis</i> (Wang, 2012)	Wang et al. 2012; Lyu et al. 2023
<i>B. jiulianensis</i> (Wang, Zeng, Lyu & Wang, 2019)	Lyu et al. 2023
<i>B. kuatunensis</i> (Pope, 1929)	Lyu et al. 2023
<i>B. leishanensis</i> (Li, Xu, Liu, Jiang, Wei & Wang, 2018)	Lyu et al. 2023
<i>B. lushuiensis</i> (Shi, Li, Zhu, Jiang, Jiang & Wang, 2021)	Wang et al. 2017b; Lyu et al. 2023
<i>B. liboensis</i> (Zhang, Li, Xiao, Li, Pan, Wang, Zhang & Zhou, 2017)	Zhang et al. 2017
<i>B. lini</i> (Wang & Yang, 2014)	Wang et al. 2014; Lyu et al. 2023
<i>B. lishuiensis</i> (Wang, Liu & Jiang, 2017)	Lyu et al. 2023
<i>B. minor</i> (Stejneger, 1926)	Lyu et al. 2023
<i>B. mirabilis</i> (Lyu, Wang & Zhao, 2020)	Lyu et al. 2020; Lyu et al. 2023
<i>B. mufumontana</i> (Wang, Lyu & Wang, 2019)	Lyu et al. 2023
<i>B. nankunensis</i> (Wang, Zeng & Wang, 2019)	Lyu et al. 2023
<i>B. nanlingensis</i> (Lyu, Wang, Liu & Wang, 2019)	Lyu et al. 2023
<i>B. obesa</i> (Wang, Li & Zhao, 2014)	Li et al. 2014; Lyu et al. 2023
<i>B. ombrophila</i> (Messenger & Dahn, 2019)	Lyu et al. 2023
<i>B. omeimontis</i> (Liu, 1950)	Lyu et al. 2023
<i>B. palpebralespinosa</i> (Bourret, 1937)	Fei et al. 2009; Lyu et al. 2023
<i>B. pepe</i> (Wang & Zeng, 2024)	Wang et al. 2024
<i>B. puningensis</i> Wang, Zeng, Lyu, Xiao & Wang, 2022	Lyu et al. 2023
<i>B. qianbeinsis</i> (Su, Shi, Wu, Li, Yao, Wang & Li, 2020)	Lyu et al. 2023
<i>B. rubrimera</i> (Tapley, Cutajar, Mahony, Chung, Dau, Nguyen, Luong & Rowley, 2017)	Tapley et al. 2017, 2018b
<i>B. sangzhiensis</i> (Jiang, Ye & Fei, 2008)	Lyu et al. 2023
<i>B. sanmingensis</i> (Lyu & Wang, 2021)	Lyu et al. 2021; Lyu et al. 2023
<i>B. shimentaina</i> (Lyu, Liu & Wang, 2020)	Lyu et al. 2020; Lyu et al. 2023
<i>B. shuichengensis</i> (Tian & Sun, 1995)	Tian and Sun 1995; Tian et al. 2000; Fei and Ye 2016
<i>B. shunhuangensis</i> (Wang, Deng, Liu, Wu & Liu, 2019)	Wang et al. 2019b; Lyu et al. 2023
<i>B. spinata</i> (Liu & Hu, 1973)	Hu et al. 1973; Lyu et al. 2023
<i>B. tongboensis</i> (Wang & Lyu, 2021)	Lyu et al. 2021; Lyu et al. 2023
<i>B. tuberogranulatus</i> (Shen, Mo & Li, 2010)	Mo et al. 2010; Fei and Ye 2016; Lyu et al. 2023
<i>B. wugongensis</i> (Wang, Lyu & Wang, 2019)	Lyu et al. 2023
<i>B. wuliangshanensis</i> (Ye & Fei, 1995)	Lyu et al. 2023
<i>B. wushanensis</i> (Ye & Fei, 1995)	Ye and Fei 1995; Fei and Ye 2016; Lyu et al. 2023
<i>B. xiangnanensis</i> (Lyu, Zeng & Wang, 2020)	Lyu et al. 2020; Lyu et al. 2023
<i>B. xianjuensis</i> (Wang, Wu, Peng, Shi, Lu & Wu, 2020)	Lyu et al. 2023
<i>B. xuefengmontis</i> Lyu & Wang, 2023	Lyu et al. 2023
<i>B. yangmingensis</i> (Lyu, Zeng & Wang, 2020)	Lyu et al. 2020; Lyu et al. 2023
<i>B. yaoshanensis</i> Qi, Mo, Lyu, Wang & Wang, 2021	Qi et al. 2021; Lyu et al. 2023
<i>B. yingdeensis</i> Qi, Lyu, Wang & Wang, 2021	Qi et al. 2021; Lyu et al. 2023
<i>B. yunkaiensis</i> Qi, Wang, Lyu & Wang, 2021	Qi et al. 2021; Lyu et al. 2023

Phylogeny

We use two partial mitochondrial genes, the 16S ribosomal RNA (16S) and the cytochrome c oxidase 1 (COI), for phylogenetic analysis. DNA extraction, PCR amplification, and sequencing protocols follow that of Liu et al. (2018). In total, 84 sequences were used in this study, including six new ones from this study and 78 attained from GenBank. Two samples of the genus *Xenophrys* were used as outgroups (Suppl. material 1).

We used Clustal X 2.0 (Thompson et al. 1997) for sequence aligning with default parameters. PartitionFinder (Lanfear et al. 2012) was used for searching the optimal partitioning schemes and the analysis determined that partitioning by gene was optimal for 16S, while partitioning by codon position was optimal for COI, with GTR+I+G identified as the best-fit nucleotide substitution model for all partitions. Phylogenetic trees were constructed using maximum likelihood (ML) implemented in RaxmlGUI v.1.3 (Silvestro and Michalak 2012), and Bayesian inference (BI) using MrBayes v.3.2.4 (Ronquist et al. 2012). For the ML analysis, an optimal tree was obtained and branch supports were evaluated with 1000 rapid bootstrapping replicates. For the BI analysis, two independent runs were conducted with each running for 10,000,000 generations and sampled every 1000 generations with the first 25% samples discarded as burn-in, resulting in a potential scale reduction factor (PSRF) of < 0.01. Then the remaining trees were used to create a consensus tree. Nodes having ML bootstrap values (BS) ≥ 70 and BI posterior probabilities (BPP) ≥ 0.90 were considered well supported.

Results

The BI and ML phylogenetic trees resulted in essentially identical topologies, with the ML phylogenetic tree shown in Fig. 2. The relationship among the *Boulenophrys* species in our trees correspond to those in previous studies (Liu et al. 2018; Lyu et al. 2023; Zeng et al. 2024; Wang et al. 2024). Our results show that all samples from eastern Fujian, China, cluster into a monophyletic group with strong nodal support (BS 100, BPP 1.00), and are distinct from all known *Boulenophrys* species occurring in Fujian. Furthermore, the corresponding specimens of the evolving lineage can be distinguished from all recognized congeners by a combination of morphological characters. As both the phylogenetic results and morphological comparisons support that the lineage from eastern Fujian represents an undescribed new species, we thus describe it below.

Taxonomic account

Boulenophrys lichun sp. nov.

<https://zoobank.org/02303B1E-ED1A-482B-8BD3-B32BC0DB9D6B>

Fig. 3

Lichun Horned Toad (in English) / lì chūn jiǎo chán (立春角蟾 in Chinese)

Material examined. Holotype. CHINA · ♂; Fujian Province, Ningde City, Jiaocheng District, Mt Nanji; 26.645774°N, 119.519939°E, ca. 230 m elev.; 4 Feb. 2024; Jian Wang, Zhao-Chi Zeng, Shi-Shi Lin and Yuan-Hang Li leg.; GEP a214.



Figure 2. Maximum-likelihood phylogenies, with ‘*’ representing BS \geq 70 or BPP \geq 0.90 and ‘-’ representing BS < 70 or BPP < 0.90.

Paratypes. CHINA • 4♂♂; same data as for holotype; CIB 121428 [field number GEP a210], GEP a211–213 • 1♀; same data as for holotype; GEP a215.

Etymology. The specific name *lichun* is derived from Chinese Pinyin Lì Chūn, i.e. 立春 in Chinese, which means the beginning of spring, the first of the 24 solar terms (24节气) of China. The specific name refers to the breeding season of the new species which begins around this period. The song of the new species heralds the spring of a year. The type specimens of the new species were also collected on “Lichun” of the Year 2024.

Diagnosis. (1) small size (SVL 33.5–37.0 mm in five adult males, SVL 47.1 mm in a single adult female); (2) canthus rostralis well developed, tongue not notched posteriorly; (3) tympanum distinct; (4) vomerine ridges and vomerine teeth present; (5) dorsal skin rough and highly granular, discontinuous X-shaped ridge on center of dorsum, discontinuous dorsolateral ridges present, sparse large tubercles on flanks, dorsal limbs with discontinuous transverse ridges and tubercles, ventral skin with dense raised tubercles; (6) outer margin

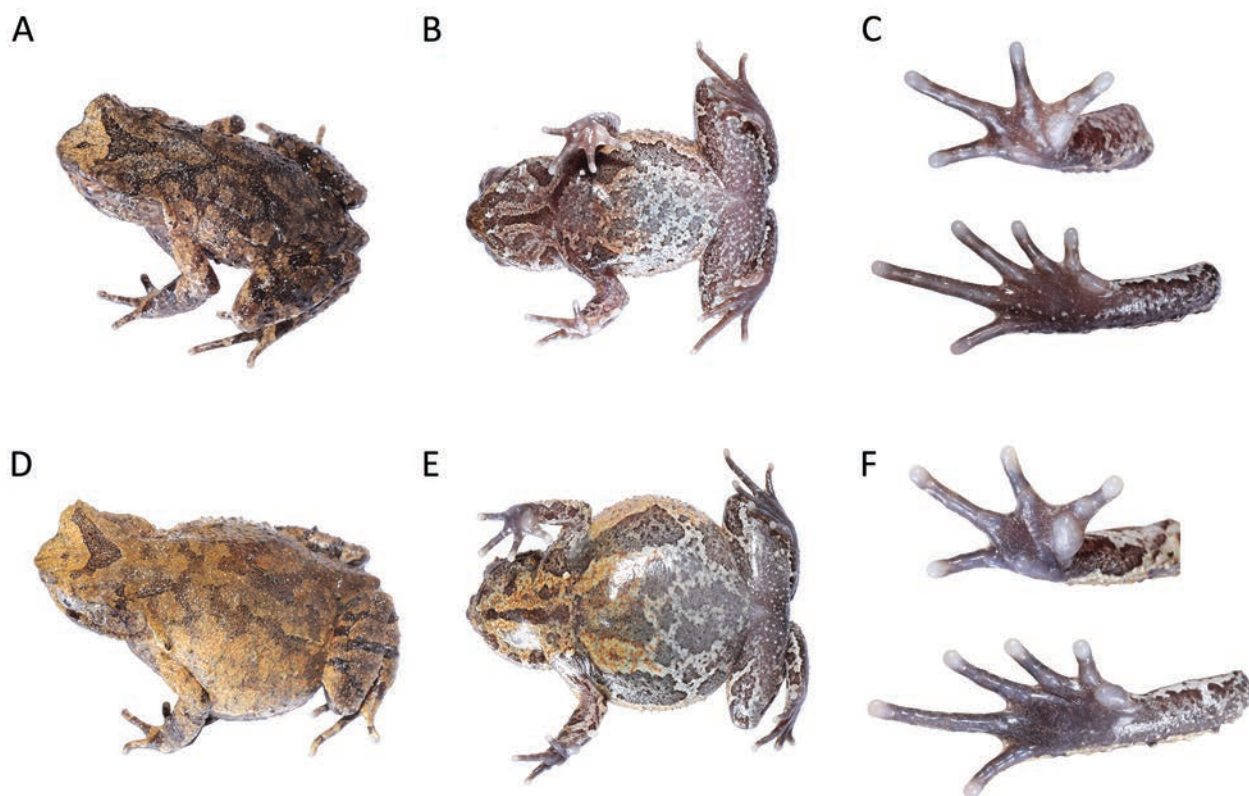


Figure 3. The male holotype (GEP a214, A–C) and the female paratype (GEP a215, D–F) of *Boulenophrys lichun* sp. nov. in life.

of upper eyelid with a small horn-like prominent tubercle, supratympanic fold distinct and narrow, curving posteroventrally to above arm; (7) two metacarpal tubercles distinct, inner one observably enlarged; relative finger lengths $I < II < IV < III$; distinct subarticular tubercle at base of each finger; (8) heels not meeting when hindlimbs folded; tibio-tarsal articulation reaching shoulder to posterior corner of eye; (9) toes without webbing and lateral fringes, inner metatarsal tubercle long ovoid, outer one absent, relative toe length $I < II < V < III < IV$; (10) dorsal surface yellowish-brown with irregular dark-brown patches, and dark-brown triangular marking between eyes, dorsal limbs and digits light brown with dark-brown transverse bands; and (11) dense nuptial spines on dorsal bases of fingers I and II in breeding adult males, subgular vocal sac present in males.

Description of holotype. Adult male. Body size small, SVL 37.0 mm. Head width larger than head length, HWD/HDL 1.04; snout rounded in dorsal view, projecting, sloping backward to mouth in profile, protruding well beyond margin of lower jaw; top of head flat; eyes moderate in size, ED 0.34 of HDL, pupil vertical, near diamond-shaped; nostril obliquely ovoid; canthus rostralis well developed; loreal region slightly oblique; internasal distance slightly larger than interorbital distance; tympanic region oblique, tympanum distinct and visible in dorsal view; tympanum moderate in size, margin clear, upper margin in contact with supratympanic fold, lower margin in contact with upper lip, TD/ED 0.55; large ovoid choanae at base of maxilla; vomerine ridge and vomerine teeth present, maxillary teeth present; margin of tongue rounded, not notched distally; presence of single subgular vocal sac.

Forearm length 0.23 of SVL, hand 0.24 of SVL; webbing absent between fingers, lateral fringes absent, relative finger length $I < II < IV < III$; tips of fingers slightly dilated, round; subarticular tubercles on base of fingers present, dis-

tinct; inner metacarpal tubercle observably enlarged, outer one slightly smaller; single nuptial pad bearing nuptial spines present on dorsal surface of first and second fingers, respectively. Hindlimbs short, tibio-tarsal articulation reaching forward to posterior corner of eye when hindlimb stretched along body; heels not meeting when flexed hindlimbs held at right angles to body axis; crus length 0.40 of SVL and foot length 0.58 of SVL; relative toe length I < II < V < III < IV; tips of toes round and slightly dilated; toes without lateral fringes and webbing; subarticular tubercles on base of toes present and distinct; inner metatarsal tubercle long ovoid and lacking outer metatarsal tubercle.

Dorsal skin rough and highly granular; dense large tubercles on flanks; single horn-like prominent tubercle on edge of upper eyelid; obvious supratympanic fold curving posteroventrally from posterior corner of eye to level above insertion of arm; upper lip, mandibular articulation, loreal, temporal region excluding tympanum, upper eyelid and surface around cloaca with conical tubercles; discontinuous X-shaped ridge on center of dorsum, discontinuous dorsolateral ridges present; ventral surface with dense raised tubercles; tubercles on ventral hindlimbs and around cloaca bearing tiny spines on their tips; small and distinct pectoral gland closer to axilla; single femoral gland positioned on posterior surface of thigh at midpoint between knee and cloaca.

Coloration of holotype. In life, dorsal surface of body yellowish-brown with irregular dark-brown patches, dark-brown X-shaped marking on center of dorsum, dark-brown triangular marking between eyes. A vertical dark-brown band present below eye. Dorsal surface of limbs with dark-brown transverse bands. Tubercles on edge of upper eyelids orange. Supratympanic fold light brown. Surface of throat and chest yellowish-brown with irregular dark brown and white patches and white and orange dots. Center of throat with black longitudinal band. Surface of abdomen white, mottled with orange dots and black patches. Surface of ventral limbs purple brown, with white mottling and dark-brown patches. Spines on tips of tubercles on ventral hindlimbs and area around cloaca black. Digits gray white; subarticular tubercles, inner and outer metacarpal tubercles and inner metatarsal tubercle grayish-brown. Pectoral glands and femoral glands white. Iris yellowish-brown with range mottling.

In preservative, the dorsal surface of the body is dark brown, with markings and patches more distinct. Surface of chest, throat and limbs are dark brown, with dark-brown markings and patches more distinct, white patches and dots faded and orange dots absent. Color of pectoral glands and femoral glands faded.

Variation. Morphometric variation is listed in Table 2. Most of the paratypes are similar to the holotype in morphology and color pattern, except for the following: tibio-tarsal articulation reaching forward to posterior corner of eye when hindlimb stretched along body in the holotype GEP a214, while reaching to shoulder in female paratype GEP a215; absence of nuptial pads and spines in the female paratype; larger body size in the female paratype.

Comparisons. *Boulenophrys lichun* sp. nov. can easily be distinguished from the following congeners by its heels not meeting when flexed hindlimbs held at right angles to body axis: *B. anlongensis*, *B. baishanzuensis*, *B. binlingensis*, *B. caudoprocta*, *B. cheni*, *B. chishuiensis*, *B. congjiangensis*, *B. daweimontis*, *B. fanjingmontis*, *B. fansipanensis*, *B. frigida*, *B. hoanglienensis*, *B. jiangi*, *B. jingdongensis*, *B. jinggangensis*, *B. jiulianensis*, *B. leishanensis*, *B. liboensis*, *B. lini*, *B. lushuiensis*, *B. mirabilis*, *B. mufumontana*, *B. nanlingensis*, *B. omeimontis*, *B. palpebralespinosa*,

Table 2. Measurements (in mm) of voucher specimens of *Boulenophrys lichun* sp. nov.; * holotype.

Voucher	CIB 121428	GEP a211	GEP a212	GEP a213	GEP a214 *	GEP a215
Sex	male	male	male	male	male	female
SVL	36.7	33.5	35.7	34.6	37.0	47.1
HDL	13.1	12.7	13.5	12.9	13.3	15.3
HDW	13.6	13.3	13.8	13.6	13.9	16.5
ED	4.5	4.0	4.5	4.5	4.8	5.5
TD	2.3	2.6	2.5	2.5	2.6	2.8
TED	1.7	1.7	1.8	1.8	1.7	2.4
SNT	4.5	4.4	4.5	4.5	4.6	4.9
IND	3.6	3.7	3.8	3.7	3.9	4.3
IOD	3.5	3.3	3.4	3.5	3.7	4.3
HDN	8.7	7.8	8.7	9.1	9.2	10.2
RAD	8.6	7.0	8.5	8.1	8.7	9.0
FTL	20.7	18.9	20.7	20.9	21.4	24.1
TIB	14.3	12.5	14.3	14.5	14.7	15.7

B. qianbeiensis, *B. sangzhiensis*, *B. sanmingensis*, *B. shimentaina*, *B. shunhuanensis*, *B. spinata*, *B. sanmingensis*, *B. tongboensis*, *B. tuberogranulata*, *B. wuliangshanensis*, *B. xianjuensis*, *B. yangmingensis*, *B. yaoshanensis*, *B. yingdeensis* (vs. heels overlapping), from *B. binchuanensis*, *B. elongata*, *B. lishuiensis*, *B. minor*, *B. xiangnanensis*, *B. xuefengmontis* (vs. heels just meeting), and from *B. angka*, *B. daiyunensis*, *B. baolongensis*, *B. wushanensis*, *B. yunkaiensis* (vs. heels just meeting or slightly overlapping).

Boulenophrys lichun sp. nov. can easily be distinguished from the following congeners by its tongue not notched distally: *B. brachykolos*, *B. insularis*, *B. pepe* (vs. tongue notched distally). *Boulenophrys lichun* sp. nov. can easily be distinguished from the following congeners by its presence of vomerine teeth: *B. acuta*, *B. boettgeri*, *B. caobangensis*, *B. daoji*, *B. hungtai*, *B. hengshanensis*, *B. kuatunensis*, *B. ombrophila*, *B. obesa*, *B. shuichengensis*, *B. wugongensis* (vs. vomerine teeth absent).

Boulenophrys lichun sp. nov. can easily be distinguished from the following congeners by its absence of lateral fringes on webbing on toes: *B. dongguanensis*, *B. fengshunensis*, *B. nankunensis*, *B. puningensis* (vs. toes with rudimentary webbing), and from *B. rubrimera* (vs. toes with narrow lateral fringes).

Distribution and natural history. Currently, *Boulenophrys lichun* sp. nov. is only known from the coastal hills of Ningde City, eastern Fujian Province, China. It inhabits flowing montane seeps and the nearby forest floor and leaf litter. The habitat is surrounded by secondary forest mixed with bamboo groves at elevations between 150–510 m. Advertisement calls of males were heard from February to May. Males were found calling in rock crevices.

Discussion

The lack of follow-up surveys can pose issues in terms of endangered species listing. *Boulenophrys lichun* is currently only known from the coastal hills of Ningde City, eastern Fujian. The development of tourism infrastructure, stream diversion and tea leaf cultivation have gradually affected and threatened the habitats of the new species. Thus, more data (i.e., distribution, population size, potential and existing risk factors, etc.) from long-term extensive surveys are urgently required to make an assessment of their endangered status.

Boulenophrys possess limited dispersal abilities and narrow ecological niches, resulting in the restricted distribution ranges of many species (Wang et al. 2019a; Lyu et al. 2023). Their high levels of morphological conservatism (Liu et al. 2018; Wang et al. 2022; Lyu et al. 2023) and the lack of follow-up surveys have led to inadequate protection due to misidentifications and deficient data. Thus, we provide a provincial key below to aid the local authorities in accurately identifying species during field identifications and data collection efforts and further serve their conservation.

Key to *Boulenophrys* species occurring in Fujian Province, China

- 1 Vomerine ridges and vomerine teeth present 2
- Vomerine ridges and vomerine teeth absent..... 3
- 2 Toes with rudimentary webbing and wide lateral fringes *B. daiyunensis*
- Toes without webbing and lateral fringes..... *B. lichun*
- 3 Toes with rudimentary webbing and lateral fringes..... 4
- Toes without webbing and lateral fringes..... *B. ombrophila*
- 4 Toes with wide lateral fringes..... 5
- Toes with narrow lateral fringes..... *B. kuatunensis*
- 5 Round light patches on the shoulder present..... *B. boettgeri*
- Round light patches on the shoulder absent..... *B. sanmingensis*

Acknowledgments

We thank Chong Xu, Xin Zhao, Qi-Feng Yan, Yu-Sen Chen, and Gen-De Yu, for their long-term monitoring of the breeding season of *Boulenophrys lichun*. We thank Chao Huang from the Australian Museum, Australia for proofreading the manuscript.

Additional information

Conflict of interest

The authors have declared that no competing interests exist.

Ethical statement

No ethical statement was reported.

Funding

This work was supported by the Project of Innovation team of General Institutes of Higher Education in Guangdong Province (2024KCXTD078), the Project of Integration of resource monitoring, epidemic diseases monitoring and rescue capability of wildlife in 2023 (ZT202304111), the Project of Innovation team of General Institutes of Higher Education in Guangdong Province (2024KCXTD078) and the Project of Background survey of biosafety in Guangdong Province (STST-2021-10).

Author contributions

Conceptualization: Jian Wang, Zhao-Chi Zeng; Data curation: Jian Wang, Zhao-Chi Zeng; Funding acquisition: Shi-Shi Lin; Investigation: All authors; Writing – original draft, review and editing: All authors.

Author ORCIDs

Shi-Shi Lin  <https://orcid.org/0000-0001-7709-7005>

Hong-Hui Chen  <https://orcid.org/0000-0001-5026-2920>

Yuan-Hang Li  <https://orcid.org/0009-0009-6543-9245>

Zhao-Ning Peng  <https://orcid.org/0009-0008-5103-2797>

Zhao-Chi Zeng  <https://orcid.org/0000-0003-4054-8399>

Jian Wang  <https://orcid.org/0000-0003-4249-7767>

Data availability

All of the data that support the findings of this study are available in the main text or Supplementary Information.

References

- Bonaparte CLJL (1850) *Conspectus Systematum Herpetologiae et Amphibiologiae*. Editio altera reformata [Lugduni Batavorum], Brill EJ, Leiden, 1 pp.
- Bourret R (1937) Notes herpétologiques sur l'Indochine française. XIV. Les batraciens de la collection du Laboratoire des Sciences Naturelles de l'Université. Descriptions de quinze especes ou variétés nouvelles. Annexe au Bulletin Général de l'Instruction Publique. Hanoi 1937: 5–56.
- Fei L, Ye CY (2016) *Amphibians of China* (Vol. 1). Science Press, Beijing, 1040 pp.
- Fei L, Ye CY, Huang YZ (1983) Two new subspecies of *Megophrys omeimontis* Liu from China (Amphibia, Pelobatidae). *Acta Herpetologica Sinica*. New Series. Chengdu 2(2): 49–52. [In Chinese with English abstract]
- Fei L, Hu SQ, Ye CY, Huang YZ (2009) *Fauna Sinica*. Amphibia. (Vol. 2). Anura. Science Press, Beijing, 503 pp. [in Chinese]
- Frost DR (2024) *Amphibian Species of the World: an online reference*. Version 6.2. American Museum of Natural History, New York, USA. <https://amphibiansoftheworld.amnh.org/index.php> [accessed 9 September 2024]
- Hu SQ, Zhao EM, Liu CC (1973) A survey of amphibians and reptiles in Kweichow province, including a herpetofaunal analysis. *Acta Zoologica Sinica/ Dong wu xue bao*, 19: 149–181.
- Inger RF, Romer JD (1961) A new pelobatid frog of the genus *Megophrys* from Hong Kong. *Fieldiana, Zoology*, 39: 533–538.
- Jiang JP, Ye CY, Fei L (2008) A new horn toad *Megophrys sangzhiensis* from Hunan, China (Amphibia, Anura). *Zoological Research* 29: 219–222. [in Chinese with English abstract] <https://doi.org/10.3724/SP.J.1141.2008.00219>
- Lanfear R, Calcott B, Ho SYW, Guindon S (2012) PartitionFinder: combined selection of partitioning schemes and substitution models for phylogenetic analyses. *Molecular Biology & Evolution* 29: 1695–1701. <https://doi.org/10.1093/molbev/mss020>
- Li YL, Jin MJ, Zhao J, Liu ZY, Wang YY, Pang H (2014) Description of two new species of the genus *Megophrys* (Amphibia: Anura: Megophryidae) from Heishiding Nature Reserve, Fengkai, Guangdong, China, based on molecular and morphological data. *Zootaxa* 3795: 449–471. <https://doi.org/10.11646/zootaxa.3795.4.5>
- Li SZ, Xu N, Liu J, Jiang JP, Wei G, Wang B (2018) A new species of the asian toad genus *Megophrys* sensu lato (Amphibia: Anura: Megophryidae) from Guizhou Province, China. *Asian Herpetological Research* 9: 224–239. <https://doi.org/10.16373/j.cnki.ahr.180072>

- Li SZ, Lu NN, Liu J, Wang B (2020) Description of a new *Megophrys* Kuhl & Van Hasselt, 1822 (Anura, Megophryidae) from Guizhou Province, China. *ZooKeys* 986: 101–126. <https://doi.org/10.3897/zookeys.986.57119>
- Liu CC (1950) Amphibians of western China. *Fieldiana. Zoology Memoires* 2: 1–397. [+ 10 pl.] <https://doi.org/10.5962/bhl.part.4737>
- Liu ZY, Chen GL, Zhu TQ, Zeng ZC, Lyu ZT, Wang J, Messenger K, Greenberg AJ, Guo ZX, Yang ZH, Shi SH, Wang YY (2018) Prevalence of cryptic species in morphologically uniform taxa – Fast speciation and evolutionary radiation in Asian frogs. *Molecular Phylogenetics and Evolution* 127: 723–731. <https://doi.org/10.1016/j.ympev.2018.06.020>
- Liu J, Li S, Wei G, Xu N, Cheng Y, Wang B, Wu J (2020) A new species of the asian toad genus *Megophrys* sensu lato (Anura: Megophryidae) from Guizhou Province, China. *Asian Herpetological Research* 11: 1–18. <https://doi.org/10.16373/j.cnki.ahr.190041>
- Luo T, Wang Y, Wang S, Lu X, Wang W, Deng H, Zhou J (2021) A species of the genus *Panophrys* (Anura, Megophryidae) from southeastern Guizhou Province, China. *ZooKeys* 1047(2):27–60. <https://doi.org/10.3897/zookeys.1047.61097>
- Lyu ZT, Li YQ, Zeng ZC, Zhao J, Liu ZL, Guo GX, Wang YY (2020) Four new species of Asian horned toads (Anura, Megophryidae, *Megophrys*) from southern China. *ZooKeys* 942: 105–140. <https://doi.org/10.3897/zookeys.942.47983>
- Lyu ZT, Zeng ZC, Wang J, Liu ZY, Huang YQ, Li WZ, Wang YY (2021) Four new species of *Panophrys* (Anura, Megophryidae) from eastern China, with discussion on the recognition of *Panophrys* as a distinct genus. *Zootaxa* 4927(1):9–40. <https://doi.org/10.11646/zootaxa.4927.1.2>
- Lyu ZT, Qi S, Wang J, Zhang SY, Zhao J, Zeng ZC, Wan H, Yang JH, Mo YM, Wang YY (2023) Generic classification of Asian Horned Toads (Anura: Megophryidae: Megophryinae) and monograph of Chinese species. *Zoological Research*. Kunming 44: 380–450. <https://doi.org/10.24272/j.issn.2095-8137.2022.372>
- Messenger KR, Dahn HA, Liang Y, Xie P, Wang Y, Lu C (2019) A new species of the genus *Megophrys* Gunther, 1864 (Amphibia: Anura: Megophryidae) from Mount Wuyi, China. *Zootaxa* 4554: 561–583. <https://doi.org/10.11646/zootaxa.4554.2.9>
- Mo XY, Shen YH, Li HH, Wu XS (2010) A new species of *Megophrys* (Amphibia: Anura: Megophryidae) from the northwestern Hunan Province, China. *Current Zoology* 56(4): 432–436. <https://doi.org/10.1093/czoolo/56.4.432>
- Nguyen TQ, Pham CT, Nguyen TT, Luong AM, Ziegler T (2020) A new species of *Megophrys* (Amphibia: Anura: Megophryidae) from Vietnam. *Zootaxa* 4722(5): 401–422. <https://doi.org/10.11646/zootaxa.4722.5.1>
- Pope CH (1929) Four new frogs from Fukien Province, China. *American Museum Novitates* 352: 1–5.
- Qi S, Lyu ZT, Wang J, Mo YM, Zeng ZC, Zeng YJ, Dai KY, Li YQ, Grismer LL, Wang YY (2021) Three new species of the genus *Boulenophrys* (Anura, Megophryidae) from southern China. *Zootaxa* 5072 (5): 401–438. <https://doi.org/10.11646/zootaxa.5072.5.1>
- Qian TY, Hu K, Mo XY, Gao Z, Zhang N, Yang DD (2023) A new species of *Boulenophrys* from central Hunan Province, China (Anura: Megophryidae). *Vertebrate Zoology* 73: 915–930. <https://doi.org/10.3897/vz.73.e100889>
- Rao DQ, Yang DT (1997) The karyotypes of Megophryinae (Pelobatinae) with a discussion on their classification and phylogenetic relationships. *Asiatic Herpetological Research* 7: 93–102. <https://doi.org/10.5962/bhl.part.18858>
- Ronquist F, Teslenko M, Van Der Mark P, Ayres D, Darling A, Höhna S, Larget B, Liu L, Suchard MA, Huelsenbeck JP (2012) Mrbayes 3.2: Efficient bayesian phylogenetic

- inference and model choice across a large model space. *Systematic Biology* 61(3): 539–542. <https://doi.org/10.1093/sysbio/sys029>
- Shen YH (1994) A new pelobatid toad of the genus *Megophrys* from China (Anura: Pelobatidae). *Collection of Articles for the 60th Anniversary of the Foundation of the Zoological Society of China*. Nanking, Zoological Society of China, 603–606.
- Shi SC, Li DH, Zhu WB, Jiang W, Jiang JP, Wang B (2021) Description of a new toad of *Megophrys* Kuhl & Van Hasselt, 1822 (Amphibia: Anura: Megophryidae) from western Yunnan Province, China. *Zootaxa* 4942: 351–381. <https://doi.org/10.11646/zootaxa.4942.3.3>
- Silvestro D, Michalak I (2012) raxmlGUI: A graphical front-end for RAxML. *Organisms, Diversity & Evolution* 12(4): 335–337. <https://doi.org/10.1007/s13127-011-0056-0>
- Su HJ, Shi SC, Wu YQ, Li GR, Yao XG, Wang B, Li SZ (2020) Description of a new horned toad of *Megophrys* Kuhl & Van Hasselt, 1822 (Anura, Megophryidae) from southwest China. *Zookeys* 974: 131–159. <https://doi.org/10.3897/zookeys.974.56070>
- Tapley B, Cutajar T, Mahony S, Nguyen CT, Dau VQ, Nguyen TT, Luong HV, Rowley JJJ (2017) The Vietnamese population of *Megophrys kuatunensis* (Amphibia: Megophryidae) represents a new species of Asian horned frog from Vietnam and southern China. *Zootaxa* 4344: 465–492. <https://doi.org/10.11646/zootaxa.4344.3.3>
- Tapley B, Cutajar TP, Mahony S, Nguyen CT, Dau VQ, Luong AM, Le DT, Nguyen TT, Nguyen TQ, Portway C, Luong HV, Rowley JJJ (2018a) Two new and potentially highly threatened *Megophrys* Horned frogs (Amphibia: Megophryidae) from Indochina's highest mountains. *Zootaxa* 4508: 301–333. <https://doi.org/10.11646/zootaxa.4508.3.1>
- Tapley B, Cutajar T, Nguyen LT, Nguyen CT, Harding L, Portway C, Van Luong H, Rowley JJ (2018b) A new locality and elevation extension for *Megophrys rubrimer* (Tapley et al., 2017) in Bat Xat Nature Reserve, Lao Cai Province, northern Vietnam. *Herpetology Notes* 11: 865–868.
- Tapley B, Cutajar T, Nguyen LT, Portway C, Mahony S, Nguyen CT, Harding L, Luong HV, Rowley JJJ (2021) A new potentially Endangered species of *Megophrys* (Amphibia: Megophryidae) from Mount Ky Quan San, north-west Vietnam. *Journal of Natural History* 54: 2543–2575. <https://doi.org/10.1080/00222933.2020.1856952>
- Thompson JD, Gibson TJ, Plewniak F, Jeanmougin F, Higgins DG (1997) The CLUSTAL_X windows interface: flexible strategies for multiple sequence alignment aided by quality analysis tools. *Nucleic Acids Research* 25: 4876–4882. <https://doi.org/10.1093/nar/25.24.4876>
- Tian YZ, Sun A (1995) A new species of *Megophrys* from China (Amphibia: Pelobatidae). *Journal of Liupanshui Teachers College* 52(3): 11–15. [in Chinese]
- Tian YZ, Gu XM, Sun AQ (2000) A new species of *Megophrys* in China (Amphibia: Pelobatidae). *Acta Zootaxonomica Sinica* 25: 462–466. [in Chinese]
- Wang YY, Zhang TD, Zhao J, Sung YH, Yang JH, Pang H, Zhang Z (2012) Description of a new species of the genus *Xenophrys* Gunther, 1864 (Amphibia: Anura: Megophryidae) from Mount Jinggang, China, based on molecular and morphological data. *Zootaxa* 3546: 53–67. <https://doi.org/10.11646/zootaxa.3546.1.4>
- Wang YY, Zhao J, Yang JH, Zhou Z, Chen GL, Liu Y (2014) Morphology, molecular genetics, and bioacoustics support two new sympatric *Xenophrys* toads (Amphibia: Anura: Megophryidae) in Southeast China. *PloS ONE* 9: e93075. <https://doi.org/10.1371/journal.pone.0093075>
- Wang J, Liu ZY, Lyu ZT, Zeng ZC, Wang YY (2017a) A new species of the genus *Xenophrys* (Amphibia: Anura: Megophryidae) from an offshore island in Guangdong Province, southeastern China. *Zootaxa* 4324: 541–556. <https://doi.org/10.11646/zootaxa.4324.3.8>

- Wang YF, Liu BQ, Jiang K, Jin W, Xu JN, Wu CH (2017b) A new species of the Horn Toad of the genus *Xenophrys* from Zhejiang, China (Amphibia: Megophryidae). Chinese Journal of Zoology 52: 19–29. [in Chinese with English abstract] <https://doi.org/10.13859/j.cjz.201701003>
- Wang J, Lyu ZT, Liu ZY, Liao CK, Zeng ZC, Zhao J, Li YL, Wang YY (2019a) Description of six new species of the subgenus *Panophrys* within the genus *Megophrys* (Anura, Megophryidae) from southeastern China based on molecular and morphological data. ZooKeys 851: 113–164. <https://doi.org/10.3897/zookeys.851.29107>
- Wang L, Deng X, Liu Y, Wu Q, Liu Z (2019b) A new species of the genus *Megophrys* (Amphibia: Anura: Megophryidae) from Hunan, China. Zootaxa 4695: 301–330. <https://doi.org/10.11646/zootaxa.4695.4.1>
- Wang B, Wu YQ, Peng JW, Shi SC, Lu NN, Wu J (2020) A new *Megophrys* Kuhl & Van Hasselt (Amphibia, Megophryidae) from southeastern China. ZooKeys 904: 35–62. <https://doi.org/10.3897/zookeys.904.47354>
- Wang J, Zeng ZC, Lyu ZT, Qi S, Liu ZY, Chen HH, Lu YH, Xiao HW, Lin CR, Chen K, Wang YY (2022) Description of three new *Boulenophrys* species from eastern Guangdong, China, emphasizing the urgency of ecological conservation in this region (Anura, Megophryidae). Zootaxa 5099(1): 91–119. <https://doi.org/10.11646/zootaxa.5099.1.4>
- Wang J, Lin SS, Gan JS, Chen HH, Yu LM, Pan Z, Xiao JJ, Zeng ZC (2024) A new species of the genus *Boulenophrys* from South China (Anura, Megophryidae). Zootaxa 5514(5): 451–468. <https://doi.org/10.11646/zootaxa.5514.5.3>
- Wu YH, Suwannapoom C, Poyarkov NA, Chen JM, Pawangkhanant P, Xu K, Jin JQ, Murphy RW, Che J (2019) A new species of the genus *Xenophrys* (Anura: Megophryidae) from northern Thailand. Zoological Research 40: 564–574. <https://doi.org/10.24272/j.issn.2095-8137.2019.032>
- Wu YQ, Li SZ, Liu W, Wang B, Wu J (2020) Description of a new horned toad of *Megophrys* Kuhl & Van Hasselt, 1822 (Amphibia, Megophryidae) from Zhejiang Province, China. ZooKeys 1005: 73–102. <https://doi.org/10.3897/zookeys.1005.58629>
- Xu N, Li SZ, Liu J, Wei G, Wang B (2020) A new species of the horned toad *Megophrys* Kuhl & Van Hasselt, 1822 (Anura, Megophryidae) from southwest China. ZooKeys 943: 119–144. <https://doi.org/10.3897/zookeys.943.50343>
- Ye CY, Fei L (1995) Taxonomic studies on the small type *Megophrys* in China including descriptions of the new species (subspecies) (Peloatidae: genus *Megophrys*). Acta Herpetologica Sinica 4–5: 72–81. [in Chinese]
- Ye CY, Fei L, Xie F (2007) A new species of Megophryidae – *Megophrys baolongensis* from China (Amphibia, Anura). Herpetologica Sinica 11: 38–41. [in Chinese]
- Zeng ZC, Wang J, Chen HH, Xiao WW, Zhan BB, Li YH, Lin SS (2024) A new species of the genus *Boulenophrys* (Anura, Megophryidae) from eastern Guangdong, China. Asian Herpetological Research 15(1): 12–21.
- Zhang Y, Li G, Xiao N, Li J, Pan T, Wang H, Zhang B, Zhou J (2017) A new species of the genus *Xenophrys* (Amphibia: Anura: Megophryidae) from Libo County, Guizhou, China. Asian Herpetological Research 8: 75–85. <https://doi.org/10.16373/j.cnki.ahr.160041>

Supplementary material 1

Localities, voucher information, and GenBank accession numbers for all samples used in this study

Authors: Shi-Shi Lin, Hong-Hui Chen, Yuan-Hang Li, Zhao-Ning Peng, Zhao-Chi Zeng, Jian Wang

Data type: xlsx

Copyright notice: This dataset is made available under the Open Database License (<http://opendatacommons.org/licenses/odbl/1.0/>). The Open Database License (ODbL) is a license agreement intended to allow users to freely share, modify, and use this Dataset while maintaining this same freedom for others, provided that the original source and author(s) are credited.

Link: <https://doi.org/10.3897/zookeys.1216.130017.suppl1>

A new epigean species of *Trichopeltis* Pocock, 1894 from southwest China (Diplopoda, Polydesmida, Cryptodesmidae)

Zhenfei Wu¹, Sihang Zhang¹, Fuxue Qin², Peiyun Cong¹

¹ Yunnan Key Laboratory for Palaeobiology & MEC International Joint Laboratory for Palaeobiology and Palaeoenvironment, Institute of Palaeontology, Yunnan University, Kunming 650500, China

² Earthquake Prevention and Disaster Reduction Bureau of Zhaoyang, Zhaotong 657099, China

Corresponding author: Sihang Zhang (eva@ynu.edu.cn)

Abstract

A new species of Cryptodesmidae, *Trichopeltis jiyue* sp. nov., is described from the Ailaoshan National Nature Reserve in Yunnan Province, southwest China. The new species is distinguished from its congeners by the gonopodal coxae with two conspicuous wing-like processes, the relatively long, stout setae on the gonopodal coxae, gonopodal telopodites glabrous and four-branched, and the acropodite curved caudolaterad. The new species is the second record of an epigean species of genus *Trichopeltis* Pocock, 1894 in China. An updated key is provided to all 14 presently known species.

Key words: Key, millipedes, taxonomy, Yunnan



Academic editor: Pavel Stoev

Received: 22 May 2024

Accepted: 9 September 2024

Published: 18 October 2024

ZooBank: <https://zoobank.org/9FAD26B7-8734-4CFC-94A6-66211BECF33F>

Citation: Wu Z, Zhang S, Qin F, Cong P (2024) A new epigean species of *Trichopeltis* Pocock, 1894 from southwest China (Diplopoda, Polydesmida, Cryptodesmidae). ZooKeys 1216: 17–26. <https://doi.org/10.3897/zookeys.1216.128080>

Copyright: © Zhenfei Wu et al.
This is an open access article distributed under terms of the Creative Commons Attribution License (Attribution 4.0 International – CC BY 4.0).

Introduction

The Polydesmida is one of the most diverse orders of Diplopoda (millipedes), containing about 5000 species in 30 families (Brewer et al. 2012) and with many species globally widespread (Shelley 2003). All Polydesmida are blind and eyeless, and metaterga usually show small to prominent lateral paranota or paraterga (Brewer and Bond 2013).

The Cryptodesmidae Karsch, 1880 is a relatively small family of Polydesmida comprising approximately 40 genera and 130 species (Golovatch et al. 2010; Liu et al. 2017). It occupies three geographic areas: Neotropical (Mexico to Argentina), Afrotropical (continental sub-Saharan Africa), and Asian + Australasian (Central Asia and the Himalayas to Japan and Papua New Guinea) (Golovatch and Vanden-Spiegel 2017). In tropical or subtropical Asia and Australasia, 12 genera and 36 species have been documented in Cryptodesmidae (Liu et al. 2017). The diagnosis of Cryptodesmidae has been revised by Enghoff et al. (2015) as follows: body incapable of volvation, strongly flattened; collum strongly enlarged, flabellate, with radiating lines; paraterga strongly developed, broad and subhorizontal; pore formula normal, but deviating; ozopores absent, or present on small tubercles, removed from lateral edge of paraterga; metaterga without cerotegument, densely setose and/or uniformly tuberculate, arranged in numerous transverse rows; limb microreticulate; epiproct exposed, from rather simple and subconical to strongly flattened

and deeply incised at lateral edges; legs without sphaerotrichomes; and gonopods without seminal chamber, often with a hairy pulvillus (Enghoff et al. 2015).

Trichopeltis Pocock, 1894 is one of the tropical or subtropical genera of Asian Cryptodesmidae. Currently, this genus encompasses 13 species, mainly documented in Indonesia, Myanmar, Laos, Vietnam, Cambodia, southern China, and the Himalayas (Golovatch 2015, 2016; Golovatch and VandenSpiegel 2017; Likhitrakarn et al. 2017; Liu et al. 2017; Liu and Wynne 2019). This genus is well defined and characterized by a tripartite or deeply notched gonopod telopodite, including a small middle to caudal solenomere branch (Golovatch et al. 2010). Six species of this genus have been reported from China, including five cavernicolous and one epigean species.

In this paper, we describe a new epigean species of *Trichopeltis* from southwest China and update the key to all known species in this genus. This new species represents the second record of an epigean species of *Trichopeltis* in China.

Materials and methods

All specimens were collected from the Ailaoshan National Nature Reserve (24°32'N, 101°01'E, 2476 m above mean sea level) in Yunnan Province, southwest China. Yunnan Province is well known for its high biodiversity (Yang et al. 2004). Ailaoshan Mountain National Nature Reserve stretches across six counties, or cities, of Yunnan, and is mainly covered with mid-montane humid evergreen broad-leaved forest with abundant wild fauna and flora resources (Qiu et al. 1998). The subtropical evergreen broadleaved forest is old-growth (>300 years) and well protected (Yang et al. 2007). All collected millipedes are preserved in 75% ethanol. The holotype and paratypes are deposited in Yunnan University, China.

The live photographs were taken in the habitats of the described species using a SONY DSC-RX1R camera. All specimens were further studied and photographed with a Nikon SMZ25 stereomicroscope and Nikon DS-Ri2 microscope camera within the laboratory. Scanning electron microscope (SEM) images were taken with a FEI Quanta FEG 650 with gold coating. All figures are prepared with Affinity Photo v. 2 and Affinity Designer v. 2. The terminology used here follows that of Golovatch and VandenSpiegel (2017).

Results

Taxonomy

Order Polydesmida Leach, 1815

Family Cryptodesmidae Karsch, 1880

Genus *Trichopeltis* Pocock, 1894

***Trichopeltis jiyue* sp. nov.**

<https://zoobank.org/77367C20-B420-457F-A095-AB493A6BB2F7>

Type material. Holotype: • ♂ (YNU-MD 0151), China, Yunnan Province, Pu'er City, Jingdong Yi Autonomous County, 24°54'78"N, 101°03'58"E, 2450 m elev., 4.X.2021, leg. Peiyun Cong, Sihang Zhang, Zhenfei Wu & Fuxue Qin. **Paratypes:** • 4 ♂, 9 ♀ (YNU-MD 0152-165) same location as the holotype.

Etymology. Jiyue (Chinese spelling) alludes to the bright white appearance when the animal emerges from the leaf mold, like the moon appearing from behind a dark rain cloud.

Diagnosis. *Trichopeltis* is characterized by the relatively long and stout setae on the gonopodal coxae, with the posterior part having two conspicuous wing-like processes (cxp); gonopodal telopodites glabrous and four-branched; and the acropodite curved caudolaterad. The living animal is uniformly bright white.

Description. Length of ♂ ca 17.2–17.8 mm, paratype ♀ ca 17.0–17.4 mm, width of midbody pro- and metazonae 2.2–2.4 mm and 5.3–5.4 mm (♂), 2.2–2.5 mm and 5.1–5.4 mm (♀), respectively.

Coloration of tergites uniformly bright white (Fig. 1A); fed 1–2 months with local mor and leaves, yellow (Fig. 1B); in alcohol, after months of preservation, whitish-yellow to yellow (Fig. 1C, D). Antenna whitish-yellow (proximal) to red-dish-purple (distal).

Adults body with 20 segments, collum plus 17 podous and 1 apodous tergites, plus 1 telson. In width, head << collum < segment 2 < 3 < 4 < 5 < 6 < 7–17, thereafter body tapered towards telson.

Head sparsely pilose, epicranial suture present (Fig. 2A). Antennae short and clavate, reaching tergite 4 when stretched ventrally; in length, antennomere 6 > 3 > 2 = 4 > 5 > 1 > 7 (Fig. 2A); antennomeres 5–7 each with a bacilliform sensilla field apico-laterally, the numbers of bacilliform sensilla are 100, 67, and 34, respectively.

Collum completely covering the head from above, inverted subtrapeziform, regularly convex at peripheric margin, caudal margin slightly concave (Fig. 2B); arranged with 12 or 13 regular, transverse rows of small, spherical, setigerous tubercles on the surface, tubercles 8-13+8-13 per row, surrounded with spherical granulations, seta on each tubercle directed caudad (Fig. 2B).

Prozona of segments following collum finely shagreened, metazona densely tuberculate and setose; fore and caudolateral margins of collum, anterolateral, lateral and caudal margins of following paraterga of segments besides telson with obvious dentiform-lobulate lobules, smallest at mid-dorsal region and slightly larger bidirectionally at caudal margins of paraterga.

Dorsum convex, postcollum paraterga flat, very broad and long, narrowly rounded laterally, axial line absent. Metatergal segments 2–16 with four or five irregular transverse rows of similarly small, spherical, setigerous tubercles. Tubercles decreasingly extend to paraterga, but each of the latter only with three or four irregular rows of similar tubercles (Fig. 2C), surrounded by spherical granulations, same to collum; following metatergal segments 17 and 18 with 6–8 rows of smaller tubercles.

Paraterga very strongly developed (Fig. 2C), regularly declivous, the tips extending down below level of venter (Fig. 2D). Segments 2–15 slightly projecting forward, each with 6–9 small, crown-like dentiform, lateral lobules (Fig. 2I) and 7–9 tongue-shaped to squarish caudolateral lobules; all evident, setigerous and microvillose segments 16–19 projecting caudally, each with 5–7 small, crown-like dentiform, lateral lobules and 9–13 tongue-shaped to squarish, caudolateral lobules; all evident, setigerous, and microvillose.

Sterna sparsely setose; axial line present; tergite stricture divided into pro- and metazone parts. Limbus, with a row of tongue-shaped lobules, microdentate apically (Fig. 2G). Pore visible, lying on the ventral paraterga of segment 5, ozopores formula not discernable.

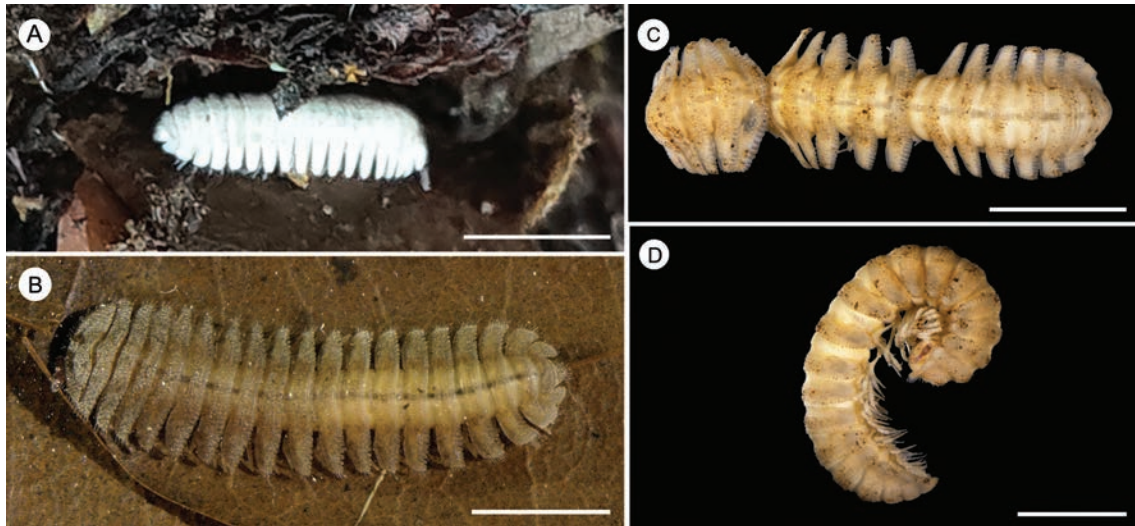


Figure 1. External morphology and colouration of *Trichopeltis jiyue* sp. nov. **A** ♂ holotype in habitus and live **B** fed 1–2 months in laboratory **C, D** ♀ paratype, after 3 months storage in 75% alcohol. Scale bars: 10 mm (**A**); 5 mm (**B–D**).

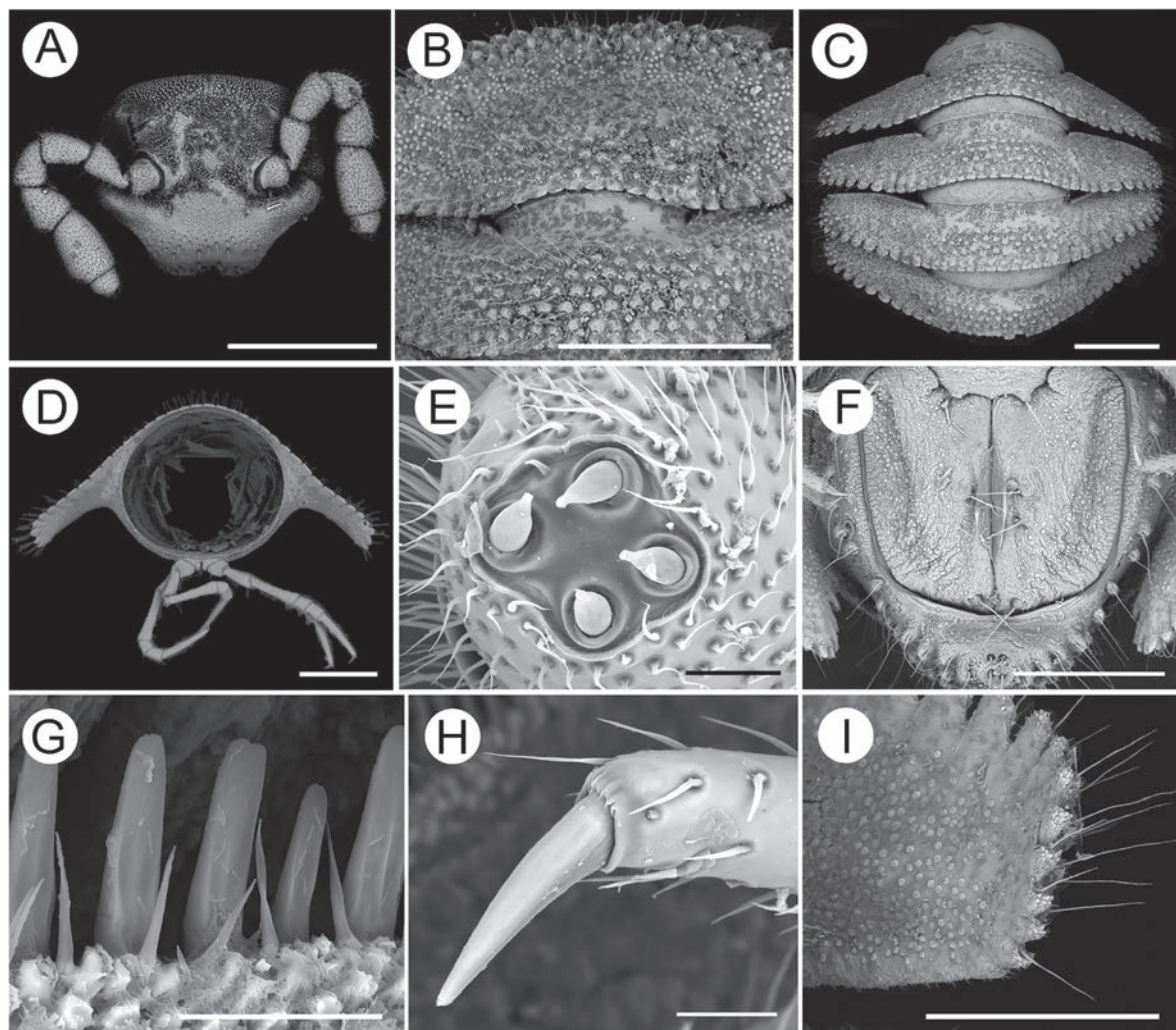


Figure 2. SEM images of *Trichopeltis jiyue* sp. nov., ♂ holotype **A** head, dorsal view **B** collum and the second segment, dorsal view **C** segments 6–9, dorsal view **D** cross-section of segment 5, caudal view **E** antenna disc coeloconic sensilla, plan view **F** telson and anal, ventral view **G** limbus of segment 5, subventral view **H** claw of leg, subventral view **I** paraterga of segment 6, ventral view. Scale bars: 1 mm (**A–D**); 50 µm (**E, H**); 20 µm (**G**); 500 µm (**F, I**).

Telson (Fig. 2F) conical, with numerous spherical granulations; epiproct flattened dorsoventrally, microtuberculate, with four strong apical papillae. Hypoproct roundly subtrapeziform, 1+1 caudal setae separated, surface rugged.

Legs (Fig. 2D, H) long and slender, without modifications, longer than paraterga when stretched straight, about 1.2 times as long as the width of paraterga. In length, femur \approx tarsus \gg prefemur $>$ coxa = tibia $>$ postfemur $>$ claw.

Gonopods complex (Figs 3, 4). Coxae with relatively long stout setae; with two conspicuous wing-like processes (cxp). Telopodite complex, with four-branched process (**p**), clearly curved (Figs 3, 4), approximately as long as coxa, divided by a notch (Fig. 3D); prefemur glabrous; femorite (**p1**) one leaf-shaped lobe on the inner side mesally; branch **p2** leaf-shaped, three times as long as **p1**, rather thick, curved caudolaterally, with dense micro-setae on surface, distal margin with serrate process; **p3** subconical, with three apical processes; **p4** leaf-shaped, close to the **p2**, the distal margin consists of numerous conical processes, forming a corolliform pulvillus; with no distinct solenomere.

Remarks. The specimens were found on a stoney roadside, which some researchers usually walk around. As compared with virgin forests, the surroundings were relatively densely populated. However, the environment is undeveloped, and it the new species seemed abundant.

Key to species of *Trichopeltis*

Modified after Liu et al. 2017.

- 1 Tegument unpigmented, pallid to light yellowish; cavernicolous species. **2**
- Tegument clearly pigmented, bright white, red- or grey-brown to blackish; epigeal species..... **7**
- 2 Central parts of metaterga with 2–4 irregular, transverse rows of setigerous tubercles; gonopodal coxite as usual, at most with only few setae ... **3**
- Central parts of metaterga with 5–6 irregular transverse rows of setigerous tubercles; gonopodal coxite unusually densely setose on lateral side; Yunnan, China **6**
- 3 Paraterga declivous; tergal setae very long, about half as long as body diameter; gonopodal telopodite clearly twisted. Guizhou, China **T. latellai Golovatch et al., 2010**
- Paraterga clearly upturned; tergal setae much shorter; gonopodal telopodite untwisted **4**
- 4 Gonopodal telopodite with a hairy pulvillus; coxite short and squarish, without seta; central parts of metaterga with 4 irregular, transverse rows of setigerous tubercles. Guangxi, China **T. liangfengdong Liu & Wynne, 2019**
- Gonopodal telopodite without pulvillus **5**
- 5 Central parts of metaterga with 2–3 subregular, transverse rows of setigerous tubercles; acropodite strongly condensed, tripartite..... **T. reflexus Liu, Golovatch & Tian, 2017**
- Central parts of metaterga with 3–4 irregular transverse rows of setigerous tubercles; Telopodite only slightly curved caudad, vaguely tripartite. Laos..... **T. cavernicola Golovatch, 2016**

- 6 Tergal setae long; gonopods relatively simple ***T. bellus* Liu, Golovatch & Tian, 2017**
- Tergal setae short; gonopods rather complex..... **12**
- 7 Central parts of metaterga with 4–6 irregular, transverse rows of setigerous tubercles **8**
- Central parts of metaterga with 2–3 irregular, transverse rows of setigerous tubercles **11**
- 8 Gonopodal telopodite with evident branches..... **13**
- Gonopodal telopodite without long branches **9**
- 9 Central parts of metaterga with 4–5 subregular, transverse rows of setigerous tubercles; gonopodal telopodite with a conspicuous accessory seminal chamber and a pulvillus but devoid of denticles laterally or mesally. Laos ***T. muratovi* Golovatch & VandenSpiegel, 2017**
- Central parts of metaterga with 5–6 subregular, transverse rows of setigerous tubercles; gonopodal telopodite without accessory seminal chamber but with a pulvillus, also abundantly denticulate either laterally or mesally **10**
- 10 Gonopodal telopodite abundantly denticulate on lateral face. Vietnam, Laos, and Cambodia and possibly endemic to the Indochina Peninsula ***T. kometis* Attems, 1938**
- Gonopodal telopodite abundantly denticulate on mesal face. Sumatra, Indonesia..... ***T. bicolor* Pocock, 1894**
- 11 Frontal margin of paraterga abundantly lobulated. Solenomere lobe-shaped, tip nearly pointed..... ***T. feae* Pocock, 1895**
- Frontal margin of paraterga entire, not lobulated. Solenomere axe-shaped, tip pointed..... ***T. watsoni* Pocock, 1895**
- 12 Each coxa with a conspicuous, high, curved, laterally densely setose process ***T. sutchariti* Likhitrakarn et al., 2017**
- Each coxa with a small process without setae ***T. intricatus* Liu, Golovatch & Tian, 2017**
- 13 Clearly 3-branched; solenomere long and slender..... ***T. doriae* Pocock, 1895**
- Clearly 4-branched; with two conspicuous wing-like process (wp) basal, one pan-shaped lobe on the inner side; acropodite reverse caudally against femorite, unfolded into sheet form. Yunnan, China..... ***T. jiyue* sp. nov.**

Comparisons

The Cryptodesmidae comprises about 40 genera. The new species can be assigned to the genus *Trichopeltis* Pocock, 1894 based on the lobulated and tuberculate-setose tergites, subcordiform gonopod aperture, four-branched telopodite, and coxa divided by a notch.

Amongst all known 14 species of *Trichopeltis*, *T. jiyue* sp. nov. is most similar to *T. kometis* Attems, 1938 (Golovatch & Akkari, 2016), *T. doriae* Pocock, 1895, *T. intricatus* Liu, Golovatch & Tian, 2017, *T. sutchariti* Likhitrakarn et al., 2017, and *T. muratovi* Golovatch & Vanden Spiegel, 2017.

The gonopodal telopodite of *T. jiyue* sp. nov. clearly differs from that of *T. doriae* in having four branches, in contrast to the gonopodal telopodite of *T. doriae* which bears three branches; also, it differs from *T. muratovi* in the telopodite, which has a conspicuous accessory seminal chamber, in contrast to the

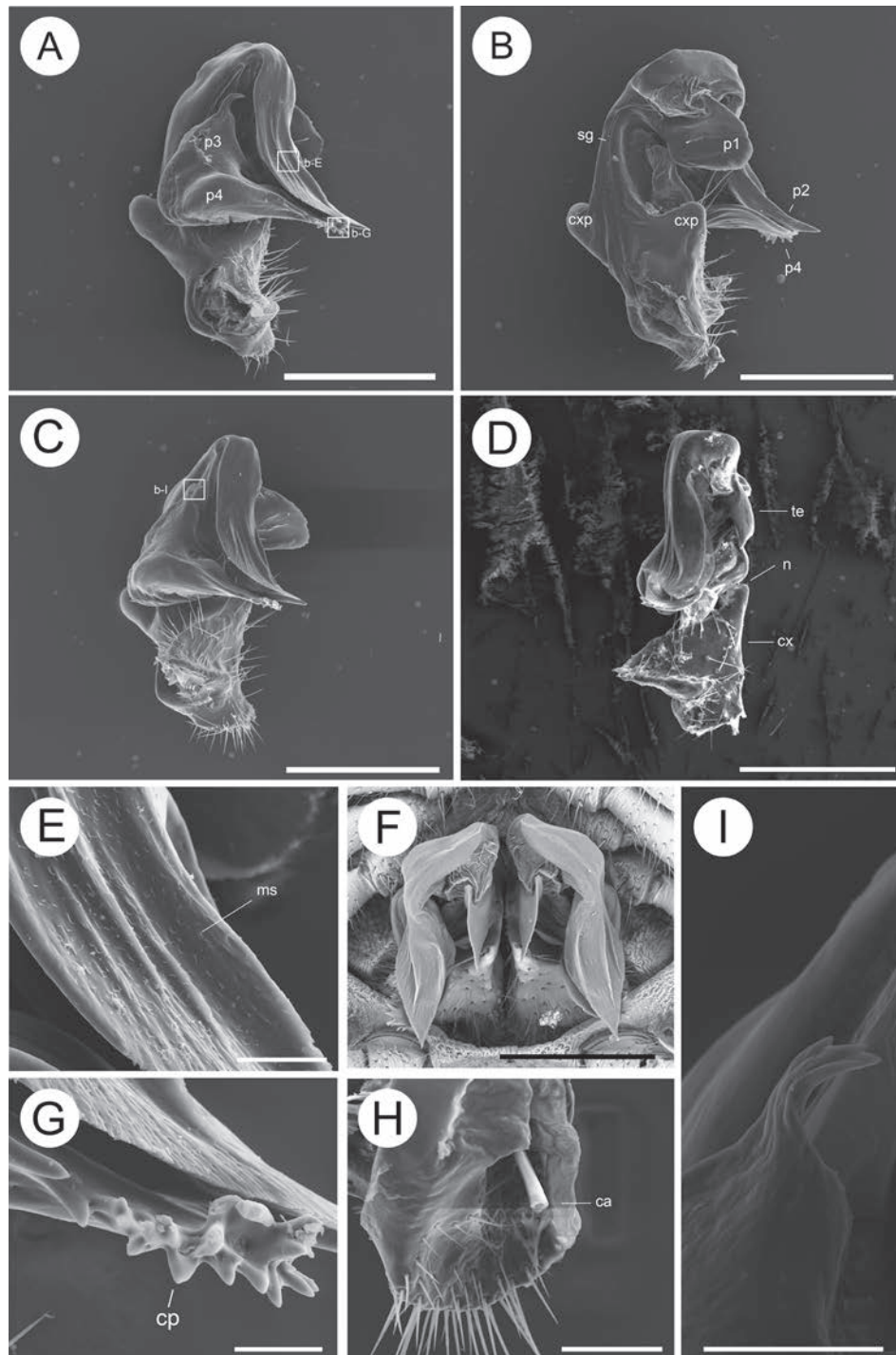


Figure 3. Gonopodal characters of *Trichopeltis jiyue* sp. nov., ♂ holotype, paratype. **A, C** right gonopod, sublateral and subfrontal views **B** left gonopod, subcaudal view **D** right gonopod, ventral view, coxite and telopodite divided by a notch **E** enlargement of box-E of A, prefemur sheet micro-setose on the surface **F** gonopod, ventral view from above **G** enlargement of box-G of A, corolliform solenomere **H** seminal groove **I** box-I of C, tripartite apical process. Abbreviations: p1, p2, p3, p4 = processes of telopodite; cp = corolliform pulvillus; cxp = coxa process; ms = microsetae; sg = seminal groove; tap = tripartite apical process; ca = cannula; cx = coxa; te = telopodite; n = notch. Scale bars: 500 μ m (**A–D, F**); 50 μ m (**E, G**); 100 μ m (**H, I**).

gonopodal telopodite of *T. jiyue* sp. nov., which is without a conspicuous accessory seminal chamber; furthermore, the gonopodal surface of the new species is relatively smooth, with dense microsetae, and differs from that of the abundantly denticulate gonopodal surface of *T. kometis* and *T. bicolor* Pocock, 1894.

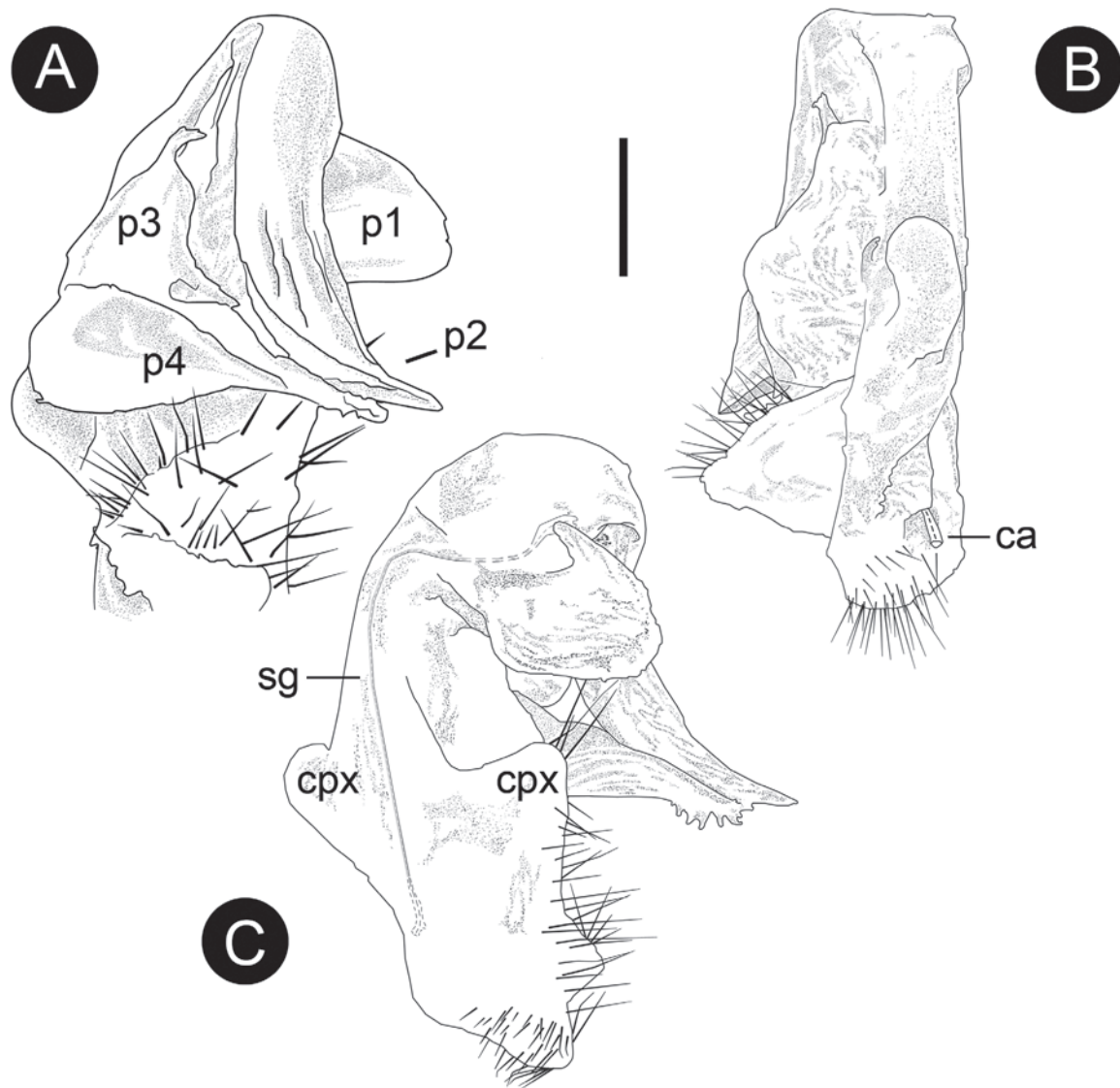


Figure 4. *Trichopeltis jiyue* sp. nov., ♂ holotype, paratype. **A** subfrontal view **B** subcaudal view **C** cadual view. Abbreviations: p1, p2, p3, p4 = processes of telopodite; cpx = coxa process; sg = seminal groove; ca = cannula. Scale bar: 200 μ m.

Trichopeltis intricatus and *T. sutchariti* were also found in Yunnan Province, China. Compared to *T. jiyue* sp. nov., the body size of *T. jiyue* sp. nov. is much larger; the length of the adult is over 17 mm, the pro- and metazonae are over 2 and 5 mm long, respectively, which is much longer than *T. intricatus*. *T. intricatus* is relatively short, ca 10 mm long, with the width of midbody pro- and metazonae 1.5 and 2.5 mm, respectively. Furthermore, the tuberculations on the collum have up to 12 or 13 irregular, transverse rows, which is more differ than the eight to nine irregular, transverse rows of *T. sutchariti*. The characters of the gonopod reveal many obvious interspecific differences.

Conclusions

Trichopeltis jiyue sp. nov. is described from Ailaoshan National Nature Reserve in Yunnan Province, southwest China. It represents the second record of an epigean species of the genus *Trichopeltis* in China. An updated identification key (modified from Liu et al. 2017) to all known species of *Trichopeltis* is provided here.

Acknowledgements

We thank Canchen Liao and Xishuangbanna Tropical Botanical Garden, Chinese Academy of Sciences for providing us scientific research field. We appreciate the valuable comments and useful suggestions on our manuscript from the associate editor and the reviewers. Last but not least, we extend our deep gratitude to Professors Sergei Golovatch, Natdanai Likhitrakarn, and Pavel Stoev for invaluable constructive feedback, and to Dr. Christopher Glasby and Dr. Robert Forsyth for polishing and revising the English of the manuscript.

Additional information

Conflict of interest

The authors have declared that no competing interests exist.

Ethical statement

No ethical statement was reported.

Funding

This work is supported by the Yunling Scholar funding and a joint grant of YNU-Yunnan Government (202201BF070001-016).

Author contributions

Data curation: FQ. Writing - original draft: ZW. Writing - review and editing: SZ, PC.

Author ORCIDs

Zhenfei Wu  <https://orcid.org/0009-0004-5586-6511>

Sihang Zhang  <https://orcid.org/0000-0002-8230-6892>

Fuxue Qin  <https://orcid.org/0009-0001-1140-3927>

Peiyun Cong  <https://orcid.org/0000-0001-9910-6478>

Data availability

All of the data that support the findings of this study are available in the main text.

References

- Brewer MS, Bond JE (2013) Ordinal-level phylogenomics of the arthropod class Diplopoda (millipedes) based on an analysis of 221 nuclear protein-coding loci generated using next-generation sequence analyses. *PLoS ONE* 8(11): e79935. <https://doi.org/10.1371/journal.pone.0079935>
- Brewer MS, Sierwald P, Bond JE (2012) Millipede taxonomy after 250 years: classification and taxonomic practices in a mega-diverse yet understudied arthropod group. *PLoS ONE* 7(5): e37240. <https://doi.org/10.1371/journal.pone.0037240>
- Enghoff H, Golovatch SI, Short M, Stoev P, Wesener T (2015) Diplopoda—taxonomic overview. *Treatise on Zoology-Anatomy, Taxonomy, Biology. The Myriapoda, Vol. 2*, Koninklijke Brill NV, Leiden, The Netherlands, 363–453. https://doi.org/10.1163/9789004188273_017
- Golovatch SI (2015) Review of the millipede genus *Ophrydesmus* Cook, 1896, with the description of a new species from southern Vietnam (Diplopoda: Polydesmida:

- Cryptodesmidae). *Tropical Natural History* 15(2): 155–165. <https://li01.tci-thaijo.org/index.php/tnh/article/view/103079>
- Golovatch SI (2016) The millipede family Cryptodesmidae in Indochina (Diplopoda: Polydesmida). *ZooKeys* 578: 33–43. <https://doi.org/10.3897/zookeys.578.7994>
- Golovatch SI, Akkari N (2016) Identity of the millipede, *Pseudoniponiella kometis* (Attems, 1938) (Diplopoda: Polydesmida: Cryptodesmidae). *Tropical Natural History* 16(1): 1–6. <https://li01.tci-thaijo.org/index.php/tnh/article/view/103069>
- Golovatch SI, VandenSpiegel D (2017) One new and two little-known species of the millipede family Cryptodesmidae from Indochina (Diplopoda, Polydesmida). *Zoologicheskii zhurnal* 96(7): 757–767. <http://doi.org/10.7868/S0044513417070066>
- Golovatch S, Geoffroy JJ, Mauriés JP, Vandenspiegel D (2010) Two new species of the millipede genus *Trichopeltis* Pocock, 1894 (Diplopoda: Polydesmida: Cryptodesmidae) from Vietnam and China. *Arthropoda Selecta* 19(2): 63–72. <https://doi.org/10.15298/arthsel.19.2.01>
- Likhitrakarn N, Golovatch SI, Srisonchai R, Panha S (2017) A new species of *Trichopeltis* Pocock, 1894 from southern China, with a checklist and a distribution map of *Trichopeltis* species (Diplopoda, Polydesmida, Cryptodesmidae). *ZooKeys* 725: 123–137. <https://doi.org/10.3897/zookeys.725.22014>
- Liu W, Wynne JJ (2019) Cave millipede diversity with the description of six new species from Guangxi, China. *Subterranean Biology* 30: 57–94. <https://doi.org/10.3897/subtbiol.30.35559>
- Liu WX, Golovatch SI, Tian M (2017). Three new cavernicolous species of the millipede genus *Trichopeltis* Pocock, 1894 from southern China (Diplopoda, Polydesmida, Cryptodesmidae). *ZooKeys* 710: 1–14. <https://doi.org/10.3897/zookeys.710.20025>
- Qiu XZ, Xie SC, Liu WY (1998). *Studies on the forest ecosystem in Ailao Mountains, Yunnan, China*. Yunnan Sciences and Technology Press, Kunming.
- Shelley RM (2003) A new polydesmid millipede genus and two new species from Oregon and Washington, USA, with a review of *Bidentogon* Buckett and Gardner, 1968, and a summary of the family in western North America (Polydesmida: Polydesmidae). *Zootaxa* 296(1): 1–12. <https://doi.org/10.11646/zootaxa.296.1.1>
- Yang Y, Tian K, Hao J, Pei S, Yang Y (2004) Biodiversity and biodiversity conservation in Yunnan, China. *Biodiversity & Conservation* 13: 813–826. <https://doi.org/10.1023/b:bioc.0000011728.46362.3c>
- Yang LP, Liu WY, Yang GP, Ma WZ, Li DW (2007) Composition and carbon storage of woody debris in moist evergreen broad-leaved forest and its secondary forests in Ailao Mountains of Yunnan Province. *Chinese Journal of Applied Ecology* 18(10): 2153–2159.

First discovery of troglobitic Paederinae (Coleoptera, Staphylinidae) from China

Cheng-Bin Wang¹, Li He^{2,3}

1 Engineering Research Center for Forest and Grassland Disaster Prevention and Reduction, Mianyang Normal University, 166 Mianxing West Road, Mianyang 621000, Sichuan, China

2 State Grid Tianfu New Area Electric Power Supply Company, Chengdu 610094, Sichuan, China

3 Sichuan Cave Exploration Team, No. 66, 5th Shuangcheng Road, Chenghua District, Chengdu 610051, Sichuan, China

Corresponding author: Li He (coleoptera@qq.com)

Abstract

An unexpected troglobitic staphylinid is described from a dolomite cave in western China as *Domene lizeyui* Wang & He, **sp. nov.** (Coleoptera, Staphylinidae, Paederinae). The habitus of both sexes and important diagnostic features are illustrated. Brief notes on the habitat, biology and taxonomic status of the new species are provided. This is the first discovery of a troglobitic representative of Paederinae from China, the first record of a troglobitic *Domene* species, and only the third cavernicolous species of Paederinae from eastern Asia.

Key words: Cavernicolous, *Domene*, new species, Paederinae, rove beetle, Sichuan, subterranean, taxonomy



Academic editor: Jan Klimaszewski

Received: 15 July 2024

Accepted: 3 October 2024

Published: 18 October 2024

ZooBank: <https://zoobank.org/2A9FFA2A-92B7-4B29-AE78-2C90D64635C4>

Citation: Wang C-B, He L (2024) First discovery of troglobitic Paederinae (Coleoptera, Staphylinidae) from China. ZooKeys 1216: 27–42. <https://doi.org/10.3897/zookeys.1216.132155>

Copyright: © Cheng-Bin Wang & Li He.
This is an open access article distributed under terms of the Creative Commons Attribution License (Attribution 4.0 International – CC BY 4.0).

Introduction

Currently in China, research on cave biodiversity is flourishing, and the first two textbooks on *Cave Biology* were published very recently (Liu 2021; Tian et al. 2023c). The last few decades have been particularly prolific in new findings of troglobitic beetles in China, for example Carabidae (Uéno and Wang 1991; Tian 2008; Tian and Clarke 2012; Deuve and Tian 2016; Tian et al. 2016, 2018, 2021, 2023a, 2023b; Chen et al. 2019; Tian and He 2020a, 2020b; Huang and Tian 2021; Jia et al. 2021), Cholevinae (Leiodidae) (Perreau and Růžička 2018), Pselaphinae (Staphylinidae) (Nomura and Wang 1991; Yin et al. 2010, 2011a, 2011b, 2015, 2016; Yin and Li 2015; Yin and Zhou 2018; Yin 2020; Yin and He 2020), and Dytiscidae (Spangler 1996; Wewalka et al. 2007; Zhao and Jia 2021). However, no obligate troglobites of Pselaphidae were known from China prior to this study—exclusive of troglaphiles according to the screening criteria of Hlaváč et al. (2006); *Lathrobium formidabile* Assing, 2013 from Sichuan of China is presumably a hypogean species, which was collected in a mixed forest, not in natural cave, probably by sifting leaf litter (Assing 2013).

Hlaváč et al. (2006) catalogued 44 species of troglobitic Staphylinidae worldwide, excluding the former Pselaphidae and Scaphidiidae. Among them, only four species are known from eastern Asia: two *Lathrobium* species

(Paederinae) from Japan, one *Uenohadesina* species (Omaliinae) from South Korea, and one *Typhlomalota* species (Aleocharinae) from northern India.

For the genus *Domene* Fauvel, 1873 (Paederinae: Lathrobiini), 33 epigeal species have been reported from eastern Asia (Koch 1939; Rougemont 1995; Assing and Feldmann 2014; Feldmann et al. 2014; Assing 2015, 2016, 2021; Peng et al. 2015, 2017; Schülke and Smetana 2015; Li 2019; Lin and Peng 2021): 24 species from Chinese mainland, two from Taiwan Island, five from Japan, two from Russia, two from Korea, two from Vietnam, and one from Myanmar; all belong to the subgenus *Macromene* Coiffait, 1982, except *D. hybrida* Assing, 2021, which was assigned to the monotypic subgenus *Lobramene* Assing, 2021 (Assing 2021).

In the present study, a fascinating troglobitic new species of *Domene* is described and illustrated from Taojindong [=Taojin Cave], a dolomite cave in Leshan Karst, Sichuan Province, western China. This species represents the first discovery of a troglobitic *Domene* species from eastern Asia. In addition, the problem of its taxonomic status is briefly discussed.

Materials and methods

Specimens were relaxed and softened in an HH-2 digital homoeothermic water bath at 44.4 °C for 5 h and then placed in distilled water for cleaning and dissection. To examine the male genitalia, the abdomens after segments VII in morphological sense were detached using dissecting needles and cleared with a trypsin enzyme solution at room temperature for 12 h. They were then placed in 70% ethanol solution to remove the remaining trypsin. After examination, the dissected parts were stored in microvials with glycerin and attached below the respective specimens to which they belonged. Habitus images were taken using a Canon 50D DSLR with a Canon EF 100 mm f/2.8L IS USM lens and a dual LED fill light was used as the light source. Images of the morphological details were taken using a Canon macrophoto lens MP-E 65 mm on a Canon 5DsR. Images of the same object at different focal planes were combined using Zerene Stacker 1.04 stacking software. Adobe Photoshop CS6 was used for postprocessing. The terminology adopted in this paper for external features of the body and genitalia follows Lawrence et al. (2011).

The material examined for this study is deposited in the following collections: **CCZC**—collection of Chao Zhou, Chengdu, China; **CLHC**—collection of Li He, Chengdu, China; **CYLD**—collection of Yuan Li, Deyang, China; **CZWC**—collection of Zhen Wang, Chengdu, China; **CZYL**—collection of Ze-Yu Li, Panzhihua, China; **MYNU**—Invertebrate Collection of Mianyang Normal University, Mianyang, China; **SNUC**—Insect Collection of Shanghai Normal University, Shanghai, China.

Morphological measurements were taken using an ocular micrometer in millimetres (mm) of the following: **abdominal length**: length between the posterior margin of elytra and the abdominal apex along midline; **abdominal width**: widest part of abdomen; **antennal length**: length between the base and the apex of antenna; **body length**: length between the anterior margin of clypeus and the abdominal apex along midline; **elytral length**: length between the apex of scutellar shield and the posterior margin of elytra along suture; **elytral width**: widest part of both elytra combined; **eye length**: length of a single compound eye in lateral view; **forebody**: length between the anterior apex of clypeus and the posterior margin of elytra along midline; **head length**: length between the

anterior margin of clypeus and the posterior constriction along midline; **head width**: widest part of head (including compound eyes); **neck region width**: widest part of neck region; **pronotal length**: length of the pronotum along midline; **pronotal width**: widest part of pronotum.

Results

Genus *Domene* Fauvel, 1873

Domene lizeyui Wang & He, sp. nov.

<https://zoobank.org/0E20A8F4-460E-4C7B-9AAA-06C071B41AF3>

Figs 1–5, 7

Common name: 李泽雨穴毒隐翅虫

Type material. Holotype: • ♂, CHINA, Sichuan, Leshan City, Hulu Town, Shiqianggou, Taojindong [=Taojin Cave] [四川省乐山市沙湾区葫芦镇石墙沟淘金洞], 29.2965°N, 103.6370°E, alt. 513 m, 28.V.2023, Li He & Ze-Yu Li legg. (MYNU).

Paratype: • 3♂♂4♀♀. 3♀♀, same data as holotype (1♀ each in CLHC, MYNU and SNUC); • 3♂♂1♀, same data as holotype except 16.VI.2024, Yuan Li & Ze-Yu Li legg. (1♂ each in CCZC, CYLD and CZYL, 1♀ in CZWC).

Etymology. The specific epithet is gratefully dedicated to one of the collectors of the type specimens, Mr Ze-Yu Li (Panzhuhua, China), an enthusiastic amateur entomologist. The name is a noun in the genitive case.

Description. Male holotype. Measurements. Body 8.5 mm long, widest at posterior angles of sternite V, 5.1 times as long as wide. Lengths of body parts: forebody 5.5 mm, head 2.0 mm, eye 0.1 mm, antenna 6.3 mm, pronotum 1.6 mm, elytra 1.2 mm, abdomen 3.0 mm; widths: head 1.4 mm, pronotum 1.0 mm, elytra 1.0 mm, abdomen 1.7 mm.

Habitus (Fig. 1A, B). Body slender, with rather long and slender appendages, matt. Body almost entirely reddish brown; head with paired blackish paramedian spots at eye level; appendages with distal parts lighter in various degree. Body predominantly covered with short, recumbent, yellowish-brown pubescence.

Head (Fig. 2B–D) oval, weakly convex dorsally, 1.4 times as long as wide, 1.4 times as wide as pronotum. Clypeus transverse, rather slightly emarginate at anterior margin; surface impunctate in anterior part. Fronto-clypeal suture absent. Frons distinctly concave. Antennal tubercles prominent, impunctate in apical parts. Surface irregularly, densely covered with fine punctures, attenuating posteriorly; interstices wider than diameter of punctures, lacking microsculpture. Eyes (Fig. 2E) extremely reduced, 0.06 times as long as postocular region in lateral view, lacking pigmentation, ommatidia unidentifiable. Neck region 3/8 width of head capsule. Gular sutures fused into longitudinally straight line, except at both ends.

Mouthparts (Fig. 2B–D). Labrum transverse, deeply emarginate in middle of anterior margin and with paired subtriangular paramedian teeth. Mandibles sickle-shaped, large and strong, constantly curved and gradually tapered towards acute apices; left mandible with four inner teeth while right one with five. Maxillary palpi with four palpomeres, long and slender, with terminal palpomere rather thin and slender. Labial palpi with three palpomeres, slender, with terminal palpomere rather thin and slenderly coniform.

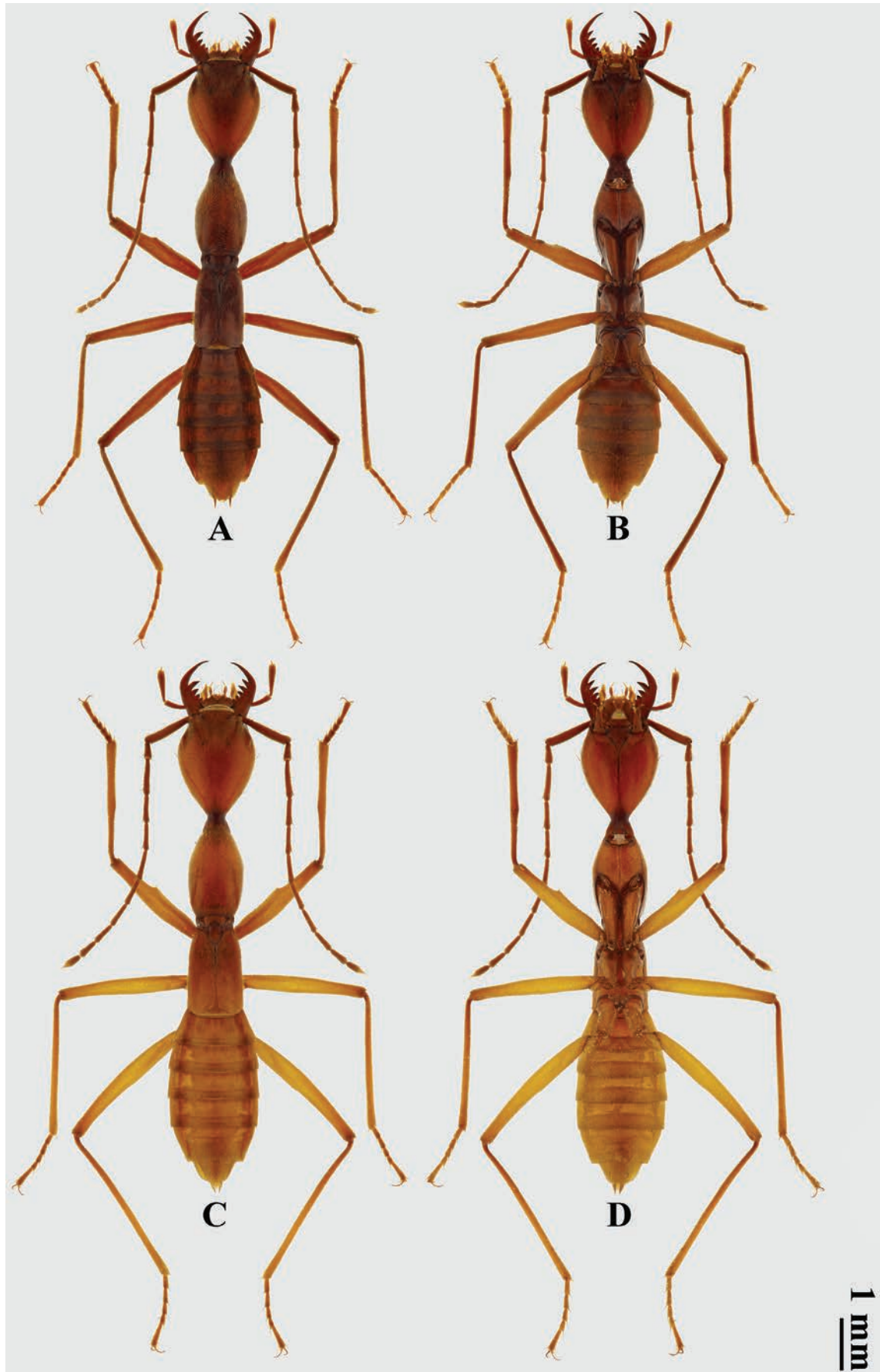


Figure 1. Habitus of *Domene lizeyui* Wang & He, sp. nov. A, B ♂, holotype C, D ♀, paratype (A, C dorsal views B, D ventral views).

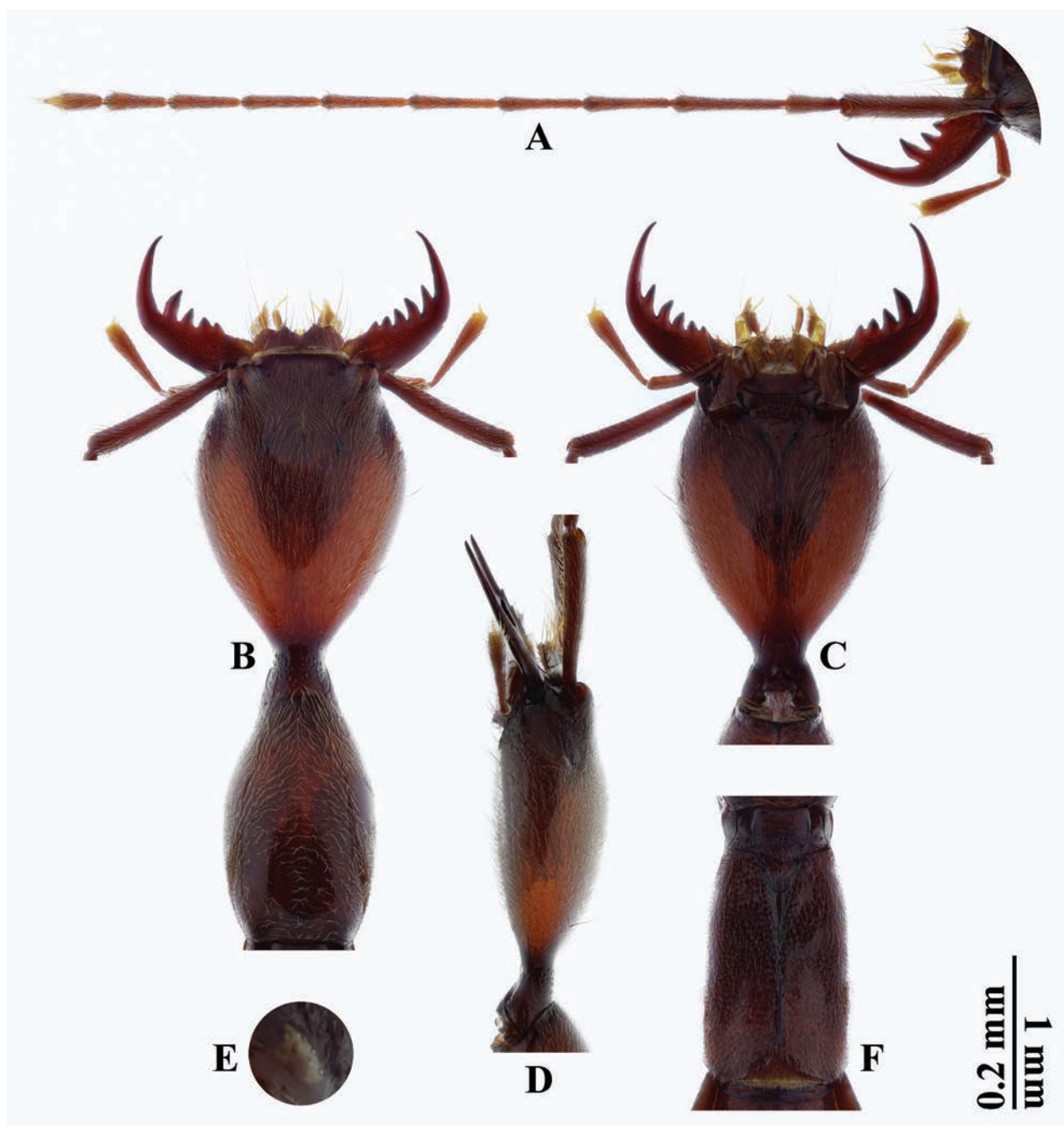


Figure 2. *Domene lizeyui* Wang & He, sp. nov., holotype, ♂ **A** left antenna **B** head and pronotum **C**, **D** head **E** left eye **F** elytra (**A**, **B**, **F** dorsal views **C** ventral view **D**, **E** lateral views). Scale bars: 1 mm (**A–D**, **F**); 0.2 mm (**E**).

Antennae (Fig. 2A) rather long and slender, 1.1 times as long as forebody and 4.5 times as long as head width. Antennomeres with length ratio from scape to antennomere 11 as follows: 2.5: 1.0: 1.9: 1.5: 1.4: 1.5: 1.5: 1.3: 1.2: 1.1: 1.0: 1.0. All antennomeres considerably longer than wide; scape longest, much thicker than other antennomeres; pedicel shortest; antennomere 3 second longest, 1.3 times as long as antennomere 4; antennomere 11 spindle-shaped, 3.2 times as long as wide.

Pronotum (Fig. 2B) slenderly oblong, distinctly constricted anteriorly, weakly convex dorsally, 1.6 times as long as wide, widest around middle. Anterior margin rather narrow and arcuate; lateral margins from middle gradually narrowed posteriorly and distinctly so anteriorly; posterior angles roundly obtuse; poste-

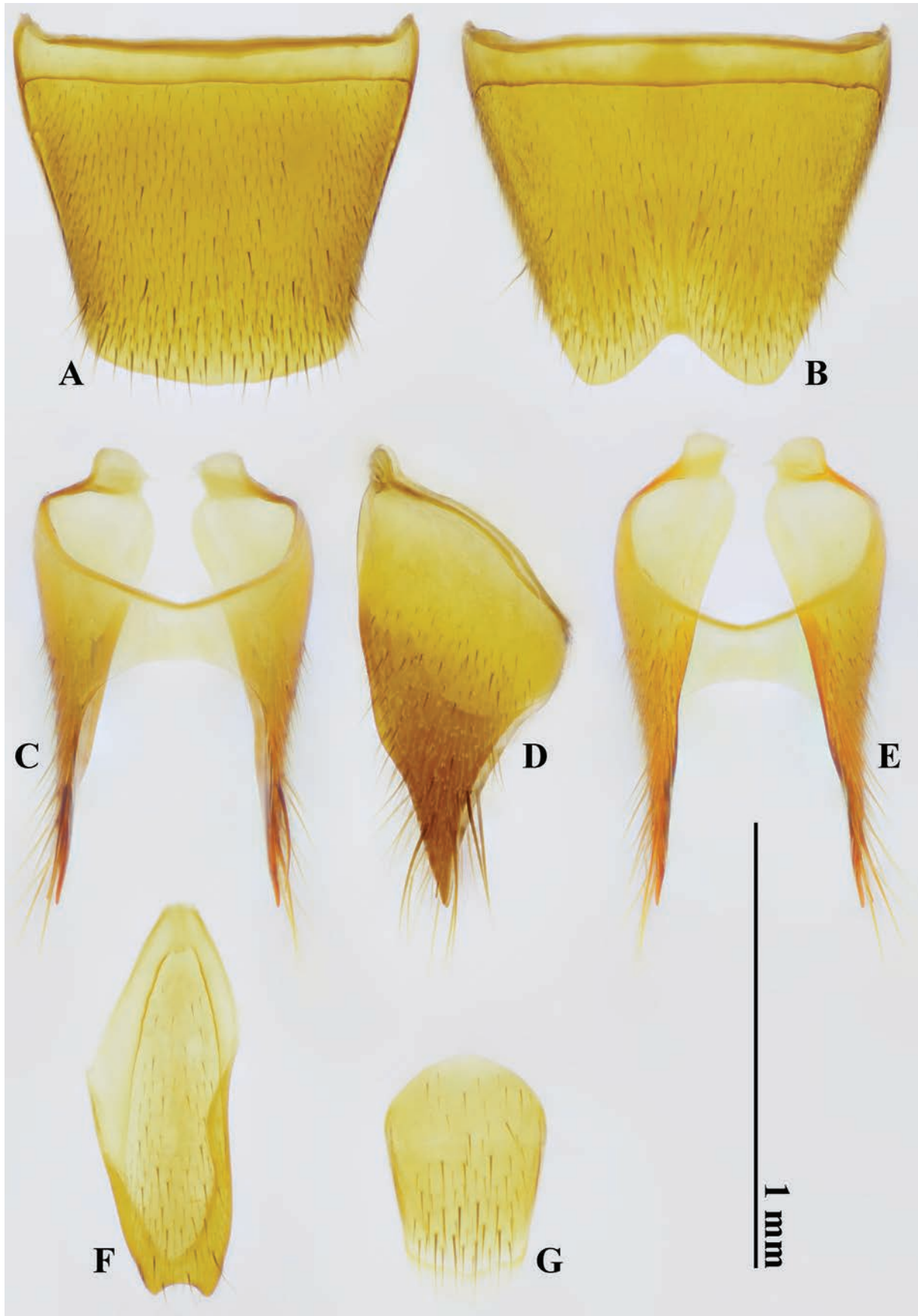


Figure 3. *Domene lizeyui* Wang & He, sp. nov., holotype, ♂ **A** tergite VIII **B** sternite VIII **C–E** tergite IX **F** sternite IX **G** tergite X (**A, C, G** dorsal views **B, E, F** ventral views **D** lateral view).

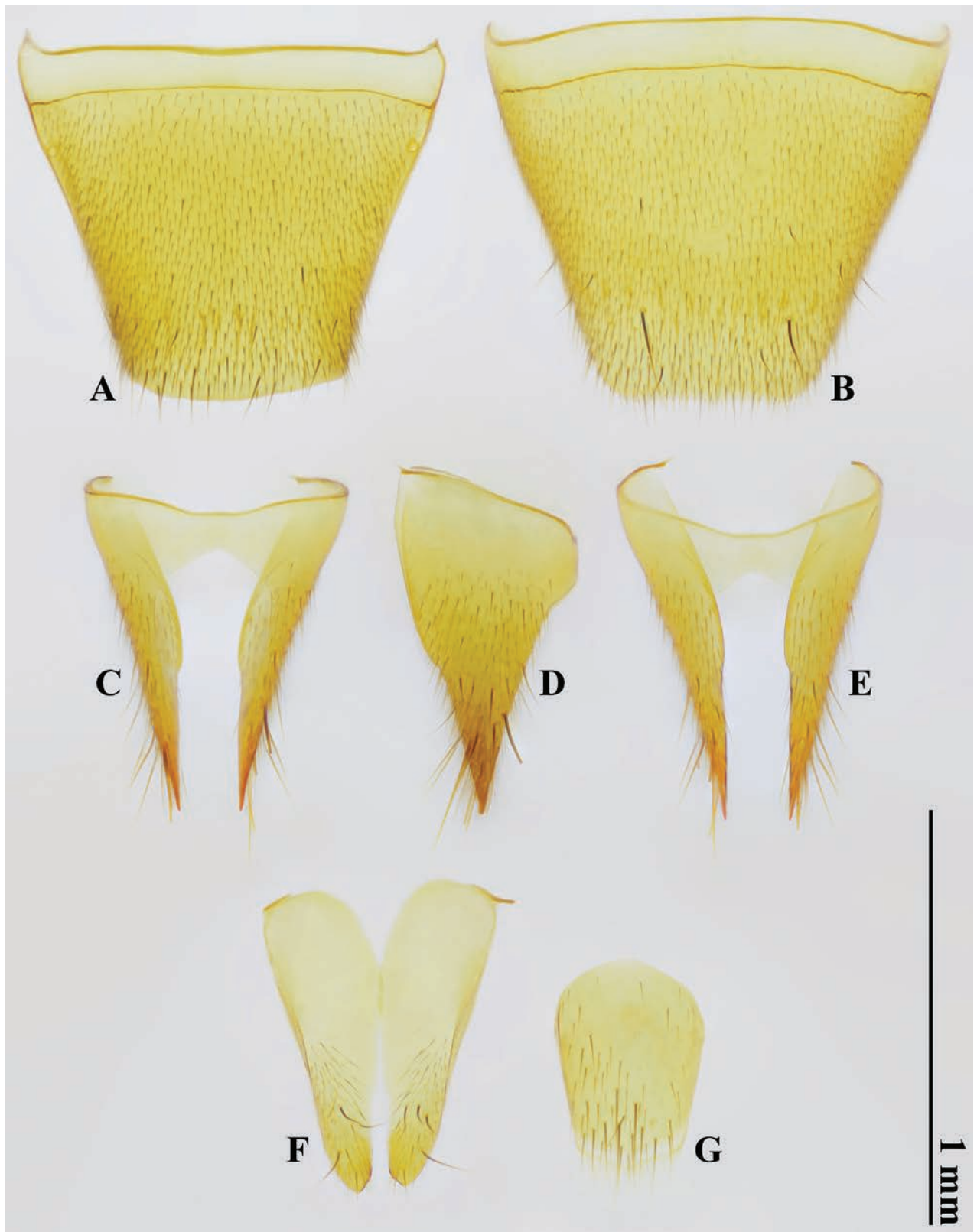


Figure 4. *Domene lizeyui* Wang & He, sp. nov., paratype, ♀ **A** tergite VIII **B** sternite VIII **C–E** tergite IX **F** sternite IX **G** tergite X (**A, C, G** dorsal views **B, E, F** ventral views **D** lateral view).



Figure 5. Aedeagus of *Domene lizeyui* Wang & He, sp. nov., holotype **A** ventral view **B** ventrolateral view **C** lateral view **D** dorsolateral view **E** dorsal view.

rior margin weakly emarginate. Dorsum with punctures similar to that of head but slightly finer; interstices without microsculpture; posterior half of median portion with shallow and impunctate sulcus.

Scutellar shield (Fig. 2F) linguiform, rounded at apex. Surface with punctures coarser than that of head; interstices microreticulate.

Elytra (Fig. 2F) long subtrapezoidal, 1.3 times as long as wide, widest at apicolateral angles, nearly as wide as and 0.8 times as long as pronotum, with apical parts distinctly apart. Lateral margins gradually divergent from humeri to apicolateral angles, then obliquely convergent to roundly obtuse apices. Dorsum slightly impressed on either side of scutellar shield and in middle portion, with punctures coarser than that of head; interstices microreticulate. Wings completely reduced.

Legs rather long and slender. Coxae elongate. Femora slender, wider but shorter than tibiae. Tibiae thin, straight, each with two substraight and rather thin spurs at apex. Protarsi faintly widened; meso- and metatarsi slender; protarsi simple, not dilated; metatarsomeres 1–5 with length ratio as follows: 1.6: 1.7: 1.2: 1.0: 2.8. Claws rather thin, simply curved.

Abdomen somewhat flattened dorsally, 1.8 times as long as wide, about half length of forebody, 1.7 times as wide as elytra, widest at posterior angles of sternite V. Tergites and sternites densely covered with fine punctures; interstices microreticulated. Tergites III–VII anteriorly with paired, ill-delimited, shallow impressions; sternites III–VII without modified setae. Tergite VII and sternite VII both unmodified, rather slightly emarginate at posterior margins.

Male Terminalia and genitalia. Tergite VIII (Fig. 3A) subtrapezoidal, without modified setae, simply curved at posterior margin; sternite VIII (Fig. 3B) without modified setae, deeply and subtriangularly excised at posterior margin. Tergite IX (Fig. 3C–E) unmodified; sternite IX (Fig. 3F) asymmetrical, longer than wide, and distinctly, roundly emarginate at posterior margin. Tergite X (Fig. 3G) shortly oblong, rounded at posterior margin. Aedeagus (Fig. 5A–E) large and symmetrical in ventral view, 1.0 mm long; posterior margin of ventral wall deeply and subtriangularly excised; ventral process absent.

Male paratypes. Body 8.2–8.6 mm long. Three male types without evident variations to the holotype.

Female paratypes. Body 8.9–9.2 mm long, similar to male in general appearance (Fig. 1C, D), but can be differentiated by the following characters: body generally larger; abdomen slightly slenderer, 1.9 times as long as wide; sternite VII with paired strong predistal setae; and the combination of following characters in terminalia and genitalia.

Female terminalia and genitalia. Tergite VIII (Fig. 4A) subtrapezoidal, lacking modified setae, simply curved at posterior margin; sternite VIII (Fig. 4B) with paired strong predistal setae, truncated at posterior margin. Tergite IX (Fig. 4C–E) unmodified; sternite IX (Fig. 4F) bilobate, both slender, each with four strong predistal setae. Tergite X (Fig. 4G) shortly oblong, rounded at posterior margin.

Habitat. The dolomite cave, Taojindong, is a shaft-type cave with a broad entrance located next to a backroad of Shiqianggou (Fig. 6A). Investigators can only descend into the cave by the single-rope technique (SRT) (Fig. 6B). During the rainy season, the water level in the cave rises, making access impossible; at other times, the cave is wet and the tunnel is spacious.

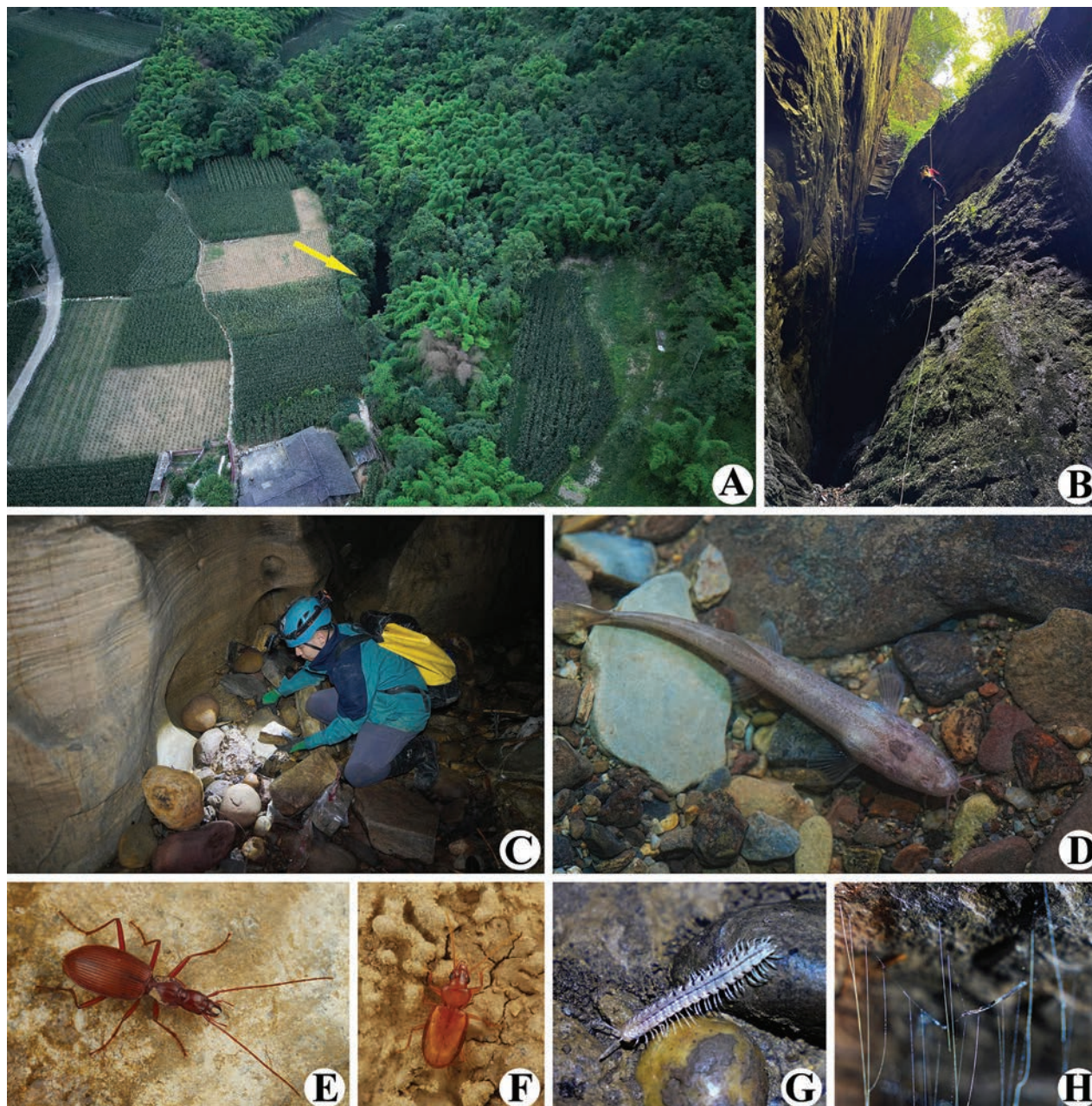


Figure 6. Taojindong [= Taojin Cave], the type locality of *Domene lizeyui* Wang & He, sp. nov. and some sympatric cave animals **A** environs of the cave (entrance shown by arrowhead) **B** Li He descending into the cave by using SRT **C** Ze-Yu Li collecting **D** *Claea* sp. (Cypriniformes, Nemacheilidae) **E** *Jujiroa duqianae* (Coleoptera, Carabidae) **F** *Paratachys* sp. (Coleoptera, Carabidae) **G** *Epanerchodus* sp. (Polydesmida, Polydesmidae) **H** *Chetoneura* sp. (Diptera, Keroplatidae) (A © Xin-Yang Zou B, D, G, H © Ze-Yu Li).

Domene lizeyui Wang & He, sp. nov. lives deep in the dark zone of the cave and was found either under rocks (Fig. 6C) or wandering on rock walls (Fig. 7; Suppl. material 1). Other troglobites found also inside the same cave were *Claea* sp. (Cypriniformes, Nemacheilidae) (Fig. 6D), *Jujiroa duqianae* Tian & He, 2023 (Coleoptera, Carabidae) (Fig. 6E), *Paratachys* sp. (Coleoptera, Carabidae) (Fig. 6F), *Epanerchodus* sp. (Polydesmida, Polydesmidae) (Fig. 6G), and *Chetoneura* sp. (Diptera, Keroplatidae) (Fig. 6H).



Figure 7. An individual of *Domene lizeyui* Wang & He, sp. nov. wandering on a rock in Taojindong (© Ze-Yu Li).

Differential diagnosis. *Domene lizeyui* Wang & He, sp. nov. has no evident relatives to other cave congeners because it lives on the opposite side of Eurasia. It is readily distinguishable from its congeners in eastern Asia by its rather unique appearance, like integument depigmented, legs and antennae rather long and slender, eyes reduced, and wings absent. Moreover, it can be differentiated from its congeners by the combination of the following characters: labrum deeply emarginate in middle of anterior margin and with paired subtriangular paramedian teeth, abdomen shortened (about half length of forebody), modified setae absent on all tergites and sternites in male, and ventral process absent on aedeagus.

Distribution. China (Sichuan).

Discussion

The new species can be assigned to the genus *Domene* by the combination of the following characters (Coiffait 1982; Li 2009): body lacking bright-colored pattern; head dorsally weakly convex; eyes shorter than half length of temples; neck region wider than 1/5 width of head capsule; maxillary palpi with terminal palpomere thin and slender, smooth and glabrous; antennae slender; pronotum dorsally weakly convex, longer than wide; profemora each with a ventral protuberance around middle; tibiae lacking setae on lateral sides; protarsi faintly widened in both sexes; metatarsomere 5 shorter than length of basal four tarsomeres.

The discovery of the troglobitic *D. lizeyui* Wang & He, sp. nov. in China is of great interest for staphylinid taxonomy and biogeography. Species of the genus *Domene* were categorized into seven nominal subgenera (some species treated as incertae sedis) (Coiffait 1982; Oromí and Hernández 1986; Assing and Feldmann 2014; Assing 2018, 2021): *Domene* (s. s.) (Western Palaearctic), *Canariomene* Oromí & Hernández, 1986 (Canary Islands), *Lathromene* Koch, 1938 (Western Mediterranean), *Lobramene* Assing, 2021 (China), *Spelaeomene* Español, 1977 (Morocco), *Neodomene* Blackwelder, 1939 (Northern India; generic assignment doubtful), and *Macromene* Coiffait, 1982 (Eastern Palaearctic and Northern Oriental). As mentioned above, the new species is very different from known epigeal species from eastern Asia in the subgenera *Lobramene* and *Macromene* by its striking troglomorphic features. Except *Spelaeomene*, other subgenera have their ventral processes on aedeagi more or less developed (absent in *Spelaeomene* and *D. lizeyui* Wang & He, sp. nov.). And the new species is easily distinguishable from *Spelaeomene* by its deeply, medially emarginate and subtriangularly, paramedianly toothed labrum on the anterior margin, and its short abdomen (about one-half length of forebody). Thus, it appears that a new subgenus needs to be established to accommodate this new species. However, as stated by Assing and Feldmann (2014: 499) "... the subgeneric concept currently in use is highly artificial. Taxa such as *Canariomene* and *Spelaeomene*, for instance, are mainly constituted by characters associated with adaptations to a hypogean habitat." Therefore, we refrain from establishing a new subgenus at present because of the unavailability of specimens of other known troglobitic *Domene* species. A comprehensive phylogenetic analysis of the genus is urgently needed.

Acknowledgements

We are deeply indebted to Yuan Li (Deyang, China) and Ze-Yu Li (Panzhihua, China) for providing specimens of the new species and assistances during the cave surveys. We would like to express our sincere gratitude to Chang-Chin Chen (Tianjin, China), Tian-Long He (Huainan, China), Zhuo-Heng Jiang (Westlake University, Hangzhou, China), Xiao-Yan Li (Langfang Normal University, Langfang, China), Ye-Jie Lin and Hong-Zhang Zhou (both Institute of Zoology, Chinese Academy of Sciences, Beijing, China), Lu Qiu (MYNU), Ming-Yi Tian (South China Agricultural University, Guangzhou, China), Zhen Wang (Chengdu, China), Zi-Wei Yin (Shanghai Normal University, Shanghai, China) and Chao Zhou (Chengdu, China) for their constant support. We are grateful to Xin-Yang Zou (Chongqing, China) for helping us to take aerial photos of the cave. Our appreciation is due also to Li-Fei Chen, Jin-Xiong Duan, Long-Jue Hu, Hao Jin, Xue-Fei Liu, Can Tang, Wei-Qi Wang, Song-Lun Xie, Yue-Hai Yu and Cheng-Xing Zhu (all Sichuan Cave Exploration Team, Chengdu) for their help in the field collection. Carabids and millipedes in the cave were kindly identified by Ming-Yi Tian and Wei-Xin Liu (South China Agricultural University, Guangzhou, China). We thank Christopher J. Glasby (Museum and Art Gallery Northern Territory, Australia) for his linguistic revision of the text. In particular, we thank Sinan Anlaş (Manisa Celal Bayar University, Manisa, Turkey) and Peter Hlaváč (National Museum, Prague, Czech Republic) for their constructive comments on earlier versions of the manuscript.

Additional information

Conflict of interest

The authors have declared that no competing interests exist.

Ethical statement

No ethical statement was reported.

Funding

This project is supported by the Natural Science Foundation of LiGeZiTaoYaoBao (NSFL-2024).

Author contributions

Conceptualization: C-B Wang. Funding acquisition: L He. Project administration: L He. Supervision: L He. Visualization: C-B Wang & L He. Writing—original draft: C-B Wang. Writing—review and editing: C-B Wang & L He.

Author ORCIDs

Cheng-Bin Wang  <https://orcid.org/0000-0002-7913-8779>

Li He  <https://orcid.org/0000-0002-4597-3442>

Data availability

All of the data that support the findings of this study are available in the main text or Supplementary Information.

References

- Assing V (2013) On the *Lathrobium* fauna of China IV. Six new species from Sichuan (Coleoptera: Staphylinidae: Paederinae). *Linzer Biologische Beiträge* 45(1): 155–170. <https://doi.org/10.21248/contrib.entomol.63.1.53-128>
- Assing V (2015) Three new species of *Domene* from China (Coleoptera: Staphylinidae: Paederinae). *Contributions to Entomology* 65(1): 31–39. <https://doi.org/10.21248/contrib.entomol.65.1.31-39>
- Assing V (2016) Two new species and additional records of *Domene* from China and Vietnam (Coleoptera: Staphylinidae: Paederinae). *Contributions to Entomology* 66(1): 113–118. <https://doi.org/10.21248/contrib.entomol.66.1.113-118>
- Assing V (2018) The third hypogean *Domene* species from Greece (Coleoptera: Staphylinidae: Paederinae). *Linzer biologische Beiträge* 50(1): 17–23.
- Assing V (2021) A new subgenus and a remarkable new species of *Domene* from South China, with additional records of the genus from China, Taiwan, and Vietnam (Coleoptera: Staphylinidae: Paederinae). *Contributions to Entomology* 71(2): 227–231. <https://doi.org/10.21248/contrib.entomol.71.2.227-231>
- Assing V, Feldmann B (2014) On *Domene scabripennis* Rougemont and its close relatives (Coleoptera: Staphylinidae: Paederinae). *Linzer Biologische Beiträge* 46(1): 499–514.
- Chen M-Z, Ma Z-J, Tian M-Y (2019) Discovery of a cavernicolous trechine species from the Sanwang Dong-Erwang Dong cave system, Wulong, Chongqing, southwestern China (Coleoptera: Carabidae: Trechinae). *Zootaxa* 4668(1): 105–114. <https://doi.org/10.11646/zootaxa.4668.1.6>

- Coiffait H (1982) Coléoptères Staphylinidae de la région paléarctique occidentale. IV. Sous famille Paederinae. Tribu Paederini 1 (Paederi, Lathrobii). Supplément à la Nouvelle Revue d'Entomologie 12(4): 1–440.
- Deuve T, Tian M-Y (2016) Descriptions de sept nouveaux Trechini cavernicoles de la Chine continentale (Coleoptera, Caraboidea). Bulletin de la Société Entomologique de France 121(3): 343–354. <https://doi.org/10.3406/bsef.2016.2174>
- Feldmann B, Peng Z, Li L-Z (2014) On the *Domene* species of China, with descriptions of four new species (Coleoptera, Staphylinidae). ZooKeys 456: 109–138. <https://doi.org/10.3897/zookeys.456.8413>
- Hlaváč P, Oromí P, Bordoni A (2006) Catalogue of troglobitic Staphylinidae (Pselaphinae excluded) of the world. Subterranean Biology 4: 19–28.
- Huang S-B, Tian M-Y (2021) Overview of cave-dwelling ground beetles in the past three decades in China. Carsologica Sinica 40(6): 1026–1031. <https://doi.org/10.11932/karst20210611>
- Jia X-Y, He L, Tian M-Y (2021) A new subgenus and three new cavernicolous species of the genus *Pterostichus* from China (Coleoptera: Carabidae: Pterostichini). Annales de la Société Entomologique de France (N.S.) 57(4): 346–358. <https://doi.org/10.1080/00379271.2021.1966320>
- Koch C (1939) Über neue und wenig bekannte paläarktische Paederinae (Col. Staph.). III. Entomologische Blätter 35(3): 156–172.
- Lawrence JF, Ślipiński A, Seago AE, Thayer MK, Newton AF, Marvaldi AE (2011) Phylogeny of the Coleoptera based on morphological characters of adults and larvae. Annales Zoologici, Warszawa 61(1): 1–217. <https://doi.org/10.3161/000345411X576725>
- Li L-Z (2019) Catalogue of Chinese Coleoptera. Vol. 3. Staphylinidae. Science Press, Beijing, [xix +] 720 pp.
- Li X-Y (2009) Taxonomy of Paederina and Lathrobiina from China (Coleoptera: Staphylinidae: Paederina). PhD Thesis, Institute of Zoology, Chinese Academy of Sciences, Beijing, [ix +] 431 pp.
- Lin X-B, Peng Z (2021) Two new species and additional records of mainland Chinese *Domene* (Coleoptera: Staphylinidae: Paederinae). Zootaxa 5081(3): 444–450. <https://doi.org/10.11646/zootaxa.5081.3.8>
- Liu Z-X (2021) Cave Biology. Science Press, Beijing, [xxi +] 255 pp.
- Nomura S, Wang F-X (1991) Description of a new cavernicolous species of the genus *Batrisodellus* (Coleoptera, Pselaphidae) from Southeast China. Elytra 19(1): 77–83.
- Oromí P, Hernández JJ (1986) Dos nuevas especies cavernícolas de *Domene* de Tenerife (Islas Canarias). Fragmenta Entomologica 19(1): 129–144.
- Peng Z, Sun Z, Li L-Z, Zhao M-J (2015) Four new species and additional records of *Domene* and *Lathrobium* from the Dayao Mountains, southern China. ZooKeys 508: 113–126. <https://doi.org/10.3897/zookeys.508.9682>
- Peng Z, Liu S-N, Xie G-G, Li L-Z, Zhao M-J (2017) New data on the genus *Domene* (Coleoptera: Staphylinidae: Paederinae) of mainland China. Zootaxa 4329(5): 449–462. <https://doi.org/10.11646/zootaxa.4329.5.3>
- Perreau M, Růžička J (2018) *Ptomaphagus troglodytes* sp. n., the first anophthalmic species of Ptomaphagina from China (Coleoptera, Leiodidae, Cholevinae, Ptomaphagini). ZooKeys 749: 135–147. <https://doi.org/10.3897/zookeys.749.24964>
- Rougemont GM de (1995) A new *Domene* (*Macromene*) Coiffait from Taiwan (Coleoptera, Staphylinidae, Paederinae) (33rd contribution to the knowledge of Staphylinidae). Bulletin of National Museum of Natural Science 5: 135–138.

- Schülke M, Smetana A (2015) Family Staphylinidae Latreille, 1802. In: Löbl I, Löbl D (Eds) Catalogue of Palaearctic Coleoptera. Vol. 2/1. Hydrophiloidea – Staphylinoidea. Revised and Updated Edition. Brill, Leiden & Boston, 304–1134.
- Spangler PJ (1996) Four new stygobiontic beetles (Coleoptera: Dytiscidae; Noteridae; Elmidae). *Insecta Mundi* 10(1–4): 241–259.
- Tian M-Y (2008) An overview to cave-dwelling carabids (Insecta: Coleoptera) in China. *Proceedings of the 14th National Congress of Speleology, Chongqing*, 333–342.
- Tian M-Y, Clarke A (2012) A new eyeless species of cave-dwelling trechine beetle from northeastern Guizhou Province, China (Insecta: Coleoptera: Carabidae: Trechinae). *Cave and Karst Science* 39(2): 66–71.
- Tian M-Y, He L (2020a) New species and new record of cavernicolous ground beetles from Sichuan Province, China (Coleoptera: Carabidae: Pterostichini and Platynini). *Zootaxa* 4881 (3): 545–558. <https://doi.org/10.11646/zootaxa.4881.3.7>
- Tian M-Y, He L (2020b) A contribution to the knowledge of cavernicolous ground beetles from Sichuan Province, southwestern China (Coleoptera, Carabidae, Trechini, Platynini). *ZooKeys* 1008: 61–91. <https://doi.org/10.3897/zookeys.1008.61040>
- Tian M-Y, Huang S-B, Wang X-H, Tang M-R (2016) Contributions to the knowledge of subterranean trechine beetles in southern China's karsts: five new genera (Insecta, Coleoptera, Carabidae, Trechinae). *ZooKeys* 564: 121–156. <https://doi.org/10.3897/zookeys.564.6819>
- Tian M-Y, Huang S-B, Wang D-M (2018) Occurrence of hypogean trechine beetles in Hanzhong Tiankeng Cluster, southwestern Shaanxi, China (Coleoptera: Carabidae: Trechinae). *Annales de la Société Entomologique de France (N.S.)* 54(1): 81–87. <https://doi.org/10.1080/00379271.2017.1417056>
- Tian M-Y, Huang X-L, Li C-L (2021) Contribution to the knowledge of subterranean ground beetles from eastern Wuling Mountains, China (Coleoptera: Carabidae: Trechinae). *Zootaxa* 4926(4): 521–534. <https://doi.org/10.11646/zootaxa.4926.4.3>
- Tian M-Y, He L, Zhou J-J (2023a) New genera and new species of cavernicolous beetles from southwestern China (Coleoptera: Carabidae: Trechini, Platynini). *Annales de la Société Entomologique de France (N.S.)* 59(1): 65–81. <https://doi.org/10.1080/00379271.2023.2169760>
- Tian M-Y, Huang S-B, Jia X-Y (2023b) A contribution to cavernicolous beetle diversity of South China Karst: eight new genera and fourteen new species (Coleoptera: Carabidae: Trechini). *Zootaxa* 5243(1): 1–66. <https://doi.org/10.11646/zootaxa.5243.1.1>
- Tian M-Y, Liu W-X, Huang S-B, Luo X-Z (2023c) *Cave Biology*. Geology Press, Beijing, [iii +] 248 pp.
- Uéno S-I, Wang F-X (1991) Discovery of a highly specialized cave trechine (Coleoptera, Trechinae) in Southeast China. *Elytra* 19(1): 127–135.
- Wewalka G, Ribera I, Balke M (2007) Description of a new subterranean hyphydrine species from Hainan (China), based on morphology and DNA sequence data (Coleoptera: Dytiscidae). *Koleopterologische Rundschau* 77: 61–66.
- Yin Z-W (2020) New species of karst-dwelling Pselaphinae from southwestern China (Coleoptera: Staphylinidae). *Acta Entomologica Musei Nationalis Pragae* 60(1): 163–168. <https://doi.org/10.37520/aemnp.2020.009>
- Yin Z-W, He L (2020) New cavernicolous Pselaphinae from Sichuan, China (Coleoptera: Staphylinidae). *The Coleopterists Bulletin* 74(4): 827–836. <https://doi.org/10.1649/0010-065X-74.4.827>

- Yin Z-W, Li L-Z (2015) *Zopherobatrus* gen. n. (Coleoptera: Staphylinidae: Pselaphinae), a new troglobitic batrisine from southwestern China. *Zootaxa* 3985 (2): 291–295. <http://dx.doi.org/10.11646/zootaxa.3985.2.8>
- Yin Z-W, Zhou G-C (2018) Two new cavernicolous Pselaphinae (Coleoptera: Staphylinidae) from southern China. *Zootaxa* 4457(4): 589–594. <https://doi.org/10.11646/zootaxa.4457.4.9>
- Yin Z-W, Li L-Z, Zhao M-J (2010) *Araneibatrus gracilipes* gen. et sp. n., a remarkable Batrisitae (Coleoptera, Staphylinidae, Pselaphinae) from P. R. China. *ZooKeys* 69: 53–58. <https://doi.org/10.3897/zookeys.69.740>
- Yin Z-W, Li L-Z, Zhao M-J (2011a) Discovery in the caves of Guangxi, China: three new troglobitic species of *Tribasodites* Jeannel (Coleoptera, Staphylinidae, Pselaphinae). *Zootaxa* 3065: 49–59. <https://doi.org/10.11646/zootaxa.3065.1.5>
- Yin Z-W, Nomura S, Zhao M-J (2011b) Taxonomic study on *Batrisodellus* Jeannel of China, with discussion on the systematic position of *Batrisodellus callissimus* Nomura & Wang, 1991 (Coleoptera, Staphylinidae, Pselaphinae). *Spixiana* 34(1): 33–38.
- Yin Z-W, Nomura S, Li L-Z (2015) Ten new species of cavernicolous *Tribasodites* from China and Thailand, and a list of East Asian cave-inhabiting Pselaphinae (Coleoptera: Staphylinidae). *Acta Entomologica Musei Nationalis Pragae* 55(1): 105–127.
- Yin Z-W, Jiang R-X, Steiner H (2016) Revision of the genus *Araneibatrus* (Coleoptera: Staphylinidae: Pselaphinae). *Zootaxa* 4097(4): 475–494. <http://doi.org/10.11646/zootaxa.4097.4.2>
- Zhao S, Jia F-L (2021) A new species of stygobiontic diving beetles from China (Coleoptera, Dytiscidae, Hydroporinae, Bidessini). *Carsologica Sinica* 40(6): 1046–1051.

Supplementary material 1

A live *Domene lizeyui* Wang & He, sp. nov. wandering on rock walls (© Ze-Yu Li)

Authors: Cheng-Bin Wang, Li He

Data type: mp4

Copyright notice: This dataset is made available under the Open Database License (<http://opendatacommons.org/licenses/odbl/1.0/>). The Open Database License (ODbL) is a license agreement intended to allow users to freely share, modify, and use this Dataset while maintaining this same freedom for others, provided that the original source and author(s) are credited.

Link: <https://doi.org/10.3897/zookeys.1216.132155.suppl1>

Two new species of the treehopper genus *Enchenopa* Amyot & Serville, 1843 (Hemiptera, Membracidae) from northwest Ecuador

María P. Rueda-Rodríguez^{1,2}, Jorge L. Montalvo-Salazar¹

¹ Universidad San Francisco de Quito USFQ, Colegio de Ciencias Biológicas y Ambientales, Instituto de Biodiversidad Tropical IBIOTROP, Laboratorio de Zoología Terrestre, Museo de Zoología, Quito 170901, Ecuador

² Tandayapa Cloud Forest Station, Colegio de Ciencias Biológicas y Ambientales, Universidad San Francisco de Quito USFQ, P.O. Box 17-1200-841, Quito, Ecuador
Corresponding author: María P. Rueda-Rodríguez (mariapazrr03@gmail.com)

Abstract

Enchenopa Amyot & Serville, 1843 is a diverse treehopper genus widespread across the New World. We describe two new *Enchenopa* species from northwest Ecuador: *Enchenopa gennyae* **sp. nov.** from urban forest remnants at the foothills of the Andes cordillera and *Enchenopa chocoandina* **sp. nov.** from secondary montane forests. *Enchenopa gennyae* **sp. nov.** is placed in the *E. biplaga* species group and is distinguished by the sexual dimorphism of the pronotal horn and lateral carina shape, the straight metopidium, 2–4 accessory carinae and the whitish dorsal spot and subapical band. *Enchenopa chocoandina* **sp. nov.** belongs to the *E. andina* species group and is diagnosed by its reddish central carina and posterior pronotal process apex, presence of an obtuse projection rather than an anterior horn, three or four irregular accessory carinae, and apical amber forewing patch. Illustrations, notes on natural history, and keys to species of the *E. biplaga* and *E. andina* species groups are also provided.

Key words: Membracinae, Membracini, Tandayapa, taxonomy, Tropical Andes, urban green spaces



Academic editor: Christopher H. Dietrich

Received: 29 March 2024

Accepted: 5 August 2024

Published: 21 October 2024

ZooBank: <https://zoobank.org/4258382E-C1BE-4969-8240-C1251459D2DD>

Citation: Rueda-Rodríguez MP, Montalvo-Salazar JL (2024) Two new species of the treehopper genus *Enchenopa* Amyot & Serville, 1843 (Hemiptera, Membracidae) from northwest Ecuador. ZooKeys 1216: 43–62. <https://doi.org/10.3897/zookeys.1216.124181>

Copyright: © María P. Rueda-Rodríguez & Jorge L. Montalvo-Salazar
This is an open access article distributed under terms of the Creative Commons Attribution License (Attribution 4.0 International – CC BY 4.0).

Introduction

Enchenopa Amyot & Serville, 1843 is a diverse New World treehopper genus belonging to Membracinae, the second most speciose subfamily of the New World Membracidae (Bartlett et al. 2018). It is differentiated from other Membracini genera by the horn-shaped anterior process or obtuse projection on the pronotum with a lateral carina running from the apex of the anterior process to, usually, the lateral margin of pronotum, and two or more pairs of accessory carinae on the metopidium (Strümpel and Strümpel 2014). *Enchenopa* is most similar to *Enchophyllum* Amyot & Serville, 1843 due to the pronotal horn and lateral carinae, but it differs mainly in the presence of the accessory carinae and the lateral carina usually surpassing the humeral angles. *Enchenopa* can be distinguished from *Membracis* Fabricius, 1775, *Folicarina* Sakakibara, 1992, and *Phyllotropis* Stål, 1869 by the non-foliaceous pronotum, presence of a pronotal horn, and the carination which is typically absent in *Membracis* and reduced in *Folicarina* and *Phyllotropis*; although *Folicarina* also has accessory carinae

(Flórez-V et al. 2015; McKamey 2022). Richter (1947, 1954) noted that some *Membracis* species occasionally have a short lateral carina and, *Enchophyllum* and *Enchenopa* can vary intraspecifically in the length of the lateral carina. Lastly, *Enchenopa* can only be differentiated accurately from *Leioscyta* Fowler, 1894 by the accessory carinae, which are absent in the latter. Some *Leioscyta* are also smaller species, lack lateral carinae, and the pronotum is rounded (Dietrich and McKamey 1995). *Enchenopa* is not supported by any synapomorphies, and phylogenetic studies have suggested that it, as well as its related genera, may not be monophyletic (Dietrich and McKamey 1995; Lin et al. 2004).

Strümpel and Strümpel (2014) revised *Enchenopa* and recognized 51 valid species, including 21 new to science, and classified them into ten species groups. They also treated *Campylenchia* Stål, 1869 as a junior synonym. Since then, only one more species of the *E. andina* species group has been described from Brazil (Lencioni-Neto and Sakakibara 2015). McKamey (2022) reinstated four more species excluded from the genus by Strümpel and Strümpel (2014) however, the types are not in a good state of preservation and he could not evaluate possible synonymy.

The biology of most species of *Enchenopa* is poorly known. Some species are solitary but occasionally congregations of adults with nymphs can be found. There is no parental care; instead, the females deposit their eggs in clusters on their host plant covered with a white wax-like substance that protects them from parasitoids (Godoy et al. 2006; Lin 2006). They have been reported to have mutualistic relationships with ants and to feed on host plants from at least 32 families of which Fabaceae and Asteraceae are the most predominant (Flórez-V et al. 2015). *Enchenopa binotata* (Say, 1824) is undoubtedly the most studied species of the genus, and its mating signals and host plant specialization suggest that this taxon comprises a complex of as many as 15 species (McNett and Coccoft 2008; Hamilton and Coccoft 2009; Deitz and Wallace 2012).

Species of *Enchenopa* are distributed from Canada to Argentina, but most species inhabit the Neotropical region. Strümpel and Strümpel (2014) recorded 12 species in Ecuador. Nevertheless, they could not review enough material, especially, from the Andean region. Previously Goding (1928) registered the species *E. lanceolata* (Fabricius, 1787), *E. quadricolor* (Walker, 1858), *E. minans* (Fairmaire, 1846) and *E. tatei* (Goding, 1928) in Ecuador not recorded by Strümpel and Strümpel (2014).

In this study, we describe two new species of *Enchenopa* from northwestern Ecuador, one of which was found in the forest remnants of a populous city at the foothills of the Andean Cordillera, and the second species from secondary montane forests. Additionally, we provide keys to species of the *Enchenopa biplaga* and *E. andina* species groups to which the newly described species belong.

Materials and methods

Fieldwork was conducted between 2023 and 2024 in two locations in north-west Ecuador, urban forest remnants of Santo Domingo (Santo Domingo de los Tsáchilas) composed of patches of secondary semi-deciduous forest and located next to water bodies between 300 and 600 m of elevation, and Tandayapa Cloud Forest Station (Pichincha), a scientific station of Universidad San Francisco de Quito founded in 2022 and located in the Tandayapa Valley at

2280 m of elevation. The station covers 53 hectares of secondary and mature Montane Forest. Specimens were collected opportunistically during the day and euthanized in 75% ethanol. Observations of natural history were recorded in situ. A light trap with a mercury lamp was set up in Tandayapa Cloud Forest Station from 6 pm to 6 m in February 2024, and all membracid specimens were collected. We also examined specimens deposited at the Museo de Zoología Universidad San Francisco de Quito, Ecuador (**ZSFQ**), where all our specimens are deposited.

The specimens were photographed and measured using an Olympus DP73 digital camera attached to the Olympus SZX16 stereomicroscope with the light diffused as adapted from Kerr et al. (2008). The measurements were taken following Strümpel and Strümpel (2014). To examine the genitalia, we removed the entire abdomens and cleared them using 10% KOH for 48 hours at room temperature and then washed with distilled water. Genitalia were photographed using an OMAX A35180U3 digital camera attached to Olympus CX22 optic microscope and afterwards preserved in a 0.2-ml microvial with glycerol pinned with their respective specimen. Images were compiled in one multifocal composition using Zerene Stacker - USDA SI-SEL Lab Bk imaging system. The illustrations were made digitally with Sketchbook, a free access illustration software. Final images were edited in Adobe Photoshop CC 2023.

Terminology of general morphology follows Deitz (1975), Dietrich et al. (2001), and Strümpel and Strümpel (2006, 2014).

Results

Key to species of *Enchenopa biplaga* species group (modified from Strümpel and Strümpel 2014)

- 1 Pronotum with one white or yellow dorsal spot **2**
- Pronotum with one white or yellow dorsal spot and one white or yellow subapical band **3**
- 2 Pronotal horn short, curved forward, dorsal spot always yellow
..... ***E. ignidorsum* Walker**
- Pronotal horn long and straight, white or yellow dorsal spot ***E. vittifera* Stål**
- 3 Pronotum with horn length shorter than distance between tips of humeral angles or horn absent **4**
- Pronotum with horn longer than distance between tips of humeral angles..... **7**
- 4 Metopidium with two accessory carinae, the posterior one half to almost as long as lateral carina **5**
- Metopidium with two to four accessory carinae, all < 1/2 length of lateral carina..... **6**
- 5 Pronotal horn curved forwards; lateral carina just surpassing the corner of humeral angles; posterior accessory carinae almost length of lateral carina. Males / females with dorsal spot 2 × / 4 × as long as subapical band
..... ***E. longimaculata* Strümpel & Strümpel**
- Pronotal horn straight; lateral carina almost touching lateral pronotal margin; posterior accessory carinae 1/2 length of lateral carina; dorsal spot and lateral band not sexually dimorphic ***E. singularis* Strümpel & Strümpel**

- 6 Metopidium convex and two to three accessory carinae. Male and female not dimorphic. Overall color brown to black.....*E. biplaga* Walker
- Metopidium straight with two to four accessory carinae. Male with narrow horn curved forwards and female with only obtuse projection; male shorter than female. Overall color black.....*E. gennyae* sp. nov.
- 7 Pronotum with horn curved, directed forward..... 8
- Pronotum with horn straight..... 9
- 8 Length from pronotum base to horn apex equal to distance from pronotum base to posterior apex of pronotum.....*E. dubia* (Fowler)
- Length from pronotum base to horn apex shorter than distance from pronotum base to posterior apex of pronotum*E. lanceolata* Fabricius
- 9 Pronotum with horn distinctly longer than body width, lateral carina just surpassing horn base.....*E. reticornuta* Strümpel & Strümpel
- Pronotum with horn slightly longer than body width, lateral carina almost touching lateral pronotum margin..... *E. richteri* Strümpel & Strümpel

***Enchenopa gennyae* sp. nov.**

<https://zoobank.org/F7605C6C-FB5D-4337-A24E-84A915713DC4>

Figs 1–4

Material examined. Holotype: ECUADOR • 1 ♀; Santo Domingo de los Tsáchilas, Santo Domingo, Río Baba -0.30295, -79.15211, 480 m; 12 May 2023; Montalvo, J. & Rueda, M. P. leg.; Ex. Manual ZSFQ-i12112. **Paratypes:** ECUADOR • 2 ♂; same labels as for holotype; ZSFQ-i12110, ZSFQ-i12111 • 2 ♀, 1 ♂ Santo Domingo de los Tsáchilas, Santo Domingo, Quebrada del Río Pove -0.25237, -79.156668, 570 m; 14 Aug. 2023; Rueda, M. P. & Montalvo, J. leg.; Ex. Manual; ZSFQ-i17766:17768 • 3 ♀, 1 ♂ same locality as paratypes; 20 Apr. 2024; Rueda, M. P. leg.; Ex. Manual; ZSFQ-i18855:18858.

Notes on the type series. All specimens are minuten-mounted. Dissected abdomens of the holotype and two female and two male paratypes were placed in vials with glycerol pinned beneath the specimens. Some paratypes are in poor condition, with legs or wings lost.

Additional material. ECUADOR • 3 5th instars; same data as paratypes; ZSFQ-i17925, 17926.

Diagnosis. Overall color black with whitish dorsal spot and subapical band; metopidium straight, two to four sub-equal accessory carinae. Sexually dimorphic: female with obtuse projection instead of horn, short lateral carina not surpassing humeral angles, dorsal spot 2× longer than subapical band, and longer than male in size; male with narrow horn slightly curved forwards, lateral carinae almost touching lateral margin of pronotum and dorsal spot subequal in length to subapical band.

Description. Female holotype (ZSFQ-i12112). **Measurements** (mm): Length from head to wings at rest: 5.7; Total length: 6.3; Head to apex of posterior process: 4.6; Pronotal length: 4.4; Head to horn apex: 2.4; Forewing length: 4.9; Body width: 1.9; Vertex width on ocellar line: 1; Head length: 1.2; Frontoclypeus length: 0.8; Frontoclypeus width: 0.7; Prothoracic tibia length: 0.9; Metathoracic tibia length: 1.4; Metathoracic tibia width: 0.3; Prothoracic tibia width: 0.3.

Color. Overall black with whitish dorsal spot and subapical band on dorsum. Dorsal spot 2× longer than subapical band. Eyes black with dark brown

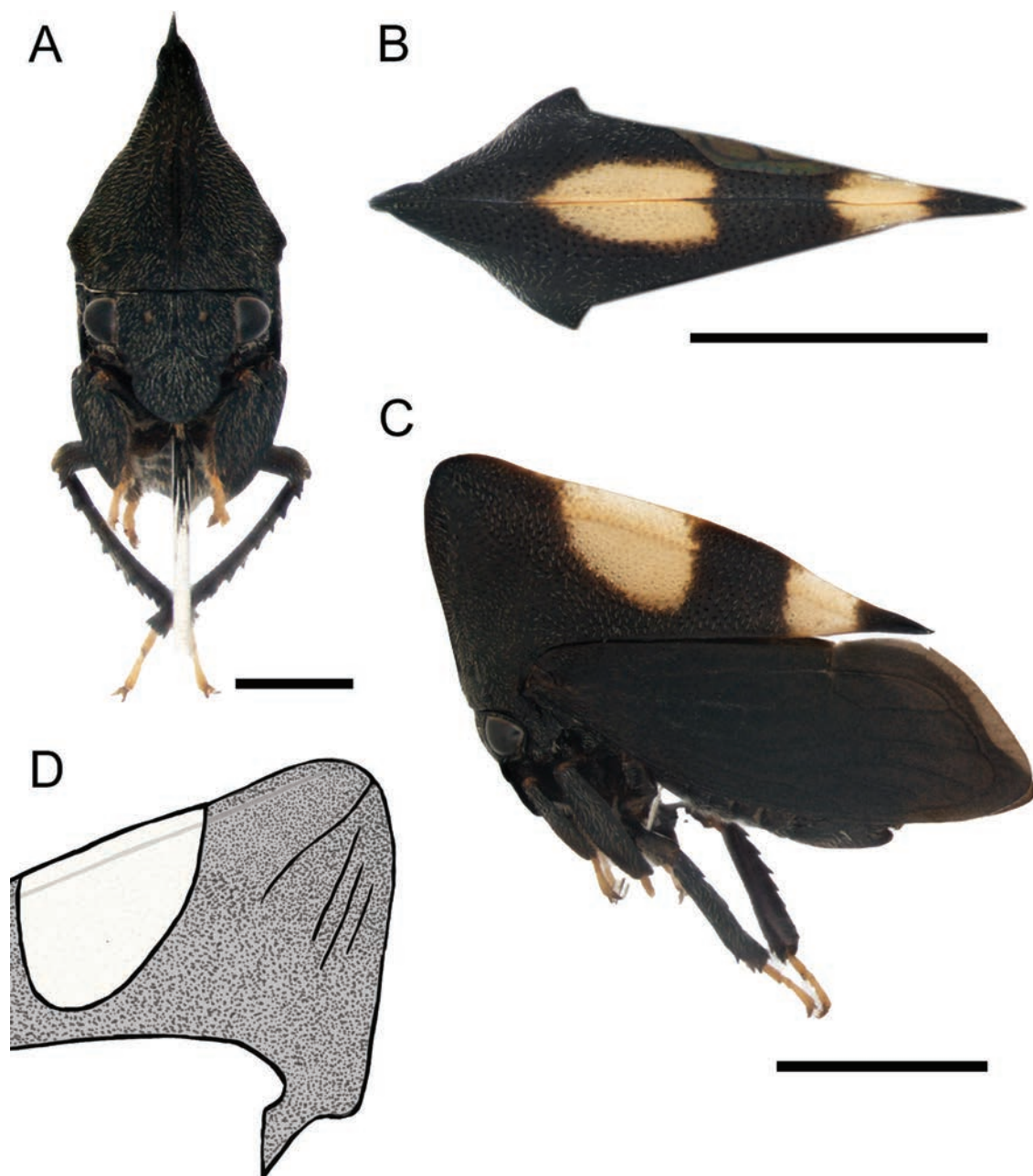


Figure 1. *Enchenopa gennyae* sp. nov. holotype female **A–C** habitus in frontal, dorsal view, and lateral views respectively **D** illustration of pronotum showing the carination. Scale bars: 1 mm (**A**); 2 mm (**B, C**).

margins, ocelli golden. Forewings opaque dull black, hind wings hyaline, veins black. Tarsi golden.

Surface. Head, pronotum, ventral sclerites of thorax, legs, and abdomen with dense golden pubescence; subcostal cell and veins of forewings with short, dispersed, almost indistinguishable golden pubescence. Pronotum (except metopidium) strongly punctured. Head, metopidium, forewings, and legs rough.

Head. Triangular, longer than wide (avoiding eyes); ocelli closer to eyes than each other; supra-antennal ledges arranged above clypeus; clypeus broad, longer than wide, anterior margin rounded; rostrum reaching hind coxae (Fig. 1A).

Thorax. Pronotum somewhat compressed, in lateral view, triangular, dorsal contour arched; metopidium straight, inclined anteriorly; horn reduced to an obtuse projection, obliquely directed dorso-anteriorly, wider than long, apex broadly round-

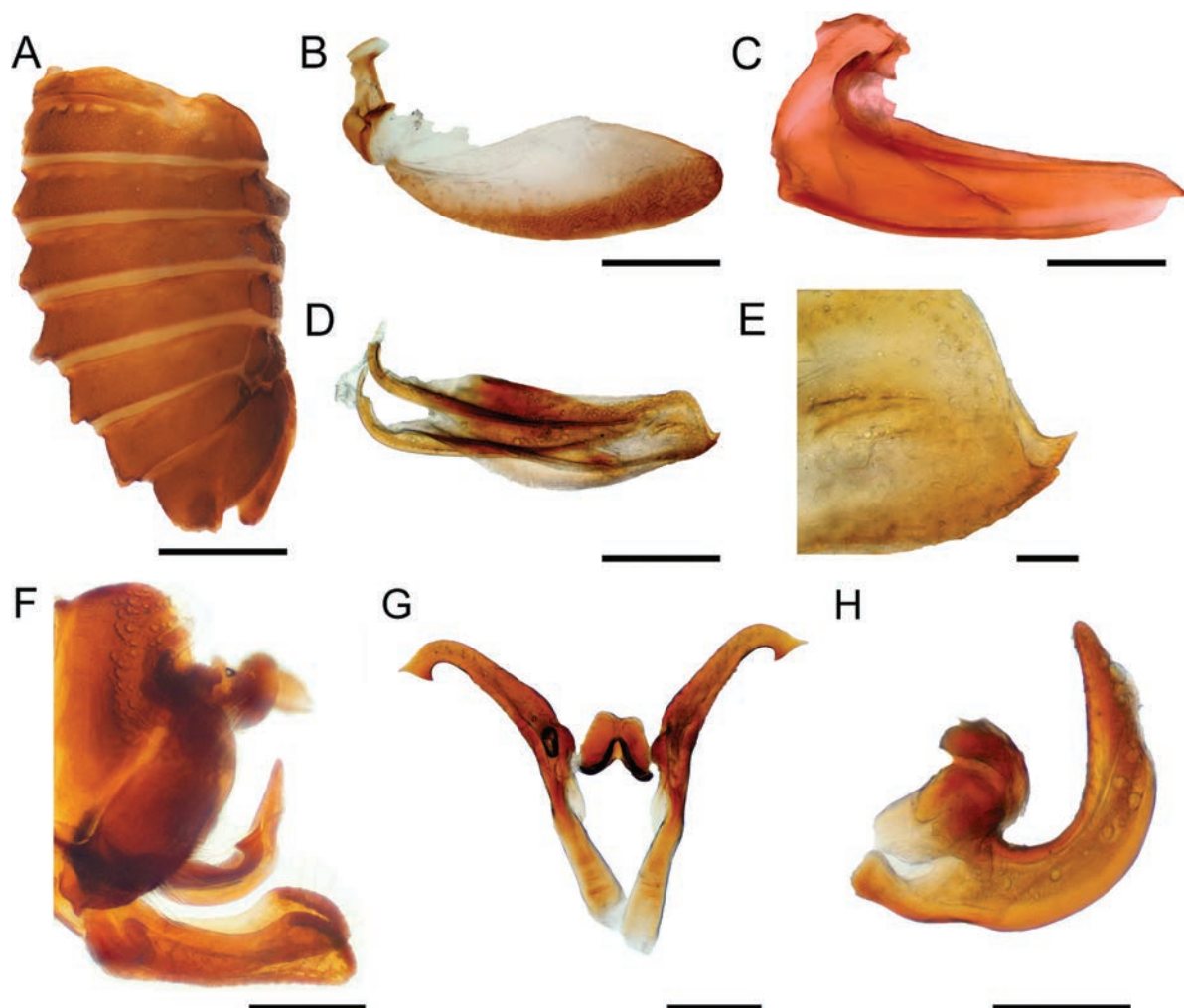


Figure 2. Abdomen and terminalia of *Enchenopa gennyae* sp. nov. **A** undissected female abdomen in lateral view **B** gonoplac in lateral view **C** first valvula in lateral view **D** second valvula in lateral view **E** close-up apex of second valvula **F** undissected male pygofer in lateral view **G** styles in dorsal view **H** aedeagus in lateral view. Scale bars: 1 mm (**A**); 0.1 mm (**B–D**); 0.01 mm (**E**); 0.2 mm (**F**); 0.05 mm (**G, H**).

ed; median carina laminated and somewhat foliaceous, especially on dorsum; lateral carina short, not extending beyond humeral angles (Fig. 1C); three parallel accessory carinae, almost as long as lateral carina extending ventroposteriorly from projection apex; posterior apex of pronotum acuminate almost reaching the apex of first apical cell (Fig. 1D); humeral angles slightly produced (Fig. 1B). Forewings with five apical cells, one discoidal cell, and one vein in the clavus, one r-m crossvein, two m-cu crossveins, and without s crossvein; apical limbus broad. Hind wings with four apical cells and one r-m crossvein. Anterior and middle tibiae foliaceous; posterior femur with apical, ventral and middle cucullate setae, metathoracic tibia compressed with spine-like cucullate setae on rows I and II, row III absent.

Abdomen. Sternum III with a transverse keel extending along the sternite and slightly projected ventrally. Dorsum of tergites VII and VIII with medial tuberosities, tergites IV–VI with reduced medial tuberosities (Fig. 2A). Genitalia. Gonoplac ventrally with few setae and more sclerotized, apex rounded (Fig. 2B). First valvula blade shaped, apex ventrally rounded, dorsally acuminate extending beyond ventral margin (Fig. 2C). Second valvula broad throughout, dorsally rounded, ventrally weakly serrated with a ventral apical tooth directed upwards (Fig. 2D, E).

Male paratype (ZSFQi-17766). Similar to female except dorsal spot as long as subapical band, pronotal horn narrow and curved forwards, lateral carina almost touching lateral margin of pronotum, metopidium with three accessory carinae at each side. Genitalia. Subgenital plate, in lateral view, 3× longer than wide, lobes diverging in first 1/4, dorsal margin concave, distally expanded (Fig. 2F). Styles 5× as long as wide, anterior projection subequal to posterior projection; shank with notch at middle of ventral margin, distally recurved and apically truncate, slightly expanded with posterior end longer and narrower than anterior end (Fig. 2G). Aedeagus U-shaped with anterior arm smaller than posterior arm and rounded; posterior arm lanceolate and abruptly narrowed at 1/3 length, anterior surface smooth, without serrations (Fig. 2H).

Variation. Measurements. Male / Female (mm): Length from head to wings: 4.4–5.1 / 5.3–5.8; Total length: 4.9–5.6 / 6.2–6.3; Head to apex of posterior process: 3.8–4.5 / 4.58–5; Pronotal length: 3.8–5.5 / 4.4–5.3; Head to horn apex: 2.2–2.7 / 2.4–2.9; Forewing length: 3.7–4.2 / 4.5–5.1; Body width: 1.6–1.7 / 1.9–2; Vertex width on ocellar line: 0.9–1 / 1.0–1.1; Head length: 1.1–1.2 / 1–1.2; Frontoclypeus length: 0.7–0.8 / 0.7–0.8; Frontoclypeus width: 0.7 / 0.7–0.8; Metathoracic tibia length: 0.8–1 / 0.9–1; Prothoracic tibia length: 1.2–1.4 / 1.4–1.8; Metathoracic tibia width: 0.2–0.3 / 0.3–0.5; Prothoracic tibia width: 0.3–0.4 / 0.3.

Females longer than males, with obtuse projection instead of horn, dorsal spot 2× longer than subapical band, lateral carina not surpassing humeral angles and, in some individuals, weakly produced; two to four secondary carinae almost as long as lateral carina. Male with horn narrow and curved forwards, dorsal spot < 2× subapical band length (Fig. 3A–C), lateral carina almost attaining lateral margin of pronotum and metopidium with three accessory carinae on each side (Fig. 3D). Independent of gender, dorsal contour of pronotum is more or less arched.

Fifth-instar nymph description. Overall color mostly white with black tarsi and scoli (Fig. 3E). One pair of abdominal scoli on each segment from III to VII; scoli length 5–6× basal width. Pronotum anteriorly with nascent horn not extended beyond head and posteriorly extended to abdominal segment III; anterior apex rounded and directed forward; posterior apex acute, dorsal margin convex in middle. Needle-like setae on chalazae distributed over whole body.

Distribution and natural history. Specimens of *Enchenopa gennyae* sp. nov. were found in two secondary forest remnants of the Western Foothills Forest from the urban area of Santo Domingo (Fig. 9): on the banks of the Baba River (Fig. 4C) and Pove River's ravine (Fig. 4D). Adult and nymph congregations were found on several occasions cohabiting together and perched on the underside of leaves and stems of an unidentified species of the genus *Piper* L. between 100 and 150 cm above the ground (Fig. 4A). Females were always more abundant than males in these congregations. Nymphs were attended by fire ants of the species *Wasmannia auropunctata* (Roger) (Fig. 4B).

Etymology. The species is dedicated to the mother of the first author, Genny Elizabeth Rodríguez Cueva, who helped to find the specimens of this species and has been a great support and inspiration throughout her life.

Remarks. Females of *Enchenopa gennyae* sp. nov. have a short lateral carina that does not extend beyond the humeral angles, while males have a long lateral carina that almost reaches the lateral margin of pronotum. In the tribe Membracini, the length of the lateral carina has not been previously reported as sexually dimorphic in any species. However, in some species of *Membracis*, it has been

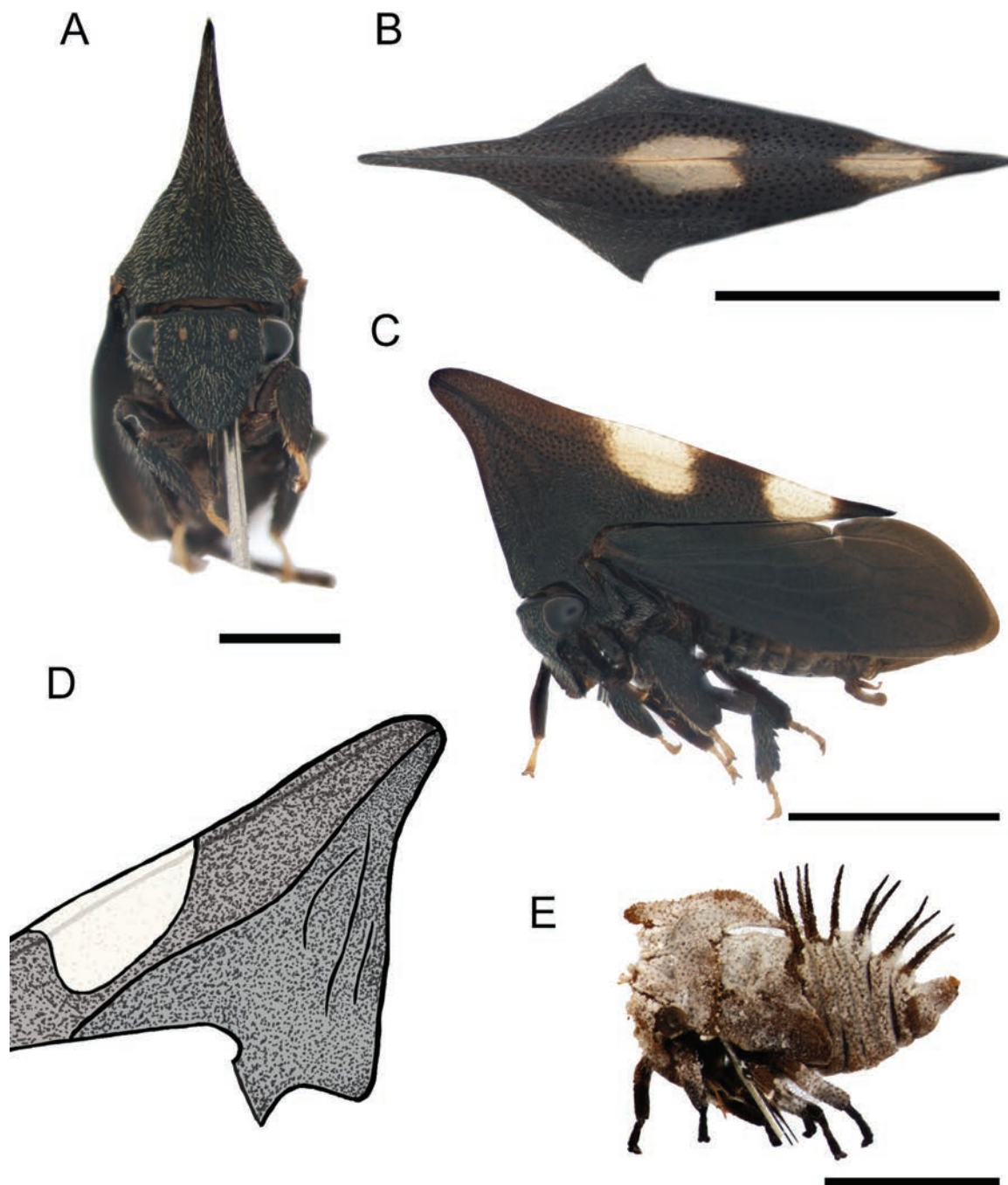


Figure 3. *Enchenopa gennyae* sp. nov. paratype male and nymph **A–C** male habitus in frontal, dorsal view, and lateral views respectively **D** illustration of male pronotum showing the carination **E** nymph habitus in lateral view. Scale bars: 1 mm (**A**); 2 mm (**B, C, E**).

noted that the lateral carina may or may not be present among individuals (Richter 1947). Likewise, Richter (1954) argued the lateral carina of some species of *Enchophyllum* and *Enchenopa* can vary in length within the same population. This species is the first known in the *Enchenopa biplaga* species group to exhibit sexual dimorphism in pronotum shape and lateral carina length. Like *Enchenopa gennyae* sp. nov., *E. longimaculata* Strümpel & Strümpel, 2014 has remarkable sexual dimorphism of the dorsal spot. However, in *Enchenopa longimaculata* the females the spot is 4× the length of the subapical band and in males 2× while in *E. gennyae* sp. nov. the spot is 2× as long in females but subequal in males.

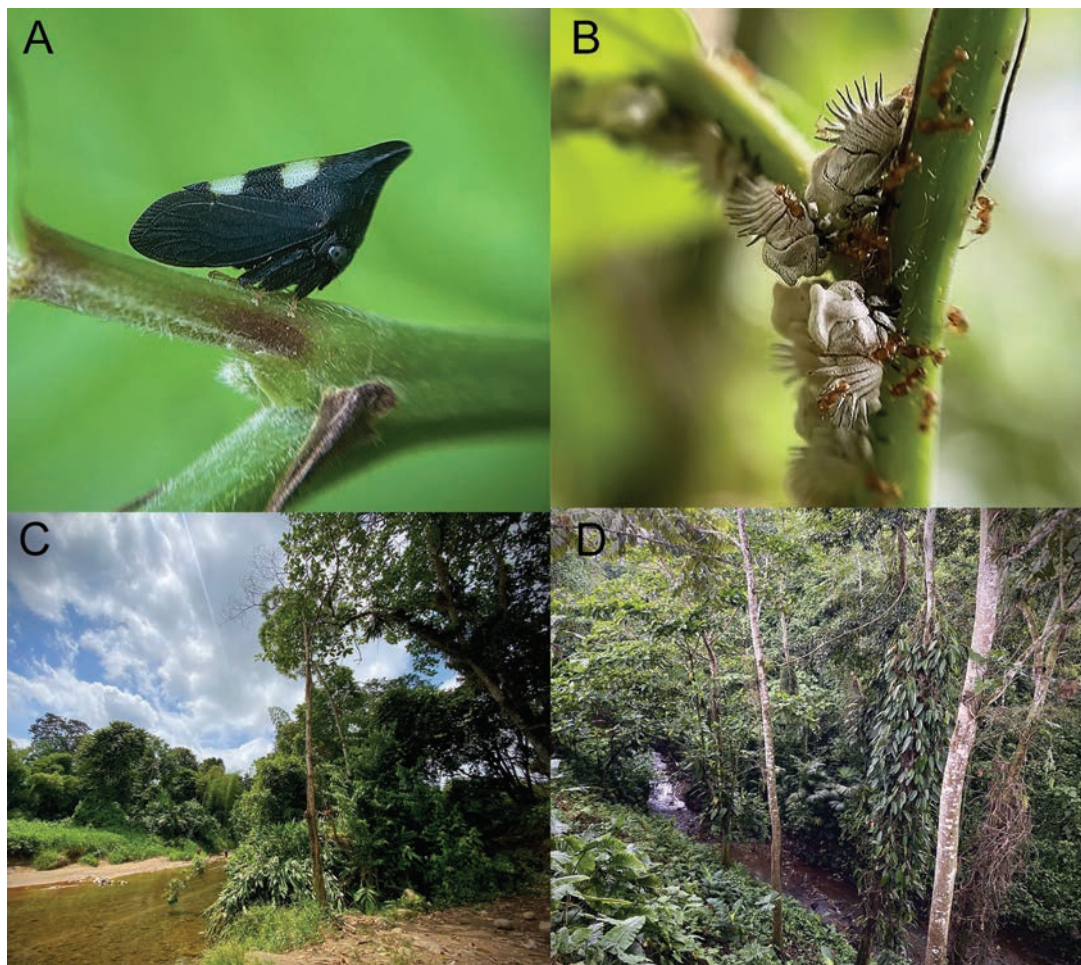


Figure 4. *Enchenopa gennyae* sp. nov. in its natural environment and habitat **A** male paratype perched on a stem of its host plant **B** nymphs attended by *Wasmannia auropunctata* (Roger) **C** shore of Baba River **D** ravine of Pove River.

Sexual dimorphism in the shape of the pronotal horn is characteristic of the *Enchenopa minuta* species group. However, *Enchenopa gennyae* sp. nov. does not belong to that group, given its coloration, the shape of the second valvula and, more importantly, the female's lack of a pronotal horn; in the *E. minuta* species group, males lack the horn and females generally have a developed horn.

Enchenopa gennyae sp. nov. belongs to the *E. biplaga* species group due to the presence of bands on dorsum of the pronotum, the second valvula with a ventral apical tooth, and forewings with one discoidal cell. *Enchenopa gennyae* sp. nov. differs from *E. ignidorsum* (Walker, 1858) and *E. vittifera* (Stål, 1869) by the two white lateral bands instead of just one yellow or white one, respectively. *Enchenopa gennyae* sp. nov. differs from *E. dubia* (Fowler, 1894), *E. lanceolata*, *E. reticornuta* Strümpel & Strümpel, 2014, and *E. richteri* Strümpel & Strümpel, 2014 by a horn shorter than the distance between the tips of humeral angles rather than longer. *Enchenopa singularis* Strümpel & Strümpel, 2014 and *E. longimaculata* have two accessory carinae with the posterior one ~ 1/2 or almost the total length, respectively, of the lateral carina, while *E. gennyae* sp. nov. has from two to four somewhat subequal accessory carinae. *E. gennyae* sp. nov. is distinguished from *E. melaleuca* Walker, 1858 by the shorter horn that is not curved forward. The new species closely resembles *Enchenopa biplaga* Walker, 1858 due to the shape of the pronotal horn, pronotum coloration, and the disposition

of the accessory carinae. However, *Enchenopa gennyae* sp. nov. has a straight metopidium, less produced horn, and sexual dimorphism. In contrast, in *E. biplaga* the metopidium is convex, the horn is large and strongly produced, and without sexual dimorphism. The females of *E. gennyae* sp. nov. have a short and straight horn while *E. biplaga* females have the horn longer than wide and curved forward. In males of *E. gennyae* sp. nov. the posterior arm of the aedeagus, in lateral view, is abruptly narrowed at one-third of its length, and the apical hook of the styles has the posterior tooth longer and narrower than the anterior tooth. In contrast, in the male of *E. biplaga* the width of the posterior arm of the aedeagus, in lateral view, slightly decreases at half of its length, and the apical hook of the styles has the posterior tooth similar in size to the anterior tooth.

McKamey (2022) reinstated *Enchenopa melaleuca* from the genus *Enchophyllum* and suggested it shares morphological similarities with some species of the *E. biplaga* species group. However, the holotype of this species has yet to be reviewed to confirm these affinities. Therefore, excluded *E. melaleuca* from the key to *E. biplaga* group species but compared it with *E. gennyae* sp. nov. in the above discussion.

In the *E. biplaga* species group, nymphs of *E. reticornuta* and *E. vittifera* are known (Strümpel and Strümpel 2014). They share with the nymph of *E. gennyae* sp. nov. the body covered with white wax-like material, black tarsi, and the presence of scoli on abdominal tergites III–VIII. However, we found the nymphs of *E. gennyae* sp. nov. differ from them mainly in the shape of the pronotum and scoli. The nymphs of *Enchenopa vittifera* have a longer horn directed forward with the posterior apex of the pronotum reaching the abdominal tergite III and have shorter scoli. While the nymphs of *Enchenopa reticornuta* have a straight horn with the posterior apex of the pronotum not touching the abdomen and longer scoli widened at the base.

Key of species of *Enchenopa andina* group (modified from Strümpel and Strümpel 2014; Lencioni-Neto and Sakakibara 2015)

- 1 Pronotal horn horizontally directed forwards ***E. loranthacina* Sakakibara & Marques**
- Pronotal horn obliquely directed upwards and forwards or horn absent and replaced by an obtuse projection **2**
- 2 Head as long as wide or wider than long **3**
- Head longer than wide **4**
- 3 Head as long as wide, body with long pubescence, forewings with a medial pale patch ***E. pilosa* Strümpel & Strümpel**
- Head wider than long, body with short pubescence, forewings without a medial pale patch ***E. eurycephala* Strümpel & Strümpel**
- 4 Median carina or just posterior apex of pronotum reddish, apical 1/3 of forewings amber **5**
- Median carina and posterior apex of pronotum concolorous, forewing with hyaline patch at apical margin **6**
- 5 Pronotal horn well produced; two to three accessory carinae well developed ***E. andina* Schmidt**
- Pronotal horn absent, replaced by obtuse projection; three to four weak and irregular accessory carinae present, some touching lateral carina ***E. chocoandina* sp. nov.**

- 6 Pronotal accessory carinae well developed; forewing apical patch occupying all of distal margin and extended basad to middle of apical cells 3 and 4.....*E. monoceros* (Germar)
- Pronotum with accessory carinae weak; forewing apical patch small, occupying only part of limb..... *E. luizae* Lencioni-Neto & Sakakibara

***Enchenopa chocoandina* sp. nov.**

<https://zoobank.org/BA0A3604-4903-4D28-B991-E3E3BB0365B2>

Figs 5–8

Material examined. Holotype: ECUADOR • 1 ♂; Pichincha, Tandayapa Cloud Forest Station -0.009645, -78.688058, 2280 m of elevation; 3 Fbr. 2024; Rueda, M. P. leg.; Ex. Manual; ZSFQ-i18060. **Paratypes:** ECUADOR • 1 ♂; same data as for holotype; ZSFQ-i18061 • 3 ♀, 1 ♂; Pichincha, Tandayapa Cloud Forest Station -0.009645, -78.688058, 2280 m of elevation; 9 Fbr. 2024; López-García, M. M., Montalvo, J. & Rueda, M. P. leg.; Ex. Mercury light; ZSFQ-i10862: 10865 • 1 ♀; Pichincha, Mindo, 0.04166, -78.77472, 1300 m of elevation; 11 Jun. 2022; Torres, D. leg.; Ex. Manual; ZSFQ-i8423 • 1 ♀, Imbabura, Seis de Julio de Cuellaje, 0.4509352, -78.525948, 2000 m of elevation; 13 Nov. 2021; Rubio, A. leg.; Ex. Manual; ZSFQ-i8196.

Note on the type series. Holotype and most paratypes are minuten-mounted. The paratype female ZSFQ-i8243 was originally pinned, but later the specimen was transferred to double mounting on a minuten pin. Dissected abdomens of holotype, one male paratype, and three female specimens placed in vials with glycerol pinned with specimens.

Diagnosis. Overall coloration black with scarlet median carina and posterior apex in females and scarlet posterior apex in males, apical 1/3 of forewing amber; pronotal horn absent, replaced by obtuse projection directed obliquely forwards, lateral carina almost touching lateral margin of pronotum; three or four weak accessory carinae, some touching lateral carinae or bifurcate.

Description. Male holotype (ZSFQ-i10860): Measurements (mm): Length from head to wings: 5.3; Total length: 5.4; Head to apex of posterior process: 4.5; Pronotal length: 4.6; Head to horn apex: 1.5; Forewing length: 4.4; Body width: 2.2; Vertex width on ocellar line: 1.2; Head length: 1.2; Frontoclypeus length: 0.7; Frontoclypeus width: 0.1; Metathoracic tibia length: 0.9; Prothoracic tibia length: 1.8; Metathoracic tibia width: 0.3; Prothoracic tibia width: 0.2.

Color. Overall color black. Eyes brownish, ocelli golden. Posterior apex of pronotum scarlet red. Forewings almost entirely opaque black with an apical translucent amber patch restricted on the third to fifth apical cells and limb around this area. Tarsi pale brownish.

Surface. Head, pronotum, ventral sclerites of thorax, legs, and abdomen with golden pubescence (Fig. 5B); sclerotized area of forewings with shorter pubescence. Pronotum (except by metopidium) and sclerotized area of forewings strongly punctured. Head, metopidium, legs, and abdomen rough.

Head. Triangular blunt, longer than wide (excluding eyes); distance between ocelli subequal to ocelli-eye distance; supra-antennal ledges arranged above clypeus; clypeus broad, longer than wide, anterior margin rounded; rostrum reaching posterior coxae (Fig. 5A).

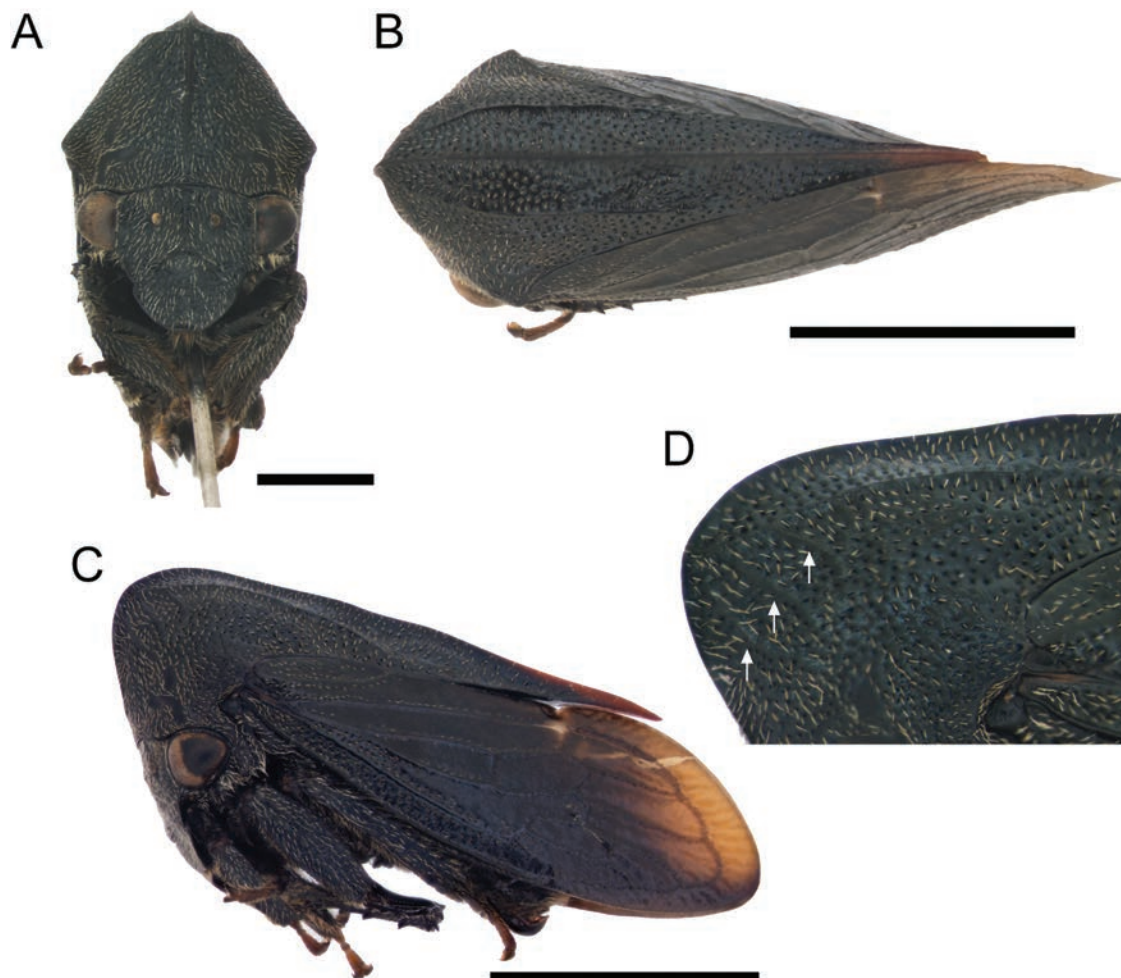


Figure 5. *Enchenopa chocoandina* sp. nov. holotype male **A–C** habitus in frontal, dorsal view, and lateral views respectively **D** approach to base of horn in lateral view, the white arrows indicate the accessory carinae. Scale bars: 1 mm (**A**); 2 mm (**B, C**).

Thorax. Pronotum, in lateral view, triangular; metopidium straight directed forwards; pronotal horn absent instead an obtuse projection with rounded apex; humeral angles slightly produced (Fig. 5B); median carina sharp; lateral carina parallel to median carina, running from apex of anterior projection to middle of the lateral margin of pronotum, almost touching the margin (Fig. 5C); three accessory carinae short (1/10 length of lateral carina), weak, irregular, sub-perpendicular to primary lateral carina, the last two diverging from the lateral carina (Fig. 5D), left side with the anterior two accessory carinae convergent; posterior apex of pronotum acuminate, just surpassing first apical cell. Forewing with one vein on clavus, two discoidal cells, two m-cu cross veins, one s cross veins which enclose second discoidal cell, and five apical cells; apical limb broad. Anterior and middle tibiae foliaceous; posterior femur with apical ventral and middle cucullate setae, posterior tibia with spine-like cucullate setae on rows I and II, row III absent.

Abdomen. Sternum III with a transversal keel extended along the sternite, strongly projected downwards and medially invaginated. Tergites III to VI with a pair of medial tuberosities, tuberosities of tergite VI strongly developed (Fig. 6D). Subgenital plate, in lateral view, 3× longer than wide, lobes diverging since the base, dorsal margin concave (Fig. 6A). Aedeagus with posterior arm lanceolate, 2× longer than anterior arm and strongly inclined forwards; anterior face of pos-

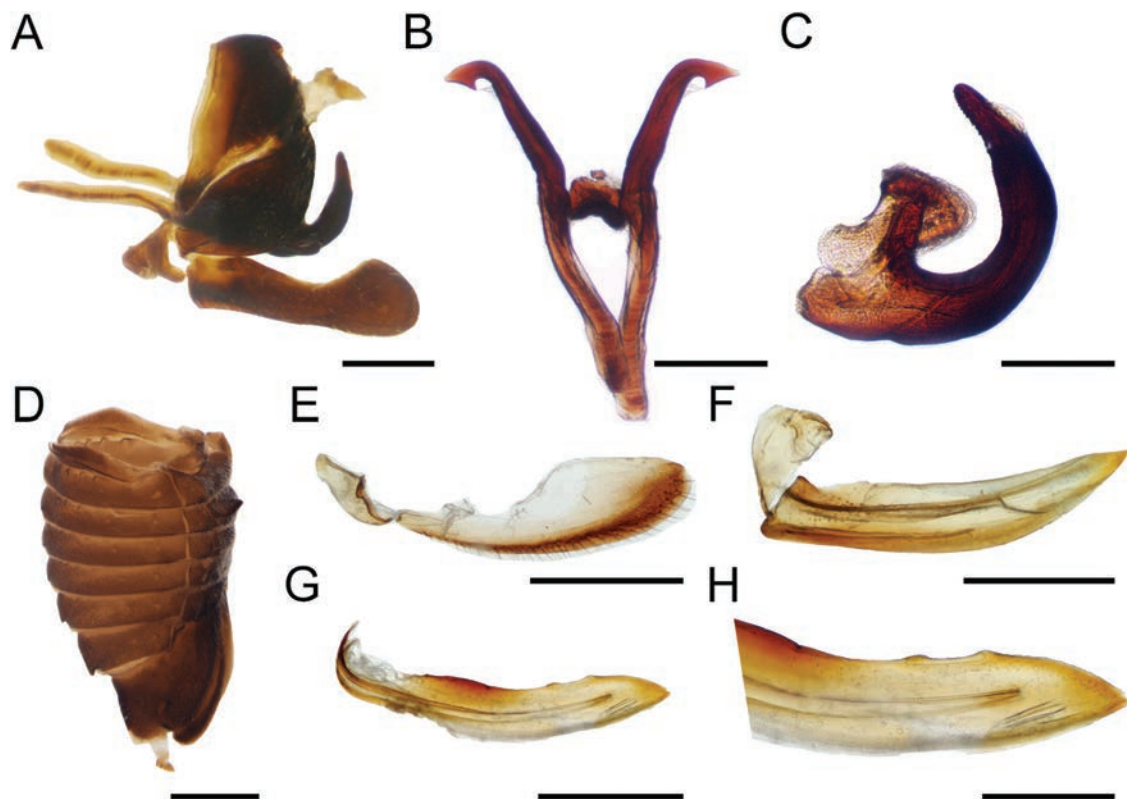


Figure 6. Abdomen and terminalia of *Enchenopa chocoandina* sp. nov. **A** undissected male pygofer in lateral view **B** styles in dorsal view **C** aedeagus in lateral view **D** undissected female abdomen in lateral view **E** gonoploc in lateral view **F** first valvula in lateral view **G** second valvula in lateral view **H** close-up apex of second valvula. Scale bars: 0.1 (**A**, **H**); 0.05 (**B**, **C**); 1 mm (**D**); 0.2 mm (**E**–**G**).

terior arm armed at apical 1/3 with small dorsal apical denticles, gonopore sub-apically (Fig. 6C). Styles distally recurved, apically truncate with anterior part longer than posterior part, spine tuft on dorsal margin just anterior to apex (Fig. 6B).

Female paratype (ZSFQ-i8423): Similar to male except for the pronotal projection more angulated and produced, central carina reddish behind humeral angles and forewings with amber patch extended from the second to fifth apical cells and limbus around this area. Genitalia. Gonoploc ventrally setose and more sclerotized than dorsally (Fig. 6E). First valvula blade shaped, basal 2/3 broad, apex acuminate (Fig. 6F). Second valvulae blade shaped with two dorsal tubercles in apical 1/2 (Fig. 6G, H).

Nymph unknown.

Variation. Measurements. Female / male (mm): Length from head to wings: 5.7–5.9 / 5.3–5.5; Total length: 5.9–6.4 / 5.4–5.7; Head to apex of posterior process: 5–5.6 / 4.3–4.5; Pronotal length: 4.9–5.5 / 4.5–4.6; Head to horn apex: 1.6–1.9 / 1.5–1.8; Forewing length: 5–5.4 / 4.4–4.8; Body width: 2.3–2.7 / 2.1–2.2; Vertex width on ocellar line: 1.2–1.4 / 1.1–1.2; Head length: 1.3–1.5 / 1.0–1.2; Frontoclypeus length: 0.7–0.9 / 0.7–0.8; Frontoclypeus width: 0.8–1.0 / 0.7–0.9; Metathoracic tibia length: 1–1.2 / 0.9–1.1; Prothoracic tibial length: 1.5–1.9 / 1.8–1.9; Metathoracic tibia width: 0.3–0.4 / 0.3–0.3; Prothoracic tibia width: 0.2–0.4 / 0.2–0.3.

Females are longer and have more produced pronotal projections than males (Fig. 7A, C), three or four accessory carinae (Fig. 7D), lateral carina behind humeral angles reddish rather than just the posterior apex of pronotum, and

the amber membrane is most extended (Fig. 7B). Independent of gender, some accessory carinae are bifurcate or converged.

Distribution and natural history. This species is distributed in the Montane forests of northwest Ecuadorian Andes (Fig. 9), between 1300 to 2300 m elevation. It inhabits the borders of secondary forests (Fig. 8B) and is a solitary species. The species has been recorded perched on the leaves or stems of different species of Asteraceae and Araceae, but more oftenly on *Munnozia pinnatipartita* (Hieron.) H. Rob. & Brettell (Asteraceae) (Fig. 8A), an endemic Ecuadorian species (Barriga et al. 2011). The species has been observed active during the day and attracted to mercury light traps at night between 8 pm and 2 am (Fig. 8C).

Etymology. The species, a noun in apposition, is named after the Andean Choco Biosphere Reserve declared by UNESCO as the seventh biosphere reserve of Ecuador, where this species lives. It honors the people who defend this territory from the metal mining that threatens the ecosystems and biodiversity of this important area.

Remarks. *Enchenopa chocoandina* sp. nov. belongs to *E. andina* species group based on the pronotum with a horn or projection shorter than the distance between the humeral angles, the forewing with transparent patches, and the blade-

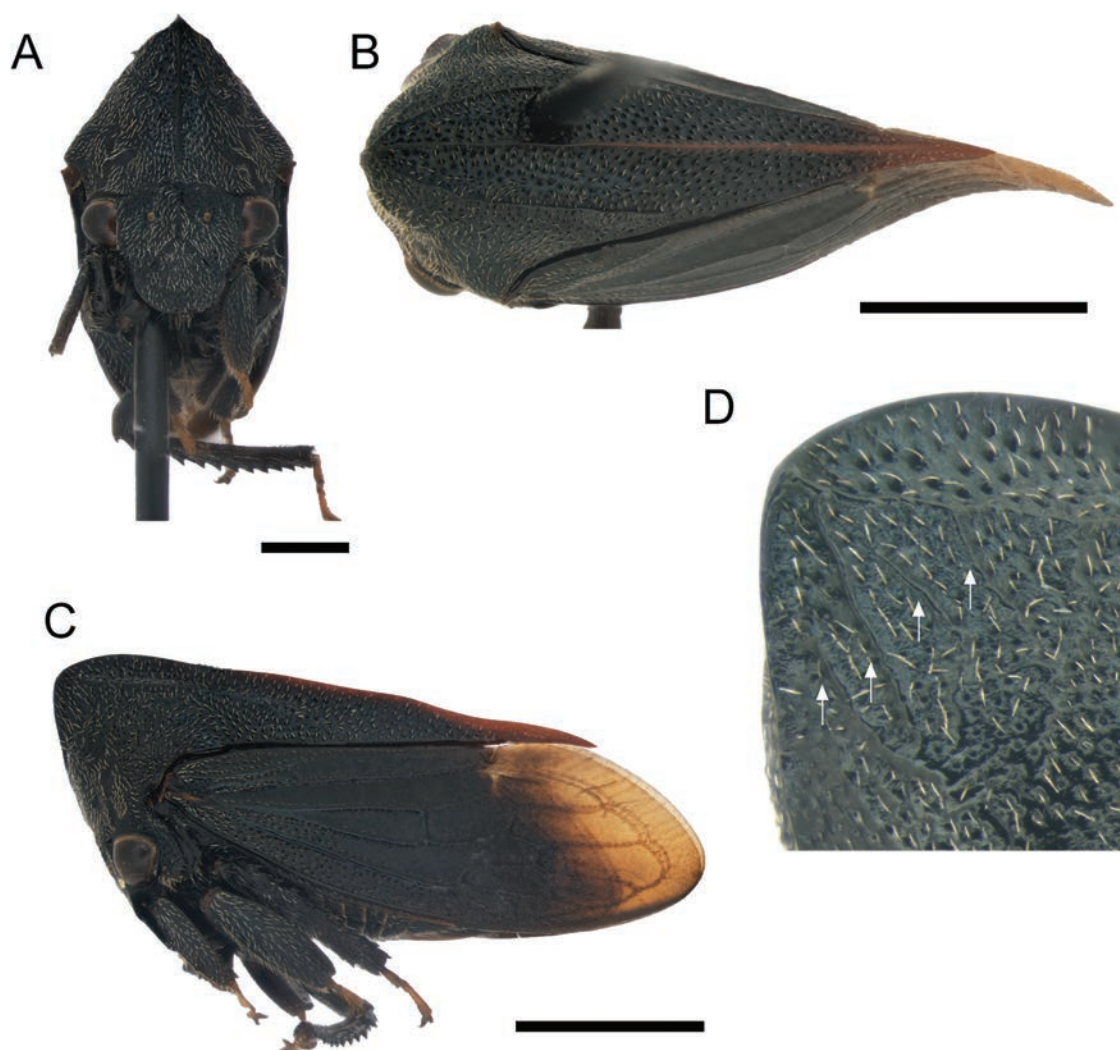


Figure 7. *Enchenopa chocoandina* sp. nov. paratype female **A–C** habitus in frontal, dorsal view, and lateral views respectively **D** approach to base of horn in lateral view, the white arrows indicate the accessory carinae. Scale bars: 1 mm (**A**); 2 mm (**B, C**).

shaped second valvulae. Moreover, some species of this group, such as *E. pilosa* and *E. eurycephala*, have dense pubescence, shared with *E. chocoandina* sp. nov.

Enchenopa chocoandina sp. nov. differs from *Enchenopa loranthacina* (Sakakibara & Marques, 2010) by the obtuse projection obliquely directed forwards rather than a horizontally inclined horn and from *E. pilosa* Strümpel & Strümpel, 2014 and *E. eurycephala* Strümpel & Strümpel, 2014 by the head longer than wide instead of as long as wide or wider than long respectively. *Enchenopa chocoandina* sp. nov. has a reddish median pronotal carina and amber forewing patches which separate it from *E. monoceros* (Germar, 1821) and *E. luizae* (Lencioni-Neto & Sakakibara, 2015) which have the median carina concolorous and forewing patches hyaline. The new species resembles *E. andina* (Schmidt, 1924) by the black overall coloration with median carina and posterior apex reddish, and the amber forewing apex; however, *E. chocoandina* sp. nov. does not have a horn instead an obtuse projection, longer and denser pubescence, and three or four weak and irregular accessory carinae instead of two or three. Moreover, the new species is considerably shorter than *E. andina* and differs in the male and female genitalia.

Enchenopa chocoandina sp. nov. lacks a distinctive horn; instead, it has an obtuse projection with a rounded apex, resembling species of the *E. beebi* species group or the males of *E. minuta* species group (Strümpel and Strümpel 2014). However, *E. chocoandina* sp. nov. properly does not fit within the *E. beebi* species group due to the absence of large punctation on the upper portion of the pronotum and dorsum, a short translucent apical patch and yellow tarsi. Neither does it

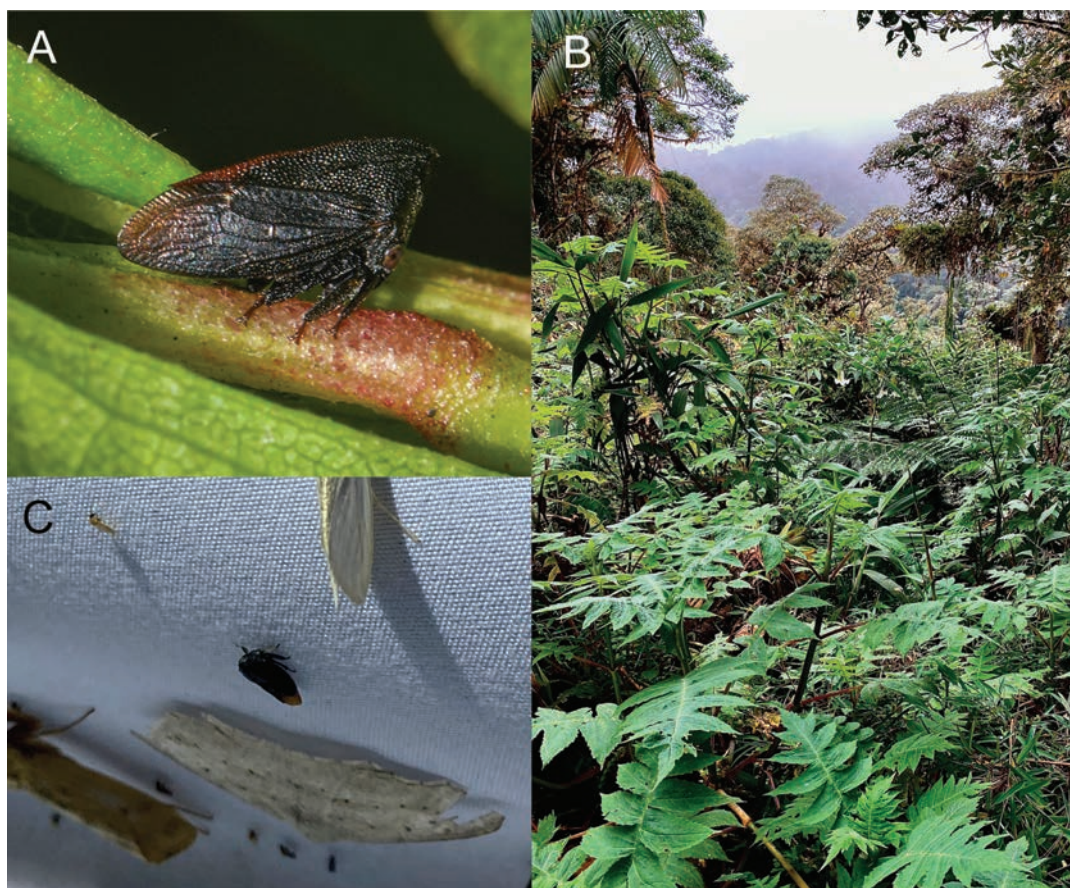


Figure 8. *Enchenopa chocoandina* sp. nov. in its natural environment and habitat **A** paratype female from Mindo by David Torres **B** border of a secondary forest at Tandayapa Cloud Forest Station **C** female paratype attracted by a light trap.

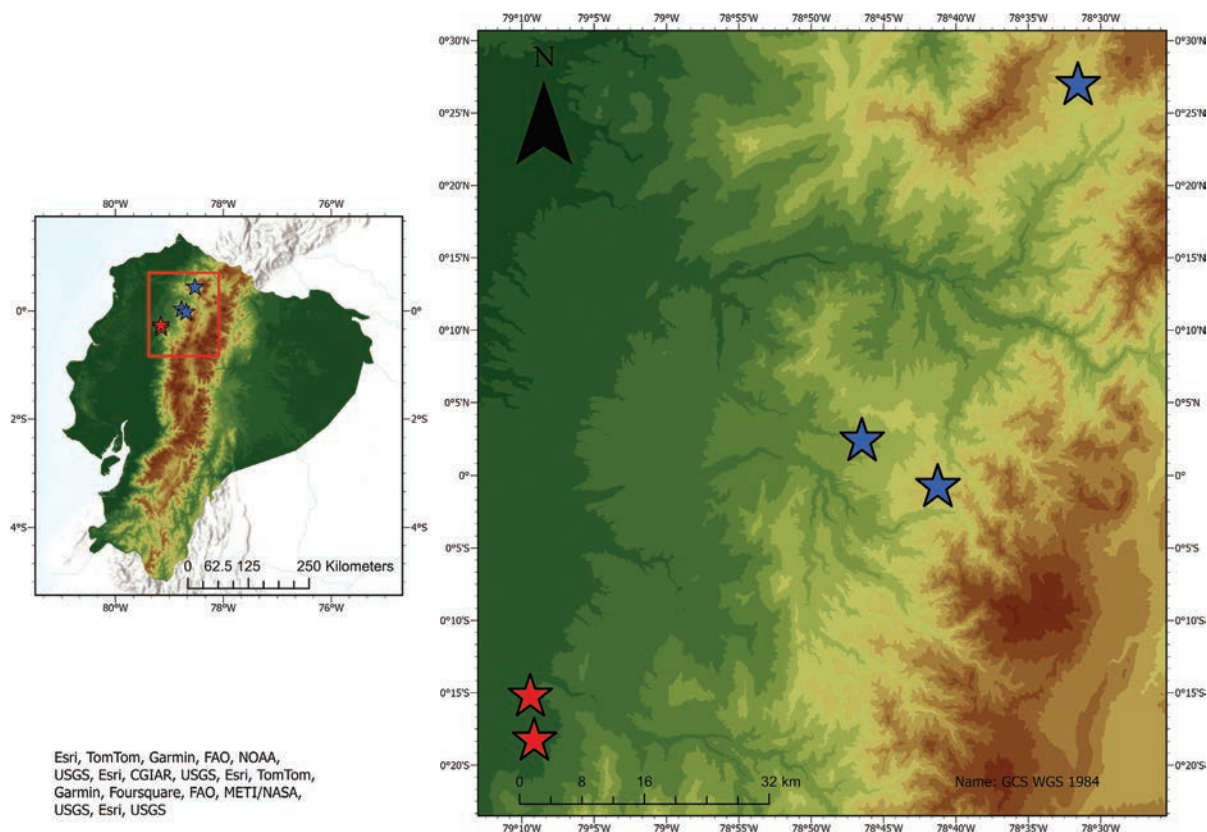


Figure 9. Distribution of the new species in Ecuador. Red stars = records of *Enchenopa gennyae* sp. nov.; blue stars = records of *Enchenopa chocoandina* sp. nov.

belong to the *E. minuta* species group due to the absence of sexual dimorphism in pronotal horn shape; in *E. chocoandina* both females and males lack a horn.

We suggest *E. andina* and *E. chocoandina* sp. nov. could be related species by the scarlet median carina and posterior apex only shared in both species. Both inhabit mountain forests of the north Andes of Ecuador however are geographically separated by the Interandean Valley.

Discussion

This study increases the number of valid *Enchenopa* species worldwide to 58 and 17 species for Ecuador. Furthermore, ten species are currently recognized within the *E. biplaga* species group and seven in the *E. andina* species group. Unfortunately, Strümpel and Strümpel (2014) did not provide specific localities from the species recorded in Ecuador; thus, based on Goding (1928), *Enchenopa gennyae* sp. nov. and *E. chocoandina* sp. nov. could be the only species known from northwestern Ecuador because most species are recorded mainly in the Amazon region and a few in the Interandean Valley and central to southwestern Ecuador. Nevertheless, further studies are needed to understand better the distribution of *Enchenopa* species within Ecuador and, likely, there are still new species to be discovered.

Strümpel and Strümpel (2014) argued that *Enchenopa* is not supported by any synapomorphies but, instead a combination of characters, some of which are shared with other Membracini genera, and therefore suggested the genus is likely a paraphyletic group. Previously, Lin et al. (2004) found in their molecular phylogeny of Membracinae that *Enchenopa* is polyphyletic and even *Campylenchia*

(currently synonymized in *Enchenopa*) belongs to a different clade together with the genera *Kronides* Kirkaldy, 1904 and *Tylopelta* Fowler, 1894. Likewise, species with intermediate characters have been found that cannot be assigned with confidence to any genera until the phylogenetic relationships within the tribe are resolved (Dietrich and McKamey 1995; McKamey 2022).

Because *Enchenopa* is a phenetic and probably non-monophyletic group, we suggest that the, *E. biplaga* and *E. andina* species groups, and likely the rest of the *Enchenopa* species groups could belong to independent lineages as they exhibit many important morphological differences and future phylogenetic studies might split them into different genera. The pronotum of the *E. biplaga* species group species is somewhat foliaceous with a dorsal spot and lateral band, and some species (e.g., *E. lanceolata*, *E. longimaculata*) even have short lateral carinae, resembling *Enchophyllum*. In contrast, in the *E. andina* group, the pronotum is not very compressed and mostly unicolorous with the horn short or reduced to a blunt projection, similar to some species of *Leioscyta*. The second valvulae of females also are strikingly different between both groups; species of the *E. biplaga* species group having the second valvule broad with a ventral-apical tooth, also shared with some species of *Enchophyllum* (Strümpel and Strümpel 2006), while in the *E. andina* species group, it is blade-shaped with dorsal blunt teeth shared with other *Enchenopa* species groups. It is likely the horn-shaped anterior process and the metopidial carination that defines *Enchenopa* could be homoplastic characters since they vary intra and interspecifically within *Enchenopa* and other Membracini (Richter 1954; Strümpel and Strümpel 2014). Until the phylogenetic relationships are resolved, however, the new species described in this study belong to the current definition of *Enchenopa*.

Enchenopa gennyae sp. nov. inhabits the forest remnants of Santo Domingo, a populous city with extensive areas dedicated to monocultures and livestock around the urban area. This city, within its urban area, harbors small patches of secondary forest, mainly around water bodies, which hold a great diversity of native and endemic insect species. Several studies have shown urban green areas, such as urban forest fragments, to be valuable reservoirs of native arthropod biodiversity and these must be integrated with plans for conservation management (Watts and Larivière 2004; Philpott et al. 2014). Membracids are particularly abundant in this kind of ecosystem because they prefer sun-exposed vegetation (Wood 1993). Thus, we reiterate the importance of urban green areas for the conservation of local biodiversity and even unnamed species.

Acknowledgments

We thank the Laboratory of Terrestrial Zoology and the Museum of Zoology, IBIOTROP Institute, Universidad San Francisco de Quito USFQ (Ecuador) for access to the specimens under their care and the equipment; to Diego F. Cisneros-Heredia and Margarita M. López-García for their valuable comments on the draft; to Emilia Peñaherrera for her help in designing the map; a special acknowledgment to David Torres and Amaru Rubio who collected some paratypes of *Enchenopa chocoandina* sp. nov. and shared in-situ photographs; to Genny Rodríguez who helped to collect some specimens of *Enchenopa gennyae* sp. nov., to Ignacio Moreno for the identification of the ant species; to Nelson Miranda for the identification of the host plants; to the administrative and field staff of

Tandayapa Cloud Forest Station USFQ, especially, to Juan Manuel Guayasamín, Sofía Carvajal, Daniela Franco, Cristian Calvachi and Dayana Rivera who support us in the fieldwork at the station; and to Camilo Flórez-V and Stuart McKamey for valuable taxonomical suggestions. The specimens were legally collected under the research permits MAAE-ARSFC-2021-1858, MAATE-ARSFC-2023-3348, MAATE-ARSFC-2023-0163, and MAATE-CMARG-2022-0603-ACT-001 issued by the Ministerio del Ambiente, Agua y Transición Ecológica de Ecuador.

Additional information

Conflict of interest

The authors have declared that no competing interests exist.

Ethical statement

No ethical statement was reported.

Funding

Our work was possible thanks to operative funds assigned to the Laboratory of Terrestrial Zoology, Institute of Tropical Biodiversity of Universidad San Francisco de Quito USFQ; and research funds granted by the Tandayapa Cloud Forest Station.

Author contributions

Conceptualization: MPRR, JLMS. Data curation: MPRR, JLMS. Formal analysis: JLMS, MPRR. Funding acquisition: JLMS, MPRR. Investigation: JLMS, MPRR. Methodology: MPRR, JLMS. Project administration: JLMS. Resources: JLMS, MPRR. Software: MPRR, JLMS. Supervision: MPRR, JLMS. Validation: JLMS, MPRR. Visualization: MPRR, JLMS. Writing - original draft: MPRR, JLMS. Writing - review and editing: MPRR, JLMS.

Author ORCIDs

María P. Rueda-Rodríguez  <https://orcid.org/0009-0002-8190-7239>

Jorge L. Montalvo-Salazar  <https://orcid.org/0009-0003-1221-0304>

Data availability

All of the data that support the findings of this study are available in the main text.

References

- Amyot CJB, Serville A (1843) Histoire naturelle des insectes. Hémiptères. Librairie encyclopédique de Roret, Paris, 676 pp. <https://doi.org/10.5962/bhl.title.8471>
- Barriga P, Toasa G, Montufar R, Tye A (2011) Asteraceae. In: León Yáñez S, Valencia R, Pitman N, Endara L, Ulloa-Ulloa C, Navarrete H (Eds) Libro Rojo de las Plantas Endémicas del Ecuador. Publicaciones del Herbario QCA, Pontificia Universidad Católica del Ecuador, Quito, 139–196.
- Bartlett CR, Deitz LL, Dmitriev DA, Sanborn AF, Soulier-Perkins A, Wallace MS (2018) The Diversity of the True Hoppers (Hemiptera: Auchenorrhyncha). In: Insect Biodiversity. John Wiley & Sons, Ltd, 501–590. <https://doi.org/10.1002/9781118945582.ch19>
- Deitz LL (1975) Classification of the higher categories of the New World treehoppers (Homoptera: Membracidae). North Carolina Agricultural Experiment Station, Technical Bulletin 255: 1–177.

- Deitz LL, Wallace MS (2012) Richness of the Nearctic Treehopper Fauna (Hemiptera: Aetalionidae and Membracidae). *Zootaxa* 3423: 1. <https://doi.org/10.11646/zootaxa.3423.1.1>
- Dietrich CH, McKamey SH (1995) Two new Neotropical treehopper genera and investigation of the phylogeny of the subfamily Membracinae (Homoptera: Membracidae). *Proceedings of the Entomological Society of Washington* 97: 1–16. <https://www.biodiversitylibrary.org/part/54714>
- Dietrich CH, McKamey SH, Deitz LL (2001) Morphology-based phylogeny of the treehopper family Membracidae (Hemiptera: Cicadomorpha: Membracoidea). *Systematic Entomology* 26: 213–239. <https://doi.org/10.1046/j.1365-3113.2001.00140.x>
- Fabricius JC (1775) *Systema Entomologiae sistens insectorum classes, ordines, species, genera, adjectis synonymis, locis, descriptionibus, observationibus*. Officina Libraria Kortii, Flensbvirgi et Lipsiae, 832 pp. <https://doi.org/10.5962/bhl.title.36510>
- Fabricius JC (1787) 2 Mantissa Insectorum. *Impensis C. G. Proft, Hafniae*, 382 pp. <https://doi.org/10.5962/bhl.title.36471>
- Fairmaire LMH (1846) Revue de la tribu des Membracides. *Annales de la Société Entomologique de France* 2: 235–320. <https://www.biodiversitylibrary.org/page/8261565#page/241/mode/1up>
- Flórez-V C, Wolff MI, Cardona-Duque J (2015) Contribution to the taxonomy of the family Membracidae Rafinesque (Hemiptera: Auchenorrhyncha) in Colombia. *Zootaxa* 3910: 1–261. <https://doi.org/10.11646/zootaxa.3910.1.1>
- Fowler WW (1894) Some new species of Membracidae. *Transactions of the Entomological Society of London*: 415–424. <https://doi.org/10.1111/j.1365-2311.1894.tb02087.x>
- Germar EF (1821) Bemerkungen über einige Gattungen der Cicadarien. *Magazin der Entomologie* 4: 1–106. <https://www.biodiversitylibrary.org/item/81944#page/15/mode/1up>
- Goding FW (1928) Membracidae of South America and Antilles, III. Subfamily Membracinae. *Journal of the New York Entomological Society* 36: 201–234. <https://www.jstor.org/stable/25004260>
- Godoy C, Miranda X, Nishida K (2006) Membrácidos de la América tropical. *Treehoppers of tropical America*, 1st ed. Instituto Nacional de Biodiversidad (INBIO), Santo Domingo de Heredia, Costa Rica, 352 pp.
- Hamilton KGA, Cocroft RB (2009) Establishing the identity of existing names in the North American *Enchenopa binotata* species complex of treehoppers (Hemiptera: Membracidae). *Entomological News* 120: 554–565. <https://doi.org/10.3157/021.120.0513>
- Kerr PH, Fisher EM, Buffington ML (2008) Dome lighting for insect imaging under a microscope. *American Entomologist* 54: 198–200. <https://doi.org/10.1093/ae/54.4.198>
- Kirkaldy GW (1904) Bibliographical and nomenclatorial notes on the Hemiptera. No. 3. *The Entomologist* 37: 279–283. <https://doi.org/10.5962/bhl.part.2885>
- Lencioni-Neto F, Sakakibara AM (2015) A new species of *Enchenopa* (Hemiptera: Membracidae) from the Brazilian Atlantic Forest. *Zoologia (Curitiba)* 32: 257–259. <https://doi.org/10.1590/S1984-46702015000300009>
- Lin C-P (2006) Social behavior and life history of membracine treehoppers. *Journal of Natural History* 40: 1887–1907. <https://doi.org/10.1080/00222930601046618>
- Lin C-P, Danforth BN, Wood TK (2004) Molecular phylogenetics and evolution of maternal care in Membracine treehoppers. *Systematic Biology* 53: 400–421. <https://doi.org/10.1080/10635150490445869>
- McKamey SH (2022) Notes on the New World Treehopper genera *Membracis* Fabricius, *Enchenopa* Amyot and Serville, and closely related taxa (Hemiptera: Membracidae):

- Membracinae). Proceedings of the Entomological Society of Washington 124: 85–97. <https://doi.org/10.4289/0013-8797.124.1.85>
- McNett GD, Cocroft RB (2008) Host shifts favor vibrational signal divergence in *Enchenopa binotata* treehoppers. Behavioral Ecology 19: 650–656. <https://doi.org/10.1093/beheco/arn017>
- Philpott SM, Cotton J, Bichier P, Friedrich RL, Moorhead LC, Uno S, Valdez M (2014) Local and landscape drivers of arthropod abundance, richness, and trophic composition in urban habitats. Urban Ecosystems 17: 513–532. <https://doi.org/10.1007/s11252-013-0333-0>
- Richter L (1947) Membracidae Colombianae. Revisión de las especies colombianas del género *Membracis*. Revista de la Academia Colombiana de Ciencias Exactas, Físicas y Naturales 8: 382–403. <https://doi.org/10.18257/raccefyn.588>
- Richter L (1954) Membracidae Colombianae. Caldasia 6: 269–387. <https://revistas.unal.edu.co/index.php/cal/article/view/32938/32975>
- Sakakibara AM (1992) Sobre alguns Membracini (Homoptera, Membracidae): notas taxonômicas edescrições de gênero e espécies novos. Revista Brasileira de Entomologia 36: 93–100.
- Sakakibara AM, Marques OM (2010) Uma nova espécie de membracídeo (Hemiptera, Membracidae) coletada em plantas da família Loranthaceae. Magistra 22: 137–139. <https://doi.org/10.1590/S1984-46702015000300009>
- Say T (1824) Appendix. Part I. Natural History. Zoology. In: Narrative of an expedition to the source of St. Peter's river, Lake Winnepeek, Lake of the Woods, &c. &c., performed in the year 1823, by the order of the Hon. J. C. Calhoun, secretary of war, under the command of Stephen H. Long, Major U. S. T. E. H. C. Carey & I. Lea, Philadelphia, 253–400. <https://www.biodiversitylibrary.org/item/48506#page/277/mode/1up>
- Schmidt E (1924) Neue Zikaden-Gattungen und Arten. Entomologische Mitteilungen Berlin 13: 285–297. <https://sdei.senckenberg.de/media/openaccess/00790.pdf>
- Stål C (1869) Bidrag till Membracidernas Kannedom. Öfversigt af Kongliga Vetenskaps-Akademiens Förhandlingar 26: 231–300. <https://www.biodiversitylibrary.org/item/100848#page/251/mode/1up>
- Strümpel VH, Strümpel R (2006) Revision of the Neotropical treehopper genus *Enchophyllum* (Hemiptera: Membracidae, Membracinae). Entomologische Mitteilungen aus dem Zoologischen Museum Hamburg 14: 335–371. <https://hamburg.leibniz-lib.de/forschung/sektionen/entomologie/zeitschrift/pdfs-publikationen/2006/14-175-335.pdf>
- Strümpel VH, Strümpel R (2014) Revision der amerikanischen Membracidengattung *Enchenopa* (Hemiptera: Auchenorrhyncha: Cicadomorpha: Membracidae) mit Beschreibungen neuer Arten. Entomologische Mitteilungen aus dem Zoologischen Museum Hamburg 17: 1–137.
- Walker F (1858) 4 Insecta Saundersiana: or, Characters of undescribed insects in the collection of William Wilson Saunders. John Van Voorst, London, 117 pp. <https://doi.org/10.5962/bhl.title.5112>
- Watts CH, Larivière M-C (2004) The importance of urban reserves for conserving beetle communities: a case study from New Zealand. Journal of Insect Conservation 8: 47–58. <https://doi.org/10.1023/B:JICO.0000027504.92727.ab>
- Wood TK (1993) Diversity in the New World Membracidae. Annual Review of Entomology 38: 409–433. <https://doi.org/10.1146/annurev.en.38.010193.002205>

Insights into phylogenetic relationships and gene rearrangements: complete mitogenomes of two sympatric species in the genus *Rana* (Anura, Ranidae)

Jingfang Li^{1,2}, Mei Xie^{1,2}, Fangpeng Zhang^{1,2}, Juan Shu³, Jun Zhang³, Zhinuo Zhang³, Hongmei Xiang², Wansheng Jiang^{1,2}

¹ College of Biology and Environmental Sciences, Jishou University, Jishou 416000, China

² National and Local United Engineering Laboratory of Integrative Utilization Technology of *Eucommia ulmoides*, Jishou University, Zhangjiajie 427000, China

³ Zhangjiajie National Forest Park, Zhangjiajie 427400, China

Corresponding authors: Hongmei Xiang (hmxiang@163.com); Wansheng Jiang (jiangwschina@163.com)

Abstract

Mitochondrial genomes (also known as mitogenomes) serve as valuable molecular markers and have found widespread applications in molecular biology and ecology. There is abundant sequence variation in vertebrate mitogenomes, and occasionally, they exhibit gene rearrangements. In this study, two Chinese endemic *Rana* species, *Rana jiemuxiensis* and *Rana hanluica*, were sequenced and analyzed to obtain their complete mitogenomes. The two species were sympatrically distributed in the Zhangjiajie National Forest Park, in Wulingyuan District, Zhangjiajie City, Hunan Province, China. The mitogenome of *R. jiemuxiensis* was 17,506 bp, while that of *R. hanluica* was 17,505 bp, each comprising 13 protein-coding genes (PCGs), 22 transfer RNA genes (tRNAs), two ribosomal RNA genes (rRNAs), and a non-coding control region (D-loop). The gene content, nucleotide composition, and evolutionary rates of each mitogenome were analyzed and compared with those of congeners. A phylogenetic analysis based on 22 mitogenomes in *Rana* revealed that the two sympatric species were in two different lineages, indicating that they were genetically separated to a certain extent. Three types of gene rearrangement patterns were identified when examining the gene orders of the 22 *Rana* mitogenomes. Most of the species shared a second and dominant gene rearrangement pattern that originated from the first ancient pattern. A “tandem duplication – multiple deletion” hypothesis was proposed to explain the evolution of these different gene rearrangement patterns. This study provided valuable data references and enhanced our understanding of the phylogenetic implications and gene rearrangements of *Rana* species.

Key words: China, genome, mitochondrial, phylogeny, Ranine, Zhangjiajie

Introduction

The amphibian genus *Rana* Linnaeus, 1758, commonly referred to as the “wood frog” or “brown frog,” represents an early-established group typified by the European wood frog, *Rana temporaria* Linnaeus, 1758. Over the past two decades, there has been significant taxonomic restructuring within the genus *Rana* and its ranine counterparts. According to the Amphibian Species of the World online



Academic editor: Anthony Herrel

Received: 12 July 2024

Accepted: 10 September 2024

Published: 21 October 2024

ZooBank: <https://zoobank.org/09044CD6-2B7C-4AD0-8B0C-074A798DEE93>

Citation: Li J, Xie M, Zhang F, Shu J, Zhang J, Zhang Z, Xiang H, Jiang W (2024) Insights into phylogenetic relationships and gene rearrangements: complete mitogenomes of two sympatric species in the genus *Rana* (Anura, Ranidae). ZooKeys 1216: 63–82. <https://doi.org/10.3897/zookeys.1216.131847>

Copyright: © Jingfang Li et al.
This is an open access article distributed under terms of the Creative Commons Attribution License (Attribution 4.0 International – CC BY 4.0).

database, the currently reclassified *Rana* encompasses 52 species distributed throughout temperate Eurasia into Indochina (Frost 2024). Notably, China hosts the largest number of *Rana* species, totaling 28, which are extensively dispersed across almost every province of the country, ranging from the north in the Heilongjiang River basin, to the south in Hainan Island, and from the west in the Tibetan plateau, to the east in the East China coastal plain (AmphibiaChina 2024).

Numerous scientific investigations concerning *Rana* have focused on taxonomy and phylogeny, as well as the discovery of new species and insights into their ecological behaviors. The first discovery of a *Rana* species in China took place in the Qinling Mountains during the late 19th century, officially named as *Rana chensinensis* David, 1875 (Boulenger 1920). However, for a long time, the Chinese wood frog *R. chensinensis* was often considered a synonym or subspecies of the European wood frog *R. temporaria* due to their morphological similarities (Liu and Hu 1961). The introduction of new phenotypic techniques and genetic tools, such as microstructure analysis, chromosome karyotyping, cytogenetics, protein analysis, isoenzymes, and DNA sequencing, has helped clarify many problematic species, identify new species, and gradually reveal phylogenetic relationships within wood frog groups (Wu 1981). For instance, Che et al. (2007) identified four well-supported clades of East Asian wood frogs through phylogenetic reconstructions using mitochondrial genes, showing significant geographic separations in the distribution patterns of some clades. Subsequently, Zhou et al. (2017) classified *Rana* species in East Asia into four species groups: *R. japonica* Boulenger, 1879, *R. maoershanensis* Lu, Li & Jiang, 2007, *R. chensinensis* and *R. amurensis* Boulenger, 1886. Their research emphasized that the *R. maoershanensis* and *R. japonica* species groups formed a monophyletic clade known as the Southern Chinese wood frogs, where the *R. japonica* species group could be further divided into *R. japonica*, *R. chaohiaoensis* Liu, 1946, and other species of the *R. longicrus* Stejneger, 1898 species group, each linked to distinct geographical regions.

Rana hanluica Shen, Jiang & Yang, 2007 and *Rana jiemuxiensis* Yan, Jiang, Chen, Fang, Jin, Li, Wang, Murphy, Che & Zhang, 2011 are two species belonging to the *R. longicrus* species group (Fei et al. 2009; Wan et al. 2020), which constitutes the largest species group within the Southern Chinese Wood Frogs. Recent studies focusing on the *R. longicrus* species group have revealed the presence of several new species in China, highlighting the incomplete understanding of this particular group of *Rana* (Pope and Boring 1940; Yan et al. 2011). Although initially discovered in a localized area in Hunan Province, distribution records of *R. jiemuxiensis* and *R. hanluica* exhibit different patterns. *Rana jiemuxiensis* has a relatively restricted distribution, being found only in the surrounding areas of its type locality, the Jiemuxi National Nature Reserve in Yuanling County (Yan et al. 2011). In contrast, the distribution range of *R. hanluica* extends beyond its type locality in Yangmingshan, Shuangpai County (Zhu et al. 2018), encompassing neighboring provinces such as Guizhou, Guangxi, Jiangxi, and even Zhejiang Province (AmphibiaChina 2024). Notably, *R. jiemuxiensis* and *R. hanluica* coexist in the Zhangjiajie National Forest Park, representing the northernmost distribution zones and likely the only coexisting area for both species to date. The reasons for the coexistence of these closely related species are multifaceted, likely stemming from their long-term evolutionary

history. Factors contributing to their coexistence may include reproductive isolation, as well as potential genetic and niche differentiations. One factor facilitating their coexistence could be the non-synchronous breeding seasons. *Rana jiemuxiensis* typically breeds from late January to mid-March, with a peak breeding period in early March (Yan et al. 2011), whereas the breeding season of *R. hanluica* typically occurs in October, around the “hanlu” or “Cold Dew Festival” (Xia et al. 2022), one of the 24 traditional Chinese solar terms, which also inspired its species name “*hanluica*” (Shen et al. 2007).

The genetic differentiations between the two sympatric species, *R. jiemuxiensis* and *R. hanluica*, may play a crucial role in their coexistence, yet this aspect has received limited attention in previous studies. Furthermore, species within the Ranoidae family typically exhibit gene rearrangements in their mitogenomes (Igawa et al. 2008), which could further contribute to genetic differentiation and potentially influence their coexistence. In this study, we employed next-generation sequencing technology to sequence and characterize the complete mitochondrial genome of *R. jiemuxiensis* and *R. hanluica*. We conducted comparative analyses of these mitogenomes with those of closely related species, focusing on mitochondrial structures and features such as nucleotide composition, codon usage, and selection pressures. Additionally, we reconstructed the phylogenetic relationships using all available mitogenomes of the genus *Rana* obtained from NCBI and analyzed gene rearrangements within this group. The primary objective of this study is to provide novel insights into the phylogenetic implications and gene rearrangements of the two sympatric species, as well as other species within the genus *Rana*.

Materials and methods

Sample collection and sequencing

Samples of *R. jiemuxiensis* and *R. hanluica* were collected from Zhangjiajie National Forest Park (29°9'39"N, 110°24'58"E), located in the Wulingyuan District of Zhangjiajie City, Hunan Province, China. Permissions for the field survey were obtained for scientific purposes from the local administrations, and the sample collections and experimental protocols were approved by the Biomedical Ethics Committee of Jishou University (Approval No: JSDX-2024-0083). In accordance with the “3R principle” (Reduction, Replacement, and Refinement) as required by the National Ministry of Science and Technology (No. 398 [2006]), only one sample of each species was utilized. Specimens were euthanized humanely and preserved in 85% ethanol as voucher specimens. These specimens were deposited at the Molecular Ecology Laboratory, Zhangjiajie Campus, Jishou University (*R. jiemuxiensis*, voucher no. JWS20211037; *R. hanluica*, voucher no. JWS20211131). A small volume of liver tissue was used for molecular experiments. Total DNA was extracted using the DNeasy Blood & Tissue Kit (Qiagen, Hilden, Germany). DNA library construction was performed using the VAHTS Universal DNA Library Prep Kit for Illumina V3 (Vazyme, Nanjing, China). High-throughput sequencing was conducted on the DNBSEQ-T7 platform (Complete Genomics and MGI Tech, Shenzhen, China), generating approximately 30 Gb of raw reads with a read length of 150 bp for each sample.

Mitogenome assembly, annotation, and character analyses

The complete mitogenomes of *R. jiemuxiensis* and *R. hanluica* were assembled using NOVOPlasty 4.3 (Dierckxsens et al. 2017), based on the raw reads generated through next-generation sequencing (NGS). The complete mitogenome and the CYTB gene (1140 bp) of *R. chensinensis* (NCBI accession No. KF898356) were used as the “reference” and “seed” sequences for assembling the mitogenomes of both *R. jiemuxiensis* and *R. hanluica*. The positions and orientations of protein-coding genes (PCGs), ribosomal RNA genes (rRNAs), transfer RNA genes (tRNAs), and the control region (D-loop) were annotated using the MITOS Web Server (<http://mitos.bioinf.uni-leipzig.de/overview.py>) (Berni et al. 2013). The site and secondary structure of tRNAs were predicted using the tRNAscan-SE 1.21 online tool (<http://lowelab.ucsc.edu/tRNAscan-SE/>) (Chan and Lowe 2019). Visualization and circularization of the complete mitogenomes were performed using the CGview online server (<https://cgview.ca/>) (Grant and Stothard 2008).

The numbers of observed transitions (s) and transversions (v) for all the PCGs were plotted using DAMBE v7.3.11 (Xia 2018). Saturation was determined based on the values of *I*ss (simple index of substitution saturation) and *I*ss.c (critical *I*ss value). Other analyses, such as nucleotide composition, AT and GC skewing, codon usage frequency of PCGs, and determination of sequence genetic distances under the Kimura two-parameter (K2P) model, were conducted in MEGA 11.0. Relative synonymous codon usage (RSCU), nucleotide diversity (*P*i), and the ratio of nonsynonymous substitution rate (*K*a) to synonymous substitution rate (*K*s) were calculated using DnaSP 6 (Rozas et al. 2017), with all stop codons removed before analysis.

Phylogenetic analysis

The complete mitogenome sequences of the available species of the genus *Rana* were downloaded from NCBI. Twenty-two species in *Rana* were involved in the final dataset, including *R. jiemuxiensis* and *R. hanluica* that we sequenced. This dataset represented the most comprehensive set of mitogenome sequences available to date. An additional species, *Odorrana jingdongensis* Fei, Ye & Li, 2001, was selected as the outgroup. Each of the 13 PCGs was extracted from the dataset of 23 mitogenomes and checked manually. Subsequently, all PCGs were aligned using the inbuilt MUSCLE module in MEGA and then concatenated to create a combined PCGs dataset. The 13 PCGs concatenated dataset was used to reconstruct the phylogenetic tree using Bayesian inference (BI) (Huelsenbeck and Ronquist 2001) and maximum likelihood (ML) (Höhler et al. 2022) methods. The optimal partition scheme and model for BI and ML were identified using PartitionFinder 2 (Lanfear et al. 2017). BI analysis was performed in MrBayes 3.2.6 with a run set to 10 million generations, sampled every 1000 generations. The initial 25% of the tree topologies were discarded as burn-in, and the consensus tree and posterior probabilities were calculated from the remaining trees. ML analysis was conducted using RAxML 8.2.0, and the support values of the tree were assessed by conducting a bootstrap test with 1000 replicates. The phylogenetic tree was visualized, checked, and improved using FigTree 1.4.2 (Rambaut 2009).

Gene rearrangement analysis

Gene rearrangement in *Rana* was analyzed by comparing the gene orders across the entire mitogenomes of the 22 species in *Rana*, most of which were assembled using NGS techniques (Van Dijk et al. 2014; Ye et al. 2014). The two species we assembled in this study were compared in detail with each other and within the broader context of gene rearrangement patterns in the *Rana* mitogenome dataset. Based on the complete mitogenomes downloaded from GenBank, we reidentified the tRNAs of each species using tRNAscan-SE (Chan and Lowe 2019) to further verify the gene orders of tRNAs. TBtools (Chen et al. 2023) was also employed to assist in the gene rearrangement analysis.

Results

Mitogenome assembly and annotation

The complete mitogenomes of *R. jiemuxiensis* and *R. hanluica* were circular DNA molecules with lengths of 17,506 bp and 17,505 bp, respectively (Fig. 1). Both species exhibited a typical mitogenome organization, consisting of 37 genes, including 13 PCGs, 22 tRNA genes, two rRNA genes, and one control region (CR) (Table 1). All genes were encoded by the heavy strand (H-strand), except for eight tRNA genes (tRNA^{His} , tRNA^{Phe} , tRNA^{Pro} , tRNA^{Leu} , tRNA^{Val} , tRNA^{Gln} , tRNA^{Cys} , tRNA^{Tyr}) and one PCG (ND6), which were encoded by the light strand (L-strand). The final complete mitogenomes, along with annotated information for both species, have been deposited in GenBank under accession numbers PP228843 and PP228844.

In *R. jiemuxiensis* and *R. hanluica*, 13 distinct but overlapping sites were found in their mitogenomes. Three of these overlapping sites were observed between contiguous PCGs, ATP8 and ATP6, ATP6 and COX3, and ND4L and ND4, respectively. Ten gene intervals were also identified, with the largest one located between ND5 and ND6 in both species, measuring 624 bp and 305 bp, respectively.

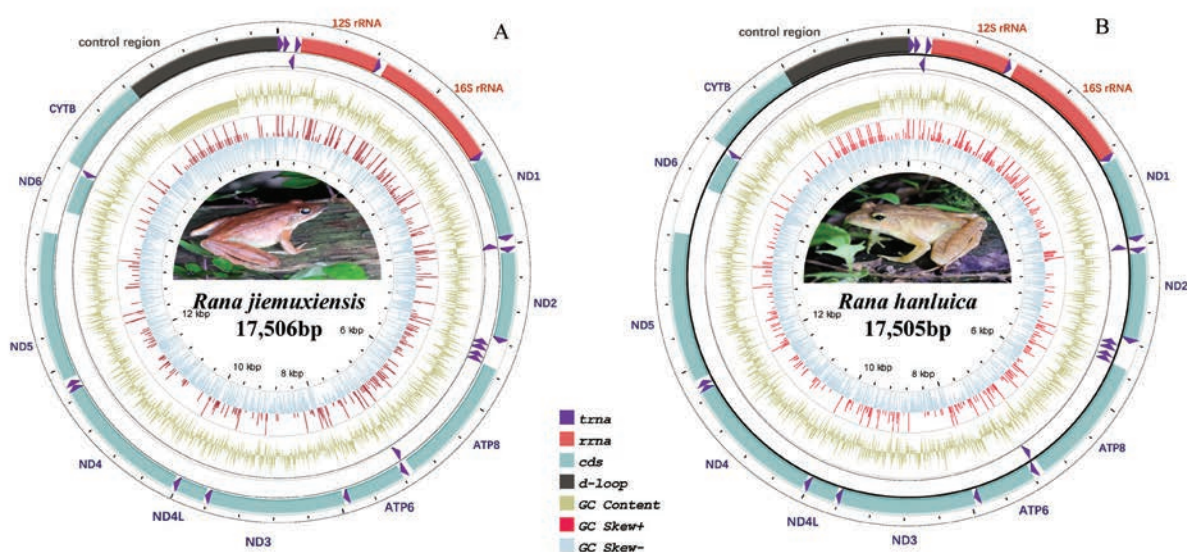


Figure 1. Mitochondrial gene maps of **A** *R. jiemuxiensis* and **B** *R. hanluica*.

Table 1. Characteristics of the mitogenomes of *R. jiemuxiensis* (RJ) and *R. hanluica* (RH).

Gene	Position				Length		Strand*	Codons				Anti codon	Intergenic nucleotide#	
	RJ		RH		RJ	RH		RJ		RH			RJ	RH
	From	To	From	To				Start codons	Stop codons	Start codons	Stop codons			
tRNA ^{Leu} (CUN)	1	74	1	74	74	74	H	-	-	-	-	TAG	0	0
tRNA ^{Thr}	75	144	75	144	70	70	H	-	-	-	-	TGT	0	0
tRNA ^{Pro}	145	213	145	213	69	69	L	-	-	-	-	TGG	1	1
tRNA ^{Phe}	215	286	215	285	72	71	H	-	-	-	-	GAA	0	0
12S rRNA	287	1216	286	1215	930	930	H	-	-	-	-	-	0	0
tRNA ^{Val}	1217	1285	1216	1284	69	69	H	-	-	-	-	TAC	0	0
16S rRNA	1286	2860	1285	2859	1575	1575	H	-	-	-	-	-	0	0
tRNA ^{Leu} (UUR)	2861	2934	2860	2933	74	74	H	-	-	-	-	TAA	47	47
ND1	2982	3935	2981	3934	954	954	H	ATT	AGG	ATT	AGG	-	-41	-41
tRNA ^{Ile}	3895	3965	3894	3964	71	71	H	-	-	-	-	GAT	1	0
tRNA ^{Gln}	3967	4037	3965	4035	71	71	L	-	-	-	-	TAA	-2	-2
tRNA ^{Met}	4036	4106	4034	4104	71	71	H	-	-	-	-	CAT	-1	-1
ND2	4106	5140	4104	5138	1035	1035	H	ATG	TAG	ATG	TAG	-	-2	-2
tRNA ^{Trp}	5139	5208	5137	5206	70	70	H	-	-	-	-	TCA	-1	-1
tRNA ^{Ala}	5208	5278	5206	5276	71	71	L	-	-	-	-	TGC	0	0
tRNA ^{Asn}	5279	5351	5277	5349	73	73	L	-	-	-	-	GTT	2	2
NCR	5354	5378	5352	5377	25	26	H	-	-	-	-	-	-2	-2
tRNA ^{Cys}	5377	5442	5376	5441	66	66	L	-	-	-	-	GCA	0	0
tRNA ^{Tyr}	5443	5509	5442	5508	67	67	L	-	-	-	-	GTA	1	1
COX1	5511	7064	5510	7063	1554	1554	H	GTG	AGG	GTG	AGG	-	-10	-10
tRNA ^{Ser} (UCN)	7055	7126	7054	7125	72	72	L	-	-	-	-	TGA	1	1
tRNA ^{Asp}	7128	7196	7127	7195	69	69	H	-	-	-	-	GTC	135	0
COX2	7332	7884	7196	7883	553	688	H	ATG	T(AA)	ATG	T(AA)	-	0	0
tRNA ^{(Lys)(Asn)}	7885	7953	7884	7952	69	69	H	-	-	-	-	TTT	1	1
ATP8	7955	8117	7954	8115	163	162	H	ATG	TAA	ATG	TAA	-	-8	-7
ATP6	8110	8823	8109	8791	714	683	H	ATG	AGT	ATG	AGT	-	-32	-1
COX3	8792	9576	8791	9575	785	785	H	ATG	TA(A)	ATG	TA(A)	-	-2	-2
tRNA ^{Gly}	9575	9644	9574	9643	70	70	H	-	-	-	-	TCC	-46	-46
ND3	9599	9948	9598	9947	350	350	H	ATG	TA(A)	ATG	TA(A)	-	35	35
tRNA ^{Arg}	9984	10053	9983	10052	70	70	H	-	-	-	-	TCG	0	0
ND4L	10054	10338	10053	10337	285	285	H	ATG	TAA	ATG	TAA	-	-7	-7
ND4	10332	11703	10331	11702	1372	1372	H	ATG	T(AA)	ATG	T(AA)	-	-12	-12
tRNA ^{His}	11692	11759	11691	11758	68	68	H	-	-	-	-	GTG	0	0
tRNA ^{Ser} (AGY)	11760	11826	11759	11825	67	67	H	-	-	-	-	GCT	32	31
ND5	11859	13646	11857	13644	1788	1788	H	ATG	AGG	ATG	AGG	-	624	305
ND6	14271	14765	13950	14444	495	495	L	ATG	AGA	ATG	AGA	-	0	0
tRNA ^{Glu}	14766	14834	14445	14513	69	69	L	-	-	-	-	TTC	3	3
CYTB	14838	15980	14517	15659	1143	1143	H	ATG	TAA	ATG	TAA	-	0	0
D-Loop	15981	17505	15660	17505	1525	1846	H	-	-	-	-	-	0	0

* H and L indicate genes transcribed on the heavy and light strand, respectively. # Positive numbers correspond to the nucleotides separating adjacent genes; negative numbers indicate overlapping nucleotides.

The shortest interval identified was only 1 bp, found in multiple locations within both species. The lengths of the 13 PCGs varied considerably. The longest gene was ND5, which was identical in length in both species at 1788 bp, while the shortest gene was ATP8, with lengths of 162 bp and 163 bp for *R. jiemuxiensis* and *R. hanluica*, respectively. Both species had ATG as the start codon for most PCGs, except for ND1 (ATT) and COX1 (GTG). Five typical stop codons, including TAG, AGG, AGA, AGT, and TAA, as well as two kinds of incomplete terminal codons (TA-, T-), were found in the PCGs within their mitogenomes.

Nucleotide composition and diversity

The overall base composition of *R. jiemuxiensis* was as follows: A (24.33%), T (29.11%), G (15.65%), C (30.49%), while that of *R. hanluica* was A (24.47%), T (29.37%), G (15.65%), C (30.49%). Both species showed an A+T bias with greater A+T than G+C content. Additionally, both species exhibited negative AT skew and GC skew, indicating a predominant bias towards T and C base pairs. The mitogenome sequences of the 22 *Rana* species compiled in this study ranged from approximately 16,000 bp to 22,000 bp in length, indicating a complex mitogenome evolution among *Rana* species. However, all species showed a similar A+T content bias and T and C base pair biases that resembled *R. jiemuxiensis* and *R. hanluica* (Table 2).

When examining the average length and nucleotide composition of each PCG (Table 3), there were generally similarities, but differences remained. The shortest PCG was ATP8, and the longest one was ND5. The ND6 gene exhibited distinct differences in AT skew and GC skew compared to other PCGs. After removing the stop codon from each PCG, the total aligned length of the final 13 PCGs dataset was 11,244 bp. Nucleotide diversity analysis of each PCG showed values ranging from 0.18 (COX3) to 0.27 (ND5). In addition to ND5 (0.27), four other PCGs exhibited relatively high nucleotide diversity, namely ND3 (0.24), ATP6 (0.24), ND2 (0.25), and ATP8 (0.26), while the remaining PCGs showed relatively low nucleotide diversity, all less than 0.2.

Table 2. Basal composition (percentage) of the mitogenomes of *R. jiemuxiensis* and *R. hanluica* and 20 other *Rana* species.

Name	T%	C%	A%	G%	Total length	(A+T)%	GC skew	AT skew	Accession number
<i>R. hanluica</i>	29.37567	30.49626	24.47528	15.65279	17505	53.85094	-0.32164	-0.091	PP228844*
<i>R. jiemuxiensis</i>	29.11775	30.73639	24.33298	15.81288	17506	53.45073	-0.3206	-0.08952	PP228843*
<i>R. dybowskii</i>	30.53428	29.31434	24.57703	15.57435	18864	55.11131	-0.30609	-0.1081	KF898355
<i>R. chensinensis</i>	30.69457	29.10062	24.94212	15.26269	18808	55.63669	-0.31192	-0.10339	KF898356
<i>R. draytonii</i>	29.67805	30.06937	25.37353	14.87905	17805	55.05158	-0.33795	-0.07819	KP013110
<i>R. huanrensis</i>	30.76512	29.04605	25.06458	15.12425	19253	55.8297	-0.31518	-0.10211	KT588071
<i>R. amurensis</i>	30.9651	29.11325	25.5609	14.36075	18470	56.526	-0.33934	-0.09561	KU343216
<i>R. chaochiaoensis</i>	30.19221	29.76508	24.68411	15.3586	18591	54.87631	-0.31927	-0.10037	KU246048
<i>R. kukunoris</i>	30.70901	29.11663	25.06005	15.11431	18863	55.76906	-0.31657	-0.10129	KU246049
<i>R. omeimontis</i>	29.75714	30.03292	24.16155	16.04839	19934	53.91869	-0.30347	-0.10378	KU246050
<i>R. temporaria</i>	30.66239	29.20228	24.90207	15.23326	16061	55.56446	-0.31437	-0.10367	MH536744
<i>R. uenoi</i>	30.60552	29.439	24.87979	15.07569	17370	55.48531	-0.32266	-0.10319	MW009067
<i>R. johnsi</i>	29.40915	30.72611	25.2981	14.56665	17837	54.70724	-0.35678	-0.07515	MZ571365
<i>R. dabieshanensis</i>	29.61744	30.22242	24.1637	15.99644	18291	53.78114	-0.3078	-0.10141	MW526989
<i>R. hanluica</i>	29.37461	30.5133	24.4907	15.62139	19395	53.86531	-0.32279	-0.09067	MZ680529
<i>R. zhenhaiensis</i>	29.16111	30.59336	24.66862	15.57691	18806	53.82973	-0.32524	-0.08346	OL681880
<i>R. wuyiensis</i>	29.43584	30.66382	25.44937	14.45097	17779	54.88521	-0.35937	-0.07263	OL467321
<i>R. catesbeiana</i>	32.8264	26.68979	25.99609	14.48773	17212	58.82248	-0.29633	-0.11612	ON746668
<i>R. arvalis</i>	30.69122	29.13442	24.81986	15.35451	16143	55.51108	-0.30974	-0.10577	MT872666
<i>R. coreana</i>	29.22448	30.46958	24.7243	15.58164	22262	53.94877	-0.32329	-0.08342	ON920705
<i>R. longicrus</i>	31.33066	28.63373	25.73209	14.30352	17833	57.06275	-0.33375	-0.09811	MZ680528
<i>R. kunyuensis</i>	31.27726	28.63373	25.8834	14.20561	22255	57.16066	-0.3368	-0.09436	KF840516
Avg.	30.24552	29.62343	24.96542	15.16564	18493	55.21094	-0.3228	-0.09564	-

*, the sequence obtained in this study.

Table 3. The average proportion of 13 PCGs in 22 *Rana* species.

Gene	T%	C%	A%	G%	(A+T)%	Total length	GC skew	AT skew
ND1	31.8	31.5	23.7	13	55.5	958	-0.41964	-0.14595
ND2	29	32	27.7	11.3	56.7	1029	-0.43921	-0.02293
COX1	29.7	28	24.8	17.4	54.5	1684	-0.26115	-0.08991
COX2	26.3	27.5	29.7	16.5	56	548	-0.22897	0.060714
ATP8	28.9	28.8	32.1	10.1	61	159	-0.48205	0.052459
ATP6	31.5	31.9	25.4	11.2	56.9	682	-0.47541	-0.10721
COX3	30.1	30.4	22.7	16.8	52.8	783	-0.28358	-0.14015
ND3	33.2	31.3	21	14.6	54.2	337	-0.38912	-0.22509
ND4L	30.1	31.8	24.6	13.5	54.7	282	-0.38073	-0.10055
ND4	30.3	31	25.9	12.9	56.2	1363	-0.40278	-0.07829
ND5	30.2	29.8	25.7	14.3	55.9	1779	-0.3573	-0.0805
ND6	34.8	10.7	17.8	36.6	52.6	491	0.02521	-0.32319
CYTB	29.2	32.8	24.1	13.9	53.3	1140	-0.35499	-0.09568

Analysis of codon usage and genetic distance

There are a total of 20 amino acids encoded by the PCGs of *R. jiemuxiensis* and *R. hanluica*. Among these amino acids, Leu, Ser, and Arg had the highest frequency, while Trp and Met had the lowest. According to the RSCU analysis, Leu, Ser, and Arg were encoded by six codons each; Pro, Thr, Val, Ala, and Gly were encoded by four codons each; Phe, Tyr, Cys, His, Gln, Asn, Lys, Asp, and Glu were encoded by two codons each; Trp and Met were encoded by only one codon each. This reflects a significant bias in codon usage in their mitogenomes (Fig. 2).

Genetic distances were analyzed among 22 *Rana* species (Fig. 3). *Rana jiemuxiensis* was found to be closely related to *R. zhenhaiensis* Ye, Fei & Matsui, 1995, *R. longicrus*, *R. hanluica*, *R. dabieshanensis* Wang, Qian, Zhang, Guo, Pan, Wu, Wang & Zhang, 2017, and *R. omeimontis* Ye & Fei, 1993, with genetic distances of 0.08327, 0.08529, 0.08547, 0.08932, and 0.09243, respectively. Conversely, *R. hanluica* was closely related to *R. dabieshanensis*, *R. omeimontis*, *R. jiemuxiensis*, *R. zhenhaiensis*, and *R. longicrus*, with genetic distances of 0.07802, 0.07793, 0.08357, 0.08398, and 0.08609, respectively. *Rana catesbeiana* Dubois, 1992 appeared to be the most genetically distant from all other *Rana* species, suggesting it may be an ancient ancestor species. Sliding window analysis along the concatenated PCGs dataset showed significant variation in nucleotide diversity (π) among different genes (Fig. 4A). Substitution saturation test indicated that $I_{ss} < I_{ss.c}$ in general, and scatter diagrams also suggested that the PCGs substitution was not saturated, making them suitable for phylogenetic analysis (Fig. 4B).

Standard deviations of K_a and K_s for the 13 PCGs across 22 species showed that the data were generally concentrated, with variances of K_s generally greater than those of K_a (Fig. 5A). ATP8 and ND6 exhibited the highest and lowest standard deviations of K_s , respectively, while ND5 and COX1 showed the highest and lowest standard deviations of K_a , respectively. The average K_a/K_s values from pairs of species among the 22 *Rana* species fell into the range of 0 to 1. Among the 13 PCGs analyzed, ND6 and ATP8 genes evolved relatively quickly, exhibiting the highest K_a/K_s values. Conversely, COX1 and CYTB had the lowest K_a/K_s ratios (Fig. 5B). However, all 13 PCGs had K_a/K_s values below 0.45, with no signals of positive selection detected.

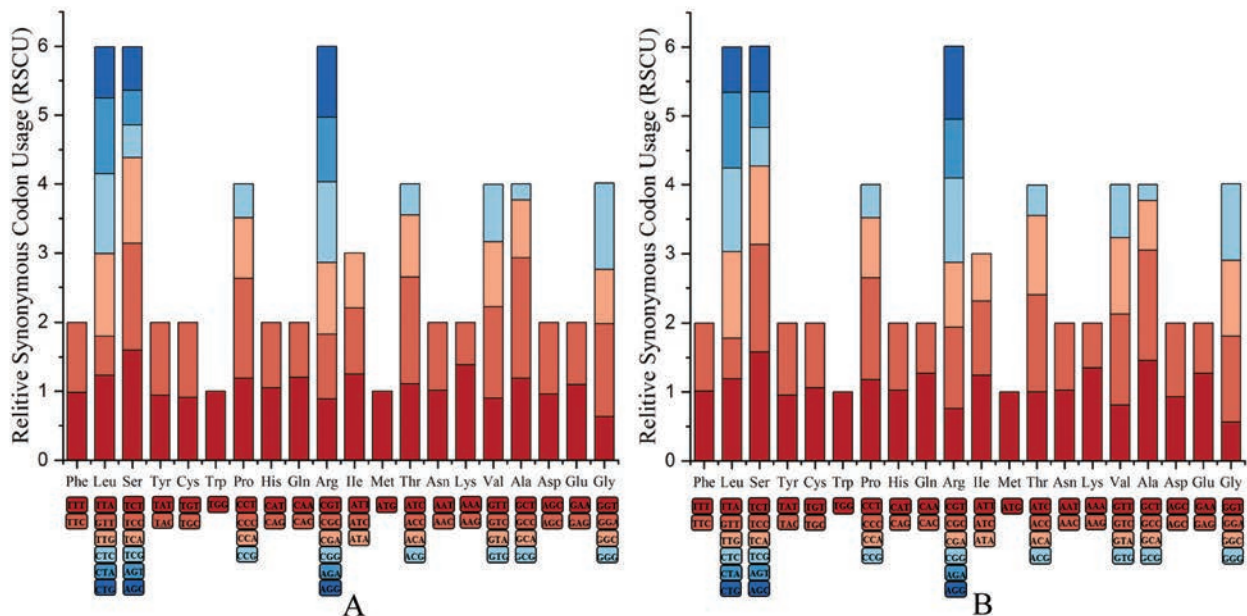


Figure 2. Relative synonymous codon usage in the protein coding genes of **A** *R. jiemuxiensis* and **B** *R. hanluica*.

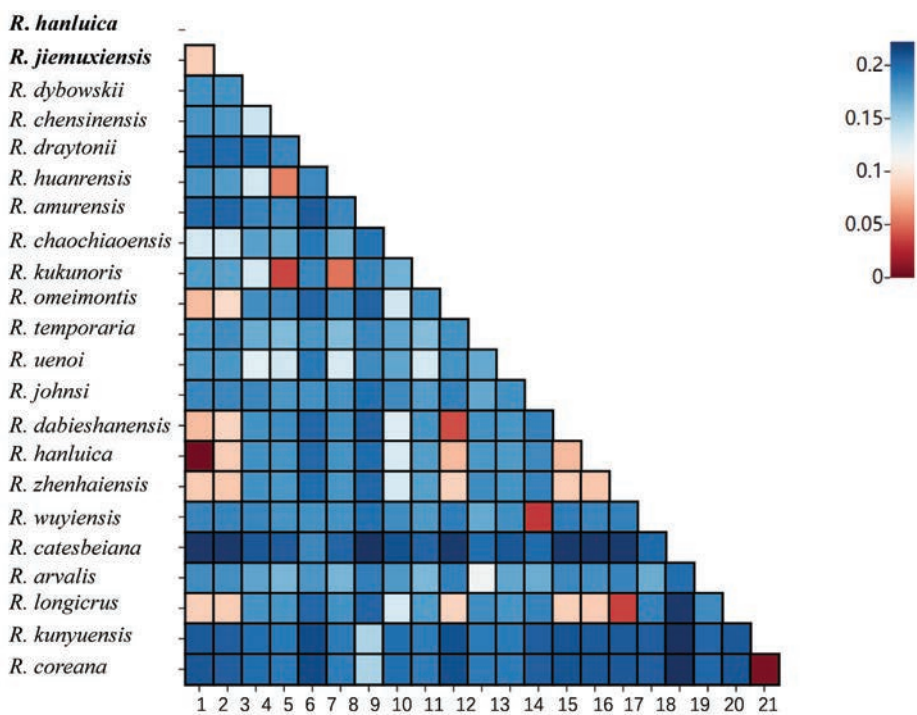


Figure 3. Genetic distance heatmap plot within 22 *Rana* species.

Phylogenetic analysis

The tree topologies resulting from BI and ML analyses were identical, with only slight differences in the support values of some nodes (Fig. 6). Generally, the support values were high in most branches. Despite their sympatric coexistence, *R. jiemuxiensis* and *R. hanluica* did not cluster together in the same subclade. *Rana jiemuxiensis* was grouped with *R. longicrus* and *R. zhenhaiensis* to form one subclade, while *R. hanluica* was grouped with *R. omeimontis* and *R. dabieshanensis* in another subclade. However, the subclades containing *R. jiemuxiensis* and

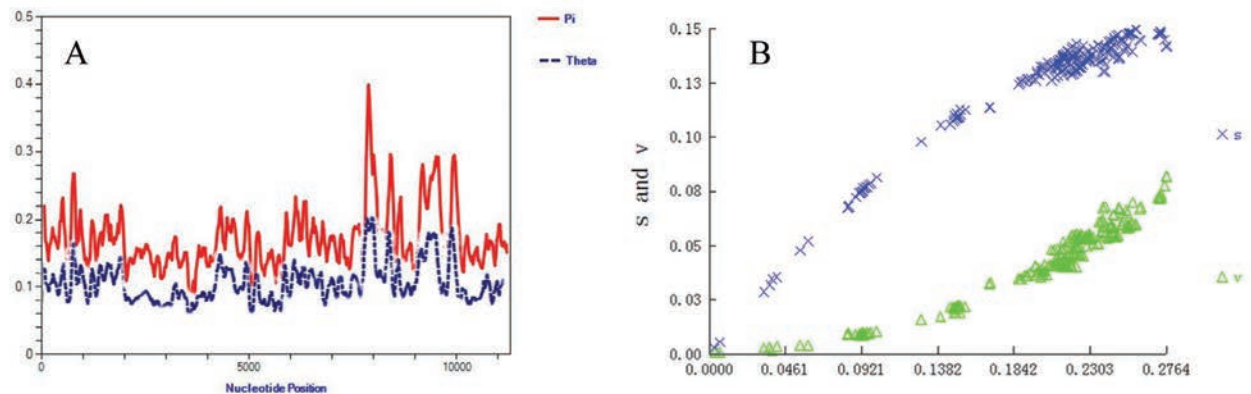


Figure 4. A Nucleotide diversities and B substitution saturation plot of the mitochondrial protein coding genes.

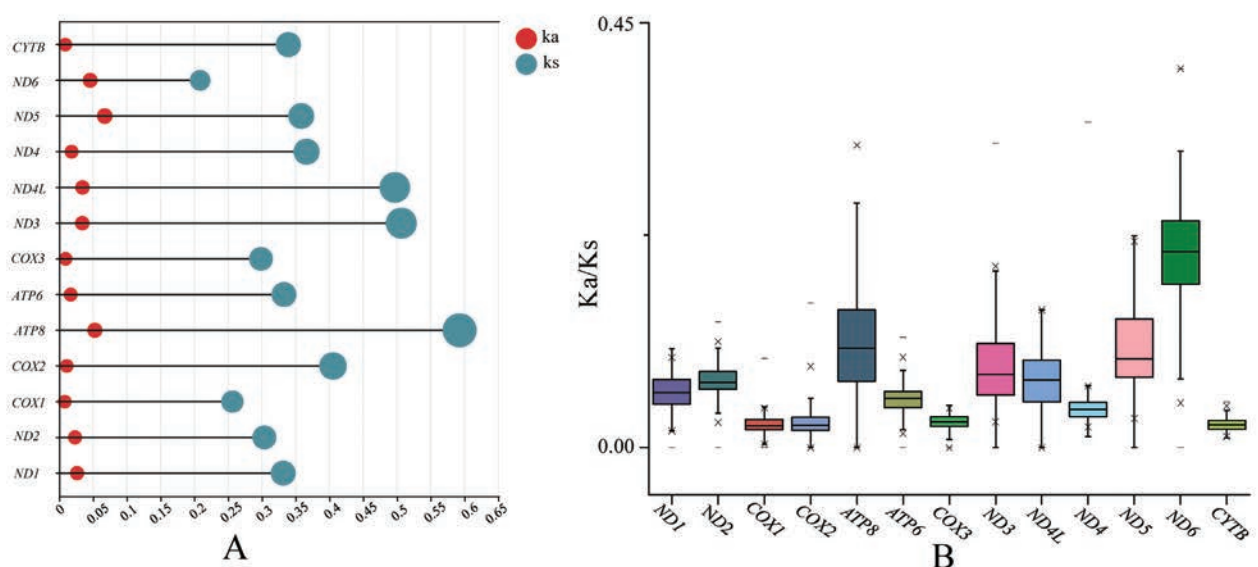


Figure 5. Standard deviation of A Ks and Ka and B the Ka/Ks ratio of 13 protein coding genes.

R. hanluica were then grouped together to form a major clade. The phylogenetic tree also revealed five other major clades, with *R. catesbeiana* and *R. draytonii* Baird & Girard, 1852 representing the two most ancient clades. Evolutionary branch lengths reflected the evolutionary history of each branch, indicating that earlier clades had longer branch lengths. Sequence lengths, distribution of altitude, and degree of threatened levels, however, did not show strong links to the phylogenetic relationships, indicating a complicated and specific evolutionary history for each species.

Gene rearrangement analysis

As expected, the mitogenomes of *Rana* species exhibited substantial gene rearrangements and were categorized into three distinct patterns (Fig. 7A). Only two species, *R. draytonii* and *R. zhenhaiensis*, retained the first pattern, which is assumed to be ancient based on its presence in most amphibian species, including the relatively close outgroup species *Odorrana jingdongensis* used in this study, as well as species from other studies such as *Leptobrachium* and *Boulenophrys* species in Anura (Zhou et al. 2023; Xiang et al. 2024) and *Tylototriton* species

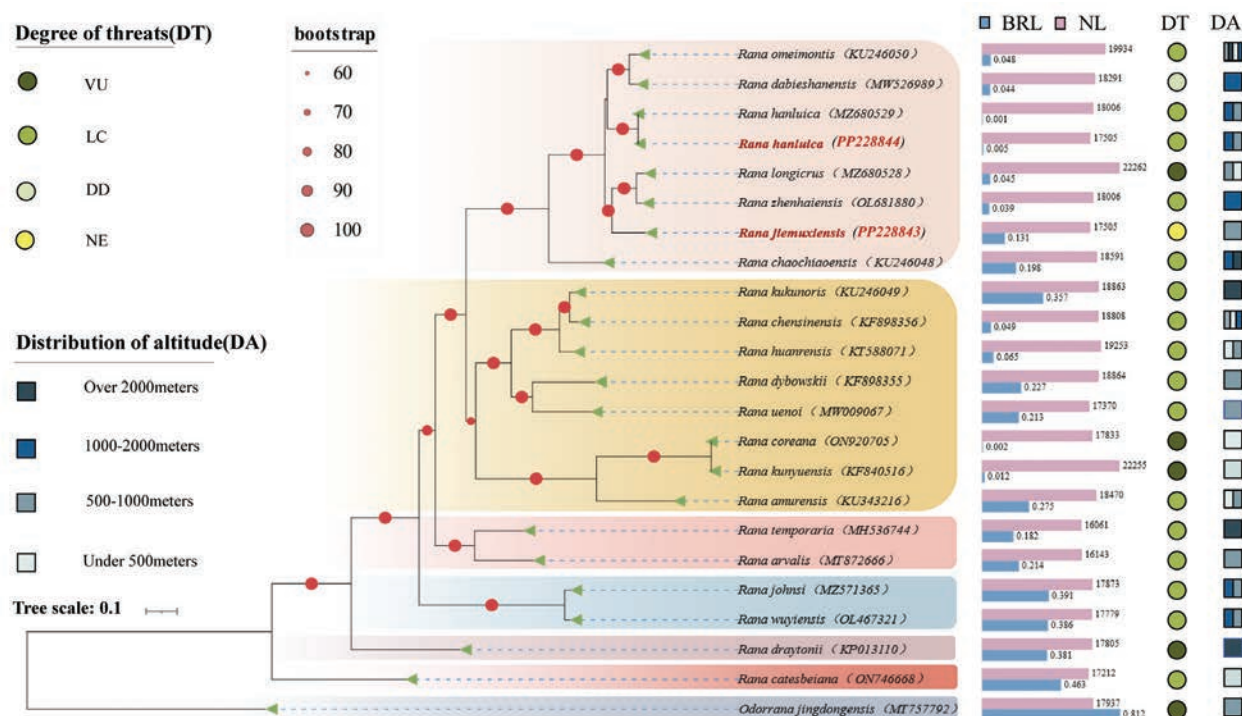


Figure 6. Phylogenetic tree of *Rana* species based on BI and ML analyses. Note: samples sequenced in this study are highlighted in red. BRL represents the length of the evolutionary branch and NL represents the length of the nucleotide sequence.

in Caudata (Wang et al. 2022). Interestingly, 18 out of the 22 examined *Rana* species shared the second and also the most dominant pattern, accounting for 82% of the species analyzed. Both *R. jiemuxiensis* and *R. hanluica*, sequenced in this study, belonged to this dominant pattern. Two other species, *R. amurensis* Boulenger, 1886 and *R. coreana* Okada, 1928, shared the third, rare pattern, which is similar to the second pattern except that the ND5 gene is transposed to a position behind the control region (D-loop). The transition from the first pattern to the second and third patterns primarily resulted from changes in the positions of tRNA genes. The gene orders of rRNAs remained unchanged, except for the rearrangement of ND5 from the second to the third pattern.

We proposed a plausible scenario to explain the mitochondrial gene rearrangements within *Rana*, considering that duplications and losses are more likely to occur among tRNAs than rRNAs and PCGs. According to the principle of parsimony, a “tandem duplication - multiple deletion” event in a sequence region spanning from ND4 to the D-loop likely triggered the transition from the first ancient pattern to the second pattern. Subsequently, a simple transposition of ND5 would have driven the second pattern to evolve into the third pattern (Fig. 7B). In the evolutionary history of *Rana*, for reasons yet unclear, the second pattern became the dominant pattern within this group. This dominance pattern in mitochondrial gene orders in *Rana* is distinct from those in other amphibian species.

Species verification based on individual genes

Species verification is crucial for publishing the complete mitogenome of a species. To verify the molecular identification of the species involved in this study, we selected the individual 16S rRNA, ND2, and CYTB genes as target genes because

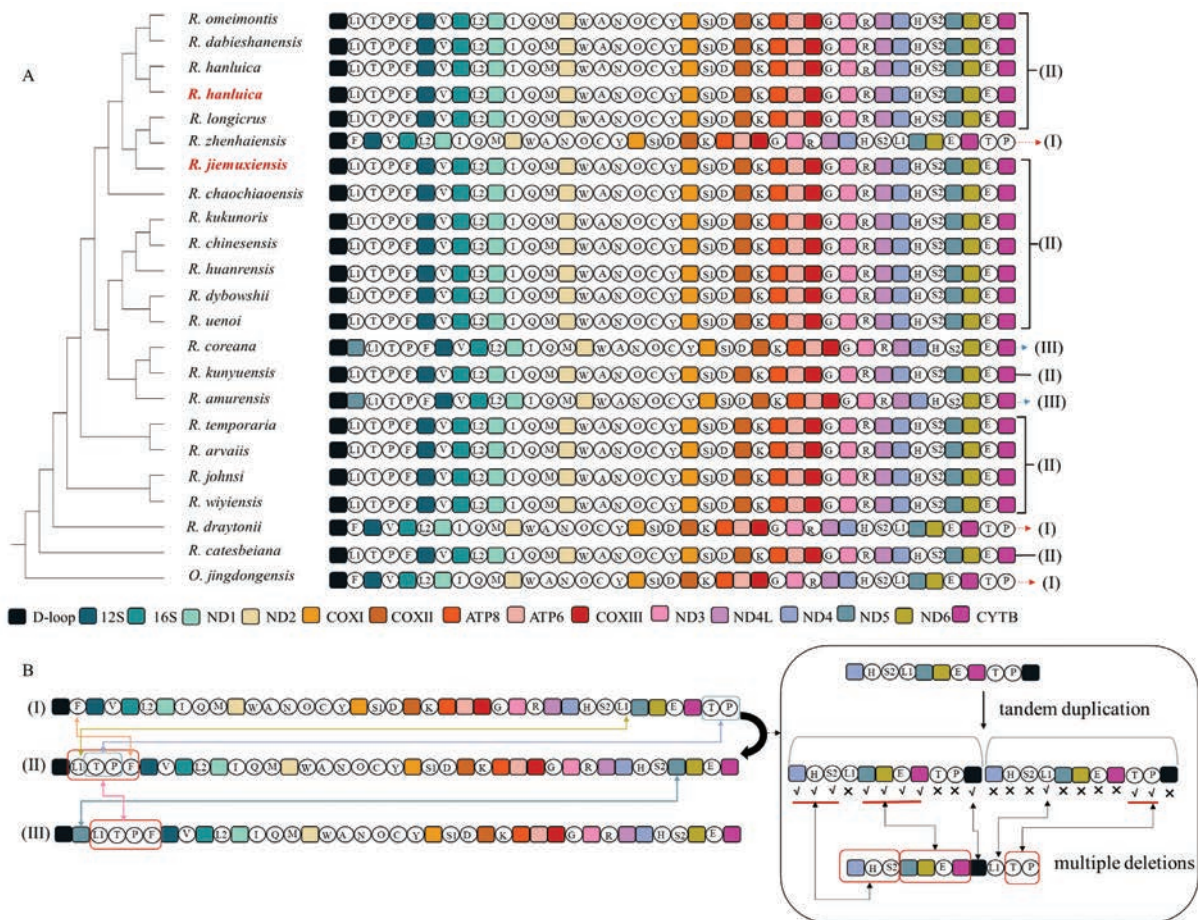


Figure 7. A Phylogenetic gene orders within 22 *Rana* species and **B** three patterns of mitochondrial gene rearrangement. Note: The icons represent tRNAs as: (1) L1: tRNA^{Leu} (CUN), (2) T: tRNA^{Thr}, (3) P: tRNA^{Pro}, (4) F: tRNA^{Phe}, (5) V: tRNA^{Val}, (6) L2: tRNA^{Leu} (UUR), (7) I: tRNA^{Ile}, (8) Q: tRNA^{Gln}, (9) M: tRNA^{Met}, (10) W: tRNA^{Trp}, (11) A: tRNA^{Ala}, (12) N: tRNA^{Asn}, (13) O: NCR, (14) C: tRNA^{Cys}, (15) Y: tRNA^{Tyr}, (16) S1: tRNA^{Ser} (UCN), (17) D: tRNA^{Asp}, (18) K: tRNA^(Lys/Asn), (19) G: tRNA^{Gly}, (20) R: tRNA^{Arg}, (21) H: tRNA^{His}, (22) S2: tRNA^{Ser} (AGY), (23) E: tRNA^{Glu}.

they have abundant resources in NCBI based on previous studies (Djebbi et al. 2018). These genes are also frequently used in DNA barcoding studies (Formenti et al. 2021; Ahmed et al. 2022). Through BLAST homology searching operations, the CYTB, ND2, and 16S rRNA fragments from our samples showed high similarities, 100%, 99.64%, and 99.79%, respectively, with the species named *R. jiemuxiensis* in NCBI, which was collected from its type locality in Yuanling County, Hunan Province. Similarly, the gene fragments of *R. hanluica* samples showed nearly 100% similarity with these genes of *R. hanluica* collected from Lishui City, Zhejiang Province. It is generally accepted that gene similarities between individuals of the same species are usually greater than 98%. Therefore, we conclude that the two species used in this study were correctly identified.

Discussion

Characteristics of the mitogenomes

Mitochondrial DNAs, or mitogenomes, often serve as valuable molecular markers and have been widely applied in molecular biology and ecological studies.

Typically, animal mitogenomes contain 2 rRNAs (12S and 16S rRNA), 22 tRNAs, 13 PCGs, and a control region (also known as the D-loop), with a sequence length usually ranging from 16 to 17 kb (Huang et al. 2016; Tang et al. 2021). Vertebrate mitogenomes are particularly conservative with several unique characteristics, including maternal inheritance, a rapid evolutionary rate, and low levels of recombination. These characteristics make mitochondrial DNA valuable in reconstructing phylogenetic relationships, testing selective pressures, and identifying species using mitochondrial barcoding genes, etc. (Jiang et al. 2023; Lan et al. 2023; Zhang et al. 2023; Xiang et al. 2024).

The utilization of mitochondrial DNA in molecular identification provides a valuable tool in taxonomic studies compared to traditional morphological approaches (Li et al. 2021). In recent years, an increasing number of species identifications have relied on the combination of morphology and molecular evidence. In some cases, such as cryptic species identifications, molecular evidence carries more weight than morphological evidence. Molecular data are commonly used in species identification and phylogenetic studies (Miya and Nishida 2015; Wang et al. 2016; Tan et al. 2018), especially with the rapid advancements in NGS technology. The two sympatric *Rana* species involved in this study, *R. jiemuxiensis* and *R. hanluica*, are morphologically similar, with a distinguishing characteristic primarily based on the number of bands on the thighs and tibia (5 or 6 in *R. jiemuxiensis* vs 8 or 9 in *R. hanluica*). In the field, these two species often seem to completely overlap, as they are sometimes found coexisting in very small areas. However, their genetic distance and phylogenetic position are distinct (Fig. 3 and Fig. 6, respectively), which is also evident in the species verification based on BLAST searches of our sequences against the NCBI database.

The nucleotide composition of both *R. jiemuxiensis* and *R. hanluica* exhibited a distinct A+T rich pattern (Table 3), which is commonly observed in the mitogenomes of other species (Rayko 1997; Franoso et al. 2023). This typical nucleotide composition is highly conserved among vertebrates (Zhou et al. 2006; Hao et al. 2016; Vinogradov and Anatskaya 2017). In *Rana* species, the A+T content generally exceeds 50% but is less than 60%. The gene structure of both sequenced species was identical and similar to other animal species, with the majority of genes, especially the PCGs, located on the H strand, while only a few are on the L strand (Boore 1999). There were 13 gene overlaps in the mitogenomes of *R. jiemuxiensis* and *R. hanluica*, which is also common in other *Rana* species (Zyla et al. 2019), indicating the compact nature of mitogenomes in regulating gene expression. However, gene intervals were also commonly present in frog mitogenomes, with the locations varying more than overlapping regions and showing species-specific patterns. For example, for the two *Rana* species here, the gene interval between tRNA^{Leu} and ND1 was 41 bp, whereas there was no interval between 12S rRNA and tRNA^{Val}. In contrast, in the mitogenomes of two *Leptobrachium* species (Zhou et al. 2023), there was no interval between tRNA^{Leu} and ND1 genes, and the interval between 12S rRNA and tRNA^{Val} was 4 bp. The usage of start and stop codons in different mitogenomes also showed species-specific patterns, which have received limited attention (Wang et al. 2022). In the two *Rana* mitogenomes sequenced here, all genes shared the start codon ATG, except for COX1 (GTG) and ND1 (ATT). In comparison, the start codons of COX1, ATP6, and ATP8 were GTG in the mitogenomes of two *Tylotriton* species. Three

rare types of stop codons (AGT, AGA, and AGG) were also identified in this study, which are less common but have been observed in other *Rana* species.

The ratio of K_a and K_s is a popular proxy for detecting adaptive evolution, with $K_a/K_s > 1$ reported in the mitochondrial PCGs of some species (Ye et al. 2017; Bi et al. 2020). However, none of the K_a/K_s values from the PCGs within *Rana* species exceeded 1 (Fig. 5A), indicating that the overall evolution pattern of *Rana* mitogenomes tends to be conservative in maintaining the functions of regularly generated proteins. The relatively high K_a/K_s ratios observed in some PCGs may represent higher evolutionary rates, such as those of the ATP6, ND3, ND5, and ND6 genes (Fig. 5B). These mitochondrial PCGs that evolve more rapidly may accumulate advantageous mutations, potentially enhancing the fitness of the species in adapting to environmental changes (Yang et al. 2018).

Phylogenetic implications and gene rearrangement evolution

Mitochondrial DNA sequences, particularly mitogenomes, are increasingly utilized in phylogenetic studies (Dhorne-Pollet et al. 2020). In this study, a phylogenetic tree of the genus *Rana* was constructed based on 13 mitochondrial PCGs from 22 species, representing the most comprehensive and detailed mitogenomic phylogenetic tree of *Rana* to date. Although coexisting in Zhangjiajie National Forest Park, *R. jiemuxiensis* and *R. hanluica* were found in distinct phylogenetic lineages (Fig. 6). *Rana jiemuxiensis* clustered with *R. longicrus* and *R. zhenhaiensis* to form a subclade, while *R. hanluica* grouped with *R. omeimontis* and *R. dabiesshanensis* in another subclade. This supports our speculation that the two sympatric species are genetically separated to a certain extent. Despite including more species, our phylogenetic tree was largely consistent with previous studies that also utilized mitogenomes in *Rana* (Chen et al. 2018; Wang et al. 2020; Zhang et al. 2020).

The differentiation of species in *Rana* is possibly associated with geographic isolation and habitat selection. The known distribution altitudes of *Rana* species were mapped onto the phylogenetic tree (Fig. 6). It revealed that *Rana* species have a wide altitudinal adaptation, ranging from over 100 meters to more than 2000 meters above sea level. However, no clear correlations were evident between phylogenetic position and distribution altitude ranges. Previous studies have shown that the skin morphological properties of *Rana* species at high altitudes differ from those at low altitudes (Zhi and Li 2016). It was further inferred that amphibians living at high altitudes, thriving in low temperatures, may have slower evaporative rates (Zyla et al. 2019). Additionally, the degree of threat for each *Rana* species, acquired from the IUCN Red List of Threatened Species of Amphibians, was also mapped onto the phylogenetic tree. Among the 22 *Rana* species in this study, five were classified as vulnerable (VN), 15 as least concern (LC), three as data deficient (DD), and four as not evaluated (NE). Generally, the species in *Rana* are experiencing a medium level of threats.

Previous studies have revealed that interspecies variations in mitochondrial gene orders are prone to occur in certain groups (Shao and Barker 2003; Liu et al. 2017), including species within *Rana* (Zhu et al. 2018). However, few studies have analyzed mitogenomic gene rearrangements in *Rana* from a phylogenetic perspective. By examining the gene orders of 22 *Rana* species in this study, three distinct patterns can be discerned (Fig. 7A). The first pattern represents a very ancient type that is shared with most amphibian species (Wang et al. 2022; Zhou

et al. 2023). The second pattern, however, is dominant in *Rana* species and mainly results from position changes of some tRNAs in their mitogenomes. The third pattern appears to be derived from the second one, with only one PCG (ND5) seemingly transposed. Interestingly, the three patterns of gene arrangements show a trend of parallel evolution, with none of them being confined to a single subclade.

A simple parsimony scenario is proposed to explain the evolutionary process of the three patterns observed in this study (Fig. 7B), which we refer to as the “tandem duplication-multiple deletion” hypothesis. This phenomenon is commonly observed in mitogenomes, where tandem duplications can occur due to strand slippage during replication, followed by gene deletions under selective pressures (Moritz and Brown 1987; Levinson and Gutman 1987). In the case of *Rana* mitochondrial genes, this duplication and loss event can drive the evolution from the first ancient pattern to the second dominant pattern. The genes involved in this process include 6 tRNAs, 4 PCGs, and a control region, with changes mainly resulting from the tRNAs. Previous studies have indicated that tRNAs in mitogenomes are relatively neutral (Downton et al. 2009; Lavrov and Pett 2016), suggesting that gene arrangements resulting from tRNA position changes may not significantly alter the conservative functions of mitochondria. Additionally, tandemly duplicated regions often favor genes that utilize stem-loop structures during replication (Stanton et al. 1994), a characteristic typical of vertebrate tRNAs (Macey et al. 1997). The involvement of one PCG (ND5) from the second to the third pattern echoes that changes in tRNAs and PCG positions are frequently observed in mitochondrial gene rearrangements in both invertebrates and vertebrates (Cantatore et al. 1989; Miya and Nishida 1999).

The study of gene rearrangement patterns can provide insights into taxonomy and elucidate the complex evolutionary history among species (Ye et al. 2021; Feng et al. 2023). However, a comprehensive phylogenetic tree comprising most species is necessary to fully understand the evolutionary background that underlies the gene rearrangements in *Rana*. As more mitogenomes, such as those of the two species in this study, become available in the future, we anticipate that the complete evolutionary history of *Rana* will gradually be unveiled.

Additional information

Conflict of interest

The authors have declared that no competing interests exist.

Ethical statement

The collection and handling of *Rana* species in this study were approved by the Biomedical Ethics Committee of Jishou University (Approval No: JSDX-2024-0083).

Funding

This work was supported by the Graduate Scientific Research Innovation Project of Hunan Province (CX20231083), National Natural Science Foundation of China (32060128), and Zhilan Foundation (2020040371B/2022010011B).

Author contributions

Conceptualization, H.X. and W.J.; methodology, J.L. and W.J.; software, M.X. and F.Z.; validation, W.J. and J.L.; formal analysis, J.L. and W.J.; investigation, M.X., F.Z., J.S., J.Z.

and Z.Z.; resources, J.S., J.Z. and Z.Z.; data curation, J.L.; writing original draft preparation, J.L.; writing review and editing, H.X. and W.J.; visualization, J.L.; supervision, W.J.; project administration, W.J.; funding acquisition, W.J. All authors have read and agreed to the published version of the manuscript.

Author ORCIDs

Hongmei Xiang  <https://orcid.org/0009-0006-3251-3726>

Wansheng Jiang  <https://orcid.org/0000-0002-6498-944X>

Data availability

The final complete mitogenomes, along with annotated information for both species, have been deposited in GenBank under accession numbers PP228843 and PP228844. All the analyses and findings of this study were based on these two sequences and other sequences that were available in GenBank.

References

- Ahmed S, Ibrahim M, Nantasenamat C, Nisar MF, Malik AA, Waheed R, Ahmed MZ, Ojha SC, Alam MK (2022) Pragmatic applications and universality of DNA barcoding for substantial organisms at species level: a review to explore a way forward. *BioMed Research International* 2022(1): 1846485. <https://doi.org/10.1155/2022/1846485>
- AmphibiaChina (2024) The database of Chinese amphibians. Kunming Institute of Zoology (CAS), Kunming, Yunnan, China. <https://www.amphibiachina.org/> [accessed on 6 Jun 2024]
- Bernt M, Donath A, Jühling F, Externbrink F, Florentz C, Fritzsche G, Pütz J, Middendorf M, Stadler PF (2013) MITOS: improved *de novo* metazoan mitogenome annotation. *Molecular Phylogenetics and Evolution* 69(2): 313–319. <https://doi.org/10.1016/j.ympev.2012.08.023>
- Bi C, Lu N, Xu Y, He C, Lu Z (2020) Characterization and analysis of the mitochondrial genome of common bean (*Phaseolus vulgaris*) by comparative genomic approaches. *International Journal of Molecular Sciences* 21(11): 3778. <https://doi.org/10.3390/ijms21113778>
- Boore JL (1999) Animal mitochondrial genomes. *Nucleic Acids Research* 27(8): 1767–1780. <https://doi.org/10.1093/nar/27.8.1767>
- Boulenger GA (1920) A monograph of the South Asian, Papuan, Melanesian and Australian frogs of the genus *Rana*. *Records of the Zoological Survey of India* 20(1): 1–223. <https://doi.org/10.26515/rzsi/v20/i1/1920/163533>
- Cantatore P, Roberti M, Rainaldi G, Gadaleta MN, Saccone C (1989) The complete nucleotide sequence, gene organization, and genetic code of the mitogenome of *Paracrotalus lividus*. *The Journal of Biological Chemistry* 264(19): 10965–10975. [https://doi.org/10.1016/S0021-9258\(18\)60413-2](https://doi.org/10.1016/S0021-9258(18)60413-2)
- Chan PP, Lowe TM (2019) tRNAscan-SE: searching for tRNA genes in genomic sequences. *Methods in Molecular Biology (Clifton, N.J.)* 1962: 1–14. https://doi.org/10.1007/978-1-4939-9173-0_1
- Che J, Pang J, Zhao EM, Matsui M, Zhang YP (2007) Phylogenetic relationships of the Chinese brown frogs (genus *Rana*) inferred from partial mitochondrial 12S and 16S rRNA gene sequences. *Zoological Science* 24(1): 71–80. <https://doi.org/10.2108/zsj.24.71>
- Chen J, Xing Y, Yao W, Zhang C, Zhang Z, Jiang G, Ding Z (2018) Characterization of four new mitogenomes from Ocyropoidea & Grapsoidea, and phylomitogenomic insights into thoracotreme evolution. *Gene* 675: 27–35, 47. <https://doi.org/10.1016/j.gene.2018.06.088>

- Chen C, Wu Y, Li J, Wang X, Zeng Z Xu J, Liu Y, Feng J, Chen H, He Y, Xia R (2023) TBtools-II: a “one for all, all for one” bioinformatics platform for biological big-data mining. *Molecular Plant* 16(11): 1733–1742. <https://doi.org/10.1016/j.molp.2023.09.010>
- Dhorne-Pollet S, Barrey E, Pollet N (2020) A new method for long-read sequencing of animal mitochondrial genomes: application to the identification of equine mitochondrial DNA variants. *BMC Genomics* 21(1): 785. <https://doi.org/10.1186/s12864-020-07183-9>
- Dierckxsens N, Mardulyn P, Smits G (2017) NOVOPlasty: *de novo* assembly of organelle genomes from whole genome data. *Nucleic Acids Research* 45(4): e18. <https://doi.org/10.1093/nar/gkw955>
- Djebbi S, Mezghani-Khemakhem M, Bouktila D, Makni H, Makni M (2018) Assessment of pea weevil *Bruchus pisorum* (Coleoptera, Bruchidae) genetic diversity based on mitochondrial COI gene sequences. *African Entomology* 26: 95–103. <https://doi.org/10.4001/003.026.0095>
- Downton M, Cameron SL, Dowavic JI, Austin AD, Whiting MF (2009) Characterization of 67 mitochondrial tRNA gene rearrangements in the Hymenoptera suggests that mitochondrial tRNA gene position is selectively neutral. *Molecular Biology and Evolution* 26(7): 1607–1617. <https://doi.org/10.1093/molbev/msp072>
- Fei L, Hu S, Ye C, Huang Y (2009) Anura Ranidae. *Fauna Sinica; Science Press: Beijing, China* 3: 1–22.
- Feng H, Lv S, Li R, Shi J, Wang J (2023) Mitochondrial genome comparison reveals the evolution of cnidarians. *Ecology and Evolution* 13(6): e10157. <https://doi.org/10.22541/au.166687211.16942420/v1>
- Formenti G, Rhie A, Balacco J, Haase B, Mountcastle J et al. (2021) Complete vertebrate mitogenomes reveal widespread repeats and gene duplications. *Genome Biology* 22(1): 120. <https://doi.org/10.1186/s13059-021-02336-9>
- Françoso E, Zuntini AR, Ricardo PC, Santos PKF, Souza Araujo N, Silva JPN, Gonçalves LT, Brito R, Gloag R, Taylor BA, Harpur BA, Oldroyd B P, Brown MJF, Arias MC (2023) Rapid evolution, rearrangements and whole mitogenome duplication in the Australian stingless bees *Tetragonula* (Hymenoptera, Apidae): a steppingstone towards understanding mitochondrial function and evolution. *International Journal of Biological Macromolecules* 242(1): 124568. <https://doi.org/10.1016/j.ijbiomac.2023.124568>
- Frost DR (2024) Amphibian Species of the World, an Online Reference. <https://amphibi-ansoftheworld.amnh.org/> [accessed on 6 Jun 2024]
- Grant JR, Stothard P (2008) The CGView Server: a comparative genomics tool for circular genomes. *Nucleic Acids Research* 36: W181–W184. <https://doi.org/10.1093/nar/gkn179>
- Hao S, Ping J, Zhang Y (2016) Complete mitochondrial genome of *Gekko chinensis* (Squamata, Gekkonidae). *Mitochondrial DNA Part A* 27(6): 4226–4227. <https://doi.org/10.3109/19401736.2015.1022751>
- Höhler D, Pfeiffer W, Ioannidis V, Stockinger H, Stamatakis A (2022) RAXML Grove: an empirical phylogenetic tree database. *Bioinformatics* 38(6): 1741–1742. <https://doi.org/10.1093/bioinformatics/btab863>
- Huang D, Su T, Qu L, Wu Y, Gu P, He B, Xu X, Zhu C (2016) The complete mitochondrial genome of the *Colletes gigas* (Hymenoptera, Colletidae, Colletinae). *Mitochondrial DNA Part A* 27(6): 3878–3879. <https://doi.org/10.3109/19401736.2014.987243>
- Huelsenbeck JP, Ronquist F (2001) MRBAYES: Bayesian inference of phylogenetic trees. *Bioinformatics* 17(8): 754–755. <https://doi.org/10.1093/bioinformatics/17.8.754>
- Igawa T, Kurabayashi A, Usuki C, Fujii T, Sumida M (2008) Complete mitochondrial genomes of three neobatrachian anurans: a case study of divergence time estimation

- using different data and calibration settings. *Gene* 407(1–2): 116–129. <https://doi.org/10.1016/j.gene.2007.10.001>
- Jiang W, Li J, Xiang H, Sun C, Chang J, Yang J (2023) Comparative analysis and phylogenetic and evolutionary implications of mitogenomes of Chinese *Sinocyclocheilus* cavefish (Cypriniformes, Cyprinidae). *Zoological Research* 44(4): 779–781. <https://doi.org/10.24272/j.issn.2095-8137.2022.439>
- Lan X, Wang J, Zhang M, Zhou Q, Xiang H, Jiang W (2023) Molecular identification of *Acrossocheilus jishouensis* (Teleostei, Cyprinidae) and its complete mitochondrial genome. *Biochemical Genetics* 62(2): 1396–1412. <https://doi.org/10.1007/s10528-023-10501-x>
- Lanfear R, Frandsen PB, Wright AM, Senfeld T, Calcott B (2017) PartitionFinder 2: new methods for selecting partitioned models of evolution for molecular and morphological phylogenetic analyses. *Molecular Biology and Evolution* 34(3): 772–773. <https://doi.org/10.1093/molbev/msw260>
- Lavrov DV, Pett W (2016) Animal mitochondrial DNA as we do not know it: Mt-genome organization and evolution in nonbilaterian lineages. *Genome Biology and Evolution* 8(9): 2896–2913. <https://doi.org/10.1093/gbe/evw195>
- Levinson G, Gutman GA (1987) Slipped-strand mispairing: a major mechanism for DNA sequence evolution. *Molecular Biology and Evolution* 4(3): 203–221. <https://doi.org/10.1093/oxfordjournals.molbev.a040442>
- Li J, Chen L, Liu B, Zhao Z, Yu L, Yin M, Zhang Y, Gong L (2021) Whole sequence determination and phylogenetic analysis of the mitochondrial genome of the blunt-toothed hairy sea-crab. *Journal of Zhejiang Ocean University* 40(3): 198–208.
- Liu C, Hu S (1961) Chinese Tailless Amphibians. Science Publishing House, Beijing, 364 pp.
- Liu H, Li H, Song F, Gu W, Feng J, Cai W, Shao R (2017) Novel insights into mitochondrial gene rearrangement in thrips (Insecta, Thysanoptera) from the grass thrips, *Anaphothrips obscurus*. *Scientific Reports* 7(1): 4284. <https://doi.org/10.1038/s41598-017-04617-5>
- Macey JR, Larson A, Ananjeva NB, Fang Z, Papenfuss TJ (1997) Two novel gene orders and the role of light-strand replication in rearrangement of the vertebrate mitogenome. *Molecular Biology and Evolution* 14(1): 91–104. <https://doi.org/10.1093/oxfordjournals.molbev.a025706>
- Miya M, Nishida M (1999) Organization of the mitogenome of a deep-sea fish *Gonostoma gracile* (Teleostei, Stomiiformes): first example of transfer RNA gene rearrangements in bony fishes. *Molecular Biology and Evolution* 14(1): 416–426. <https://doi.org/10.1007/pl00011798>
- Miya M, Nishida M (2015) The mitogenomic contributions to molecular phylogenetics and evolution of fishes: a 15-year retrospect. *Ichthyological Research* 62: 29–71. <https://doi.org/10.1007/s10228-014-0440-9>
- Moritz C, Brown WM (1987) Tandem duplications in animal mitochondrial DNAs: variation in incidence and gene content among lizards. *Proceedings of the National Academy of Sciences of the United States of America* 84(20): 7183–7187. <https://doi.org/10.1073/pnas.84.20.7183>
- Pope CH, Boring AM (1940) A survey of Chinese Amphibia. *Peking Natural History Bulletin* 15: 13–86.
- Rambaut AA (2009) FigTree. Tree Figure Drawing Tool, Version 1.4.2. <http://tree.bio.ed.ac.uk/software/figtree/> [accessed on 6 Jun 2024]
- Rayko E (1997) Organization, generation and replication of amphimeric genomes: a review. *Gene* 199(1–2): 1–18. [https://doi.org/10.1016/S0378-1119\(97\)00357-0](https://doi.org/10.1016/S0378-1119(97)00357-0)

- Rozas J, Ferrer-Mata A, Sánchez-DelBarrio JC, Guirao-Rico S, Librado P, Ramos-Onsins SE, Sánchez-Gracia A (2017) DnaSP 6: DNA sequence polymorphism analysis of large data sets. *Molecular Biology and Evolution* 34(12): 3299–3302. <https://doi.org/10.1093/molbev/msx248>
- Shao R, Barker SC (2003) The highly rearranged mitogenome of the plague thrips, *Thrips imaginis* (Insecta, Thysanoptera): convergence of two novel gene boundaries and an extraordinary arrangement of rRNA genes. *Molecular Biology and Evolution* 20(3): 362–370. <https://doi.org/10.1093/molbev/msg045>
- Shen Y, Jiang J, Yang D (2007) A new species of the genus *Rana*, *Rana hanluica* sp. nov. from Hunan Province China (Anura, Ranidae). *Acta Zoologica Sinica* 53(3): 481–488.
- Stanton DJ, Daehler LL, Moritz CC, Brown WM (1994) Sequences with the potential to form stem-and-loop structures are associated with coding-region duplications in animal mitochondrial DNA. *Genetics* 137(1): 233–241. <https://doi.org/10.1093/genetics/137.1.233>
- Tan M, Gan H, Lee YP, Linton S, Grandjean F (2018) Order within the chaos: insights into phylogenetic relationships within the *Anomura* (Crustacea, Decapoda) from mitochondrial sequences and gene order rearrangements. *Molecular Phylogenetics and Evolution* 127: 320–331. <https://doi.org/10.1016/j.ympev.2018.05.015>
- Tang X, Lyu B, Lu H, Tang J, Meng R, Cai B (2021) The mitochondrial genome of a parasitic wasp, *Chouioiacunea* Yang (Hymenoptera, Chalcidoidea, Eulophidae) and phylogenetic analysis. *Mitochondrial DNA Part B* 6(3): 872–874. <https://doi.org/10.1080/23802359.2021.1886008>
- Van Dijk EL, Auger H, Jaszczyszyn Y, Thermes C (2014) Ten years of next-generation sequencing technology. *Trends in Genetics* 30(9): 418–426. <https://doi.org/10.1016/j.tig.2014.07.001>
- Vinogradov AE, Anatskaya OV (2017) DNA helix: the importance of being AT-rich. *Mammalian Genome* 28(9–10): 455–464. <https://doi.org/10.1007/s00335-017-9713-8>
- Wan HL, Yu Z, Qi S, Liu L, Wang Y (2020) A new species of the *Rana japonica* group (Anura, Ranidae, *Rana*) from China, with a taxonomic proposal for the *R. johnsi* group. *ZooKeys* 942: 141–158. <https://doi.org/10.3897/zookeys.942.46928>
- Wang Y, Shen Y, Feng C, Zhao K, Song Z, Zhang Y, Yang L, He S (2016) Mitogenomic perspectives on the origin of Tibetan loaches and their adaptation to high altitude. *Scientific Reports* 6: 690. <https://doi.org/10.1038/srep29690>
- Wang Z, Shi X, Guo H, Tang D, Bai Y, Wang Z (2020) Characterization of the complete mitochondrial genome of *Uca lacteus* and comparison with other Brachyuran crabs. *Genomics* 112(1): 10–19. <https://doi.org/10.1016/j.ygeno.2019.06.004>
- Wang J, Lan X, Luo Q, Gu Z, Zhou Q, Zhang M, Zhang Y, Jiang W (2022) Characterization, comparison of two new mitogenomes of crocodile newts *Tylotriton* (Caudata, Salamandridae), and phylogenetic implications. *Genes* 13(10): 1878. <https://doi.org/10.3390/genes13101878>
- Wu Z (1981) Karyotype of Chinese wood frogs from Beijing. *Journal of Genetics* 8: 138–144.
- Xia X (2018) DAMBE7: New and improved tools for data analysis in molecular biology and evolution. *Molecular Biology and Evolution* 35(6): 1550–1552. <https://doi.org/10.1093/molbev/msy073>
- Xia X, Li Y, Yang D, Pi Y (2022) Habitat characteristics during the breeding season of the cold-dew wood frog (*Rana pipiens*) and the main factors affecting its habitat selection. *Journal of Ecology* 41(9): 1740–1745.
- Xiang H, Zhou Q, Li W, Shu J, Gu Z, Jiang W (2024) Insights into phylogenetic positions and distribution patterns: Complete mitogenomes of two sympatric Asian horned

- toads in *Boulenophrys* (Anura: Megophryidae). *Ecology and Evolution* 14(7): e11687. <https://doi.org/10.1002/ece3.11687>
- Yan F, Jiang K, Chen H, Fang P, Jin J, Yi Li, Wang S, Murphy RW, Che J, Zhang Y (2011) Matrilineal history of the *Rana longicrus* species group (*Rana*, Ranidae, Anura) and the description of a new species from Hunan, southern China. *Asian Herpetological Research* 2(2): 61–71. <https://doi.org/10.3724/SP.J.1245.2011.00061>
- Yang H, Li T, Dang K, Bu W (2018) Compositional and mutational rate heterogeneity in mitochondrial genomes and its effect on the phylogenetic inferences of Cimicomorpha (Hemiptera, Heteroptera). *BMC Genomics* 19(1): 264. <https://doi.org/10.1186/s12864-018-4650-9>
- Ye F, Samuels DC, Clark T, Guo Y (2014) High-throughput sequencing in mitochondrial DNA research. *Mitochondrion* 17: 157–163. <https://doi.org/10.1016/j.mito.2014.05.004>
- Ye N, Wang X, Li J, Bi C, Xu Y, Wu D, Ye Q (2017) Assembly and comparative analysis of complete mitochondrial genome sequence of an economic plant *Salix suchowensis*. *PeerJ* 5: e3148. <https://doi.org/10.1186/s12864-021-07490-9>
- Ye F, Li H, Xie Q (2021) Mitogenomes from two specialized subfamilies of Reduviidae (Insecta, Hemiptera) reveal novel gene rearrangements of true bugs. *Genes* 12(8): 1134. <https://doi.org/10.3390/genes12081134>
- Zhang Y, Gong L, Lu X, Jiang L, Liu B, Liu L, Lü Z, Li P, Zhang X (2020) Gene rearrangements in the mitochondrial genome of *Chiromantes eulimene* (Brachyura, Sesamidae) and phylogenetic implications for Brachyura. *International Journal of Biological Macromolecules* 162: 704–714. <https://doi.org/10.1016/j.ijbiomac.2020.06.196>
- Zhang M, Zhou Q, Xiang H, Wang J, Lan X, Luo Q, Jiang W (2023) Complete mitochondrial genome of *Rectoris luxiensis* (Teleostei, Cyprinidae): characterization and phylogenetic implications. *Biodiversity Data Journal* 11: e96066. <https://doi.org/10.3897/BDJ.11.e96066>
- Zhi M, Li W (2016) Comparison of skin histostructures in three species of genus *Rana*. *Chinese Journal of Zoology* 51(5): 844–852.
- Zhou K, Li H, Han D, Bauer AM, Feng J (2006) The complete mitochondrial genome of *Gekko gecko* (Reptilia: Gekkonidae) and support for the monophyly of Sauria including *Amphisbaenia*. *Molecular Phylogenetics and Evolution* 40(3): 887–892. <https://doi.org/10.1016/j.ympev.2006.04.003>
- Zhou Y, Wang S, Zhu H, Li P, Yang B, Ma J (2017) Phylogeny and biogeography of South Chinese brown frogs (Ranidae, Anura). *PLOS ONE* 12(4): e175113. <https://doi.org/10.1371/journal.pone.0175113>
- Zhou Q, Xiang H, Zhang M, Liu Y, Gu Z, Lan X, Wang J, Jiang W (2023) Two complete mitochondrial genomes of *Leptobrachium* (Anura, Megophryidae, Leptobrachiinae): characteristics, population divergences, and phylogenetic implications. *Genes* 14(3): 768. <https://doi.org/10.3390/genes14030768>
- Zhu S, Zhang X, Zhang S, Zhang R, Liu S, Xiong R (2018) Molecular identification of a *Rana hanluica* population distributed in Youyang County, Chongqing City in China. *Open Journal of Nature Science* 6(1): 1–8. <https://doi.org/10.12677/ojns.2018.61001>
- Zyla J, Marczyk M, Domaszewska T, Kaufmann SHE, Polanska J, Weiner J (2019) Gene set enrichment for reproducible science: comparison of CERNO and eight other algorithms. *Bioinformatics* 35(24): 5146–5154. <https://doi.org/10.1093/bioinformatics/btz447>

Afrotropical *Centistidea* Rohwer, 1914 (Hymenoptera, Braconidae) with description of four new species

Zhen Liu^{1,2,3} , Andrew Polaszek² 

¹ Changde Key Innovation Team for Wetland Biology and Environmental Ecology, College of Life and Environmental Sciences, Hunan University of Arts and Science, Changde 415000, China

² Natural History Museum, London, UK

³ State Key Laboratory of Development Biology of Freshwater Fish Sub-Center for health aquaculture, Hunan University of Arts and Science, Changde 415000, China

Corresponding authors: Zhen Liu (zhen.liu@nhm.ac.uk); Andrew Polaszek (a.polaszek@nhm.ac.uk)

Abstract

The braconid parasitoid wasp genus *Centistidea* Rohwer, 1914 is revised for the Afrotropical region, with four new species described; *Centistidea areolaris* Liu & Polaszek, **sp. nov.**, *C. linearis* Liu & Polaszek, **sp. nov.**, *C. longipedes* Liu & Polaszek, **sp. nov.**, and *C. turneri* Liu & Polaszek, **sp. nov.** are described based on specimens from the Natural History Museum, United Kingdom, and the Royal Museum for Central Africa, Belgium. An illustrated key to species in the Afrotropical region is provided.

Key words: Africa, leaf-miner, Miracinae, *Mirax*, new taxa



Academic editor: Kees van Achterberg

Received: 26 July 2024

Accepted: 11 September 2024

Published: 22 October 2024

ZooBank: <https://zoobank.org/04C335D9-5252-499F-A004-7C9C2220C88C>

Citation: Liu Z, Polaszek A (2024) Afrotropical *Centistidea* Rohwer, 1914 (Hymenoptera, Braconidae) with description of four new species. ZooKeys 1216: 83–100. <https://doi.org/10.3897/zookeys.1216.133127>

Copyright: © Zhen Liu & Andrew Polaszek. This is an open access article distributed under terms of the Creative Commons Attribution License (Attribution 4.0 International – CC BY 4.0).

Introduction

Miracinae (Hymenoptera, Braconidae) are quite rare in all collections worldwide, with only 70 species known from all geographical regions (Yu et al. 2016; Ghramh et al. 2019; Ranjith et al. 2019, 2023; Slater-Baker et al. 2022). Three miracine genera have been described: *Mirax* Haliday, 1833, *Centistidea* Rohwer, 1914, and *Rugosimirax* Ranjith & van Achterberg, 2023 (Yu et al. 2016; Ranjith et al. 2023; Liu and Polaszek 2024). The miracine fauna of the Afrotropical region is only by the report of four species in the genus *Centistidea*, viz., *C. africana* (Brues, 1926), *C. leucopterae* (Wilkinson, 1936), *C. mubilibana* (de Saeger, 1944), and *C. tihamica* Ahmad & Pandey, 2019. The first three species listed above were originally placed in *Mirax*, but this generic placement was questioned recently (Liu and Polaszek 2024).

Here we describe four new species of *Centistidea* from Cameroon, South Africa, and Uganda, together with a preliminary revision of this group in the Afrotropical region as part of our ongoing project on worldwide Miracinae.

Materials and methods

Specimens studied are deposited in the Natural History Museum, UK (**NHMUK**) and the Royal Museum for Central Africa, Belgium (**RMCA**). Descriptions and measurements were made using a stereomicroscope (Zeiss® Stemi SV6). Pho-

tographs were taken and processed using a digital camera (Zeiss AxioZoom combined with Helicon software or Hirox HRX-01). The images were further processed using Adobe Photoshop® CS6. Morphological terms for body structures and measurements mainly follow Ranjith et al. (2023) and Slater-Baker et al. (2022). The wing vein terminology follows the modified Comstock-Needham system (van Achterberg 1993). The terminology of the cuticular sculpture follows Harris (1979). Abbreviations used in this research are as follows: POL = postocellar line, OOL = ocular-ocellar line, OD = ocellar diameter; T1 = 1st tergite of metasoma, T2 = 2nd tergite of metasoma, T3 = 3rd tergite of metasoma.

Taxonomy

Key to species of *Centistidea* from the Afrotropical region

- 1 Propodeum with lateral carinae alongside median longitudinal carina, and with reticulate sculpture between lateral carinae (Fig. 1k).....**2**
 - Propodeum without lateral carinae alongside median longitudinal carina, at most with indistinct punctures anterolaterally (e.g. Figs 2h, 3i, 4j, 6h)**3**
- 2 Scutellar sulcus greatly reduced and not impressed; temple obliquely narrowed behind eyes; vein 1-CU1 as long as 2-CU1... ***C. africana* (Brues, 1926)**
 - Scutellar sulcus obviously depressed (Fig. 1e); temple roundly narrowed behind eyes (Fig. 1b); vein 1-CU1 0.6 × length of 2-CU1 (Fig. 1g)
..... ***C. areolaris* Liu & Polaszek, sp. nov.**
- 3 Scutellar sulcus not depressed (Fig. 2e); temple strongly constricted behind eyes (Fig. 2b); eyes nearly 4.0 × longer than temple in dorsal view (Fig. 2b) ***C. leucopterae* (Wilkinson, 1936)**
 - Scutellar sulcus obviously depressed, even when with crenulation (e.g. Fig. 3e); temple less constricted behind eyes (e.g. Fig. 3b); eyes 1.5–2.0 × longer than temple in dorsal view (e.g. Fig. 3b) **4**
- 4 Propodeum rugulose with median carina bifurcated at apical third (Fig. 5d); vein r of fore wing hardly visible (Fig. 5e) ***C. mubilibana* (de Saeger, 1944)**
 - Propodeum smooth with median carina bifurcated medially (e.g. Fig. 6h) or nearly to apex with some transverse rugae beside the median carina (e.g. Figs 3i, 4j); vein r of fore wing developed (e.g. Figs 3g, 4g, 6g) **5**
- 5 Medio-posterior depressions of scutellum distinctly separated (Fig. 3e). **6**
 - Medio-posterior depressions of scutellum touching each other (Figs 4e, 6e) **7**
- 6 Vein 1-SR of fore wing absent; vein r of fore wing very prominent; median longitudinal carina bifurcated at middle of propodeum
..... ***C. tihamica* Ahmad & Pandey, 2019**
 - Vein 1-SR of fore wing present (Fig. 3g); vein r of fore wing less prominent (Fig. 3g); median longitudinal carina bifurcated at nearly apical extremity of propodeum (Fig. 3i) ***C. linearis* Liu & Polaszek, sp. nov.**
- 7 Propodeum with regular short transverse rugae along median carina (Fig. 4j); T3 polished (Fig. 4k); vein 1-R1 of fore wing present (Fig. 4g)
..... ***C. longipedes* Liu & Polaszek, sp. nov.**
 - Propodeum without regular short rugae along median carina (Fig. 6h); T3 longitudinally striate (Fig. 6k); vein 1-R1 of fore wing absent (Fig. 6g)
..... ***C. turneri* Liu & Polaszek, sp. nov.**

***Centistidea africana* (Brues, 1926)**

Mirax africana Brues, 1926: 292. Holotype in Durban Museum and Art Gallery, Durban, South Africa (not examined).

Mirax africana: De Saeger 1944: 37; Shenefelt 1973: 676.

Diagnosis. Body length 1.7 mm, yellow-brown; occiput deeply emarginate; head matte, without median groove on vertex; ocelli in small equilateral triangle, about the distance to each eye; antenna shorter than body, first three flagellomeres of equal length, the fourth and following becoming shorter and more slender; notauli very distinct anteriorly, less so behind; mesoscutum and central part of scutellum minutely granular, matte; scutellar sulcus greatly reduced and not impressed; scutellum depressed at sides, with a large subtriangular, smooth, margined impression on each side, and a pair of small round foveae at apex, the two enclosed together in an oval margined line; propodeum with distinct median and a lateral longitudinal carina, more or less irregularly reticulate between the carinae, more coarsely posteriorly; T1 narrow; pterostigma less than half as wide as long, with vein r emitted from its middle, 1-CU1 as long as 2-CU1 (following Brues 1926).

Distribution. South Africa.

Host. Unknown.

Note. No specimens were available for this study.

***Centistidea areolaris* Liu & Polaszek, sp. nov.**

<https://zoobank.org/712D4603-E764-40FD-86C9-821AD4505472>

Fig. 1

Diagnosis. Body length 2.0 mm, light red-brown; eyes $1.8 \times$ longer than temple in dorsal view; temple smooth, superficially punctate, indistinctly constricted behind eyes in dorsal view; hind ocelli in a shallow depression, distance between fore and a hind ocellus $1.2 \times$ longer than minor axis of a hind ocellus, POL:OD:OOL = 1.3:1.0:2.9; vertex between eye and hind ocellus nearly smooth except some extremely fine transverse wrinkles; face nearly polished except some punctures along eyes, not convex medially, $1.5 \times$ wider than high; antenna nearly as long as body length, with 1st, 2nd, penultimate and ultimate flagellomeres 4.9, 5.5, 2.7 and $3.0 \times$ longer than wide, 1st indistinctly longer than 2nd; mesoscutum with superficial and weakly-defined punctures anteriorly and laterally, largely smooth dorsally, notauli less obvious, weakly crenulated near to anterior 1/3; scutellar sulcus concave but not crenulated; medio-posterior depressions of scutellum large and oblong, both enclosed by a margined line; propodeum with distinct median carina and carinate-areolate elements medio-apically; pterostigma narrow, $2.9 \times$ as long as its widest part; vein 1-R1 attenuated to 0.3 of length of pterostigma; T1 $3.9 \times$ longer than its maximum width, radially striate at lateral membranous area; T2 triangular part $1.3 \times$ wider than median length; T3 $1.9 \times$ longer than T2.

Description. Female. Body length 2.0 mm, fore wing length 2.5 mm (Fig. 1a).

Head. $1.8 \times$ as wide as long, $1.2 \times$ wider than mesoscutum. Eyes $1.8 \times$ longer than temple in dorsal view (Fig. 1b). Temple a little shiny, smooth, superficially punctate, sparsely pubescent, indistinctly constricted behind eyes in dorsal view. Ocelli small, hind ocelli in a shallow dimple, distance between fore and a hind

ocellus $1.2 \times$ longer than minor axis of a hind ocellus, POL:OD:OOL = 1.3:1.0:2.9. Frons flat and polished. Vertex between eye and hind ocellus shiny and nearly smooth except some extremely fine transverse wrinkles. Face (Fig. 1c) shiny, nearly polished except some punctures along eyes, not convex medially, transverse, $1.5 \times$ wider than high. Clypeus $2.0 \times$ wider than medial length, nearly polished. Length of malar space $1.4 \times$ longer than width of mandible. Antenna (Fig. 1d) nearly as long as body length, with scape, pedicel and 1st, 2nd, penultimate and ultimate flagellomeres 1.4 , 1.6 , 4.9 , 5.5 , 2.7 and $3.0 \times$ longer than wide, 1st indistinctly longer (nearly $1.1 \times$) than 2nd, flagellomeres gradually shortened to apex.

Mesosoma. Length:width:height = $1.4:1.0:1.2$. Mesoscutum (Fig. 1c) shiny with superficial and weakly defined punctures anteriorly and laterally, largely

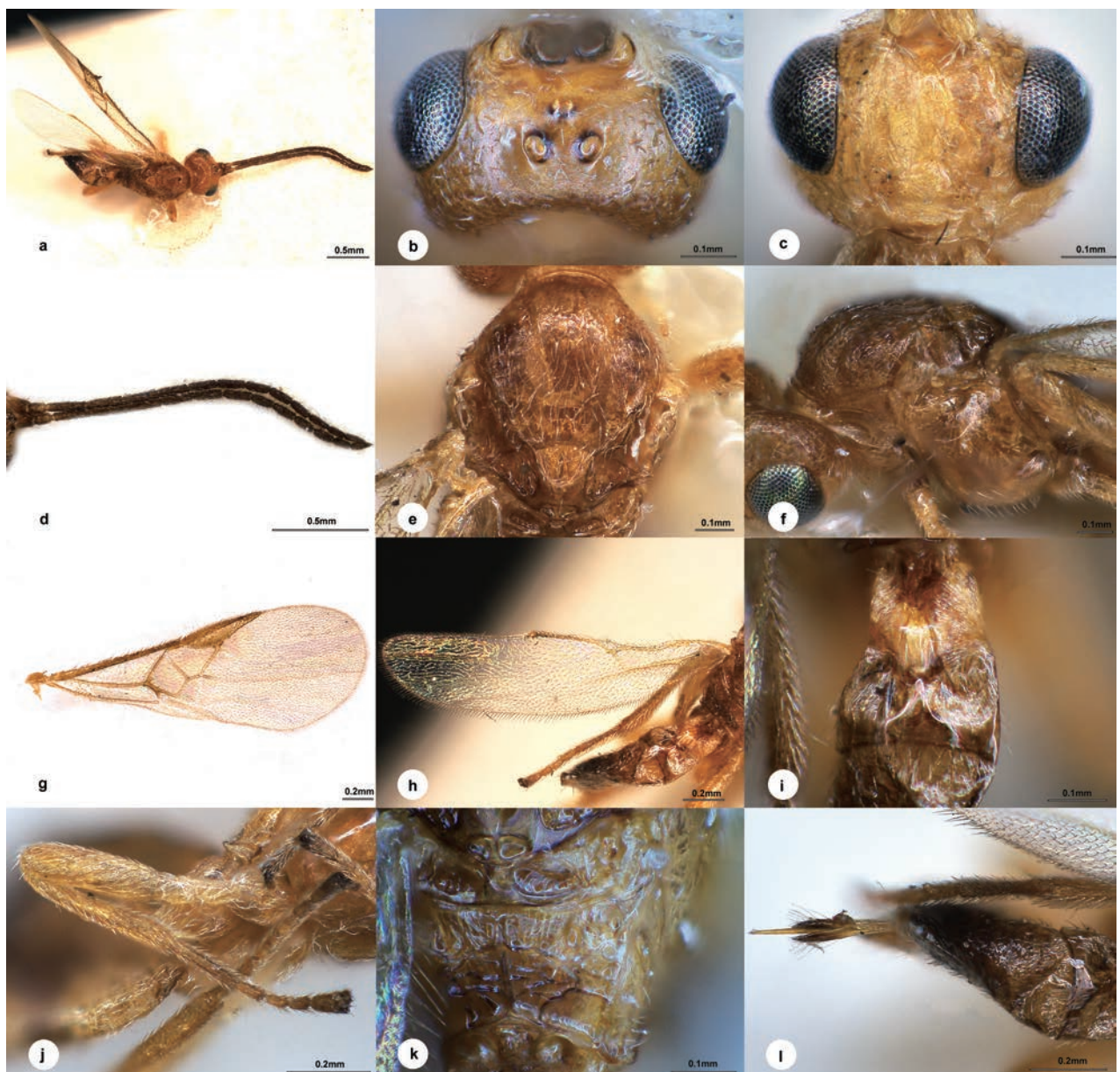


Figure 1. *Centistidea areolaris* Liu & Polaszek, sp. nov., female, holotype **a** habitus, dorsal view **b** head, dorsal view **c** head, frontal view **d** antenna **e** mesosoma, dorsal view **f** mesosoma, lateral view **g** fore wing **h** hind wing **i** T1–T3, dorsal view **j** hind leg **k** propodeum, dorsal view **l** ovipositor sheath.

smooth dorsally, notauli less obvious, weakly crenulated near to anterior 1/3. Scutellar sulcus slightly curved, concave, not crenulated. Scutellum shiny, sculptured as dorsal mesoscutum, medio-posterior depressions large and oblong, both enclosed by a margined line. Propodeum (Fig. 1k) shiny with distinct median carinae reaching posterior margin, rugulose anteriorly, with carinate-areolate elements medio-apically. Mesopleuron (Fig. 1f) highly polished, impunctate.

Legs. Hind femur (Fig. 1j) 3.7 × as long as its widest part. Length of hind femur:tibia:basitarsus = 2.0:2.4:1.0. Basitarsus of hind leg 0.6 × as long as tarsomeres 2–5.

Wings. Fore wing (Fig. 1g): pterostigma narrow, 2.9 × as long as its widest part (Fig. 1b); vein 1-R1 attenuated to 0.3 length of pterostigma; vein r:2-SR:2-M = 1.0:7.7:3.0, 1-SR:1-M = 1.0:6.1, 1-CU1:2-CU1 = 1.0:1.7; first discal cell of fore wing nearly 1.2 × wider than high. Hind wing (Fig. 1h): vein M+CU:1-M:r-m = 2.0:2.2:1.0.

Metasoma. 0.9 × length of mesosoma. T1 (Fig. 1i) highly polished, spatula-shaped, 3.9 × longer than its maximum width, distinctly narrowed anterior-medially, radially striate at lateral membranous area. T2 triangular part 1.3 × wider than median length, longitudinally striate at lateral membranous area. T3 1.9 × longer than T2, weakly longitudinally striate. Hypopygium shorter than length of metasoma. Ovipositor sheath (Fig. 1l) 1.3 × longer than hind basitarsus, with long and dense setae apically.

Colour. Light red-brown, except apex of metasoma darker brown (Fig. 1a). Palpi and spurs pale yellow. Antenna and apical ovipositor sheath dark brown. Legs yellow except apical tarsomeres. Wing membrane hyaline, pterostigma yellow-brown, vein 1-SR, 1-M and 1-CU1 brown, other veins brown.

Male. Unknown.

Host. Unknown.

Material examined (NHMUK). **Holotype:** • 1♀, SOUTH AFRICA, Port St. John, Pondoland, RE Turner, 12–30.VI.1923, Brit. Mus 1923-363, No. NHMUK010639675. **Paratype:** • 1♀, same data except IX.1923, Brit. Mus 1923-510, No. NHMUK010639676.

Distribution. South Africa.

Etymology. The specific name “*areolaris*” refers to the propodeum with carinate-areolate elements medio-apically.

Remarks. This species is similar to the Neotropical species, *C. vertus* (Papp, 2013). Its peculiar propodeum is very rare in Miracinae with both median carina and areola present, but differs in the following: antenna slightly shorter than body length, with penultimate flagellomere 2.7 × longer than wide (antenna 1.2 × longer than body length, with penultimate flagellomere 4.0 × longer than wide in *C. vertus*); medio-posterior depressions on scutellum distinct in an enclosed oval margined line (absent in *C. vertus*); and T2 gradually wider basally (narrowly parallel-sided basally in *C. vertus*).

***Centistidea leucopterae* (Wilkinson, 1936)**

Fig. 2

Mirax leucopterae Wilkinson, 1936: 385. Holotype in NHMUK, examined.

Mirax leucopterae: De Saeger 1944: 36; Decelle 1962: 189; Nixon 1965: 9; Shenefelt 1973: 678.

Diagnosis. Body length 1.5–2.0 mm, mostly black (Fig. 2a); head exceedingly minutely punctate, more densely so on the face than on the frons and vertex (Fig. 2b, c); ocelli in a small equilateral triangle which about the length to each eye; flagellum of female rather shorter, and of male rather longer, than body; mesoscutum and disc of scutellum (Fig. 2e) throughout regularly, minutely punctate; notauli very distinct on anterior declivity; scutellar sulcus greatly reduced; propodeum (Fig. 2h) with a very strong median longitudinal carina, which bifurcates at about the middle and forms a pair of very strong, diverging carinae, punctate and setiferous anterolaterally, impunctate elsewhere; vein r (Fig. 2g) emitted before middle of pterostigma; T1 long and narrow, broadened in apical half; T2 (Fig. 2l) entirely smooth except two or three minute punctures, membranous lateral basal areas with fine longitudinal aciculation; T3

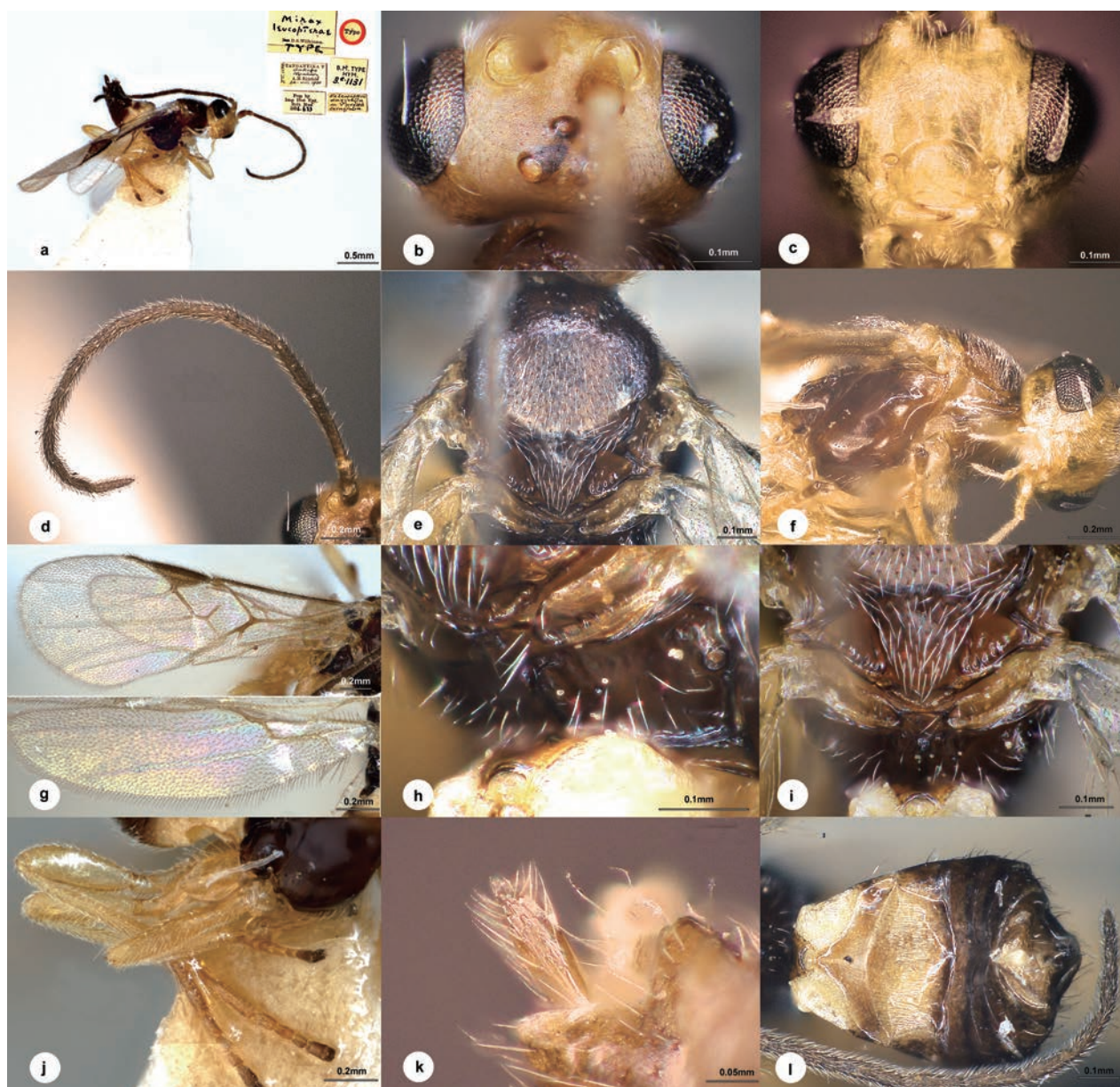


Figure 2. *Centistidea leucopterae* (Wilkinson, 1936), female, holotype **a** habitus, lateral view **b** head dorsal view **c** head, frontal view **d** antenna **e** mesosoma, dorsal view **f** mesosoma, lateral view **g** wings **h** propodeum **i** scutellum **j** hind leg **k** ovipositor sheath **l** metasoma, dorsal view.

with some minute punctures across apical third or fourth, otherwise almost throughout with fine longitudinal aciculation.

Material examined. Holotype: • 1 ♀, [Tanzania] Tanganyika T[erritory], Bukoba, Nyakato, AH Ritchie, 24.VIII.1935, ex *Leucoptera daricella* on *Pavetta ternifolia*, type No. B.M.TYPE HYM. 3.C.1131, No. NHMUK010639681; **paratypes:** • 9 ♂♂, same data as holotype Nos. NHMUK010635732, 010639360, 010639353, 010639367, 010639480, 010639377, 010639403, 010639362, 010639384.

Other materials. • 3 ♀♀3 ♂♂, MADAGASCAR, Fianarantsoa, 19.III.1968, C.I.E. A2287, ex *Leucoptera*, det. Nixon, 1968, Nos. NHMUK010639677 (2), 010639678 (2), 010639679 (2); • 3 ♀♀, MADAGASCAR, Tulear Berenty 12 km, N.W. Amboasary, JS Noyes, MC Day, 5-15.V.1983, B.M.1983-201, Nos. NHMUK010639735, 010639730, 010639744; • 1 ♀, KENYA, Diani Beach, VII.1951, NLH Krauss, B.M.1951-541, No. NHMUK010639745; • 1 ♀, SOUTH AFRICA, Port St. John, Pondoland, 25-31.III.1923, RE Tuner, Brit.Mus. 1923-241, No. NHMUK010639726; • 1 ♀3 ♂♂, ZIMBABWE Chipinga Dist., Masasimn, 20.VII.1990, ex larvae of *Leucoptera meyricki*, IIE 21643, det. AK Walker, 1991, No. NHMUK010639680.

Host. *Crobylophora daricella* [*Pavetta ternifolia*], *Leucoptera* sp. [*Cremaspora*, *Cremaspora hirsutus*, *pavetta*], *Leucoptera coffeella*, and *Leucoptera coma* (Yu et al. 2016; Decelle 1962).

Distribution. New records for Kenya, Madagascar, South Africa, Zimbabwe; Democratic Republic of Congo, Tanzania.

***Centistidea linearis* Liu & Polaszek, sp. nov.**

<https://zoobank.org/AB062463-62D2-4E1B-9483-8F2076BD8851>

Fig. 3

Diagnosis. Body length 2.6 mm, dark brown; head 1.7 × as wide as long, 1.5 × wider than mesoscutum; eyes 2.0 × longer than temple in dorsal view; temple slightly shiny, small setose punctures with transverse wrinkles in between, not constricted behind eyes in dorsal view; distance between fore and a hind ocellus 1.5 × longer than minor axis of a hind ocellus, POL:OD:OOL = 1.3:1.0:3.1; clypeus 1.6 × wider than medial length, weakly defined punctate; antenna 1.2 × longer than body length, with 1st, 2nd, penultimate and ultimate flagellomeres 5.2, 4.9, 4.1 and 4.3 × longer than wide, 1st about as long as 2nd; mesoscutum with superficial and extremely small punctures, intervals with extremely fine wrinkles, notauli obvious, crenulated near to anterior 1/2; scutellar sulcus slightly curved, indistinctly crenulated; medio-posterior depressions of scutellum large and oblong, interval 3/4 of depression diameter; propodeum with distinct median carinae reaching beyond weak defined costulae, anterior parts with indistinct punctures anteriorly except wrinkles elsewhere as posterior parts, anterior part 2.8 × longer than median length of metanotum; vein 1-R1 0.3 of length of pterostigma; T1 2.8 × longer than its maximum width; T2 2.6 × wider than median length; T3 1.7 × longer than T2.

Description. Female. Body length 2.6 mm, fore wing length 2.6 mm (Fig. 3a).

Head. Transverse in dorsal view, 1.7 × as wide as long, 1.5 × wider than mesoscutum. Eyes 2.0 × longer than temple in dorsal view (Fig. 3b). Temple a little shiny, with small setose punctures and with transverse wrinkles in between, not constricted behind eyes in dorsal view. Ocelli small, distance between fore and a hind ocellus 1.5 × longer than minor axis of a hind ocellus, POL:OD:OOL = 1.3:1.0:3.1.

Frons flat and nearly polished except extremely fine transverse wrinkles. Vertex between eye and hind ocellus shiny and sculptured as temple. Face (Fig. 3c) shiny, with fine setose punctures, indistinctly convex medially, transverse, 1.3 × wider than high. Clypeus 1.6 × wider than medial length, weakly defined punctate. Length of malar space as long as basal width of mandible. Antenna (Fig. 3d) 1.2 × longer than body length, with scape, pedicel and 1st, 2nd, penultimate and ultimate flagellomeres 2.0, 1.7, 5.2, 4.9, 4.1 and 4.3 × longer than wide, 1st about as long as 2nd, flagellomeres gradually shortened to apex.

Mesosoma. Length:width:height = 10:4.2:6.3. Mesoscutum (Fig. 3e) shiny with superficial and extremely small punctures, intervals with extremely fine wrinkles, notauli distinct, crenulated near to anterior 1/2. Scutellar sulcus slightly curved, indistinctly crenulated. Scutellum strongly shiny, sculptured as mesoscutum, medio-posterior depressions large and oblong, widely separated,



Figure 3. *Centistidea linearis* Liu & Polaszek, sp. nov., female, holotype **a** habitus, lateral view **b** head, dorsal view **c** head, frontal view **d** antenna **e** mesosoma, dorsal view **f** mesosoma, lateral view **g** fore wing **h** hind wing **i** propodeum **j** ovipositor sheath **k** hind leg **l** T1–T3, dorsal view.

interval 3/4 of depression diameter). Propodeum (Fig. 3i) shiny, with distinct median carinae reaching beyond weakly defined costulae, anterior parts with indistinct punctures anteriorly except wrinkles elsewhere as posterior parts, anterior part 2.8 × longer than median length of metanotum. Mesopleuron (Fig. 3f) highly polished, impunctate.

Legs. Hind femur (Fig. 3k) 3.3 × as long as its widest part. Length of hind femur:tibia:basitarsus = 1.5:1.9:1.0. Basitarsus of hind leg 0.9 × as long as tarsomeres 2–5.

Wings. Fore wing (Fig. 3g): pterostigma, 2.6 × as long as its widest part; vein 1-R1 0.3 length of pterostigma; vein r:2-SR:2-M = 1.0:5.5:2.3, 1-SR:1-M = 1.0:4.1, 1-CU1:2-CU1 = 1.0:1.7; first discal cell of fore wing nearly 1.2 × wider than high. Hind wing (Fig. 3h): vein M+CU:1-M:r-m = 2.0:2.2:1.0.

Metasoma. Indistinctly longer than mesosoma. T1 (Fig. 3l) highly polished, spatula-shaped, 2.8 × longer than its maximum width, distinctly narrowed anterior-medially. T2 transverse, 2.6 × wider than median length. T3 1.7 × longer than T2, weakly longitudinally striate. Hypopygium shorter than length of metasoma. Ovipositor sheath (Fig. 3j) 0.8 length of hind basitarsus, with long and dense setae apically.

Colour. Dark brown, except metasoma more or less brown dorsally (Fig. 3a). Palpi and spurs pale yellow. Antenna and apical ovipositor sheath dark brown. Legs yellow to yellow-brown on all tarsi and hind tibia. Wing membrane hyaline, pterostigma brown, vein r, 2-SR, 1-SR, 1-M and 1-CU1 darker brown, other veins brown.

Male. Unknown.

Host. Unknown.

Material examined (NHMUK). *Holotype*: • 1♀, CAMEROON, Nkoémvon, D. Jackson, VII–VIII.1979, No. NHMUK010639762.

Distribution. Cameroon.

Etymology. The specific name “*linearis*” derives from the Latin, referring to the fine wrinkles on head and mesosoma.

Remarks. This species is similar to *C. africana* but differs in the following: antenna 1.3 × longer than body (antenna shorter than body in *C. africana*); medio-posterior depressions on scutellum oblong, far away from each other, interval 3/4 of depression diameter (oval and close to each other in *C. africana*); and scutellar sulcus indistinctly crenulated (not crenulated or concave in *C. africana*).

***Centistidea longipedes* Liu & Polaszek, sp. nov.**

<https://zoobank.org/3164ADDF-C71B-4EB8-BB2A-A719EE211873>

Fig. 4

Diagnosis. Body length 2.2 mm, dark brown; head 1.7 × as wide as long, 1.3 × wider than mesoscutum; eyes 1.5 × longer than temple in dorsal view; temple with transverse wrinkles in between, not constricted behind eyes in dorsal view; distance between fore and a hind ocellus 1.2 × longer than minor axis of a hind ocellus, POL:OD:OOL = 1.2:1.0:3.2; frons flat and nearly polished except extremely fine transverse wrinkles; vertex between eye and hind ocellus shiny and sculptured as temple; face shiny, with extremely fine setose punctures, indistinctly convex medially, transverse, 1.4 × wider than high; clypeus 2.2 × wider than medial length, nearly polished; antenna 1.2 × longer than body length, with 1st, 2nd, penul-

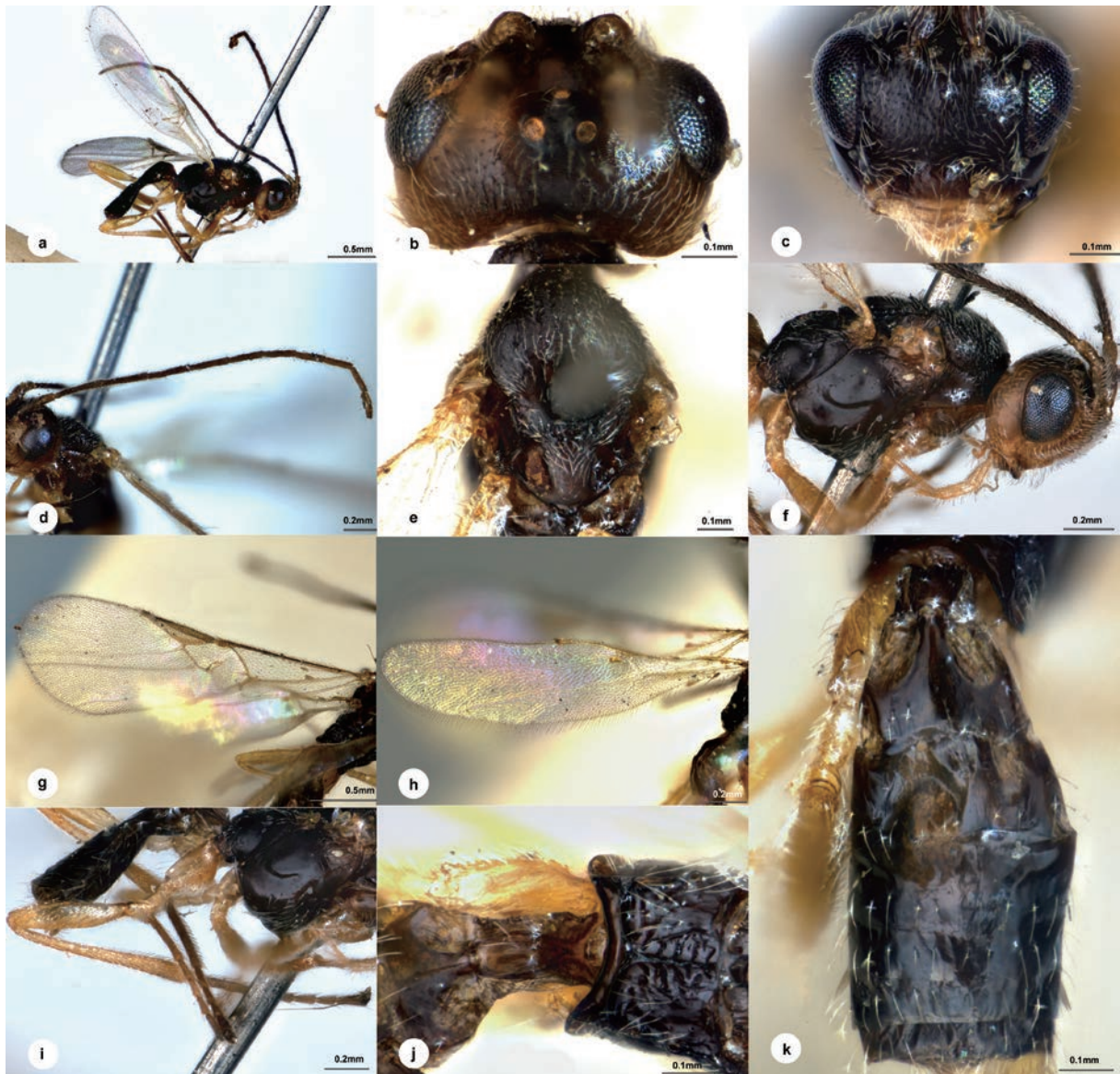


Figure 4. *Centistidea longipedes* Liu & Polaszek, sp. nov., male, holotype **a** habitus, lateral view **b** head, dorsal view **c** head, frontal view **d** antenna **e** mesosoma, dorsal view **f** mesosoma, lateral view **g** fore wing **h** hind wing **i** hind leg **j** propodeum and T1 **k** metasoma, dorsal view.

timate and ultimate flagellomeres 6.3, 6.7, 3.8, and 4.6 × longer than wide, 1st 1.1 × longer than 2nd; mesoscutum with superficial and extremely small punctures, intervals with extremely fine wrinkles, notauli obvious, crenulated to anterior 1/3; scutellar sulcus straight and crenulated; medio-posterior depressions on scutellum large and oblong, virtually touching each other; propodeum with distinct median carinae just reach costulae, anterior parts with indistinct punctures and several short rugae alongside median carinae, 2.5 × longer than median length of metanotum, posterior parts polished; hind leg extremely long, 2.6 × than metasoma; pterostigma narrow, 3.7 × as long as its widest part; vein 1-R1 0.3 of length of pterostigma; T1 poorly defined, 2.8 × longer than its maximum width; T2 1.2 × wider than median length; T3 0.9 × length of T2, not longitudinally striate.

Description. Male. Body length 2.2 mm, fore wing length 2.6 mm (Fig. 4a).

Head. Transverse in dorsal view, 1.7 × as wide as long, 1.3 × wider than mesoscutum. Eyes 1.5 × longer than temple in dorsal view (Fig. 4b). Tem-

ple slightly shiny, small setose punctures with transverse wrinkles in between, not constricted behind eyes in dorsal view. Ocelli small, distance between fore and a hind ocellus $1.2 \times$ longer than minor axis of a hind ocellus, POL:OD:OOL = 1.2:1.0:3.2. Frons flat and nearly polished except extremely fine transverse wrinkles. Vertex between eye and hind ocellus shiny and sculptured as temple. Face (Fig. 4c) shiny, with extremely fine setose punctures, indistinctly convex medially, transverse, $1.4 \times$ wider than high. Clypeus $2.2 \times$ wider than medial length, nearly polished. Length of malar space $1.6 \times$ basal width of mandible. Antenna (Fig. 4d) $1.2 \times$ longer than body length, with scape, pedicel and 1st, 2nd, penultimate and ultimate flagellomeres 2.3, 1.9, 6.3, 6.7, 3.8 and $4.6 \times$ longer than wide, 1st $1.1 \times$ longer than 2nd, flagellomeres gradually shortened to apex.

Mesosoma. Length:width:height = 10:4.6:6.5. Mesoscutum (Fig. 4e) shiny with superficial and extremely small punctures, intervals with extremely fine wrinkles, notauli obvious, crenulated to anterior 1/3. Scutellar sulcus slightly curved, crenulated. Scutellum shiny, sculptured as mesoscutum, medio-posterior depressions large and oblong, virtually touching each other. Propodeum (Fig. 4j) highly shiny, with distinct median carinae just reaching costulae, anterior parts with indistinct punctures and several short rugae alongside median carinae, $2.5 \times$ longer than median length of metanotum, posterior parts polished. Mesopleuron (Fig. 4f) highly polished, impunctate.

Legs. Hind leg (Fig. 4i) remarkably long, $2.6 \times$ than metasoma. Hind femur $4.1 \times$ as long as its widest part. Length of hind femur:tibia:basitarsus = 2.2:3.2:1.0. Basitarsus of hind leg $0.6 \times$ as long as tarsomeres 2–5.

Wings. Fore wing (Fig. 4g): pterostigma narrow, $3.7 \times$ as long as its widest part; vein 1-R1 0.3 of length of pterostigma; vein r:2-SR:2-M = 1.0:5.3:3.4, 1-SR:1-M = 1.0:4.0, 1-CU1:2-CU1 = 1.0:2.2; first discal cell of fore wing nearly 1/5 wider than high. Hind wing (Fig. 4h): vein M+CU:1M:1r-m = 1.5:1.9:1.0.

Metasoma. Indistinctly longer than mesosoma. T1 (Fig. 4k) highly polished, poorly defined, spatula-shaped, $2.8 \times$ longer than its maximum width, distinctly narrowed anterior-medially. T2 $1.2 \times$ wider than median length; T3 $0.9 \times$ length of T2, smooth without longitudinal striae.

Colour. Dark brown (Fig. 4a). Palpi and spurs honey yellow. Antenna dark brown. Legs yellow, except apical 1/3 of hind tibia and hind tarsus brown. Wing membrane hyaline, pterostigma yellow-brown, vein r, 2-SR, 1-SR, 1-M and 1-CU1 yellow-brown, other veins pale.

Female. Unknown.

Host. Unknown.

Material examined (NHMUK). **Holotype:** • 1♂, CAMEROON, Mt Cameroon, Mann's Quelle (2256 m), M Steele, 4.II.1932, B.M.1934-240, No. NHMUK010639754. **Paratype:** • 1♂, UGANDA, Ruwenzori Range, Bigo (3475 m), DS Fletcher, 20–22.VII.1952, No. NHMUK010639740.

Distribution. Cameroon, Uganda.

Etymology. The specific name "*longipedes*" derives from Latin, referring to the extremely long hind legs.

Remarks. This species is similar to *C. leucopterae* (Wilkinson, 1936) but differs in the following: temple not constricted behind eyes in dorsal view (distinctly constricted in *C. leucopterae*); T2 $1.2 \times$ wider than median length ($3.3 \times$ wider in *C. leucopterae*); and T3 polished (longitudinally striate in *C. leucopterae*).

***Centistidea mubilibana* (de Saeger, 1944)**

Fig. 5

Mirax mubilibana de Saeger, 1944: 34. Holotype in RMCA, examined.

Mirax mubilibana: Shenefelt 1973: 678.

Diagnosis. Body length 2–3 mm, colour variable, mostly black; face, vertex and occiput very finely punctate, shiny; temple smooth; eyes a third longer than wide; length of the ocellar triangle approximately equal to the distance which separates it from each eye; antenna nearly as long as body, 1st flagellomere a little longer and thinner than the following; mesoscutum regularly and finely punctate, more densely than the face, more sparsely laterally and disc of the scutellum, notauli present anteriorly; scutellar sulcus weakly arched, narrow and foveated; medio-posterior depressions of scutellum very small, round; propodeum rough, with carinae arranged as in *M. leucopterae*, but median carinae more wide, more or less divided, the apical area comprises approximately a third the length of propodeum; vein r almost completely absent; T1 2.5 × longer than its greatest width, striate or rugose; T2 smooth and shiny, with a small tubercle basal medially; T2 and T3 of the same length; T3 with slightly stronger longitudinal aciculation than T2; ovipositor sheath a little shorter than metatarsus III.

Host. Unknown.

Material examined (RMCA). *Holotype*: • 1♀, CONGO BELGE: PNA Mubiliba (Vol. Nyamuragira), 2000 m, 14–26.VI.1935, G.F.de Witte: 1499, Coll. Mus. Congo (ex coll. I.P.N.C.B).

Distribution. Democratic Republic of Congo, Rwanda.

***Centistidea tihamica* Ahmad & Pandey, 2019**

Centistidea tihamica Ahmad & Pandey, 2019: 43. Holotype in the Insect Collection of the Department of Zoology, Aligarh Muslim University, Aligarh, India (not examined).

Diagnosis. Body length 1.8 mm, mostly yellow-brown; length of eye 1.5 × temple in dorsal view; head and vertex indistinctly punctate; 1st flagellomere 1.25 × longer than 2nd; penultimate flagellomere 2.5–3.0 × as long as wide; mesoscutum shiny with few distinct punctures, notauli only anteriorly impressed; scutellar sulcus distinct, present as a narrow groove and crenulated; medio-posterior depressions of scutellum semicircular and separated (from the original image); propodeum almost smooth with a complete median longitudinal carina bifurcate posteriorly, median carina of propodeum absent behind level of costulae; pterostigma with a long slender, apical expansion, 2.2 × longer than wide; vein r very prominent and 0.2 × as long as the height of pterostigma; vein 1-SR absent (from the original image); T1 4.0 × as long as its maximum width; T2 subtriangular, smooth, laterally membranous, and longitudinally striated; T3 longitudinally striated; ovipositor sheaths 0.15 × as long as fore wing (following Ghramh et al. 2019).

Host. Unknown.

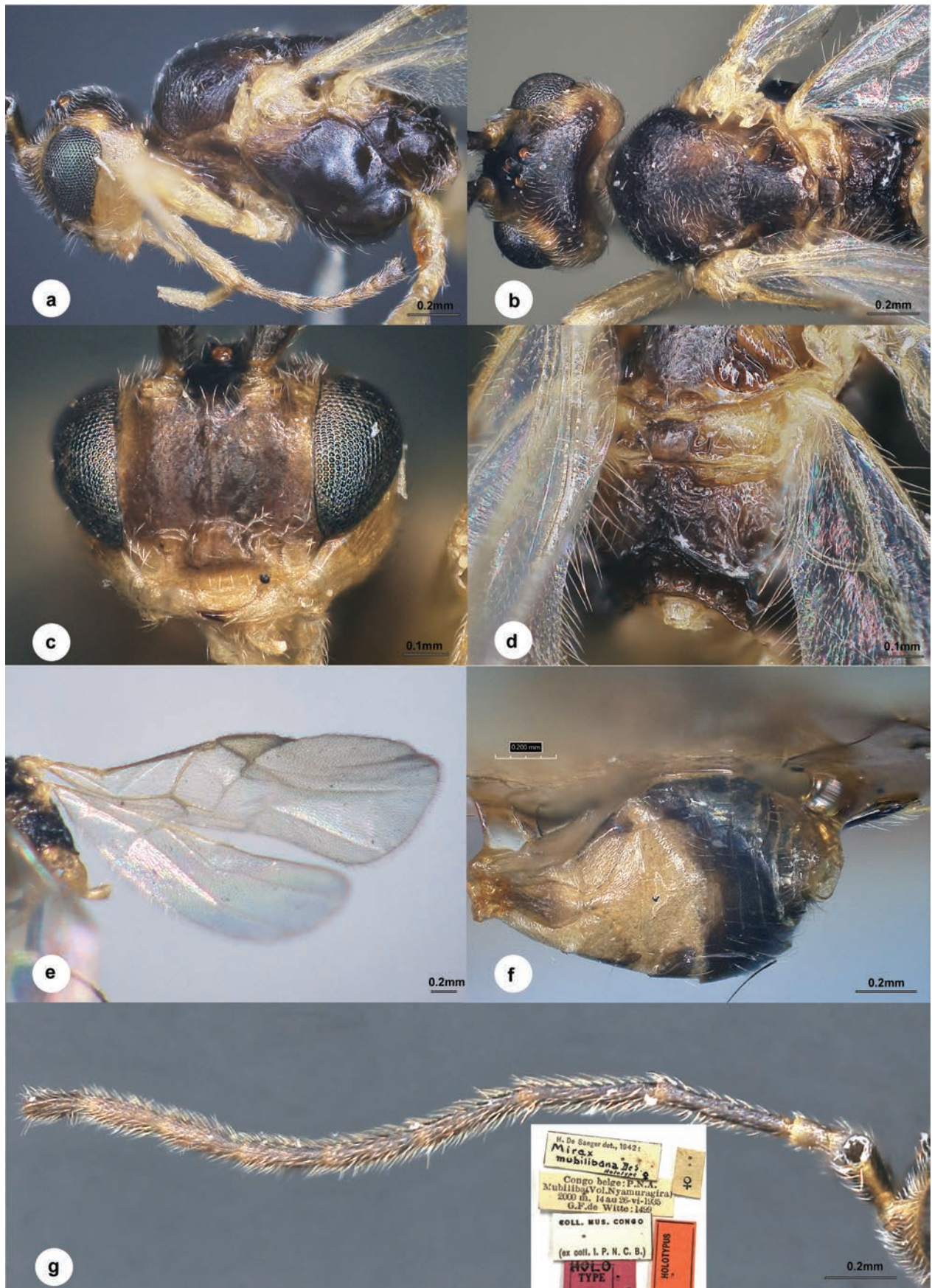


Figure 5. *Centistidea mubilibana* (de Saeger, 1944), female, holotype **a** head and mesosoma, lateral view **b** head and mesosoma, dorsal view **c** face, frontal view **d** propodeum **e** wings **f** metasoma, dorsal view **g** antenna.

Distribution. Saudi Arabia. Although not strictly in the Afrotropical region, the species is included here for future reference, in case it should eventually be discovered in the region.

Note. No specimens were available for this study. Ghramh et al. (2019) described it as the first species of *Centistidea* from the Afrotropical region. However, when we examined the original descriptions and images and related specimens, all species originally described as *Mirax* including *africana*, *leucopterae*, and *mubilibana* in this area are all *Centistidea* by possessing medio-longitudinal carina on propodeum and more or less impressed notauli on anterior mesoscutum.

***Centistidea turneri* Liu & Polaszek, sp. nov.**

<https://zoobank.org/C0CE598F-E087-488B-AB29-87091DC0C8AD>

Fig. 6

Diagnosis. Body length 1.7 mm, light red-brown; eyes 1.8 × longer than temple in dorsal view; temple smooth, superficially punctate, a little constricted behind eyes in dorsal view; hind ocelli in a shallow depression, distance between fore and a hind ocellus 1.3 × longer than minor axis of a hind ocellus, POL:OD:OOL = 1.5:1.0:2.5; vertex between eye and hind ocellus shiny and polished; face polished, 1.4 × wider than high; antenna slightly shorter than body length, with penultimate and ultimate flagellomeres 2.2 and 2.5 × longer than wide, 1st slightly longer (1.1 ×) than 2nd; mesoscutum with superficial and fine dense punctures anteriorly and laterally, more shallow and sparser dorsally, notauli hardly visible, only slightly depressed at anterior extremity; scutellar sulcus slightly curved, shallowly concave without crenulation; medio-posterior depressions of scutellum oblong, touching each other; propodeum with median carina reaching half way to hind margin, and bifurcated to two-thirds of lateral margin, largely polished elsewhere; pterostigma 2.8 × as long as its widest part, vein 1-R1 virtually absent; T1 polished, 2.5 × longer than its maximum width, strongly narrowed anterior-medially; T2 1.9 × wider than median length, not longitudinally striate at lateral membranous area; T3 1.4 × longer than T2, weakly longitudinally striate.

Description. Female. Body length 1.7 mm, fore wing length 1.8 mm (Fig. 6a).

Head. Transverse in dorsal view, 1.8 × as wide as long, 1.3 × wider than mesoscutum. Eyes 1.8 × longer than temple in dorsal view (Fig. 6b). Temple slightly shiny, smooth, indistinctly punctate, sparsely pubescent, a little constricted behind eyes in dorsal view (Fig. 6c). Ocelli small, hind ocelli in a shallow depression, distance between fore and a hind ocellus 1.3 × longer than minor axis of a hind ocellus, POL:OD:OOL = 1.5:1.0:2.5. Frons flat and polished. Vertex between eye and hind ocellus shiny and polished. Face (Fig. 6c) indistinctly convex medially, transverse, 1.4 × wider than high. Clypeus 2.0 × wider than medial length, slightly polished. Length of malar space 1.5 × longer than width of mandible. Antenna (Fig. 6d) slightly shorter than body length, with scape, pedicel and 1st, 2nd, penultimate and ultimate flagellomeres 2.0, 1.6, 4.5, 4.5, 2.2, and 2.5 × longer than wide, 1st slightly longer (1.1 ×) than 2nd, flagellomeres gradually shortened to penultimate flagellomeres.

Mesosoma. Length:width:height = 1.8:1.0:1.3. Mesoscutum (Fig. 6e) shiny with superficial and fine dense punctures anteriorly and laterally, more shallow and sparser dorsally, notauli hardly visible dorsally, only slightly depressed at



Figure 6. *Centistidea turneri* Liu & Polaszek, sp. nov., female, holotype **a** habitus, lateral view **b** head, dorsal view **c** head, frontal view **d** antenna **e** mesosoma, dorsal view **f** mesosoma, lateral view **g** wings **h** propodeum **i** hind leg **j** ovipositor sheath **k** metasoma, dorsal view.

anterior extremity. Scutellar sulcus slightly curved, shallowly concave with crenulation. Scutellum shiny, sculptured as dorsal mesoscutum, medio-posterior depressions oblong, touching each other. Propodeum (Fig. 6h) shiny, with median carina reaching halfway to hind margin, and bifurcated to two thirds of lateral margin, largely polished elsewhere. Mesopleuron highly polished, impunctate.

Legs. Hind femur (Fig. 6i) 3.3 × as long as its widest part. Length of hind femur:tibia:basitarsus = 1.9:2.9:1.0. Basitarsus of hind leg 0.7 × as long as tarsomeres 2–5.

Wings. Fore wing (Fig. 6g): pterostigma 2.8 × as long as its widest part; vein 1-R1 virtually absent; vein r:2-SR:2-M = 1.0:6.7:3.0, 1-SR:1-M = 1.0:4.4, 1-CU1:2-CU1 = 1.0:1.6; first discal cell of fore wing indistinctly wider than high. Hind wing (Fig. 6g): vein M+CU:1-M:r-m = 2.0:2.5:1.0.

Metasoma. Nearly as long as mesosoma. T1 (Fig. 6k) polished, spatula-shaped, 2.5 × longer than its maximum width, strongly narrowed antero-medially, transversely striate at lateral membranous area. T2 1.9 × wider than median length, not longitudinally striate at lateral membranous area. T3 1.4 × longer than T2, weakly longitudinally striate. Hypopygium not shorter than length of metasoma. Ovipositor sheath (Fig. 6j) 1.3 × longer than hind basitarsus, with long and dense setae at apical third.

Colour. Light red-brown, terga posterior to T3 dark brown (Fig. 6a). Palpi and spurs light red-yellow. Antenna and basal half ovipositor sheath (apical half dark brown) yellow-brown. Legs yellow-brown except apical tarsomeres. Wing membrane hyaline, pterostigma pale yellow, vein 1-SR, 1-M and 1-CU1 brown, other veins pale yellow.

Variation. Body colour varying from light yellow to dark brown on trunk of body among specimens. Specimens from Mossel Bay and Ceres from Cape Province tend to be darker when compared with the light yellow specimens from Pondoland of Port St. John in South Africa and Uganda. Body length varies from very small (1.2 mm) to large (2.2 mm).

Male. Similar to female, but body smaller with darker metasoma and longer antenna.

Host. Leaf-miner in castor (*Ricinus communis*).

Material examined (NHMUK). Holotype: • 1 ♀, SOUTH AFRICA, Cape Province, Swellendam, RE Turner, II.1932, Brit. Mus 1932-145, No. NHMUK010639682.

Paratypes: • 1 ♀, South Africa, Cape Province, Somerset East, RE Turner, 23–31. XII.1930, Brit. Mus 1931-61, No. NHMUK010639720; • 2 ♀♀, SOUTH AFRICA, Cape Province, Mossel Bay, RE Turner, IV.1921, Brit. Mus 1921-210, Nos. NHMUK010639718, 010639716; • 1 ♀, same data except V.1921, Brit. Mus 1921-248, No. NHMUK010639719; • 6 ♀♀, same data except VI.1921, Brit. Mus 1921-294, Nos. NHMUK010639717, 010639706, 010639700, 010639710, 010639701, 010639686; • 2 ♀♀, same data except 5–31.VII.1921, Brit. Mus 1921-315, Nos. NHMUK010639715, 010639714; • 7 ♀♀, same data except VIII.1921, Brit. Mus 1921-353, Nos. NHMUK010639711, 010639712, 010639707, 010639708, 010639692, 010639687, 010639713; • 6 ♀♀, same data except IX.1921, Brit. Mus 1921-412, Nos. NHMUK010639705, 010639703, 010639695, 010639693, 010639697, 010639699; • 7 ♀♀ 1 ♂, same data except X.1921, Brit. Mus 1921-450, Nos. NHMUK010639696, 010639709, 010639683, 010639689, 010639694, 010639684, 010639691, 010639690; • 1 ♀, same data except 18–30.XI.1921, Brit. Mus 1922-2, No. NHMUK010639688; • 1 ♀, same data except I.1922, Brit. Mus 1922-67, No. NHMUK010639704; • 1 ♀, same data except II.1922, Brit. Mus 1922-97, No. NHMUK010639698; • 2 ♀♀, SOUTH AFRICA, Cape Province, Ceres (457 m), RE Turner, I.1921, Brit. Mus 1921-78, Nos. NHMUK010639685, 010639702; • 2 ♀♀, same data except II.1921, Brit. Mus 1921-115, Nos. NHMUK010639629 010639640; • 11 ♀♀, same data except III.1921, Brit. Mus 1921-150, Nos. NHMUK010639661, 010639654, 010639666, 010639650, 010639645, 010639674, 010639663, 010639655, 010639660, 010639671, 010639630; • 1 ♀, same data except II.1925, Brit. Mus 1925-116, No. NHMUK010639633; • 9 ♀♀, same data except III.1925, Brit. Mus 1925-161, Nos. NHMUK010639644, 010639638, 010639659, 010639636, 010639635, 010639651, 010639658, 010639668; • 1 ♀, same data except IV.1925, Brit. Mus 1925-210, No. NHMUK010639538; • 1 ♂, SOUTH AFRICA, Cape Province, Katberg (1219 m), RE Turner, X.1932, Brit. Mus 1932-521, No. NHMUK010639599;

• 1♀, SOUTH AFRICA, Port St. John, Pondoland, RE Turner, 12–30.VI.1923, Brit. Mus 1923-363, No. NHMUK010639652; • 1♀, same data except 15–31.VIII.1923, Brit. Mus 1923-463, No. NHMUK010639541; • 1♀, same data except 1–13.III.1924, Brit. Mus 1924-177, No. NHMUK010639617; • 1♀1♂, same data except XII.1923, Brit. Mus 1924-54, Nos. NHMUK010639542, 010639549; • 1♀, same data except I.1924, Brit. Mus 1924-97, No. NHMUK010639605; • 1♀, same data except 29.I–5.II.1924, Brit. Mus 1924-109, No. NHMUK010639580; • 1♂, same data except 6-25.II.1924, Brit. Mus 1924-136, No. NHMUK010639557; • 1♀, same data except 18–31.III.1924, Brit. Mus 1924-191, No. NHMUK010639607; • 8♀♀, UGANDA, Kampala, 7.V.1934, ex leaf-miner in castor (*Ricinus communis*), Nos. NHMUK010639764, 010639759, 010639742, 010639729, 010639749, 010639758, 010639755, 010639733.

Distribution. South Africa, Uganda.

Etymology. The specific name “*turneri*” expresses our gratitude to the late R.E. Turner for the large quantity of this species collected in South Africa.

Remarks. From a short apical extension of the pterostigma to distinctly longer and equaling the length of pterostigma, vein 1-R1 is often present in *Centistidea*. In this species, however, it is absent compare to its Afrotropical allies; it is similar to *C. mubilibana* (de Saeger, 1944) for the carination of propodeum but differs in the following: length of the ocellar triangle nearly half of the distance which separates it from each eye (approximately equal in *C. mubilibana*); vein 1-SR present (almost completely absent in *C. mubilibana*); and T1 polished (striate or rugose in *C. mubilibana*).

Acknowledgements

We are grateful to the collectors for their efforts in the field. We also thank Dr Gavin Broad, Natural History Museum, UK and Dr Stéphane Hanot from Royal Museum for Central Africa, Belgium for their help during the course of this study.

Additional information

Conflict of interest

The authors have declared that no competing interests exist.

Ethical statement

No ethical statement was reported.

Funding

Funding for this study was provided by the China Scholarship Council (202208430072), Scientific Research Fund of Hunan Provincial Education Department (23B0654) and Hunan Provincial Natural Science Foundation of China (2023JJ30434).

Author contributions

Conceptualization: AP, ZL. Data curation: AP, ZL. Formal analysis: ZL. Funding acquisition: ZL. Supervision: AP. Writing - original draft: ZL. Writing - review and editing: AP.

Author ORCIDs

Zhen Liu  <https://orcid.org/0000-0002-8670-0205>

Andrew Polaszek  <https://orcid.org/0000-0002-7171-3353>

Data availability

All of the data that support the findings of this study are available in the main.

References

- Brues CT (1926) Studies on Ethiopian Braconidae, with a Catalogue of the African Species. *Proceedings of the American Academy of Arts and Sciences* 61(8): 205–436. <https://doi.org/10.2307/20026158>
- de Saeger H (1944) Microgastrinae (Hymenoptera: Apocrita). *Exploration du parc National Albert: Mission G.F. de Witte* 47: 1–342.
- Decelle J (1962) The leaf-miner of robusta coffee, *Leucoptera coma*. *Parasitica* 18(3): 177–198.
- Ghramh HA, Ahmad Z, Pandey K (2019) Three new species of the genus *Centistidea* Rohwer, 1914 (Hymenoptera, Braconidae, Miracinae) from India and Saudi Arabia. *ZooKeys* 889: 37–47. <https://doi.org/10.3897/zookeys.889.34942>
- Harris RA (1979) Glossary of surface sculpturing. *Occasional Papers in Entomology of the California Department of Food and Agriculture* 28: 1–31.
- Liu Z, Polaszek A (2024) First records of Miracinae (Hymenoptera: Braconidae) from Borneo with description of two new species. *European Journal of Taxonomy* 935: 283–292. <https://doi.org/10.5852/ejt.2024.935.2563>
- Nixon GEJ (1965) A reclassification of the tribe Microgasterini (Hymenoptera: Braconidae). *Bulletin of the British Museum (Natural History) Entomology Supplement* 2: 1–284. <https://doi.org/10.5962/p.144036>
- Papp J (2013) Eleven new *Mirax* Haliday, 1833 species from Colombia and Honduras and key to the sixteen Neotropical *Mirax* species (Hymenoptera: Braconidae: Miracinae). *Acta Zoologica Academiae Scientiarum Hungaricae* 59(2): 97–129.
- Ranjith AP, van Achterberg C, Priyadarsanan DR, Kim IK, Keloth R, Mukundan S, Nasser M (2019) First Indian record of *Centistidea* Rohwer (Hymenoptera: Braconidae, Miracinae) with description of eight new species. *Insect Systematics and Evolution* 50(3): 407–444. <https://doi.org/10.1163/1876312X-00002194>
- Ranjith AP, van Achterberg C, Priyadarsanan DR (2023) A new genus in the braconid subfamily Miracinae from the Oriental region, with descriptions of seven new species from India and Sri Lanka. *Zootaxa* 5318(4): 451–473. <https://doi.org/10.11646/zootaxa.5318.4.1>
- Shenefelt RD (1973) Braconidae 5, Microgastrinae and Ichneutinae. In: van der Vecht J, Shenefelt RD (Eds) *Hymenopterorum Catalogus*, Part 9, 669–812.
- Slater-Baker MR, Austin AD, Whitfield JB, Fagan-Jeffries EP (2022) First record of miracine parasitoid wasps (Hymenoptera: Braconidae) from Australia: molecular phylogenetics and morphology reveal multiple new species. *Austral Entomology*, 61: 49–67. <https://doi.org/10.1111/aen.12582>
- van Achterberg C (1993) Illustrated key to the subfamilies of the Braconidae (Hymenoptera: Ichneumonoidea). *Zoologische Verhandelingen* 283: 1–189.
- Wilkinson DS (1936) On two braconids (Hym.) bred from economic hosts. *Bulletin of Entomological Research* 27(3): 385–388. <https://doi.org/10.1017/S0007485300058247>
- Yu DS, van Achterberg C, Horstmann K (2016) *World Ichneumonoidea 2015. Taxonomy, Biology, Morphology and Distribution*. Nepean, Ottawa, Canada. [database on flash-drive]

A pictorial key to the adult and larval nasal mites (Halarachnidae) of marine mammals

Morgan M. Shields¹, Tara Roth², Risa Pesapane^{1,3}

¹ Department of Veterinary Preventive Medicine, College of Veterinary Medicine, The Ohio State University, 1920 Coffey Rd., Columbus, OH 43210, USA

² San Mateo County Mosquito and Vector Control District, 1351 Rollins Rd., Burlingame, CA 94010, USA

³ School of Environment and Natural Resources, College of Food, Agricultural, and Environmental Sciences, The Ohio State University, 2021 Coffey Rd., Columbus, OH 43210, USA

Corresponding author: Risa Pesapane (pesapane.1@osu.edu)

Abstract

Mites in the family Halarachnidae are common endoparasites infesting the nasal tissues of a variety of marine mammals. These mites are easily transmissible and compromise the health of their hosts, especially in captive environments. While these mites are noted by marine mammal caretakers, they may easily be misidentified due to repeated revisions to halarachnid mite taxonomy and reclassification of misidentified specimens. Species identification currently requires multiple taxonomic keys, knowledge of revisions to species classifications through time, and training in acarology, which is impractical for marine mammal clinicians. Therefore, to summarize the known taxonomy and aid in future identification of halarachnid mites, we present a pictorial key composed of illustrations based on existing literature and images obtained by scanning electron microscopy (SEM) and high-resolution light microscopy (LM). Illustrations are organized into flow charts for the identification of both adult and larval stages. Dorsal shield silhouettes are also provided to facilitate the identification of adults. We hope that this key be used to simplify future taxonomic research, provide a standard for species identification, and aid in the diagnosis of halarachnid infestations in captive and rehabilitated marine mammal populations.

Key words: Acari, dichotomous key, *Halarachne halichoeri*, *Halarachne laysanae*, *Halarachne miroungae*, *Orthohalarachne attenuata*, *Orthohalarachne diminuta*



Academic editor: Vladimir Pesic

Received: 24 August 2024

Accepted: 25 September 2024

Published: 23 October 2024

ZooBank: <https://zoobank.org/32FD4431-2584-45C6-8217-674194343808>

Citation: Shields MM, Roth T, Pesapane R (2024) A pictorial key to the adult and larval nasal mites (Halarachnidae) of marine mammals. ZooKeys 1216: 101–114. <https://doi.org/10.3897/zookeys.1216.135359>

Copyright: © Morgan M. Shields et al.
This is an open access article distributed under terms of the Creative Commons Attribution License (Attribution 4.0 International – CC BY 4.0).

Introduction

Five extant species of mites from two genera in the family Halarachnidae are known to infest a variety of marine mammals, including both captive and wild populations of pinnipeds and lutrinids (Furman and Dailey 1980; Pesapane et al. 2018). A sixth species, *Halarachne americana* Banks, 1899, once infested the Caribbean monk seal (*Neomonachus tropicalis* (Gray, 1850)) but is presumed extinct along with its host (Kenyon 1977; Furman and Dailey 1980). All species of halarachnids are parasitic and can be harmful to their hosts, impairing respiration by way of mucopurulent respiratory exudate, rhinitis, nasopharyngitis, bronchitis, and severe turbinate lysis (Dunlap and Piper 1976; Baker

1987; Alonso-Farré et al. 2012; Dent et al. 2019; Ebmer et al. 2022). Accurate identification of halarachnid mites is important for understanding host-parasite relationships, how to care for captive marine mammals, and the impact mite infestations may have on wild populations.

The family Halarachnidae has undergone numerous taxonomic revisions (Fig. 1), which have invalidated some pre-existing keys and species descriptions (Domrow 1974; Furman and Dailey 1980), meaning that identification requires an in-depth literature review. Additionally, the limited number of well-preserved voucher specimens of some halarachnid species, similarity in morphology among halarachnid taxa, and varying degrees of host overlap by halarachnid mites have compounded the challenge of accurate identification. Although publications for halarachnid mite identification exist, they often focus on a single genus or describe a single species, meaning many documents are needed. Some of these publications are also difficult to obtain or describe extinct species such as *H. americana*. As a result, marine mammal clinicians find it challenging to accurately identify these mites, potentially missing valuable information on host specificity and behavior that could be used to identify sources of infestation and appropriate control methods. Parasite misidentification can stem from a lack of good quality specimens, training in acarology, and the use of outdated identification keys

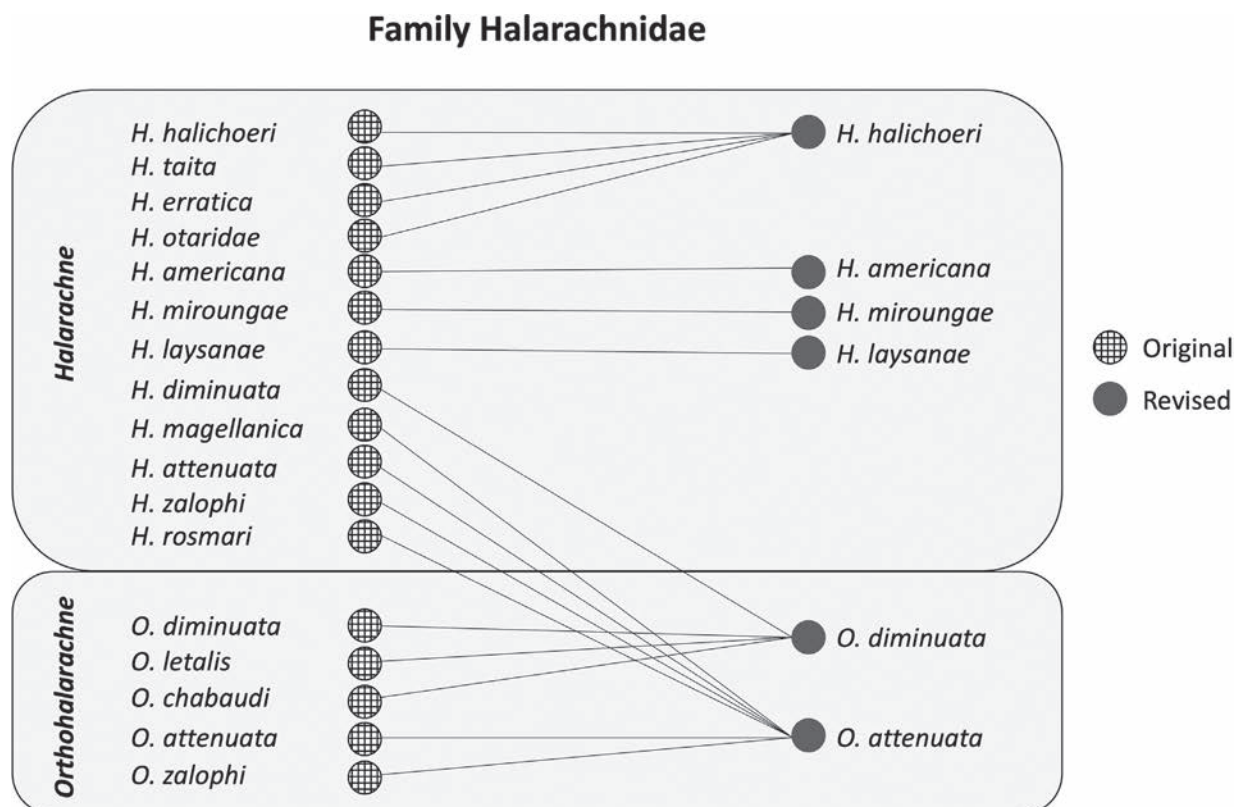


Figure 1. Graphic depiction of Halarachnidae systematics illustrating numerous taxonomic revisions from original species descriptions to revised current described species. Gridded and solid circles represent original and revised species names, respectively, and lines indicate synonymy.

(Bush et al. 2021). Misidentification of parasites by veterinary pathologists or researchers can create error cascades leading to persistent misidentification of species in the literature and incorrect assumptions about parasite behavior and host preferences. While routine collaboration with acarologists is ideal, in practice this does not always happen due to logistical constraints or resource limitations. Therefore, pictorial guides that are accessible and understandable to clinicians and students can help avoid the consequences associated with misidentification. A composite morphological key is useful for both experts and non-experts in parasitology; the former because it ensures accurate taxonomy and future research, and the latter to recognize and accurately document trends in halarachnid infestations to improve marine mammal welfare.

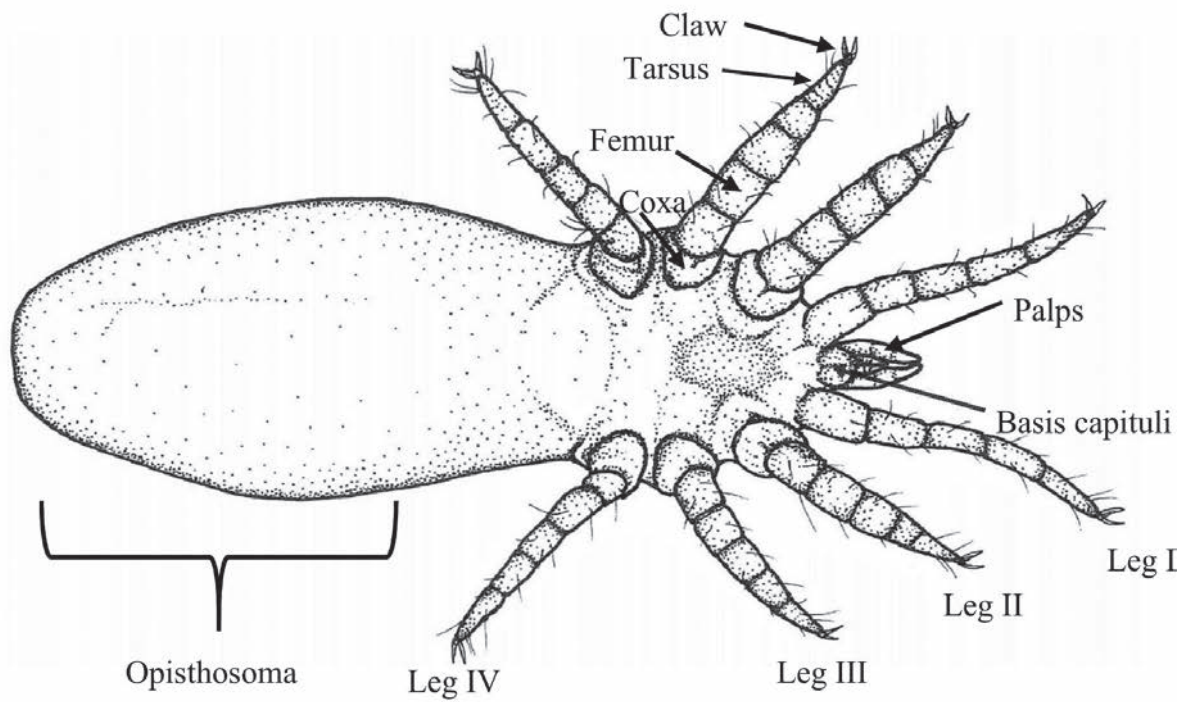
We have produced a simple yet comprehensive pictorial guide to halarachnids based on published keys to increase accessibility and to aid in consistent identification of these mite species independent of their hosts. Our goal is for this key to be accessible to both parasitology experts and non-experts in order to further document and understand the impact of halarachnid infestations in both captive and free-ranging marine mammals.

Methods

A singular pictorial key for identifying larval and adult nasopulmonary mites from both *Halarachne* and *Orthohalarachne* was created using previously published morphologically distinguishing criteria and the most current taxonomic descriptions (Domrow 1962; Furman and Smith 1973; Furman and Dailey 1980; Alonso-Farré et al. 2012; Gastal et al. 2016; Rolbiecki et al. 2018; Ebmer et al. 2022). These criteria are clearly outlined in Figs 2, 3. The focus is on extant species, so *H. americana* is excluded from our key.

Fine-scale resolution of important defining morphologic characteristics were obtained from high-resolution light microscope (LM) images of 357 specimens of *H. halichoeri* Allman, 1847, *H. miroungae* Ferris, 1925, *O. attenuata* Banks, 1910, and adult *O. diminuata* Doetschman, 1944 in our archive using a Nikon SMZ25 stereomicroscope with DS-Ri2 camera (Nikon Inc., Melville, NY, USA). Additional images of *O. attenuata*, *O. diminuata*, and *H. miroungae* generated by both LM and scanning electron microscopy (SEM), and illustrations of *H. laysanae* Furman & Dailey, 1980 were gleaned from existing literature (Furman and Dailey 1980; Pesapane et al. 2018, 2021; Ebmer et al. 2022). Using these images, illustrations for the pictorial key were then hand drawn with pen and ink and organized into a flow chart figure for use in identifying both larval (Figs 4, 5) and adult (Fig. 6) halarachnids. This key also contains a figure depicting the body shape outline (Fig. 7) and dorsal shield shape of each adult species (Fig. 8). Dorsal shield and body morphology were outlined and excised from SEM and LM images using tools in the software NIS-Elements Basic Research (Nikon Inc., Melville, NY, USA), and images and descriptions from previous literature using GNU Image Manipulation Program (GIMP) v. 2.10.24 (<https://www.gimp.org>).

H. halichoeri adult ventral view:



H. halichoeri adult dorsal view:

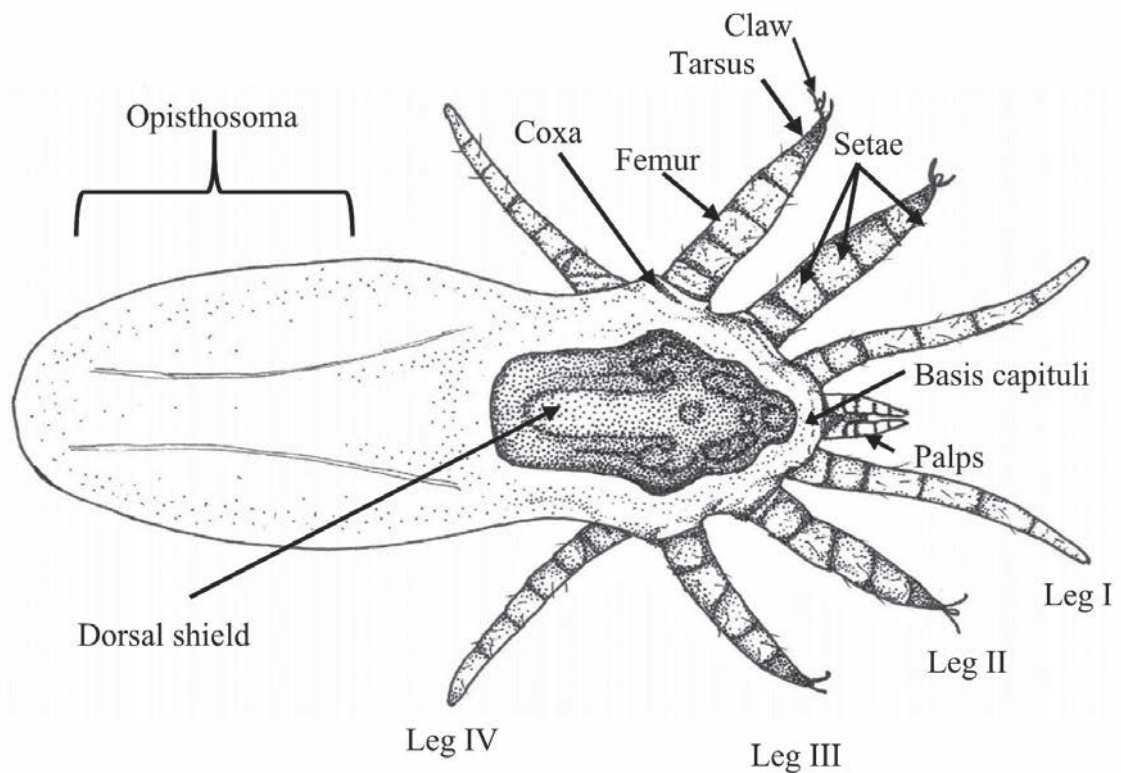
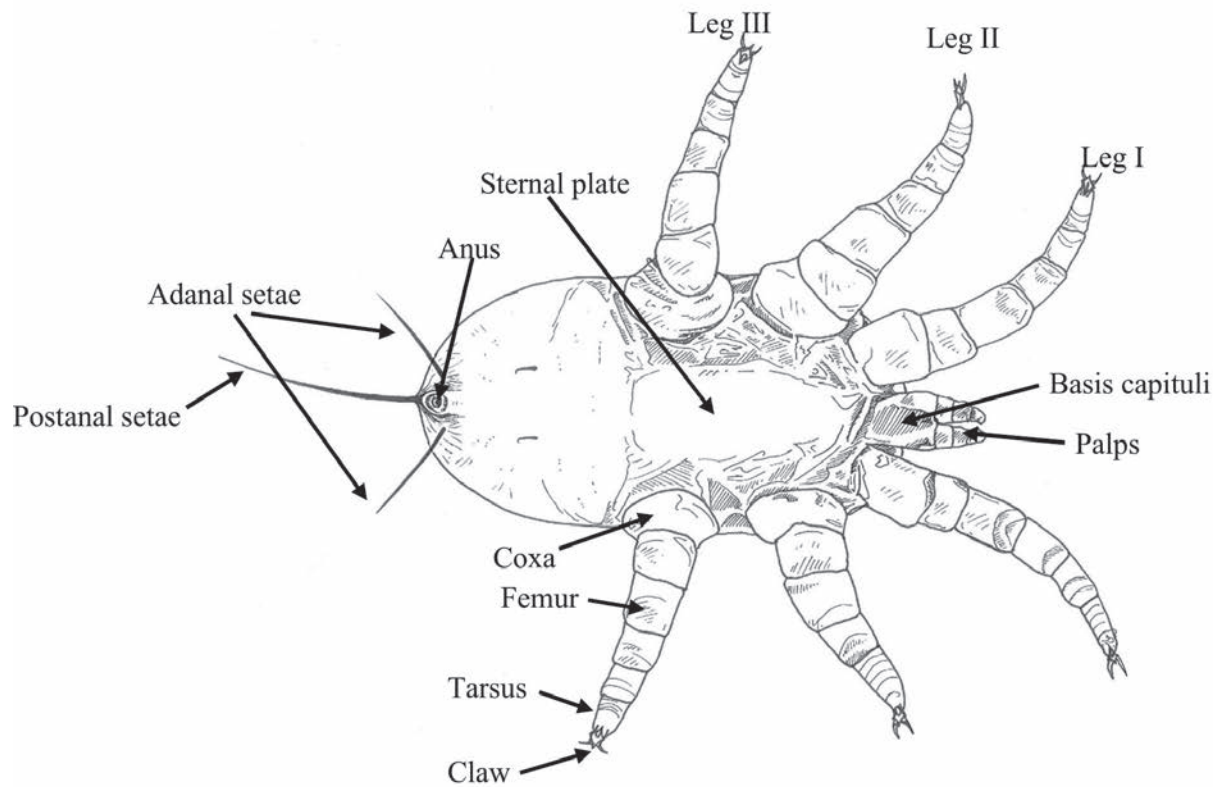


Figure 2. Key distinguishing morphological features of adult nasal mites (Halarachnidae).

H. halichoeri larvae ventral view:



H. halichoeri larvae dorsal view:

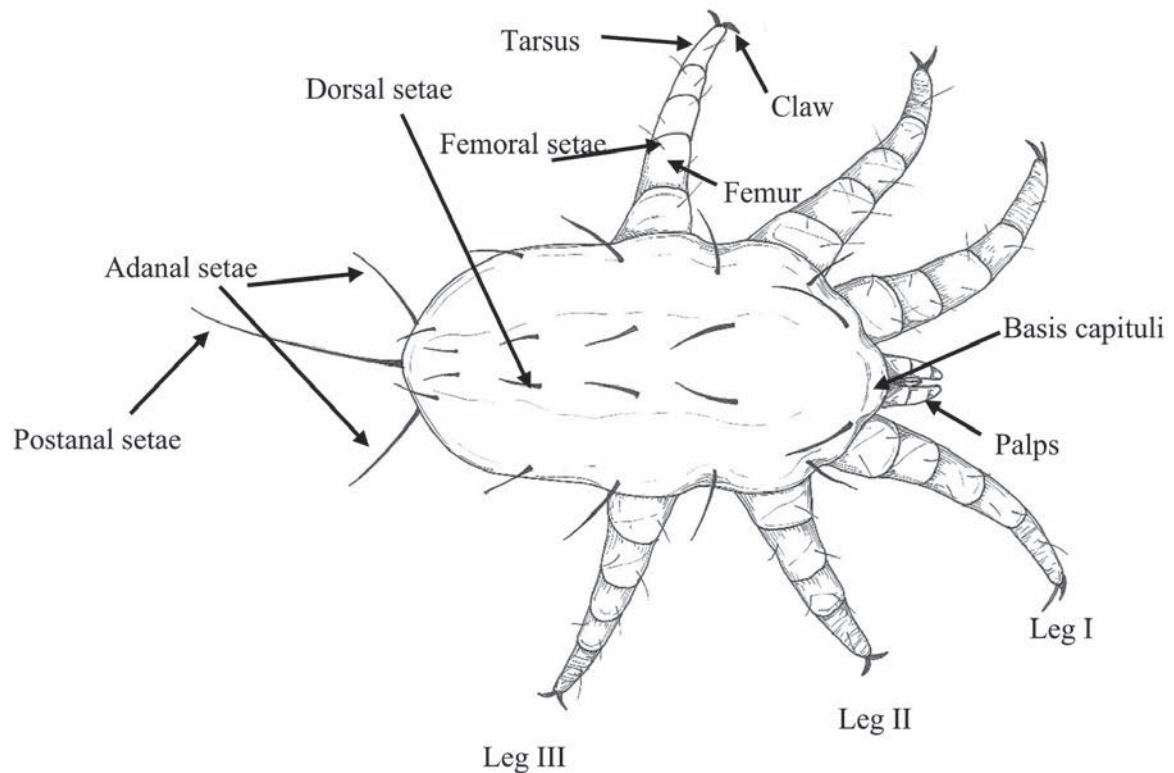


Figure 3. Key distinguishing morphological features of larval nasal mites (Halarachnidae).

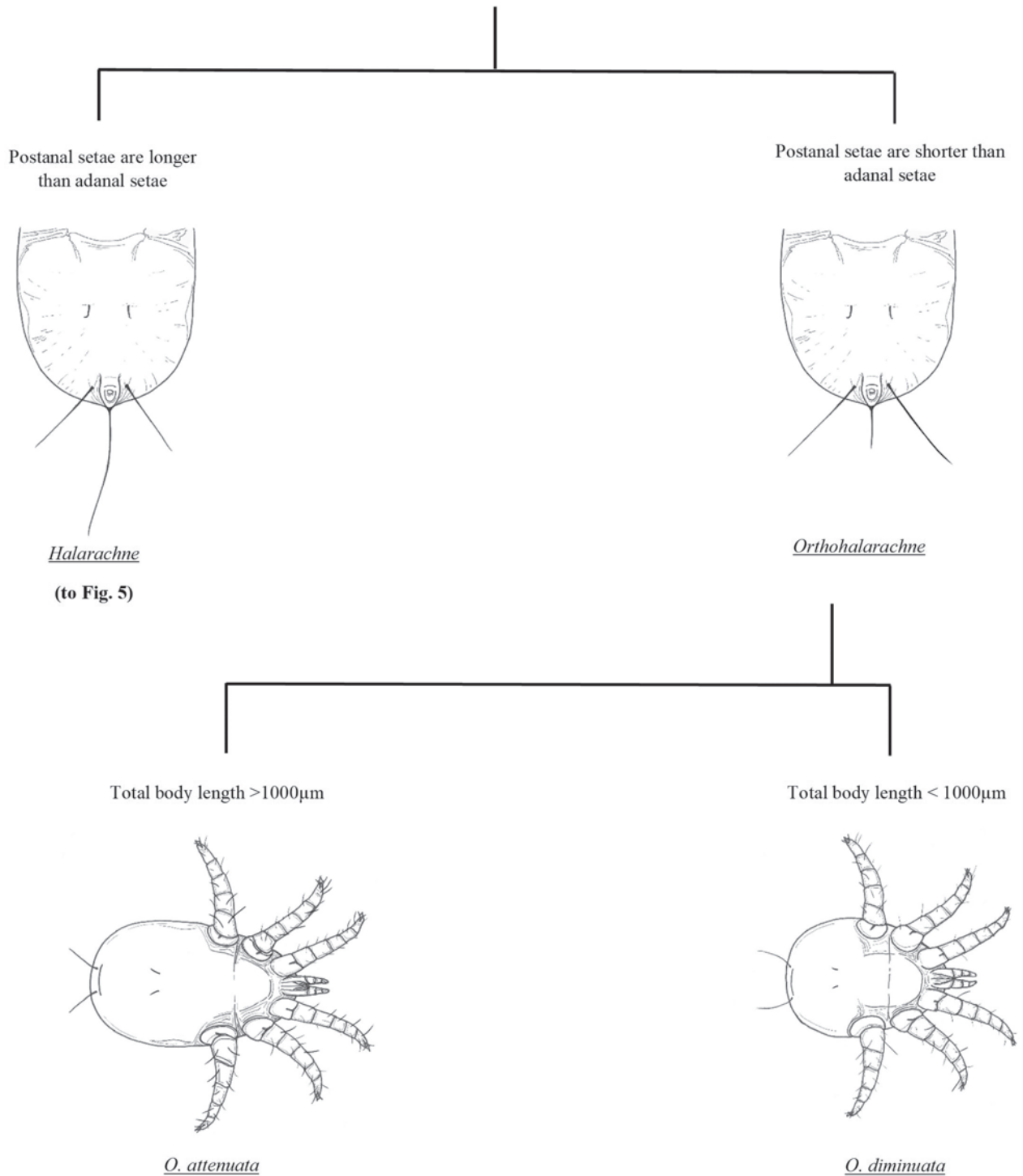
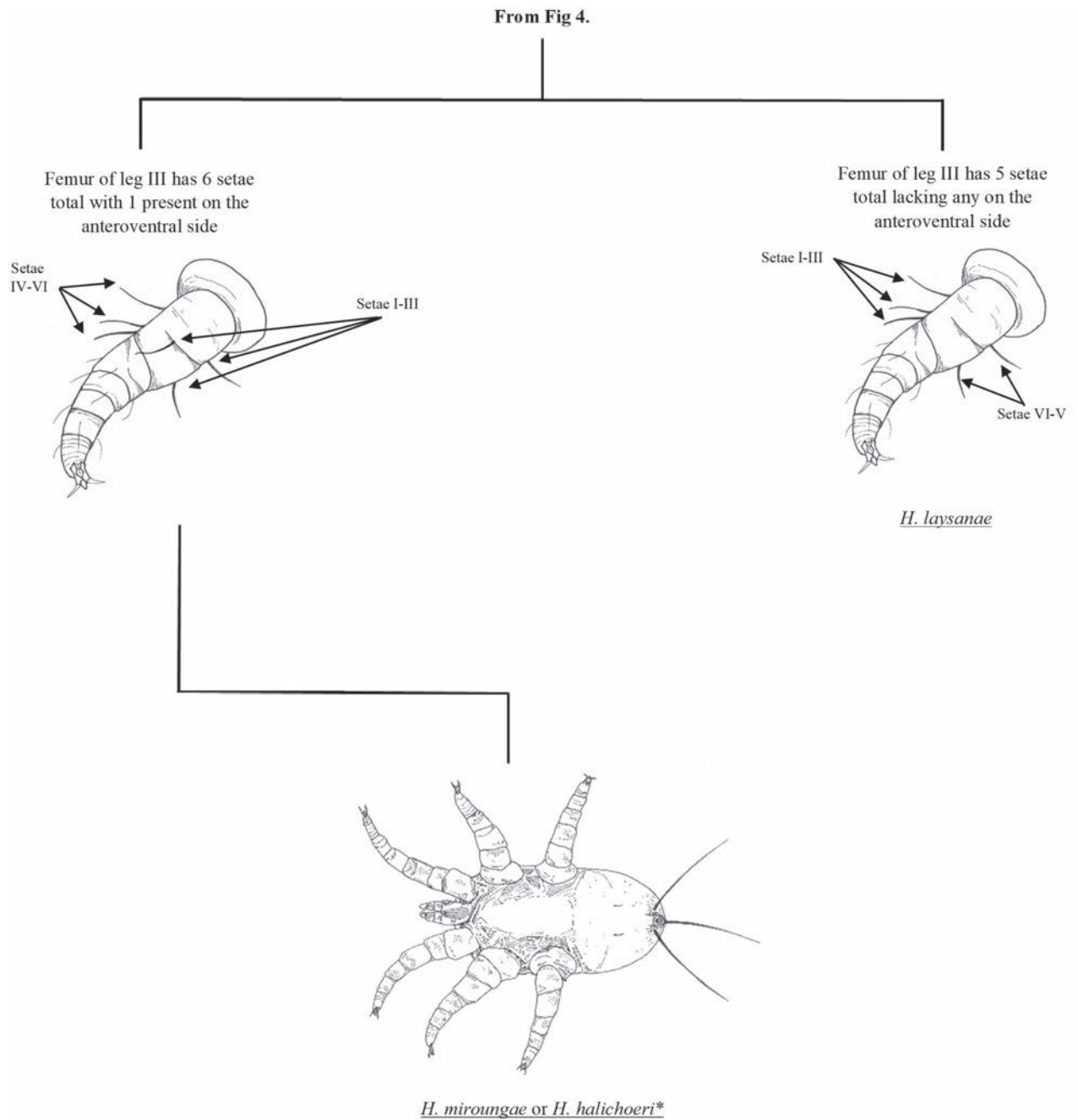


Figure 4. Pictorial key to the larval nasal mites (Halarachnidae) of marine mammals. Larvae are distinguishable from adult mites by the presence of six legs.



*Currently indistinguishable based on available specimens. Anecdotally *H. miroungae* may have longer postanal and adanal setae (>1000µm and >790µm long respectfully) compared to *H. halichoeri* (~632µm and ~376µm long). However this trait has been reported as variable by Furman and Dailey (1980) and without adequate numbers of larval stages for direct comparison this trait cannot confidently be used to distinguish the two.

Figure 5. Pictorial key to the larval nasal mites (Halarachnidae) of marine mammals. Larvae are distinguishable from adult mites by the presence of six legs.

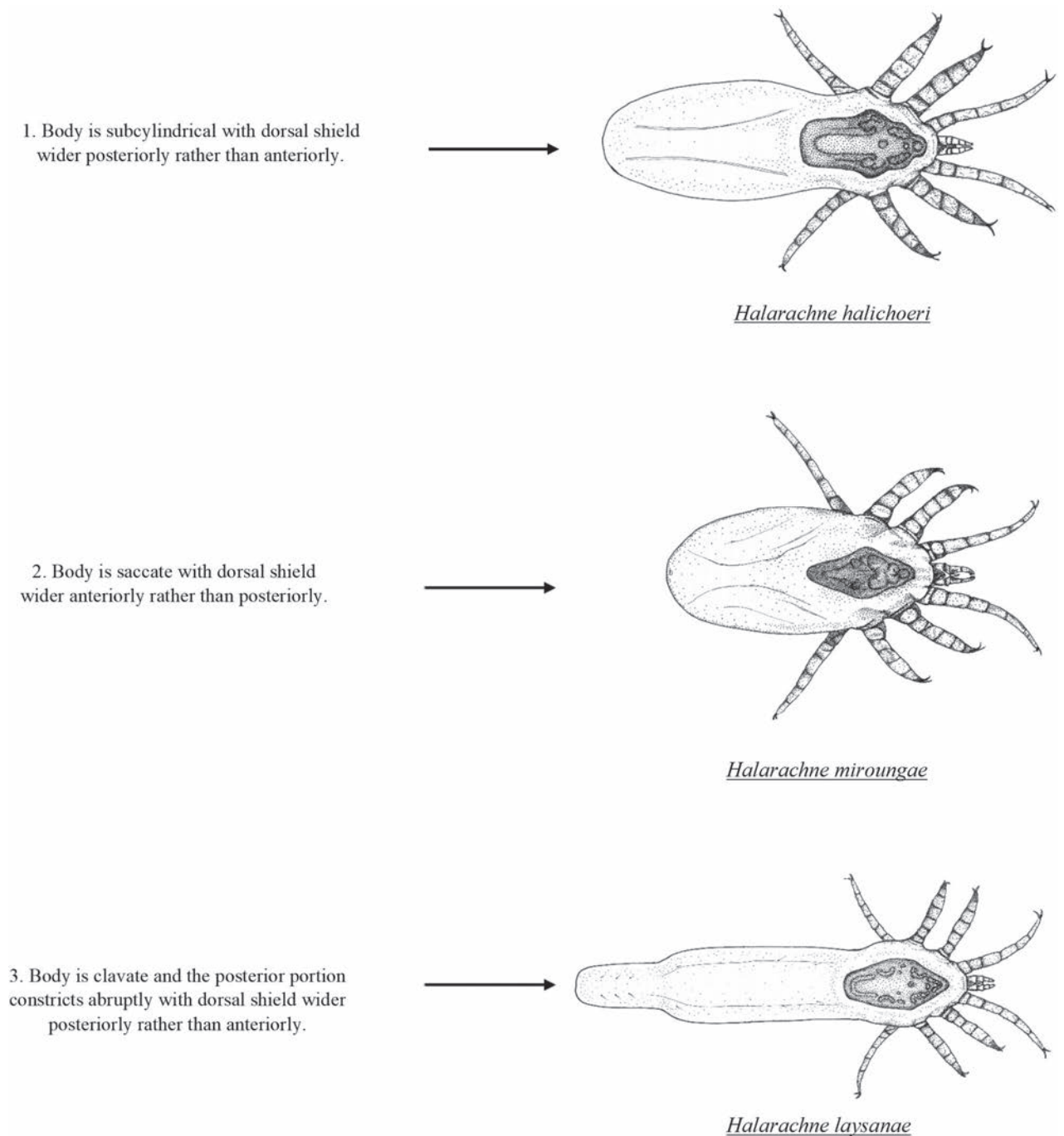


Figure 6. Pictorial key to the adult nasal mites (Halarachnidae) of marine mammals. Adult mites are distinguishable from the larval stage by the presence of eight legs.

Discussion

Adult halarachnid have distinct differences in body and dorsal shield shape making differentiation (particularly between genera) straightforward in this pictorial key. Adult *H. halichoeri* and *H. miroungae* share very similar morphology with two notable differences: *H. miroungae* opisthosoma (posterior end of the body) is more saccate (sack-like) than the subcylindrical (cigar-like) opisthosoma of *H. halichoeri* and the posterior portion of the dorsal shield of *H. halichoeri* is blunt and wider than the anterior portion, whereas in *H. miroungae* the posterior portion

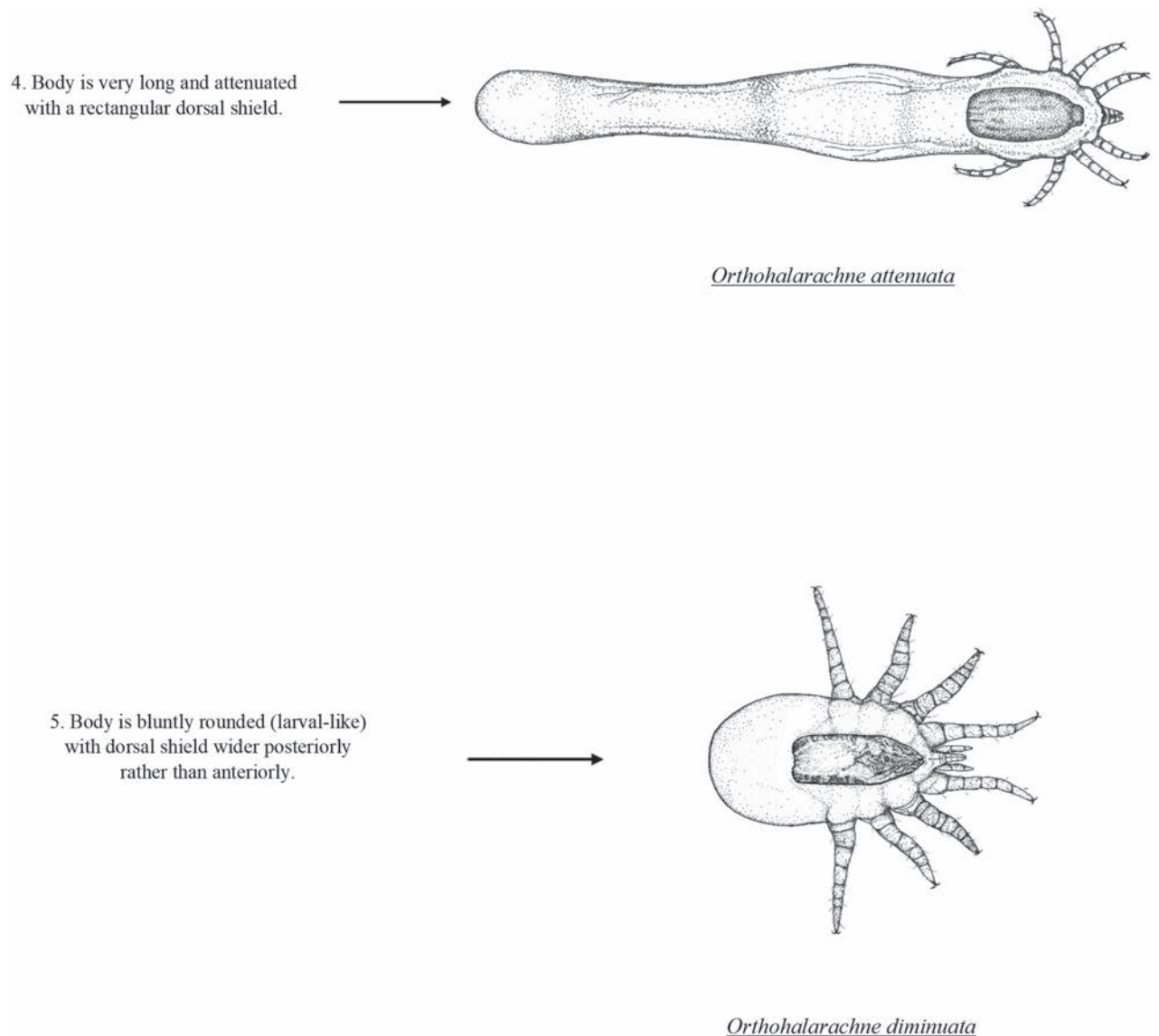


Figure 6. Continued.

of the dorsal shield is pointed and narrower than the anterior portion. Adult *O. attenuata* are the most readily identified of the halarachnid mites because of their long opisthosoma that attenuates (becomes narrower) anteriorly to posteriorly. In contrast, the bluntly elliptical (rounded) opisthosoma of *O. diminuata* mimics the larval body form. Few images of well-preserved *O. diminuata* exist in the literature, making some features challenging to distinguish. For example, in Gastal et al. (2016) the shape of the dorsal shield was not well defined. The dorsal shield illustrations for *O. diminuata* included in this pictorial key are based on LM of our archival specimens, which agree with the shape depicted in Ebmer et al. (2022).

Identification of juvenile halarachnid mites is more challenging than adults. Larvae can be reliably identified to genus, but *H. miroungae* and *H. halichoeri* cannot be conclusively determined based on the current literature. While *H. miroungae* often has longer postanal and adanal setae compared to *H. halichoeri*, Furman and Dailey (1980) noted that this may be a variable characteristic, and we did not have larvae of *H. miroungae* in our archive for direct comparison. We have decided to forego using this feature in our key as a probable distinction

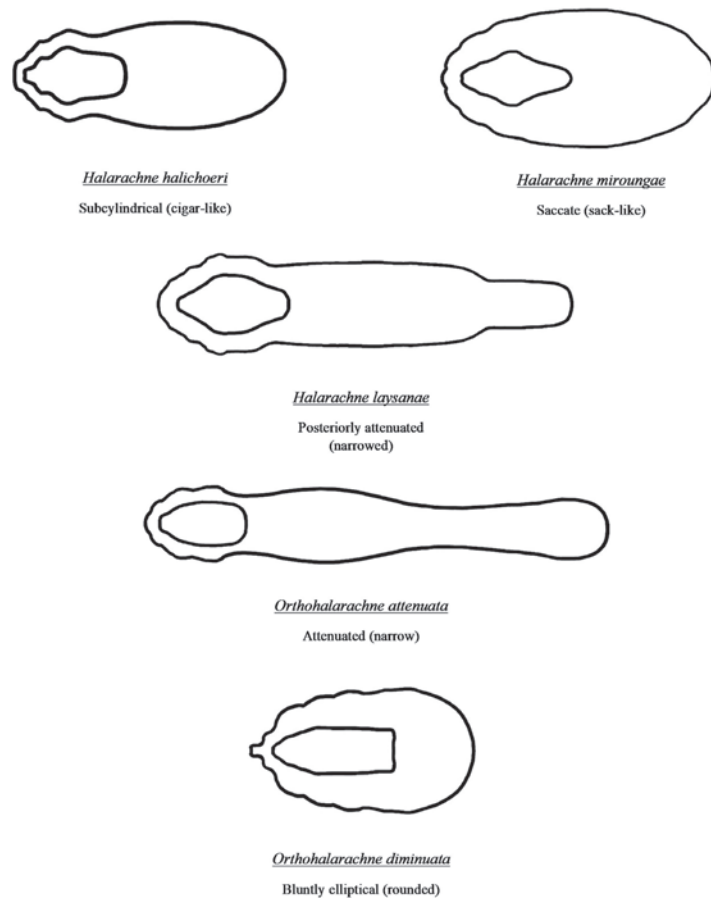


Figure 7. Body and dorsal shield outlines for simplified identification of adult halarachnids (anterior to the left, posterior to the right).

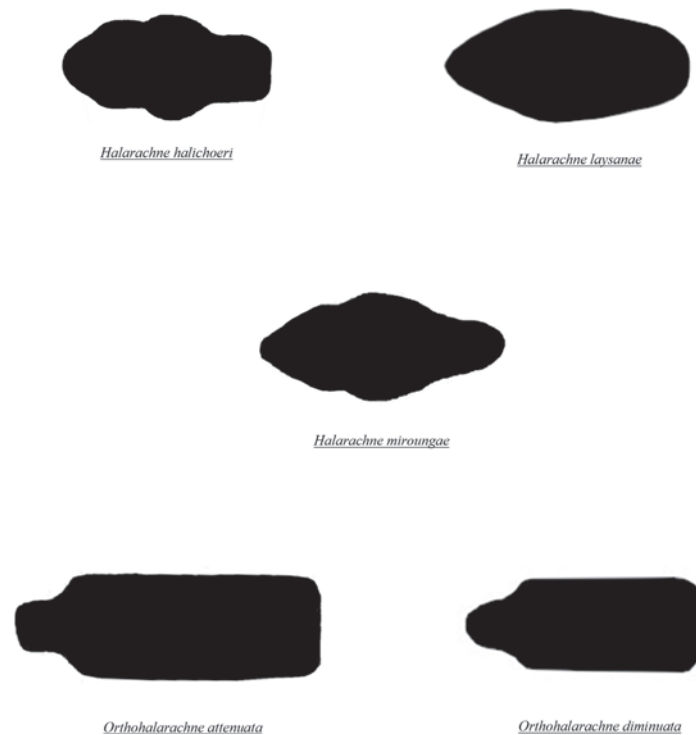


Figure 8. Dorsal shield shapes of adult halarachnids (anterior to the left, posterior to the right).

between the two species as we note that a morphometric study of large sample sizes of both *Halarachne* species larvae is needed to confirm whether this characteristic is consistent enough for reliable species differentiation. Nymphal stages of halarachnid mites of either genus are rarely seen because these stages are teneral and of very short duration making them challenging for taxonomic identification by non-experts. For this reason, we have not included them in our pictorial key and recommend these specimens always be reviewed by an expert.

Halarachnid mites exhibit varying degrees of host specificity. Genus *Halarachne* infests primarily phocids and mustelids, while genus *Orthohalarachne* infests primarily otariids and odobenids (Rolbiecki et al. 2018; Pesapane et al. 2021). Within the genus *Halarachne*, *H. halichoeri* infests primarily harbor seals (*Phoca vitulina* (Linnaeus, 1758)) and sea otters (*Enhydra lutris* (Linnaeus, 1758)), while *H. miroungae* infests elephant seals (*Mirounga* spp. Gray, 1827), harbor seals, and sea otters (Fay and Furman 1982; Pesapane et al. 2018; Rolbiecki et al. 2018). The third species of this genus, *H. laysanae*, has only been found to infest Hawaiian monk seals (*Neomonachus schauinslandi* (Matschie, 1905)) (Fay and Furman 1982). Within genus *Orthohalarachne*, *O. attenuata* primarily infests northern fur seals (*Callorhinus ursinus* (Linnaeus, 1758)), Cape fur seals (*Arctocephalus pusillus* (Schreber, 1775)), California sea lions (*Zalophus californianus* (Lesson, 1828)), Guadalupe fur seals (*Arctocephalus townsendi* (Merriam, 1897)), and walrus (*Odobenus rosmarus* (Linnaeus, 1758)), while *O. diminuta* infests Stellar sea lions (*Eumetopias jubata* (Schreber, 1776)), California sea lions, cape fur seals, and northern fur seals (Furman and Dailey 1980; Kim et al. 1980; Rolbiecki et al. 2018; Ebmer et al. 2022).

Although a relatively high degree of host specificity is a hallmark of the family Halarachnidae, some species may share hosts with other halarachnids. For example, *H. halichoeri* has been found to occasionally infest spotted seals (*Phoca largha* Pallas, 1811), hooded seals (*Cystophora cristata* (Erxleben, 1777)), California sea lions, and southern elephant seals (*Mirounga leonine* (Linnaeus, 1758)) (Rolbiecki et al. 2018). Accidental host spillover events have also been reported. *Halarachne halichoeri* was found in a captive Gentoo penguin (*Pygoscelis papua* (Forster, 1781)) (Rolbiecki et al. 2018) and has been reported co-infesting a northern elephant seal (*Mirounga angustirostris* (Gill, 1866)) along with *H. miroungae* (Pesapane et al. 2021). *Orthohalarachne attenuata* and *O. diminuta* may co-infest cape fur seals, California sea lions, northern fur seals, and Stellar sea lions (Rolbiecki et al. 2018). Additionally, *O. attenuata* was recently identified as the first reported nasopulmonary mite infestation in the threatened Guadalupe fur seal, suggesting it may infest additional host species outside of those reported (Pesapane et al. 2021).

The host specificity of halarachnid mites may be a product of host behavior (such as dive depth) and anatomical adaptations. For example, *H. halichoeri* employs the use of a reinforced elastic tracheal trunk that can stay open at depths of 30–40 m (Pugh 1996a), whereas it is unlikely that *H. miroungae* employs the same methods, as the host it parasitizes often frequent depths of 300–400 m and the pressure at that depth would be too high for the tunica intima to hold the airway open (Pugh 1996a). This may explain why *H. halichoeri* seems to prefer shallow divers such as sea otters and harbor seals (Pesapane et al. 2018; Reckendorf et al. 2019). Generalist *Halarachne* larvae, unlike other

acarids, do not seem to possess the olfactory chemoreceptors or sensilla required to distinguish between host species (Pugh 1996b). It is possible that such structures are not required as their hosts tend to form large rookeries, making it likely that larvae will come into contact primarily with conspecific hosts (Pugh 1996b).

The ecology of halarachnid mites and their effect on their associated host species can only be described through correct taxonomic identification. We have attempted to unite the myriad verbal descriptions, images, and revisionist publications of these genera into a single taxonomic key. This is an understudied group of organisms that may reveal interesting adaptations and behaviors to cope with changes in pressure, blood flow, temperature, or other environmental stresses. The accurate identification of these species is necessary to enable future behavioral and ecological research.

Conclusion

The taxonomy of halarachnid mites has been subject to numerous revisions, and some publications on host associations have been controversial. Although some halarachnid species are readily distinguished, species within *Halarachne* are morphologically very similar, with only slight differences in the shape of certain attributes such as the dorsal shield or opisthosoma. Existing keys are numerous, frequently focus on a single genus or species, and contain relative comparisons like “more saccate” or “more subcylindrical”, which are difficult because they are subjective, and accuracy of species identification is best done via direct comparison. In this key, we compile all current taxonomic characteristics for species differentiation for both genera into a singular key with accompanying illustrations to aid in the easy and accurate identification of halarachnid mites in marine mammal hosts.

Misidentification of parasites has become a major issue (Bush et al. 2021), and this may lead to further errors in disease treatment and management, complicating animal recovery (Laga et al. 2021). This key will enable accurate halarachnid mite identification among experts and non-experts alike and can help alleviate some of the underlying drivers of misidentification. Improved accuracy and reporting of halarachnid mite infestations will also contribute to ongoing efforts to understand host–parasite relationships, managing mites in captive marine mammal populations, and evaluating the impact of mite infestations on wild populations.

Acknowledgements

We thank our collaborators at the California Department of Fish and Wildlife Marine Wildlife Veterinary Care and Research Center, The Marine Mammal Center, and the National Marine Life Center for providing the mite specimens examined in this work.

Additional information

Conflict of interest

The authors have declared that no competing interests exist.

Ethical statement

No ethical statement was reported.

Funding

Acquisition of specimens was supported by the Sea Otter Foundation and Trust (<https://seaotterfoundationtrust.org/>). M.S. was supported by the Boehringer Ingelheim Veterinary Scholars Program. R.P. received funding from The Ohio State University College of Veterinary Medicine (<https://vet.osu.edu/>) and the College of Food, Agricultural, and Environmental Sciences (<https://cfaes.osu.edu/>).

Author contributions

Conceptualization: MMS, RP. Data curation: MMS, TR. Formal analysis: MMS. Funding acquisition: RP. Investigation: MMS. Methodology: TR, RP, MMS. Project administration: MMS. Resources: MMS. Supervision: RP. Visualization: TR. Writing - original draft: MMS. Writing - review and editing: RP, TR, MMS.

Author ORCIDs

Morgan M. Shields  <https://orcid.org/0009-0006-9268-413X>

Tara Roth  <https://orcid.org/0000-0002-6046-0653>

Risa Pesapane  <https://orcid.org/0000-0001-9318-9911>

Data availability

All of the data that support the findings of this study are available in the main text.

References

- Alonso-Farré JM, D'Silva JD, Gestal C (2012) Naso-pharyngeal mites *Halarachne halichoeri* (Allman, 1847) in grey seals stranded on the NW Spanish Atlantic coast. *Veterinary Parasitology* 183: 317–322. <https://doi.org/10.1016/j.vetpar.2011.08.002>
- Baker JR (1987) Causes of mortality and morbidity in wild juvenile and adult grey seals (*Halichoerus grypus*). *British Veterinary Journal* 143: 203–220. [https://doi.org/10.1016/0007-1935\(87\)90083-2](https://doi.org/10.1016/0007-1935(87)90083-2)
- Bush SE, Gustafsson DR, Tkach VV, Clayton DH (2021) A misidentification crisis plagues specimen-based research: a case for guidelines with a recent example (Ali et al., 2020). *The Journal of Parasitology* 107: 262–266. <https://doi.org/10.1645/21-4>
- Dent CES, Miller MA, Batac F, Dodd E, Smith W, Pesapane R, Foley J (2019) Pathology and epidemiology of nasopulmonary acariasis (*Halarachne* sp.) in southern sea otters (*Enhydra lutris nereis*). *International Journal for Parasitology: Parasites and Wildlife* 9: 60–67. <https://doi.org/10.1016/j.ijppaw.2019.03.009>
- Domrow R (1962) *Halarachne miroungae* Ferris redescribed. *Pacific Insects* 4: 859–863. <https://archive.org/details/pacific-insects-4-859>
- Domrow R (1974) Notes on halarachnine larval morphology and a new species of *Pneumonyssus* Banks (Acari: Dermanyssidae). *Australian Journal of Entomology* 13: 17–26. <https://doi.org/10.1111/j.1440-6055.1974.tb02286.x>
- Dunlap JS, Piper RC (1976) Lesions associated with *Orthohalarachne attenuata* (Halarachnidae) in the northern fur seal (*Callorhinus ursinus*). *Journal of Wildlife Diseases* 12: 42–44. <https://doi.org/10.7589/0090-3558-12.1.42>
- Ebmer D, Kniha E, Strauss V, Kübber-Heiss A, Komornik L, Balfanz F, Hering-Hagenbeck S, Walochnik J, Gärtner U, Prosl H, Taubert A, Voracek T, Hermosilla C (2022) First

- report of a severe nasopulmonary acariasis caused by *Orthohalarachne diminuata* Doetschman, 1944 (Acari: Halarachnidae) in a captive South American sea lion (*Otaria flavescens* Shaw, 1800). *International Journal for Parasitology: Parasites and Wildlife* 19: 248–256. <https://doi.org/10.1016/j.ijppaw.2022.10.005>
- Fay FH, Furman DP (1982) Nasal mites (Acari: Halarachnidae) in the spotted seal, *Phoca largha* Pallas, and other pinnipeds of Alaskan waters. *Journal of Wildlife Diseases* 18: 63–68. <https://doi.org/10.7589/0090-3558-18.1.63>
- Furman DP, Dailey MD (1980) The genus *Halarachne* (Acari: Halarachnidae), with the description of a new species from the Hawaiian monk seal. *Journal of Medical Entomology* 17: 352–359. <https://doi.org/10.1093/jmedent/17.4.352>
- Furman DP, Smith AW (1973) In vitro development of two species of *Orthohalarachne* (Acarina: Halarachnidae) and adaptations of the life cycle for endoparasitism in mammals. *Journal of Medical Entomology* 10: 415–416. <https://doi.org/10.1093/jmedent/10.4.415>
- Gastal SB, Mascarenhas CS, Ruas JL (2016) Infection rates of *Orthohalarachne attenuata* and *Orthohalarachne diminuata* (Acari: Halarachnidae) in *Arctocephalus australis* (Zimmermann, 1783) (Pinnipedia: Otariidae). *Comparative Parasitology* 83: 245–249. <https://doi.org/10.1654/4797s.1>
- Kenyon KW (1977) Caribbean Monk seal extinct. *Journal of Mammalogy* 58: 97–98. <https://doi.org/10.2307/1379738>
- Kim KC, Haas VL, Keyes MC (1980) Populations, microhabitat preference and effects of infestation of two species of *Orthohalarachne* (Halarachnidae: Acarina) in the northern fur seal. *Journal of Wildlife Diseases* 16: 45–51. <https://doi.org/10.7589/0090-3558-16.1.45>
- Laga AC, Granter SR, Mather TN (2021) Proficiency at tick identification by pathologists and clinicians is poor. *The American Journal of Dermatopathology* 44: 111–114. <https://doi.org/10.1097/DAD.0000000000001977>
- Pesapane R, Dodd E, Javeed N, Miller M, Foley J (2018) Molecular characterization and prevalence of *Halarachne halichoeri* in threatened southern sea otters (*Enhydra lutris nereis*). *International Journal for Parasitology: Parasites and Wildlife* 7: 386–390. <https://doi.org/10.1016/j.ijppaw.2018.09.009>
- Pesapane R, Archibald W, Norris T, Fontaine C, Halaska B, Duignan P, Javeed N, Miller M, Foley J (2021) Nasopulmonary mites (Halarachnidae) of coastal Californian pinnipeds: identity, prevalence, and molecular characterization. *International Journal for Parasitology: Parasites and Wildlife* 16: 113–119. <https://doi.org/10.1016/j.ijppaw.2021.08.005>
- Pugh PJA (1996a) The respiratory system of *Halarachne halichoeri* (Halarachnidae: Gamasida: Anactinotrichida). *Journal of Zoology* 239: 285–300. <https://doi.org/10.1111/j.1469-7998.1996.tb05452.x>
- Pugh PJA (1996b) The structure and function of the tarsus I sensillar field in mites of the genus *Halarachne* (Halarachnidae: Gamasida). *Journal of Natural History* 30: 1069–1086. <https://doi.org/10.1080/00222939600770571>
- Reckendorf A, Wohlsein P, Lakemeyer J, Stokholm I, von Vietinghoff V, Lehnert K (2019) There and back again—the return of the nasal mite *Halarachne halichoeri* to seals in German waters. *International Journal for Parasitology: Parasites and Wildlife* 9: 112–118. <https://doi.org/10.1016/j.ijppaw.2019.04.003>
- Rolbiecki L, Izdebska JN, Bidziński K, Jankowska-Jarek M (2018) Nasopharyngeal mites *Halarachne halichoeri* (Allman, 1847) parasitizing the gray seal *Halichoerus grypus* (Fabricius, 1791) in the Baltic Sea with notes on other parasitic Halarachnidae associated with marine mammals. *Oceanological and Hydrobiological Studies* 47: 398–404. <https://doi.org/10.1515/ohs-2018-0037>

First contribution to the genera *Branchiobaetis* and *Megabranchiella* (Ephemeroptera, Baetidae) in China, with descriptions of two new species

Xiaoli Tong¹, Zhiheng Zhou¹, Bangyi Wu¹

¹ Department of Entomology, College of Plant Protection, South China Agricultural University, Guangzhou 510642, Guangdong Province, China
Corresponding author: Xiaoli Tong (xtong@scau.edu.cn)

Abstract

Branchiobaetis Kaltenbach, Kluge & Gattolliat, 2022 and *Megabranchiella* Phlai-ngam & Tungpairajwong, 2022 (Ephemeroptera: Baetidae) are newly recorded in China. Two new species, *Branchiobaetis borealis* **sp. nov.** based on larval stage and *Branchiobaetis megasinus* **sp. nov.** based on larval and imaginal stages associated by laboratory rearing, are described. *Megabranchiella longusa* Phlai-ngam & Tungpairajwong, 2022, previously only distributed from Thailand, is recorded from China for the first time.

Key words: Baetid, mayflies, new record, Southeast Asia, subtropical China

Introduction

The family Baetidae is ubiquitous in freshwater habitats with the highest species diversity amongst mayflies, often being a major benthic component of freshwater ecosystems (Barber-James et al. 2008; Jacobus et al. 2019). It is almost worldwide distributed but is mostly diversified in the tropics (Gattolliat and Nieto 2009; Kaltenbach et al. 2022a, b). Southeast Asia, known for its expanses of tropical rainforests and river systems representing one of the most biologically diverse ecosystems on the Earth, harbours a unique and diverse mayfly fauna, which is one of the most species-rich hotspots of mayflies at the global scale (Gattolliat and Nieto 2009; Kaltenbach et al. 2023a). For a long time, however, systematics of mayflies (Baetidae in particular) has received little attention by taxonomists compared with those from Europe and North America. Although many Ephemeroptera taxonomists, such as Ulmer (1939), Kimmins (1947), Gillies (1949, 1951), and Müller-Liebenau (1980, 1981, 1984a, b) have made great contributions to the study of baetid fauna in the region, the knowledge of the baetid systematics is still sparse (Gattolliat and Nieto 2009), and baetid species diversity of Southeast Asia is under severe threat of extinction because of rapid economic development and urbanization. Encouragingly, significant progress has been made in baetid systematics in the region during the past decade or so. A large number of new genera and species of Baetidae have emerged like mushrooms after spring rain in Southeast Asia and its neighbouring areas. For example, eight new genera were established, *Asiobaetodes*



Academic editor: Ben Price
Received: 15 June 2024
Accepted: 15 September 2024
Published: 23 October 2024

ZooBank: <https://zoobank.org/2312FE20-8C12-48B2-8D97-CFC920CCF5C2>

Citation: Tong X, Zhou Z, Wu B (2024) First contribution to the genera *Branchiobaetis* and *Megabranchiella* (Ephemeroptera, Baetidae) in China, with descriptions of two new species. ZooKeys 1216: 115–148. <https://doi.org/10.3897/zookeys.1216.129803>

Copyright: © Xiaoli Tong et al.
This is an open access article distributed under terms of the Creative Commons Attribution License (Attribution 4.0 International – CC BY 4.0).

Gattolliat (in Gattolliat 2012), *Acerobiella* Gattolliat (in Gattolliat 2012), *Procerobaetis* Kaltenbach & Gattolliat (in Kaltenbach et al. 2020b), *Cymbalocloeon* Suttinun, Gattolliat & Boonsong (in Suttinun et al. 2020), *Philibaetis* Kaltenbach & Gattolliat (in Kaltenbach et al. 2021), *Branchiobaetis* Kaltenbach, Kluge & Gattolliat (in Kaltenbach et al. 2022b), *Megabranchiella* Phlai-ngam & Tungpaiojwong (in Phlai-ngam et al. 2022), *Arcobaetis* Kaltenbach, Kluge & Gattolliat (in Kaltenbach et al. 2023a), and dozens of new baetid species were described (e.g. Tong and Dudgeon 1999, 2021; Kluge and Novikova 2011, 2017; Gattolliat 2012; Shi and Tong 2014, 2015a, b, 2019; Tong et al. 2014; Kaltenbach and Gattolliat 2018, 2019, 2020, 2021, 2023; Kaltenbach et al. 2020a, 2023b; Kluge and Suttinun 2020; Suttinun et al. 2021, 2022; Li et al. 2023).

The baetid fauna of South China and Southwest China (e.g., Guangdong, Hong Kong, Hainan, Guangxi, Yunnan) shows important affinities with those of the mainland Southeast Asia and even share many baetid taxa with the insular Southeast Asia (Tong and Dudgeon 2002; Shi and Tong 2014, 2015a, b, 2019). In our present surveys, two genera of Baetidae, formerly described only from Southeast Asia, are newly recorded from China, i.e., the genus *Branchiobaetis*, recently established by Kaltenbach et al. (2022b), is a small genus with seven species and these are previously known only from the archipelagic Southeast Asia (Indonesia, Malaysia, and Philippines); the genus *Megabranchiella* was erected by Phlai-ngam et al. (2022) from Thailand with two species, of which *Megabranchiella longusa* Phlai-ngam & Tungpaiojwong, 2022 is recorded from China for the first time. Here, we describe two new species of *Branchiobaetis* found from Guangdong, Hong Kong, Yunnan, China, and report the new record of *M. longusa* from Yunnan, China.

Materials and methods

The larvae were collected with a D-frame net and then placed into vials containing 90% ethanol in the field, while some living mature larvae with black wing pads were transported to the laboratory in a plastic container containing stream water for rearing. Each reared subimago and imago together with its final instar exuviae and subimaginal skin were stored in a single vial containing 90% ethanol. The larvae were dissected in ethanol under a stereomicroscope, with subsequent mounting on slides by Hoyer's solution. Photographs were taken using a Canon EOS 5D Mark IV camera with MP-E 65 mm macro lens and the microscope with a digital camera attached. Water physicochemical parameters were measured by portable multi-parameter meter (Hach sensION™156) in the field. The distribution map was downloaded from the National Platform for Common GeoSpatial Information Services (<https://www.tianditu.gov.cn/>). Type specimens have been deposited in the Insect Collection, South China Agricultural University (SCAU), Guangzhou, China.

Results

Branchiobaetis borealis sp. nov.

<https://zoobank.org/7E13C47C-A248-40C6-A77E-8F0BBBAEB188>

Figs 1–7

Type material. Holotype. CHINA • male larva in alcohol (mature); Yunnan, Lushui City, Chengan Town, a tributary of the Nujiang River (26.2605°N, 98.8792°E,

altitude 1036 m); 21.iii.2019; leg. Xiaoli Tong. **Paratypes** (in alcohol): • 41 mature larvae (2 on slide), locality and date as holotype, leg. Xiaoli Tong, Lin Hong, Jian Jiang • 10 larvae (1 on slide); Yunnan, Weixi County, Tacheng Town, Lapu River (a tributary of the Jinsha River, 99.3507°E, 27.5728°N, altitude 2523 m); 8.xi.2018; leg. Xiaoli Tong, Lin Hong, Haoyang Chen • 13 larvae (1 on slide), Yunlong County, Caojian Town, a tributary of the Lancang River (25.6339°N, 99.1123°E, altitude 1824 m); 23.iii.2019; leg. Xiaoli Tong, Lin Hong, Jian Jiang.

Description. Mature larva (Fig. 1a–e). Body length (mm): female 7.2–8.5, male larvae slightly shorter than female, 6.0–7.5; antenna 2.0–3.0; cerci 3.0–4.0, paracercus ~ 3/4 length of cerci.

Cuticular colouration. Body mainly creamy yellow with brown maculae dorsally. Vertex and pronotum creamy yellow with irregular brown marks, meso- and metanotum creamy yellow with longitudinal brown streaks. Antennal scape and pedicel mainly off-white, flagellum pale brown. Femur of foreleg mainly off-white with dark brown apex and brown streaks along dorsal and ventral margins; tibia off-white; tarsus off-white with apical 1/2 dark brown; midlegs and hindlegs similar to forelegs in colour pattern. Abdominal tergites cream yellow with contrasting brown maculae as in Fig. 1a–e, tergite hypodermal colour uniformly without maculae or pigmentation (Fig. 7d); sternites with cream shading to pale brown backwardly. Gills white with transparent main trunk and branches of tracheae. Caudalii cream to yellow-brown with brown primary swimming bristles.

Precursors of turbinate eyes in last instar male larvae normal, without elevated area with well-expressed facets.

Antenna (Fig. 1b–e). Antenna ~ 3–4× head width; scape smooth with fine setae sparsely; pedicel surface with fine setae and one row of tiny, rounded setae along distal margin, inner margin with tiny, triangular denticles distolaterally (Fig. 2a).

Labrum (Fig. 2b) nearly rectangular, width/length ratio ~ 1.6; anterior margin bordered with long and feathered setae and a deep notch; dorsally with submedial pair of long, robust bristles and submarginal arc of ~ 5 long, robust bristles on each side of midline, several fine setae scattered proximally; ventral surface with dense, fine setae medially and 6–8 short, pointed setae laterally and disto-laterally.

Left mandible (Fig. 2c). Incisor and kinetodontium fused; incisor with three denticles, kinetodontium with three main denticles decreasing in length and one additional minute denticle between incisor and kinetodontium; prostheca robust, apex with five or six blunt denticles and two or three slender, pointed denticles; margin between prostheca and mola straight; apex of mola without tuft of setae.

Right mandible (Fig. 2d). Incisor and kinetodontium fused; incisor with three denticles; kinetodontium with four denticles, inner margin of innermost denticle with three or four small denticles; prostheca slender with slightly wider base, apex toothbrush-like, with many sharp denticles on inner margin; margin between prostheca and mola slightly concave; apex of mola with a tuft of straight setae.

Hypopharynx and superlinguae (Fig. 4d). Lingua subequal to superlinguae in length, with numerous fine setae apically. Superlinguae distally rounded with numerous fine setae along apical margin.

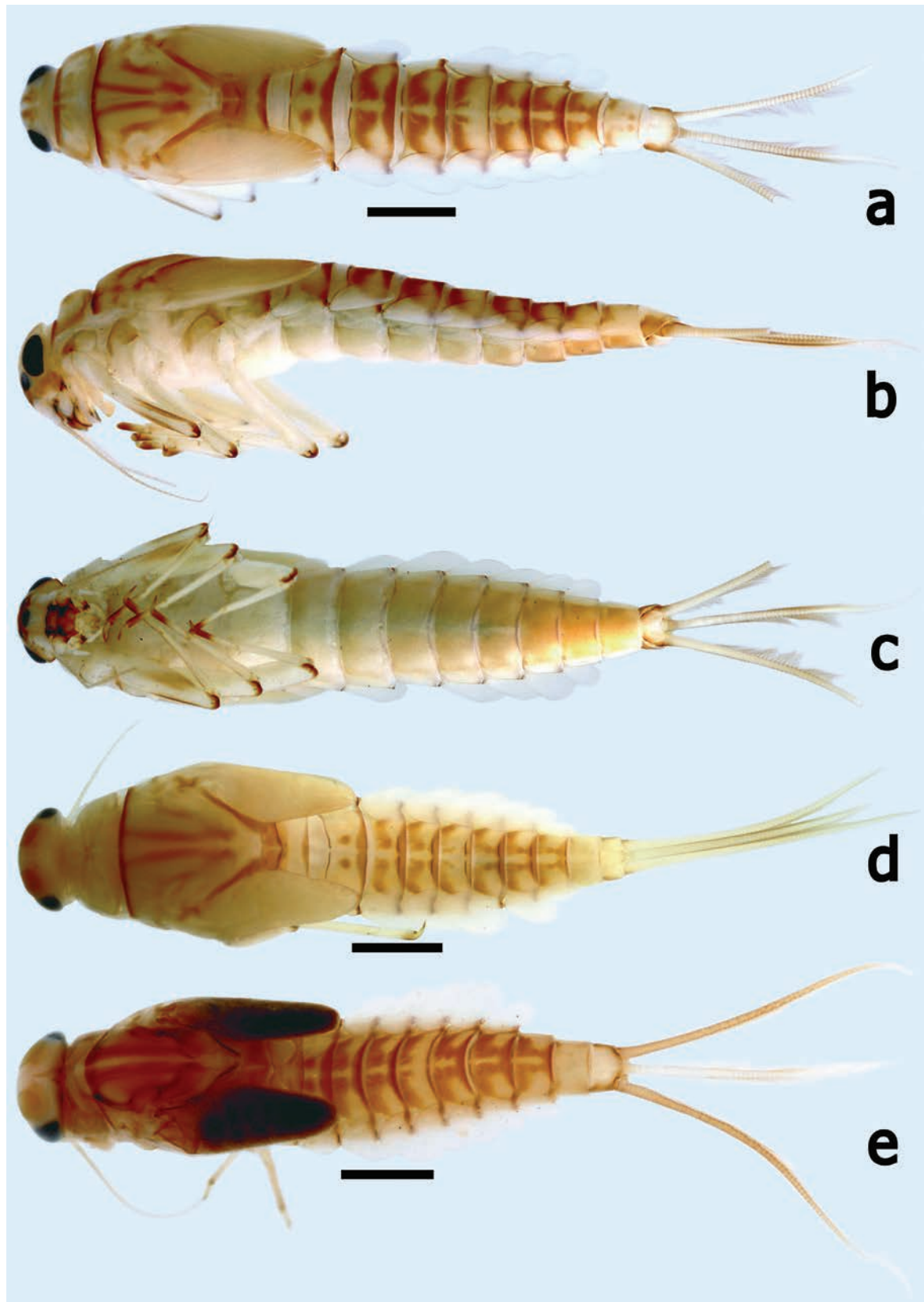


Figure 1. *Branchiobaetis borealis* sp. nov. Larval habitus **a** female larva (dorsal view) **b** female larva (lateral view) **c** female larva (ventral view) **d** male larva (dorsal view) **e** final instar male larva (dorsal view). Scale bars: 1.0 mm.

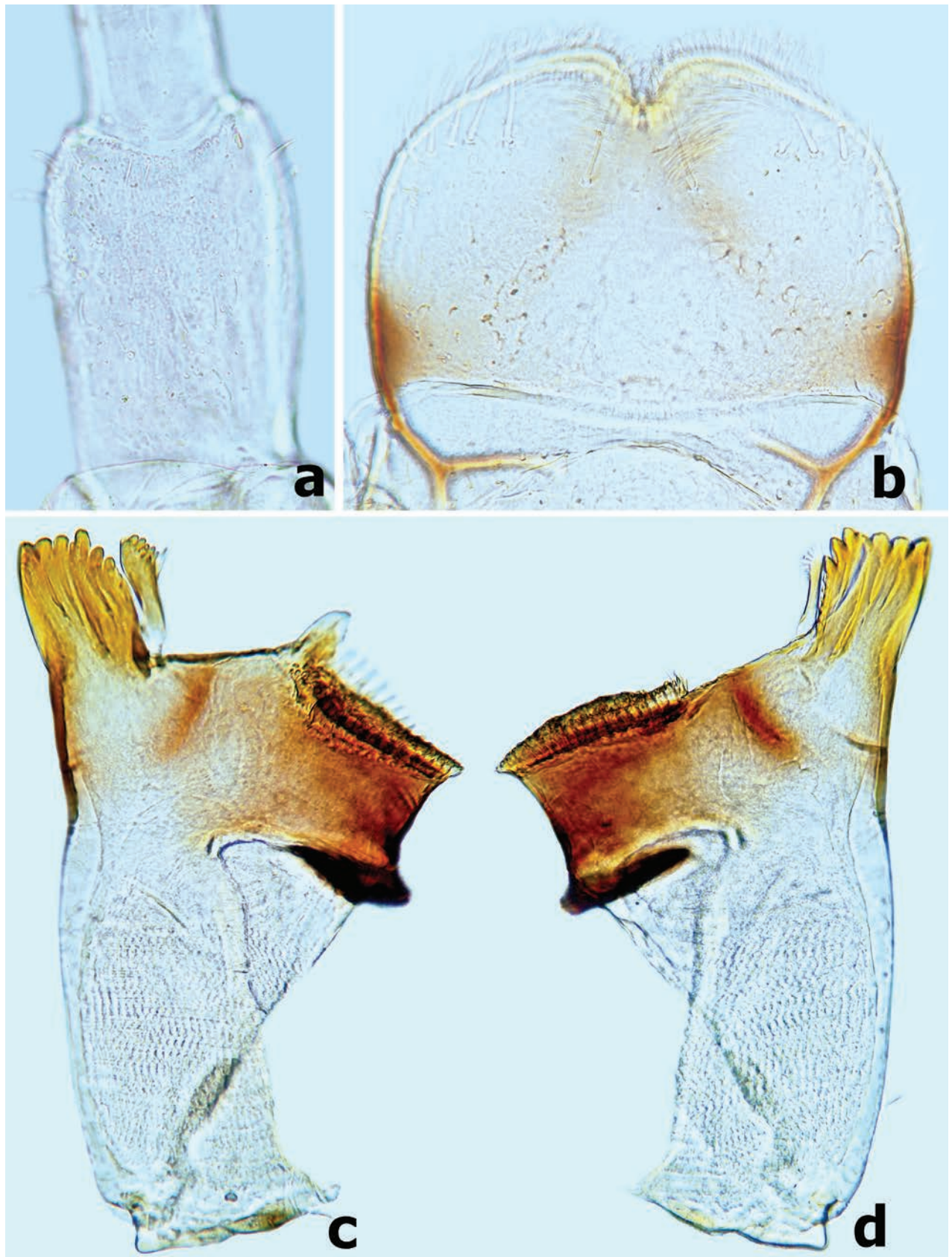


Figure 2. *Branchiobaetis borealis* sp. nov. **a** antennal pedicel **b** labrum **c** left mandible **d** right mandible.

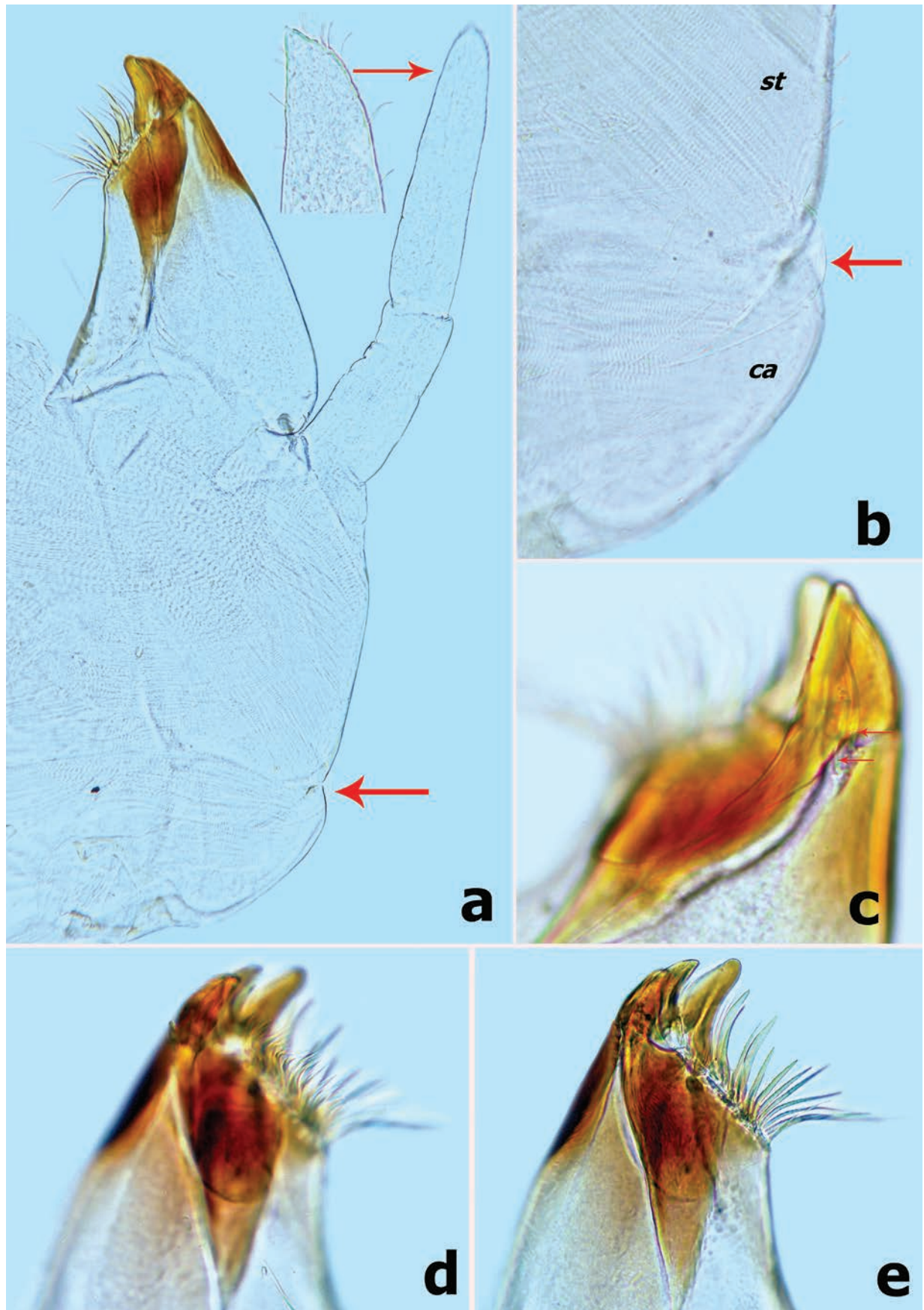


Figure 3. *Branchiobaetis borealis* sp. nov. **a** maxilla **b** accessory gill between stipes and cardo of maxilla **c–e** apex of maxilla. Abbreviations: st: stipes, ca: cardo.

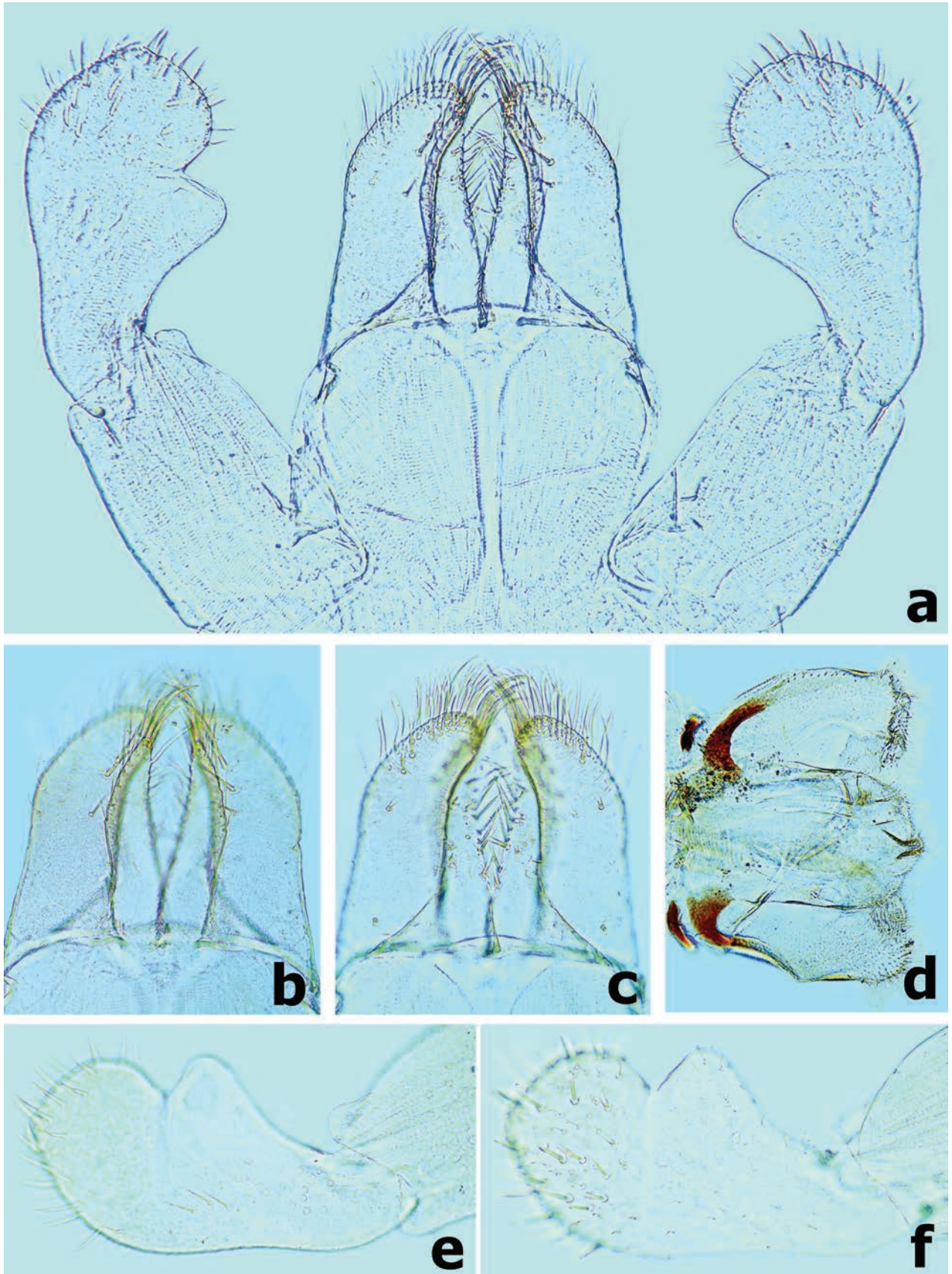


Figure 4. *Branchiobaetis borealis* sp. nov. **a** labium **b** glossae & paraglossae (dorsal view) **c** glossae and paraglossae (ventral view) **d** hypopharynx and superlinguae **e** segments II & III of labial palp (dorsal view) **f** segments II and III of labial palp (ventral view).

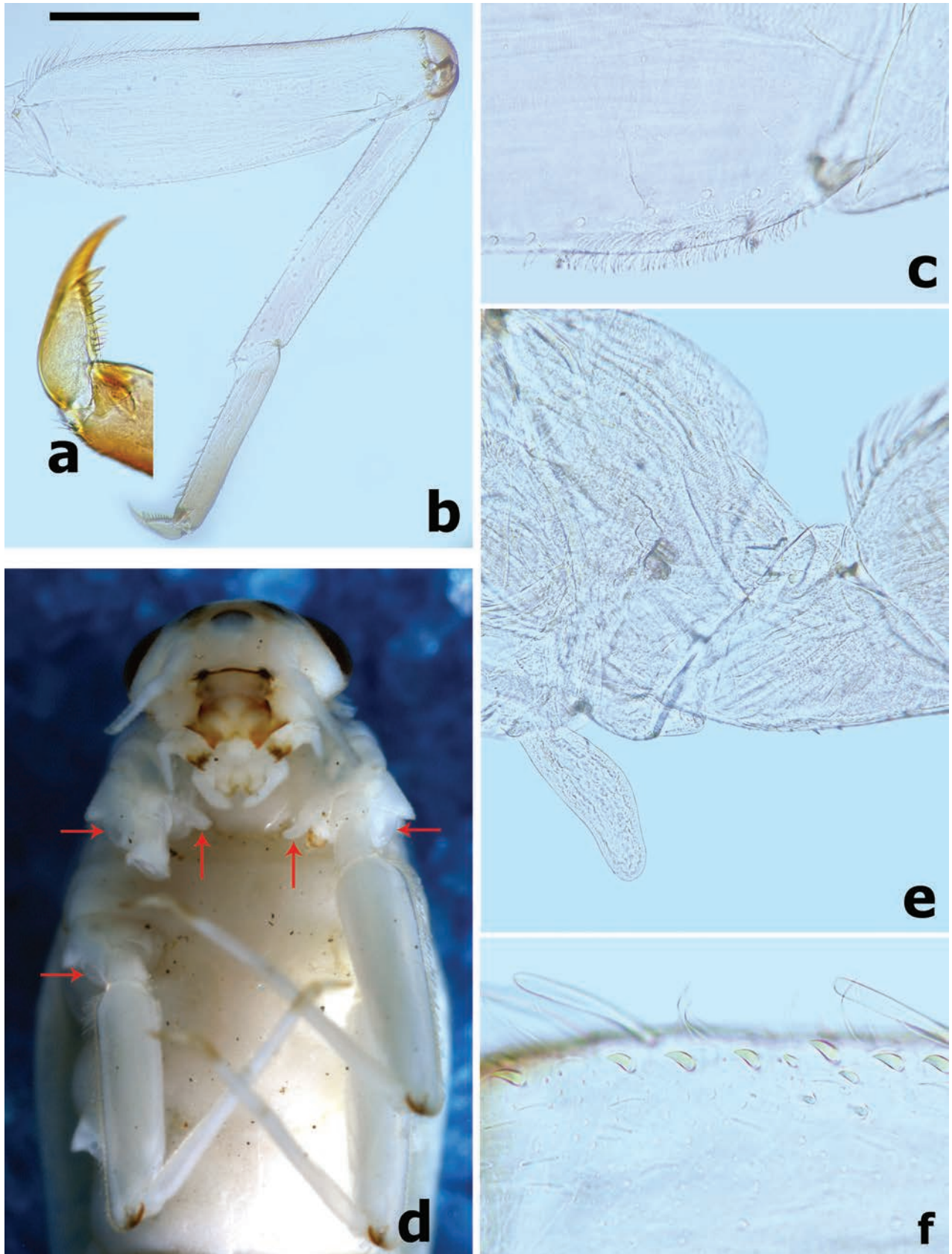


Figure 5. *Branchiobaetis borealis* sp. nov. **a** claw **b** foreleg **c** villopore of femur **d** accessory gills (vertical arrows) between coxa and prosternum on foreleg and bubble-like membranous swellings (horizontal arrows) **e** detail of accessory gill on foreleg **f** distally curved hook-like setae on dorsal margin of femur. Scale bar: 0.5 mm.

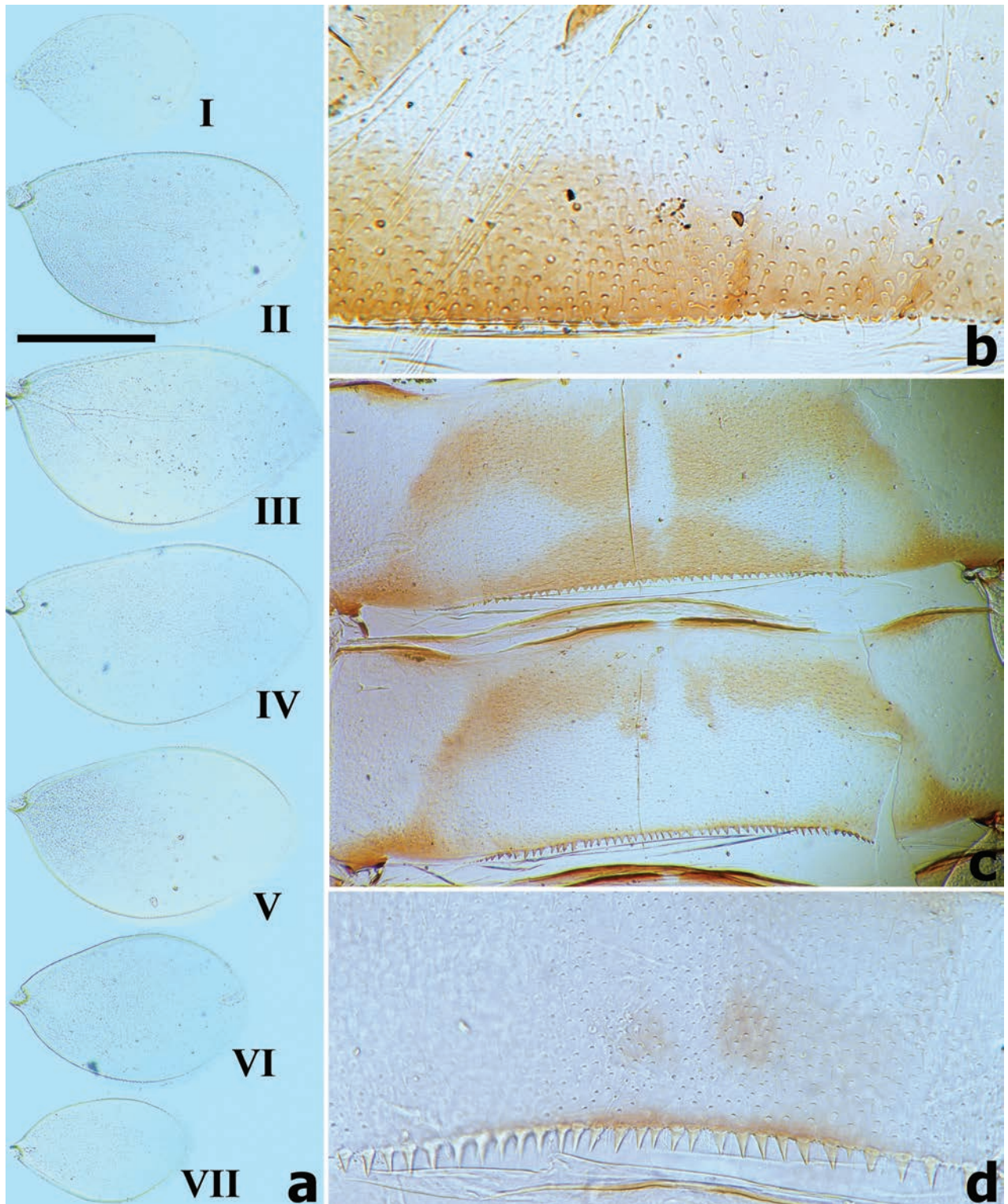


Figure 6. *Branchiobaetis borealis* sp. nov. **a** gills I–VII **b** posterior margin of abdominal tergite I **c** posterior margin of abdominal tergites IV–V **d** posterior margin of abdominal tergite IX. Scale bars: 0.5 mm.

Maxilla (Fig. 3a). Galea-lacinia with three robust canines; crown of galea-lacinia with one regular row of 10–13 medium-size arcuate, simple setae (Fig. 3d), second row composed of three dentisetae and a row of 7–9 elongated pectinate setae (Fig. 3e), 1st dentisetate robust, canine-like with wide base, other

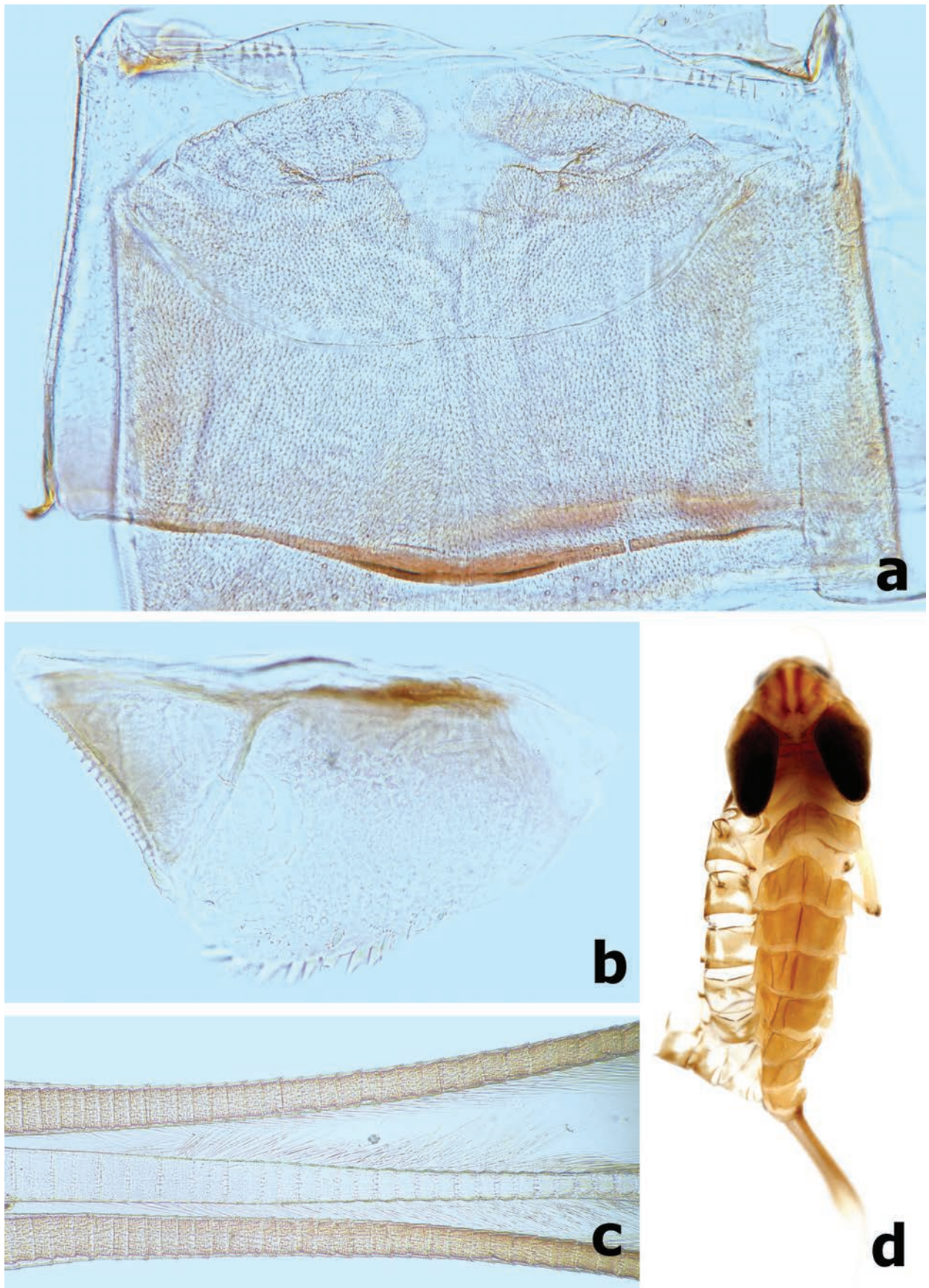


Figure 7. *Branchiobaetis borealis* sp. nov. **a** gonostyli bud under cuticle of last instar male larva **b** paraproct **c** part of caudalii **d** subimaginal female extracted from last instar larva before emergence.

dentisetae slender, bifid, and pectinate; ventrally with two simple, apical setae under canines (Fig. 3c). Medially with one row of five or six long, simple setae and one spine-like seta perpendicular to lacinia margin. Maxillary palp 2-segmented, longer than galea-lacinia, segment I shorter than segment II, apex of segment II with single tiny scale on small cone-shaped projection (Fig. 3a). Small tongue-like accessory gill located on outer side of the articulation between stipes and cardo (Fig. 3a, b).

Labium (Fig. 4a). Glossae shorter and narrower than paraglossae, triangular with wide base, narrowing toward apex, inner margin of glossae with 10–12 spine-like, simple setae and outer margin with six or seven long, simple setae, apex with three robust setae; paraglossae with three rows of long, robust, distally pectinate and curved setae distoventrally and one short, simple seta in proximolateral area (Fig. 4c); dorsal surface on distal 1/2 with one longitudinal row of five or six long, robust, spine-like setae near inner margin (Fig. 4b); labial palp 3-segmented; segment I slightly shorter than segments II and III combined, with many micropores dorsally; segment II triangular with distinct protuberance apico-laterally, ~ 1.3× wider than base of segment III, dorsal surface with one longitudinal row of three or four medium spine-like simple setae and many micropores (Fig. 4e); segment III similar to asymmetrical onion-shaped dome, dorsally with pointed simple setae near apex, ventral surface covered with many blunt pointed spatulate setae accompanied by fine setae (Fig. 4f).

Hind wing pads well developed.

Forelegs (Fig. 5b). Ratio of foreleg segments (femur to claw) 6.8:5.4:3.0:1.0. **Femur**. Length ~ 3.4× maximum width. Dorsal surface covered with many small oval spatulate setae accompanied by fine setae; ventral face with sparse, small, spatulate setae and fine setae. Outer margin with two rows of different type setae: one row of 13–17 medium-sized, robust, clavate setae and proximal row of 17–22 long, slender setae; additional row of small, teardrop-shaped, distally curved, hook-like setae along dorsal margin (Fig. 5f); ventral margin with small, apically pointed or rounded, spatulate setae basally. Apex rounded with short, stout setae anteriorly, dorsoapical setal patch formed by two stout clavate setae. Villopore present and well developed (Fig. 5c). A transparent finger-like accessory gill on inner side of coxal articulation (between coxa and prosternum) (Fig. 5d, e); hyaline bubble-like membranous swelling between coxa and trochanter (Fig. 5d). **Tibia**. Outer margin with one row of fine setae and several small, curved hook-like setae; ventral margin with row of short, stout spine-like setae. Tibio-patellar suture present. Both surfaces covered with small, apically pointed or rounded, spatulate setae alternating with hair-like setae. **Tarsus**. Outer margin with fine setae and one row of small, distally curved hook-like setae; ventral margin with one row of ~ 10 stout spine-like pointed setae increasing in length towards apex; both surfaces covered with small, spatulate setae alternating with hair-like setae. **Claws** hooked (Fig. 5a), with one row of ~ 10 acute teeth, subapical setae absent.

Middle and hind legs similar to foreleg in structure except for lacking the finger-like accessory gills on base of coxa and the villopore larger and more obvious than that of forelegs.

Abdominal tergites and sternites both densely covered with crescent-shaped scale bases, several triangular spatulate setae, and hair-like setae. Posterior margins of tergites I–X with triangular spines increasing in length from I to X

(Fig. 6b–d). Posterior margins of sternites I–IX smooth medially, but with row of dentate protuberances laterally (as Fig. 14b).

Gills (Fig. 6a) present on segments I–VII and well tracheated with a transparent main trunk and branches of tracheae, ratio of gill length from I–VII = 1.1:1.7:1.9:1.8:1.7:1.3:1.0. External margins of all gills with small denticles intercalating fine hair-like setae, without any marginal spines or spatulate setae.

Paraproct (Fig. 7b). Surface scattered with many micropores and hair-like setae, two or three small oval spatulate setae present near posterior margin; posterior margin with nine or ten triangular spines; surface of cercotractor smooth, with 19–22 spines marginally.

Caudalii (Fig. 7c). Cerci with a row of swimming bristles on inner side of intersegment, each segment with row of pointed spines distally; paracercus with swimming bristles on both sides of intersegment.

Gonostyli bud. Subimaginal gonostyli folded under cuticle of last instar larvae, segments II and III sharply bent towards middle (Fig. 7a).

Etymology. The specific epithet *borealis* is the Latin masculine adjective, meaning “northern”, referring to the fact that this new species may represent the northernmost distribution of the genus in the Oriental Region.

Distribution (Fig. 23). China: Yunnan (Lushi, Weixi, and Yunlong).

Larval habitat (Fig. 22b). *Branchiobaetis borealis* sp. nov. was found in moderately rapid to swift unshaded streams with gravel substrates at altitudes from 1036 m to 2523 m in Yunnan, China. The three collection sites of the new species are respectively located in catchments of the Jinsha River (the upper reaches of the Yangtze River), Nujinag River (the upper reaches of Salween River), and Lancang River (the upper reaches of Mekong River), suggesting that *B. borealis* sp. nov. may be common in the Three Parallel Rivers of Yunnan Protected Areas.

***Branchiobaetis megasinus* sp. nov.**

<https://zoobank.org/59F827E6-DFA2-4020-9B44-36480650CD3F>

Figs 8–17

Type material. Holotype. CHINA • male larva in alcohol (mature); Guangdong, Shenzhen, Wutongshan River (22.5972°N, 114.2067°E); 30.xii.2023–1.i.2024; leg. Zhiheng Zhou. **Paratypes** (in alcohol): • 9 mature larvae, locality and date as holotype • 3 larvae, 1 male imago (reared specimen) on slide; Tai Po Kau Forest Stream, Hong Kong; 25.ii.1999; leg. Xiaoli Tong; 1 larva (on slide); Tai Po Kau Forest Stream, Hong Kong; 19.xi.1996; leg. Xiaoli Tong; 1 larva; Tai Po Kau Forest Stream, Hong Kong; 26.ii.1997; leg. Maria Salas; 1 larva (on slide); Shing Mum, Hong Kong; 7.i.1997; leg. Xiaoli Tong • 2 larvae; Ma Po Mei, Hong Kong; 10.x.1997; leg. Xiaoli Tong; 1 larva (on slide); Ma Po Mei, Hong Kong; 7.iii.1998; leg. Xiaoli Tong; 1 larva (on slide); Mt. Nankunshan, Longmen County, Guangdong; 16.ix.1994; leg. Xiaoli Tong • 3 larvae (1 on slide), Mt. Luofushan, Boluo County, Guangdong; 31.x.2023; leg. Xiaoli Tong, Zhiheng Zhou & Bangyi Wu • 5 larvae (1 on slide); upper reaches of Liuxihe River, Conghua, Guangzhou, Guangdong; 23–24.iii.2024; leg. Zhiheng Zhou & Bangyi Wu.

Description. Larva (Fig. 8a–e). Body length (mm): female 7.0–8.5, male larvae slightly shorter than female, 6.0–7.5; antenna 3.0–4.0; cerci 3.0–4.0, paracercus ~ 4/5 length of cerci.

Cuticular colouration. Body mainly brown or brownish green (in life) dorsally. Vertex uniformly brown. Antennal scape brown with off-white apex, pedicel off-white, flagellum pale brown. Pronotum mainly brown with irregular dark brown marks, meso- and metanotum mainly brown with irregular cream marks near base of forewing pads and a pair of small cream spots submedially. Legs contrasting bicoloured. Femur off-white with a large dark brown band medially and dark brown macula proximally and apically; tibia off-white with dark brown macula basally and distally; tarsus off-white with dark brown band apically. Abdominal tergites I–IV and VI–IX brown with a pair of cream stripes laterally; V brown with a cream, oval macula anterior medially and a pair of cream stripes laterally; X with yellow-brown shading to cream in the anterior portion and brown in posterior 1/2; tergites II–VIII with a pair of oblique dark brown medio-anterior sigilla and a pair of medioposterior sigilla (Figs 13e, 14a). Abdominal sternites with cream shading to pale brown posteriorly. Cerci cream to yellow-brown with dark brown bands medially and distally (Figs 8a–e, 15f); paracercus cream to yellow-brown with dark brown band near terminal; primary swimming bristles dark brown.

Precursors of turbinate eyes (Figs 8d, e, 15a, b) in last instar male larvae normal, without elevated area with well-expressed facets.

Antenna (Fig. 8a–c). Antenna ~ 3–4× of head width; scape smooth, without noticeable setae; inner margin of pedicel with tiny triangular denticles distolaterally (Fig. 9a, b).

Labrum (Fig. 9c) nearly rectangular, width/length ratio ~ 1.5; anterior margin bordered with long and feathered setae and a median notch; dorsally with submedial pair of long, robust bristles and submarginal arc of six or seven long, robust bristles on each side of midline, several fine setae scattered proximally; ventral surface with densely fine setae medially and six or seven short, pointed setae laterally and disto-laterally.

Left mandible (Fig. 9d). Incisor and kinetodontium fused; incisor with three denticles, kinetodontium with four main denticles decreasing in length and one additional minute denticle between incisor and kinetodontium; prostheda robust, apex with four bluntly denticles and two or three long, pointed denticles; margin between prostheda and mola straight with two or three fine, pointed minute spines; apex of mola without tuft of setae.

Right mandible (Fig. 9e). Incisor and kinetodontium fused; incisor with three denticles; kinetodontium with four denticles, inner margin of innermost denticle with three small denticles (Fig. 10a); prostheda slender and toothbrush-like, with many sharp denticles on inner margin apically; margin between prostheda and mola slightly concave, occasionally with 1–3 fine, pointed minute spines; apex of mola with a tuft of straight setae.

Hypopharynx and superlinguae (Fig. 10b). Lingua slightly longer than superlinguae, with numerous fine setae apically. Superlinguae distally rounded with numerous fine setae along apical margin.

Maxilla (Fig. 10e). Galea-lacinia with three robust canines; crown of galea-lacinia with one regular row of 13–15 medium-size arcuate simple setae, second row compound of three dentisetae and row of 7–9 elongated pectinate setae; ventrally with two simple, apical setae under canines. Base of lacinia with one row of five or six long simple setae and one seta perpendicular to lacinia margin. Maxillary palp 2-segmented, longer than galea-lacinia, two seg-

ments subequal in length; apex of segment II with single tiny scale on small cone-shaped projection (Fig. 10d). Small tongue-like accessory gill located on outer side of the articulation between stipes and cardo (Fig. 10c, e).

Labium (Fig. 11a). Glossae shorter and narrower than paraglossae, triangular with wide base, narrowing toward apex, inner margin of glossae with 7–10 long, simple setae and distal 1/3 of outer margin with ~ 5 long, simple setae, apex with three robust setae; paraglossae with two rows of long, robust, curved setae distoventrally, dorsal surface on distal 1/2 with one longitudinal row of two or three long, robust, spine-like setae near inner margin (Fig. 11b); labial palp 3-segmented, segment I longer than segments II and III combined, with many micropores dorsally; segment II triangular with distinct protuberance apico-laterally, ~ 1.1× wider than base of segment III, dorsal surface with one longitudinal row of three medium simple setae and many micropores (Fig. 11c); segment III similar to asymmetrical onion-shaped dome, apex usually with a small cone-shaped projection, ventral surface covered with many spine-like, simple setae accompanied by fine setae distally (Fig. 11c).

Hind wing pads well developed.

Forelegs (Fig. 12b–f). Ratio of foreleg segments (femur to claw) 6.9:5.9:3.5:1.0. *Femur*. Length ~ 3.5× maximum width. Dorsal surface covered with numerous crescent scale bases accompanied by fine setae; ventral face with sparse crescent scale bases and fine setae. Outer margin with two rows of different type setae: one row of 10–13 long, robust, blunt pointed setae and proximal row of 13–17 slender long setae (Fig. 12d); additional row of small, decurved hook-like setae along dorsal margin; ventral margin with small, apically pointed or rounded, spatulate setae. Apex rounded with many short, stout, hook-like setae anteriorly, dorsoapical setal patch formed by two stout setae. Villopore present and well developed (Figs 10f, 12d). A finger-like accessory gill on inner side of coxal articulation (between coxa and prosternum); hyaline bubble-like membranous swelling between coxa and trochanter (Fig. 12a). *Tibia*. Outer margin with one row of small, apically decurved hook-like setae and fine setae; ventral margin with row of longer, stout spine-like setae. Tibio-patellar suture present (Fig. 12e). Both surfaces covered with crescent-shaped scale bases, apically oval or pointed spatulate setae alternating with hair-like setae. *Tarsus*. Outer margin with fine setae and one row of short, curved hook-like setae; ventral margin with one row of ~ 11 stout spine-like pointed setae increasing in length toward apex (Fig. 12f), apex with single robust, spine-like pointed seta. Both surfaces covered with crescent scale bases. *Claws* hooked (Fig. 12c), with one row of 11–13 acute teeth, subapical setae absent.

Middle and hind legs similar to foreleg in structure except for lacking the finger-like accessory gills on base of coxa.

Abdominal tergites and sternites. Both tergites and sternites densely covered with crescent scale bases and sparse hair-like setae, without any spatulate setae. Posterior margins of tergites I–X with triangular spines increasing in length from I to X (Figs 13c–e, 14a). Posterior margins of sternites I–IX smooth medially, but with row of dentate protuberances laterally (Fig. 14b).

Gills (Fig. 13a) present on segments I–VII and well tracheated, ratio of gill length from I–VII = 1.0:1.8:2.0:1.9:1.6:1.3:1.0. External margins of all gills with small denticles intercalating fine hair-like setae (Fig. 13b), without any marginal spines or spatulate setae.

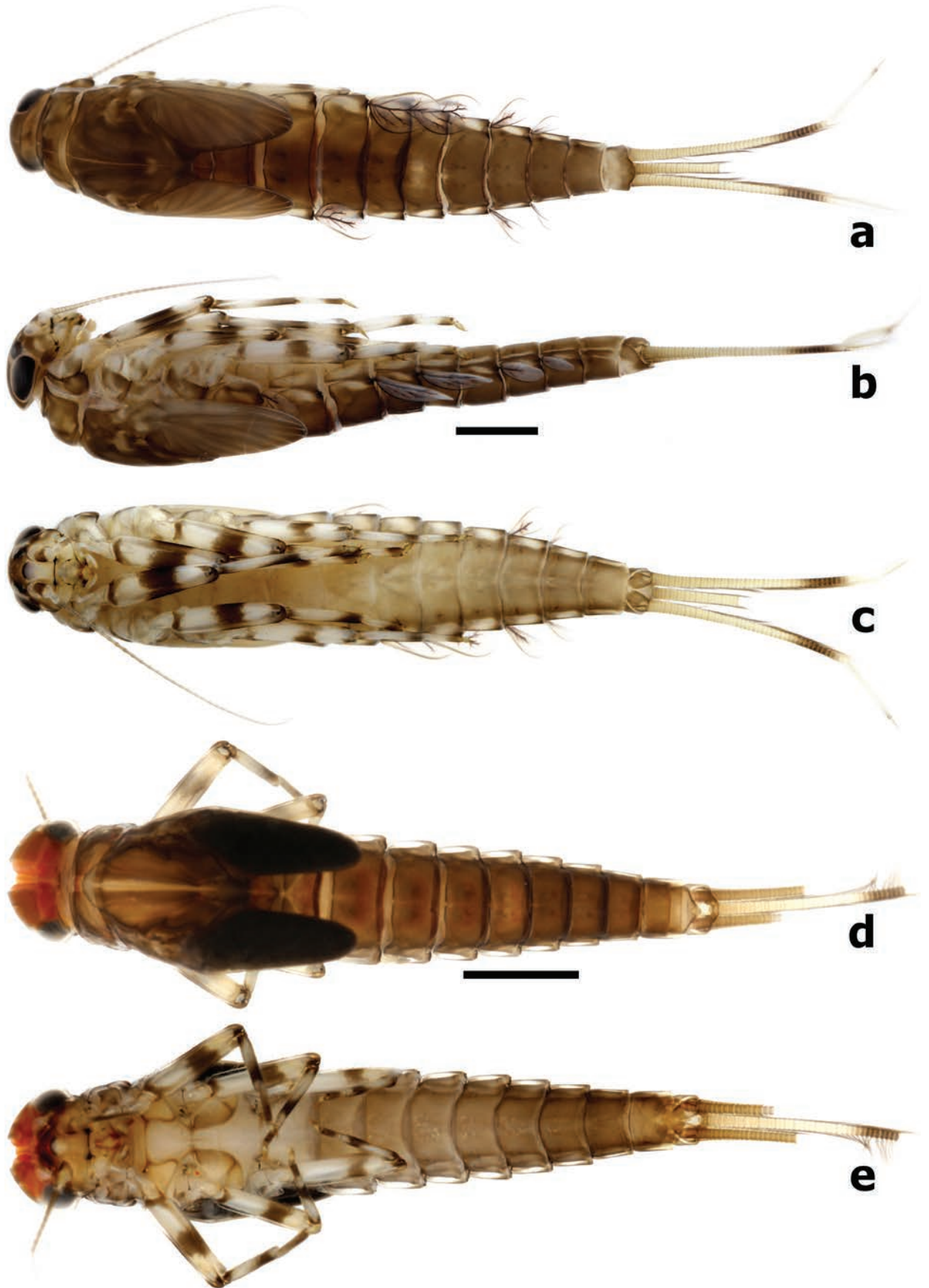


Figure 8. *Branchiobaetis megasinus* sp. nov. larval habitus **a** female larva (dorsal view) **b** female larva (lateral view) **c** female larva (ventral view) **d** final instar male larva (dorsal view) **e** final instar male larva (ventral view).

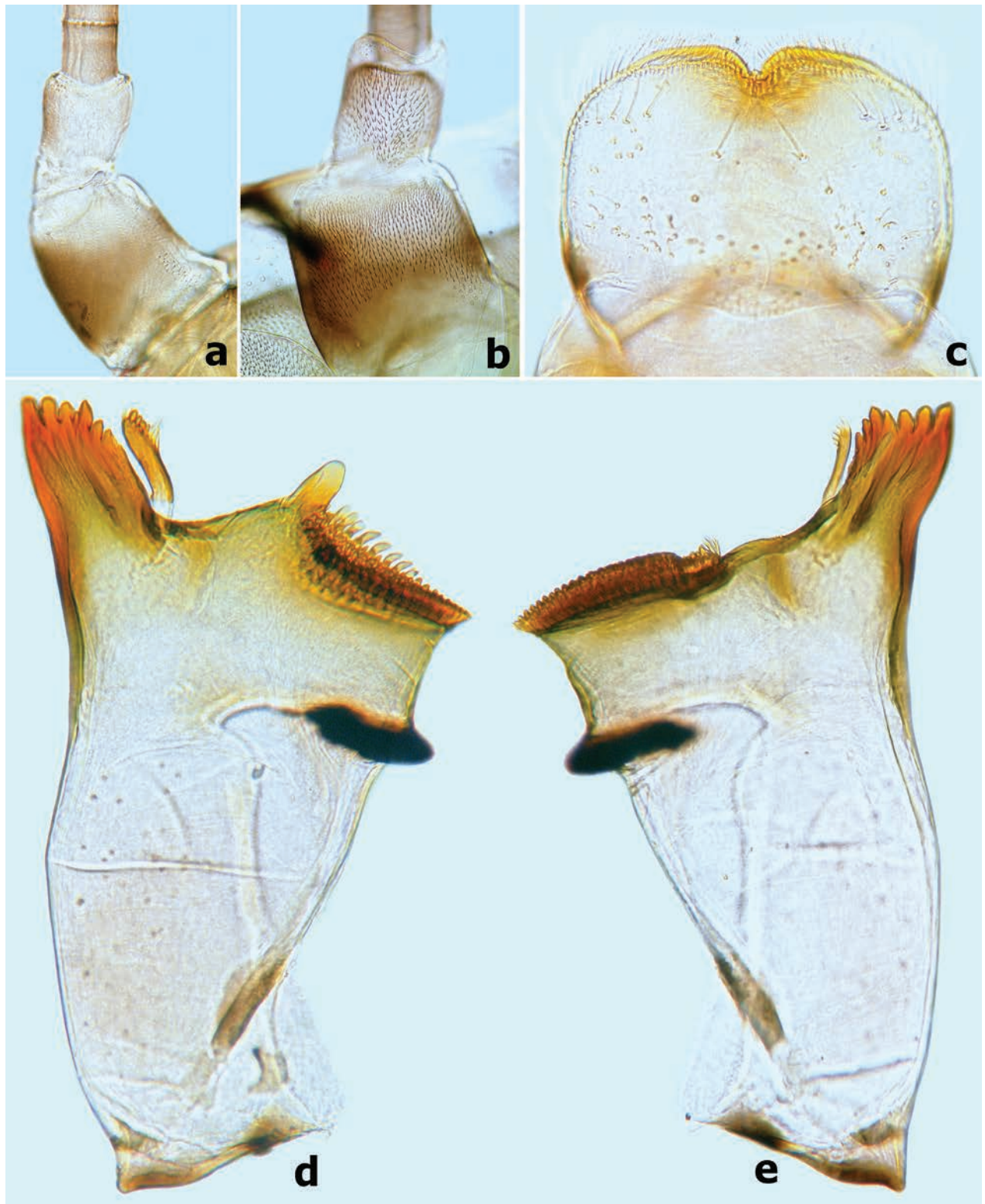


Figure 9. *Branchiobaetis megasinus* sp. nov. **a** antennal scape and pedicel **b** antennal scape and pedicel (final instar) **c** labrum **d** left mandible **e** right mandible.

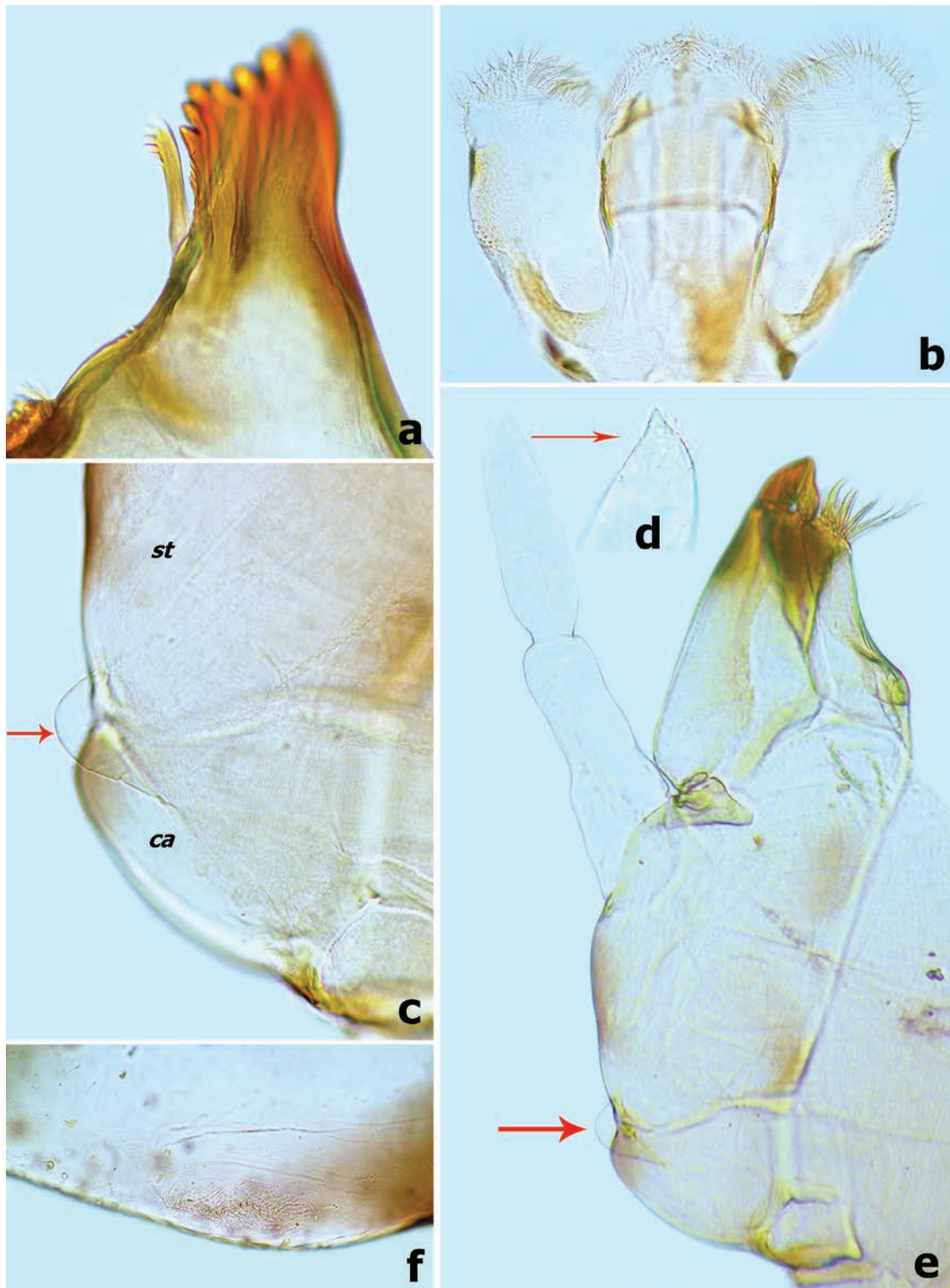


Figure 10. *Branchiobaetis megasinus* sp. nov. **a** apex of right mandible **b** hypopharynx and superlinguae **c** accessory gill between stipes and cardo of maxilla **d** apex of maxillary palp **e** maxilla **f** villopore of femur. Abbreviations: st: stipes, ca: cardo. Red arrows indicate the tongue-like accessory gill (**c**, **e**).

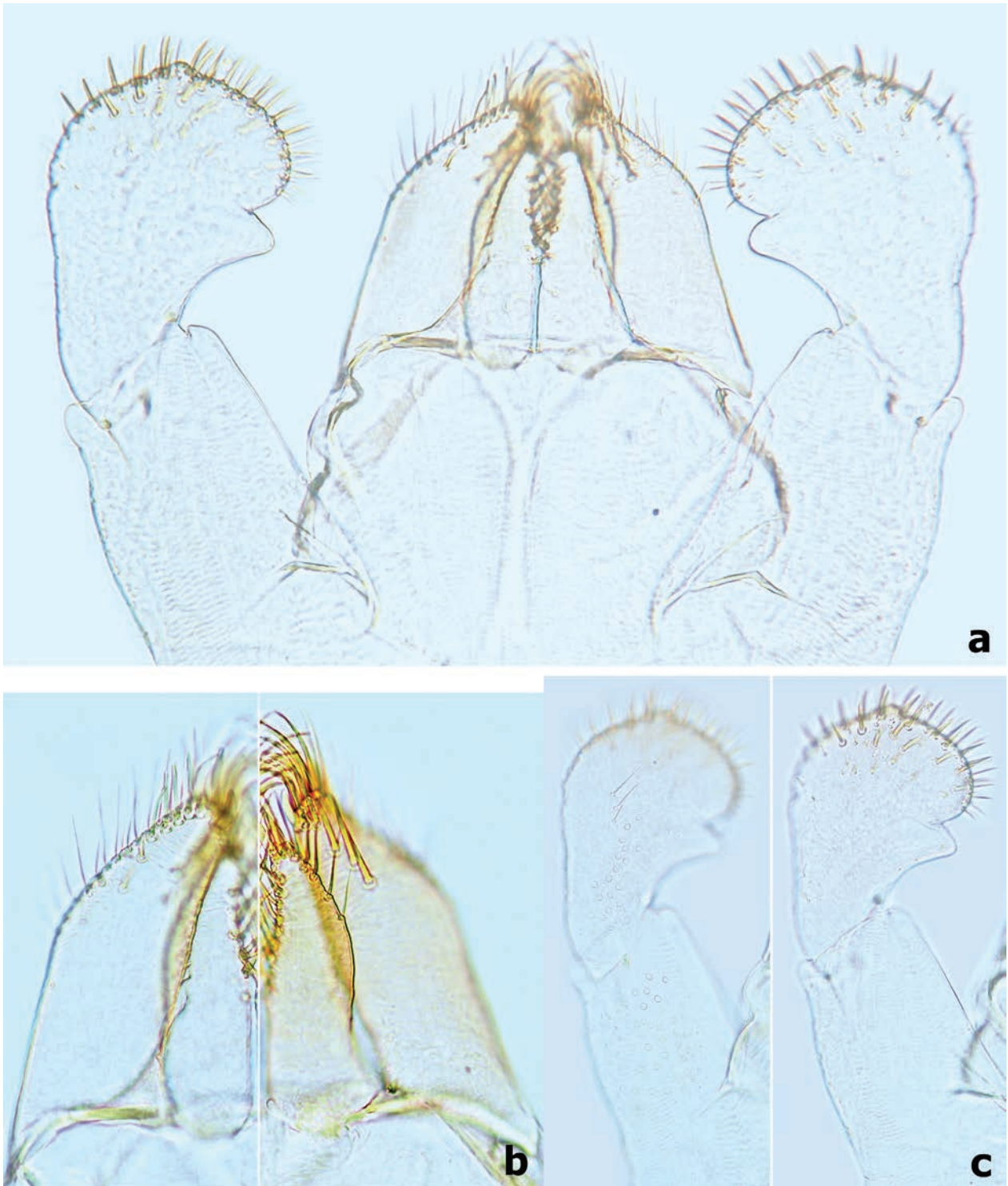


Figure 11. *Branchiobaetis megasinus* sp. nov. **a** labium **b** glossae and paraglossae (left: ventral view; right: dorsal view) **c** labial palp (left: dorsal view; right: ventral view).

Paraproct (Fig. 14d). Surface scattered with several crescent scale bases, fine setae and many micropores; margin with ~ 12 triangular spines; surface of cercotractor smooth, with 12–15 spines marginally.

Caudalii (Fig. 15f). Cerci with a row of swimming bristles on inner side of intersegment, each segment with row of pointed spines distally; paracercus with swimming bristles on both sides of intersegment.

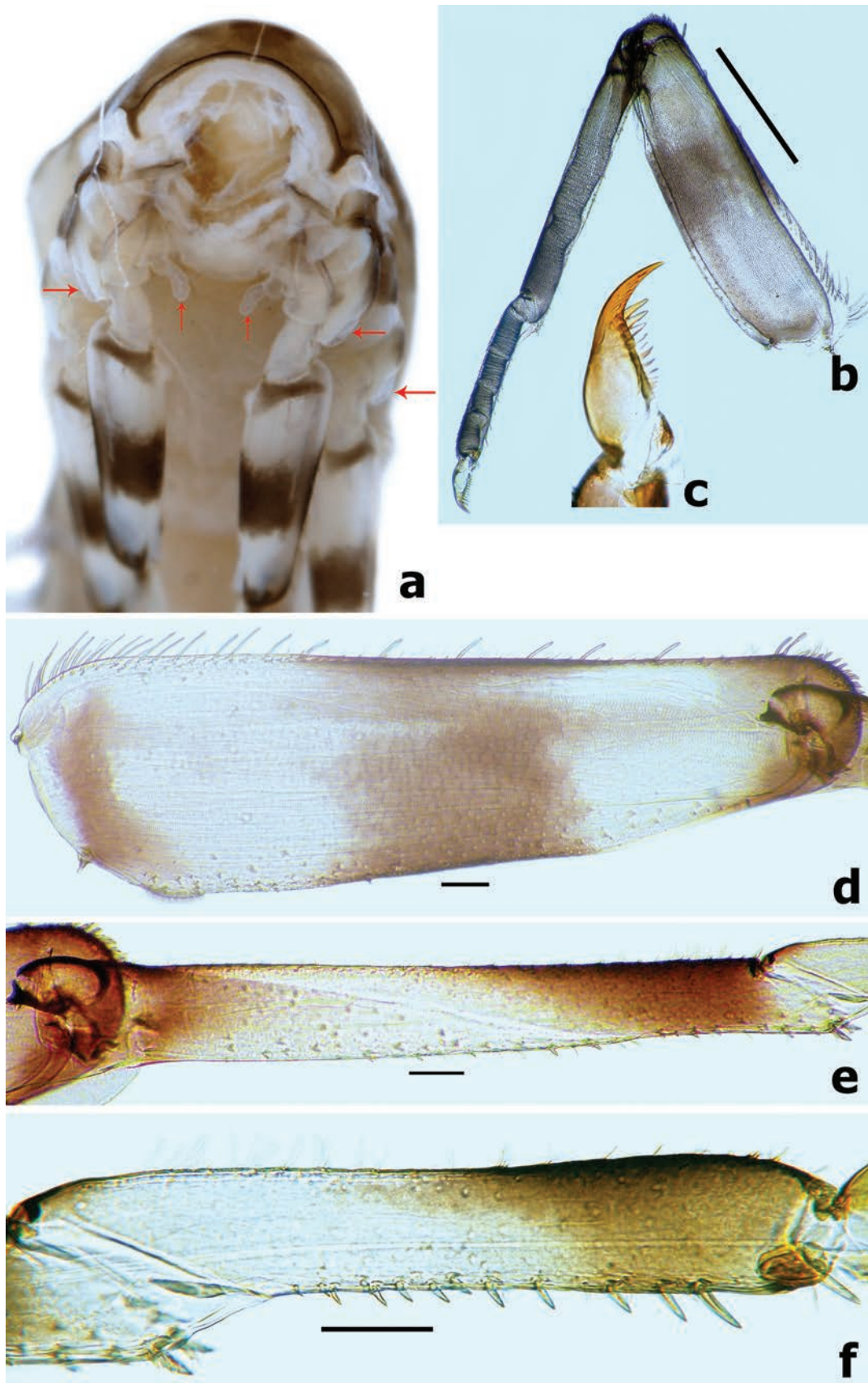


Figure 12. *Branchiobaetis megasinus* sp. nov. **a** accessory gills (vertical arrows) between coxa and prosternum on foreleg and bubble-like membranous swellings (horizontal arrows) **b** foreleg of final instar larva **c** claw **d** foreleg femur **e** foreleg tibia **f** foreleg tarsus. Scale bars: 0.5 mm (**b**); 0.1 mm (**d**, **e**, **f**).

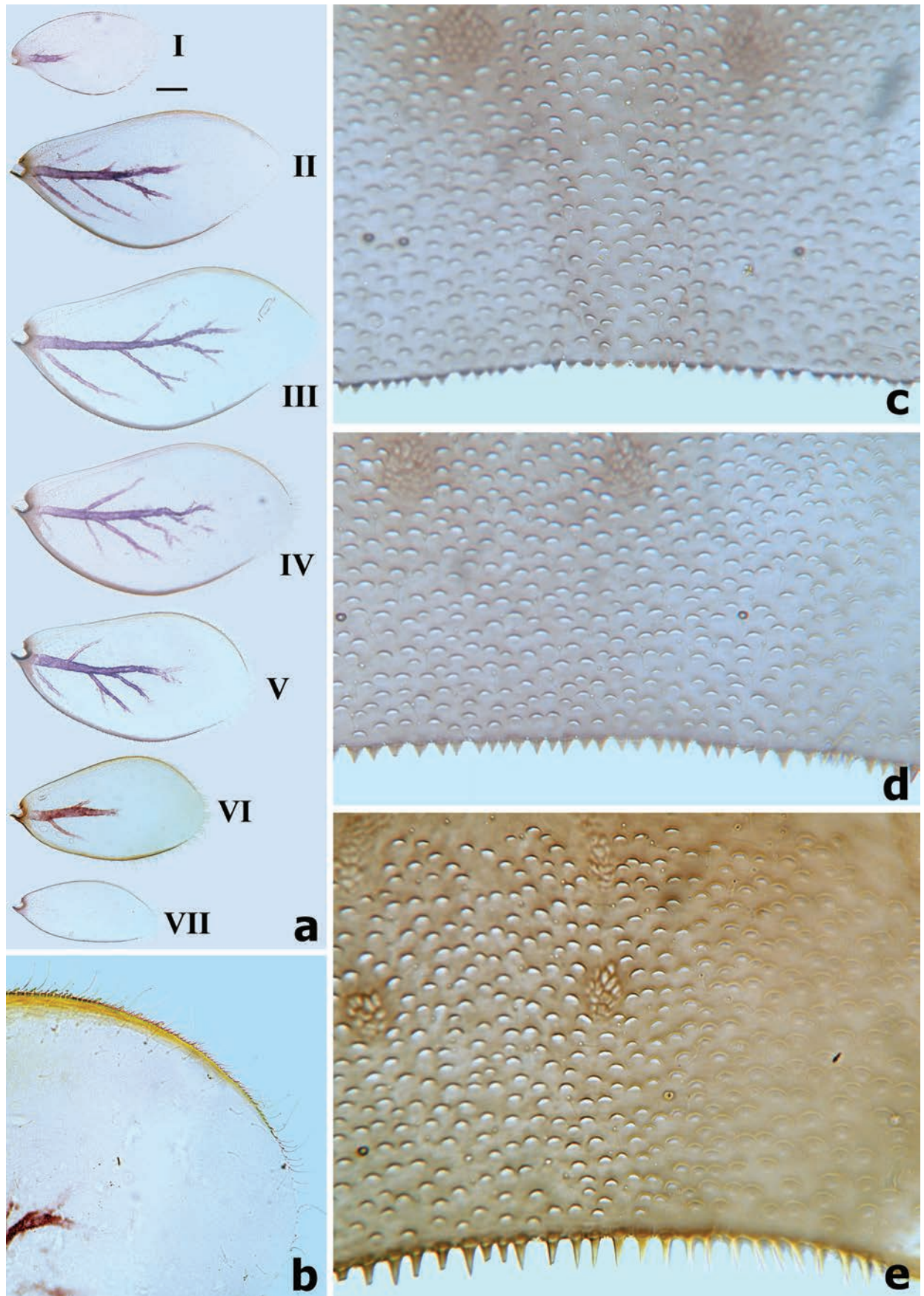


Figure 13. *Branchiobaetis megasinus* sp. nov. **a** gills I–VII **b** external margin of gill **c** posterior margin of abdominal tergite II **d** posterior margin of tergite IV **e** posterior margin of tergite VIII.

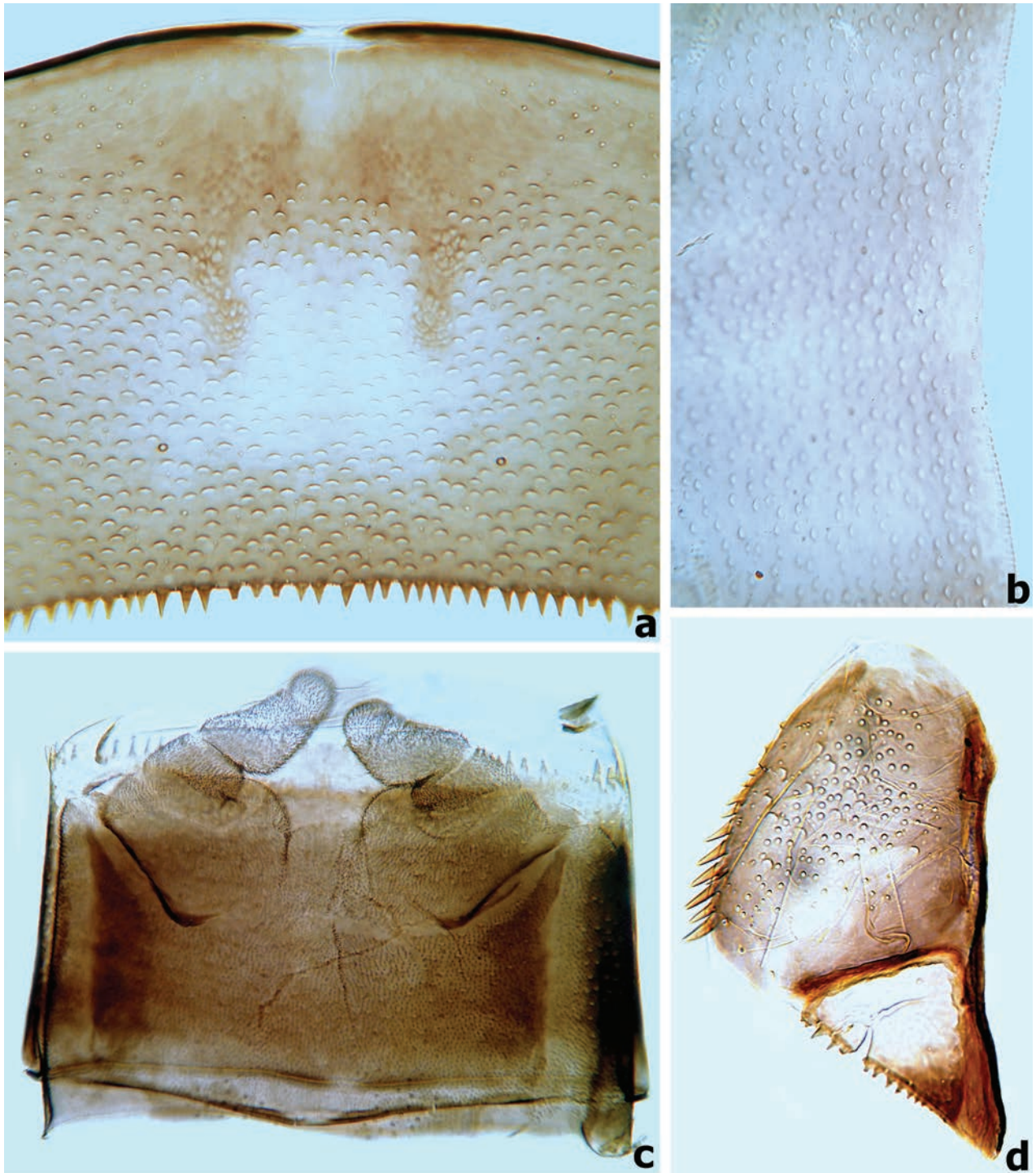


Figure 14. *Branchiobaetis megasinus* sp. nov. **a** middle part of abdominal tergite V **b** posterior margin of sternite VII **c** gonostyli bud under cuticle of last instar male larva **d** paraproct.

Gonostyli bud folded under cuticle of last instar larvae, segment II of gonostylus bud sharply bent towards middle and segment III sharply bent towards posterolaterally (Fig. 14c); subimaginal gonostyli extracted from last instar larva as Fig. 15e.

Male imago. Body length 6.4 mm. Forewing 6.3 mm. Cerci 18.0 mm. Turbinate eyes cylindrical (Fig. 17b, c), slightly widened apically, stalk and faceted



Figure 15. *Branchiobaetis megasinus* sp. nov. **a, b** head of final instar male larva before emergence **c** female abdomen extracted from last instar larva before emergence **d** male abdomen extracted from last instar larva before emergence **e** subimaginal gonostyli extracted from last instar larva **f** caudalii.

surface orange; ocelli off-white with dark brown basal ring. Antennae longer than head capsule; flagella pale brown, pedicels and scapes cream. Pronotum pale with dark brown maculae medially; mesonotum pale to pale brown with brown markings medially and posterolaterally; metanotum yellow-brown to dark brown; thorax dark brown laterally. Forewings hyaline (Fig. 17d), longitudinal veins and paired marginal intercalaries yellow-brown, double intercalary veins longer than distance between corresponding longitudinal veins; costa serrated with pointed spines on basal portion (Fig. 16b), pterostigma area transparent washed pale yellow-brown, with four or five slanting cross veins (Figs 16c, 17d); hindwings (Fig. 17e) with acute costal process and three longitudinal veins. Fore femur pale, arched medially (Fig. 17g), fore tibia yellow-brown, fore tarsus pale yellow-brown; ratio of foreleg femur/tibia/tarsus = 1:1.4:1.4; ratio of foreleg tarsal segments = 1.0:6.6:5.7:3.3:2.0; middle and hind legs similar to foreleg

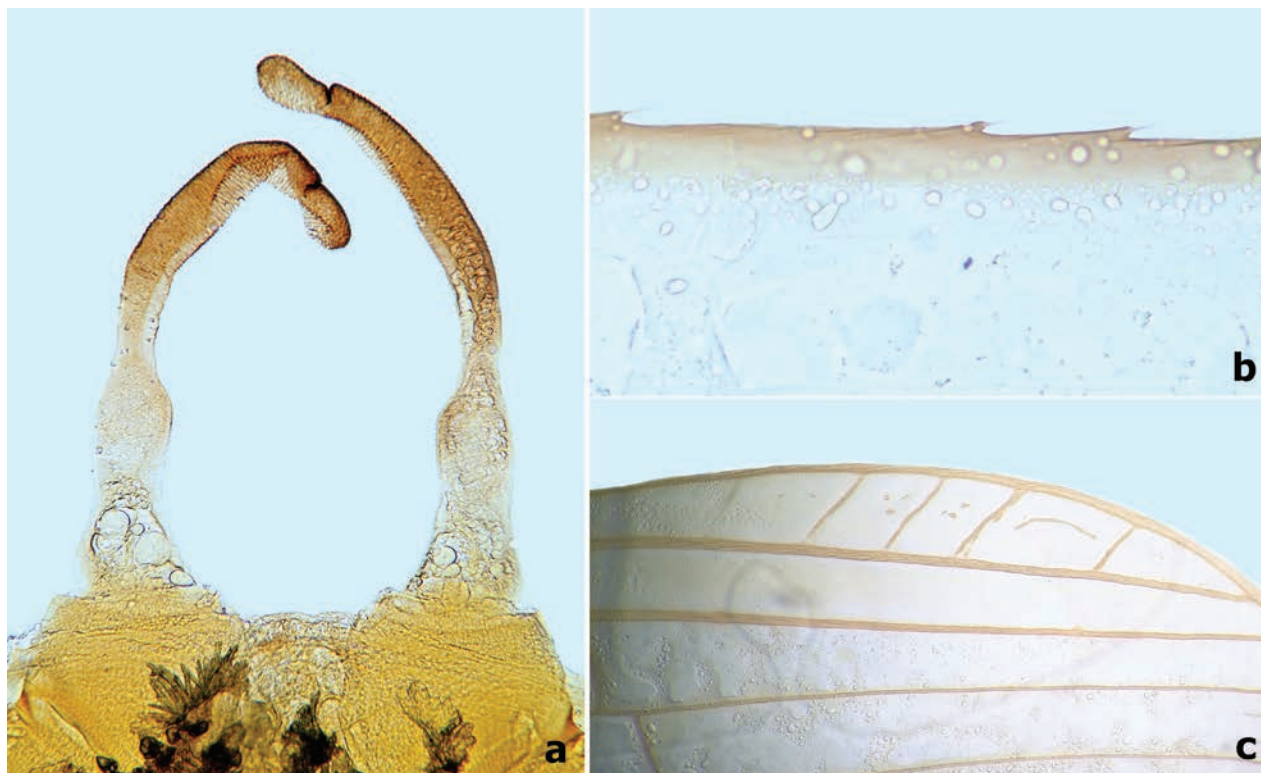


Figure 16. Male imago of *Branchiobaetis megasinus* sp. nov. **a** genitalia **b** costa of fore wing on basal portion **c** pterostigma area of fore wing.

in colouration except with straight femora and apical spine on fused 1st+2nd and 3rd tarsal segments (Fig. 17f); all claws with one oval lobe and one pointed curved hook. Abdominal tergites I–VIII rust-red with anterior submedial pair of pale streaks, each with single purple-brown transverse streak along posterior margin, tergites IX–X pale. Genitalia (Figs 16a, 17a): unistyliger cylindrical, inner margin of segment I of gonostylus with distomedial swelling and outer margin with protuberance basally (Fig. 17a), segment III of gonostylus oblong. Cerci grey-white with rust tints basally.

Female imago. Unknown.

Etymology. The specific epithet is a combination of *mega-* (derived from the Greek, meaning huge, large) and *sinus* (from Latin masculine adjective meaning bay or gulf). Thus, the name refers to the fact that the type series of the new species was found from the Guangdong-Hong Kong-Macao Greater Bay Area (Greater Bay Area).

Distribution (Fig. 23). China: Guangdong (Shenzhen, Guangzhou, Boluo, Longmen) and Hong Kong (Tai Po Kau Forest Stream, Shing Mun, Chuen Lung, Ma Po Mei, Ng Tung Chai, Mui Tsz Lam, Shek Mun Kap).

Larval habitat (Fig. 22a). The species usually live in moderately rapid, well-aerated riffles at low-altitude (< 300 m a.s.l.) forest streams with gravel and cobble substrates. The physicochemical parameters of the type locality (Wutongshan River, Shenzhen in December) are as follows: river width 5–7 m, water depth 10–20 cm, water temperature 18.3 °C, current velocity 0.25 m/s, DO 9.4 mg/l, pH 8.0 and TDS 43.9 mg/l.

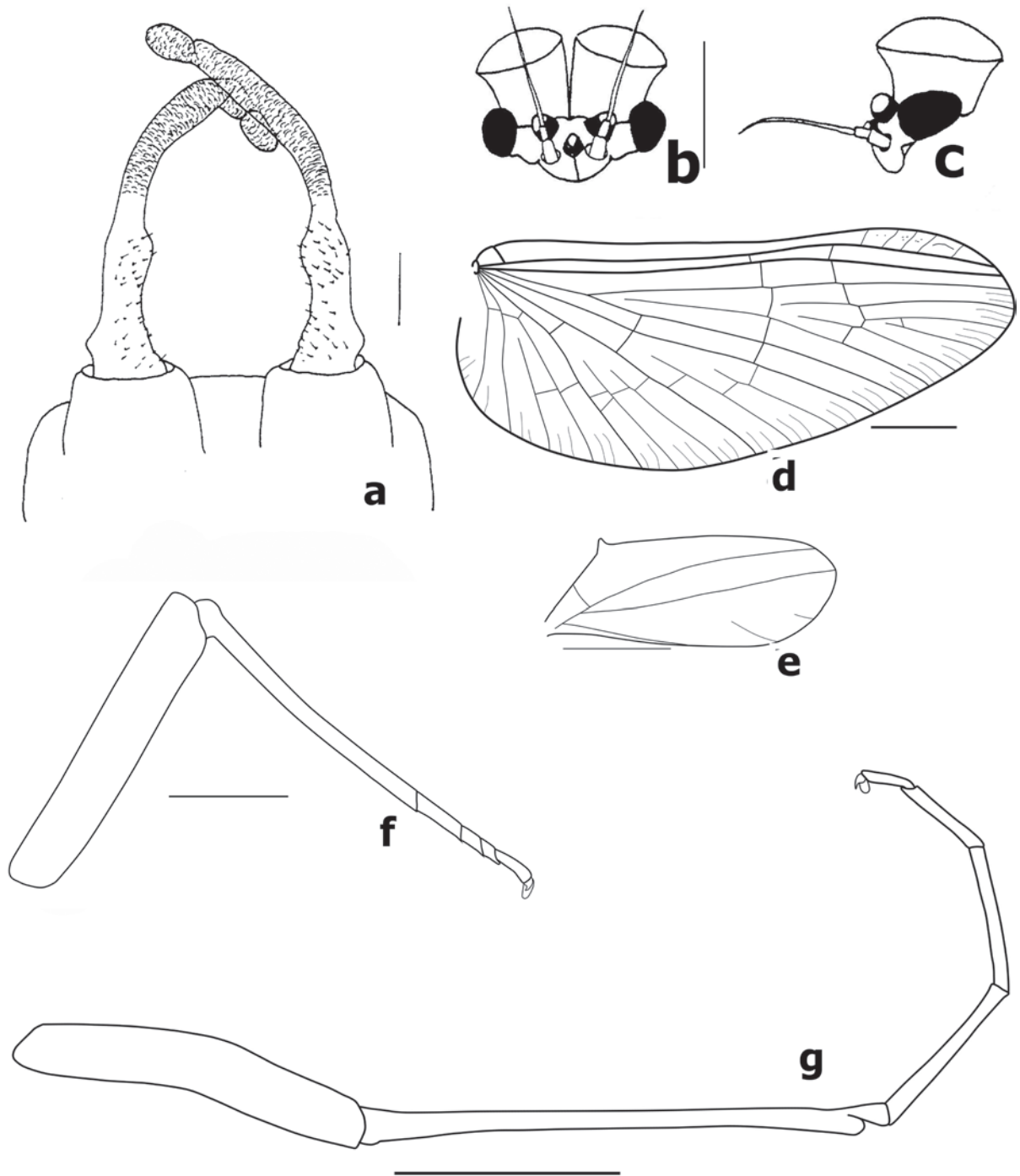


Figure 17. Male imago of *Branchiobaetis megasinus* sp. nov. **a** genitalia **b** head (anterior view,) **c** head (lateral view) **d** fore wing **e** hind wing (enlarge,) **f** hind leg **g** foreleg. Scale bars: 0.1 mm (**a**); 0.5 mm (**e**, **f**); 1.0 mm (**b**, **d**, **g**).

***Megabranchiella longusa* Phlai-ngam & Tungpairojwong, 2022**

Figs 18–21

Megabranchiella longusa: Phlai-ngam & Tungpairojwong in Phlai-ngam et al. 2022: 16.

Material examined. One female larva on slide; Yunnan, Lushui, Bajiao River (a tributary of the Nujiang River, altitude 1112 m); 21.iii.2019; leg. Xiaoli Tong.

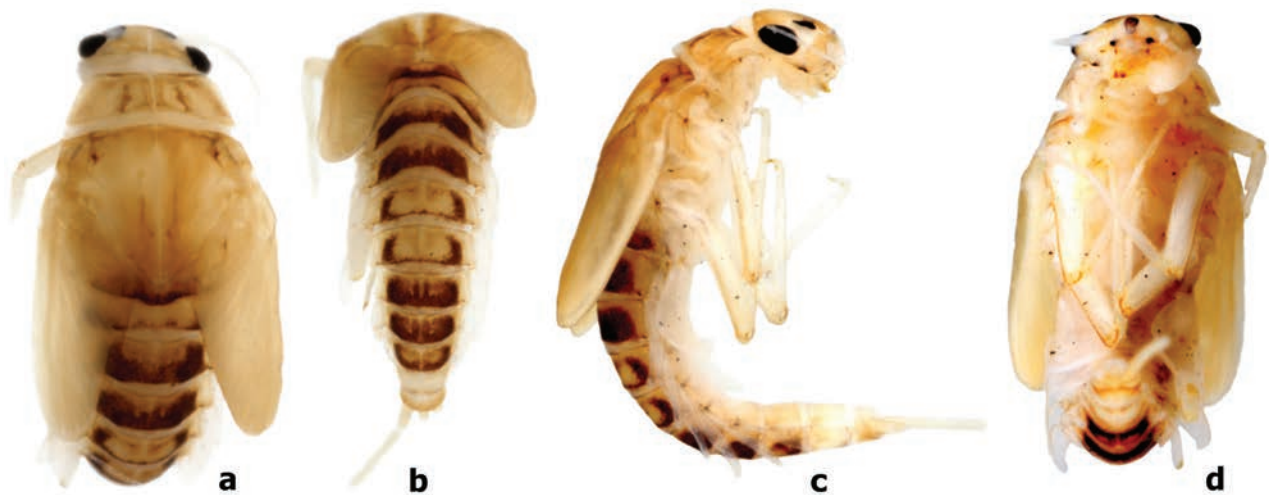


Figure 18. Larval habitus of *Megabranchiella longusa* **a, b** female larva (dorsal view) **c** female larva (lateral view) **d** female larva (ventral view).

Diagnosis. Female larva (Fig. 18a–d), body short and flattened, length ~ 4.0 mm; body colour pattern as Fig. 18a–c. **Head.** Labrum nearly semicircular, ~ 1.4× wider than long; anteromedian notch deep with a small, rounded lobe at base; dorsal surface in distal 1/2 with one pair of long, simple setae near mid-line and irregular row of three medium, simple setae (Fig. 19c). Left mandible (Fig. 19a), incisor and kinetodontium fused, incisor with four denticles, kinetodontium with six denticles decreasing in length, prostheca robust, apex with six bluntly denticles and one or two long, spine-like denticles; incisor of right mandible with four denticles, kinetodontium with four denticles, inner margin of innermost denticle with row of small denticles; prostheca robust, apex with comb-like structure, with many denticles apically (Fig. 19b). Maxilla (Fig. 19e), galea-lacinia of with three robust canines, base of lacinia with one row of four long, simple setae and one seta perpendicular to lacinia margin; maxillary palp 2-segmented, apex of segment II with a small cone-shaped projection. Labium (Fig. 19d, f), glossae shorter and narrower than paraglossae, paraglossae with three rows of long curved setae distoventrally, dorsal surface on distal 1/2 with one longitudinal row of two or three long, spine-like setae near inner margin; labial palp 3-segmented, segment I longer than segments II and III combined, segment II triangular with small protuberance apico-laterally, dorsal surface of segment II with row of two robust, simple setae near distal margin (Fig. 19g). **Thorax.** Hindwing pads reduced (Fig. 20b). Forelegs (Fig. 21c), femur with a row of long, robust, pointed setae along dorsal margin, surface with notched scales anteromedially (Fig. 20c), villopore present (Fig. 20d); tibia with a row of long, pointed setae and short, blunt spatulate setae, tibio-patellar suture present; ventral margin of tarsus with one row of four robust, spine-like setae; claws hooked (Fig. 21b) with one row of 13 acute teeth, subapical setae absent. Middle and hind legs similar to foreleg in structure. **Abdomen.** Abdominal tergites and sternites with smooth posterior margins (Fig. 21a); gills present on abdominal tergites I–VII, gill I oriented ventrally, extremely enlarged and elongated (Fig. 20a), covering abdominal sternites II–VI (Fig. 18c), gills II–VII oriented dorsolaterally, elongated oval similar to tongue blade (Figs 18c, 20a), gill margins with long, fine, hair-like setae, ratio of gill length from I–VII = 3.2:1.7:1.7:1.7:1.5:1.3:1.0;

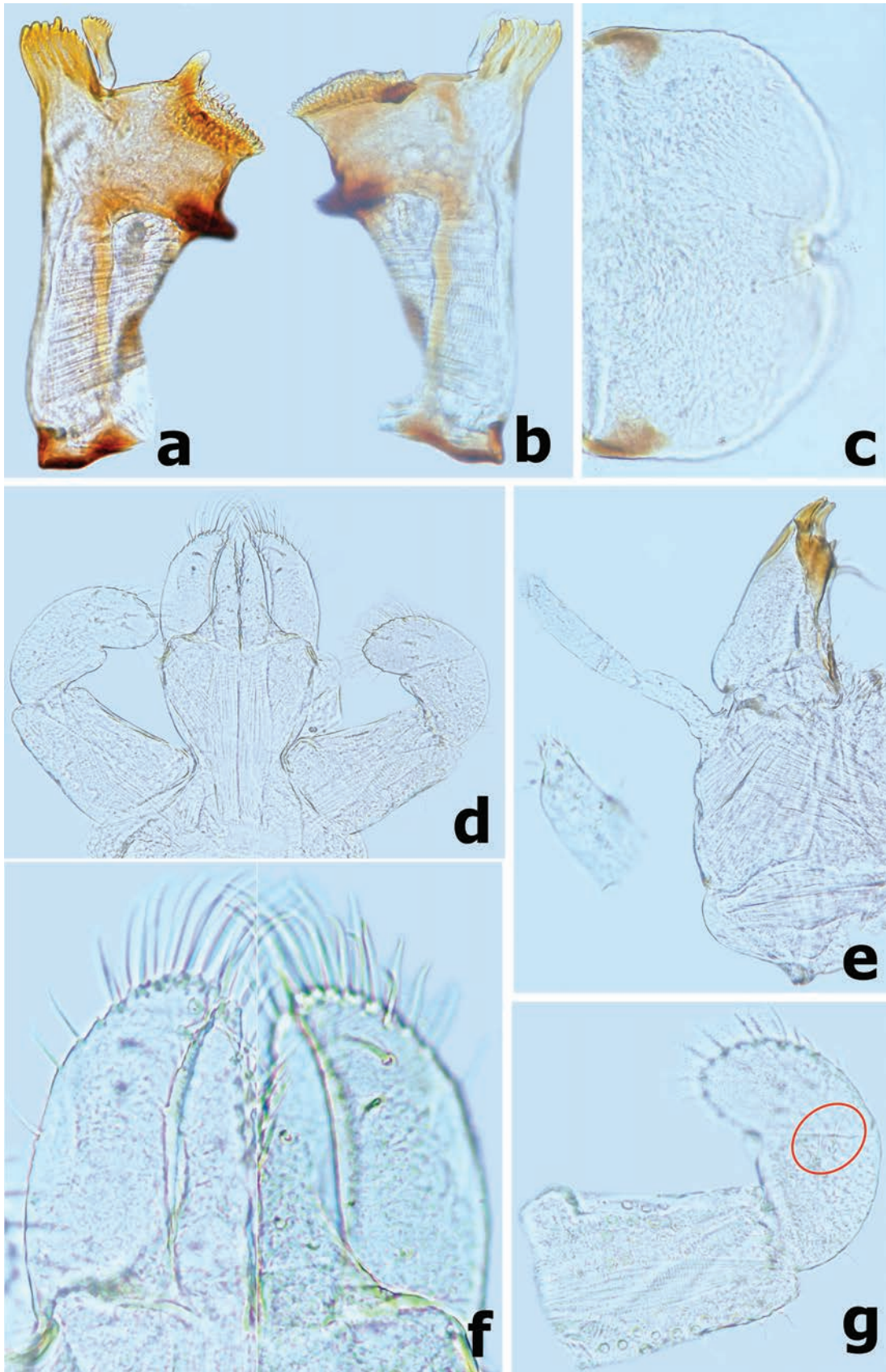


Figure 19. *Megabranchiella longusa* **a** left mandible **b** right mandible **c** labrum **d** labium **e** maxilla **f** glossae and paraglossae (left: dorsal view; right: ventral view) **g** labial palp (dorsal view). Red ellipse encloses dorsal setae.

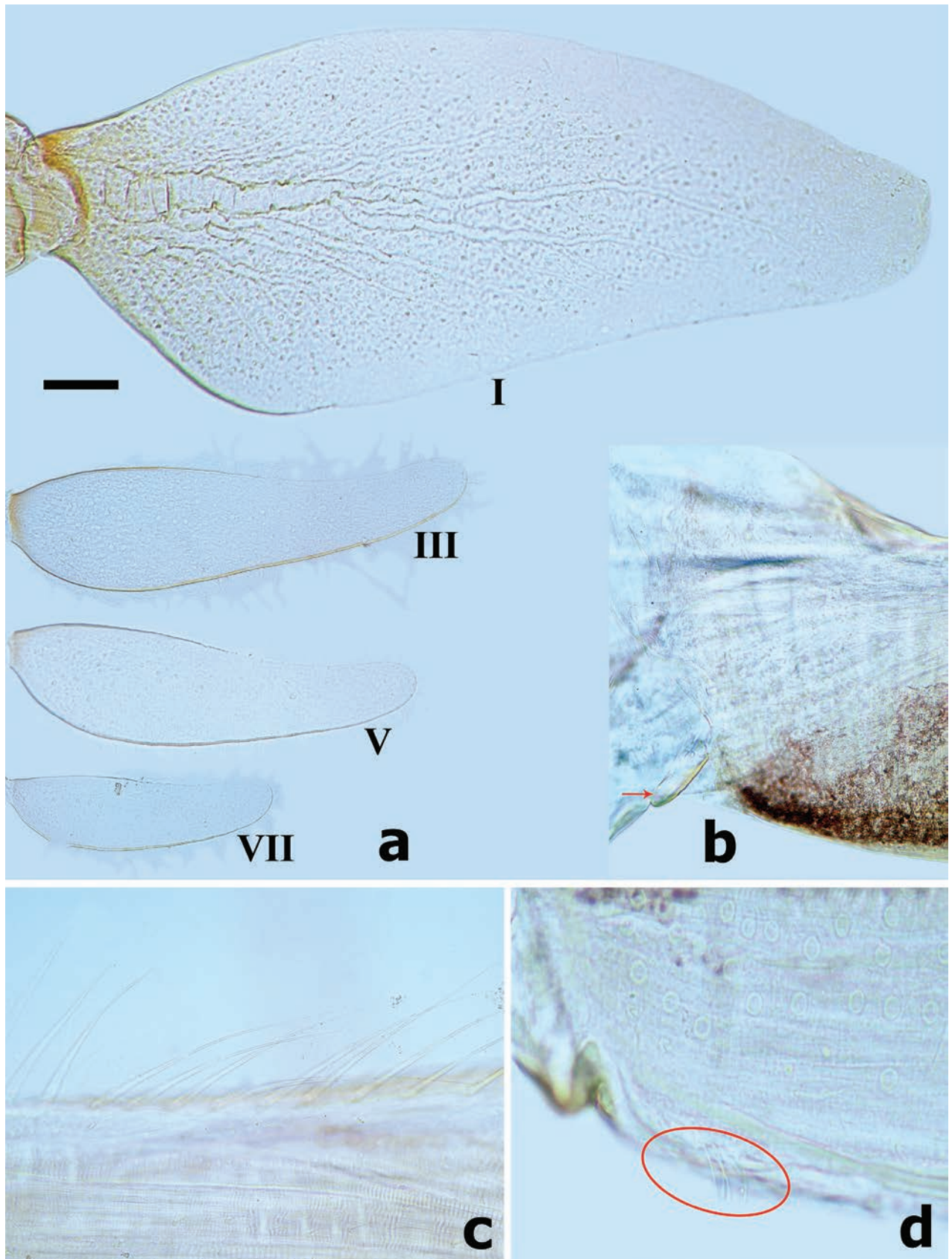


Figure 20. *Megabranchiella longusa* **a** gills I, III, V, VII **b** hindwing pad **c** dorsal margin of femur **d** villopore of femur. Red arrow indicates hindwing pad. Red ellipse encloses villopore. Scale bar: 0.1 mm.

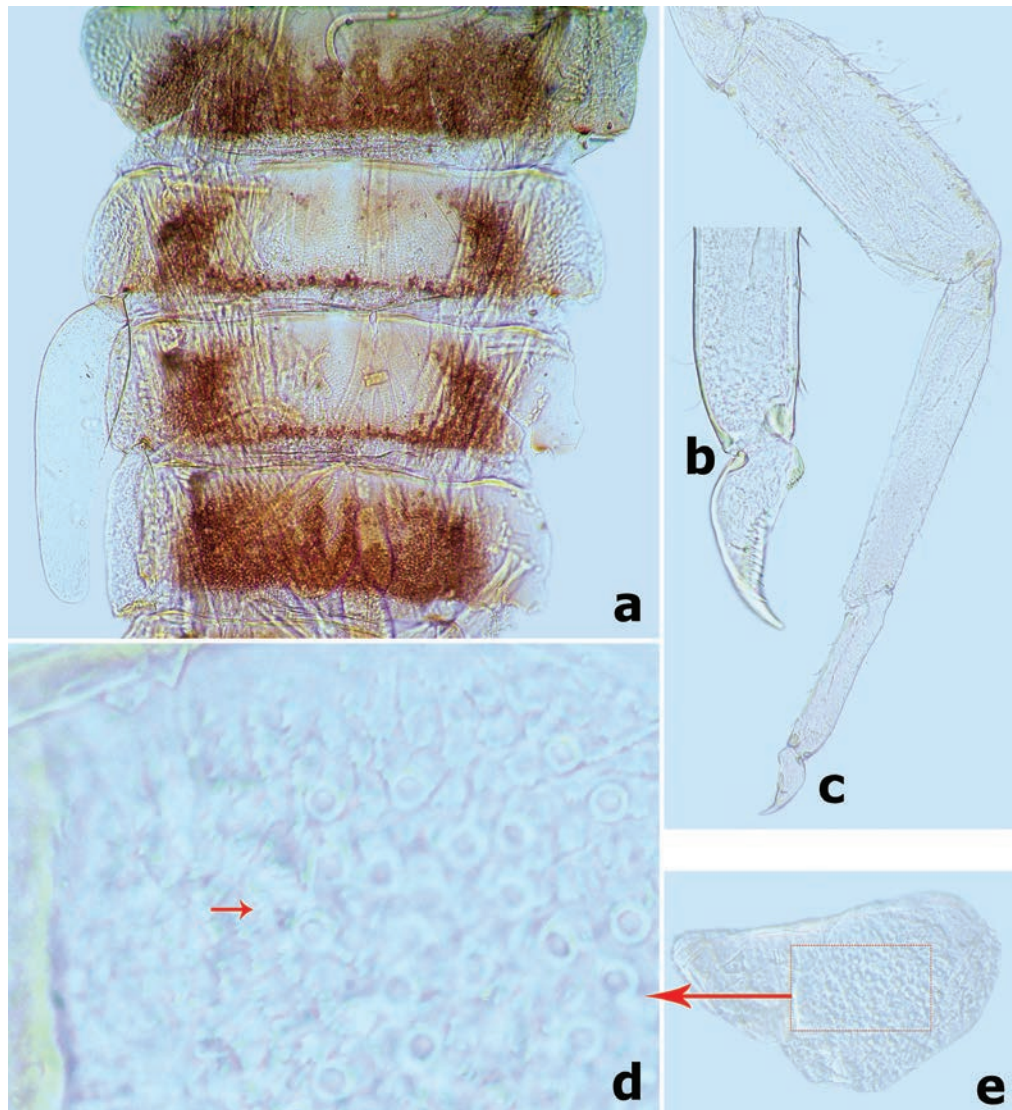


Figure 21. *Megabranchiella longusa* **a** abdominal tergites III–VI **b** claw **c** foreleg **d** notched scales on paraproct surface **e** paraproct.

paraproct with smooth margin, without marginal spines or spatulate setae, surface with micropores and patch of notch scales (Fig. 21d, e).

Distribution (Fig. 23). Thailand (Chiang Mai and Nan Provinces) and China (Yunnan Province).

Larval habitat (Fig. 22c). The species was collected in a swift, unshaded stream with cobble substrate at an altitude of ~ 1100 m in Yunnan, China.

Remarks. Geographically, this record represents the farthest distribution north of the genus *Megabranchiella* so far. We expect that more species of the genus will be discovered with the expansion of the investigation range in China.

Discussion

The morphological characters of *B. borealis* sp. nov. and *B. megasinus* sp. nov. are slightly different from other known species of the genus by the following characters in the larval stage: (1) antennal scape smooth without spatulate se-



Figure 22. Representative sites of larval habitat **a** *Branchiobaetis megasinus* sp. nov. Upper reaches of Liuxihe River, Conghua, Guangdong **b** *Branchiobaetis borealis* sp. nov. Lapu River, Weixi, Yunnan **c** *Megabranchiella longusa* Phlai-ngam & Tungpairajwong. Bajiao River, Lushui, Yunnan.



Figure 23. Distribution map of the genera *Branchiobaetis* and *Megabranchiella* in China.

tae, inner margin of pedicel with tiny triangular denticles distolaterally; (2) mandible without blade-like incisor; (3) maxillary accessory gill reducing to small tongue-like structure. However, the presence of the following combination of characteristics confirms that they belong to the genus *Branchiobaetis*: (1) one finger-like accessory gill ventrally on coxal articulation of foreleg; (2) accessory gill outside laterally between stipes and cardo at the base of maxillae; (3) bubble-like membranous swelling between coxa and trochanter of legs; (4) one row of row of small, apically decurved hook-like setae along dorsal margin of femur, tibia, and tarsus on legs. In addition to these three differences, the new species can be distinguished from other known species of *Branchiobaetis* by the following combination of characters in the larvae.

In *B. borealis* sp. nov.: (1) abdominal tergites with contrasting colour pattern as Fig. 1; (2) paraglossae of labium with three rows of long, robust, distally pectinate setae distoventrally; (3) femur with row of long, stout, clavate setae along dorsal margin, villopore well developed on all legs; (4) claw without subapical seta; (5) untypical folding way of gonostyli bud.

In *B. megasinus* sp. nov.: (1) abdominal tergites almost uniformly brown except for with a cream oval macula anterior medially on tergite V, legs with contrasting cream and brown alternating bands as Fig. 8; (2) paraglossae of labium with two rows of long, robust, distally pectinate setae distoventrally; (3) femur with row of long, stout, blunt pointed setae along dorsal margin, villopore well developed on all legs; (4) claw without subapical seta.

Branchiobaetis megasinus sp. nov. is the second species in the genus that is known with a male imago. Compared with male imago of *Branchiobaetis javanicus* (Ulmer, 1913) (in Kaltenbach et al. 2022b), the new species can be distinguished by the following combination of characters: (1) precursors of turbinate eyes are normal based on the exuviae of last instar male larva (vs with elevated area with well-expressed facets in *B. javanicus* (Kaltenbach et al. 2022b: fig. 5c); (2) forewing costa serrated with pointed spines on basal portion (Fig. 16b), pterostigma area almost transparent with four or five– slanting cross veins (vs costa smooth and pterostigma area brown with at least ten slanting cross veins or veinlets in *B. javanicus*); (3) femur of foreleg arched medially (Fig. 17g). In *B. javanicus*, the femur is straight, but the tibia is slightly arched medially (Kaltenbach et al. 2022b: fig. 8a); (4) genitalia: inner margin of segment I of gonostylus with distomedial expansion and outer margin with protuberance basally (Fig. 17a), segment III of gonostylus oblong (vs segment I of gonostylus with projected blunt angle proximad of its middle; segment III short and triangular in *B. javanicus*). Consequently, as Kaltenbach et al. (2022b) pointed out, the imaginal generic diagnosis is currently still difficult to define until more male imagos are described.

The most striking characteristic of *Branchiobaetis* is the presence of the accessory gills (the etymology of the genus is derived from this character), i.e., coxal gills (located between coxae and prosterna) and maxillary gills (located between stipes and cardo). An overview of accessory gills among mayflies and a discussion of the possibility of their respiratory function is given by Kaltenbach et al. (2022b). Other than that, another interesting character of the genus is the presence of a bubble-like, membranous swelling located between the coxa and trochanter and between the coxa and pleurite, and the branches of tracheae are observed under the swelling. These thin-walled, air sac-like structures on the articulation of legs are rare in Baetidae, even in Ephemeroptera.

It is unclear whether they serve as the accessory respiratory organs, or the air sacs are formed by tracheal dilatation for adjusting their respiration or buoyancy (Harrison et al. 2023).

In aquatic ecosystems, dissolved oxygen (DO) concentration is not only the primary limiting factor that determines aquatic insect physiology and behaviour, but also a critical measure of habitat quality and river health. Thus, DO concentrations are one of major factors influencing biological diversity and productivity of freshwater ecosystems worldwide (Dudgeon 2008; Jacobus et al. 2019). According to our rearing experience, when transferring the larvae of the new species together with other baetid larvae (e.g., *Baetis* spp., *Labiobaetis* sp., *Liebebiella vera*) to indoors for rearing, we found that the mortality rate of *B. borealis* sp. nov. and *B. megasinus* sp. nov. was much higher than those of other baetid larvae without such accessory gills, even with the aid of portable air pump during transportation. In addition, the same is true of *Branchiobaetis javanicus* (Ulmer, 1913) in Southeast Asia as the “larvae are unable to live for a long time in stagnant water” (Kaltenbach et al. 2022b). One possible explanation is that they are possibly a sensitive species to low dissolved oxygen or hypoxia owing to their relatively high oxygen demand in water. In present study, the two new species occur most commonly in very clean, cool, and well-oxygenated mountainous or forest streams in subtropical China. For example, the dissolved oxygen concentration is up to 9.4 mg/L in the type locality of *B. megasinus* sp. nov. In general, as the water temperature increases, the dissolved oxygen concentration decreases. Thus, the average water temperature of rivers in Southeast Asia is usually warmer than that of rivers in subtropical China (Dudgeon 2008). The accessory gills on maxillae of the new species are less developed and reduced to a small tongue-like structure (Figs 3b, 10c). In contrast, the maxillary gills of the species in Southeast Asia are well developed (Kaltenbach et al. 2022b: figs 1a, 18j), which may be an adaptation to low dissolved oxygen environment in Southeast Asia, as only by increasing the absorption area of maxillary gills can they absorb enough dissolved oxygen in water. Nevertheless, it remains unclear if the contribution of coxal gills or maxillary gills to oxygen uptake is significant or negligible. The establishment of these two new species will facilitate the subsequent in-depth studies on their morphological anatomy, oxygen uptake, and other biological traits.

Acknowledgements

This work was supported by the National Natural Science Foundation of China (No. 31872265) and the Science & Technology Fundamental Resources Investigation Program (No. 2022FY100504). Thanks are due to Lin Hong, Jian Jiang, Haoyang Chen, Lijia Qiu, and Prof. Xingmin Wang for help with the fieldwork and to the reviewers for their advice and constructive comments.

Additional information

Conflict of interest

The authors have declared that no competing interests exist.

Ethical statement

No ethical statement was reported.

Funding

This work was supported by the National Natural Science Foundation of China (No. 31872265) and the Science & Technology Fundamental Resources Investigation Program (No. 2022FY100504).

Author contributions

Investigation and rearing, XT, ZZ, BW; writing and editing, XT; slide preparation, photography and figures, XT.

Author ORCIDs

Xiaoli Tong  <https://orcid.org/0000-0003-1731-229X>

Zhiheng Zhou  <https://orcid.org/0009-0009-0763-8713>

Bangyi Wu  <https://orcid.org/0009-0005-6398-5243>

Data availability

All of the data that support the findings of this study are available in the main text.

References

- Barber-James HM, Gattolliat J-L, Sartori M, Hubbard MD (2008) Global diversity of mayflies (Ephemeroptera, Insecta) in freshwater. *Hydrobiologia* 595: 339–350. <https://doi.org/10.1007/s10750-007-9028-y>
- Dudgeon D (2008) *Tropical Stream Ecology* (1st edn.). Academic Press. Elsevier Science, London, UK.
- Gattolliat J-L (2012) Two new genera of Baetidae (Ephemeroptera) from Borneo (East Kalimantan, Indonesia). *Annales de Limnologie – International Journal of Limnology* 48(2): 187–199. <https://doi.org/10.1051/limn/2012012>
- Gattolliat J-L, Nieto C (2009) The family Baetidae (Insecta: Ephemeroptera): synthesis and future challenges. *Aquatic Insects* 31(sup1): 41–62. <https://doi.org/10.1080/01650420902812214>
- Gillies MT (1949) Notes on some Ephemeroptera Baetidae from India and South-East Asia. *Transactions of the Royal Entomological Society of London* 100: 161–177.
- Gillies MT (1951) Further notes on Ephemeroptera from India and South East Asia. *Proceedings of the Royal Entomological Society of London B* 20: 121–130. <https://doi.org/10.1111/j.1365-3113.1951.tb01009.x>
- Harrison JF, McKenzie EKG, Talal S, Socha JJ, Westneat MW, Matthews PGD (2023) Air sacs are a key adaptive trait of the insect respiratory system. *Journal of Experimental Biology* 226: jeb245712. <https://doi:10.1242/jeb.245712>
- Jacobus LM, Macadam CR, Sartori M (2019) Mayflies (Ephemeroptera) and their contributions to ecosystem services. *Insects* 10(6): 1–26. <https://doi.org/10.3390/insects10060170>
- Kaltenbach T, Gattolliat J-L (2018) The incredible diversity of *Labiobaetis* Novikova & Kluge in New Guinea revealed by integrative taxonomy (Ephemeroptera, Baetidae). *ZooKeys* 804: 1–136. <https://doi.org/10.3897/zookeys.804.28988>
- Kaltenbach T, Gattolliat J-L (2019) The tremendous diversity of *Labiobaetis* Novikova & Kluge in Indonesia (Ephemeroptera, Baetidae). *ZooKeys* 895: 1–117. <https://doi.org/10.3897/zookeys.895.38576>
- Kaltenbach T, Gattolliat J-L (2020) *Labiobaetis* Novikova & Kluge in Borneo (Ephemeroptera, Baetidae). *Zookeys* 914: 43–79. <https://doi.org/10.3897/zookeys.914.47067>

- Kaltenbach T, Gattolliat J-L (2021) New species of *Labiobaetis* Novikova & Kluge from Southeast Asia and New Guinea (Ephemeroptera, Baetidae). *ZooKeys* 1067: 159–208. <https://doi.org/10.3897/zookeys.1067.72251>
- Kaltenbach T, Gattolliat J-L (2023) New species of *Nigrobaetis* from Southeast Asia (Ephemeroptera, Baetidae). *ZooKeys* 1166: 175–234. <https://doi.org/10.3897/zookeys.1166.102941>
- Kaltenbach T, Garces JM, Gattolliat J-L (2020a) The success story of *Labiobaetis* Novikova & Kluge in the Philippines (Ephemeroptera, Baetidae), with description of 18 new species. *ZooKeys* 1002: 1–114. <https://doi.org/10.3897/zookeys.1002.58017>
- Kaltenbach T, Garces JM, Gattolliat J-L (2020b) A new genus of Baetidae (Insecta, Ephemeroptera) from Southeast Asia. *European Journal of Taxonomy* 612(612): 1–32. <https://doi.org/10.5852/ejt.2020.612>
- Kaltenbach T, Garces JM, Gattolliat J-L (2021) *Philibaetis* gen. nov., a new genus from the Philippines (Ephemeroptera, Baetidae). *Deutsche Entomologische Zeitschrift* 68(1): 1–20. <https://doi.org/10.3897/dez.68.59462>
- Kaltenbach T, Garces J, Gattolliat J-L (2022a) First contribution to *Labiobaetis* Novikova & Kluge in Cambodia (Ephemeroptera, Baetidae), with description of two new species. *ZooKeys* 1123: 63–81. <https://doi.org/10.3897/zookeys.1123.90308>
- Kaltenbach T, Kluge NJ, Gattolliat J-L (2022b) A widespread new genus of Baetidae (Baetidae, Ephemeroptera) from Southeast Asia. *ZooKeys* 1135: 1–59. <https://doi.org/10.3897/zookeys.1135.93800>
- Kaltenbach T, Kluge NJ, Gattolliat J-L (2023a) A new, widespread genus of Baetidae from South Asia (Insecta, Ephemeroptera). *ZooKeys* 1168: 231–266. <https://doi.org/10.3897/zookeys.1168.104844>
- Kaltenbach T, Phlai-ngam S, Suttinun C, Gattolliat J-L (2023b) First report of the Afrotropical genus *Securiops* Jacobus, McCafferty & Gattolliat (Ephemeroptera, Baetidae) from Southeast Asia, with description of a new species. *ZooKeys* 1157: 127–143. <https://doi.org/10.3897/zookeys.1157.99642>
- Kimmins DE (1947) New species of Indian Ephemeroptera. *Proceedings of the Royal Entomological Society of London* B16: 92–100. <https://doi.org/10.1111/j.1365-3113.1947.tb00865.x>
- Kluge NJ, Novikova EA (2011) Systematics of the mayfly taxon *Acentrella* (Ephemeroptera, Baetidae), with description of new Asian and African species. *Russian Entomological Journal* 20(1): 1–56. <https://doi.org/10.15298/rusentj.20.1.01>
- Kluge NJ, Novikova EA (2017) Occurrence of *Anafroptilum* Kluge, 2012 (Ephemeroptera: Baetidae) in Oriental Region. *Zootaxa* 4282(3): 453–472. <https://doi.org/10.11646/zootaxa.4282.3.2>
- Kluge NJ, Suttinun C (2020) Review of the Oriental genus *Indocloeon* Müller-Liebenau 1982 (Ephemeroptera: Baetidae) with descriptions of two new species. *Zootaxa* 4779(4): 451–484. <https://doi.org/10.11646/zootaxa.4779.4.1>
- Li B, Shi W, Li X, Tong X (2023) Two new species of the genus *Nigrobaetis* Kazlauskas (in Novikova & Kluge), 1987 (Ephemeroptera: Baetidae) from Southwest China. *Zootaxa* 5315(2): 131–149. <https://doi.org/10.11646/zootaxa.5315.2.3>
- Müller-Liebenau I (1980) A new species of the genus *Platybaetis* Müller-Liebenau 1980, *P. bishopi* sp. n. from Malaysia (Insecta, Ephemeroptera). *Gewässer und Abwässer* 66/67: 95–101.
- Müller-Liebenau I (1981) Review of the original materiel of the baetid genera *Baetis* and *Pseudocloeon* from the Sunda Islands and the Philippines described by G. Ulmer,

- with some general remarks (Insecta: Ephemeroptera). *Mitteilungen aus dem Hamburgischen Zoologischen Museum und Institut* 78: 197–208.
- Müller-Liebenau I (1984a) New genera and species of the family Baetidae from West-Malaysia (River Gombak) (Insecta: Ephemeroptera). *Spixiana* 7: 253–284.
- Müller-Liebenau I (1984b) Baetidae from Sabah (East Malaysia) (Ephemeroptera). In: Landa V, Soldán T, Tonner M (Eds) *Proceedings of the Fourth International Conference on Ephemeroptera*, Czechoslovak Academy of Sciences, Budejovice, 85–89.
- Phlai-ngam S, Boonsoong B, Gattolliat J-L, Tungpairajwong N (2022) *Megabranchiella* gen. nov., a new mayfly genus (Ephemeroptera, Baetidae) from Thailand with description of two new species. *ZooKeys* 1125: 1–31. <https://doi.org/10.3897/zookeys.1125.90802>
- Shi W, Tong X (2014) The genus *Labiobaetis* (Ephemeroptera: Baetidae) in China, with description of a new species. *Zootaxa* 3815(3): 397–408. <https://doi.org/10.11646/zootaxa.3815.3.5>
- Shi W, Tong X (2015a) First record of the genus *Gratia* Thomas (Ephemeroptera, Baetidae) from China with the description of a new species. *Zookeys* 478:129–137. <https://doi.org/10.3897/zookeys.478.8995>
- Shi W, Tong X (2015b) Taxonomic notes on *Baetiella* Uéno from China, with the descriptions of three new species (Ephemeroptera: Baetidae). *Zootaxa* 4012: 553–569. <https://doi.org/10.11646/zootaxa.4012.3.9>
- Shi W, Tong X (2019) Genus *Bungona* Harker, 1957 (Ephemeroptera: Baetidae) from China, with descriptions of three new species and a key to Oriental species. *Zootaxa* 4586 (3): 571–585. <https://doi.org/10.11646/zootaxa.4586.3.12>
- Suttinun C, Gattolliat J-L, Boonsong B (2020) *Cymbalcloeon* gen. nov., an incredible new mayfly genus (Ephemeroptera: Baetidae) from Thailand. *PLoS ONE* 15(10): 1–17. <https://doi.org/10.1371/journal.pone.0240635>
- Suttinun C, Kaltenbach T, Gattolliat J-L, Boonsoong B (2021) A new species and first record of the genus *Procerobaetis* Kaltenbach & Gattolliat, 2020 (Ephemeroptera, Baetidae) from Thailand. *ZooKeys* 1023: 13–28. <https://doi.org/10.3897/zookeys.1023.61081>
- Suttinun C, Gattolliat J-L, Boonsoong B (2022) First report of the genus *Tenuibaetis* (Ephemeroptera, Baetidae) from Thailand revealing a complex of cryptic species. *ZooKeys* 1084: 165–182. <https://doi.org/10.3897/zookeys.1084.78405>
- Tong X, Dudgeon D (1999) Two new species of *Platybaetis* from Sulawesi, Indonesia (Ephemeroptera: Baetidae). *Entomological News* 110 (5): 290–296.
- Tong X, Dudgeon D (2002) *Platybaetis*, a newly recorded genus of Baetidae from China (Insecta: Ephemeroptera). *Wuyi Science Journal* 18: 24–26.
- Tong X, Dudgeon D (2021) A new species of the genus *Cloeon* Leach, 1815 from China (Ephemeroptera: Baetidae). *Aquatic Insects* 42:1: 12–22. <https://doi.org/10.1080/01650424.2020.1867747>
- Tong X, Dudgeon D, Shi W (2014) A new species of the genus *Baetis* from China (Ephemeroptera: Baetidae). *Entomological News* 123(5): 333–338. <https://doi.org/10.3157/021.123.0503>
- Ulmer G (1939) Eintagsfliegen (Ephemeropteren) von den Sunda-Inseln. *Archiv für Hydrobiologie* 16: 443–692.

Caribbean Amphipoda (Crustacea) of Panama. Part III: parvorder Lysianassidira

Kristine N. White¹ 

¹ Aquatic Sciences Center, Department of Biological and Environmental Sciences, Georgia College & State University, Milledgeville, GA 31061, USA
Corresponding author: Kristine N. White (kristine.white@gcsu.edu)

Abstract

Amphipods in the parvorder Lysianassidira are scavengers, often collected in sediment, coral rubble, algae, or among other invertebrates. Members of the parvorder have a head that is deeper than long, large coxae, lacinia mobilis present only on the left molar, and a mitten-shaped gnathopod 2 propodus with a long ischium. Nine species from two families within the parvorder are documented from Bocas del Toro, Panama. This research documents range extensions for eight species and an identification key to the species of Caribbean Lysianassidira of Panama is provided.

Resumen

Los anfípodos del parvorden Lysianassidira son carroñeros, a menudo recolectados en sedimentos, escombros de coral, algas o entre otros invertebrados. Los miembros del parvorden tienen una cabeza que es más profunda que larga, con coxas grandes, lacinia mobilis presenta solo en el molar izquierdo y un gnatópodo 2 en forma de manopla con un isquion largo. Nueve especies de dos familias dentro del parvorden están documentadas en Bocas del Toro, Panamá. Esta investigación documenta extensiones de rango para ocho especies y se proporciona una clave de identificación para las especies de Lysianassidira caribeña de Panamá.

Key words: Bocas del Toro, identification key, Lysianassidae, Lysianassoidea, Tryphosidae



This article is part of:
Caribbean Amphipoda of Panama
Edited by Kristine N. White

Academic editor: Alan Myers
Received: 21 August 2024
Accepted: 4 October 2024
Published: 24 October 2024

ZooBank: <https://zoobank.org/67B6C273-62C5-4F89-AE63-316B73D65D55>

Citation: White KN (2024) Caribbean Amphipoda (Crustacea) of Panama. Part III: parvorder Lysianassidira. ZooKeys 1216: 149–171. <https://doi.org/10.3897/zookeys.1216.135258>

Copyright: © Kristine N. White.
This is an open access article distributed under terms of the Creative Commons Attribution License (Attribution 4.0 International – CC BY 4.0).

Introduction

Parvorder Lysianassidira Dana, 1849 is comprised of 1243 species around the world, with several listed as *incertae sedis* (Horton et al. 2024). Members of the parvorder are characterized by having the head that is deeper than long, antenna 1 with callynophore, large coxae, lacinia mobilis present only on the left molar, and a distally mitten-shaped gnathopod 2 propodus with a long ischium (Lowry and Myers 2017). The parvorder contains 33 families of amphipods: Alcellidae Lowry & DeBroyer, 2008 (17 spp.), Parargissidae Lowry & Myers, 2017 (two spp.), Podopronidae Lowry & Stoddart, 1996 (four spp.), Valettidae Stebbing, 1888 (two spp.), Valettiopsidae Lowry & DeBroyer, 2008 (12 spp.), Vemaniidae Lowry & Myers, 2017 (five spp.), Stegocephalidae Dana, 1852 (110 spp.), Adeliellidae Lowry & Myers, 2017 (three spp.), Amaryllididae Lowry & Stoddart,

2002 (37 spp.), Cebocaridae Lowry & Stoddart, 2011 (15 spp.), Cyclocaridae Lowry & Stoddart, 2011 (four spp.), Cyphocarididae Lowry & Stoddart, 1997 (21 spp.), Eurytheneidae Stoddart & Lowry, 2004 (10 spp.), Hirondelleidae Lowry & Stoddart, 2010a (20 spp.), Lysianassidae Dana, 1849 (130 spp.), Opisidae Lowry & Stoddart, 1995 (19 spp.), Scopelocheiridae Lowry & Stoddart, 1997 (27 spp.), Tryphosidae Lowry & Stoddart, 1997 (389 spp.), Uristidae Hurley, 1963 (190 spp.), Acidostomatidae Stoddart & Lowry, 2012 (11 spp.), Ambasiidae Lowry & Myers, 2017 (three spp.), Aristiidae Lowry & Stoddart, 1997 (42 spp.), Conicostomatidae Lowry & Stoddart, 2012 (19 spp.), Derjugianidae Lowry & Myers, 2017 (one sp.), Endeavouridae Lowry & Stoddart, 1997 (19 spp.), Izinkalidae Lowry & Stoddart, 2010c (two spp.), Kergueleniidae Lowry & Stoddart, 2010d (26 spp.), Lepidepcrellidae Stoddart & Lowry, 2010 (12 spp.), Pakynidae Lowry & Myers, 2017 (38 spp.), Sophrosynidae Lowry & Stoddart, 2010b (14 spp.), Thoriellidae Lowry & Stoddart, 2011 (seven spp.), Trischizostomatidae Lilljeborg, 1865 (18 spp.), Wandinidae Lowry & Stoddart, 1990 (four spp.). Only 30 species in the parvorder have been previously reported from the Caribbean Sea, representing ten families (Aristiidae, Cyphocarididae, Endeavouridae, Eurytheneidae, Lysianassidae, Parargissidae, Stegocephalidae, Tryphosidae, Uristidae, Vemanidae). Four species, *Concarnes concavus* (Shoemaker, 1933), *Eclecticus eclecticus* Lowry & Stoddart, 1997, *Paracentromedon carabicus* Barnard, 1964, and *Vemana compressa* Barnard, 1964 have been previously reported from Caribbean Panama (LeCroy et al. 2009; Miloslavich et al. 2010; Martín et al. 2013). Miloslavich et al. (2010) listed *Parargissa galathea americana* Barnard, 1961 from Caribbean Panama without locality details, but Barnard (1961) stated that it was collected from the Pacific. Andres (1977) documented *P. galathea americana* from the eastern Atlantic, but the author can find no reports of this species from the Caribbean and, thus, do not include it herein.

Within the parvorder Lysianassidira, nine species of amphipods were collected from Bocas del Toro, Panama, with representatives from the families Lysianassidae and Tryphosidae. Regional diagnoses for each species collected during this study are provided herein. An identification key is provided to distinguish between the Lysianassidira species known from the Caribbean waters of Panama.

Methods

Coral rubble, sand, algae, and sponges were collected by hand and placed into buckets or plastic bags from various sites around Bocas del Toro, Panama at depths of 0–15 m. Coral rubble, sand, and algae were elutriated with fresh water to remove amphipods, and sponges were sorted through by hand. Live amphipods were sorted to morphospecies, placed in clove oil for imaging, and preserved in 99.5% EtOH for later examination. Preserved specimens were transferred to glycerol, measured from the tip of the rostrum to the base of the telson, and dissected under a stereomicroscope. Specimens were illustrated using a Meiji MT5900L phase contrast microscope with an Olympus U-DA drawing tube. Illustrations were digitally inked following Coleman (2003) in Adobe Illustrator 2024 using a Wacom® Intuos Pro Pen Tablet. Abbreviations used in figures are as follows: Hd, head; Mx2, maxilla 2; G, gnathopod; P, pereopod; E, epimeron; Ur: urosome; U, uropod; T, telson. Size ranges of each species collected from Bocas del Toro, Panama are provided at the beginning of each

material examined section. Specimens are deposited in the Smithsonian Institution, U.S. National Museum of Natural History (**USNM**) and the Gulf Coast Research Laboratory Museum (**GCRL**).

Results

Parvorder Lysianassidira Dana, 1849

Superfamily Lysianassoidea Dana, 1849

Family Lysianassidae Dana, 1849

Genus *Aruga* Holmes, 1908

Diagnosis. Antenna 1 with strong callynophore in male and female. Antenna 2 flagellum elongate in male. Epistome not produced; upper lip produced. Maxilla 2 inner plate narrow. Gnathopod 1 simple. Gnathopod 2 minutely chelate. Uropod 2 inner ramus with dorsal notch, gradually narrowing distally. Uropod 3 outer ramus 2-articulate. Telson entire.

***Aruga holmesi* J.L. Barnard, 1955**

Figs 1, 10A

Aruga holmesi J.L. Barnard, 1955: 100, pls 27, 28; J.L. Barnard 1958: 90; J.L. Barnard 1959: 18; Gurjanova 1962: 299–301, figs 98, 99; J.L. Barnard 1964: 79, chart 1; Barnard and Karaman 1991: 469; Lowry and Stoddart 1997: 47–53, figs 17–20; LeCroy 2007: 575, fig. 497.

Lysianopsis holmesi: Hurley 1963: 74, 75, fig. 21b.

Lysianassa holmesi: J.L. Barnard 1966a: 25; J.L. Barnard 1966b: 69; J.L. Barnard 1979: 12, 130; Austin 1985: 600; Stepien and Brusca 1985: 97–101, fig. 2F; Stretch 1985: 129–133.

Material examined. PANAMA • 4.8 mm • 1 ♀; Bocas del Toro, Crawl Cay; 9.2376°N, 82.1438°W; depth 1.5–3 m, among coral rubble; 11 Aug 2021; K.N. White leg.; USNM 1739772.

Diagnosis. Upper lip projecting well beyond epistome; epistome concave. Gnathopod 1 propodus posterodistal margin slightly concave. Epimeron 3 posteroventral corner subquadrate, without tooth. Uropod 3 peduncle length at least 2 × width. Telson distal margin truncate, slightly emarginate, with two short setae on each side.

Distribution. USA: Folly Island, South Carolina; Florida from Perdido Key to the lower Florida Keys (LeCroy 2007); Pacific California (Lowry and Stoddart 1997); Ecuador (Lowry and Stoddart 1997); Panama: Pacific side of Isthmus of Panama (Lowry and Stoddart 1997); Bocas del Toro (present study).

Ecology and remarks. These amphipods are associated with coral rubble and seagrass beds at depths of 1.5–120 m. Panamanian specimens agree closely with previous descriptions of the species. Lowry and Stoddart (1997) recorded this species from the Gulf of Mexico for the first time, noting that it was previously only known from the Pacific side of the Isthmus of Panama. Panamanian specimens are white in color when alive.

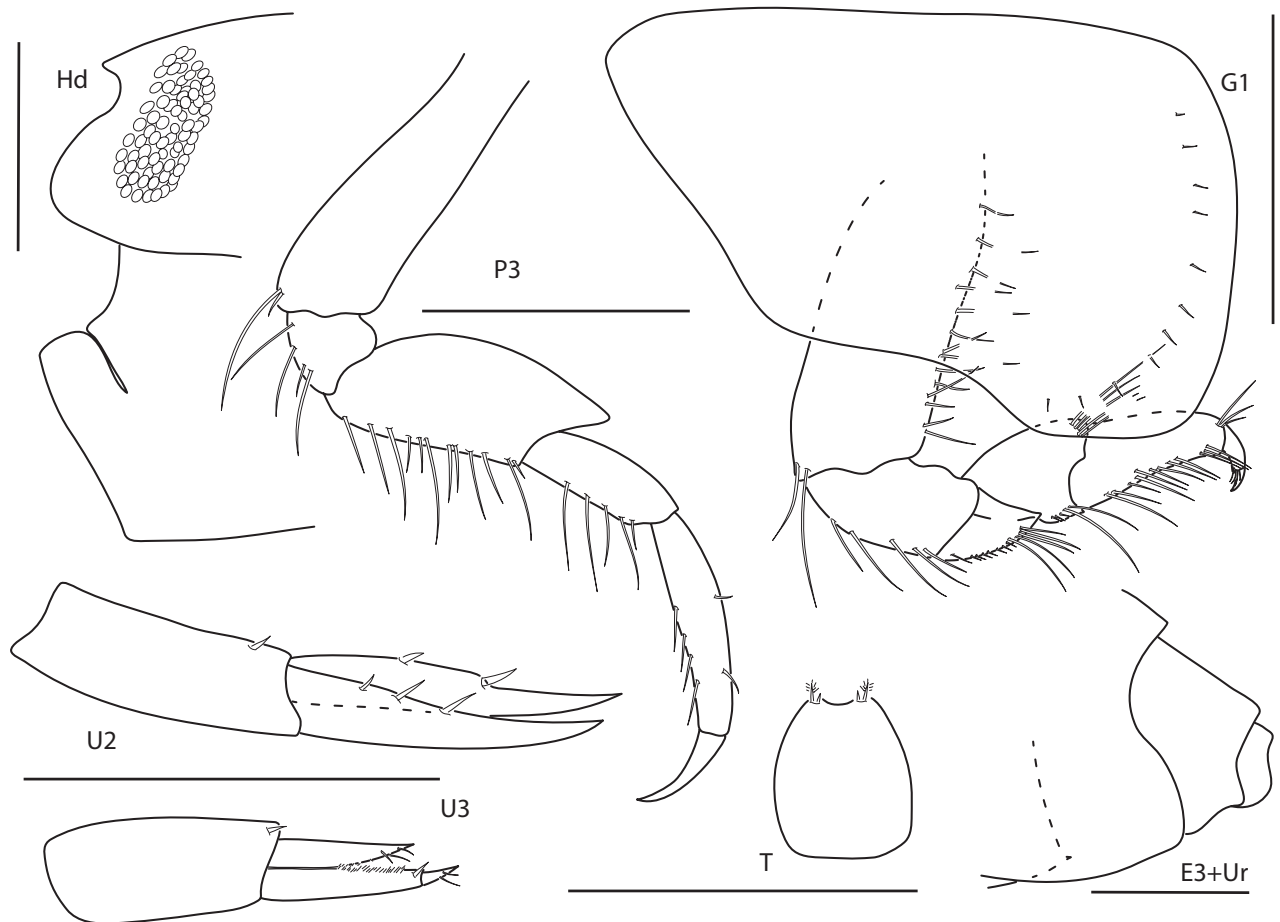


Figure 1. *Aruga holmesii*, female, 4.8 mm, head, epistome and upper lip, pereopod 3, gnathopod 1 lateral, uropod 2, uropod 3, telson, epimeron 3 and urosome. Scale bars: 0.5 mm.

Genus *Bonassa* Barnard & Karaman, 1991

Diagnosis. Antenna 1 with strong callynophore in male. Antenna 2 flagellum elongate in male. Epistome and upper lip produced. Maxilla 2 inner plate narrow. Gnathopod 1 simple. Gnathopod 2 minutely chelate. Uropod 2 inner ramus with dorsal notch, gradually narrowing distally. Uropod 3 outer ramus 1-articulate. Telson entire.

Bonassa bonairensis (Stephensen, 1933)

Figs 2, 10B

Lysianassa (?) *bonairensis* Stephensen, 1933a: 416–420, figs 1, 2; Stephensen 1948: 1, 3.

Lysianassa bonairensis J.L. Barnard, 1958: 94; Ortiz 1979: 19.

Bonassa bonairensis Barnard & Karaman, 1991: 472; Lowry and Stoddart 1997: 54–58, figs 21–23.

Material examined. PANAMA • 2–3 mm • 1 ♀; Bocas del Toro, Swan Cay; 9.4533°N, 82.2983°W; depth 2–3 m, among algae; 4 Aug 2005; S. DeGrave leg.; GCRL 6655 • 1 ♀; Bocas del Toro, Drago; 9.418056°N, 82.3375°W; depth 2–3 m, among coral rubble, 9 Aug 2021; K.N. White leg.; USNM 1739773 • 1 juvenile;

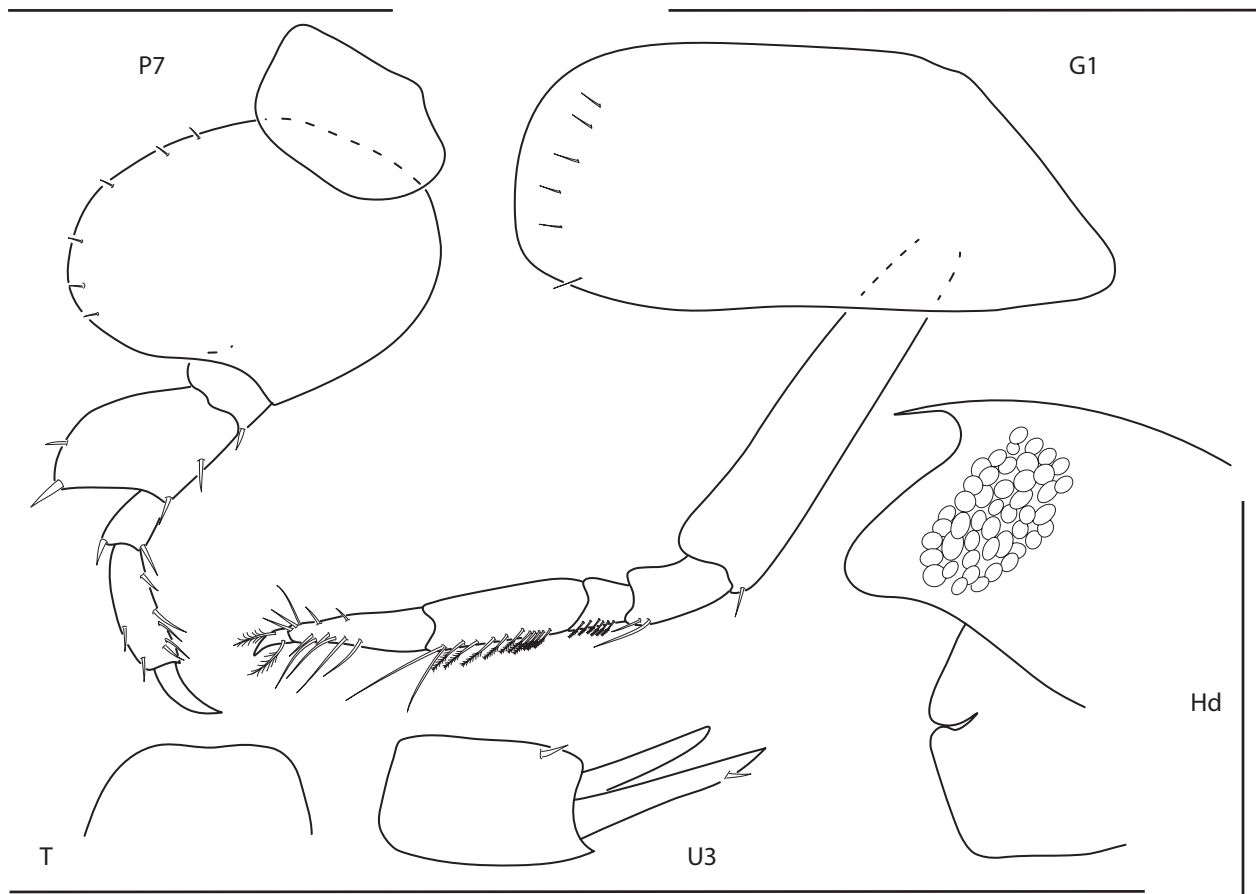


Figure 2. *Bonassa bonairensis*, female, 2.8 mm, pereopod 7, gnathopod 1 lateral, telson, uropod 3, head, epistome and upper lip. Scale bars: 0.5 mm.

Bocas del Toro, Hospital Point; 9.331967°N, 82.214817°W; depth 1–3 m, among coral rubble; 22 June 2023; K.N. White leg.; USNM 1739774.

Diagnosis. Epistome produced, rounded, subequal to produced upper lip. Antenna 1 with strong callynophore in female. Gnathopod 1 propodus distally narrowing. Pereopod 7 basis greatly expanded, posteriorly rounded; merus greatly expanded, approximately 3 × width of carpus. Uropod 3 rami narrow, apically acute, and lacking plumose setae in female. Telson distal margin truncate, slightly emarginate.

Distribution. Lesser Antilles: Bonaire Island (Stephensen 1933a; Lowry and Stoddart 1997); Panama: Bocas del Toro (present study).

Ecology and remarks. These amphipods occur among algae and coral rubble at depths of 1–3 m. Panamanian specimens agree closely with previous descriptions of the species, with the exception of a slightly emarginate telson, with the exception of the uropod 3, which is documented for the first time in a female. This species is easily distinguishable based on the expanded pereopod 7 basis and merus. Panamanian specimens are a translucent white color when alive.

Genus *Concarnes* Barnard & Karaman, 1991

Diagnosis. Antenna 1 with strong callynophore in male, lacking in female. Antenna 2 flagellum short in male and female. Epistome and upper lip produced.

Mouthparts forming quadrate bundle. Maxilla 2 inner plate broad. Gnathopod 1 simple. Uropod 2 inner ramus with dorsal notch, gradually narrowing distally. Uropod 3 outer ramus 2-articulate. Telson weakly cleft.

***Concarnes concavus* (Shoemaker, 1933)**

Figs 3, 10C

Socarnes concavus Shoemaker, 1933: 247–248, fig. 1; J.L. Barnard 1958: 99; Gurjanova 1962: 304; Ortiz 1979: 19.

Concarnes concavus Barnard & Karaman, 1991: 477; Lowry and Stoddart 1997: 58–63, figs 24–26; LeCroy 2007: 576, fig. 493.

Material examined. PANAMA • 5–6 mm • 1 ♀; Bocas del Toro, Crawl Cay; 9.2475°N, 82.1290°W; depth 5 m, among coral rubble; 12 Aug 2021; K.N. White leg.; USNM 1739775 • 1 ♀; Bocas del Toro, Crawl Cay; 9.2460°N, 82.1369°W; depth 1–4 m, among coral rubble; 25 June 2023; K.N. White leg.; USNM 1739776.

Diagnosis. Head ocular lobe subacute. Epistome produced, rounded, subequal to produced upper lip. Gnathopod 1 basis slender, elongate; propodus distally narrowing. Gnathopod 2 minutely subchelate. Telson partially cleft, lobes apically rounded.

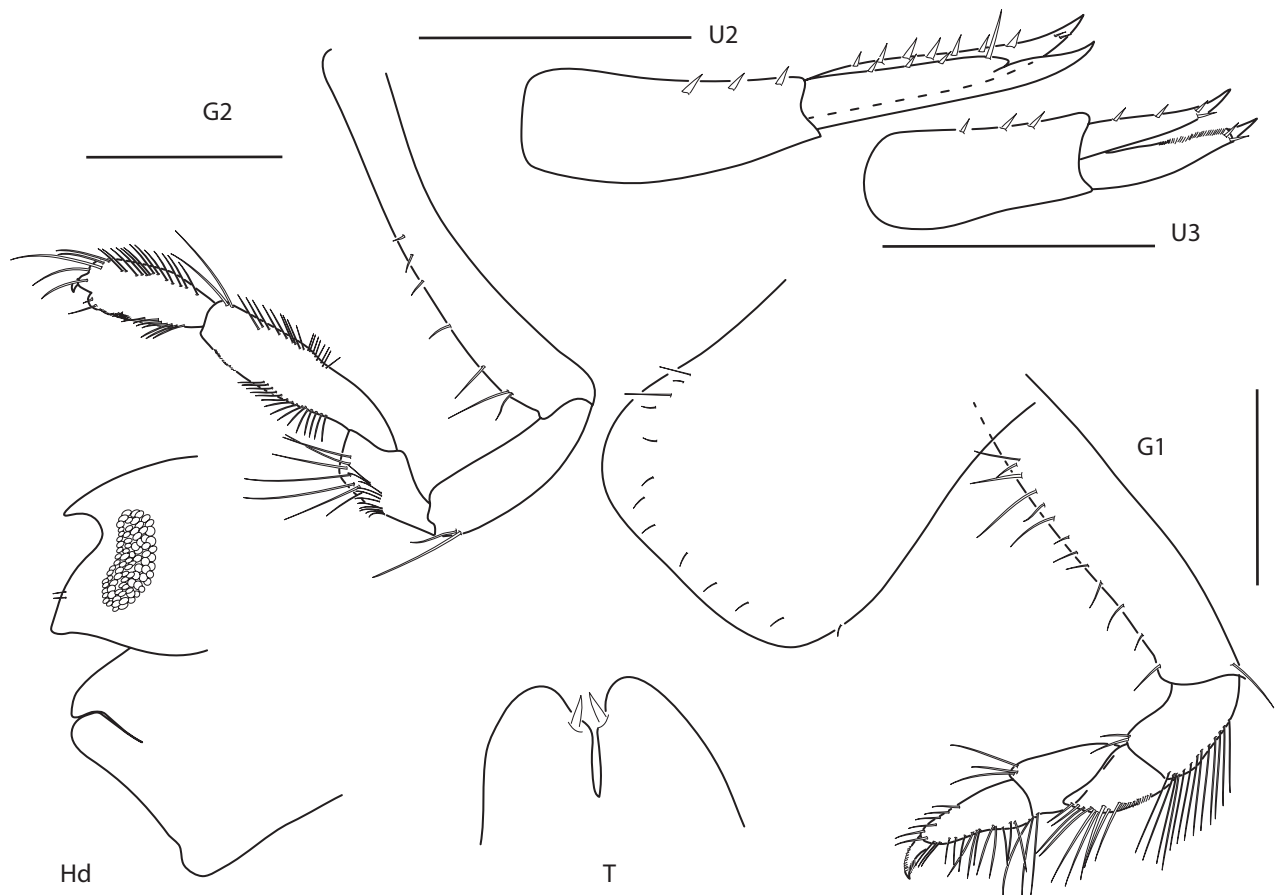


Figure 3. *Concarnes concavus*, female, 6.0 mm, gnathopod 2 lateral, uropod 2, uropod 3, head, epistome, and upper lip, telson, gnathopod 1 medial. Scale bars: 0.5 mm.

Distribution. USA: Santee River, South Carolina (LeCroy 2007); off Sapelo and Little Tybee Islands, Georgia (LeCroy 2007); Dry Tortugas (Shoemaker 1933); Gulf of Mexico from Florida Keys to Panama City (Thomas 1993; Lowry and Stoddart 1997; LeCroy 2007); Belize (Thomas 1993); Panama: Bocas del Toro (Miloslavich et al. 2010; present study).

Ecology and remarks. These amphipods are associated with coral rubble and coarse sand at depths of 1–80 m. Panamanian specimens agree closely with previous descriptions of the species. This species is easily recognizable by the subacute ocular lobe, produced epistome and upper lip, and slender, elongate basis of gnathopod 1. Panamanian specimens have a distinct red coloration on the tips of antennae and on the anterior half of the body and have a white snowflake pattern on the posterior half of the body when alive.

Genus *Lysianopsis* Holmes, 1903

Diagnosis. Antenna 1 with strong callynophore in male, weak or lacking in female. Antenna 2 flagellum short in male and female. Epistome not produced; upper lip produced. Maxilla 2 inner plate narrow. Gnathopod 1 simple. Gnathopod 2 minutely chelate. Uropod 2 inner ramus with dorsal notch, gradually narrowing distally. Uropod 3 outer ramus 1-articulate. Telson entire.

Lysianopsis hummelincki (Stephensen, 1933)

Figs 4, 10D

Lysianassa hummelincki Stephensen, 1933b: 438–440, fig. 1; Pirlot 1936: 256; Stephensen 1948: 1, 3, table 1; J.L. Barnard 1958: 94; Hurley 1963: 72; Ortiz 1979: 19.

Lysianassa falcata Stephensen, 1933b: 440–441, fig. 2; Stephensen 1948: 1, 4, table 1; J.L. Barnard 1958: 94; Ortiz 1979: 19.

Lysianopsis alba Barnard & Karaman, 1991: 499 (in part).

Falcanassa falcata Barnard & Karaman, 1991: 486.

Lysianopsis hummelincki Lowry & Stoddart, 1997: 82–89, figs 37–39.

Material examined. PANAMA • 4 mm • 1 ♂; Bocas del Toro, Hospital Point; 9.3320°N, 82. 2148°W; depth 1–3 m, among coral rubble; 22 June 2023; K.N. White leg.; USNM 1739777.

Diagnosis. Upper lip produced well beyond epistome; epistome straight. Gnathopod 1 of male prehensile. Pereopod 7 basis slightly expanded, posterior margin almost straight, merus slightly expanded, approximately 1.4 × width of carpus. Uropod 3 peduncle length about 1.5 × width; outer ramus 1-articulate. Telson distal margin rounded.

Distribution. Lesser Antilles: Curaçao (Stephensen 1933b); Panama: Bocas del Toro (present study).

Ecology and remarks. These amphipods are associated with sand and coral rubble at depths of intertidal 0–12 m. Panamanian specimens agree closely with previous descriptions with the exception of the almost straight posterior margin on the pereopod 7 basis, which was described by Lowry and Stoddart

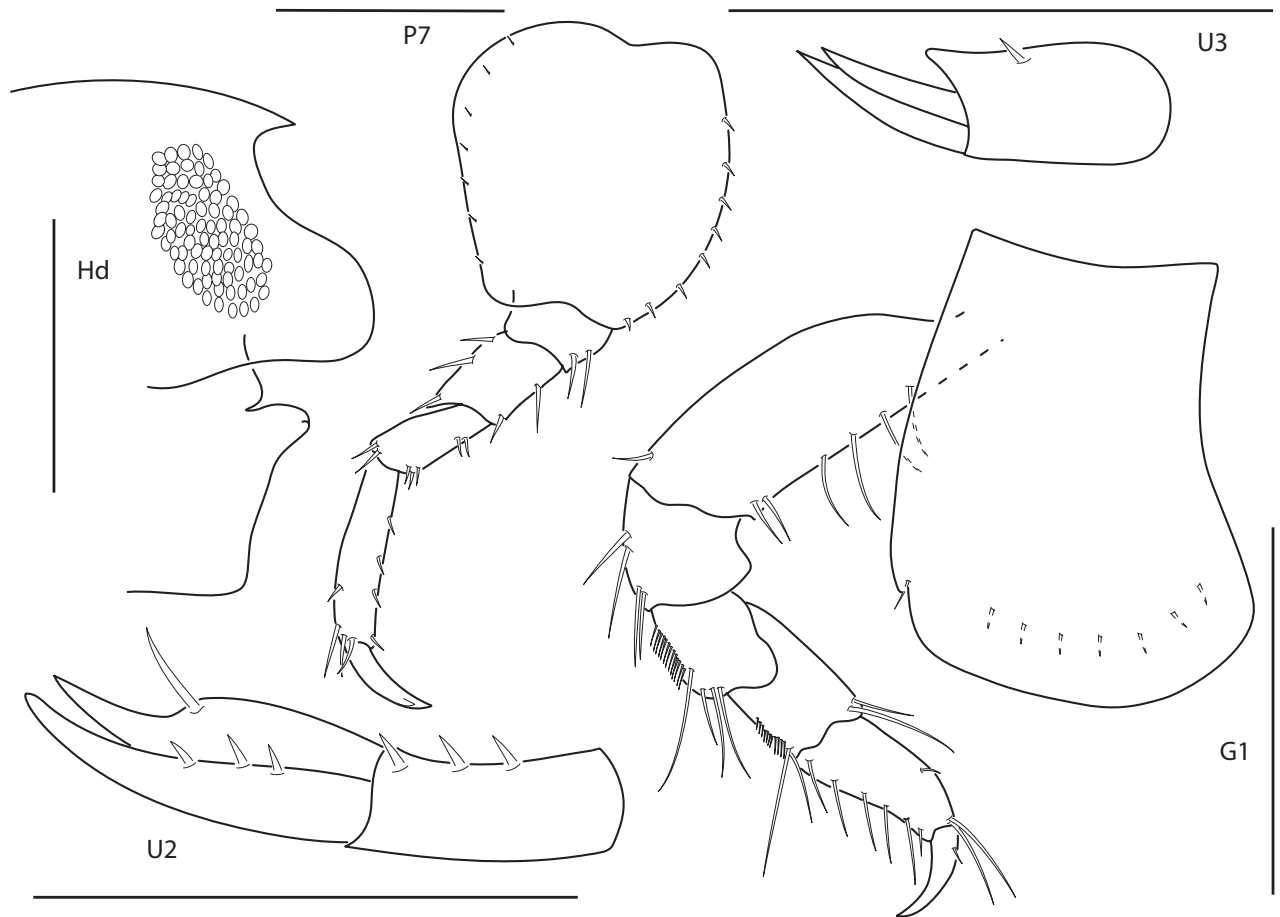


Figure 4. *Lysianopsis hummelincki*, male 4.0 mm, head, upper lip, and epistome, pereopod 7, gnathopod 1, uropod 2, uropod 3. Scale bars: 0.5 mm.

(1997) as slightly concave. This species is easily recognizable by the 1-articulate outer ramus on uropod 3 and the prehensile gnathopod 1 in males. Panamanian specimens are white with brown spots when alive.

***Lysianopsis ozona* Lowry & Stoddart, 1997**

Figs 5, 10E

Lysianopsis ozona Lowry & Stoddart, 1997: 87–91, figs 40–42.

Material examined. PANAMA • 3.2–8.5 mm • 2 ♀; Bocas del Toro, Bastamientos; depth 0–1 m, mangrove scrapings; 1 Aug 2005; T.A. Haney leg.; GCRL 6656. • 2 ♂; Bocas del Toro, Hospital Bight; 9.3045°N, 82.3160°W; depth 1.5 m, among coral rubble; 7 Aug 2005; T.A. Haney leg.; GCRL 6657 • 1 ♀; Bocas del Toro, Marina Bocas; depth 0–1 m, associated with *Phallusia nigra* ascidian; 5 June 2009; R. Rocha leg.; GCRL 6658 • 1 ♂; Bocas del Toro, Isla Solarte; 9.2901°N, 82.1897°W; depth 1–5 m, associated with solitary ascidian; 8 Aug 2021; K.N. White leg.; USNM 1739778.

Diagnosis. Epistome concave, subequal to upper lip. Gnathopod 1 propodus posterodistal margin straight; not sexually dimorphic. Uropod 3 peduncle

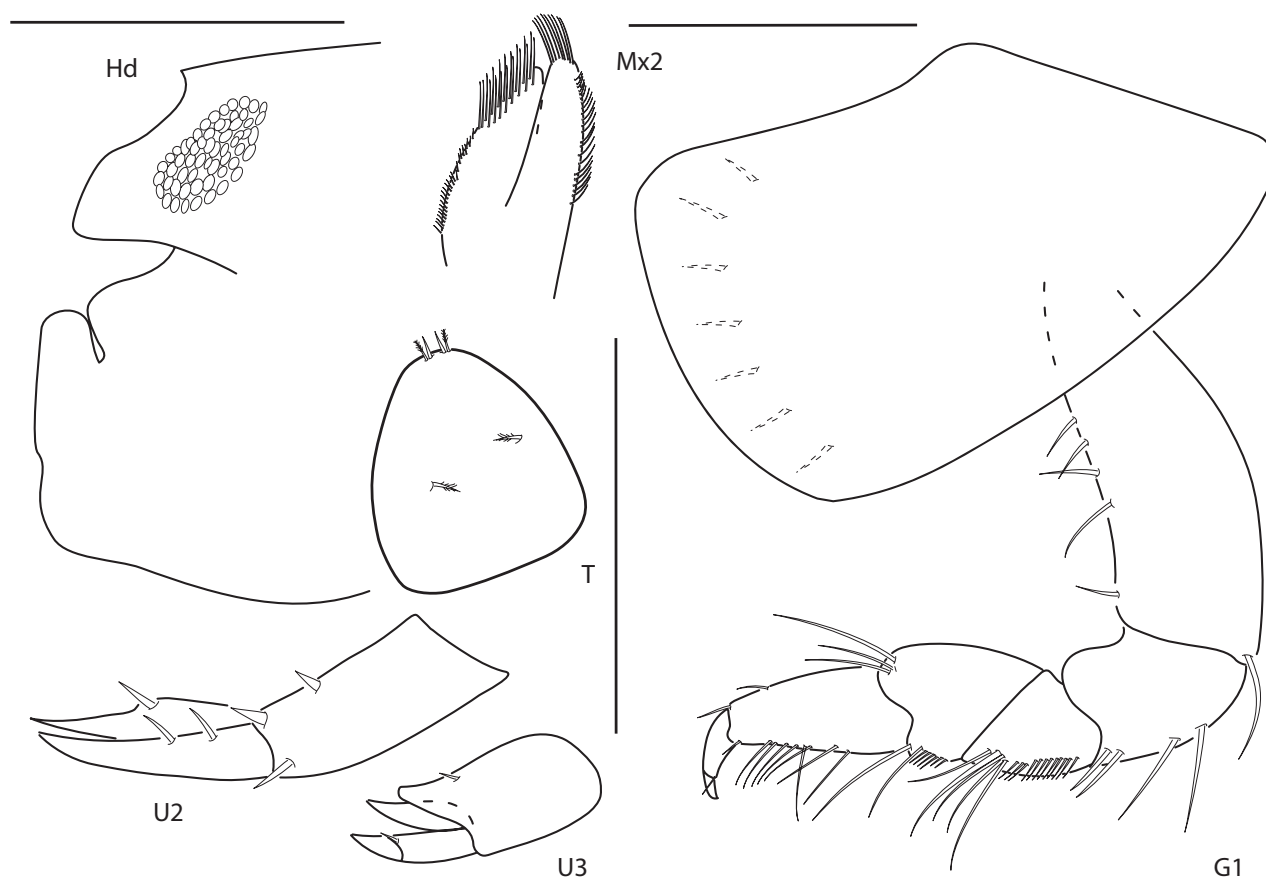


Figure 5. *Lysianopsis ozona*, male, 3.2 mm, head, upper lip, and epistome, uropod 2, uropod 3, gnathopod 1 lateral; male, 6.5 mm, maxilla 2, telson. Scale bars: 0.5 mm.

length approximately $1.5 \times$ width; outer ramus 2-articulate. Telson apical margin slightly truncate, apical margin with four short setae medially.

Distribution. USA: Eastern Gulf of Mexico (Lowry and Stoddart 1997); Panama: Bocas del Toro (present study).

Ecology and remarks. These amphipods are associated with sand, coral rubble, and various invertebrates at depths of 0–29 m. Panamanian specimens agree closely with the description provided by Lowry and Stoddart (1997). This species is easily recognizable by the concave epistome and the short uropod 3 peduncle and 2-articulate outer ramus. Panamanian specimens have an orange-brown coloration with white stripes along the pereonite edges when alive.

Genus *Shoemakerella* Pirlot, 1936

Diagnosis. Antenna 1 with weak callynophore in male, lacking in female. Antenna 2 flagellum short in male and female. Epistome not produced; upper lip produced. Maxilla 2 inner plate wider than outer plate. Gnathopod 1 simple. Pereopods 3–4 merus not enlarged compared to carpus. Uropod 2 inner ramus with dorsal notch, abruptly narrowing distally. Uropod 3 outer ramus 1-articulate. Telson entire, dorsal setae inserted proximally (compared to other genera).

***Shoemakerella cubensis* (Stebbing, 1897)**

Figs 6, 11A

Lysianax cubensis Stebbing, 1897: 29–30, pl. 7B; Hurley 1963: 70–71, fig. 20 b, c; Lowry and Stoddart 1989: 236–237.

Lysianassa cubensis Stebbing, 1906: 38; Shoemaker 1935: 232–234, fig. 1.

Lysianopsis alba Pearse, 1912: 369, fig. 1 (in part); Shoemaker 1921: 99.

Shoemakerella nasuta Pirlot, 1936: 265–266; Pirlot 1939: 47–48; Shoemaker 1948: 1–2; J.L. Barnard 1969: 180; Ortiz and Lalana Rueda 1993: 26; Ortiz and Lemaitre 1994: 124.

Lysianopsis cubensis Hurley, 1963: fig. 21a.

Lysianassa nasuta Ortiz, 1978: 8; Ortiz 1979: 19; Lalana Rueda and Pérez Moreno 1985: 51; Lalana Rueda et al. 1989: 210; Lalana Rueda and Ortiz 1990: 196; Ortiz and Lalana Rueda 1992: 40.

Shoemakerella cubensis Barnard & Karaman, 1991: 530; Lowry and Stoddart 1997: 92–98, figs 43–45; LeCroy 2007: 588, fig. 495.

Material examined. PANAMA • 1.5–4 mm • 3 ♀, 1 juvenile; Bocas del Toro, Hospital Point; 9.3336°N, 82.2188°W; depth 15 m, among coral rubble and

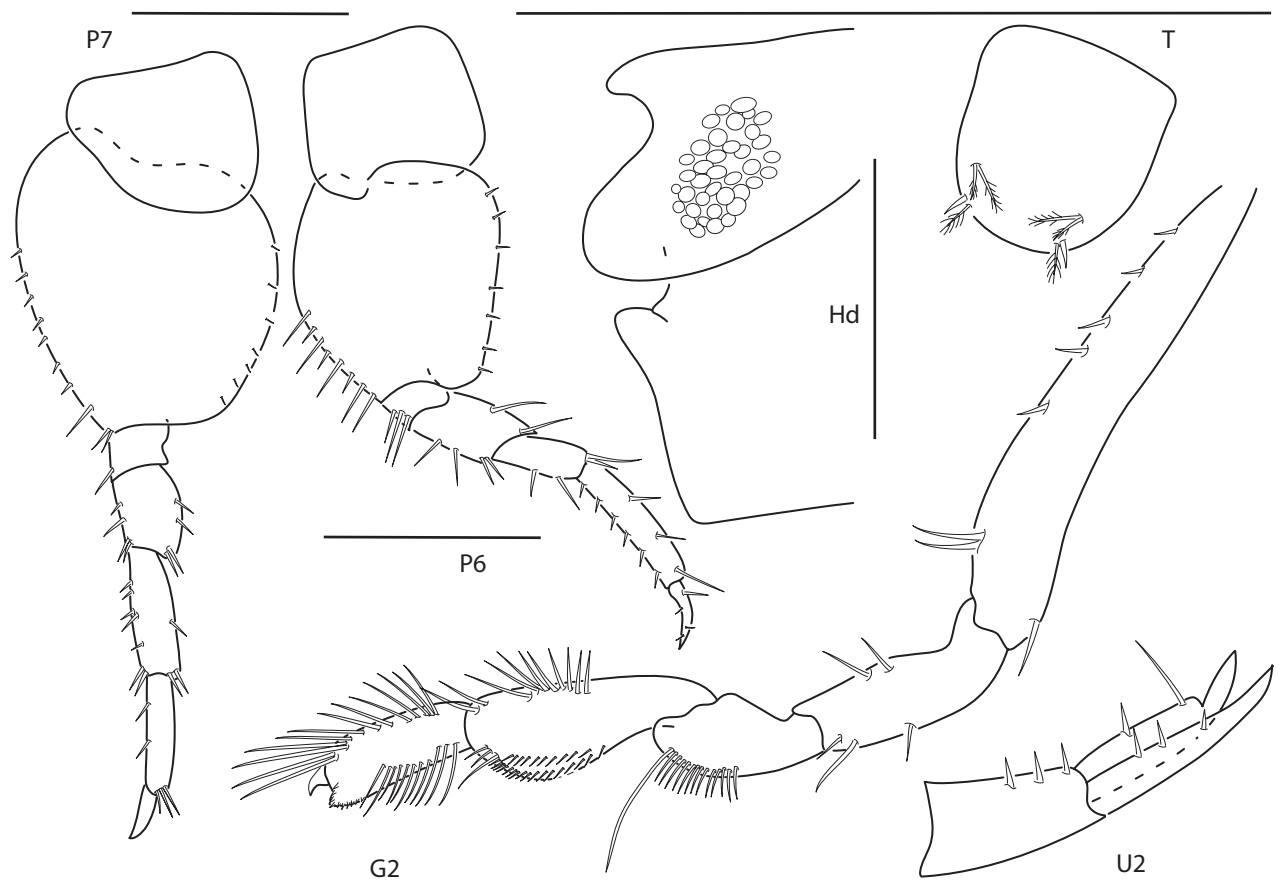


Figure 6. *Shoemakerella cubensis*, male, 4.0 mm, pereopod 7, pereopod 6, head, epistome, and upper lip, telson, gnathopod 2 lateral, uropod 2. Scale bars: 0.5 mm.

Halimeda; 6 Aug 2005; S. DeGrave and M. Salazar leg.; GCRL 6659 • 2 ♂, 9 ♀, 11 juvenile; Bocas del Toro, Lime Point; 9.4149°N, 82.3323°W; depth 0.2–0.5 m, among coral rubble and red algae; 5 Aug 2005; S. DeGrave and M. Salazar leg.; GCRL 6660 • 1 juvenile; Bocas del Toro, Juan Point; 9.3015°N, 82.2940°W; depth 10 m, among coral rubble; 7 Aug 2021; K.N. White leg.; USNM 1739779 • 1 ♂, 2 juvenile; Bocas del Toro, Isla Solarte; 9.29011°N, 82.1897°W; depth 1–5 m, mangrove scrapings; 8 Aug 2021; K.N. White leg.; USNM 1739780, USNM 1739781.

Diagnosis. Head and body with tiny setules. Epistome strongly concave. Pereopod 6 basis posterior margin nearly straight. Pereopod 7 propodus length ~5 × width. Telson apex rounded.

Distribution. USA: Panama City to Dry Tortugas, Florida (Lowry and Stoddart 1997; LeCroy 2007); Cuba (Stebbing 1897); Panama: Bocas del Toro (present study).

Ecology and remarks. These amphipods are associated with algae and coral rubble at depths of 2–69 m. Panamanian specimens closely resemble previously described specimens and can be readily distinguished from *Shoemakerella lowryi* Gable & Lazo-Wasem, 1990 based on the pereopod 6 basis posterior margin, pereopod 7 propodus length relative to the carpus length, and the telson apex. Panamanian specimens are yellow-orange in color when alive.

***Shoemakerella lowryi* Gable & Lazo-Wasem, 1990**

Figs 7, 11B

Lysianassa punctata Kunkel, 1910: 8–10, fig. 1; Johnson 1986: 377, fig. 124.
Shoemakerella lowryi Gable & Lazo-Wasem, 1990: 727–733, figs 5–7.

Material examined. PANAMA • 2–5.5 mm • 1 ♂; Bocas del Toro, San Cristobal; 9.2625°N, 82.2350°W; depth 15 m, among coral rubble; 10 August 2021; K.N. White leg.; USNM 1739782 • 1 ♀; Bocas del Toro, Swan Cay; 9.4536°N, 82.300033°W; depth 2 m, among sponges; 24 Jun 2023; K.N. White leg.; USNM 1739783 • 2 ♀; Bocas del Toro, Crawl Cay; 9.245967°N, 82.136867°W; depth 1–4 m, among coral rubble; 25 June 2023; K.N. White leg.; USNM 1739784 • 4 ♀; Bocas del Toro, Cayo Zapatilla 1; 9.2700°N, 82.0587°W; depth 10–11 m, among coral rubble; 28 June 2023; K.N. White leg.; USNM 1739785.

Diagnosis. Head and body with tiny setules. Epistome weakly concave. Pereopod 6 basis posterior margin slightly concave. Pereopod 7 propodus length ~9 × width. Telson apex truncate.

Distribution. Bermuda (Gable and Lazo-Wasem 1990); Panama: Bocas del Toro (present study).

Ecology and remarks. These amphipods are associated with algae, seagrass, and coral rubble at depths of 0.5–9 m. Panamanian specimens closely resemble previously described specimens and can be readily distinguished from *Shoemakerella cubensis* based on the pereopod 6 basis posterior margin, pereopod 7 propodus length relative to the carpus length, and the telson apex. Panamanian specimens are transparent white in color with brown spots when alive.

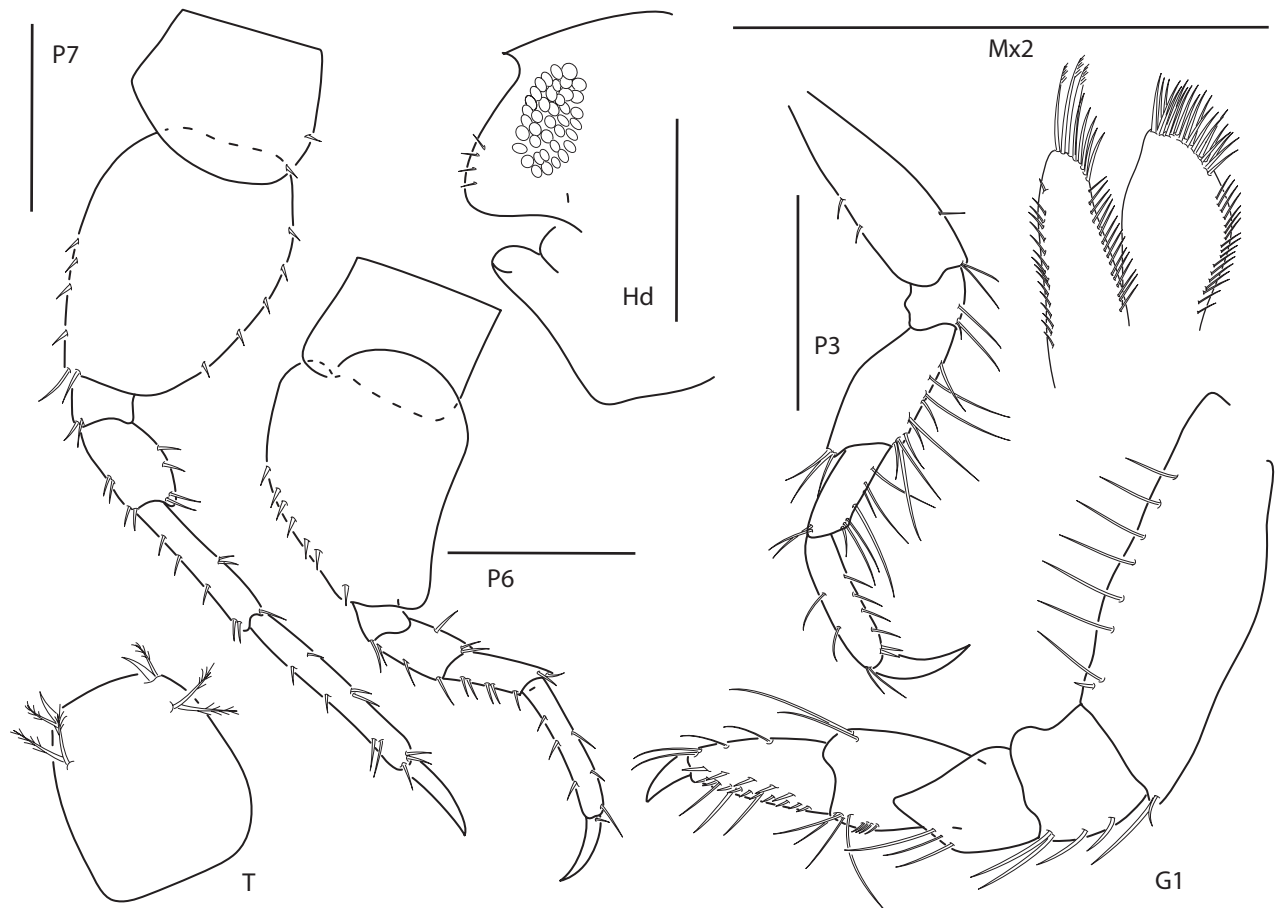


Figure 7. *Shoemakerella lowryi*, male, 4.5 mm, pereopod 7, pereopod 6, head, epistome and upper lip, pereopod 3, maxilla 2, telson, gnathopod 1 lateral. Scale bars: 0.5 mm.

Family Tryphosidae Lowry & Stoddart, 1997

Genus *Lepidepecreum* Bate & Westwood, 1868

Diagnosis. Antenna 1 with strong callynophore in male and weak callynophore in female. Antenna 2 of male elongate. Antenna 2 peduncular article 3 elongate in male and female. Maxilla 2 inner plate narrow. Gnathopod 1 subchelate; coxa large, about as long as coxa 2; carpus long (length 2 to 4 × width). Uropod 2 inner ramus without distinct dorsal notch. Uropod 3 outer ramus 2-articulate. Telson cleft.

Lepidepecreum cf. *magdalenensis* (Shoemaker, 1942)

Figs 8, 11C

Orchomenella magdalenensis Shoemaker, 1942: 4–7, fig. 1.

Lepidepecreum magdalenensis Lowry & Stoddart, 2002: 173–174; LeCroy 2007: 580, fig. 492.

Material examined. PANAMA • 2–3 mm • 6 ♂, 16 ♀; Bocas del Toro, Drago Beach; 9.4172°N, 82.3248°W; depth 0–1 m, in sand; 27 June 2023; K.N. White leg.; USNM 1739786.

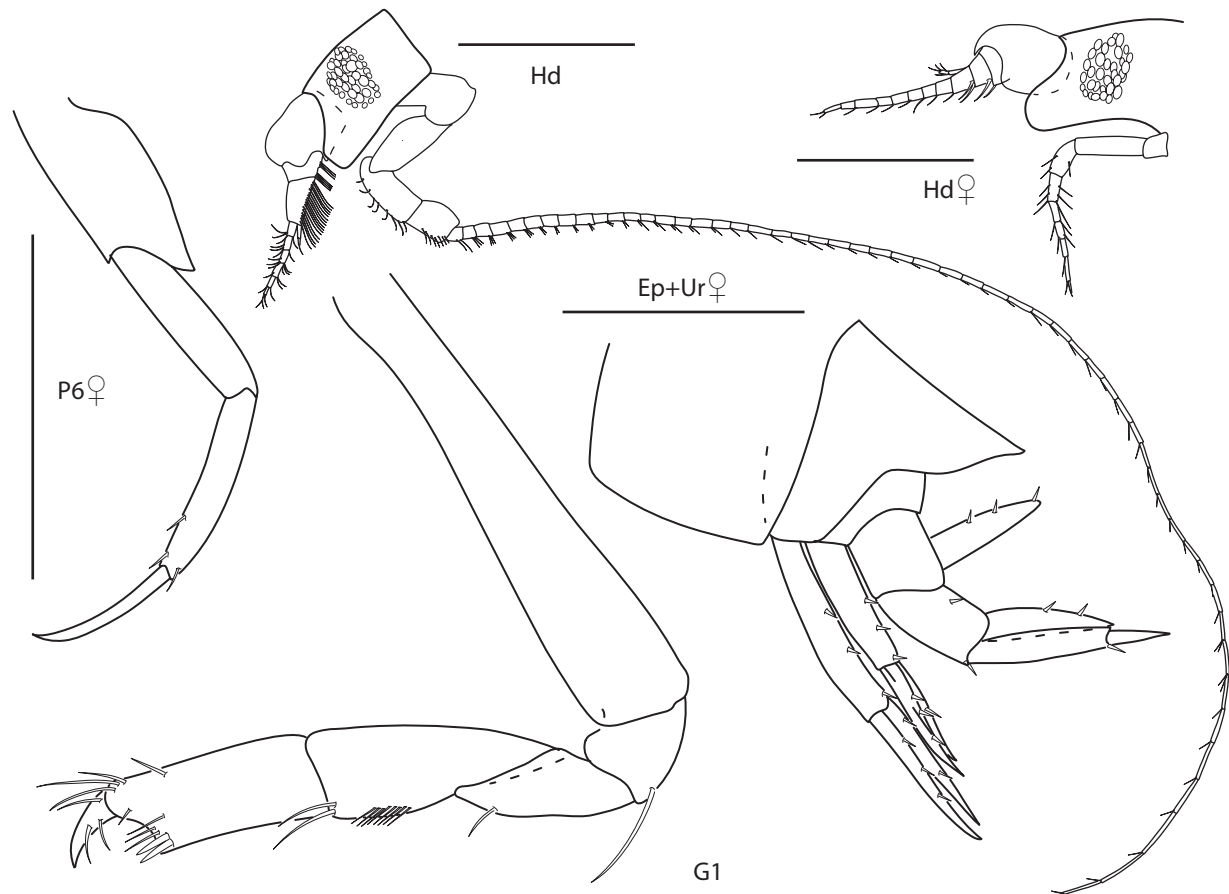


Figure 8. *Lepidepecreum magdalenensis*, female, 3.0 mm, head, epimeron 3 and urosome, pereopod 6; male, 2.8 mm, head, gnathopod 1 lateral. Scale bars: 0.5 mm.

Diagnosis. Head ocular lobe subrectangular. Gnathopod 1 carpus as long as propodus. Epimeron 3 posteroventral corner subquadrate. Urosomite 1 with dorsodistally acute carina. Uropod 3 inner ramus with two marginal spines.

Distribution. USA: Pacific California (Shoemaker 1942); Florida from Cape Romano to the lower Florida Keys (LeCroy, 2007); Cuba? (Ortiz 1978); Panama: Bocas del Toro (present study).

Ecology and remarks. These amphipods are associated with sand at depths of 0.5–27 m. Panamanian specimens closely resemble previously described specimens, except for a weak callynophore in females (strong in original description) and uropod 3 inner ramus having 2 marginal spines (3 in original description). LeCroy (2007) notes that Florida specimens of *L. cf. magdalenensis* have only one spine, suggesting that this may vary among specimens of this genus. The weak callynophore on antenna 1 of females may suggest that *L. magdalenensis* represents a species complex, but this can only be resolved with further examination of all collections. Panamanian specimens are white in color when alive.

Genus *Orchomenella* Sars, 1890

Diagnosis. Antenna 2 of male flagellum elongate. Antenna 2 peduncular article 3 short. Maxilla 2 inner plate narrow. Gnathopod 1 subchelate; carpus short (length less than 2 × width). Uropod 2 inner ramus without distinct dorsal notch. Telson cleft.

***Orchomenella thomasi* Lowry & Stoddart, 1997**

Figs 9, 11D

Orchomenella thomasi Lowry & Stoddart, 1997: 109–113, figs 52–53; LeCroy 2007: 586, fig. 502.

Material examined. PANAMA • 1.5 mm • 1 ♀; Bocas del Toro, Cayo Zapatilla 1; 9.2700°N, 82.0587°W; depth 10–11 m, among coral rubble; 28 June 2023; K.N. White leg.; USNM 1739787.

Diagnosis. Head ocular lobe subtriangular. Gnathopod 1 carpus shorter than propodus. Epimeron 3 posteroventral corner acute. Urosomite 1 with dorsodistally acute carina. Uropod 3 inner ramus bare; outer ramus 2-articulate.

Distribution. USA: from Sanibel Island, Florida to Louisiana (Lowry and Stoddart 1997; LeCroy 2007); Panama: Bocas del Toro (present study).

Ecology and remarks. These amphipods are associated with sand and coral rubble at depths of 10–73 m. Panamanian specimens closely resemble previously described specimens. Panamanian specimens are white in color when alive.

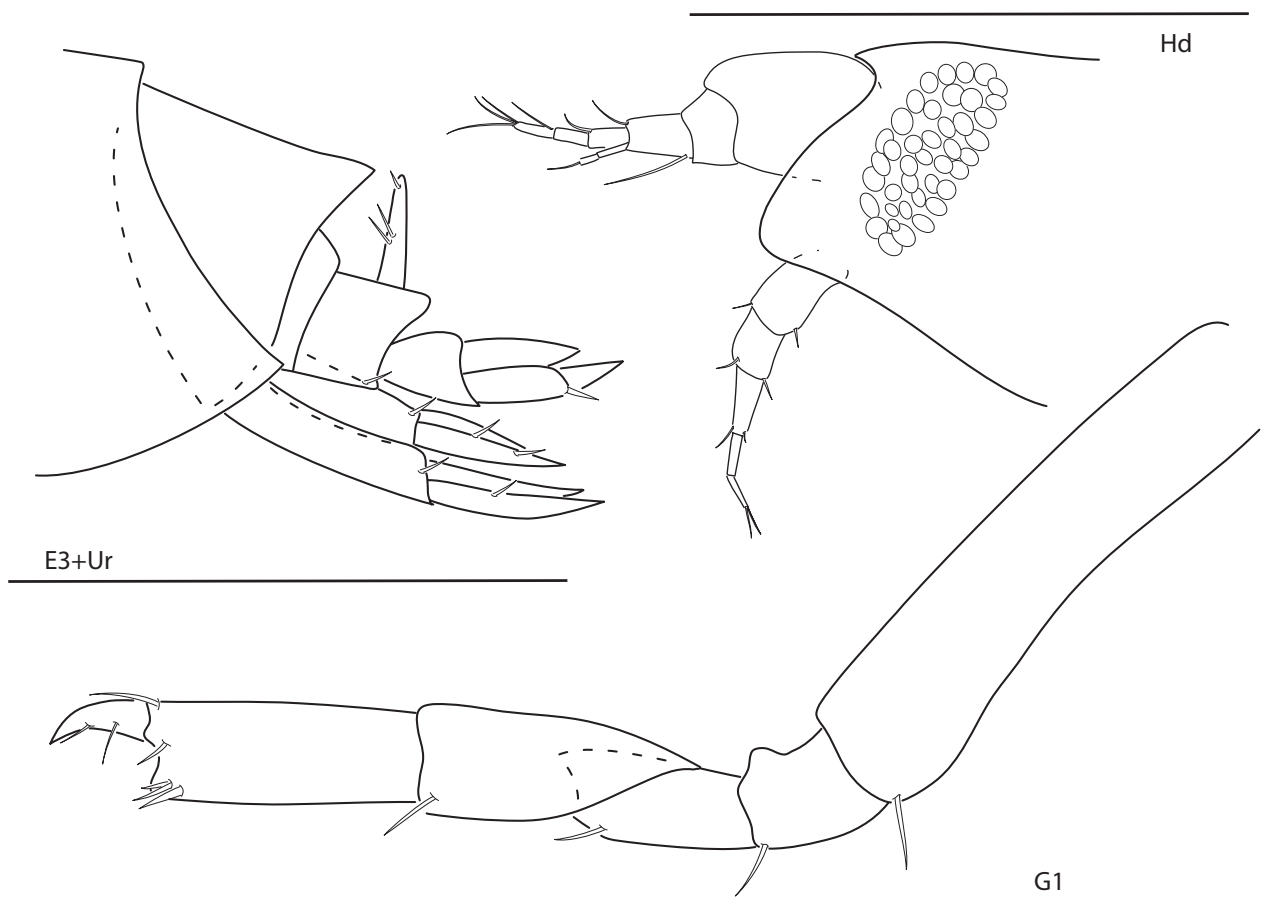


Figure 9. *Orchomenella thomasi*, female, 1.5 mm, head, epimeron 3 and urosome, gnathopod 1 lateral. Scale bars: 0.5 mm.

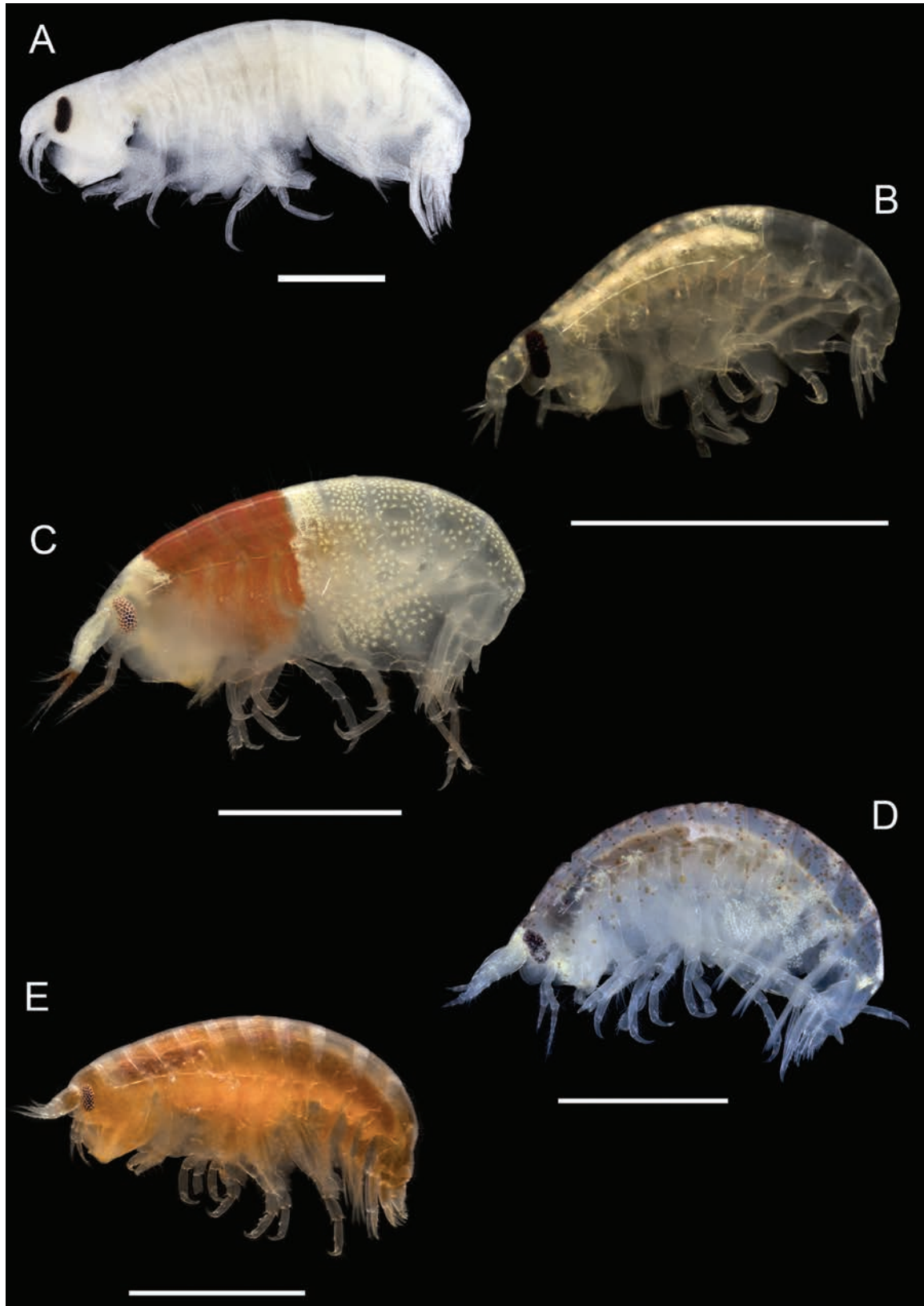


Figure 10. Photographs of live specimens unless noted **A** *Aruga holmesi* (ethanol preserved specimen) **B** *Bonassa bonai-rensis* **C** *Concarnes concavus* **D** *Lysianopsis hummelincki* **E** *Lysianopsis ozona*. Scale bars: 1.0 mm.

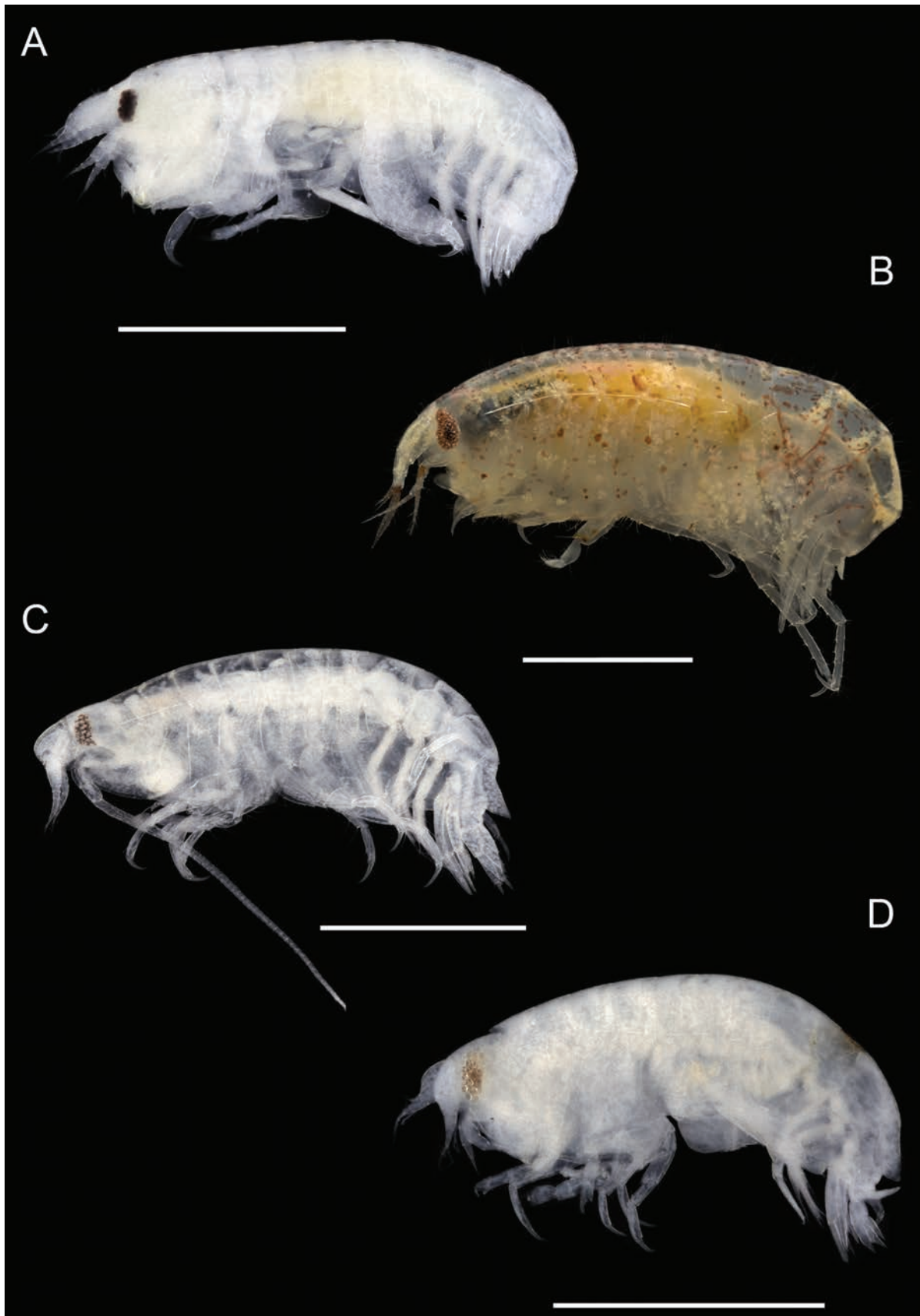


Figure 11. Photographs of live specimens unless noted **A** *Shoemakerella cubensis* (ethanol preserved specimen) **B** *Shoemakerella lowryi* **C** *Lepidepecreum magdalenensis* (ethanol preserved specimen) **D** *Orchomenella thomasi* (ethanol preserved specimen). Scale bars: 1.0 mm.

Identification Key to the Caribbean Lysianassidira of Panama

- 1 Eye absent; pereopod 5 basis narrowly expanded **2**
- Eye present, well developed; pereopod 5 basis broadly expanded **3**
- 2 Head ocular lobe produced; epimeron 3 posteroventral margin with acute tooth; telson deeply cleft, about 75% ***Paracentromedon carabicus***
- Head ocular lobe evenly rounded; epimeron 3 posteroventral margin rounded; telson shallowly cleft, less than 50% ***Vemana compressa***
- 3 Gnathopod 1 subchelate; urosomite 1 with dorsodistally acute carina; uropod 2 inner ramus without distinct dorsal notch (Figs 8, 9) **4**
- Gnathopod 1 simple; urosomite 1 without dorsodistal carina; uropod 2 inner ramus with distinct dorsal notch (Fig. 1) **5**
- 4 Antenna 2 peduncle article 3 long in female; head ocular lobe subrectangular; gnathopod 1 carpus as long as propodus; epimeron 3 posteroventral corner subquadrate; uropod 3 inner ramus with marginal spines (Fig. 8) ***Lepidepecreum magdalenensis***
- Antenna 2 peduncle article 3 short in female; head ocular lobe subtriangular; gnathopod 1 carpus shorter than propodus; epimeron 3 posteroventral corner acute; uropod 3 inner ramus bare (Fig. 9) ***Orchomenella thomasi***
- 5 Gnathopod 1 dactylus reduced, complex, covered in long, slender cuticular teeth; telson entire ***Eclecticus eclecticus***
- Gnathopod 1 dactylus not reduced, simple; telson entire or partially cleft **6**
- 6 Gnathopod 2 minutely subchelate; telson partially cleft (Fig. 3) ***Concarnes concavus***
- Gnathopod 2 minutely chelate (Figs 5, 6); telson entire (Figs 1, 6) **7**
- 7 Maxilla 2 inner plate wider than outer plate (Fig. 7); uropod 2 abruptly narrowing at notch (Fig. 6) **8**
- Maxilla 2 inner plate narrow, similar in width to outer plate (Fig. 5); uropod 2 gradually narrowing at notch (Fig. 1) **9**
- 8 Pereopod 6 basis posterior margin nearly straight; pereopod 7 propodus length ~5 × width; telson apex rounded (Fig. 6) ***Shoemakerella cubensis***
- Pereopod 6 basis posterior margin slightly concave; pereopod 7 propodus length ~9 × width; telson apex truncate (Fig. 7) ***Shoemakerella lowryi***
- 9 Epistome rounded; uropod 3 outer ramus 1-articulate (Fig. 2) **10**
- Epistome concave; uropod 3 outer ramus 2-articulate (Fig. 1) **11**
- 10 Epistome produced, subequal to produced upper lip; gnathopod 1 basis slender; pereopod 7 basis greatly expanded, posteriorly rounded, merus greatly expanded, approximately 3 × width of carpus (Fig. 2) ***Bonassa bonairensis***
- Epistome not produced, upper lip produced; gnathopod 1 basis stout; pereopod 7 basis slightly expanded, posterior margin almost straight, merus slightly expanded, approximately 1.4 × width of carpus (Fig. 4) ***Lysianopsis hummelincki***
- 11 Upper lip projecting well beyond epistome; gnathopod 1 propodus posterodistal margin slightly concave; uropod 3 peduncle long, length at least 2 × width; telson apical margin slightly emarginate (Fig. 1) ***Aruga holmesi***
- Upper lip subequal to epistome; gnathopod 1 propodus posterodistal margin straight; uropod 3 peduncle short, length approximately 1.5 × width; telson apical margin slightly truncate (Fig. 5) ***Lysianopsis ozona***

Discussion

The results of this study represent range extensions for eight species of lysianassid amphipods to include the Caribbean waters of Panama. One species collected in this study, *Concarnes concavus*, has been recorded from the Caribbean of Panama by Miloslavich et al. (2010), yet those authors did not provide any specific locality information, so it is unclear what the exact range of this species is in the Caribbean waters of Panama. Two species documented here have a distribution pattern spanning the eastern Pacific and western Caribbean (*Aruga holmesi* and *Lepidepecreum magdalenensis*). These distribution patterns may suggest that the species were established more than 3 mya, before the isthmus of Panama closed, or that we have species complexes that need to be investigated further.

Characters that have been used to identify lysianassid amphipods in the past, such as setae patterns on the dorsal surface of the body appear to be variable in Panamanian specimens and should not be used for identification. Sexual dimorphism is also used frequently but can be problematic when you have only one specimen or gender. Mouthparts are also often used as diagnostic characters which can be difficult for non-experts; thus, I included as many other characters as possible in this identification key.

Acknowledgements

Logistical support and facilities were provided by Georgia College & State University Department of Biological and Environmental Sciences and the Smithsonian Tropical Research Institute (STRI). Special thanks to Carolina Cesar and Valentina Cardona for assistance with diving and collecting in Bocas del Toro. The author also wishes to thank Dr Lauren Hughes and the Amphipod Taxonomy Course members for collecting assistance in 2023. Special thanks go to Sara LeCroy for her loan of specimens collected in 2005 and to Sally Sir, Sara LeCroy, and Tammy Horton for suggestions to improve the manuscript.

Additional information

Conflict of interest

The authors have declared that no competing interests exist.

Ethical statement

No ethical statement was reported.

Funding

Funding for this study was provided by a National Science Foundation grant: Collaborative Research: ARTS: Understanding Tropical Invertebrate Diversity Through Integrative Revisionary Systematics and Training (1856421).

Author contributions

Conceptualization: KNW. Data curation: KNW. Formal analysis: KNW. Funding acquisition: KNW. Investigation: KNW. Methodology: KNW. Project administration: KNW. Writing - original draft: KNW. Writing - review and editing: KNW.

Author ORCIDs

Kristine N. White  <https://orcid.org/0000-0002-5203-1656>

Data availability

All of the data that support the findings of this study are available in the main text or Supplementary Information.

References

- Andres HG (1977) Gammaridea (Crustacea, Amphipoda) aus dem Iberischen Tiefseebecken Auswertung des materials der Fahrten 3 und 15 von F. S. Meteor. Meteor Forschungsergebnisse (Reihe D) 25: 54–67.
- Austin WC (1985) An Annotated Checklist of Marine Invertebrates in the Cold Temperate Northeast Pacific. Cowichan, B.C., Khoyatan Marine Laboratory, 682 pp.
- Barnard JL (1955) Notes on the amphipod genus *Aruga* with the description of a new species. Bulletin of the Southern California Academy of Sciences 54(2): 97–103.
- Barnard JL (1958) Index to the families, genera, and species of the gammaridean Amphipoda (Crustacea). Allan Hancock Foundation Publications, Occasional Paper 19: 1–145.
- Barnard JL (1959) Estuarine Amphipoda. Allan Hancock Foundation Publications, Occasional Paper 21: 13–9.
- Barnard JL (1961) Gammaridean Amphipoda from depths of 400 to 6000 meters. Galathea Report 5: 23–128.
- Barnard JL (1964) Deep-sea Amphipoda (Crustacea) collected by the R/V “Vema” in the eastern Pacific Ocean and the Caribbean and Mediterranean seas. Bulletin of the American Museum of Natural History 127(1): 1–46.
- Barnard JL (1966a) Benthic Amphipoda of Monterey Bay, California. Proceedings of the United States National Museum 119: 1–41. <https://doi.org/10.5479/si.00963801.119-3541.1>
- Barnard JL (1966b) Submarine canyons of southern California. Part V. Systematics: Amphipoda. Allan Hancock Pacific Expeditions 27(5): 1–166.
- Barnard JL (1969) Gammaridean Amphipoda of the rocky intertidal of California: Monterey Bay to La Jolla. United States National Museum Bulletin 258: 1–230. <https://doi.org/10.5479/si.03629236.258.1>
- Barnard JL (1979) Littoral gammaridean Amphipoda from the Gulf of California and the Galapagos Islands. Smithsonian Contributions to Zoology 271: 1–149. <https://doi.org/10.5479/si.00810282.271>
- Barnard JL, Karaman GS (1991) The families and genera of marine gammaridean Amphipoda (Except marine Gammaroidea). Records of the Australian Museum Supplement 13 (Part 2): 419–866. <https://doi.org/10.3853/j.0812-7387.13.1991.367>
- Bate CS, Westwood JO (1868) A History of the British sessile-eyed Crustacea. Vol. 11. John Van Voorst, London, 401–536.
- Coleman CO (2003) “Digital inking”: how to make perfect line drawings on computers. Organisms Diversity & Evolution 3(14): 1–14. <https://doi.org/10.1078/1439-6092-00081>
- Dana JD (1849) Synopsis of the genera of Gammaracea. American Journal of Science and Arts, Series 2, 8: 135–140.
- Dana JD (1852) On the classification of the Crustacea Choristopoda or Tetracapoda. The American Journal of Science and Arts, Second Series 14(41): 297–316.

- Gable MF, Lazo-Wasem EA (1990) Lysianassidae (Amphipoda: Lysianassoidea) of Bermuda. *Journal of Crustacean Biology* 10(4): 721–734. <https://doi.org/10.2307/1548416>
- Gurjanova EF (1962) Amphipoda of the northern part of the Pacific Ocean (Amphipoda-Gammaridea). Part 1. *Akademiya Nauk SSSR, Opredeliteli po Faune SSSR* 74: 1–440.
- Holmes SJ (1903) Synopses of North-American invertebrates. XVIII. The Amphipoda. *American Naturalist* 37: 267–292. <https://doi.org/10.1086/278286>
- Holmes SJ (1908) The Amphipoda collected by the U.S. Bureau of Fisheries steamer Albatross off the west coast of North America, in 1903 and 1904, with descriptions of a new family and several new genera and species. *Proceedings of the United States National Museum* 35: 489–543. <https://doi.org/10.5479/si.00963801.35-1654.489>
- Horton T, Lowry J, De Broyer C, Bellan-Santini D, Copilaş-Ciocianu D, Corbari L, Costello MJ, Daneliya M, Dauvin J-C, Fišer C, Gasca R, Grabowski M, Guerra-García JM, Hendrycks E, Hughes L, Jaume D, Jazdzewski K, Kim Y-H, King R, Krapp-Schickel T, LeCroy S, Lörz A-N, Mamos T, Senna AR, Serejo C, Souza-Filho JF, Tandberg AH, Thomas JD, Thurston M, Vader W, Väinölä R, Valls Domedel G, Vonk R, White K, Zeidle, W (2024) World Amphipoda Database. [on 2024-07-05] <https://doi.org/10.14284/368>
- Hurley DE (1963) Amphipoda of the family Lysianassidae from the west coast of North and Central America. *Allan Hancock Foundation Publications, Occasional Paper* 25: 1–160.
- Johnson SE (1986) Order Amphipoda. In: Sterrer W (Ed.) *Marine Fauna and Flora of Bermuda*. John Wiley & Sons, New York, 372–381.
- Kunkel BW (1910) The Amphipoda of Bermuda. *Transactions of the Connecticut Academy of Arts and Sciences* 16: 1–116.
- Lalana Rueda R, Ortiz M (1990) Zoobentos de Cayo Hicacos, SE de la Isla de la Juventud, Cuba. *Revista de Investigaciones Marinas* 11(3): 191–199.
- Lalana Rueda R, Pérez Moreno M (1985) Estudio cualitativo y cuantitativo de la fauna asociada a las raíces de *Rhizophora mangle* en la cayería este de la Isla de la Juventud. *Revista Investigaciones Marinas* 6(2–3): 45–57.
- Lalana Rueda R, Capetillo R, Brito E, Diaz E, Cruz R (1989) Estudio del zoobentos asociado a *Laurencia intricata* en un área de juveniles de langosta, al SE de la Isla de la Juventud, Cuba. *Revista Investigaciones Marinas* 10(3): 207–218.
- LeCroy SE (2007) An Illustrated Identification Guide to the Nearshore Marine and Estuarine Gammaridean Amphipoda of Florida Volume 4: Families Anamixidae, Eusiridae, Hyalellidae, Hyalidae, Iphimediidae, Ischyroceridae, Lysianassidae, Megaluroipidae, and Melphidippidae. Florida Department of Environmental Protection Annual Report Contract No. WM724 1: 1–195.
- LeCroy SE, Gasca R, Winfield I, Ortiz M, Escobar-Briones E (2009) Amphipoda (Crustacea) of the Gulf of Mexico. In: Felder DL, Camp DK (Eds) *Gulf of Mexico: Origin, Waters, and Biota*. Texas A&M University Press, Texas, 941–972.
- Lilljeborg W (1865) Bidrag till kannedomen om underfamiljen Lysianassina inom underordningen Amphipoda bland kraftdjuren. *Nova Acta Regiae Societatis Scientiarum Upsaliensis* 3: 1–25.
- Lowry JK, DeBroyer (2008) Alicellidae and Valettiopsidae, two new callynophorate families (Crustacea, Amphipoda). *Zootaxa* 1843: 57–66. <https://doi.org/10.11646/zootaxa.1843.1.5>
- Lowry JK, Myers AA (2017) A Phylogeny and Classification of the Amphipoda with the establishment of the new order Ingolfiellida (Crustacea: Peracarida). *Zootaxa* 4265(1): 1–89. <https://doi.org/10.11646/zootaxa.4265.1.1>

- Lowry JK, Stoddart HE (1989) *Shoemakerella* Pirlot, 1936 (Crustacea, Amphipoda): proposed designation of *Lysianax cubensis* Stebbing, 1897, as type species. *Bulletin of Zoological Nomenclature* 46(4): 236–238. <https://doi.org/10.5962/bhl.part.550>
- Lowry JK, Stoddart HE (1990) The Wandinidae, a new indo-pacific family of Lysianassoidea Amphipoda (Crustacea). *Records of the Australian Museum* 42: 159–171. <https://doi.org/10.3853/j.0067-1975.42.1990.113>
- Lowry JK, Stoddart HE (1995) The Amphipoda (Crustacea) of Madang Lagoon: Lysianassidae, Opisidae, Uristidae, Wandinidae and Stegocephalidae. In: Lowry JK (Ed.) *Amphipoda (Crustacea) of the Madang Lagoon, Papua New Guinea*. *Records of the Australian Museum, Supplement* 22: 97–174. <https://doi.org/10.3853/j.0812-7387.22.1995.122>
- Lowry JK, Stoddart HE (1996) New lysianassoid amphipod species from Namibia and Madagascar (Lysianassidae Dana, 1849 and Podoprionidae fam. nov.). *Bolletino del Museo Civico di Storia Naturale di Verona*. 20(1): 225–247.
- Lowry JK, Stoddart HE (1997) Amphipoda Crustacea IV. Families Aristiidae, Cyphocarididae, Endeavouridae, Lysianassidae, Scopelocheiridae, Uristidae. *Memoirs of the Hourglass Cruises* 10: 1–148.
- Lowry JK, Stoddart HE (2002) The Amaryllididae of Australia (Crustacea: Amphipoda: Lysianassoidea). *Records of the Australian Museum* 54(2): 129–214. <https://doi.org/10.3853/j.0067-1975.54.2002.1363>
- Lowry JK, Stoddart HE (2010a) The deep-sea scavenging genus *Hirondellea* (Crustacea: Amphipoda: Lysianassoidea: Hirondelleidae fam. nov.) in Australian waters. *Zootaxa* 2329: 37–55. <https://doi.org/10.11646/zootaxa.2329.1.3>
- Lowry JK, Stoddart HE (2010b) Sophrosynidae, a new family in the Lysianassoidea (Crustacea: Amphipoda) with a revision of the genus *Sophrosyne*. *Zootaxa* 2370(1): 1–35. <https://doi.org/10.11646/zootaxa.2370.1.1>
- Lowry JK, Stoddart HE (2010c) The family Izinkalidae fam. nov. (Crustacea: Amphipoda: Lysianassoidea) in Australian waters. *Zootaxa* 2532(1): 64–68. <https://doi.org/10.11646/zootaxa.2532.1.3>
- Lowry JK, Stoddart HE (2010d) Kergueleniidae fam. nov. (Crustacea: Amphipoda: Lysianassoidea) in Australian waters. *Zootaxa* 2564(1): 1–30. <https://doi.org/10.11646/zootaxa.2564.1.1>
- Lowry JK, Stoddart HE (2011) The new deep-sea families Cebocaridae fam. nov., Cyclocaridae fam. nov. and Thoriellidae fam. nov. (Crustacea: Amphipoda: Lysianassoidea). *Zootaxa* 2747: 53–68. <https://doi.org/10.11646/zootaxa.2747.1.4>
- Lowry JK, Stoddart HE (2012) Australian and South African conicostomatine amphipods (Amphipoda: Lysianassoidea: Lysianassidae: Conicostomatinae subfam. nov.). *Zootaxa* 3248: 43–65. <https://doi.org/10.11646/zootaxa.3248.1.4>
- Martín A, Díaz Y, Miloslavich P, Escobar-Briones E, Guerra-García JM, Ortiz M, Valencia B, Giraldo A, Klein E (2013) Regional diversity of Amphipoda in the Caribbean Sea. *Revista de Biología Tropical* 61(4): 1681–1720. <https://doi.org/10.15517/rbt.v61i4.12816>
- Miloslavich P, Díaz JM, Klein E, Alvarado JJ, Díaz C, Gobin J, Escobar-briones E, Cruz-motta JJ, Weil E, Cortés J, Bastidas AC, Robertson R, Zapata F, Martín A, Castillo J, Kazandjian A, Ortiz M (2010) Marine biodiversity in the Caribbean: regional estimates and distribution patterns. *PLoS ONE* 5(8): e11916. <https://doi.org/10.1371/journal.pone.0011916>
- Ortiz M (1978) Invertebrados marinos bentosicos de Cuba. I. Crustacea, Amphipoda, Gammaridea. *Ciencias* 38: 3–10.

- Ortiz M (1979) Lista de especies y bibliografía de los anfípodos (Crustacea: Amphipoda) del Mediterráneo Americano. *Ciencias (La Habana), Series 8, Investigaciones Marinas* 43: 1–40.
- Ortiz M, Lalana Rueda R (1992) Parasites de anfípodos (Gammaridea) de Cuba. *Revista Investigaciones Marinas* 13(1): 39–48.
- Ortiz M, Lalana Rueda R (1993) Adición a la lista de especies y bibliografía de los anfípodos (Crustacea: Amphipoda) del Mediterráneo Americano. *Revista Investigaciones Marinas* 14(1): 16–37.
- Ortiz M, Lemaitre R (1994) Crustaceos Anfípodos (Gammaridea) Colectados en Las Costas del Caribe Colombiano, al sur de Cartagena. *Anales del Instituto de Investigaciones Marinas de Punta de Betin* 23: 119–127.
- Pearse AS (1912) Notes on certain amphipods from the Gulf of Mexico, with descriptions of new genera and new species. *Proceedings of the United States National Museum* 43: 369–379. <https://doi.org/10.5479/si.00963801.43-1936.369>
- Pirlot JM (1936) Les amphipodes de l'expédition du Siboga. Deuxième partie: Les amphipodes gammarides, II. - Les amphipodes de la mer profonde. 3: Addendum et partie générale. III. - Les amphipodes littoraux. 1: Lysianassidae, Ampeliscidae, Leucothoidae, Stenothoidae, Phliantidae, Colomastigidae, Ochlesidae, Liljeborgiidae, Oedicerotidae, Synopiidae, Eusiridae, Gammaridae. *Siboga-Expeditie, Monographie* 33e: 237–328.
- Pirlot JM (1939) Amphipoda. Résultats scientifiques des croisières du navire-école Belge 'Mercator'. *Mémoires du Musée Royal d'Histoire Naturelle de Belgique, Series 2, 15*: 47–80.
- Sars GO (1890) An Account of the Crustacea of Norway, with Short Descriptions and Figures of all the Species. Vol. I. Amphipoda. Parts 1–3. Christiania, Alb. Cammermeyer, 68 pp.
- Shoemaker CR (1921) Report on the amphipods collected by the Barbados-Antigua Expedition from the University of Iowa in 1918. *University of Iowa Studies in Natural History* 9(5): 99–102.
- Shoemaker CR (1933) Amphipoda from Florida and the West Indies. *American Museum Novitates* 598: 1–24.
- Shoemaker CR (1935) The amphipods of Porto Rico and the Virgin Islands. *Scientific Survey of Porto Rico and the Virgin Islands (New York Academy of Sciences)* 15: 229–253.
- Shoemaker CR (1942) Amphipod crustaceans collected on the Presidential Cruise of 1938. *Smithsonian Miscellaneous Collections* 101(11): 1–52.
- Shoemaker CR (1948) The Amphipoda of the Smithsonian-Roebling Expedition to Cuba in 1937. *Smithsonian Miscellaneous Collections* 110(3): 1–15. <https://doi.org/10.5962/bhl.part.9028>
- Stebbing TRR (1888) Report on the Amphipoda collected by H.M.S. Challenger during the years 1873–1876. *Zoology* 29: 1–1737.
- Stebbing TRR (1897) Amphipoda from the Copenhagen Museum and other sources. *Transactions of the Linnean Society, London, Series 2, Zoology* 7: 25–45 [pls 6–14]. <https://doi.org/10.1111/j.1096-3642.1897.tb00400.x>
- Stebbing TRR (1906) Amphipoda I. Gammaridea. *Das Tierreich* 21: 1–806.
- Stephensen K (1933a) Zoologische Ergebnisse einer Reise nach Bonaire, Curaçao und Aruba im Jahre 1930. No. 8. Fresh- and brackish-water Amphipoda from Bonaire, Curaçao and Aruba. *Zoologische Jahrbucher. Abteilung fur Systematik, Okologie und Geographie der Tiere* 64(3/5): 415–436.

- Stephensen K (1933b) Zoologische Ergebnisse einer Reise nach Bonaire, Curaçao und Aruba im Jahre 1930. No. 9. Amphipoda from the marine salines of Bonaire and Curaçao. Zoologische Jahrbucher. Abteilung fur Systematik, Okologie un Geographie der Tiere 64(3/5): 437–446.
- Stephensen K (1948) Amphipods from Curaçao, Bonaire, Aruba and Margarita. Studies on the Fauna of Curaçao, Aruba, Bonaire and the Venezuelan Islands 3(11): 1–20.
- Stepien CA, Brusca RC (1985) Nocturnal attacks on nearshore fishes in southern California by crustacean zooplankton. Marine Ecology Progress Series 25: 91–105. <https://doi.org/10.3354/meps025091>
- Stoddart HE, Lowry JK (2004) The deep-sea lysianassoid genus *Eurythenes* (Crustacea, Amphipoda, Eurytheneidae n. fam.). Zoosystema 26(3): 425–468.
- Stoddart HE, Lowry JK (2010) Lepidepcrellidae fam. nov. (Crustacea: Amphipoda: Lysianassoidea) in Australian waters. Zootaxa 2634: 63–68. <https://doi.org/10.11646/zootaxa.2634.1.5>
- Stoddart HE, Lowry JK (2012) Revision of the lysianassoid genera *Acidostoma* and *Shackletonia* (Crustacea: Amphipoda: Acidostomatidae fam.nov.). Zootaxa 3307: 1–34. <https://doi.org/10.11646/zootaxa.3307.1.1>
- Stretch JJ (1985) Quantitative sampling of demersal zooplankton: reentry and airlift dredge sample comparisons. Journal of Experimental Marine Biology and Ecology 91: 125–136. [https://doi.org/10.1016/0022-0981\(85\)90225-4](https://doi.org/10.1016/0022-0981(85)90225-4)
- Thomas JD (1993) Identification manual for marine Amphipoda (Gammaridea): I. Common coral reef and rocky bottom amphipods of South Florida. Florida Department of Environmental Protection Final Report Contract No. SP290: 1–83.

Supplementary material 1

Locality table

Author: Kristine N. White

Data type: xlsx

Copyright notice: This dataset is made available under the Open Database License (<http://opendatacommons.org/licenses/odbl/1.0/>). The Open Database License (ODbL) is a license agreement intended to allow users to freely share, modify, and use this Dataset while maintaining this same freedom for others, provided that the original source and author(s) are credited.

Link: <https://doi.org/10.3897/zookeys.1216.135258.suppl1>

Revision of the genus *Digonis* (Lepidoptera, Geometridae): new species and new genera

Mario I. Ramos-González^{1,2}, María Francisca Venegas-González¹, Carlos Zamora-Manzur³, Luis E. Parra¹

¹ Departamento de Zoología, Facultad de Ciencias Naturales y Oceanográficas, Universidad de Concepción, Casilla 160-C, Concepción, Chile

² Programa de Doctorado en Sistemática y Biodiversidad, Facultad de Ciencias Naturales y Oceanográficas, Universidad de Concepción, Concepción, Chile

³ Departamento de Ecología, Facultad de Ciencias, Universidad Católica de la Santísima Concepción, Alonso de Rivera 2850, Concepción, Chile

Corresponding author: Mario I. Ramos-González (marioramos@udec.cl)

Abstract

The taxonomic study of the Chilean Ennomini genera is still in its early stages. Within this group, the maculation patterns of Chilean species are uniform and often inadequate for distinguishing between many species, compounded by a lack of taxonomic revisions focused on the genera within the tribe. In this study, the genus *Digonis* Butler, 1882, is reviewed and redefined based on characteristics of wing patterns and genitalia. *Digonis* comprises the following five species: *D. aspersa* Butler, 1882, *D. cervinaria* (Blanchard, 1852), *D. punctifera* Butler, 1882, *D. gungnir* Ramos-González & Parra, **sp. nov.**, and *D. apocrypha* Ramos-González & Parra, **sp. nov.** Additionally, *D. cuprea* Butler, 1882 is synonymized with *D. cervinaria* (Blanchard, 1852), and all varieties of *D. punctifera* Butler, 1882, and *D. cuprea* are synonymized with their respective species. Furthermore, two new genera are introduced: *Phasmadigonis* Ramos-González & Parra, **gen. nov.**, erected for *P. alba* (Butler, 1882), **comb. nov.**, and *Gugnelve* Ramos-González & Parra, **gen. nov.**, established for *G. butleri* Ramos-González & Parra, **sp. nov.** With the species and genus descriptions, a comparative diagnosis, genitalia illustrations for all species, and wing venation for each genus are provided.

Key words: Andean Region, Argentina, Chile, Ennominae, Ennomini, Nacophorini, taxonomy



Academic editor: Axel Hausmann

Received: 27 June 2024

Accepted: 27 September 2024

Published: 24 October 2024

ZooBank: <https://zoobank.org/1BBB8E67-1398-4D4F-B9CE-B56B2B7A471C>

Citation: Ramos-González MI, Venegas-González MF, Zamora-Manzur C, Parra LE (2024) Revision of the genus *Digonis* (Lepidoptera, Geometridae): new species and new genera. ZooKeys 1216: 173–200. <https://doi.org/10.3897/zookeys.1216.129923>

Copyright: © Mario I. Ramos-González et al. This is an open access article distributed under terms of the Creative Commons Attribution License (Attribution 4.0 International – CC BY 4.0).

Introduction

Ennominae is the most diversified subfamily, comprising approximately half of the described species within Geometridae (Gaston et al. 1995; Scoble 1999; Pitkin 2002; Scoble and Hausmann 2007; Rajaei et al. 2022). However, due to this extensive diversity (approximately 10,000 species), the taxonomic classification at the tribal level has remained in constant flux, and there is still no consensus on the taxonomic affinities of the recognized tribes, particularly when considering taxa from the New World (Holloway 1993; Scoble 1995; Pitkin 2002; Beljaev 2006; Öunap et al. 2011; Brehm et al. 2019).

The most diverse tribes within the Chilean Ennominae, which are also better studied, correspond to Odontoperini with almost 50 species (Rindge 1973,

1983; Parra and Henriquez-Rodriguez 1993; Pitkin 2002; Brehm et al. 2019), and Diptychini with approximately 40 species (Rindge 1986; Parra 1999a, 1999b; Pitkin 2002; Parra et al. 2010; Parra and Hernández 2010; Brehm et al. 2019). In contrast, there have been few taxonomic studies conducted on the other tribes (e.g., Gnophini: Parra and Vargas 2000; Macariini: Vargas et al. 2005, 2020; Boarmiini: Vargas 2007, 2021; Nacophorini: Rindge 1973, 1983; Parra 2018; Ennomini: Bocaz et al. 2016). Therefore, there is a great uncertainty regarding the monophyly of many genera and their position in the systematics of the group (Hausmann and Parra 2009; Brehm et al. 2019).

The tribe Ennomini is characterized by having a vinculum divided ventrally by a membranous area, a paired m3 muscle inserted distally in the median invagination in the basal portion of the juxta. Among Chilean genera of Ennomini, there is notable variability in wing maculation patterns, which has posed challenges in correctly recognizing species. This is exemplified in genera such as *Syncirsodes* Butler, 1882 (Bocaz and Parra 2005; Bocaz et al. 2016), *Hasodima* Butler, 1882 (Parra and Pascual-Toca 2003; Parra et al. 2009), *Perusia* Herrich-Schäffer, 1855 (CZ-M, unpublished data), and *Digonis* Butler, 1882.

Digonis was described by Butler (1882) based on the wing shape and the simple antennae of adults. The forewings exhibit a very acute apex, followed by a concave outer margin that extends to vein M_3 , where it terminates in a new acute angle, giving the wings the appearance of having two pointed extensions along their outer margin (Pitkin 2002).

Scoble (1999) recognized five species within *Digonis*: four originally described by Butler (1882): *D. aspersa*, *D. alba*, *D. punctifera*, including the varieties *maculosa*, *acuminata*, *terranea*, and *fumosa*, and *D. cuprea*, including the varieties *olivacea* and *fusca*. Additionally, Scoble (1999) included one species, *D. cervinaria* (Blanchard, 1852). Subsequently, in his review of neotropical Ennominae genera, Pitkin (2002) identified the species comprising the genus as *D. aspersa*, *D. cervinaria*, *D. cuprea*, and *D. punctifera*, excluding *D. alba* due to significant differences in male genitalia.

Despite the general characterization of the genus provided by Pitkin (2002), uncertainty still needs to be resolved surrounding the validity of the described species and varieties. The maculation patterns are deceptively uniform and insufficient for species recognition (e.g., Hausmann and Parra 2009). Therefore, the aim of this contribution is to characterize the genus *Digonis* through a taxonomic revision based on external morphology and genital structures. To achieve this, we redescribe the genus *Digonis*, presenting its diagnostic characters; we provide an illustrated and annotated systematic species list, along with new taxonomic changes, and describe two new genera and three new species.

Materials and methods

This study was based on 107 adult specimens deposited in the collections mentioned below. The type material examined for each taxon is specified in the Results section.

NHMUK	The Natural History Museum, London (UK)
MNHN	Muséum National d'Histoire Naturelle, Paris (France)
MNNC	Museo Nacional de Historia Natural, Santiago (Chile)

MHNC	Museo de Historia Natural de Concepción, Concepción (Chile)
MZUC-UCCC	Museo de Zoología de la Universidad de Concepción, Concepción (Chile)
ZSM	Zoologische Staatssammlung München, Munich (Germany)

For specimen identification and comparison, we used the original descriptions and type material when available. Adult specimens were externally photographed using a Sony Cybershot DSC-HX300 compact camera. Wing and genitalia slides were prepared following the methods outlined in Parra (1991). Nomenclature for genitalia and external characteristics followed Klots (1970) and Scoble (1995), respectively. All prepared slides were photographed using a Motic SMZ-171-TL trinocular stereoscopic microscope equipped with a 5-Mpx Moticam Motic2500 digital camera. These photographs were then used to create detailed illustrations of the microscopic preparations.

Information on the flight period and species distribution was obtained from the labels accompanying each examined specimen. This information was supplemented with records from the citizen science platform iNaturalist (<https://www.inaturalist.org>). All iNaturalist records cited were identified by the first author as part of the “Polillas de Chile” project (<https://inaturalist.mma.gob.cl/projects/polillas-de-chile>).

All species were assigned to the biogeographical provinces proposed by Morrone (2015). The newly described genera were diagnosed through comparison with the type species of other closely related genera in the region, based on both external and internal morphological similarities.

Results

Taxonomy

Tribe Ennomini Duponchel, 1845

Digonis Butler, 1882

Digonis Butler, 1882: 360; Bartlett-Calvert 1886: 333; Angulo and Casanueva 1981: 12; Scoble 1999: 229; Pitkin 2002: 248.

Type species. *Digonis aspersa* Butler, 1882. By original designation.

Diagnosis. *Digonis* resembles *Digonodes* Warren, 1895, *Gonogala* Butler, 1882, and the newly proposed genus *Phasmadigonis* gen. nov. particularly due to the mucronate shape of the wings. However, it is distinguished from *Digonodes* by the presence of a mucronate outer margin on the M_3 of the hindwings and the presence of filiform (not bipectinate) antennae. It is recognized as distinct from *Gonogala* by the absence of bipectinate antennae and M_2 in the hindwings. It differs from *Phasmadigonis* by the presence of two accessory areoles in the forewings, R_2 arising from R_{3+4} , and the absence of a vein connecting $Sc+R_1$ to the discal cell in the hindwings. The monophyly of *Digonis* is supported by the following genital characters: a U-shaped gnathos with a plate or a pair of denticulate lobes, a concave, sclerotized process on the costa with an extended cucullus, a furca armed with spines, an aedeagus without cornuti, and a strongly denticulate annular signum.

Redescription. Antennae serrate in males and filiform in females. Thorax and abdomen with brown to grayish scales. Forewings castaneous yellowish, gray, brown, or coppery; costal margin in the apical area slightly arched; outer margin concave between apex and M_3 vein. Wing venation (Fig. 1). Two accessory cells; Sc in contact with first accessory cell, R_1 originates near apex of second accessory cell, R_{2+3+4} from apex of second accessory cell, R_3 and R_4 stalked, R_5 terminates at termen; M_2 equidistant between M_1 and M_3 , M_3 slightly arched and ending in small mucronate apex; CuA_1 originates 1/10 before end of cell, CuA_2 originates near the midpoint of the cell. Hindwings paler than forewings, with multiple dark brown scattered spots; medial band conspicuous or faint; outer margin slightly mucronate. $Sc+R_1$ in contact with radial stem up to middle of cell, R_s originates 1/10 before end of cell, M_2 absent. Male genitalia with conical uncus; gnathos “U” shaped, with a pair of prominences or a denticulated plate; subrectangular valvae with a strong sclerotized and concave costal process; spiny furca; aedeagus unarmed. Female genitalia with subpyriform corpus bursae, annular and strongly denticulated signum.

Distribution. This genus is distributed between latitudes 30°S and 47°S, spanning the provinces from Elqui to Capitán Prat in Chile.

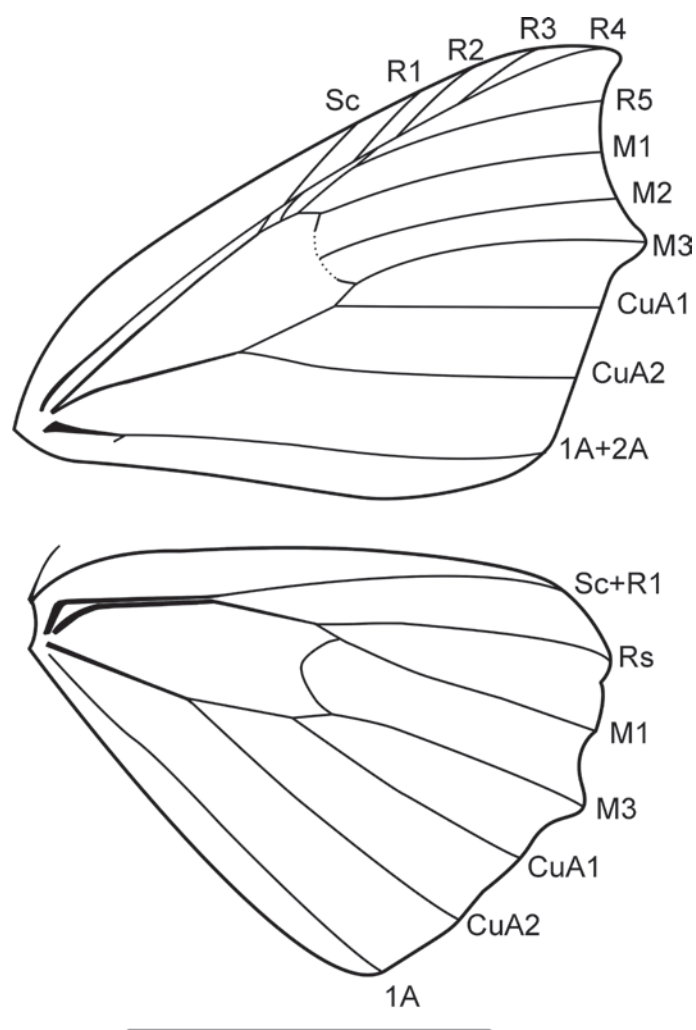


Figure 1. Wing venation of *Digonis* Butler, 1882. Scale bar: 10 mm.

***Digonis aspersa* Butler, 1882**

Figs 2A–D, 3

Digonis aspersa Butler, 1882: 361; Bartlett-Calvert 1886: 333; Angulo and Casanueva 1981: 12; Scoble 1999: 229; Pitkin 2002: 248.

Material examined. Syntype. CHILE • 1 male; Pines Valley; “XII” [labeled]; “Chili, 82-107” [labeled]; “Type” [red labeled]; T. Edmonds leg.; NHMUK.

Other material examined. CHILE — **San Antonio Prov.** • Algarrobo; 10-I-1950; n.n. leg.; MZUC-UCCC. — **Diguillín Prov.** • 1 male; Ninhue; 19-IV-2011; G. Moreno leg.; MZUC-UCCC • Las Trancas; III-2013; -36.889694, -71.471611; “Mirg-006” [genitalia slide]; MZUC-UCCC • Las Trancas; 16-IV-2010; G. Moreno leg.; “UCCC-MZUC-Lep 0258” [Museum ID]; MZUC-UCCC • 1 female; Las Trancas; 8-II-2011; G. Moreno leg.; “UCCC-MUZ-Lep-1056” [Museum ID]; “Mirg-022” [genitalia slide]; MZUC-UCCC • Las Trancas; 20-I-2012; G. Moreno leg.; “UCCC-MZUC-Lep 0377” [Museum ID]; MZUC-UCCC. — **Concepción Prov.** • 2 males; Concepción; 8-I-2001; J. Artigas leg.; MZUC-UCCC • 1 male; Concepción, Cerro Caracol; 15-II-2001; J. Artigas leg.; “Mirg-003” [genitalia slide]; MZUC-UCCC • 1 male; Concepción, Cerro Caracol; 30-II-2002; J. Artigas leg.; MZUC-UCCC • 1 male; Concepción; 3-II-1960; Trampas leg.; MZUC-UCCC • Concepción; 22-I-1960; Trampas leg. MZUC-UCCC • Concepción; 1-IV-1960; Trampas leg.; MZUC-UCCC • Concepción; 5-III-1959; Trampas leg.; MZUC-UCCC • Concepción; 21-III-1962; Trampas leg.; MZUC-UCCC • Concepción; 30-IX-2001; J. Artigas leg.; MZUC-UCCC • Concepción, Cerro Caracol; 30-II-2002; J. Artigas leg.; MZUC-UCCC • Concepción; 7-I-1961; Trampas leg.; MZUC-UCCC • 3 males; Concepción, Barrio Universitario; 4-V-1985; Carrasco leg.; MZUC-UCCC • Concepción; 29-XII-1958; Trampas leg.; MZUC-UCCC • Concepción; 16-III-1960; Trampas leg.; MZUC-UCCC. — **Arauco Prov.** • 1 male; Lanahue; 22-I-2018; L. Parra leg.; “Mirg-001” [genitalia slide]; MZUC-UCCC • Lanahue; 23-I-2018; L. Parra leg.; MZUC-UCCC. — **Biobío Prov.** • P.N. Laguna del Laja; 6-XII-2008; G. Moreno leg.; MZUC-UCCC. — **Malleco Prov.** • Nahuelbuta; Río Picoyquen; 22-XII-1960; Fetis leg.; MZUC-UCCC • Collipulli; 24-X-2014; E. Sepulveda leg.; “UCCC-MZUC-Lep 0308” [Museum ID]; MZUC-UCCC • Río Blanco; 19/25-II-1995; H. Thöny leg.; ZSM. — **Valdivia Prov.** 1 male; Valdivia; 30-IX-1987; Trampas leg.; MZUC-UCCC • 1 male; Valdivia; “5003” [Museum ID]; MNNC. — **Llanquihue Prov.** • Katalapi; 22-IV-2011; MZUC-UCCC. — **Coyhaique Prov.** • Coyhaique; I-1934; E. Ureta leg.; “Museo 5004” [Museum ID]; MNNC • 1 female; Lago Verde, R.N. Coyaique; 21-I-2007; MZUC-UCCC. — **Aysen Prov.** • 1 female; Río Maca, Cuenca Cuervo; -45.114703, -73.016065; 21-II-2008; “Mirg-020” [genitalia slide]; MZUC-UCCC. — **Capitán Prat Prov.** • Los Mellizos; 22-I-2008; Muñoz-Escobar leg.; MZUC-UCCC.

Additional records. CHILE. — **Itata Prov.** • La Palma; -36.567368, -72.689177; 9-IX-2021; observed by Claudio Maureira and submitted to iNaturalist in: <https://inaturalist.mma.gob.cl/observations/100908464>. — **Concepción Prov.** • Concepción; 4-XII-2021; -36.834994, -73.011375; observed by Flor Susana and submitted to iNaturalist in: <https://inaturalist.mma.gob.cl/observations/102608301>. • Concepción; 5-V-2023; -36.8354793349, -73.0287251249; observed by Luis Chavarriga and submitted to iNaturalist in: <https://inaturalist.mma.gob.cl/observations/159871318>. • Coliumo; 9-II-2023; -36.5526014, -72.9574049; observed by fpizarro and submitted to iNaturalist in:

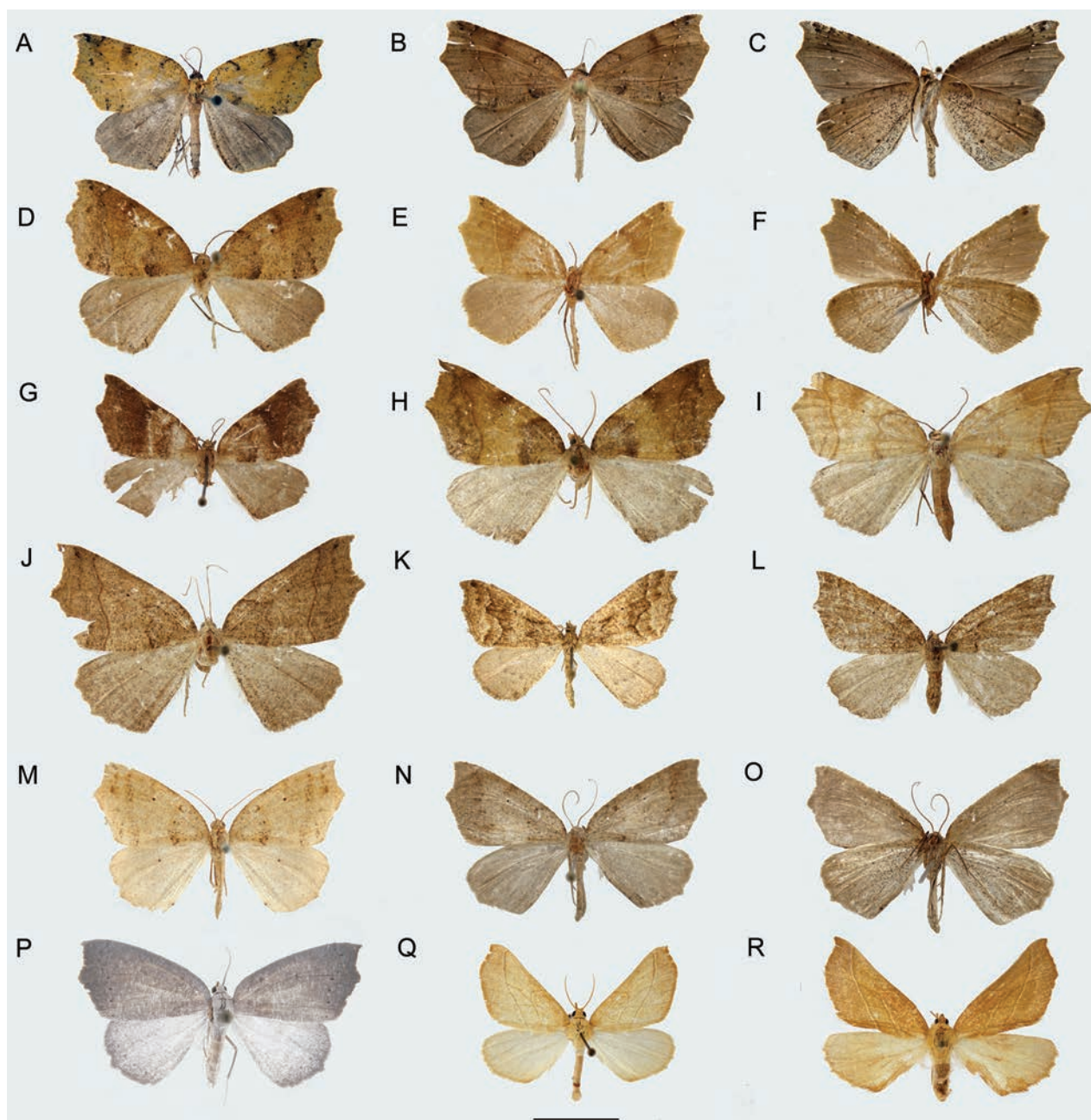


Figure 2. Habitus of *Digonis* adults **A** *Digonis aspersa* (male in dorsal view) **B** *Digonis aspersa* (male brown-morpho in dorsal view) **C** *Digonis aspersa* (male brown-morpho in ventral view) **D** *Digonis aspersa* (female in dorsal view) **E** *Digonis cervinaria*, stat. rev. (male olivaceous-morpho in dorsal view) **F** *Digonis cervinaria*, stat. rev. (male olivaceous-morpho in ventral view) **G** *Digonis cervinaria*, stat. rev. (male fuscous-morpho in dorsal view) **H** *Digonis cervinaria*, stat. rev. (female in dorsal view) **I** *Digonis cervinaria*, stat. rev. (female olivaceous-morpho in ventral view) **J** *Digonis cervinaria*, stat. rev. (female brown-morpho in ventral view) **K** *Digonis punctifera* (male in dorsal view; photo courtesy of A. Hausmann) **L** *Digonis punctifera* (female in dorsal view) **M** *Digonis gungnir* Ramos-González & Parra, sp. nov. (holotype in dorsal view) **N** *Digonis apocrypha* Ramos-González & Parra, sp. nov. (holotype in dorsal view) **O** *Digonis apocrypha* Ramos-González & Parra, sp. nov. (holotype in ventral view) **P** *Phasmadigonis alba*, comb. nov. (male in dorsal view) **Q** *Gugnelve butleri* Ramos-González & Parra, sp. nov. (holotype in dorsal view) **R** *Gugnelve butleri* Ramos-González & Parra, sp. nov. (allotype in dorsal view). Scale bar: 10 mm.

<https://inaturalist.mma.gob.cl/observations/148464516>. • Concepción; 20-XII-2023; -36.8263187829, -73.0265376168; observed by Antonio Maureira Navarrete and submitted to iNaturalist in: <https://inaturalist.mma.gob.cl/observations/144894518> • Concepción; 15-XII-2022; -36.7784506232,

-73.0294558602; observed by Antonio Maureira Navarrete and submitted to iNaturalist in: <https://inaturalist.mma.gob.cl/observations/144446815>. • Concepción; 20-XII-2023; -36.8263187829, -73.0265376168; observed by Antonio Maureira Navarrete and submitted to iNaturalist in: <https://inaturalist.mma.gob.cl/observations/144894518> – **Biobío Prov.** • Polcura; -37.285095, -71.718547; 20-III-2022; observed by Flor Susana and submitted to iNaturalist in: <https://inaturalist.mma.gob.cl/observations/110011024>. – **Osorno Prov.** • Osorno; -40.565175, -73.161816; 19-VI-2021; observed by Ricardo Huenuanca and submitted to iNaturalist in: <https://inaturalist.mma.gob.cl/observations/83672367> • Osorno; -40.565183, -73.161729; 02-V-2021; observed by Ricardo Huenuanca and submitted to iNaturalist in: <https://inaturalist.mma.gob.cl/observations/76765927> • Osorno; -40.565303, -73.162031; 09-I-2021; observed by Ricardo Huenuanca and submitted to iNaturalist in: <https://inaturalist.mma.gob.cl/observations/67836032>.

Diagnosis. This species can be easily distinguished from *D. punctifera* (Butler), *D. gungnir* Ramos-González & Parra, sp. nov., and *D. cervinaria* by its brownish forewings crossed by slightly sinuous bands and bicolored spots in the postmedial band at the level of veins R_3 , R_4 , R_5 , M_1 , M_2 , M_3 , CuA_1 , CuA_2 , and $1A+2A$. Externally, it differs from *D. apocrypha* Ramos-González & Parra, sp. nov. because its bicolored spots appear on both sides of both pairs of wings with an equal proportion of white and black scales. It can be easily distinguished from its congeners by three other genitalia characters: a tongue-shaped furca that does not surpass the height of the transtilla, the presence of lateral spines in the distal half of the furca, and anterior apophyses directed towards the tergum.

Redescription. Male (Fig. 2A–C). Head: antennae slightly serrate; palpi long, one-third larger than eye diameter and slightly pointing upward; frons and vertex covered with mottled brownish gray scales. Thorax: patagia covered with elongated scales of same color as background; tegulae covered with piliform scales of same color as background; tibial spur formula 0-2-4. Forewings: subtriangular with acute apex and outer margin excavated between apex and M_3 , with a slight mucronate extension; fovea absent; background color variable, ranging from yellowish brown to dark brown with numerous small scattered blackish spots on the surface; antemedial band dark brown to blackish, slightly arched and marked by three bicolored spots (proximal half with whitish scales and distal half with blackish scales) at the level of radial, cubital, and anal veins respectively; medial band diffuse, blackish to smoky brown, more noticeable along the costal margin; postmedial band dark brown, slightly sinuous with the costal sector, strongly arched, with bicolored spots (proximal half with blackish scales and distal half with whitish scales) at the level of veins R_3 , R_4 , R_5 , M_1 , M_2 , M_3 , CuA_1 , CuA_2 , and $1A+2A$, also visible on ventral side; subterminal band diffuse and marked only by dark spots in subapical region, at the level of medial veins and along the anal margin; discal spot visible, punctiform, and blackish. Hindwings: subrectangular with small mucronate apex at the level of M_3 ; background color grayish brown; postmedial band slightly smoky dark brown, marked by bicolored spots (proximal half with blackish scales and distal half with whitish scales) at the level of veins, also visible on ventral surface; discal spot visible only on ventral surface. Male genitalia (Fig. 3A, B). Uncus conical, apically club-shaped; gnathos U-shaped with expanded apex forming a pair of spiny lobes; valvae subrectangular, costa strongly sclerotized with distal lobe before apex, crescent-shaped, slightly convex, and

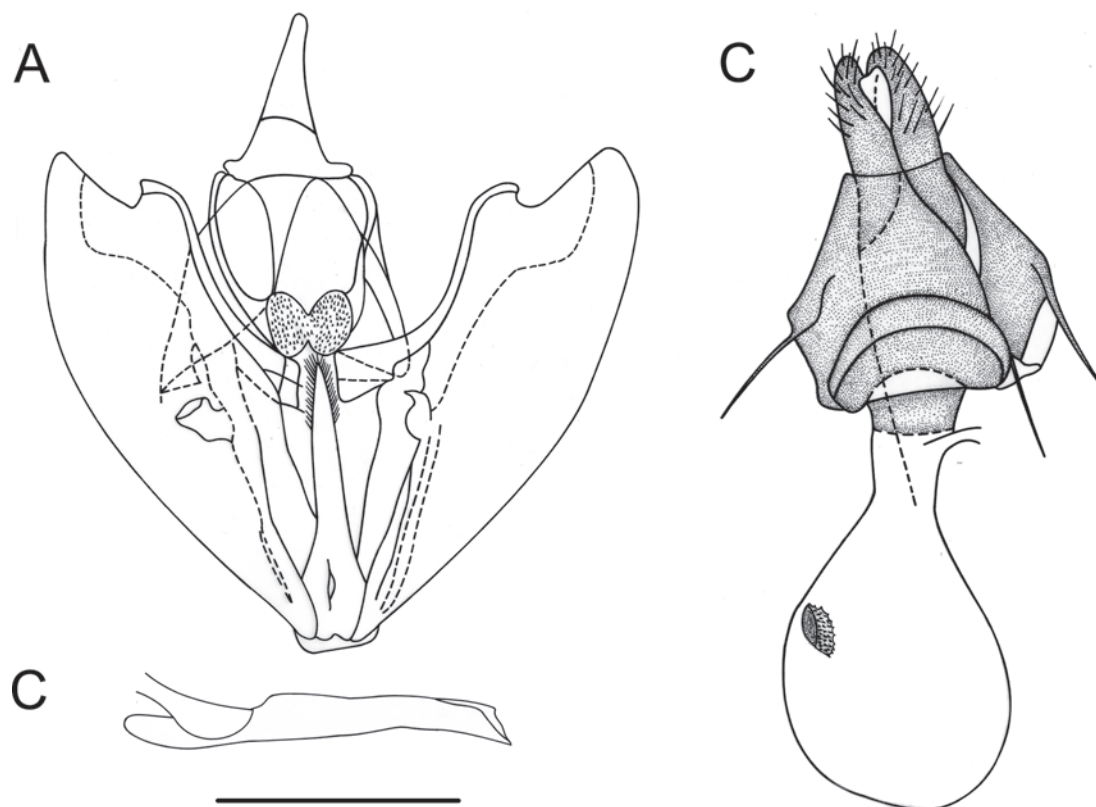


Figure 3. Genitalia of *Digonis aspersa* **A** male genitalia in ventral view **B** aedeagus in lateral view **C** female genitalia in ventral view. Scale bar: 1 mm.

cucullus extending beyond apex of costa; transtilla truncated; saccus subrectangular; juxta emarginated anteriorly, with a median dimple, and furca straight, short, does not surpass the height of the transtilla, tongue-shaped, spiny only laterally in the distal half; anellus sclerite weak, pentagonal in shape. Aedeagus tubular, straight; vesica without cornuti.

Female (Fig. 2D). Similar to male, but with simple antennae and well-defined Σ -shaped antemedial band. Female genitalia (Fig. 3C). Ductus bursae one-sixth the length of corpus bursae; lamella antevaginalis wide, strongly sclerotized; corpus bursae membranous, subpyriform with an annular, hollow, strongly denticulated signum anteriorly; posterior apophyses twice as long as anterior apophyses, anterior apophyses slightly bent towards tergite.

Distribution. This species is found between the Chilean provinces of San Antonio and Capitán Prat, with records in Neuquén, Argentina (Chalup 2020). It is distributed in parts of the biogeographic provinces of Santiago, Central Chilean subregion; Maule and Valdivian Forest, Subantarctic subregion, in the Andean region.

Flight period. Specimens were captured or observed in January, February, March, April, May, June, September, October, and December. There are no records for other months.

Remarks. Although the holotype stands out due to its yellowish tone, most examined specimens exhibit a brownish coloration. There is no evidence to suggest that this color variation reflects sexual dimorphism. The genitalia of these brown specimens are congruent with those of the holotype, indicating high variability in wing coloration.

***Digonis cervinaria* (Blanchard, 1852), stat. rev.**

Figs 2E–J, 4

Ennomos cervinaria Blanchard, 1852: 89.

Drepanogynis eversaria Guenée, 1858: 93 (unnecessary replacement name)

Digonis cervinaria (Blanchard, 1852); Scoble 1999: 229; Pitkin 2002: 248.

Digonis cuprea Butler, 1882: 362; Bartlett-Calvert 1886: 333; Angulo and Casanueva 1981: 12; Scoble 1999: 229; Pitkin 2002: 248. syn. nov.

Digonis cuprea fusca Butler, 1882: 362; Bartlett-Calvert 1886: 333; Angulo and Casanueva 1981: 12; Scoble 1999: 229; Pitkin 2002: 248. syn. nov.

Digonis cuprea olivacea Butler, 1882: 362; Bartlett-Calvert 1886: 333; Angulo and Casanueva 1981: 12; Scoble 1999: 229; Pitkin 2002: 248. syn. nov.

Material examined. Syntypes . CHILE • 1 female; Coquimbo; C. Gay leg.; “*Digonis cervinaria*” [labeled]; MNHN • 1 female; Valparaíso; T. Edmonds leg.; “*Digonis cuprea*” [labeled]; “Chili, 82-107”; “Type” [labeled]; NHMUK • 2 males; same data as for preceding but “*var. fusca*” [labeled]; “Type” [labeled] “Chili, 82-107” [labeled] and “*cuprea olivacea*” [labeled]; “Type” [labeled]; “Chili, 82-107” [labeled]; all NHMUK.

Other material examined. CHILE — **Valparaíso Prov.** • Viña del Mar; 8-VIII-1954; “Museo 5343” [Museum ID]; MNNC) • 1 female; Viña del Mar; 18-IV-1953; “Museo 5018” [Museum ID]; “Mirg-015” [genitalia slide]; MNNC; • 1 male; Viña del Mar; 15-X-1953; “Museo 5349” [Museum ID]; MNNC • 1 male; Viña del Mar; 15-VIII-1953; “Museo 5342” [Museum ID]; MNNC • 1 female; Viña del Mar; 12-IX-1953; “Museo 5350” [Museum ID]; MNNC • 1 male; Laguna Verde; 10-X-1936; E. Ureta leg.; “Museo 5014” [Museum ID]; MNNC. — **Marga Marga Prov.** • 1 male; Poza Azul, Marga Marga; 14-XII-1953; “Museo 5346” [Museum ID]; MNNC. — **Cordillera Prov.** • 1 male; La Obra; 26-III-1953; “Museo 5373” [Museum ID]; MNNC. — **Cachapoal Prov.** • 1 female; Termas de Cauquenes; 11-I-1953; E. Ureta leg.; “Museo 5006” [Museum ID]; “Mirg-013” [genitalia slide] • 1 male; Termas de Cauquenes; 11-I-1953; E. Ureta leg.; “Museo 5023” [Museum ID]; MNNC. — **Talca Prov.** • 1 female; Panguilemo, La Calor; 1-II-2005; L. Parra leg.; “Mirg-009” [genitalia slide]; MZUC-UCCC. — **Diguillín Prov.** • 1 female; Las Trancas; 29-V-2011; G. Moreno leg.; “Mirg-016” [genitalia slide]; MZUC-UCCC. — **Concepción Prov.** • 1 female; Concepción; 6-I-1961; Trampas leg.; MZUC-UCCC. — **Malleco Prov.** • 1 female; Río Blanco, Curacautín; II-1995; H. Thöny leg.; ZSM. — **Cautín Prov.** • 1 female; Termas de Río Blanco; III-1951; MZUC-UCCC. — **Valdivia Prov.** • 1 female; Valdivia; I-1974; Cameron leg.; MZUC-UCCC. — **Osorno Prov.** • 1 female; Puerto Octay; 11-III-1956; Oehrens leg.; “Museo” [labeled]; MNNC. — **Palena Prov.** • Fjord Comau, Huinay Station, -42.381111, -72.414722, 20 m; 8-I-2008; A. Hausmann leg.; ZSM.

Additional records. CHILE — **Itata Prov.** • La Palma; -36.567339, -72.689122; 09-VI-2021; observed by Claudio Maureira and submitted to iNaturalist in: <https://inaturalist.mma.gob.cl/observations/85725251>. — **Concepción Prov.** • Concepción; -36.7928173278, -73.0525010616; 13-XII-2022; observed by Antonio Maureira Navarrete and submitted to iNaturalist in: <https://inaturalist.mma.gob.cl/observations/144446817>. — **Cautín Prov.** • Molco; -39.3393898652, -72.0921077239; 25-XII-2022; observed by Michael Weymann and submitted to iNaturalist in: <https://inaturalist.mma.gob.cl/observations/145759642>. • Molco; -39.3394188914, -72.0921402457; 25-XII-2022; observed by Michael Weymann and submitted to iNaturalist in: <https://inaturalist.mma.gob.cl/observations/145759626>. **Osorno**

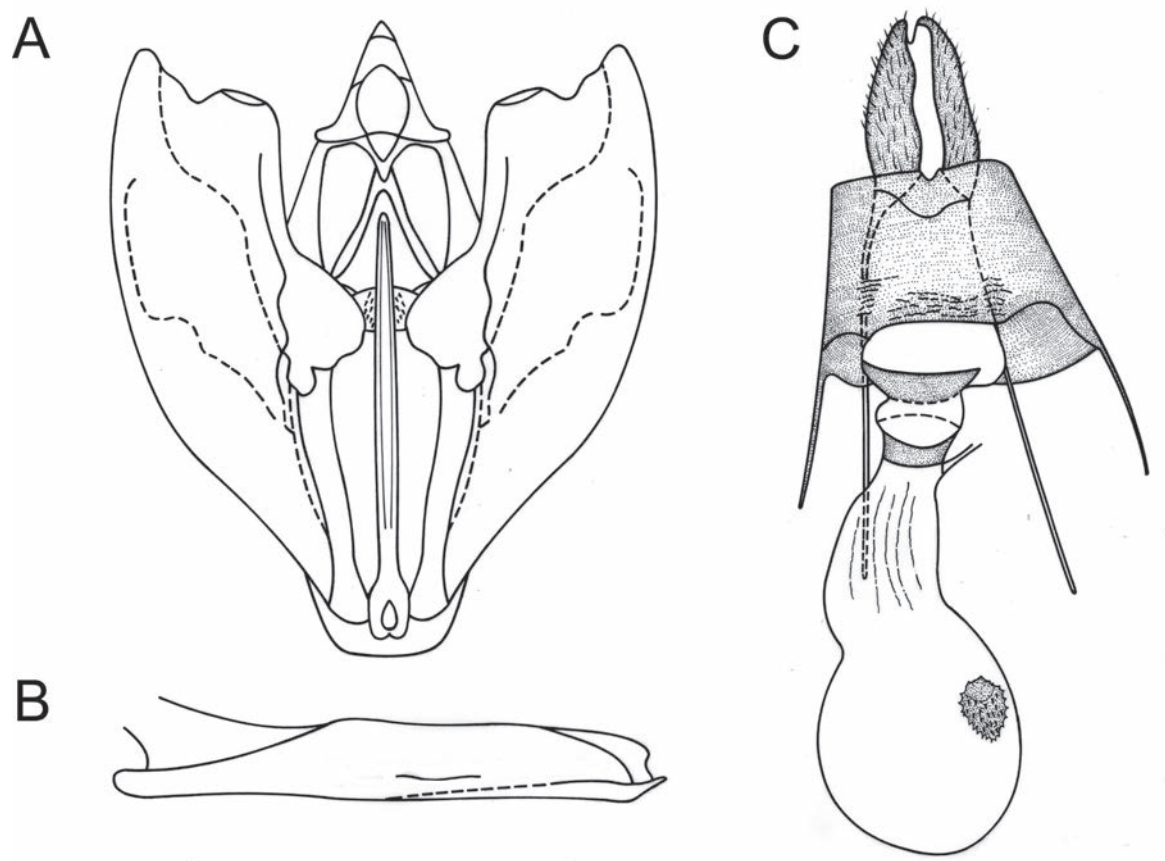


Figure 4. Genitalia of *Digonis cervinaria*, stat. rev. **A** male genitalia in ventral view **B** aedeagus in lateral view **C** female genitalia in ventral view. Scale bars: 1 mm.

Prov. • Osorno; -40.565282, -73.161883; 31-I-2021; observed by Ricardo Huenuanca and submitted to iNaturalist in: <https://inaturalist.mma.gob.cl/observations/68898181> • Osorno; -40.565277, -73.162024; 3-I-2021; observed by Ricardo Huenuanca and submitted to iNaturalist in: <https://inaturalist.mma.gob.cl/observations/67871022>. — **Llanquihue Prov.** • Las Cascadas; -41.0799870456, -72.6350197924; 6-V-2023; observed by Mario Ramos and submitted to iNaturalist in: <https://inaturalist.mma.gob.cl/observations/164957877>. — **Chiloé Prov.** • Punta; -42.119003, -73.81765; 27-II-2022; observed by Waldo Moyano and submitted to iNaturalist in: <https://inaturalist.mma.gob.cl/observations/107842416>.

Diagnosis. This species can be distinguished externally from other *Digonis* species by having elongated whitish spots at the level of veins R3, R4, R5, M1, M2, M3, CuA1, CuA2, and 1A+2A in postmedial region, also visible on ventral view. Male genitalia are characterized by the presence of a needle-shaped furca that surpasses the height of the transtilla, with only apical spines; costa strongly sclerotized with distal lobe, expanded before apex with truncated edge, and spatulate transtilla; aedeagus with a narrow and elongated caecum, one-third of the total length of the aedeagus.

Redescription. Male (Fig. 2E–G). Head: antennae slightly serrate; palpi short, subequal to eye diameter, porrect; frons and vertex covered with juxtaposed brownish scales. Thorax: patagia covered with elongated scales of same color as background; tegulae covered with piliform scales of same color as background; tibial spur formula 0-2-4. Forewings: subtriangular with acute apex and

outer margin excavated between apex and M_3 , with slight mucronate extension; fovea absent; background color variable, ranging from olive-brown to dark brown; antemedial band dark brown to blackish, slightly sinuous; medial band diffuse, blackish to smoky brown, slightly oblique and in contact with postmedial band near anal margin; postmedial band dark brown, slightly sinuous with the costal sector, near apex, strongly arched, and with elongated whitish spots at the level of veins R_3 , R_4 , R_5 , M_1 , M_2 , M_3 , CuA_1 , CuA_2 , and $1A+2A$, also visible on ventral view; subterminal band diffuse and marked only by dark spots in subapical region; discal spot visible, punctiform, and blackish. Hindwings: subrectangular with small mucronate apex at the level of M_3 ; background color grayish brown; postmedial band dark brown, slightly smoky, marked by elongated whitish spots at the level of veins, only visible on ventral surface; discal spot visible only on ventral surface. Male genitalia (Fig. 4A, B). Uncus conical, apically halberd-shaped; gnathos U-shaped with an expanded apex forming a pair of spiny lobes; valvae subrectangular, costa strongly sclerotized with a distal lobe before the apex, truncated, slightly convex, and cucullus extending beyond the apex of the costa; transtilla spatulate; saccus membranous; juxta emarginated anteriorly, with a median dimple, and furca straight, longitudinally striated, long, surpassing the height of the transtilla, needle-shaped, spiny only apically; anellus sclerite weakly defined. Aedeagus tubular, straight; caecum narrow and elongated, one-third of the total length of the aedeagus; vesica without cornuti.

Female (Fig. 2H–J). Similar to male, but with simple filiform antennae, Σ -shaped antemedial band, and zigzagging subterminal band. Female genitalia (Fig. 4C). Ductus bursae one-fourth the length of the corpus bursae; lamella antevaginalis, sclerotized; corpus bursae membranous, subpyriform with an annular, hollow, strongly denticulated signum anteriorly; posterior apophyses three times longer than the anterior apophyses.

Distribution. This species is found between the Elqui and Palena provinces. It is distributed in parts of the biogeographic provinces of Coquimbo and Santiago, Central Chilean subregion; Maule and Valdivian Forest, Subantarctic subregion, in the Andean region.

Flight period. Specimens were captured or observed in January, February, March, April, May, June, August, September, October, and December. There are no records for other months.

***Digonis punctifera* Butler, 1882**

Figs 2K, L, 5

Digonis punctifera Butler, 1882: 363; Bartlett-Calvert 1886: 333; Angulo and Casanueva 1981: 12; Pitkin 2002: 248.

Digonis punctifera acuminata Butler, 1882: 363; Bartlett-Calvert 1886: 333; Angulo and Casanueva 1981: 12; Pitkin 2002: 248. syn. nov.

Digonis punctifera fumosa Butler, 1882: 363; Bartlett-Calvert 1886: 333; Angulo and Casanueva 1981: 12; Pitkin 2002: 248. syn. nov.

Digonis punctifera maculosa Butler, 1882: 363; Bartlett-Calvert 1886: 333; Angulo and Casanueva 1981: 12; Pitkin 2002: 248. syn. nov.

Digonis punctifera terranea Butler, 1882: 363; Bartlett-Calvert 1886: 333; Angulo and Casanueva 1981: 12; Pitkin 2002: 248. syn. nov.

Material examined. Syntypes. CHILE • 1 male; Valparaíso; T. Edmonds Leg; “Type” [labeled]; “Chili, 82-107” [labeled]; NHMUK • 1 female; Valparaíso; T. Edmonds leg.; “*var. acuminata*” [labeled]; “Type” [labeled]; “Chili, 82-107” [labeled]; NHMUK • 1 male; Valparaíso; T. Edmonds leg.; “*var. fumosa*” [labeled]; “Type” [labeled]; “Chili, 82-107” [labeled]; NHMUK • 2 females; same data as for preceding but “*var. maculosa*” [labeled]; “Type” [labeled]; “Chili, 82-107” [labeled]; all NHMUK • 1 male; same data as for preceding but “*var. terranea*” [labeled]; “Type” [labeled]; “Chili, 82-107” [labeled]; NHMUK.

Other material examined. CHILE — **Limarí Prov.** • Ovalle, Quebrada Seca; 28/29-XI-1997; ZSM • 1 female; Ovalle, Los Molles; 16/19-X-1994; ZSM. — **Petorca Prov.** • 1 male and 1 female; Cachagua, Quebrada Aguas Claras; 5-III-1997; ZSM. — **Valparaíso Prov.** • 1 female; Viña del Mar; 4-IV-1953; “Mirg-011” [genitalia slide]; MNMC. • 3 males and 1 female; Valparaíso; 10-III-2006; H. Thoeny leg.; ZSM. — **Diguillín Prov.** • 1 male; Las Trancas; 8-II-2011; G. Moreno leg.; MZUC-UCCC.

Additional records. CHILE. — **Limarí Prov.** • P.N. Fray Jorge; -30.658155, -71.66439; 21-VII-2016; observed by Bastian Riveros and submitted to iNaturalist in: <https://inaturalist.mma.gob.cl/observations/87956647>.

Diagnosis. Externally, *D. punctifera* is characterized by the presence of a sinuous postmedial band that follows the shape of the wing’s outer margin. The female genitalia are distinguished by a ductus bursae that is half the length of the corpus bursae and posterior apophyses five times longer than the anterior apophyses.

Redescription. Male (Fig. 2K). Head: antennae slightly serrate; palpi long, one-third longer than the eye diameter and slightly pointing upward; frons and vertex covered with mottled grayish brown scales. Thorax: patagia covered with elongated grayish brown and dark brown scales; tegulae covered with piliform scales of same color as patagia; tibial spur formula 0-2-4. Forewings: subtriangular with acute apex and outer margin excavated between apex and M_3 , with slight mucronate extension; fovea absent; background color variable, ranging from yellowish brown to dark brown, with numerous small blackish spots scattered on surface; antemedial band faint, brownish dark, Σ -shaped; postmedial band dark brown, sinuous following the shape of the wing’s outer margin, with a strip or whitish points toward the distal margin, not visible on ventral surface; subterminal band diffuse and marked only by dark spots in subapical region, at the level of medial veins and on anal margin; discal spot visible, punctiform, and blackish. Hindwings: subrectangular with small mucronate apex at the level of M_3 ; background color grayish brown; postmedial band dark brown, zigzagging, slightly smoky, and marked by blackish spots at the level of veins, also visible on ventral surface; discal spot visible, punctiform, and blackish. Male genitalia. Unknown.

Female (Fig. 2L). Similar to male but with simple filiform antennae and more defined antemedial band, also Σ -shaped. Female genitalia (Fig. 5). Ductus bursae half the length of the corpus bursae; lamella antevaginalis sclerotized; corpus bursae membranous, subpyriform with an annular, hollow, strongly denticulated signum anteriorly, located to the right of the corpus bursae; posterior apophyses five times longer than the anterior apophyses.

Distribution. This species is found between the Limarí and Diguillín provinces. It is distributed in parts of the biogeographic provinces of Coquimbo and Santiago, Central Chilean subregion; Maule, Subantarctic subregion, Andean region.

Flight period. Specimens were captured or observed in February, March, April, July, October, and November. There are no records for other months.

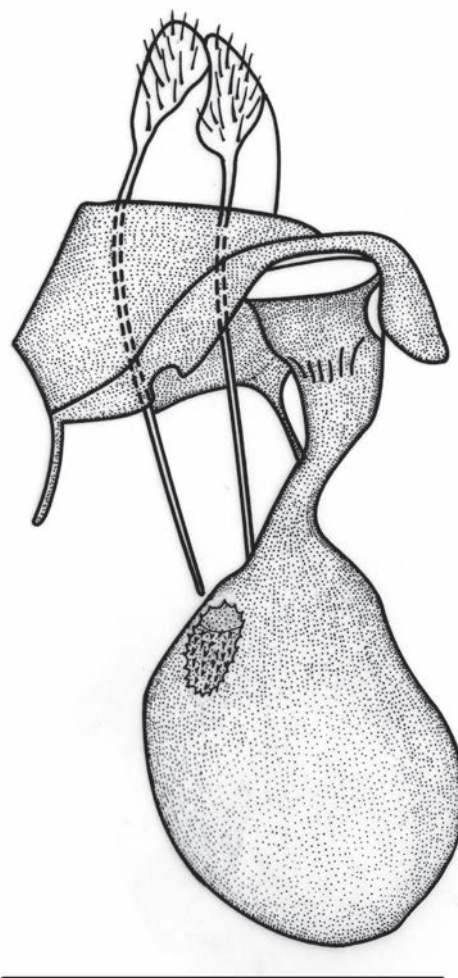


Figure 5. Female genitalia of *Digonis punctifera*. Scale bar: 1 mm.

***Digonis gungnir* Ramos-González & Parra, sp. nov.**

<https://zoobank.org/2BE6459A-9B57-400B-91F1-844437B57E79>

Figs 2M, 6

Type material. Holotype. CHILE — 1 male; pinned; Coquimbo, Elqui, Huanta; 1936 (year without more data); E. Ureta leg.; “Holotype *Digonis gungnir*” [red handwritten label]; “5024” [Museum ID]; “Mirg-019” [genitalia slide]; MNNC.

Paratypes. CHILE — 1 male; pinned; Llanquihue Prov., Maullín; II-1943; S. Barros leg.; MZUC-UCCC • 1 male; pinned; Magallanes Prov., Punta Arenas, Tres Puentes; XII-1952; n.n. leg.; MZUC-UCCC.

Diagnosis. Externally, *D. gungnir* Ramos-González & Parra, sp. nov. is characterized by straw-colored wings and a straight postmedial band with pale points bordered in dark brown at veins R_4 , R_5 , M_1 , M_2 , and M_3 on the forewings. Male genitalia feature a presence of a poorly defined juxta, a slightly arched spear-shaped furca, and dense dorsal spines on the furca.

Description. Male (Fig. 2M). Head: antennae slightly serrate; palpi long, one-third longer than the eye diameter, porrect; frons and vertex covered with juxtaposed whitish scales. Thorax: patagia covered with elongated whitish scales; tegulae covered with very pale yellowish piliform scales; tibial spur formula

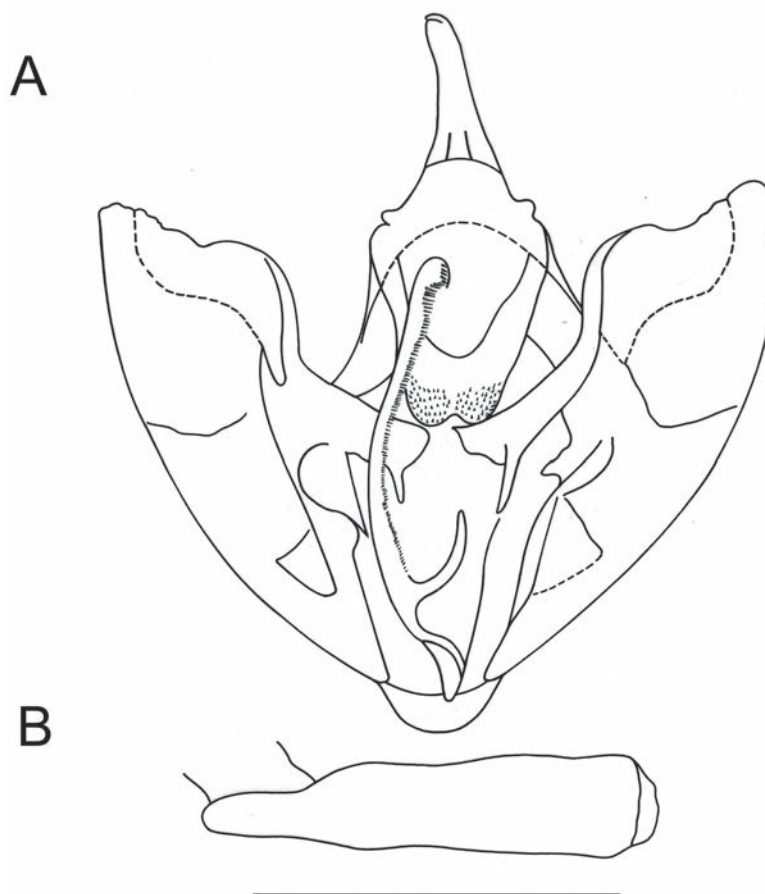


Figure 6. Genitalia of *Digonis gungnir* Ramos-González & Parra, sp. nov. (holotype) **A** male genitalia in ventral view **B** aedeagus in lateral view. Scale bar: 1 mm.

0-2-4. Forewings: subtriangular with acute apex and outer margin excavated between apex and M_3 , with slight mucronate extension; fovea absent; background color straw-colored; antemedial band diffuse, marked by three light brown points at the level of radial, cubital, and anal veins respectively; medial band diffuse, light brown, slightly arched and more noticeable between the discal spot and the costa, zigzagging to the anal margin; postmedial band straight, diffuse, light brown, with five white points bordered in dark brown at the level of veins R_4 , R_5 , M_1 , M_2 , and M_3 , visible only on ventral surface; subterminal band diffuse and demarcated only by dark spots in subapical region, at the level of medial veins and on anal margin; discal spot visible, punctiform, and blackish. Hindwings: subrectangular with small mucronate apex at the level of M_3 ; background color pale ashy; postmedial band light brown, slightly smoky, marked by elongated light brown spots at the level of veins, only visible on ventral surface; discal spot visible. Male genitalia (Fig. 6). Uncus conical, apex club-shaped; gnathos U-shaped with an expanded apex forming a pair of spinous lobes; valvae subrectangular, costa strongly sclerotized with a distal lobe before the apex, rounded, and cucullus extended beyond the apex of the costa; transtilla bifid; saccus subrounded; juxta poorly defined, pointed anteriorly, with a central depression, and with a furca curved to the left, long, surpassing the height of the transtilla, slightly arched spear-shaped, densely spiny dorsally, apex rounded; anellus sclerite weakly defined, only two subtriangular sclerites near the base of the furca are visible. Aedeagus tubular, straight; vesica without cornuti.

Female. Unknown.

Etymology. The species name is a noun in apposition, referring to Odin's spear (the chief god in Norse mythology), due to its longer and more armed furca within the genus. Gungnir is treated here as a neuter noun.

Distribution. This species is found between the provinces of Elqui and Magallanes. It is distributed in parts of the biogeographic provinces of Coquimbo and Santiago, Central Chilean subregion; Maule, Valdivian Forest, and Magellanic Forest, Subantarctic subregion, Andean region.

Flight period. Specimens were captured in December and February. There are no records for other months.

***Digonis apocrypha* Ramos-González & Parra, sp. nov.**

<https://zoobank.org/458C9CE8-3466-4EEE-99A0-35F4E244557C>

Figs 2N, O, 7

Type material. Holotype. CHILE: 1 male; pinned; Ñuble, Las Trancas; 31-III-2011; G. Moreno leg.; "Holotype *Digonis apocrypha*" [red handwritten label], "UCCC_MZUC_Lep_0300" [Museum ID], "Mirg-021" [genitalia slide] (MZUC-UCCC). **Paratypes.** CHILE — **Diguillín Prov.** • 1 male; pinned; Ñuble, Recinto; 06-II-2011; G. Moreno leg.; MZUC-UCCC • 1 male; pinned; same data as holotype but "UCCC_MZUC_Lep_0304" [Museum ID] (MZUC-UCCC) • 2 males; pinned; same data as holotype but 12-IV-2013; "UCCC_MZUC_Lep_1729" and "UCCC_MZUC_Lep_1730" [Museum ID]; MZUC-UCCC • 2 males; pinned; same data as holotype but 20-III-2011; "UCCC_MZUC_Lep_0330" and "UCCC_MZUC_Lep_0320" [Museum ID]; MZUC-UCCC • 1 male; pinned; same data as holotype but 16-IV-2010; "UCCC_MZUC_Lep_0303" [Museum ID]; MZUC-UCCC • 2 males; pinned; same data as holotype but 7-IV-2010; MZUC-UCCC • 1 male; pinned; same data as holotype but "UCCC_MZUC_Lep_0301" [Museum ID]; MZUC-UCCC • 1 male; pinned; same data as holotype but 29-V-2011; "UCCC_MZUC_Lep_0302" [Museum ID]; MZUC-UCCC • 1 male; pinned; same data as holotype but 18-III-2012; "UCCC_MZUC_Lep_1160" [Museum ID]; MZUC-UCCC. — **Valdivia Prov.** • 1 male; pinned; 09-IV-2010; Huilo-Huilo, Mocho-Choshuenco volcano; -39.911943; -71.969167; L. Roa and D. Vergara leg.; MZUC-UCCC. — **Capitán Prat Prov.** • 1 male; pinned; Cochrane; 11-IV-2008; Parra and Alvarado leg.; "sampled in scrub of Notro-Ñirre" [labeled] (*Embothrium coccineum* (Proteaceae) - *Nothofagus antarctica* (Nothofagaceae)); MZUC-UCCC.

Diagnosis. This species is distinguished from the other species in the genus by the presence of elongated blackish marks with small whitish point at the level of veins in the postmedial band of the forewings, which are not visible in ventral view. In the male genitalia, it differs from *D. aspersa* by the elongated and striated furca, more similar to that of *D. cervinaria*. It also differs from *D. cervinaria* because it has spines around the distal half of the furca. This species stands out for the presence of a U-shaped gnathos with an expanded apex like a denticulate plate, transtilla with a digitiform process at the apex, and aedeagus with a fine and elongated caecum, half the total length of the aedeagus.

Description. Male (Fig. 2N, O). Head: antennae slightly serrate; palpi long, one-third longer than the eye diameter, porrect; frons and vertex covered with grayish brown scales. Thorax: patagia covered with elongated scales of same color as background; tegulae covered with piliform scales of same color as background;

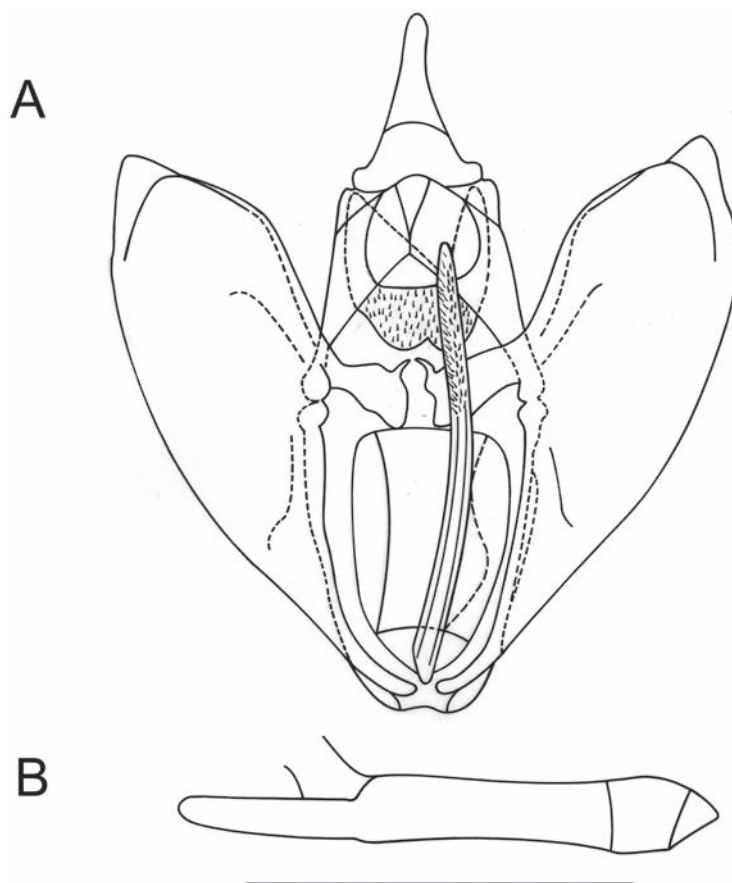


Figure 7. Genitalia of *Digonis apocrypha* Ramos-González & Parra, sp. nov. (holotype) **A** male genitalia in ventral view **B** aedeagus in lateral view. Scale bar: 1 mm.

tibial spur formula 0-2-4. Forewings: subtriangular with acute apex and outer margin excavated between apex and M_3 , with slight mucronate extension; fovea absent; pale ashy background with a large number of small blackish spots scattered over the surface; antemedial band diffuse, slightly zigzagging, marked by three dark brown points at the level of radial, cubital, and anal veins respectively; medial band light brown, diffuse; postmedial band, diffuse, light brown, with bicolored spots (elongated blackish mark with the center marked by a whitish point) at the level of veins R_4 , R_5 , M_1 , M_2 , M_3 , CuA_1 , CuA_2 , and $1A+2A$, not visible on ventral surface. Hindwings: subrectangular with small mucronate apex at the level of M_3 ; pale ashy background, without visible bands or spots; discal spot visible. Male genitalia (Fig. 7). Uncus conical, apex club-shaped; gnathos U-shaped with an expanded apex like a denticulate plate; valvae subrectangular, costa strongly sclerotized with a distal lobe before the apex, rounded, and cucullus extended beyond the apex of the costa; transtilla bifid; saccus membranous, weakly defined; juxta poorly defined, with a central depression and furca, long, surpassing the height of the gnathos, club-shaped with two longitudinal stripes, densely spiny towards the distal half; anellus sclerite weakly defined. Aedeagus tubular, straight; fine, elongated caecum, half the total length of the aedeagus; vesica without cornuti.

Female. Unknown.

Etymology. The species name is an adjective from Greek *apocryphos* ("not genuine"), referring to the deceptive maculation pattern, superficially resembling *Digonis aspersa* Butler.

Distribution. This species is found between the provinces of Diguillín and Capitán Prat. It is distributed in parts of the biogeographic provinces of Maule, Valdivian Forest, Magellanic Forest, Subantarctic subregion, in the Andean region.

Flight period. Specimens were captured in February, March, April, and May. There are no records for other months.

***Phasmadigonis* gen. nov.**

<https://zoobank.org/F0922815-E334-4247-9CE0-9F98FD0DABE0>

Type species. *Digonis alba* Butler, 1882.

Diagnosis. *Phasmadigonis* bears resemblance to *Digonodes* Warren, 1895, *Digonis* Butler, 1882, and *Gonogala* Butler, 1882, particularly due to the mucronate shape of the wings. However, *Phasmadigonis* can be distinguished by the presence of vein Sc connected by a vein to the single accessory cell in the forewings and by having vein Sc+R1 connected to radial trunk by a weak vein in the hindwings. *Phasmadigonis* is distinguished by the following genitalia characters: gnathos V-shaped with the absence of lobes or spines, spatulate transtilla, broad shovel-shaped juxta, furca armed with small sagittal spines and a dimple in the sclerite at its base, aedeagus with a digitiform apex, and vesica armed with a large spine.

Description. Antennae serrated in males and filiform in females. Thorax and abdomen with grayish scales. Forewings gray-lilac reticulated with white, lacking bands, subterminal region delimited only by a series of blackish spots at the level of R2, R3, R4, M1, M2, M3, CuA1, CuA2, and 1A+2A; costa margin in apical zone is slightly arched; outer margin is concave between apex and M3. Wing venation (Fig. 8): one accessory cell; Sc connected with accessory cell through a short vein, R1 and R2 arise from accessory cell, R3 and R4 are pedunculate, R5 terminates at termen; M2 equidistant from M1 and M3, M3 slightly arched and ending in small mucronate apex; CuA1 arises 1/10 before end of cell, CuA2 arises near middle of cell. Hindwings paler than forewings, with subterminal region delimited by series of dark spots at the level of veins. Sc+R1 connected to radial trunk by a weak transverse vein, Rs arises 1/6 before end of cell, M2 is absent. Male genitalia with rod-like uncus; gnathos V-shaped; valvae suboval; transtilla spatulate; furca spiny; vesica with prominent spine.

Etymology. The generic name is formed by combining the Greek *phasma* (meaning phantom or apparition), with *Digonis* in reference to the false resemblance to moths of the genus *Digonis* Butler and the wing coloration; its gender is neuter.

Distribution. Similar to its sole species, *P. alba* (Butler)

***Phasmadigonis alba* (Butler, 1882), comb. nov.**

Figs 2P, 9

Digonis alba Butler, 1882: 361; Bartlett-Calvert 1886: 333; Angulo and Casanueva 1981: 12; Scoble 1999: 229; Pitkin 2002: 248.

Material examined. Syntype. CHILE • 1 female; pinned; Mountains of the hacienda of Cauquenes; T. Edmonds leg.; “Chili, 82-107” [labeled]; “Type” [labeled]; NHMUK.

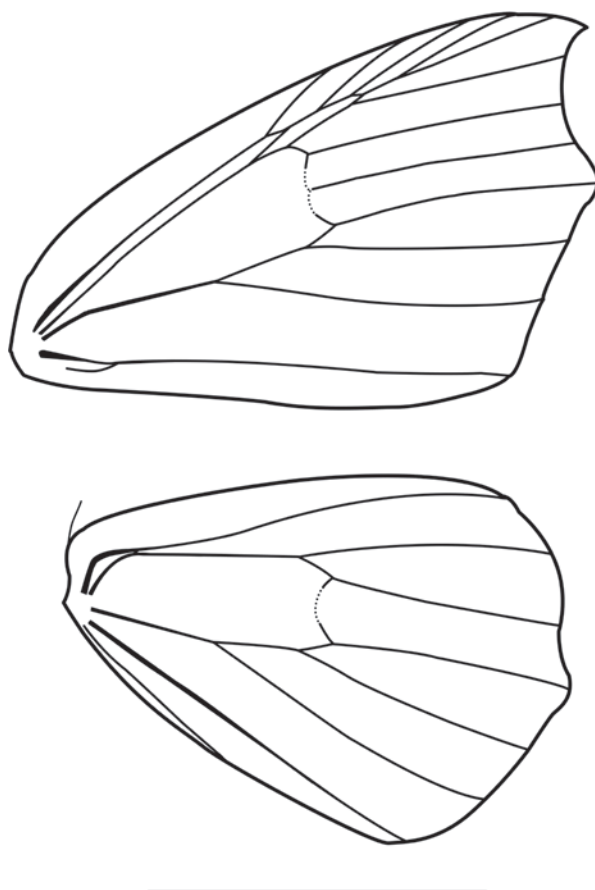


Figure 8. Wing venation of *Phasmadigonis* Ramos-González & Parra, gen. nov. Scale bar: 10 mm.

Other material examined. CHILE — • 1 male; Chile; “Museo 5022” [Museum ID]; MNNC. — **Diguillín Prov.** • 1 male; Ñuble, Las Trancas; 18-III-2012; G. Moreno leg.; “UCCC-MUZC-Lep1173” [Museum ID]; “MMA1173” [genitalia slide]; MZUC-UCCC. — **Araucanía Region** • 1 male; Araucanía, II-1888, coll. n.n, “Museo 5029” [Museum ID]; MNNC; • 2 males; same data as for precedings but “Museo 5027” [Museum ID] and “Museo 5028” [Museum ID]; all MNNC. — **Chiloé Prov.** • 1 male; Mocopulli, Ruta 5 Sur km 1170, -42.368000, -73.728833, 182 m; 3-II-2017, leg. M. Ramos-G, M. Ramos-SM & C. Rose.

ARGENTINA — • 1 male; Río Negro Prov., Bariloche; 29-I-1991; H. Ibarra-Vidal leg.; “HIV-0034” [Museum ID]; MHNC.

Additional records. CHILE. — **Talca Prov.** • Cipreses hydroelectric plant; -35.7867249, -70.8078157; 16-XII-2023; observed by César Picar and submitted to iNaturalist in: <https://inaturalist.mma.gob.cl/observations/196336300>. • Cipreses hydroelectric plant; -35.7865833685, -70.8078496903; 21-I-2024; observed by César Picar and submitted to iNaturalist in: <https://inaturalist.mma.gob.cl/observations/197310545>.

Diagnosis. As for the genus.

Redescription. Male (Fig. 2P). Head: antennae slightly serrated; short palpi, subequal to eye diameter, porrect; frons and vertex covered with juxtaposed brownish scales. Thorax: patagia covered with elongated scales of same color as background; tegulae covered with piliform scales of same color as background; tibial spur formula 0-2-4. Forewings: subtriangular with acute apex and outer

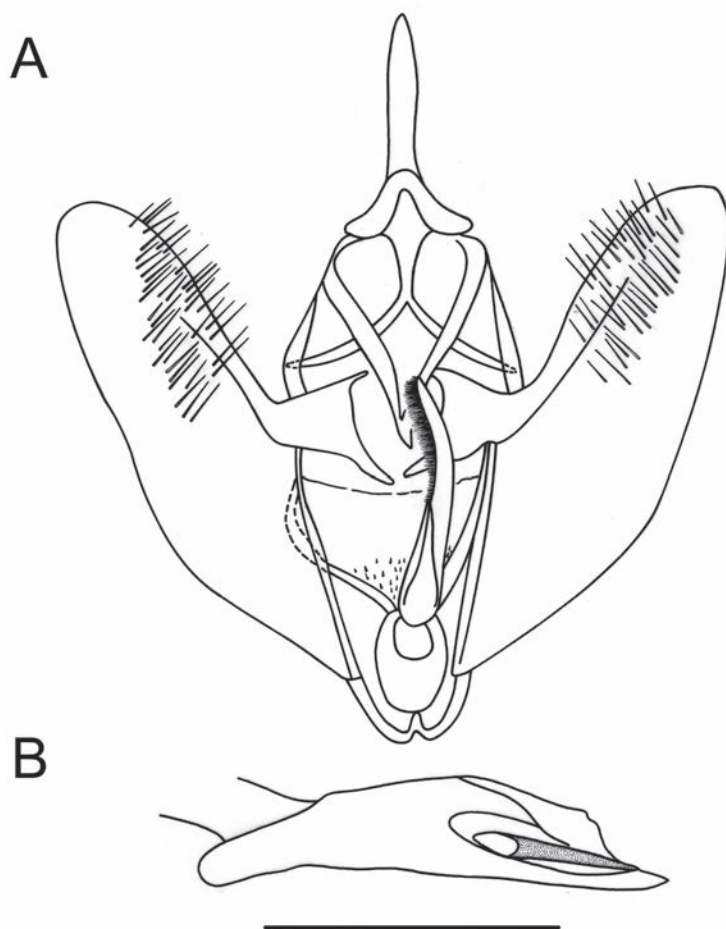


Figure 9. Genitalia of *Phasmadigonis alba*, comb. nov. **A** male genitalia in ventral view **B** aedeagus in lateral view. Scale bar: 1 mm.

margin excavated between apex and M_3 , with a slight mucronated extension; fovea absent; ground color gray-lilac reticulated with white; bands absent, only observable on wing surface are blackish points in subterminal area at the level of veins R_2 , R_3 , R_4 , M_1 , M_2 , M_3 , CuA_1 , CuA_2 , and $1A+2A$, also visible on ventral side; discal spot visible, punctiform, and blackish. Hindwings: subrectangular with small mucronated apex at the level of M_3 ; ground color ash-white, termen grayish; bands absent, only observable on wing surface is a row of blackish dots in subterminal area at the level of veins $Sc+R_1$, Rs , M_1 , M_3 , CuA_1 , CuA_2 , and $1A$; discal spot visible. Male genitalia (Fig. 9). Uncus straight, apex rod-like; gnathos V-shaped; valvae suboval, valvula and cucullus slightly setose, costa sclerotized; transtilla spatulate with sharp, projected vertices; saccus obcordate; juxta shovel-shaped, dorsally flattened and extended, with finger-shaped furca curved to the left, short, not surpassing the height of the transtilla, densely spiny sagittally; anellus sclerite weakly defined. Aedeagus tubular, straight, apex digitiform; vesica armed with a large spine.

Female. Unknown.

Distribution. This species is found between the provinces of Cachapoal and Chiloé (Chile) and Río Negro (Argentina). It is distributed in parts of the biogeographic provinces of Santiago, Central Chile subregion; Maule and Valdivian Forest, Subantarctic subregion, in the Andean region.

Flight period. Specimens were captured in December, January, February, and March. There are no records for other months.

Tribe Nacophorini Forbes, 1948

Gugnelve gen. nov.

<https://zoobank.org/5D5F1234-1907-4D23-A970-C051EF3D8DEA>

Type species. *Gugnelve butleri* Ramos-González & Parra, sp. nov.

Diagnosis. Externally, *Gugnelve* resembles *Euangerona* Butler and *Dectochilus* Warren. All three genera have an oblique curved band in the central area of the forewings. However, *Euangerona* and *Dectochilus* have a wavy termen, unlike *Gugnelve*, which has a smooth termen and a slightly falcate apex. The wing shape and antennae are similar to those of *Laninia* Orfila & Schajovskoy and *Macrolyrcea* Butler, but they differ significantly in various genital structures, such as the gnathos with a posteriorly directed apex and distally lobulated costa in *Laninia* and the spatulate uncus and wide oval valvae in *Macrolyrcea*. The V-shaped gnathos with a longitudinal row of spicules is reminiscent of *Euangerona* and *Dectochilus*, but in both of those genera, the anellus process is directed anteriorly, while in *Gugnelve*, it is oriented lateroposteriorly. The uncus and juxta resemble those of *Malleco* Rindge, but in *Gugnelve*, the uncus is glabrous, and the anellus process is trifid, while the gnathos of *Malleco* has multiple spicules on the lateral arms and apex. Finally, the new genus differs considerably in external characteristics and genitalia from other Andean Nacophorini like *Catophoenissa* Warren, 1894, *Catocalopsis* Rindge, 1971, *Talca* Rindge, 1971, and *Wichanraran* Parra, 2018. *Gugnelve* is distinguished by the following combination of genital characters: V-shaped gnathos with a row of 11 spicules at the apex, forked transtilla, halberd-shaped juxta laterally extended into a pair of tri-spined anellus processes, strongly sclerotized and glabrous, vesica armed with a series of cornuti, signum with a long blade-like ridge on a sclerotized patch.

Description. Antennae thickened and slightly serrated in males, filiform in females. Robust thorax with yellowish brown piliform scales. Abdomen with belt of white scales on A1 and A2. Forewings yellowish brown, subtriangular, slightly falcate, with sinuous and inclined antemedial and postmedial bands. Wing venation (Fig. 10). Two accessory cells, second twice as long as first; Sc in contact with first accessory cell, R1 originates from middle of second accessory cell, R2 and R3+4 connate, R3 and R4 pedunculate, R5 terminates at termen; M2 equidistant from M1 and M3, M3 slightly arched; CuA1 originates 1/8 before end of cell, CuA2 originates near middle of cell. Hindwings paler than forewings, with yellowish brown piliform scales on the termen. Sc+R1 in contact with radial trunk up to middle of cell, Rs originates 1/12 before end of cell, M2 absent. Male genitalia with V-shaped gnathos, expanded apex with 11 small variably-sized denticles towards the center; valvae sub-rhomboidal; juxta sub-halberd-shaped, laterally extended into a pair of tri-spined, strongly sclerotized processes. Female genitalia with signum with long blade-like ridge on sclerotized patch.

Etymology. The generic name is derived from the Mapudungun language (spoken by the Mapuche, the largest indigenous group in Chile), *wünyelfe*, meaning bright star or Venus, in reference to its yellowish coloration; its gender is neuter.

Distribution. As for its only species, *G. butleri* Ramos-González & Parra, sp. nov.

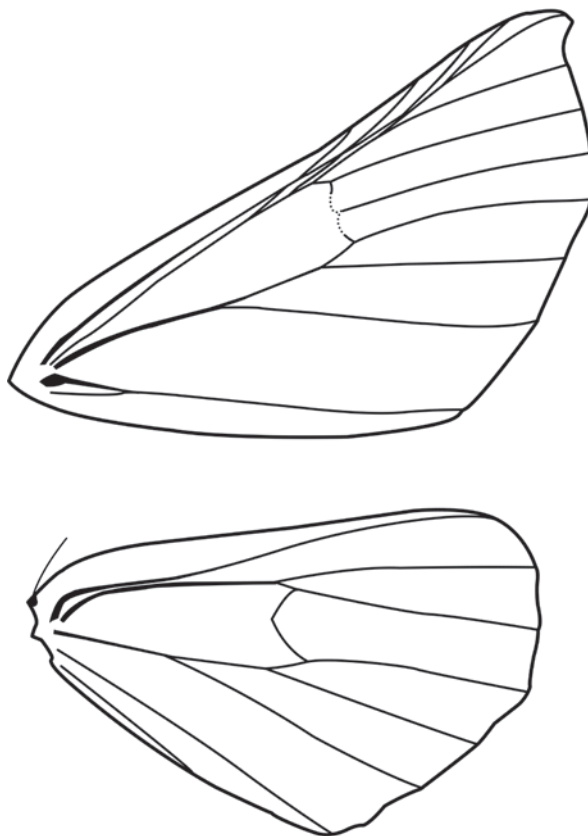


Figure 10. Wing venation of *Gugnelve* Ramos-González & Parra, gen. nov. Scale bar: 10 mm.

***Gugnelve butleri* Ramos-González & Parra, sp. nov.**

<https://zoobank.org/80882365-C942-46DB-AAD3-FC68E5CE32D8>

Figs 2Q, R, 11

Erosina cervinaria (Blanchard, 1852); Butler 1882: 347 pl. 16, fig. 4; Bartlett-Calvert 1886: 331; Angulo and Casanueva 1981: 12 [misidentification of *Ennomos cervinaria* Blanchard].

Type material. Holotype. CHILE • 1 male; Cordillera Prov., Santiago, Guayacan; XII-1950; "Holotype *Gugnelve butleri*" [red handwritten label], "Mirg-017" [genitalia slide] (MZUC-UCCC). **Allotype.** Chile • 1 female, Cordillera Prov., Santiago, Guayacan; I-1951; "Allotype *Gugnelve butleri*" [red handwritten label], "Mirg-018" [genitalia slide] (MZUC-UCCC). **Paratypes.** CHILE – **Limarí Prov.** • 2 males, Ovalle, Quebrada Seca; 28/29-XI-1997; ZSM. – **Cordillera Prov.** • 4 females and 1 male, same data as Holotype; • 1 female and 1 male, same data as allotype.

Other material examined. CHILE – **Cachapoal Prov.** • 1 female; Termas de Cauquenes; 11-I-1953; "Museo 4516" [Museum ID]; MNNC.

Additional records. CHILE. – **Cachapoal Prov.** • Mountains of the hacienda of Cauquenes; January; T. Edmonds leg.; NHMUK (Butler, 1882) – **Talca Prov.** • Parque Natural Tricahue; -35.70869903, -71.08727243; 5-I-2020; observed by Vicente Pantoja and submitted to iNaturalist in: <https://inaturalist.mma.gob.cl/observations/37300513>. • Cipreses hydroelectric plant; -35.8099272997, -70.8359745; 17-XII-2022; observed by César Picar and submitted to iNaturalist

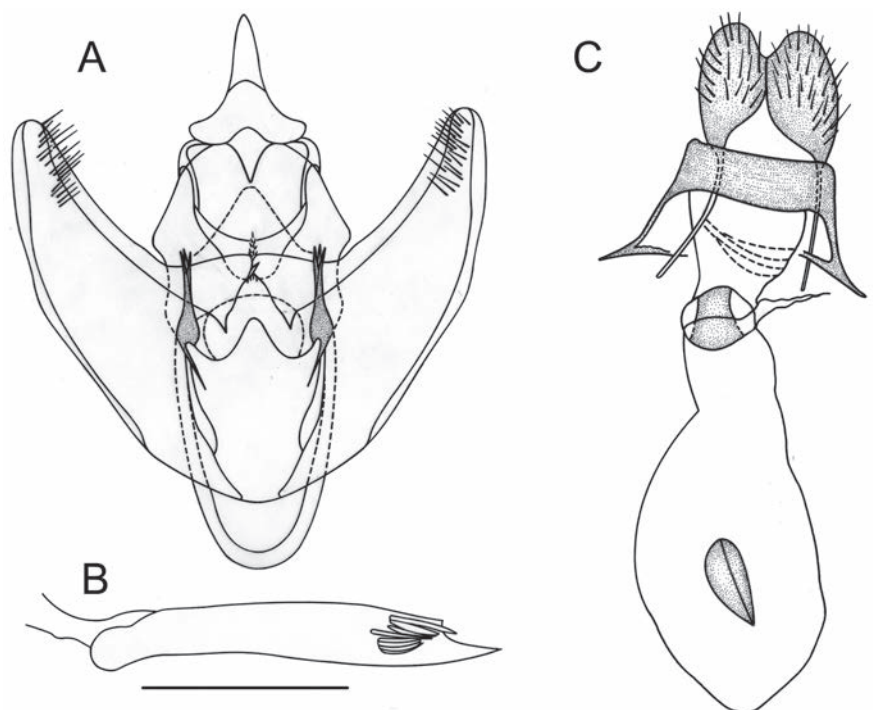


Figure 11. Genitalia of *Gugnelve butleri* Ramos-González & Parra, sp. nov. (holotype and allotype) **A** male genitalia in ventral view **B** aedeagus in lateral view **C** female genitalia in ventral view. Scale bars: 1 mm.

in: <https://iNaturalist.mma.gob.cl/observations/144651054>. • Cipreses hydroelectric plant; -35.8096577, -70.8353316; 10-I-2024; observed by César Picar and submitted to iNaturalist in: <https://iNaturalist.mma.gob.cl/observations/196337433>.

Diagnosis. As for the genus.

Description. Male (Fig. 2Q). Head: antennae slightly serrated; palpi short, subequal to the eye diameter, porrect; frons and vertex covered with juxtaposed brownish scales. Thorax: Patagia covered with elongated scales of same color as background; tegulae covered with piliform scales of same color as background; tibial spur formula 0-2-4. Forewings: slightly falcate, subtriangular; fovea absent; background color yellowish brown; antemedial band dark yellowish brown, externally bordered by pale brown, oblique, extending toward the medial area, near the end of the discal cell where it curves toward the antemedial sector to the costa, forming an acute arc; postmedial band dark yellowish brown, externally bordered by pale brown, slightly sinuous, oblique, and slightly curved, extending to the subapical sector; discal spot not visible. Hindwings: suboval; background color pale brown without bands; discal spot not visible. Male genitalia (Fig. 11A, B). Uncus conical; socii slightly setose; gnathos V-shaped with sinuous arms, expanded apex with 11 small denticles of varying sizes toward the center; valvae sub-rhomboidal, costa and anterior margin sclerotized; transstilla fork-shaped; saccus suboval; juxta sub-halberd-shaped, laterally extended into a pair of tri-spined strongly sclerotized processes; anellus sclerite weakly defined. Tubular aedeagus, straight; vesica armed with cornuti, formed by 11 grouped spines of different sizes.

Female (Fig. 2R). Similar to male but with simple filiform antennae, dark yellowish brown falcate forewings, and slightly crenulated pale brownish gray subrectangular hindwings. Female genitalia (Fig. 11C). Ductus bursae half the

length of the corpus bursae; antrum funnel-like; corpus bursae membranous, subpyriform, signum with a long blade-like ridge on a sclerotized patch; posterior apophyses three times longer than anterior apophyses.

Etymology. The specific name is dedicated to Arthur Gardiner Butler, an ornithologist, arachnologist, and entomologist of the 19th century, for his contribution to the study of Lepidoptera in Chile.

Distribution. This species is found between the provinces of Limarí and Talca. It is distributed in parts of the biogeographic provinces of Coquimbo and Santiago, Central Chilean subregion; Maule, Subantarctic subregion, in the Andean region.

Flight period. Specimens were captured in November, December, and January. There are no records for other months.

Discussion

The genus *Digonis*, described by Butler in 1882, initially included *D. aspersa*, *D. cuprea*, *D. punctifera*, and *D. alba*. Additionally, Butler (1882) described various varieties for *cuprea* and *punctifera*, differentiating them based on the coloration of the forewings. However, the analysis of the genital structures of *D. punctifera* indicates that these differences in coloration are not sufficient to separate them into distinct species or subspecies within the genus, which is why they are synonymized.

The inclusion of the species *D. gungnir* Ramos-González & Parra, sp. nov. and *D. apocrypha* Ramos-González & Parra, sp. nov. in the genus *Digonis* is justified by the congruence in their external characteristics and genitalia. The distinction from their sister species is primarily focused on male genitalia characteristics. Therefore, the genus *Digonis* is composed of the following five species: *D. aspersa*, *D. cervinaria*, *D. punctifera*, *D. gungnir* Ramos-González & Parra, sp. nov., and *D. apocrypha* Ramos-González & Parra, sp. nov. Its validity as a taxon within the tribe Ennomini is supported by the presence of a membranous and weakly developed saccus, valvae with well-sclerotized outstanding costa, and well-developed furca (Beljaev 2008).

Based on the analysis of genital structures and wing venation, a strong incongruence is recognized between the species *D. alba* Butler and the rest of the species in *Digonis*. This aligns with what Pitkin (2002) indicated, suggesting that *D. alba* should be excluded from the genus due to certain incongruences with genital characters. The main differences between both genera lie in the shape of the valvae, furca, and wing venation configuration, a combination of characters not present in any other Ennomini genus in the Andean region (e.g., *Syncirsodes* Butler, *Gonogala* Butler, *Microclysia* Butler, *Perusia* Herrich-Schäffer, *Eusarca* Hübner), which supports the proposal of *Phasmadigonis* as a new genus. Additionally, we report the first record of this taxon for Argentina, specifically for the province of Río Negro.

The different species of the genus *Digonis* have distributions that cover most of the vegetation formations (sensu Luebert and Plischoff 2018) in central-southern Chile. However, the highest species richness appears to be associated with the high-Andean deciduous forest of the Cordillera de Chillán (sensu Gajardo 1994). The lack of records in other areas may be due to a lack of comprehensive sampling, particularly in the central-northern zone of Chile

(north of Santiago). Future studies should address the rearing of different species to describe their host plants and immature stages, currently unknown.

Blanchard (1852) described the species *Ennomos cervinaria* based on a specimen from Coquimbo, providing a brief and imprecise description, and without including figures. Later, Guenée (1858) redescribed it in more detail, characterizing it by the elongated whitish marks on the wing veins, visible in both dorsal and ventral views. Furthermore, Guenée proposed a new name for this species, arguing that “*cervinaria*” was already used for a species of *Eubolia* Duponchel, 1829 (current *Larentia clavaria* Duponchel, 1845). Subsequently, Butler (1882) incorporated this species into the genus *Erosina* Guenée, 1858, arguing that, if his determination of the specimen used is correct, it has a second oblique but indistinct angular line from the costa to the inner margin, almost parallel to the line described by Blanchard (1852) in his description. Additionally, Butler (1882) added a sketch of the species for easier future determination. Finally, Scoble (1999) included it in the genus *Digonis*. However, the analysis of the type material reveals that the specimens determined as *Ennomos cervinaria* by Butler (1882) and subsequent authors are not congruent with the holotype of *Ennomos cervinaria* Blanchard. The external characteristics and genitalia of *Ennomos cervinaria* correspond to those of *Digonis cuprea* and its varieties, so these are synonymized.

The analysis of specimens incorrectly determined as *E. cervinaria* by Butler reflects a morphological correspondence with the concept of “Nacophorini” (sensu Rindge 1973, 1983), which brought together the Ennominae with a broad and “hairy” thorax that now form parts of the tribes Euangeronini, Odontoperini, and Nacophorini in part (Brehm et al. 2019). The most characteristic feature in the male genitalia corresponds to the row of spicules in the sagittal plane of the gnathos and the trifid, strongly sclerotized posterolaterally directed process of the anellus. This form and configuration of the gnathos are present in the genera *Euangerona* Butler and *Dectochilus* Butler; however, the process of the anellus is not congruent with both genera or any other Euangeronini, which show a process of the anellus pointing anteriorly and a highly developed setose socius (possible synapomorphies of the tribe). On the other hand, it shares with *Mallomus* Blanchard the spine-shaped form of the anellus process; however, in *Mallomus*, it appears as a single sclerotized spine, and the valvae have various modifications absent in *Gugnelve* gen. nov. such as a membranous harpe and digitiform processes on the cucullus. It was also not possible to assign this species to any of the Nacophorini genera in southern South America treated by Rindge (1973, 1983), Pitkin (2002), Parra and Pascual-Toca (2003), or Parra (2018). For this reason, *Gugnelve butleri* Ramos-González & Parra, gen. et sp. nov. is provisionally included in the Nacophorini.

Finally, this revision will serve as the basis for future molecular phylogenetic analyses that will help clarify the evolutionary relationships among species and related taxa. With this work, the number of Ennomini species present in Chile increases to 36 (Parra et al. 2009; Bocaz et al. 2016; Brehm et al. 2019), and the Nacophorini to 20 (Pitkin 2002; Brehm et al. 2019). These numbers are likely to increase in the future, considering that there have been few taxonomic revisions of Ennominae in the Andean region so far.

Acknowledgements

We would like to express our gratitude to M.J. Scoble and L. Pitkin (NHMUK) for their assistance during L.E. Parra's visit to the Natural History Museum. We also thank the staff at MHNC for their help during M.R.-G.'s visits. Our thanks extend to Joël Minet (MNHN) and Mario Elgueta (MNNC) for their cooperation in allowing the study of specimens deposited in their institutions. We are grateful to Axel Hausmann (ZSM) for sharing data and permitting the use of photographs of some specimens from the collection. We also acknowledge the support of the staff at the Museum of Zoology at the Universidad de Concepción, Chile (MZUC-UCCC) during the study of specimens. Additionally, we extend our sincere gratitude to Claudio Maureira, Flor Susana, Luis Chavarriga, Fpizarro, Antonio Maureira Navarrete, Ricardo Huenanuca, Michael Weymann, and Waldo Moyano for their contributions to the iNaturalist platform, particularly in observations of *Digonis* species. We extend our gratitude to Fundación Mongen (Chile) for sponsoring and supporting the field campaign in Las Cascadas (Los Lagos, Chile) during May 2023, which enabled the recording of a *Digonis* species. Thanks to Carolina Rose and Mario Ramos San Martín who collaborated in the field collection of specimens in Chiloé. M.R.-G. and C.Z.-M. acknowledge financial support from the "Beca Doctorado Nacional" ANID No. 21210517 and CONICYT No. 21161423, respectively.

Additional information

Conflict of interest

The authors have declared that no competing interests exist.

Ethical statement

No ethical statement was reported.

Funding

This research was supported by the Vicerectoría de Investigación y Desarrollo at the Universidad de Concepción (VRID 214.113.087-1.0).

Author contributions

Conceptualization: LEP, MFVG, MIRG. Data curation: MIRG, MFVG, CZM. Funding acquisition: LEP. Investigation: MIRG. Methodology: MIRG. Project administration: MIRG. Resources: MFVG. Supervision: LEP. Visualization: CZM, MIRG. Writing - original draft: MIRG, CZM, MFVG, LEP. Writing - review and editing: CZM, MFVG, MIRG, LEP.

Author ORCIDs

Mario I. Ramos-González  <https://orcid.org/0000-0002-5385-6836>

Carlos Zamora-Manzur  <https://orcid.org/0000-0001-7755-4077>

Luis E. Parra  <https://orcid.org/0000-0002-3271-0037>

Data availability

All of the data that support the findings of this study are available in the main text.

References

- Angulo AO, Casanueva ME (1981) Catálogo de los lepidópteros geométridos de Chile (Lepidoptera: Geometridae). Boletín de la Sociedad de Biología de Concepción (Chile) 51: 7–34.
- Bartlett-Calvert W (1886) Catálogo de los lepidópteros Rhopalóceros i Heteróceros de Chile. Anales de la Universidad de Chile 69: 314–352.
- Beljaev EA (2006) A morphological approach to the Ennominae phylogeny (Lepidoptera, Geometridae). Spixiana 29(3): 215–216.
- Beljaev EA (2008) A new concept of the generic composition of the geometrid moth tribe Ennomini (Lepidoptera, Geometridae) based on functional morphology of the male genitalia. Entomological Review 88(1): 50–60. <https://doi.org/10.1134/S0013873808010089>
- Blanchard E (1852) Fauna Chilena. Insectos. Orden VI. Lepidópteros. In: Gay C (Ed.) Historia física y política de Chile. Imprenta de Maulde et Renou, Paris, 1–112.
- Bocaz P, Parra LE (2005) Revisión y bionomía del género *Syncirsodes* Butler, 1882 (Lepidoptera: Geometridae). Revista Chilena de Historia Natural 78: 89–111. <https://doi.org/10.4067/S0716-078X2005000100007>
- Bocaz P, Sepúlveda-Zuniga E, Zamora-Manzur C, Parra LE (2016) Filogenia del género *Syncirsodes* (Lepidoptera: Geometridae). Revista Colombiana de Entomología 42(1): 75–80. <https://doi.org/10.25100/socolen.v42i1.6673>
- Brehm G, Murillo-Ramos L, Sihvonen P, Hausmann A, Schmidt BC, Öunap E, Moser A, Mörtter R, Bolt D, Bodner F, Lindt A, Parra LE, Wahlberg N (2019) New World geometrid moths (Lepidoptera: Geometridae): Molecular phylogeny, biogeography, taxonomic updates and description of 11 new tribes. Arthropod Systematics & Phylogeny 77(3): 457–486. <https://doi.org/10.26049/ASP77-3-2019-5>
- Butler AG (1882) Heterocerous Lepidoptera collected in Chili by Tomas Edmonds, Esq. Part III—Geometrites. Transactions of the Entomological Society of London 30(3): 339–427. <https://doi.org/10.1111/j.1365-2311.1882.tb01580.x>
- Chalup A (2020) The biodiversity of the family Geometridae for Argentina. In: Juñent SA, Claps LE, Morrone JJ (Eds) Biodiversidad de artrópodos argentinos. Vol. 4. INSUE-UNT Ediciones, San Miguel de Tucumán, Argentina, 47–62.
- Gajardo R (1994) La vegetación natural de Chile: Clasificación y distribución geográfica. Editorial Universitaria, Santiago, Chile, 165 pp.
- Gaston KJ, Scoble MJ, Crook A (1995) Patterns in species description: a case study using the Geometridae (Lepidoptera). Biological Journal of the Linnean Society 55: 225–237. <https://doi.org/10.1111/j.1095-8312.1995.tb01061.x>
- Guenée MA (1858) Histoire naturelle des insectes; espèces générales lépidoptères. Vol. 10 Uranides et Phalénites. Librairie Encyclopédique de Roret, Paris, 584 pp.
- Hausmann A, Parra LE (2009) An unexpected hotspot of moth biodiversity in Chilean northern Patagonia (Lepidoptera, Geometridae). Zootaxa 1989: 23–38. <https://doi.org/10.11646/zootaxa.1989.1>
- Holloway J (1993) The moths of Borneo, part 11: Family Geometridae, subfamily Ennominae. Malayan Nature Journal 47: 1–309.
- Klots AB (1970) Lepidoptera. In: Tuxen SL (Ed.) Taxonomist's glossary of genitalia in insects, 115–130. Second Enlarged Edition. Munksgaard, Copenhagen, 359 pp.
- Luebert F, Plissock P (2018) Sinopsis bioclimática y vegetacional de Chile. 2nd edn. Editorial Universitaria, Santiago, Chile.

- Morrone JJ (2015) Biogeographical regionalisation of the Andean region. *Zootaxa* 3936(2): 207–236. <https://doi.org/10.11646/zootaxa.3936.2.3>
- Õunap E, Javoiš J, Viidalepp J, Tammaru T (2011) Phylogenetic relationships of selected European Ennominae (Lepidoptera: Geometridae). *European Journal of Entomology* 108(2): 267–273. <https://doi.org/10.14411/eje.2011.036>
- Parra LE (1991) Revisión y filogenia del género *Pachrophylla* Blanchard, 1852 (*sensu auctorum*) (Geometridae: Larentiinae: Trichopterygini). *Gayana Zoología (Chile)* 55(2): 145–199.
- Parra LE (1999a) Revision of the Neotropical genus *Psilaspilates* (Lepidoptera: Geometridae). *Annals of the Entomological Society of America* 92: 460–472. <https://doi.org/10.1093/aesa/92.4.460>
- Parra LE (1999b) Revisión del género *Euclidiodes* Warren, 1895 (Lepidoptera: Geometridae). *Revista Chilena de Historia Natural* 72: 643–659.
- Parra LE (2018) A new genus of Nacophorini (Geometridae) from Chile. *Journal of the Lepidopterologist Society* 72(4): 265–269. <https://doi.org/10.18473/lepi.72i4.a3>
- Parra LE, Henriquez-Rodríguez JL (1993) Aportes al conocimiento de las polillas del género *Mallomus* Blanchard, 1852 (Geometridae, Nacophorini). *Boletín de la Sociedad de Biología de Concepción (Chile)* 64: 171–187.
- Parra LE, Hernández CE (2010) Estudio filogenético de los géneros de Lithinini de Sudamérica Austral (Lepidoptera, Geometridae): una nueva clasificación. *Revista Brasileira de Entomologia* 54(1): 1–27. <https://doi.org/10.1590/S0085-56262010000100001>
- Parra LE, Pascual-Toca M (2003) Revisión taxonómica de los géneros *Oratha* Walker, 1863 y *Hasodima* Butler, 1882 (Lepidoptera: Geometridae). *Revista Chilena de Historia Natural* 76: 117–128. <https://doi.org/10.4067/S0716-078X2003000100011>
- Parra LE, Vargas HA (2000) Revisión del género *Neorumia* Bartlett-Calvert, 1893 (Lepidoptera: Geometridae). *Revista Chilena de Entomología* 27: 91–98.
- Parra LE, Villagrán-Mella R, Marquet PA (2009) Phylogeny of the genera *Euclidiodes* and *Hasodima* (Lepidoptera: Geometridae) and description of two new species from the Fray Jorge relict forest in northern Chile. *Zootaxa* 2273: 59–68. <https://doi.org/10.11646/zootaxa.2273.1.3>
- Parra LE, Villagrán-Mella R, Hernández EA, Hernández CE (2010) Filogenia del género *Psilaspilates* (Butler 1893) (Lepidoptera: Geometridae) con la descripción de una nueva especie del bosque relicto Fray Jorge, Chile. *Gayana* 74(2): 94–101. <https://doi.org/10.4067/S0717-65382010000200003>
- Pitkin LM (2002) Neotropical ennomine moths: a Review of the genera (Lepidoptera: Geometridae). *Zoological Journal of the Linnean Society* 135(2-3): 121–401. <https://doi.org/10.1046/j.1096-3642.2002.00012.x>
- Rajaei H, Hausmann A, Scoble MJ, Wanke D, Plotkin D, Brehm G, Murillo-Ramos L, Sihvonen P (2022) An online taxonomic facility of Geometridae (Lepidoptera), with an overview of global species richness and systematics. *Integrative Systematics* 5(2): 145–192. <https://doi.org/10.18476/2022.577933>
- Rindge FH (1973) Notes on and descriptions of South American Nacophorini (Lepidoptera, Geometridae). *American Museum Novitates* 2531: 1–42.
- Rindge FH (1983) A generic revision of the new world Nacophorini (Lepidoptera, Geometridae). *Bulletin of the American Museum of Natural History* 175(2): 147–262.
- Rindge FH (1986) Generic descriptions of new world Lithinini (Lepidoptera, Geometridae). *American Museum Novitates* 2838: 1–68.

- Scoble MJ (1995) The Lepidoptera: Form, Function and Diversity. The Natural History Museum & Oxford University Press, London, 416 pp.
- Scoble MJ (1999) Geometrid moths of the world: a catalogue (Lepidoptera, Geometridae). CSIRO Publishing. Natural History Museum, London, 1016 pp. <https://doi.org/10.1071/9780643101050>
- Scoble MJ, Hausmann A (2007) Online list of valid and available names of the Geometridae of the World. Lepidoptera Barcode of Life. https://www.lepbarcoding.org/geometridae/species_checklists.php [accessed on 15 Feb 2022]
- Vargas HA (2007) Dos nuevas especies de *Iridopsis* Warren (Lepidoptera, Geometridae) del norte de Chile. *Revista Brasileira de Entomologia* 51(2): 138-141. <https://doi.org/10.1590/S0085-56262007000200003>
- Vargas HA (2021) *Iridopsis socoromaensis* sp. n., a geometrid moth (Lepidoptera, Geometridae) from the Andes of northern Chile. *Biodiversity Data Journal* 9: e61592. <https://doi.org/10.3897/BDJ.9.e61592>
- Vargas HA, Parra LE, Hausmann A (2005) *Macaria mirthae*: una nueva especie de Ennominae (Lepidoptera: Geometridae) de Chile. *Neotropical Entomology* 34(4): 571-576. <https://doi.org/10.1590/S1519-566X2005000400006>
- Vargas HA, Hausmann A, Parra LE (2020) A new species of *Macaria* Curtis (Lepidoptera: Geometridae: Ennominae) from the Andes of northern Chile. *Revista Brasileira de Entomologia* 64(2): e20200016. <https://doi.org/10.1590/1806-9665-RBENT-2020-0016>

Updated checklist, habitat affinities, and changes over time of the Indiana (USA) caddisfly fauna (Insecta, Trichoptera)

David C. Houghton¹, R. Edward DeWalt²

¹ Department of Biology, Hillsdale College, 33 East College Street, Hillsdale, MI 49242, USA

² Illinois Natural History Survey, 1816 South Oak Street, Champaign, IL 61820, USA

Corresponding author: David C. Houghton (dhoughton@hillsdale.edu)

Abstract

Based on recent collecting and a synthesis of ~100 years of historical data, 219 caddisfly species are reported from the state of Indiana. Seventeen species are reported herein from the state for the first time, including two previously thought to be endemic to the southeastern USA. Species records are also presented herein organized by drainage basin, ecoregion, glacial history, and waterbody type for two distinct time periods: before 1983 and after 2005. More species were reported from the state before 1983 than after 2005, despite collecting almost 3× the number of occurrence records during the latter period. Species occurrence records were greater for most families and functional feeding groups (FFGs) for the post-2005 time period, although the Limnephilidae, Phryganeidae, Molannidae, and Lepidostomatidae, particularly those in the shredder FFG, instead had greater records before 1983. This loss of shredders probably reflected the ongoing habitat degradation within the state. While species rarefaction predicts only a few more species to be found in Indiana, many regions still remain under-sampled and 44 species have not been collected in >40 years.

Key words: Biological diversity, conservation, distribution, insect, Upper Midwest



Academic editor: Ana Previšić

Received: 18 June 2024

Accepted: 4 October 2024

Published: 25 October 2024

ZooBank: <https://zoobank.org/30C9BC9B-83C6-42AC-98C9-E31DE60F9B79>

Citation: Houghton DC, DeWalt RE (2024) Updated checklist, habitat affinities, and changes over time of the Indiana (USA) caddisfly fauna (Insecta, Trichoptera). ZooKeys 1216: 201–218. <https://doi.org/10.3897/zookeys.1216.129914>

Copyright: ©

David C. Houghton & R. Edward DeWalt.

This is an open access article distributed under

terms of the Creative Commons Attribution

License (Attribution 4.0 International – CC BY 4.0).

Introduction

The caddisflies (Trichoptera) constitute an important group of aquatic organisms due to their high overall abundance, high species richness, high ecological diversity, and differing sensitivities to various anthropogenic disturbances (Barbour et al. 1999; Morse et al. 2019). Determining caddisfly distributions and habitat affinities, therefore, is valuable for assessing water quality and other aspects of ecosystem integrity (Dohet 2002; Houghton and DeWalt 2021). Assessing changes in such data over time can be especially valuable (Houghton and Holzenthal 2010).

The caddisflies of the Upper Midwest region of the United States (MAFWA 2023) have been studied for nearly 100 years, starting with the Illinois fauna (Ross 1938, 1944), including more recent comprehensive studies of Kentucky (Floyd et al. 2012), Michigan (Houghton et al. 2018, Minnesota (Houghton 2012), Missouri (Moulton and Stewart 1996), Ohio (Armitage et al. 2011), and Wisconsin (Hilsenhoff 1995), and culminating with an overall checklist of the entire region (Houghton et al. 2022). The last paper included 131 new state spe-

cies records combined from eight different states, including five from Indiana, demonstrating that even well-collected areas still contain undiscovered species.

Research on the Indiana caddisfly fauna encompasses two approximate time periods. The first period began in the 1930s and concluded with Waltz and McCafferty's (1983) checklist of 190 species. Specimens from this period are housed primarily in the Purdue University Entomological Research Collection (PERC) and the Illinois Natural History Survey Insect Collection (INHS). After a ~20-year pause, caddisfly collecting renewed in the early 2000s with subsequent studies by DeWalt et al. (2016a) and Bolton et al. (2019), as well as many specimens accessioned into the PERC, INHS and, more recently, the Hillsdale College Insect Collection (HCIC). This nearly 100-year collecting history provided an opportunity to assess any changes in the caddisfly fauna over time.

Indiana is composed of a single USEPA Level I ecoregion and three secondary ecoregions: Central Plains, Mixed Wood Plains, and Southeastern Plains (Fig. 1). The predominant land use is agriculture in the form of row crops and pasture, especially in the northern two thirds of the state. Land use corresponds strongly with glacial history, as the low-gradient environments and abundant glacial till of the more recent Wisconsin glaciation are more conducive to farming than the higher-gradient and more eroded older landscapes of the Illinoian glaciation and unglaciated regions.

The primary objective of this study was to update the state caddisfly checklist for Indiana and relate the occurrences of all species to drainage basin, ecoregion, glacial history, and waterbody type. We also assessed the rarity of all Indiana species. Since >40 years had passed since the last state checklist, we assessed any notable changes to the fauna during this period. Further, we used species rarefaction to predict total species richness for the state and assessed the importance of collecting effort on a regional level.

Materials and methods

Our primary sampling devices included two types of ultraviolet light traps: an unattended 8-watt light placed over a white pan filled with ethanol, and an attended 12-watt light suspended from a white sheet with two pans filled with ethanol at its base. Such devices were set out at dusk near aquatic habitats and retrieved approximately two hours later (Houghton 2004; Wright et al. 2013; DeWalt et al. 2016a). The nocturnally active caddisfly adults were attracted to the lights and either fell into the pan or were hand-collected (Fabian et al. 2024). Sampling the winged adults is necessary for taxonomic and conservation studies since, unlike larvae, they are usually identifiable to the species level. Moreover, since adults are attracted to lights irrespective of their specific natal microhabitat or functional feeding group (FFG), inferences on ecology and biotic integrity can be made about an ecosystem without the sampling bias that affects benthic studies (Cao and Hawkins 2011). We and our colleagues collected 194 of these ultraviolet light samples from 2005–2023 (Fig. 2, Suppl. material 1). We also databased specimens from the INHS and PERC going back to the early 1900s. These specimens represented collections of unknown effort. Thus, Fig. 2 makes the distinction between “collections” (unknown effort) and “samples” (the ultraviolet light sampling regime described above). All specimens are housed in either the HCIC, INHS, or PERC institutional collection.

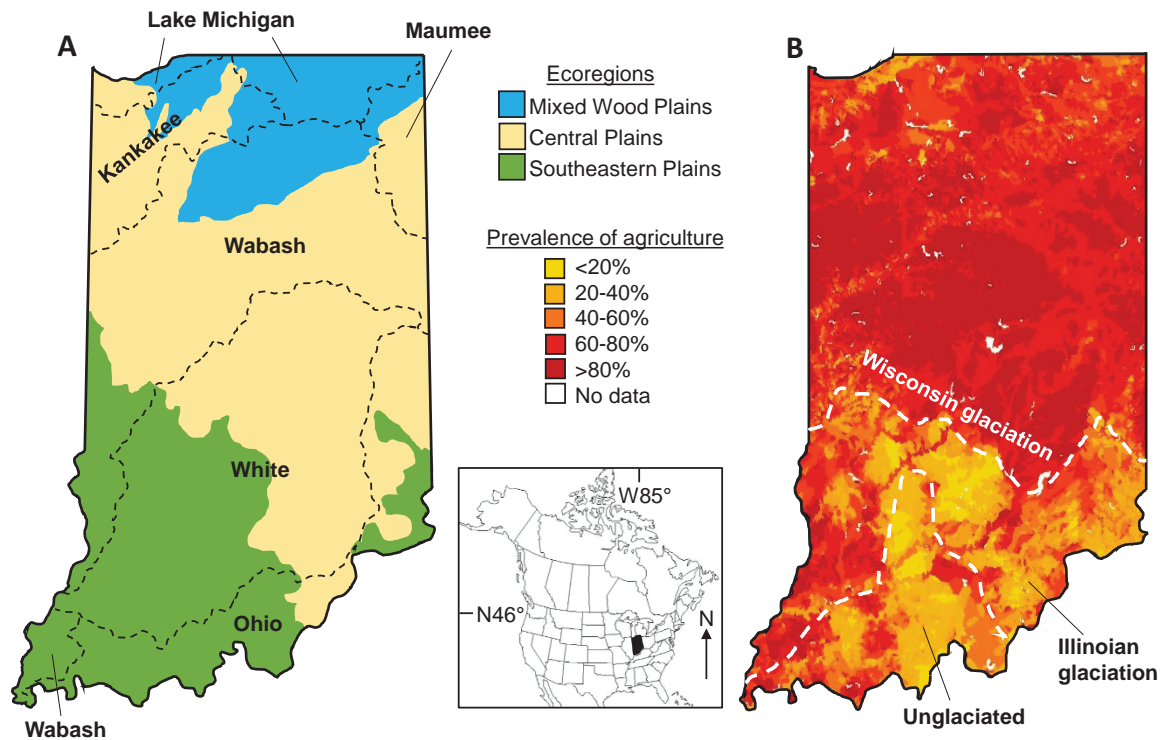


Figure 1. Location of the state of Indiana showing the approximate boundaries of drainage basins and ecoregions (**A**), and prevalence of agriculture and Pleistocene glacial history (**B**).

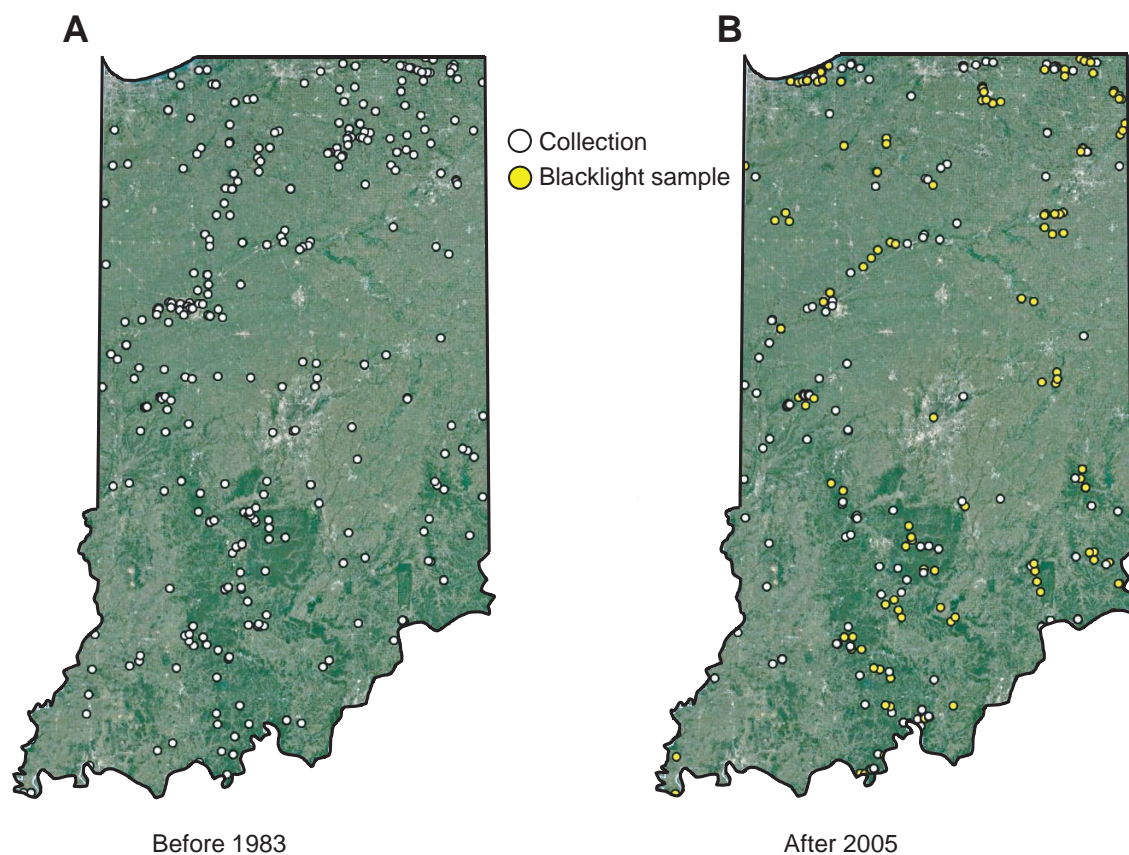


Figure 2. Collecting localities of Indiana caddisflies before 1983 (**A**) and after 2005 (**B**). White markers represent collections of unknown sampling effort whereas yellow markers represent ~2 h ultraviolet blacklight samples. Base map © Google, NOAA.

We associated all 1116 unique collecting localities with drainage basin, ecoregion, glacial maximum, and waterbody type. Our approach for dividing the state into geographic and ecological regions was a balance between having divisions specific enough to reflect biological differences, yet large enough to maintain a consistent collecting effort between them. Thus, we divided the state by United States Environmental Protection Agency Level II ecoregions (<https://www.epa.gov/eco-research/ecoregions-north-america>) and Hydrologic Unit Code (HUC) 6 drainages (<https://water.usgs.gov/GIS/huc.html>). For the latter we combined smaller watersheds with a common outlet (e.g., the various HUC6 drainages all draining into the Ohio River) into their larger drainages (Fig. 1). While slightly nonstandard, we prefer this categorization over attempting to compare small drainages with minimal collecting effort to those with hundreds of collections. We also divided the state based on glacial maximum (Gray and Letsinger 2011). Lastly, we categorized specific sampling sites by lake or size of stream (<https://www.epa.gov/waterdata>).

To estimate total species richness for the state, a species rarefaction curve based on all species and samples collected was produced using the program EstimateS for Windows v. 9.1 (<https://www.robertkcolwell.org/pages/estimates>). In addition to the basic curve, two maximum species richness estimators were calculated. The abundance-based coverage estimator (ACE) predicted total species richness based on a proportion of rare to common species, defining “rare” as any species represented by <10 specimens. The incidence-based coverage estimator (ICE) made the same prediction, but defined “rare” as any species found in <10 samples.

To assess the importance of sampling effort in collecting species, simple linear regression models were calculated for the number of species collected from each of the primary watershed, ecoregion, glacial maximum, and waterbody type designations (dependent variable) based on the accumulated number of unique collections and samples combined (independent variable). Separate models were calculated for the pre-1983 and post-2005 time periods. The number of species associated with each geographic and habitat designation was treated as an independent observation even though each sample or collection was associated with designations of all four types.

Results

A total of 219 caddisfly species among 18 families and 62 genera were determined to occur in the state of Indiana, including 17 species reported for the first time herein (Table 1). An additional seven species were removed from the state checklist due to misidentified specimens, taxonomic changes, or dubious identifications lacking voucher specimens (Table 2). The determined species are based on 80,298 total specimens representing 5223 species occurrence records from 711 unique collecting events before 1983 and 405 events after 2005 (Suppl. material 1). Because a detailed taxonomic history, including all synonymies, and regional distributions of all 219 species have already been treated in Houghton et al. (2022) and Rasmussen and Morse (2023), we do not reproduce those data herein.

Of the known species, 100 (46%) were considered abundant or common, whereas 75 (34%) were considered rare, and 44 (20%) have not been collected in the last 40 years and, thus, were considered data deficient (Table 1). Leptoce-
ridae (43 species), Hydroptilidae (42), and Hydropsychidae (38) were the most

species rich families. They were also the families with the greatest number of total species occurrence records, collectively encompassing nearly 75% of all such records (Fig. 3). Species found only either before 1983 or after 2005 occurred in similar proportions for most families. The exceptions were the Limnephilidae and Phryganeidae, which collectively included 11 species found only before 1983 and none found only after 2005 (Fig. 4). The genera *Fabria*, *Oligostomis* (both Phryganeidae), and *Hydatophylax* (Limnephilidae) were found only before 1983, whereas *Ithytrichia* and *Leucotrichia* (both Hydroptilidae) were found only after 2005.

Table 1. The 219 caddisfly species known to occur in Indiana based on all historical and contemporary collecting and sampling. All taxa are arranged alphabetically by order and family. Species reported from the state for the first time are in boldface font. Species records displayed based on those found before 1983 and after 2005. Rarity designation based on number of records after 2005: >20 = abundant, 6–20 = common, 1–5 = rare, 0 = data deficient to determine if the species still exists in the state. Most recent known collection year of data-deficient species are in the last column.

	Records before 1983	Records after 2005	Rarity	Most recent
BRACHYCENTRIDAE (5)				
<i>Brachycentrus lateralis</i> (Say, 1823)	1	0	Deficient	1903
<i>Brachycentrus numerosus</i> (Say, 1823)	9	4	Rare	–
<i>Micrasema rusticum</i> (Hagen, 1868)	3	4	Rare	–
<i>Micrasema scotti</i> Ross, 1947	2	0	Deficient	1977
<i>Micrasema wataga</i> Ross, 1938	0	2	Rare	–
DIPSEUDOPSIDAE (2)				
<i>Phylocentropus lucidus</i> (Hagen, 1961)	1	0	Deficient	1980
<i>Phylocentropus placidus</i> (Banks, 1905)	3	6	Common	–
GLOSSOSOMATIDAE (11)				
<i>Agapetus gelbae</i> Ross, 1947	2	0	Deficient	1946
<i>Agapetus illini</i> Ross, 1938	1	2	Rare	–
<i>Agapetus spinosus</i> Etnier & Way, 1973	0	1	Rare	–
<i>Glossosoma intermedium</i> (Klapálek, 1892)	3	2	Rare	–
<i>Glossosoma nigrior</i> Banks, 1911	1	6	Common	–
<i>Protophila erotica</i> Ross, 1938	1	13	Common	–
<i>Protophila georgiana</i> Denning, 1948	0	1	Rare	–
<i>Protophila lega</i> Ross, 1941	0	1	Rare	–
<i>Protophila maculata</i> (Hagen, 1861)	7	36	Abundant	–
<i>Protophila palina</i> Ross, 1941	1	0	Deficient	1948
<i>Protophila tenebrosa</i> (Walker, 1852)	1	0	Deficient	1936
GOERIDAE (1)				
<i>Goera stylata</i> Ross, 1938	1	1	Rare	–
HELICOPSYCHIDAE (1)				
<i>Helicopsyche borealis</i> (Hagen, 1861)	30	59	Abundant	–
HYDROPSYCHIDAE (38)				
<i>Cheumatopsyche analis</i> (Banks, 1908)	44	111	Abundant	–
<i>Cheumatopsyche aphantia</i> Ross, 1938	3	4	Rare	–
<i>Cheumatopsyche burksi</i> Ross, 1941	2	17	Common	–
<i>Cheumatopsyche campyla</i> Ross, 1938	37	103	Abundant	–
<i>Cheumatopsyche lasia</i> Ross, 1938	1	1	Rare	–
<i>Cheumatopsyche minuscula</i> (Banks, 1907)	1	0	Deficient	1957
<i>Cheumatopsyche oxa</i> Ross, 1938	24	58	Abundant	–
<i>Cheumatopsyche pasella</i> Ross, 1941	9	49	Abundant	–
<i>Cheumatopsyche sordida</i> (Hagen, 1861)	4	15	Common	–
<i>Cheumatopsyche speciosa</i> (Banks, 1904)	7	2	Rare	–
<i>Diplectronea metaqui</i> Ross, 1970	2	3	Rare	–
<i>Diplectronea modesta</i> Banks, 1908	26	18	Common	–

	Records before 1983	Records after 2005	Rarity	Most recent
<i>Homoplectra doringa</i> (Milne, 1936)	3	3	Rare	–
<i>Hydropsyche aerata</i> Ross, 1938	6	6	Common	–
<i>Hydropsyche alternans</i> (Walker, 1852)	2	0	Deficient	1951
<i>Hydropsyche arinale</i> Ross, 1938	1	1	Rare	–
<i>Hydropsyche betteni</i> Ross, 1938	31	88	Abundant	–
<i>Hydropsyche bronta</i> Ross, 1938	17	71	Abundant	–
<i>Hydropsyche cheilonis</i> Ross, 1938	14	31	Abundant	–
<i>Hydropsyche cuanis</i> Ross, 1938	8	8	Common	–
<i>Hydropsyche depravata</i> Hagen, 1861	5	11	Common	–
<i>Hydropsyche dicantha</i> Ross, 1938	9	10	Common	–
<i>Hydropsyche frisoni</i> Ross, 1938	4	11	Common	–
<i>Hydropsyche hageni</i> Banks, 1905	1	0	Deficient	1950
<i>Hydropsyche incommoda</i> Hagen, 1861	44	68	Abundant	–
<i>Hydropsyche morosa</i> Hagen, 1861	43	7	Common	–
<i>Hydropsyche phalerata</i> Hagen, 1861	13	23	Abundant	–
<i>Hydropsyche placoda</i> Ross, 1941	0	1	Rare	–
<i>Hydropsyche scalaris</i> Hagen, 1861	5	5	Rare	–
<i>Hydropsyche simulans</i> Ross, 1938	27	66	Abundant	–
<i>Hydropsyche slossonae</i> Banks, 1905	8	8	Common	–
<i>Hydropsyche sparna</i> Ross, 1938	17	58	Abundant	–
<i>Hydropsyche valanis</i> Ross, 1938	8	1	Rare	–
<i>Macrostemum carolina</i> (Banks, 1909)	10	11	Common	–
<i>Macrostemum transversum</i> (Walker, 1852)	2	1	Rare	–
<i>Macrostemum zebratum</i> (Hagen, 1861)	14	11	Common	–
<i>Potamyia flava</i> (Hagen, 1861)	46	92	Abundant	–
HYDROPTILIDAE (42)				
<i>Agraylea multipunctata</i> Curtis, 1834	5	12	Common	–
<i>Dibusa angata</i> Ross, 1939	1	0	Deficient	1950
<i>Hydroptila ajax</i> Ross, 1938	2	19	Common	–
<i>Hydroptila albicornis</i> Hagen, 1861	1	2	Rare	–
<i>Hydroptila amoena</i> Ross, 1938	1	0	Deficient	1976
<i>Hydroptila angusta</i> Ross, 1938	8	66	Abundant	–
<i>Hydroptila armata</i> Ross, 1938	7	77	Abundant	–
<i>Hydroptila consimilis</i> Morton, 1905	6	56	Abundant	–
<i>Hydroptila delineata</i> Morton, 1905	2	0	Deficient	1937
<i>Hydroptila grandiosa</i> Ross, 1938	5	53	Abundant	–
<i>Hydroptila gunda</i> Milne, 1939	0	10	Common	–
<i>Hydroptila hamata</i> Morton, 1905	1	26	Abundant	–
<i>Hydroptila jackmanni</i> Blicke, 1963	1	0	Deficient	1976
<i>Hydroptila perdita</i> Morton, 1905	10	72	Abundant	–
<i>Hydroptila scolops</i> Ross, 1938	0	2	Rare	–
<i>Hydroptila spatulata</i> Morton, 1905	3	16	Common	–
<i>Hydroptila vala</i> Ross, 1938	1	0	Deficient	1976
<i>Hydroptila waubesiana</i> Betten, 1934	16	128	Abundant	–
<i>Ithytrichia clavata</i> Morton, 1905	0	4	Rare	–
<i>Leucotrichia pictipes</i> (Banks, 1911)	0	1	Rare	–
<i>Mayatrichia ayama</i> Mosely, 1937	1	1	Rare	–
<i>Neotrichia minutisimella</i> (Chambers, 1873)	1	1	Rare	–
<i>Neotrichia okopa</i> Ross, 1939	0	1	Rare	–
<i>Neotrichia vibrans</i> Ross, 1938	0	3	Rare	–
<i>Ochrotrichia eliaga</i> (Ross, 1941)	3	0	Deficient	1975
<i>Ochrotrichia riesi</i> Ross, 1944	1	0	Deficient	1945
<i>Ochrotrichia tarsalis</i> (Hagen, 1861)	6	26	Abundant	–
<i>Ochrotrichia wojcickyi</i> Blicke, 1963	1	0	Deficient	1980
<i>Ochrotrichia xena</i> (Ross, 1938)	3	0	Deficient	1976

	Records before 1983	Records after 2005	Rarity	Most recent
<i>Orthotrichia aegerfasciella</i> (Chambers, 1873)	5	63	Abundant	–
<i>Orthotrichia baldufi</i> Kingsolver & Ross, 1961	0	2	Rare	–
<i>Orthotrichia cristata</i> Morton, 1905	5	43	Abundant	–
<i>Oxyethira coercens</i> Morton, 1905	2	2	Rare	–
<i>Oxyethira dualis</i> Morton, 1905	0	1	Rare	–
<i>Oxyethira forcipata</i> Mosely, 1934	1	19	Common	–
<i>Oxyethira grisea</i> Betten, 1834	2	0	Deficient	1937
<i>Oxyethira novasota</i> Ross, 1944	0	1	Rare	–
<i>Oxyethira obtatus</i> Denning, 1947	0	4	Rare	–
<i>Oxyethira pallida</i> (Banks, 1904)	7	102	Abundant	–
<i>Oxyethira serrata</i> Ross, 1938	0	3	Rare	–
<i>Oxyethira zeronia</i> Ross, 1941	0	8	Common	–
<i>Stactobiella delira</i> (Ross, 1938)	1	1	Rare	–
LEPIDOSTOMATIDAE (3)				
<i>Lepidostoma liba</i> Ross, 1941	3	1	Rare	–
<i>Lepidostoma sommermanae</i> Ross, 1946	2	0	Deficient	1980
<i>Lepidostoma togatum</i> (Hagen, 1861)	0	11	Common	–
LEPTOCERIDAE (43)				
<i>Ceraclea alagma</i> (Ross, 1938)	4	12	Common	–
<i>Ceraclea ancylus</i> (Vorhies, 1909)	6	5	Rare	–
<i>Ceraclea annulicornis</i> (Stephens, 1836)	1	1	Rare	–
<i>Ceraclea cancellata</i> (Betten, 1934)	14	19	Common	–
<i>Ceraclea diluta</i> (Hagen, 1861)	6	0	Deficient	1975
<i>Ceraclea enodis</i> Whitlock & Morse, 1994	0	1	Rare	–
<i>Ceraclea flava</i> (Banks, 1904)	3	5	Rare	–
<i>Ceraclea maculata</i> (Banks, 1899)	24	96	Abundant	–
<i>Ceraclea mentiea</i> (Walker, 1852)	1	3	Rare	–
<i>Ceraclea nepha</i> (Ross, 1944)	0	2	Rare	–
<i>Ceraclea ophioderus</i> (Ross, 1938)	1	0	Deficient	1947
<i>Ceraclea punctata</i> (Banks, 1894)	0	4	Rare	–
<i>Ceraclea resurgens</i> (Walker, 1852)	4	0	Deficient	1975
<i>Ceraclea spongillovorax</i> (Resh, 1974)	2	0	Deficient	1974
<i>Ceraclea tarsipunctata</i> (Vorhies, 1909)	19	90	Abundant	–
<i>Ceraclea transversa</i> (Hagen, 1861)	19	42	Abundant	–
<i>Leptocerus americanus</i> (Banks, 1899)	20	82	Abundant	–
<i>Mystacides interjectus</i> (Banks, 1914)	4	1	Rare	–
<i>Mystacides sepulchralis</i> (Walker, 1852)	13	23	Abundant	–
<i>Nectopsyche albida</i> (Walker, 1852)	4	9	Common	–
<i>Nectopsyche candida</i> (Hagen) 1861	27	45	Abundant	–
<i>Nectopsyche diarina</i> (Ross, 1944)	14	27	Abundant	–
<i>Nectopsyche exquisita</i> (Walker, 1852)	8	14	Common	–
<i>Nectopsyche pavidata</i> (Hagen, 1861)	6	41	Abundant	–
<i>Oecetis avara</i> (Banks, 1895)	7	27	Abundant	–
<i>Oecetis cinerascens</i> (Hagen, 1861)	27	85	Abundant	–
<i>Oecetis ditissa</i> Ross, 1966	8	11	Common	–
<i>Oecetis inconspicua</i> (Walker, 1852)	46	159	Abundant	–
<i>Oecetis immobilis</i> (Hagen, 1861)	9	1	Rare	–
<i>Oecetis nocturna</i> Ross, 1966	14	24	Abundant	–
<i>Oecetis ochracea</i> Curtis, 1825	2	2	Rare	–
<i>Oecetis osteni</i> Milne, 1934	12	3	Rare	–
<i>Oecetis persimilis</i> (Banks, 1907)	7	47	Abundant	–
<i>Setodes oligius</i> (Ross, 1938)	3	2	Rare	–
<i>Triaenodes aba</i> Milne, 1935	1	15	Common	–
<i>Triaenodes flavescens</i> Banks, 1900	3	0	Deficient	1980
<i>Triaenodes ignitus</i> (Walker, 1852)	3	26	Abundant	–

	Records before 1983	Records after 2005	Rarity	Most recent
<i>Triaenodes injustus</i> (Hagen, 1861)	12	50	Abundant	–
<i>Triaenodes marginatus</i> Sibley, 1926	3	34	Abundant	–
<i>Triaenodes melacus</i> Ross, 1947	1	16	Common	–
<i>Triaenodes nox</i> Ross, 1941	3	2	Rare	–
<i>Triaenodes perna</i> Ross, 1938	0	4	Rare	–
<i>Triaenodes tardus</i> Milne, 1934	17	57	Abundant	–
LIMNEPHILIDAE (20)				
<i>Anabolia bimaculata</i> (Walker, 1852)	4	2	Rare	–
<i>Anabolia consocia</i> (Walker, 1852)	7	3	Rare	–
<i>Frenesia missa</i> (Milne, 1935)	5	1	Rare	–
<i>Hydatophylax argus</i> (Harris, 1869)	5	0	Deficient	1980
<i>Ironoquia kaskaskia</i> (Ross, 1944)	1	0	Deficient	unknown
<i>Ironoquia lyrata</i> (Ross, 1938)	1	0	Deficient	1978
<i>Ironoquia punctatissima</i> (Walker, 1852)	3	10	Common	–
<i>Limnephilus indivisus</i> Walker, 1852	8	4	Rare	–
<i>Limnephilus ornatus</i> Banks, 1897	2	0	Deficient	1946
<i>Limnephilus rhombicus</i> (Linnaeus, 1758)	1	0	Deficient	1960
<i>Limnephilus submonilifer</i> Walker, 1852	16	4	Rare	–
<i>Platycentropus radiatus</i> (Say, 1824)	9	11	Common	–
<i>Pseudostenophylax uniformis</i> (Betten, 1934)	3	2	Rare	–
<i>Pycnopsyche guttifera</i> (Walker, 1852)	6	14	Common	–
<i>Pycnopsyche indiana</i> (Ross, 1938)	7	30	Abundant	–
<i>Pycnopsyche lepida</i> (Hagen, 1861)	6	5	Rare	–
<i>Pycnopsyche luculenta</i> (Betten, 1934)	4	0	Deficient	1981
<i>Pycnopsyche rossi</i> Betten, 1950	2	0	Deficient	1980
<i>Pycnopsyche scabripennis</i> (Rambur, 1842)	9	3	Rare	–
<i>Pycnopsyche subfasciata</i> (Say, 1828)	15	17	Common	–
MOLANNIDAE (4)				
<i>Molanna blenda</i> Sibley, 1926	2	0	Deficient	1981
<i>Molanna tryphena</i> Betten, 1934	0	7	Common	–
<i>Molanna ulmerina</i> Navas, 1934	3	0	Deficient	1960
<i>Molanna uniophila</i> Vorhies, 1909	10	6	Common	–
ODONTOCERIDAE (1)				
<i>Marilia flexuosa</i> Ulmer, 1905	2	2	Rare	–
PHILOPOTAMIDAE (7)				
<i>Chimarra aterrima</i> Hagen, 1861	10	12	Common	–
<i>Chimarra feria</i> Ross, 1941	3	9	Common	–
<i>Chimarra moselyi</i> Denning, 1948	1	0	Deficient	unknown
<i>Chimarra obscura</i> (Walker, 1852)	8	98	Abundant	–
<i>Dolophilodes distinctus</i> (Walker, 1852)	6	6	Common	–
<i>Wormaldia moesta</i> (Banks, 1914)	4	7	Common	–
<i>Wormaldia shawnee</i> (Ross, 1938)	1	2	Rare	–
PHRYGANEIDAE (11)				
<i>Agrypnia straminea</i> Hagen, 1873	2	0	Deficient	1948
<i>Agrypnia vestita</i> (Walker, 1852)	6	5	Rare	–
<i>Banksiola crotchii</i> Banks, 1943	1	6	Common	–
<i>Fabria inornata</i> (Banks, 1907)	1	0	Deficient	1966
<i>Oligostomis ocelligera</i> (Walker, 1852)	1	0	Deficient	1978
<i>Phryganea cinerea</i> Walker, 1852	1	4	Rare	–
<i>Phryganea sayi</i> Milne, 1931	3	4	Rare	–
<i>Ptilostomis angustipennis</i> (Hagen, 1873)	1	0	Deficient	1950
<i>Ptilostomis ocellifera</i> (Walker, 1852)	7	28	Abundant	–
<i>Ptilostomis postica</i> (Walker, 1852)	4	4	Rare	–
<i>Ptilostomis semifasciata</i> (Say, 1828)	2	9	Common	–

	Records before 1983	Records after 2005	Rarity	Most recent
POLYCENTROPODIDAE (20)				
<i>Cerrotina calcea</i> Ross, 1938	0	15	Common	–
<i>Cerrotina spicata</i> Ross, 1938	4	24	Abundant	–
<i>Cynellus fraternus</i> (Banks, 1913)	17	67	Abundant	–
<i>Holocentropus flavus</i> Banks, 1909	1	0	Deficient	1981
<i>Holocentropus glacialis</i> Ross, 1938	5	4	Rare	–
<i>Holocentropus interruptus</i> Banks, 1914	4	1	Rare	–
<i>Neureclipsis crepuscularis</i> (Walker, 1852)	18	50	Abundant	–
<i>Neureclipsis piersoni</i> Frazer & Harris, 1991	1	2	Rare	–
<i>Nyctiophylax affinis</i> (Banks, 1897)	9	12	Common	–
<i>Nyctiophylax moestus</i> Banks, 1911	5	57	Abundant	–
<i>Plectrocnemia cinerea</i> (Hagen, 1861)	20	48	Abundant	–
<i>Plectrocnemia clinei</i> (Milne, 1936)	0	1	Rare	–
<i>Plectrocnemia crassicornis</i> (Walker, 1852)	2	3	Rare	–
<i>Plectrocnemia nascotius</i> (Ross, 1941)	0	4	Rare	–
<i>Plectrocnemia remotus</i> Banks, 1911	4	2	Rare	–
<i>Polycentropus centralis</i> Banks, 1914	7	24	Abundant	–
<i>Polycentropus chelatus</i> Ross & Yamamoto, 1965	1	0	Deficient	1976
<i>Polycentropus confusus</i> Hagen, 1861	0	12	Common	–
<i>Polycentropus elarus</i> Ross, 1944	1	0	Deficient	1963
<i>Polycentropus pentus</i> Ross, 1941	0	1	Rare	–
PSYCHOMYIIDAE (2)				
<i>Lype diversa</i> (Banks, 1914)	3	42	Abundant	–
<i>Psychomyia flavida</i> Hagen, 1861	3	37	Abundant	–
RHYACOPHILIDAE (6)				
<i>Rhyacophila fenestra</i> Ross, 1938	6	15	Common	–
<i>Rhyacophila glaberrima</i> Ulmer, 1907	1	0	Deficient	1948
<i>Rhyacophila ledra</i> Ross, 1939	5	4	Rare	–
<i>Rhyacophila lobifera</i> Betten, 1934	7	20	Common	–
<i>Rhyacophila parantra</i> Ross, 1948	6	1	Rare	–
<i>Rhyacophila vibox</i> Milne, 1936	1	2	Rare	–
THREMMATIDAE (3)				
<i>Neophylax ayanus</i> Ross, 1938	2	4	Rare	–
<i>Neophylax concinnus</i> MacLachlan, 1871	13	22	Abundant	–
<i>Neophylax fuscus</i> Banks, 1903	3	0	Deficient	1958
Total records	1399	3824		–
Total genera	60	59		–
Total species	191	175		–

Table 2. The seven species listed as occurring in Indiana (Rasmussen and Morse 2023) that should be removed from the state checklist due to misidentified specimens, taxonomic changes, or dubious identification without voucher specimens.

Taxon	Reference	Reason
<i>Cheumatopsyche harwoodi</i> Denning, 1948	Waltz and McCafferty 1983	Misidentified. Specimens are actually <i>C. analis</i>
<i>Hydropsyche alvata</i> Denning, 1949	Waltz and McCafferty 1983	Junior synonym of <i>H. incommoda</i> (Korecki 2006)
<i>Hydropsyche bidens</i> Ross, 1938	Waltz and McCafferty 1983	Junior synonym of <i>H. incommoda</i> (Korecki 2006)
<i>Hydropsyche orris</i> Ross, 1938	Waltz and McCafferty 1983	Junior synonym of <i>H. incommoda</i> (Korecki 2006)
<i>Hydropsyche rossi</i> Flint et al., 1979	Waltz and McCafferty 1983	Junior synonym of <i>H. simulans</i> (Korecki 2006)
<i>Hydropsyche venularis</i> Banks, 1914	Bright (1985)	Larval record without voucher specimens
<i>Pycnopsyche antica</i> (Walker, 1852)	Wojtowicz (1982)	Junior synonym of <i>P. scabripennis</i> (Green 2023)

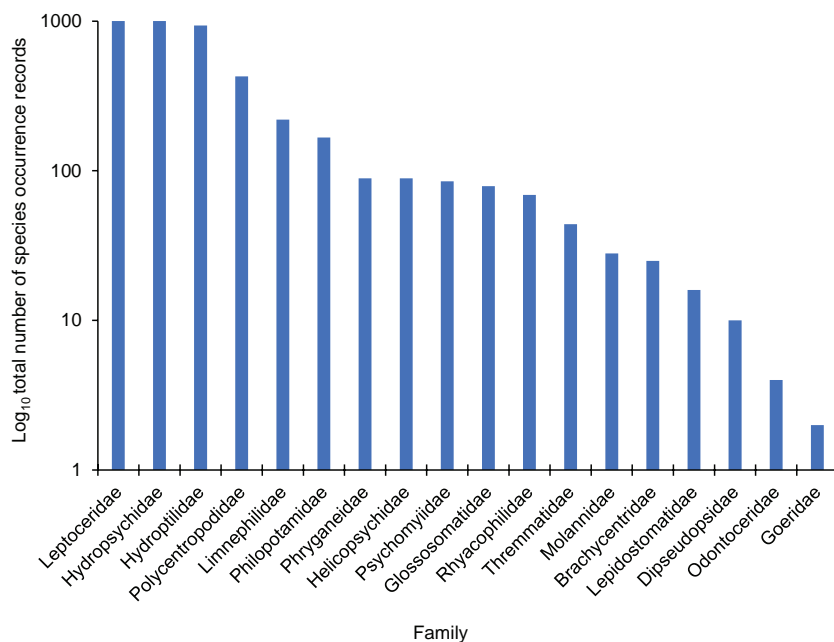


Figure 3. Log₁₀ number of species occurrence records for each of the 18 caddisfly families known from Indiana based on all historical and contemporary collecting and sampling.

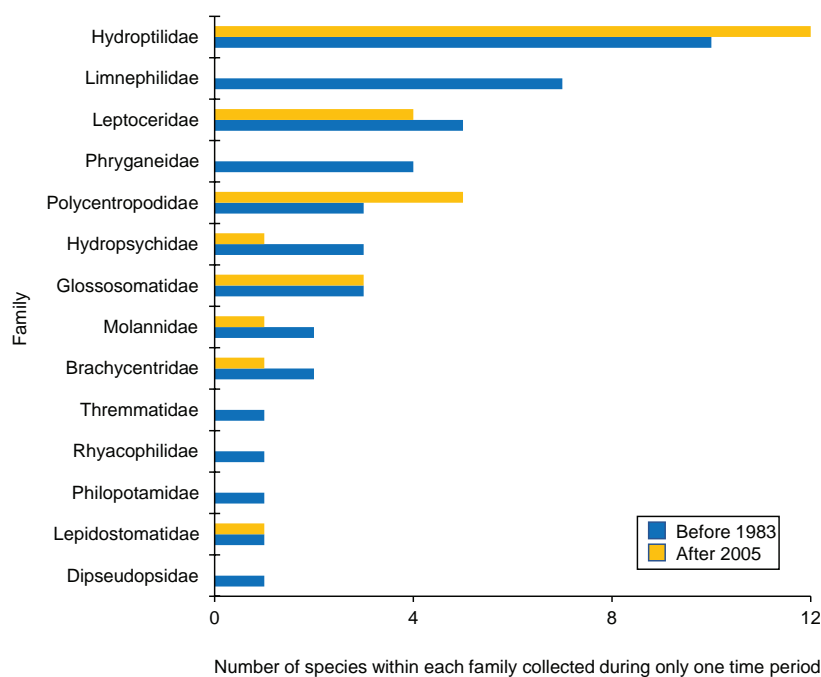


Figure 4. The 72 species collected either before 1983 or after 2005, but not during both periods, organized by family.

On average, species for 12 of the 18 families had an equal or greater number of occurrence records after 2005 than they did before 1983. The exceptions were the Lepidostomatidae (-11%), Phryganeidae (-12%), Thremmatidae (-13%), Molannidae (-31%), Dipseudopsidae (-33%), and Limnephilidae (-42%) (Fig. 5). Similarly, all FFGs had an equal or greater number of occurrence records after 2005 than they did before 1983, except for shredders which decreased by nearly 30% (Fig. 6).

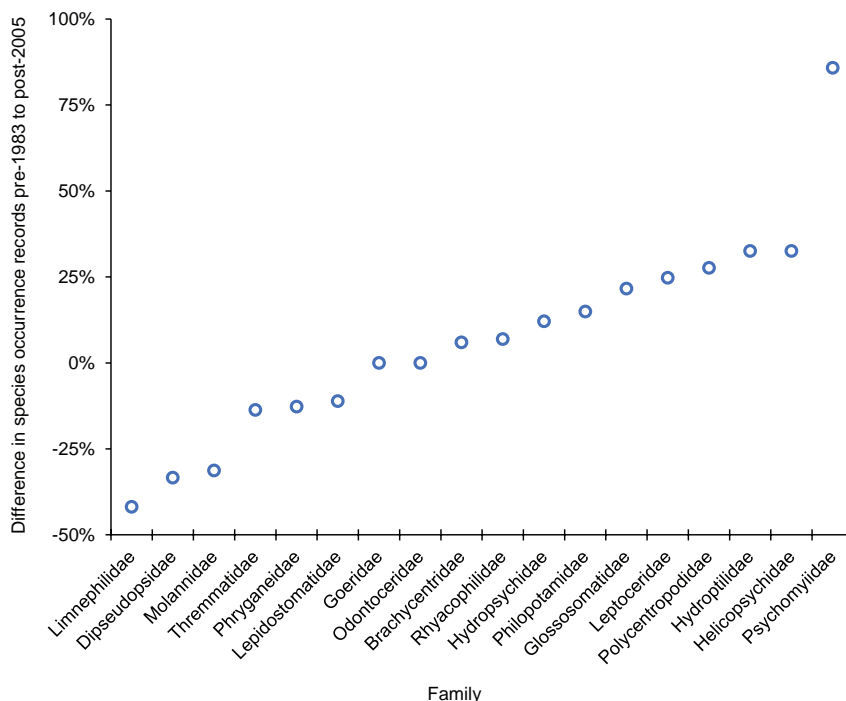


Figure 5. Mean difference between the two time periods of the study in the number of total species occurrence records among the 18 caddisfly families known from Indiana. Difference per species was calculated by subtracting the number of pre-1983 records from the number of post-2005 records and then dividing the result by the total number of records. These values were then averaged to determine the mean difference per family. A positive value signified a greater number of post-2005 records, whereas a negative value signified a greater number of pre-1983 records. Species occurrence data taken from Table 1.

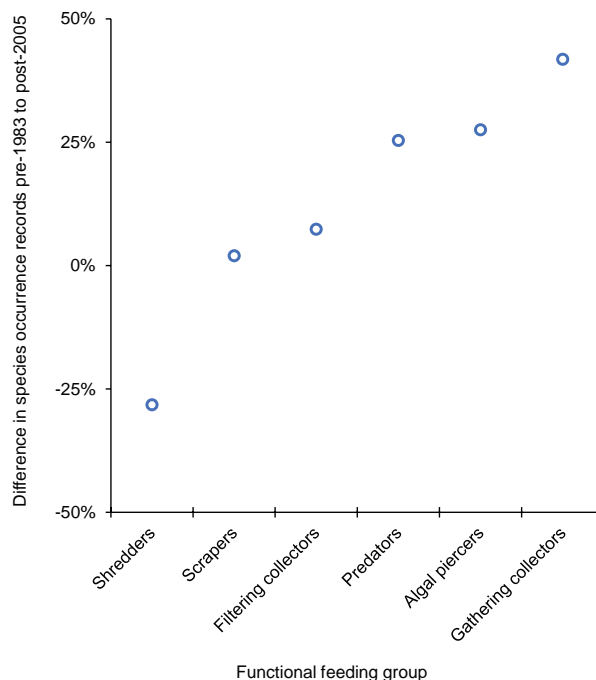


Figure 6. Mean difference between the two time periods of the study in the number of total species occurrence records among the five primary functional feeding groups (FFGs) known from Indiana. Difference per species was calculated by subtracting the number of pre-1983 records from the number of post-2005 records and then dividing the result by the total number of records. These values were then averaged to determine the mean difference per FFG. A positive value signified a greater number of post-2005 records, whereas a negative value signified a greater number of pre-1983 records. Species occurrence data taken from Table 1. FFG data taken from Merritt et al. (2019).

Individual associations between species and the various geographic and habitat designations are in Suppl. material 2 and summarized in Suppl. material 1. Overall species richness differences between the different designations were unremarkable, with the number of unique collecting events being a strong predictor of species richness for both pre-1983 and post-2005 time periods (Fig. 7). Fewer species were caught after 2005 (175) than before 1983 (191) despite having nearly 3× the species occurrence records in the post-2005 time period (Table 1). Total species richness for Indiana was predicted to be 225 and 228 species by ACE and ICE respectively (Fig. 8).

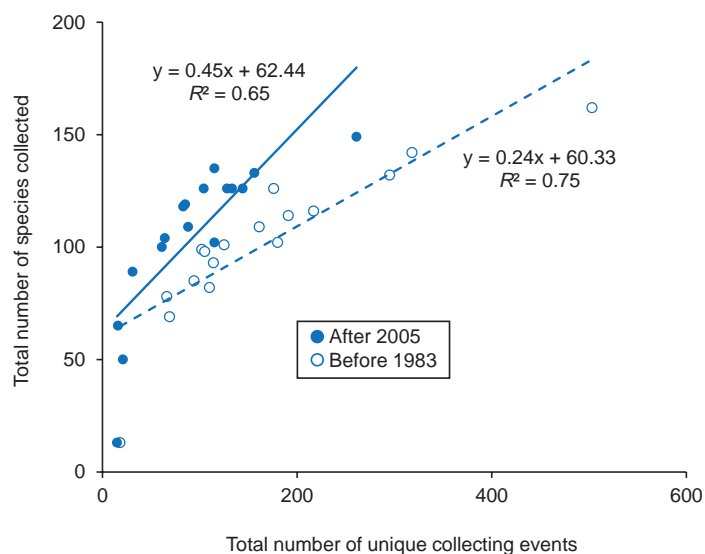


Figure 7. Simple linear regression models of caddisfly species richness (dependent variable) based on the total number of combined collections and samples taken (independent variable) for the two time periods of the study based on all geographic and ecological subunits of Indiana (Suppl. material 2).

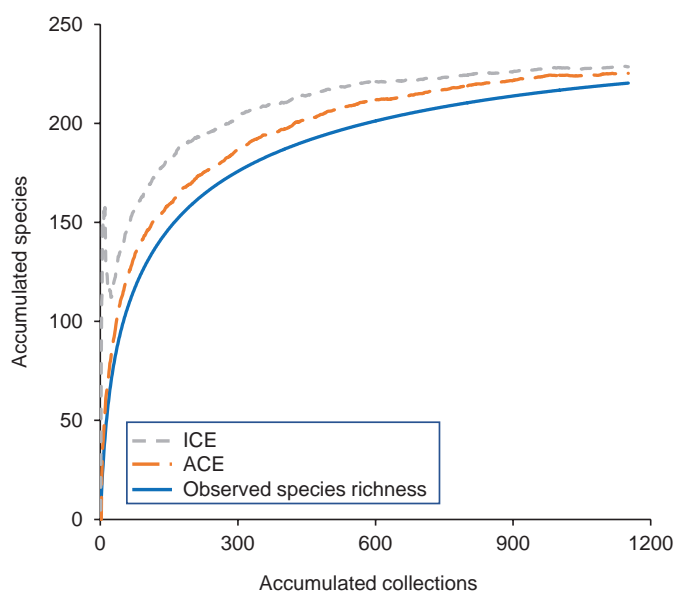


Figure 8. Species rarefaction curves for all historical and recent collections and samples, showing the accumulated number of species and two estimators: the abundance-based coverage estimator (ACE) and the incidence-based coverage estimator (ICE) of actual species richness. For each series, 50 randomized combinations of sample order were calculated and a mean value determined and displayed.

Discussion

Overall species richness within the state was not particularly remarkable or regionally distinctive, which probably reflected a general lack of habitat diversity within Indiana relative to nearby states like Michigan or Wisconsin (Omernik and Griffith 2014). Indiana has no known endemic caddisflies (Rasmussen and Morse 2023). Total species richness of Indiana lagged behind that of the adjacent states of Michigan (319 species), Kentucky (296), Wisconsin (284), and Ohio (276), but was slightly ahead of Illinois (218) (Houghton et al. 2022). Perhaps the most noteworthy difference was the higher richness in the northern half of the state despite having higher agricultural disturbance than the southern half. The Lake Michigan watershed was particularly rich despite having one of the smallest areas. This difference may be due to the high sampling effort of the region. It may also be that the northern portion of Indiana has naturally high species richness due to naturally high groundwater input or its position as an ecotone between prairie and forest (Omernik and Griffith 2014; DeWalt et al. 2016b). In the absence of disturbance, Houghton and DeWalt (2023) predicted the Wisconsin glaciated area in the northern region of the state to have ~1.5× the caddisfly richness per stream than the Illinoian or unglaciated areas. The age of the habitats might also be important, as the more heterogeneous substrates left behind by the recent Wisconsin glaciation probably increased the microhabitat diversity of streams relative to the older eroded landscapes of the Illinoian and unglaciated regions (Benn and Evans 2010).

Differences in caddisfly species occurrence records between the pre-1983 and post-2005 sampling periods indicated the effects of continued habitat degradation in the state. The goal of the current study was to sample the caddisflies with a greater effort than had been done during the pre-1983 sampling period. It is difficult to state definitively that this goal has been accomplished due to the unclear effort of pre-1983 collections; however, the almost 3× greater number of species occurrence records overall and for most families and FFGs in the post-2005 sampling period suggested that it has. Most exceptions were species that were physically large, such as those of Limnephilidae, Molannidae, and Phryganeidae, and in the shredder FFG, such as those of Lepidostomatidae, Limnephilidae, and Phryganeidae. The other two decreasing families, Dipseudopsidae and Thremmatidae have only a few species and, thus, may be more prone to stochastic variation. Houghton and Holzenthal (2010) noted a similar decrease in species occurrence records for large shredders in the Limnephilidae and Phryganeidae in Minnesota. In a study of the Upper Midwest region of the USA, Houghton and DeWalt (2021) observed that >50% of richness loss in shredder species was explained by watershed disturbance, which was more than that of any other FFG. Since shredders are directly dependent on the input of their coarse allochthonous food source, it is expected that they would most directly correlate with intact habitat, especially that of the riparian zone (Houghton et al. 2011; Dohet et al. 2014; Entekin et al. 2020; Houghton 2021; Williams and Houghton 2024). Moreover, larger caddisfly species in the Limnephilidae and Phryganeidae tend to be uni- or semivoltine (Merritt et al. 2019) and their longer larval period would expose them to habitat disturbances for more time than a multivoltine species would experience. Such a phenomenon has been previously noted for stoneflies in Illinois (DeWalt et al. 2005).

Collection data for new state species records are in Suppl. material 3. The majority of these records are not surprising, as they have previously been found in at least one state adjacent to Indiana. The two notable exceptions were *Agapetus spinosus* Etnier & Way, 1973 and *Protophila georgiana* Denning, 1948 (both Glossosomatidae). Both of these species were previously thought to be endemic to the southeastern USA, with *A. spinosus* known only from Alabama, South Carolina, and Tennessee, and *P. georgiana* from Alabama, Georgia, Maryland, North Carolina, and Virginia (Rasmussen and Morse 2023). Interestingly, both species were collected from the same site: Marble Creek, downstream of the Big Oaks Wildlife Refuge (BONWR) in Jefferson County (38.8983, -85.4646). The BONWR is one of the least disturbed habitats in Indiana and also one of the least studied, with no known previous collections from it.

Due to the recent sampling effort, most known Indiana species are still presumed extant in the state. Nonetheless, 44 species have not been seen in >40 years and remain data deficient. Eighteen of these species have not been collected in the state since the 1950s and, thus, could have been extirpated by the agricultural development that began after World War II (Omernik 1987). Most notably, *Brachycentrus lateralis* (Say, 1823) has not been seen in Indiana for 121 years.

Future research should include additional sampling. While the species rarefaction curve only predicts a few more species to be found in Indiana, the strong relationship between sampling effort and species caught within the various geographic and habitat designations suggests that a “Wallacean Shortfall” – a lack of detailed data on species distributions (Lomolino 2004) – still remains within the state, and that additional sampling is needed. This shortfall may be pronounced in some autumn-emergent species of Lepidostomatidae and Limnephilidae, due to the difficulty of collecting during the autumn flight period. Since species records for both of these families have decreased since the pre-1983 time period, more autumn sampling is necessary to clarify the reason for this decrease. Conservation efforts in Indiana should probably focus on the 75 rare species, all of which have been collected during the last 2–6 years and are presumed to be extant. Specifically, more information on the life history and specific habitat needs of rare species is necessary to formulate more specific plans for their conservation. Lastly, known or suspected habitats of the 44 data-deficient species should be sampled to ascertain whether these species remain extant in Indiana.

Acknowledgements

We appreciate the efforts of all who have collected, sorted, and identified Indiana caddisflies, including Kiralyn Brakel, Maliq Brock, Abrial Cocelli, Henrey Deese, Erin Flaherty, Janae Israel, Ryan Lardner, Caitlin Lowry, Jeremy Luce, Katelyn Mitchell, Evan Newman, Christina Peterson, Megan Phelps, Parker Reed, Joseph Ritzer, David Ruitter, Kayari Sukanuma, Noah Youtz, and Molly Williams. Collecting from the Indiana Dunes National Lakeshore was granted under permit INDU-2013-SCI-007. Philip Hogan helped produce Fig. 1. The valuable comments of Bob Haack and Kiralyn Brakel improved an earlier version of the manuscript. Google Earth base maps were used following permission guidelines (<https://www.google.com/permissions/geoguidelines/attr-guide/>). This is paper #40 of the GH Gordon BioStation Research Series.

Additional information

Conflict of interest

The authors have declared that no competing interests exist.

Ethical statement

No ethical statement was reported.

Funding

Funding for this study came from Indiana Department of Natural Resources grants to DCH (64742) and RED (40777) and from the Hillsdale College biology department.

Author contributions

Conceptualization (DCH), obtaining funding (DCH and RED), sampling (DCH and RED), specimen identification (DCH and RED), data analysis (DCH), manuscript preparation (DCH), manuscript editing (DCH and RED). Both authors contributed to the article and approved the submitted version.

Author ORCIDs

David Houghton  <https://orcid.org/0000-0001-6946-4864>

R. Edward DeWalt  <https://orcid.org/0000-0001-9985-9250>

Data availability

All of the data that support the findings of this study are available in the main text or Supplementary Information.

References

- Armitage BJ, Harris SC, Schuster GA, Usis JD, MacLean DB, Foote BA, Bolton MJ, Garono RJ (2011) Atlas of Ohio aquatic insects, Volume 1: Trichoptera. Ohio Biological Survey, Hilliard, Ohio.
- Barbour MT, Gerritsen J, Snyder BD, Stribling JB (1999) Rapid Bioassessment Protocols for Use in Streams and Rivers: Periphyton, Benthic Macroinvertebrates, and Fish, 2nd ed. EPA841-B-99-002. Office of Water, US Environmental Protection Agency, Washington, DC.
- Benn DI, Evans DJ (2010) Glaciers and Glaciation, 2nd ed. Arnold, London.
- Bolton MJ, Macy SK, DeWalt RE, Jacobus LM (2019) New Ohio and Indiana records of aquatic insects (Ephemeroptera, Plecoptera, Trichoptera, Coleoptera: Elmidae, Diptera: Chironomidae). Ohio Biological Survey Notes 9: 1–15.
- Bright GB (1985) Notes on the caddisflies of the Kankakee River in Indiana. Indiana Academy of Science 95: 191–194.
- Cao Y, Hawkins CP (2011) The comparability of bioassessments: a review of conceptual and methodological issues. Journal of the North American Benthological Society 30: 680–70. <https://doi.org/10.1899/10-067.1>
- DeWalt RE, Favret C, Webb DW (2005) Just how imperiled are aquatic insects? A case study of stoneflies (Plecoptera) in Illinois. Annals of the Entomological Society of America 98: 941–950. [https://doi.org/10.1603/0013-8746\(2005\)098\[0941:JHIAAI\]2.0.CO;2](https://doi.org/10.1603/0013-8746(2005)098[0941:JHIAAI]2.0.CO;2)
- DeWalt RE, South EJ, Robertson DR, Marburger JE, Smith WW, Brinson V (2016a) Mayflies, stoneflies, and caddisflies of streams and marshes of Indiana Dunes National Lakeshore, USA. ZooKeys 556: 43–63. <https://doi.org/10.3897/zookeys.556.6725>

- DeWalt R, Grubbs S, Armitage B, Baumann R, Clark S, Bolton M (2016b) Atlas of Ohio aquatic insects: volume II, Plecoptera. *Biodiversity Data Journal* 4: e10723. <https://doi.org/10.3897/BDJ.4.e10723>
- Dohet A (2002) Are caddisflies an ideal group for the assessment of water quality in streams? In: Mey W (Ed.) *Proceedings of the 10th International Symposium on Trichoptera*, 30 July–05 August, Potsdam, Germany. *Nova Supplementa Entomologica*, Keltern, Germany, 507–520.
- Dohet A, Hlúbiková D, Wetzel CE, L’Hoste L, Iffly JF, Hoffmann L, Ector L (2014) Influence of thermal regime and land use on benthic invertebrate communities inhabiting head-water streams exposed to contrasted shading. *Science of the Total Environment* 505: 1112–1126. <https://doi.org/10.1016/j.scitotenv.2014.10.077>
- Entrekin SA, Rosi EJ, Tank JL, Hoellein TJ, Lamberti GA (2020) Quantitative food webs indicate modest increases in the transfer of allochthonous and autochthonous C to macroinvertebrates following a large wood addition to a temperate headwater stream. *Frontiers in Ecology and Evolution* 8:114. <https://doi.org/10.3389/fevo.2020.00114>
- Fabian ST, Sondhi Y, Allen PE, Theobald JC, Lin H-T (2024) Why flying insects gather at artificial light. *Nature Communications* 15: 689. <https://doi.org/10.1038/s41467-024-44785-3>
- Floyd MA, Moulton JK, Schuster GA, Parker CR, Robinson J (2012) An annotated checklist of the caddisflies (Insecta: Trichoptera) of Kentucky. *Journal of the Kentucky Academy of Science* 73: 4–40. <https://doi.org/10.3101/1098-7096-73.1.4>
- Gray HH, Letsinger SL (2011) A history of glacial boundaries in Indiana. *Indiana Geological Survey Special Report 71*. Indiana University, Bloomington.
- Green M (2023) Revision, description, and diagnosis of adult and larval *Pycnopsyche* spp. (Trichoptera: Limnephilidae) using morphological and molecular methods. PhD dissertation, Clemson University, 436 pp. https://tigerprints.clemson.edu/all_dissertations/3286/
- Hilsenhoff WH (1995) Aquatic insects of Wisconsin. Keys to Wisconsin genera and notes on biology, habitat, distribution and species. Publication No. 3, Natural History Museums Council, University of Wisconsin-Madison, 79 pp.
- Houghton DC (2004) Minnesota caddisfly biodiversity (Insecta: Trichoptera): delineation and characterization of regions. *Environmental Monitoring and Assessment* 95: 153–181. <https://doi.org/10.1023/B:EMAS.0000029890.07995.90>
- Houghton DC (2012) Biological diversity of Minnesota caddisflies. *ZooKeys Special Issues* 189: 1–389. <https://doi.org/10.3897/zookeys.189.2043>.
- Houghton DC (2021) A tale of two habitats: whole-watershed comparison of disturbed and undisturbed river systems in northern Michigan (USA), based on adult Ephemeroptera, Plecoptera, and Trichoptera assemblages and functional feeding group biomass. *Hydrobiologia* 848: 3429–3446. <https://doi.org/10.1007/s10750-021-04579-w>
- Houghton DC, DeWalt RE (2021) If a tree falls in the forest: terrestrial habitat loss predicts caddisfly (Insecta: Trichoptera) assemblages and functional feeding group biomass throughout rivers of the north-central United States. *Landscape Ecology* 36: 3061–3078. <https://doi.org/10.1007/s10980-021-01298-4>
- Houghton DC, DeWalt RE (2023) The caddis aren’t alright: modeling Trichoptera richness in the northcentral United States reveals substantial species loss. *Frontiers in Ecology and Evolution* 11: 1163922. <https://doi.org/10.3389/fevo.2023.1163922>
- Houghton DC, Holzenthal RW (2010) Historical and contemporary biological diversity of Minnesota caddisflies: a case study of landscape-level species loss and trophic com-

- position shift. *Journal of the North American Benthological Society* 29: 480–495. <https://doi.org/10.1899/09-029.1>
- Houghton DC, Berry EA, Gilchrist A, Thompson J, MA Nussbaum (2011) Biological changes along the continuum of an agricultural stream: influence of a small terrestrial preserve and the use of adult caddisflies in biomonitoring. *Journal of Freshwater Ecology* 26: 381–397. <https://doi.org/10.1080/02705060.2011.563513>
- Houghton DC, DeWalt RE, Pytel AJ, Brandin CM, Rogers SE, Ruiter DE, Bright E, Hudson PL, Armitage BJ (2018) Updated checklist of the Michigan (USA) caddisflies, with regional and habitat affinities. *ZooKeys* 730: 57–74. <https://doi.org/10.3897/zookeys.730.21776>
- Houghton DC, DeWalt RE, Hubbard T, Schmude KL, Dimick JJ, Holzenthal RW, Blahnik RJ, Snitgen JL (2022) Checklist of the caddisflies (Insecta: Trichoptera) of the Upper Midwest region of the United States. *ZooKeys* 1111: 287–300. <https://doi.org/10.3897/zookeys.1111.72345>
- Korecki J (2006) Revision of the males of the *Hydropsyche scalaris* group in North America (Trichoptera: Hydropsychidae). MS thesis, Clemson University, 211 pp. https://tigerprints.clemson.edu/all_theses/44/
- Lomolino MV (2004) Conservation biogeography. In: Lomolino MV, Heaney LR (Eds) *Frontiers of Biogeography: New Directions in the Geography of Nature*. Sinauer Associates, Sunderland, MA, 293–296.
- MAFWA (2023) Midwest Association of Fish and Wildlife Agencies. <https://www.mafwa.org/> [Accessed 25 October 2023]
- Merritt RW, Cummins KW, Berg MB (2019) *An introduction to the aquatic insects of North America*, 5th ed. Kendall/Hunt, Dubuque, IA.
- Morse JC, Frandsen PB, Graf W, Thomas JA (2019) Diversity and ecosystem services of Trichoptera. *Insects* 10: e125. <https://doi.org/10.3390/insects10050125>
- Moulton SR, Stewart KW (1996) Caddisflies (Trichoptera) of the interior highlands of North America. *Memoirs of the American Entomological Institute* 56: 1–313.
- Omernik JM (1987) Ecoregions of the conterminous United States. *Annals of the Association of American Geologists* 77: 118–125. <https://doi.org/10.1111/j.1467-8306.1987.tb00149.x>
- Omernik JM, Griffith GE (2014) Ecoregions of the conterminous United States: evolution of a hierarchical spatial framework. *Environmental Management* 54: 1249–1266. <https://doi.org/10.1007/s00267-014-0364-1>
- Rasmussen AK, Morse JC (2023) Distributional checklist of Nearctic Trichoptera (2022 Revision). Florida A&M University, Tallahassee, FL, 541 pp. <http://www.trichoptera.org/>
- Ross HH (1938) Descriptions of Nearctic caddis flies (Trichoptera) with special reference to the Illinois species. *Bulletin of the Illinois Natural History Survey* 21: 101–183. <https://doi.org/10.21900/j.inhs.v21.261>
- Ross HH (1944) The caddis flies, or Trichoptera, of Illinois. *Bulletin of the Illinois Natural History Survey* 23: 1–326. <https://doi.org/10.21900/j.inhs.v23.199>
- Waltz RD, McCafferty WP (1983) *The caddisflies of Indiana*. Agricultural Experimental Station Bulletin 978, Purdue University, Lafayette, IN.
- Williams MF, Houghton DC (2024) Influence of a protected riparian corridor on the benthic aquatic macroinvertebrate assemblages of a small northern Michigan (USA) agricultural stream. *Journal of Freshwater Ecology* 39: 1–17. <https://doi.org/10.1080/02705060.2024.2312807>
- Wojtowicz JA (1982) A review of the adult and larvae of the genus *Pycnopsyche* (Trichoptera: Limnephilidae) with revision of the *Pycnopsyche scabripennis* (Rambur)

and *Pycnopysche lepida* (Hagen) complexes. PhD Dissertation, University of Tennessee, Knoxville, 292 pp. https://trace.tennessee.edu/utk_graddiss/1492/
Wright DR, Pytel AJ, Houghton DC (2013) Nocturnal flight periodicity of the caddisflies (Insecta: Trichoptera) in a large Michigan river. *Journal of Freshwater Ecology* 28: 463–476. <https://doi.org/10.1080/02705060.2013.780187>

Supplementary material 1

Summary of our collection data by ecological regions and habitat types

Authors: David C. Houghton, R. Edward DeWalt

Data type: xlsx

Copyright notice: This dataset is made available under the Open Database License (<http://opendatacommons.org/licenses/odbl/1.0/>). The Open Database License (ODbL) is a license agreement intended to allow users to freely share, modify, and use this Dataset while maintaining this same freedom for others, provided that the original source and author(s) are credited.

Link: <https://doi.org/10.3897/zookeys.1216.129914.suppl1>

Supplementary material 2

Historical (before 1983), recent (after 2005), and combined species occurrence records for the 219 known Indiana caddisfly species

Authors: David C. Houghton, R. Edward DeWalt

Data type: xlsx

Copyright notice: This dataset is made available under the Open Database License (<http://opendatacommons.org/licenses/odbl/1.0/>). The Open Database License (ODbL) is a license agreement intended to allow users to freely share, modify, and use this Dataset while maintaining this same freedom for others, provided that the original source and author(s) are credited.

Link: <https://doi.org/10.3897/zookeys.1216.129914.suppl2>

Supplementary material 3

Specific collection data for the new Indiana state caddisfly species records reported herein

Authors: David C. Houghton, R. Edward DeWalt

Data type: xlsx

Copyright notice: This dataset is made available under the Open Database License (<http://opendatacommons.org/licenses/odbl/1.0/>). The Open Database License (ODbL) is a license agreement intended to allow users to freely share, modify, and use this Dataset while maintaining this same freedom for others, provided that the original source and author(s) are credited.

Link: <https://doi.org/10.3897/zookeys.1216.129914.suppl3>

Taxonomic review of the grasshopper genus *Pteropera* Karsch, 1891 (Orthoptera, Acrididea, Catantopinae) with description of three new species and a preliminary phylogeny of the Cameroonian species

Jeanne Agrippine Yetchom Fondjo^{1,2}, Armand Richard Nzoko Fiemapong³, Maurice Tindo¹, Tarekegn Fite Duressa^{2,4}, Slobodan Ivković², Martin Husemann²

1 Zoology Unit, Laboratory of Biology and Physiology of Animal Organisms, Graduate School in Fundamental and Applied Sciences, University of Douala, Douala, Cameroon

2 Staatliches Museum für Naturkunde Karlsruhe, Karlsruhe, Germany

3 University of Neuchâtel, Neuchâtel, Switzerland

4 School of Plant Sciences, College of Agriculture and Environmental Sciences, Haramaya University, Dire Dawa, Ethiopia

Corresponding author: Jeanne Agrippine Yetchom Fondjo (jayetchomfondjo@gmail.com)



Academic editor: Jun-Jie Gu

Received: 22 June 2024

Accepted: 31 August 2024

Published: 25 October 2024

ZooBank: <https://zoobank.org/1221A319-03DC-4157-A7F9-F5A18E20E1FF>

Citation: Yetchom Fondjo JA, Nzoko Fiemapong AR, Tindo M, Duressa TF, Ivković S, Husemann M (2024) Taxonomic review of the grasshopper genus *Pteropera* Karsch, 1891 (Orthoptera, Acrididea, Catantopinae) with description of three new species and a preliminary phylogeny of the Cameroonian species. ZooKeys 1216: 219–264. <https://doi.org/10.3897/zookeys.1216.130270>

Copyright:

© Jeanne Agrippine Yetchom Fondjo et al.
This is an open access article distributed under terms of the Creative Commons Attribution License (Attribution 4.0 International – CC BY 4.0).

Abstract

The Afrotropical grasshopper genus *Pteropera* Karsch, 1891, is reviewed. Some species present in Cameroon are described, *Pteropera augustini* Donskoff, 1981, is recorded for the first time in the country, and three new species are described from Cameroon, *Pteropera kennei* Yetchom & Husemann, **sp. nov.**, *Pteropera matzkei* Yetchom & Husemann, **sp. nov.** and *Pteropera missoupi* Yetchom & Husemann, **sp. nov.**, increasing the number of *Pteropera* species in Cameroon from eight to 12, and overall to 30 species in Central Africa. An updated key of *Pteropera* is provided. Photographs with data on the distributions of all known species are given. In addition, a phylogenetic tree was constructed using maximum likelihood and Bayesian inference on the basis of a concatenated dataset of COI, 16S, and 12S markers of available Cameroonian species. The maximum likelihood and Bayesian inference analyses of the concatenated datasets resulted in a well-resolved phylogeny of the group and species of *Pteropera* were recovered as monophyletic, largely with high support. In all cases, the discrimination of all studied species based on barcode information was congruent with the species limits determined by traditional taxonomy. Our findings show the potential of integrative taxonomy to resolve the relationships among grasshoppers below the family level. Further analyses, including more comprehensive taxon sampling and additional nuclear markers, are needed, and the occurrence of several taxa still needs to be confirmed in African rainforests.

Keywords: DNA barcodes, integrated taxonomy, short-horned grasshopper, tropical Africa

Introduction

Pteropera Karsch, 1891, is a micropterous Afrotropical grasshopper genus belonging to the subfamily Catantopinae. This flightless grasshopper genus is morphologically similar to its close relative *Serpusia* Karsch (Johnston 1956;

Rowell et al. 2018). Species of the genus are common in forests, at forest edges, and in agrosystems, and most of them have restricted distribution ranges.

Pteropera was originally described for a single species, *Pteropera verrucigena* Karsch, and remained monotypic until the description of *P. pictipes* by Bolívar in 1908. Moreover, *P. karschi* (Bolívar, 1905), previously included in the genus *Aresceutica* Karsch, 1896, was included in the genus *Pteropera* by Donskoff (1981). After 12 years, *P. uniformis* Bruner, 1920 was described. Shortly thereafter, Ramme (1929) revised the genus on the basis of external morphology, described two additional species (*P. carnapi* Ramme, 1929, *P. zenkeri* Ramme, 1929), and transferred *P. spleniata* (Karsch, 1896) and *P. femorata* (Giglio-Tos, 1907), originally placed in the genus *Serpusia*, into the genus *Pteropera*. Moreover, Ramme (1929) proposed two keys to *Pteropera* species (one based on males and one on females), which included eight species distinguished on the basis of external morphological features and coloration. Thereafter, Ramme (1929) indicated *P. pictipes* as synonyms of *P. femorata*. Fifty-two years later, Donskoff (1981) conducted a complete revision of the genus on the basis of external morphology, coloration, and features of the genitalia and described 21 new species; by then, the genus comprised 27 valid species described from Central African forests only. Since, no further taxonomic work dedicated to this genus has been done. Given the large areas where no inventory works have been conducted thus far, it is likely that *Pteropera* is more diverse than currently known. Furthermore, to date, no molecular data for this genus are available. Thus, the main objective of this work is to shed light on the taxonomic status of grasshopper species of the genus *Pteropera* through an integrative approach, including morphometric, morphological, and molecular analyses. Herein, a description of three species new to science, distribution maps, an updated key to species, an annotated list, and photographs of all species of *Pteropera*, and the first phylogenetic tree for Cameroonian species are provided.

Materials and methods

Specimen collection and morphological studies

Field surveys were conducted from June 2017 to April 2022 at various locations situated in the central (Ongot), eastern (Somalomo, Dja), and littoral (Sohock, Koukoué, Iboti) regions of Cameroon. The grasshopper samples were collected using sweep nets and hand catches.

Specimens were identified using the identification key of Donskoff (1981). A total of six species of *Pteropera*, including three species new to science in the study area, were identified. In addition, type specimens held in the Muséum Nationale d'Histoire Naturelle Paris, France (**MNHN**) and the Museum für Naturkunde Berlin, Germany (**MfN**) were examined. Fresh samples were stored in absolute ethanol for further DNA analysis. They are kept as vouchers in the entomological collection at the Staatliches Museum für Naturkunde Karlsruhe, Germany (**SMNK**).

To study male genitalia, the standard methods of Kevan et al. (1969) and Martinelli et al. (2017) for the extraction and preparation of internal genitalia were followed. The genitalia were extracted from the grasshopper body using finely hooked forceps. The extracted internal genitalia were placed in a 1.5 mL microcentrifuge tube containing a solution of 5 µL of proteinase K (20 mg/mL)

and 25 μL of buffer (pH 8.0, 10 mM Tris-Cl, 25 mM EDTA, 100 mM NaCl, 0.5% SDS) and were incubated overnight in an incubator at 55 °C. The next day, the genitalia were gently separated from the digestion solution and then kept at 95 °C for 10 min to inactivate the enzyme; the preparations were then washed with double distilled water (ddH_2O). The terminology of male genitalia and female spermatheca follows Donskoff (1981) and Rowell (2013).

Photographs of the habitus of types and allotypes held by the MNHN were captured with a Nikon D60 digital camera. Photographs of some samples were taken at the Zoologisches Museum Hamburg, Germany (**ZMH**) with a high-resolution DUN Inc. stacking system (DUN Inc. California, USA). Images of male and female genitalia were also taken at the ZMH with a Keyence VHX-7000 digital microscope (London, UK).

Measurements were obtained using a digital caliper (at a scale of 0.01 mm). All the measurements are given in millimeters (mm). For all traits, male and female samples were measured separately. For each sample, the following measurements were taken: **HeadL**: length of the head; **HeadW**: width of the head; **AntenL**: length of the antenna; **I.O.D.**: interocular distance; **FastigL**: length of the fastigium of vertex; **PronotL**: length of the pronotum in the midline; **PronotW**: pronotum width; **TegL**: length of the tegmina; **TL**: hind tibia length; **FL**: maximum length of the hind femur; **FW**: width of the hind femur, measured as the distance between the two parallel lines running through the dorsal and ventral extremities of the femur, drawn parallel to the long axis of the femur; and **BodyL**: body length, measured from the tip of the front to the hindmost tip of the abdomen. The measurements of the samples (Table 1) correspond to the average value of the different body parts of the grasshoppers plus the standard deviation (SD).

Distributional data were obtained from geographical coordinates recorded during field observations and from locality records taken from specimen labels in the ZMH and the MNHN collections. The distribution maps of all the species were generated via QGIS 3.28.3.

Depositories

ANSP	Academy of Natural Science of Philadelphia
EMT	Egyptian Museum of Turin
MfN	Museum für Naturkunde Berlin, Germany
MNHN	Muséum National d'Histoire Naturelle Paris, France
RMCA	Royal Museum for Central Africa Tervuren, Belgium
RBINS	Royal. Belgian Institute of Natural Sciences
SMNK	Staatliches Museum für Naturkunde Karlsruhe, Germany
ZMH	Zoologisches Museum Hamburg, Germany

DNA extraction, PCR amplification, and sequencing

To perform molecular analyses, genomic DNA was extracted from the femoral muscle tissue of 41 *Pteropera* specimens and 11 outgroups samples (Table 3) stored in 96% ethanol at the ZMH. DNA was isolated using a high-salt extraction protocol (Paxton et al. 1996). To amplify the nucleotide sequences of the grasshopper COI, 16S and 12S markers, the primer pairs LCO

(5'-GTCAACAAATCATAAAGATATTGG) and HCO (5'-AAACTTCAGGGTGACCAAAAAATCA) (Folmer et al. 1994), 16S-F (5'-CGCCTGTTTAACAAAAACAT) and 16S-R (5'-CCGGTCTGAACTCAGATCACGT) (Palumbi et al. 1991), 12S-F (5'-AAACTAGGATTAGATACCCTATTAT) and 12S-R (5'-AAGAGCGACGGGCGATGTGT) (Bruvo-Madrić et al. 2005) were used.

The master mix contained 10.78 µL of nuclease-free H₂O, 1.5 µL of DreamTaq Buffer 10× (Thermo Fischer Scientific, Waltham, Massachusetts), 0.75 µL of the respective forward and reverse primers, 0.12 µL of dNTPs (VWR International, Radnor, Pennsylvania), 0.2 µL of DreamTaq DNA Polymerase (Thermo Fischer Scientific, Waltham, Massachusetts), and 1 µL of the template.

The PCR profile for the COI gene consisted of an initial denaturation step of 3 min at 94 °C, followed by 35 cycles of 30 s at 94 °C, an annealing step of 45 s at 50 °C, an extension step of 1 min at 72 °C, with a final extension of 10 min at 72 °C.

The PCR profile for the 16S gene consisted of an initial denaturation step of 3 min at 95 °C, followed by 35 cycles of 30 s at 95 °C, an annealing step of 45 s at 61 °C, an extension step of 1 min at 72 °C, with a final extension of 10 min at 72 °C.

The PCR profile for the 12S gene consisted of an initial denaturation step of 3 min at 95 °C, followed by 35 cycles of 30 s at 95 °C, an annealing step of 30 s at 60 °C, an extension step of 1 min at 72 °C, with a final extension of 5 min at 72 °C.

The PCR amplicons were checked on 1% agarose gels stained with GelRed (Biotium, Remont, CA, USA). Successfully amplified samples were purified with an ExoSap Enzyme cocktail (VWR, Pennsylvania, USA). The purified PCR products were then sequenced in both directions by MacroGen Europe (Amsterdam, Netherlands).

The newly obtained sequences were deposited in GenBank under the accession numbers indicated in Table 3.

For our study, the outgroups were selected among representatives from a few genera of the subfamily Catantopinae, on the basis of their close relationship with the ingroup. These include *Catantops stramineus* (Walker, 1870), *Exopropacris modica* (Karsch, 1893) and *Parapropacris notatus* (Karsch, 1891). In addition, we successfully sequenced the 16S fragment from 43 samples including 35 *Pteropera* samples and 8 samples from outgroups. For the 12S fragment, we sequenced 38 samples, including 34 *Pteropera* samples and four samples from outgroups.

The DNA sequences were edited using the BioEdit Sequence Alignment Editor v. 7.7.1 (Hall 1999). The sequences were further assembled and aligned in Geneious Pro (Kearse et al. 2012) using the MUSCLE algorithm (Edgar 2004). The aligned sequences were further visualized in SeaView (<https://doua.prabi.fr/software/seaview>). We checked for pseudogenes (numts) by translating sequences into amino acids using the invertebrate mitochondrial code and checking for frameshifts. Furthermore, NCBI BLAST databases were used to check for species identity and hence any contamination.

With our molecular datasets, we conducted one multilocus analysis (COI_16S_12S) with maximum likelihood (ML) and Bayesian inference (BI) methods. Phylogenetic tree based on the maximum likelihood (ML) method was reconstructed using the IQ-Tree software v. 1.6.12 (Nguyen et al. 2015). A bootstrap analysis was performed with 1000 replicates. The Bayesian analyses were performed using MrBAYES v. 3.2.7a (Ronquist et al. 2012b). Analyses were run for 1 million generations, with sampling every 100 generations for a total of 10,000 trees. The first 25% of the samples were discarded as burn-in.

The average split frequencies were less than 0.01, indicating convergence of the analyses. The final trees were visualized with FigTree v. 1.4.2 (<https://github.com/rambaut/figtree/releases>; Rambaut 2010).

Results

Phylogenetic analysis

The COI fragment was sequenced from 35 *Pteropera* specimens and 11 outgroup sample (Table 3). After trimming, the final alignment of the COI marker comprised 658 bp for 46 sequences of 11 taxa (including outgroups). In total, 43 sequences of the 16S from ten species (including outgroups), each 510 bp, were analyzed. Three outgroup sequences were missing compared with those in the COI datasets. The analyses of 16S alone yielded an unresolved tree. We analyzed a total of 352 bp for 37 sequences of 12 taxa (including outgroups) in the 12S region. The 12S topologies within *Pteropera* based on both ML and BI also resulted in largely unresolved trees. We concatenated all the loci and constructed two phylogenetic trees (one with ML and one with BI), on the basis of the concatenated sequence alignments of the three individual gene datasets (COI = 658 bp, 16S = 510 bp, 12S = 352 bp). The concatenated sequence alignment had a length of 1520 bp. Fig. 1 shows the combined majority-rule consensus tree obtained through the maximum likelihood and Bayesian inference analyses of the concatenated dataset. We recovered all included species of *Pteropera* as monophyletic, with high bootstrap values and posterior probabilities (Fig. 1). The ML and BI analyses of the combined dataset revealed a similar topology. In both the ML and BI datasets, the nine *Pteropera* species included in this work were grouped into five clades: (1) clade 1, containing *P. karschi zenkeri*; (2) clade 2, containing *P. augustini* + *P. descampsi* + *P. uniformis* + *P. verrucigena*; (3) clade 3, containing *P. kennei* sp. nov.; (4) clade 4, containing *P. carnapi* + *P. matzkei* sp. nov.; and (5) clade 5, containing *P. missoupi* sp. nov. In addition, the basal taxon to the remaining *Pteropera* species was recovered by *P. karschi zenkeri* with high support (PP > 0.95). Although the subclade formed by *P. carnapi* was reconstructed with ML analyses with high support, this was not supported by BI analyses (92% in ML; PP = 0.89 in BI analyses). In general, the delimitation of taxonomic units on the basis of genetic analyses was in line with the species limits obtained with traditional taxonomy.

Taxonomic account

Family Acrididae MacLeay, 1821

Subfamily Catantopinae Brunner von Wattenwyl, 1893

Genus group Serpusiae Johnston, 1956

Genus *Pteropera* Karsch, 1891

Pteropera Karsch, 1891: 185 (type species: *Pteropera verrucigena* Karsch, 1891, by original monotypy); Kirby 1910: 473; Ramme 1929: 358–360; Johnston 1956: 291; Sjöstedt 1931: 28–29; Johnston 1968: 239; Dirsh 1965: 338–339; Donskoff 1981: 33–88; Otte 1995: 331–333; Yetchom Fondjo et al. 2019: 317.

Diagnosis. Of medium size (22.5 mm; 30.0 mm); integument moderately rugous dorsally and smooth ventrally; body and legs with inconspicuous hairs; antennal organ on the fifth segment before the apex; frons oblique (~ 45°); frontal ridge slightly curved, depressed near the median ocelli, with parallel carinae; fastigium of vertex short, triangular to hexagonal, more or less elongated, with

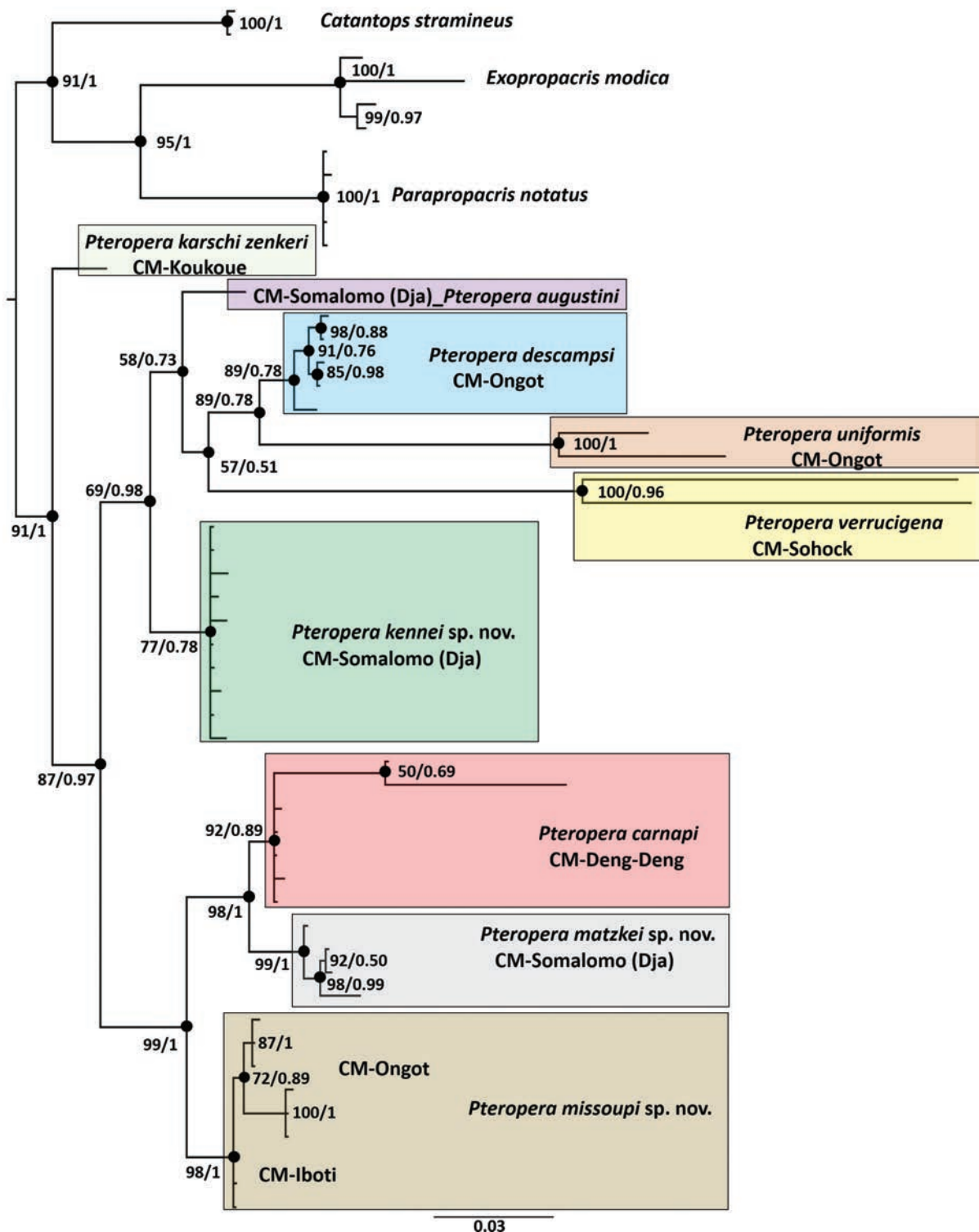


Figure 1. Phylogenetic tree built from the maximum likelihood (ML) and Bayesian inference (BI) analyses of the concatenated (COI/16S/12S) dataset. The numbers close to the nodes of the tree are the bootstrap support (%) and the Bayesian posterior probabilities (PP). The collection localities are also indicated preceded by CM (Cameroon).

the upper area very small, almost flat above; interocular distance narrower than or equal to the antennal scape; eyes large, globular, oval in profile, bean-shaped in dorsal view; ocelli large; pronotum cylindrical in cross-section at the typical groove, crossed by three transverse furrows; median carina faintly visible, lateral carina absent; metazona twice shorter than the prozona; anterior margin always notched, posterior margin excurved or notched; prosternal tubercle subconical, prominent, elevated, isolated; mesosternal lobes rounded. Tegmina lobiform, 3× longer than its width, covering the larger tympanum; wings less developed. Last article of the anterior and medial tarsi longer than the other two combined; Hind femur longer than wide; chevrons continuous and rounded in the outer median area; upper carinae serrate; upper basal lobe larger than the lower; hind tibia shorter than the femur, slightly S-curved, external apical spine absent, 8–10 spines on each upper margin; last tarsal segment as long as the other two combined; arolium larger and longer than the spurs. Supra-anal plate triangular, elongated; cerci slightly curved, conical, acute or truncated, sometimes with internal preapical lobules; male subgenital plate short, conical, or truncated; valves of ovipositor narrow, with curved apices, lower valves with small or no lateral projection; male genitalia: epiphallus bridge-shaped; bridge usually short, straight or arched, curved forward, reinforced in the vertical plane by a tubercle-like thickening and as prominent downwards as the lateral plates; ancorae short; lophi plate-shaped, aligned or forming an angle greater than 70°, posterior process not very prominent; oval sclerites small, rounded to subtriangular; cingulum horseshoe-shaped; rami of the cingulum not curved ventrally; ectophallus with two lower and two upper spiculated sheaths; intromission organ of aedeagus having four sclerotized blades and two upper spiculated sheaths; lower valves typically shorter than upper ones.

List of *Pteropera* species known from African rainforests

The complete list of the currently known *Pteropera* species and subspecies with the specimen ID, type category, collection location, date of collection and depository, are presented in Table 2. In addition, we present the images of the holotypes, allotypes, paratypes, and neallotypes of each species whenever possible (Figs 2–11). In the case of *P. femorata*, we downloaded existing photographs of the type specimen from the Orthoptera Species File website (Cigliano et al. 2024).

***Pteropera augustini* Donskoff, 1981**

Figs 2A, B, 7A, B

Pteropera augustini Donskoff, 1981: 51–52.

Type materials examined. *Holotype* • ♂; GABON. Near Youmi, in forest habitat; 0°24.617'N, 9°26.200'E; 11 Jun. 1974; M. Donskoff & J. Le Breton leg.; MNHN, MNHN-EO-CAELIF11462.

Other material examined. CAMEROON • 1 ♀, subadult; Somalomo, in the Dja Biosphere Reserve, cocoa farm; 3°23.650'N, 12°53.583'E, 606 m a.s.l.; 11 Apr. 2022; J.A. Yetchom Fondjo leg.; SMNK.

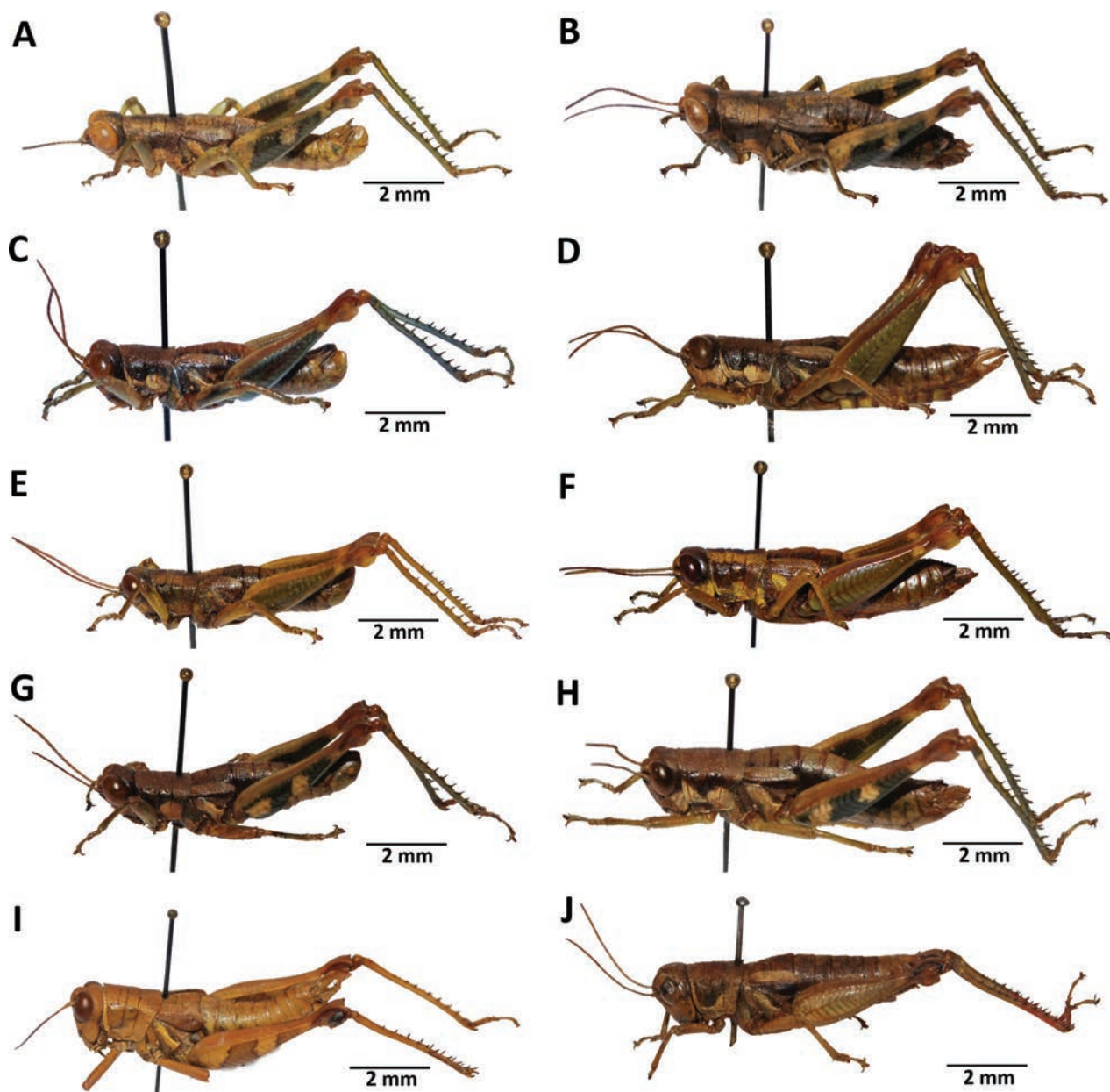


Figure 2. Images of holotypes, allotypes, and paratypes of *Pteropera* species in lateral view **A** *P. augustini* (holotype ♂) **B** *P. augustini* (allotype ♀) **C** *P. balachowskyi* (holotype ♂) **D** *P. balachowskyi* (allotype ♀) **E** *P. bertii* (holotype ♂) **F** *P. bertii* (paratype ♀) **G** *P. brosetti* (holotype ♂) **H** *P. brosetti* (allotype ♀) **I** *P. basilewskyi* (paratype ♀) **J** *P. bredoi* (holotype ♀).

Morphological characteristics. Two subocellar facial spots; posterior margin of the pronotum slightly indented; no marked difference between the upper half and lower half of the elytra; shiny black line along the lower margin; metathoracic episternites almost entirely pale; outer area of the hind femora green with pale spots, widely spread on the upper carina, median spot rounded, small, basal spot triangular; lower basal half of the inner area greenish-brown, pale spot rounded and small; only the lower inner area brownish; hind tibiae green.

Female subgenital plate pentagonal; egg-guide short; anterior apodemes narrow, short; medio-dorsal pocket narrow; basivalvar sclerites broad, slightly fused, almost perpendicular to each other; end of the copulatory bursa enlarged in the shape of a bubble; spermatheca ampulla arched, both diverticula

of different diameters; recurrent distal trunk of the lateral diverticulum 4–5× longer than the proximal trunk.

Remarks. This species is known by both males and females. The last female subadult stage was collected during this study and represents the first signalization of this species in Cameroon.

Distribution. Gabon; Cameroon (Fig. 16A).

***Pteropera carnapi* Ramme, 1929**

Figs 3A, B, 8A, B

Pteropera biloloca Sjöstedt 1931: 28; Dirsh 1965: 339.

Pteropera carnapi Ramme 1929: 364; Donskoff 1981: 59.

Type material examined. Holotype. CAMEROON • ♂; Yaoundé; 3°50.883'N, 11°30'7"E; Jun. 1887; V. Carnap leg.; MfN, BA000180S01-DORSA.

Other material examined. CAMEROON • 4 ♀♀; Ongot; 3°42.517'N, 11°15.167'E; 15 Jun. 2020; J.A. Yetchom Fondjo leg.; SMNK. CAMEROON • 2 ♂♂; Iboti, Ebo forest; 4°27.001'N, 10°27.002'E, 731 m a.s.l.; 7 Jan. 2022; J.A. Yetchom Fondjo leg.; SMNK. CAMEROON • 9 ♂♂, 4 ♀♀; Deng-Deng National Park; 3°21.364'N, 12°44.615'E, 731 m a.s.l.; 12 Jun. 2022; A.R. Nzoko Fiemapong leg.; SMNK.

Redescription. Frontal ridge raised above the median ocelli, prominent between the antennae; head and pronotum with well contrasted pale and dark colors; subocellar facial spot large; lower margin of elytra shiny black; meso- and metathoracic episternites yellow in their center; front legs, ventral area of hind femora yellow-green; dorsal area of the body and upper areas of hind femora more or less dark brown; hind tibiae bluish-green; male pallium and supra-anal plate raised; male cerci bilobate, with inner lobe equal to or longer than the outer lobe. **Epiphallus** (Fig. 15A): Ancorae small and closer to each other; bridge arched; anterior projections prominent, triangular. **Phallic complex** (Fig. 15B–D): dorsal arch of cingulum U-shaped, apodemes slender, clearly overhanging or exceeding level of separation of endophallic valves, with strongly incurved apex; upper ectophallic sheath very long in profile; lower ectophallic sheath not covering or enveloping the base of the rami; rami not bent; aedeagus valves in the form of a thin blade; latero-ventral sclerite triangular.

Distribution. Cameroon; Central African Republic; Gabon; Congo (Fig. 16B).

***Pteropera descampsi* Donskoff, 1981**

Figs 3G, H, 8G, H

Type materials examined. Holotype. CAMEROON • ♂; Yaoundé, Ongot [Onguot]; 3° 50.899'N, 11°30.133'E; 2–4 Nov. 1975; M. Descamps leg.; MNHN, MNHN-EO-CAELIF11456.

Other material examined. CAMEROON • 4 ♂♂, 3 ♀♀; Ongot; 3°51.517'N, 11°22.367'E; 15 Jun. 2020; J.A. Yetchom Fondjo & A.R. Nzoko Fiemapong leg.; SMNK. CAMEROON • 1 ♀; Meyomessala; 3°6.431'N, 12°14.703'E; 18 Aug. 2021; J.A. Yetchom Fondjo leg.; SMNK). CAMEROON • 5 ♀♀; Ongot; 3°51.517'N, 11°22.367'E; 5 Dec. 2021; J.A. Yetchom Fondjo leg.; SMNK. CAMEROON • 6 ♂♂,

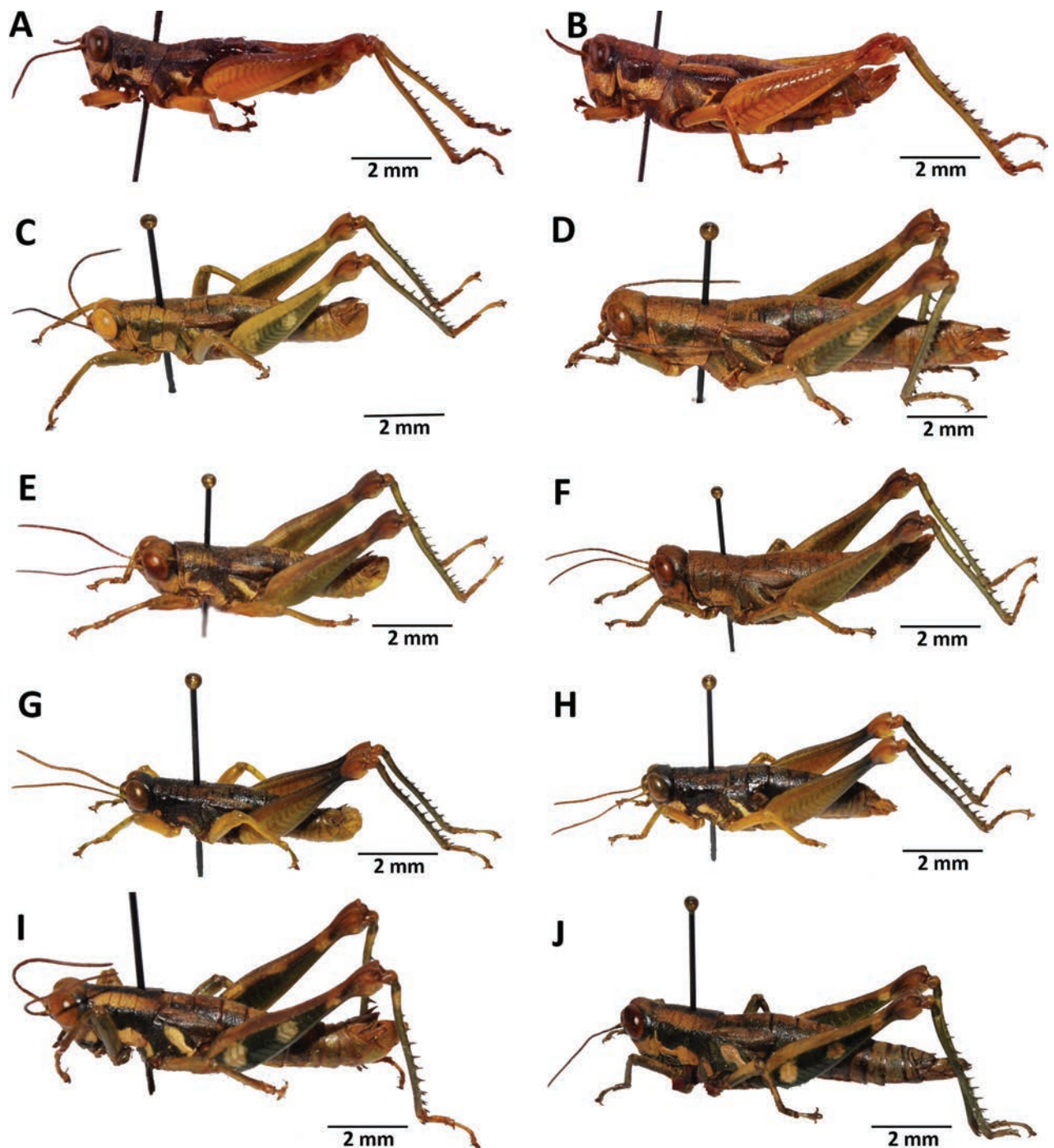


Figure 3. Images of holotypes and allotypes of *Pteropera* species in lateral view **A** *P. carnapi* (holotype ♂) **B** *P. carnapi* (paratype ♀) **C** *P. congoensis* (holotype ♂) **D** *P. congoensis* (allotype ♀) **E** *P. cornici* (holotype ♂) **F** *P. cornici* (allotype ♀) **G** *P. descampsi* (holotype ♂) **H** *P. descampsi* (allotype ♀) **I** *P. descarpentriesi* (holotype ♂) **J** *P. descarpentriesi* (allotype ♀).

2 ♀♀; Ongot; 3°51.517'N, 11°22.367'E; 20 Mar. 2022; J.A. Yetchom Fondjo & A.R. Nzoko Fiemapong leg.; SMNK.

Redescription. Subocellar facial spot V-shaped, wide; dark median longitudinal band on the pronotum disc not very distinct; the two contiguous pale bands present; lower part of body very pale on living specimen; pronotum disc shiny brownish; pale basal posterior spots on the lateral lobes of the pronotum extending almost to the lower margin; lower half of elytra shiny black, upper half brown; meso- and metathoracic episternites with pale, narrow, median and

basal band; front and middle legs pale green; outer and inner sides of hind femora pale, greenish yellow with apical third gradually darkening towards the pregenicular black ring; knees pale brown; hind tibiae green, sometimes very dark; male subgenital plate truncated; male cerci with a small inner preapical lobe.

Epiphallus (15E): of smaller size, ancorae small, anterior projections and lateral plates wide. **Phallic complex** (Fig. 15F–H): dorsal arch of cingulum V-shaped, open, apodemes reaching apex of endophallic sclerites; rami bent; upper ectophallic sheath short; lower ectophallic sheath not capping base of rami; latero-ventral sclerite subtriangular.

Distribution. Cameroon (Fig. 16B).

***Pteropera karschi zenkeri* Ramme, 1929**

Figs 4I, J, 9G, H

Type material examined. Holotype. CAMEROON • ♂; Bipindi, “Urwald”; 3°4.657'N, 10°24.607'E; Sep. 1898; G. Zenker leg.; MfN, BA000178S01-DORSA.

Other material examined. CAMEROON • 2 ♂♂, 1 ♀; Koukoué, on shrubs in palm plantations; 4°2.400'N, 10°7.002'E; 19 Sep. 2018; J.A. Yetchom Fondjo leg.; SMNK.

Redescription. Male: medium size; generally greenish; tegument weakly granular; head conical and oblique; fastigium of vertex short with obtuse apex; interocular space narrow; pronotum rugous, without lateral carinae, with straight median carina crossed by three furrows and with rounded posterior margin slightly indented in the middle, anterior margin incised in the middle; longitudinal median band of the pronotal disc darker and wider than the adjoining clear bands; prozona longer than the metazona; prosternal tubercle short conical and flattened at the base, forming an outline of a collar with the prothoracic presternite; mesosternal space open and longer than its wide; dorsal carina of hind femur finely toothed, distal end pointed; arolium large; outer area of hind femora with three pale spots; inner areas of hind femora with a median pale spot; inner and lower areas of hind femora, hind tibiae orange; middle area of male supra-anal plate with a transverse groove and tubercles on the sides; basal area with two digital tubercles; male subgenital plate conical, with a short tubercle at the apex; male cerci long conical, extending beyond the end of the supra-anal plate, with a wide internal pre-apical lobule. **Epiphallus** (Fig. 15I): bridge short and arched, convex; ancorae well developed, curved inwards and with an obtuse apex; anterior projections narrow, triangular; lophi broadly lobiform, slightly curved anteriorly; lateral plates broad, subparallel; oval sclerite large. **Phallic complex** (Fig. 15J–L): dorsal arch of cingulum U-shaped, closed, not rectangular; rami of cingulum not angular; apodemes thin and very short, reaching only the end of ejaculatory sac with incurved apices; endophallic apodemes short; aedeagus curved upward, straight, oblique in lateral view; lower ectophallic sheath not enveloping the base of rami.

Female: subgenital plate pentagonal; egg-guide short; anterior apodemes short, narrow, with projecting posterior margin; valves of ovipositor robust, curved towards the apex; external margins of the dorsal valves saw-toothed; spermatheca with medium-sized axial diverticulum; distal trunk, recurrent of the lateral diverticulum of the spermatheca 1.5× longer than the proximal trunk.

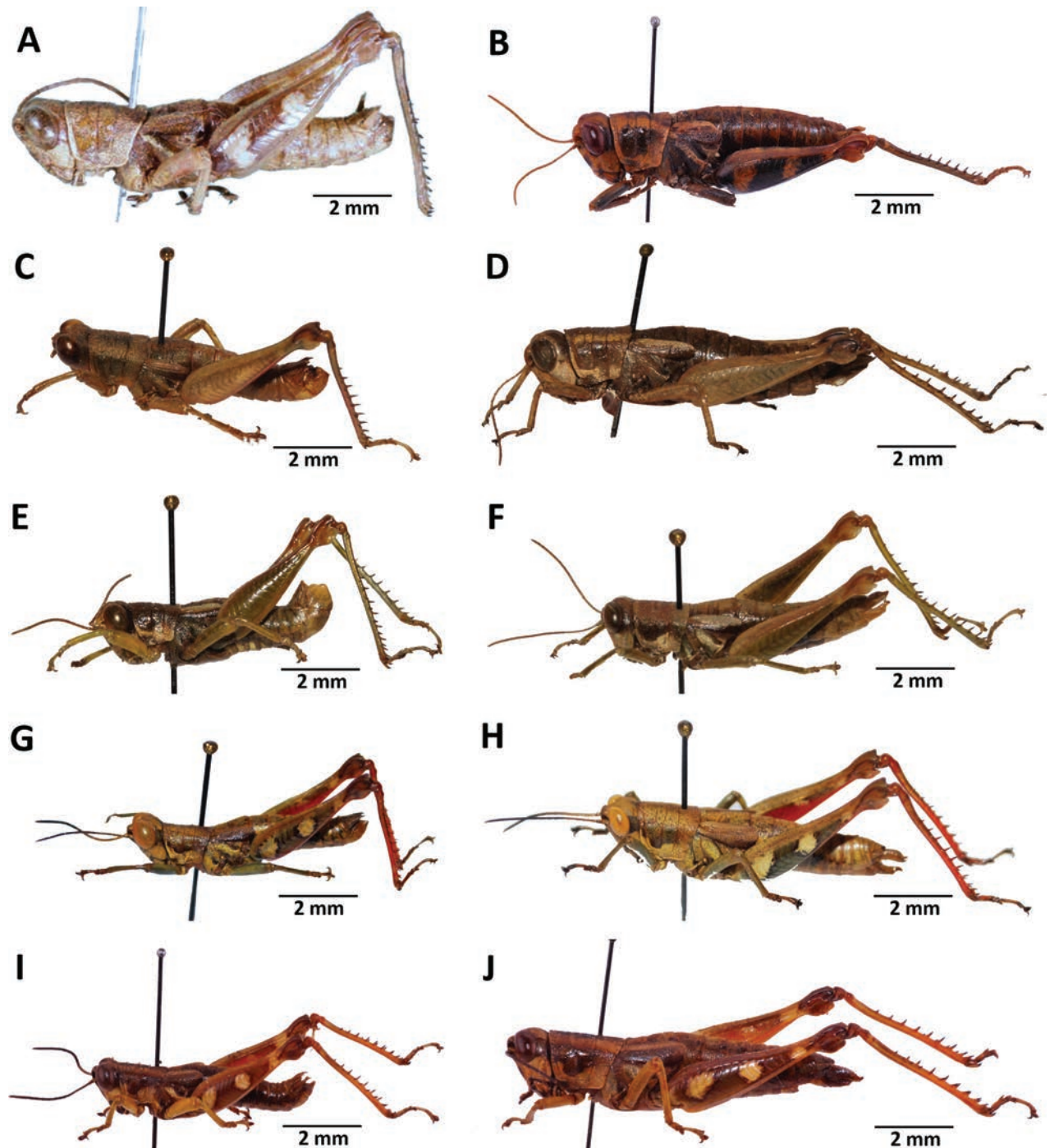


Figure 4. Images of holotypes, allotypes and paratypes of *Pteropera* species and subspecies in lateral view **A** *P. femorata* (holotype ♂; Cigliano et al. 2024) **B** *P. femorata* (♀) **C** *P. grilloti* (holotype ♂) **D** *P. meridionalis* (holotype ♀) **E** *P. jeanninae* (holotype ♂) **F** *P. jeanninae* (allotype ♀) **G** *P. karschi karschi* (♂) **H** *P. karschi karschi* (♀) **I** *P. karschi zenkeri* (holotype ♂) **J** *P. karschi zenkeri* (allotype ♀).

Remarks. Donskoff distinguished *Pteropera karschi karschi* from *Pteropera karschi zenkeri* on the basis of external morphology and described the genitalia structures of *P. karschi karschi* as representative of both subspecies. *Pteropera karschi zenkeri* resembles *P. karschi karschi* in several genitalia features but can easily be distinguished by a convex epiphallus bridge (concave in *P. karschi karschi*), with the apex of the aedeagus curved upward, oblique in lateral view

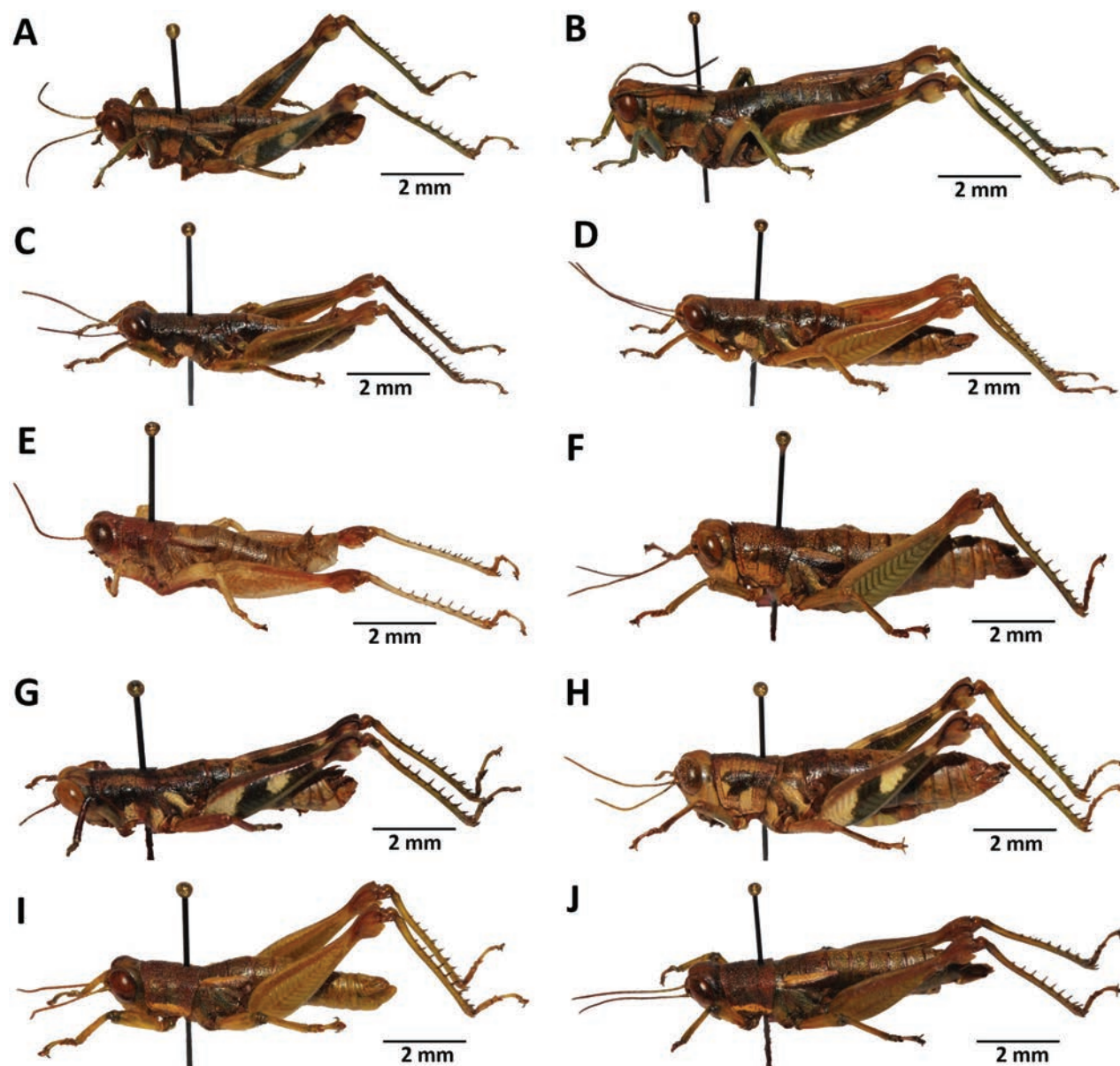


Figure 5. Images of Holotypes and Allotypes of *Pteropera* species in lateral view **A** *P. menieri* (Holotype ♂) **B** *P. menieri* (Allotype ♀) **C** *P. mirei* (Holotype ♂) **D** *P. mirei* (Allotype ♀) **E** *P. morini* (Holotype ♂) **F** *P. morini* (Allotype ♀) **G** *P. pillaulti* (Holotype ♂) **H** *P. pillaulti* (Allotype ♀) **I** *P. poirieri* (Holotype ♂) **J** *P. poirieri* (Allotype ♀).

(horizontal, in line with valves in *P. karschi karschi*), apodemes of the cingulum curved inwards in its apical part (straight in *P. karschi karschi*); and the distal trunk of the lateral diverticulum of the spermatheca being 1.5× longer than the proximal trunk (5–6× longer than the proximal trunk in *P. karschi karschi*). The juvenile of this species is unknown.

Distribution. Cameroon; Equatorial Guinea; Gabon (Fig. 17B).

***Pteropera uniformis* Bruner, 1920**

Figs 6K, 11I, 15M–P

Type material examined. Holotype. CAMEROON • ♂; Batanga; 2°50.795'N, 9°53.699'E; Apr. 1914; F.H. Hope leg.; ANSP.

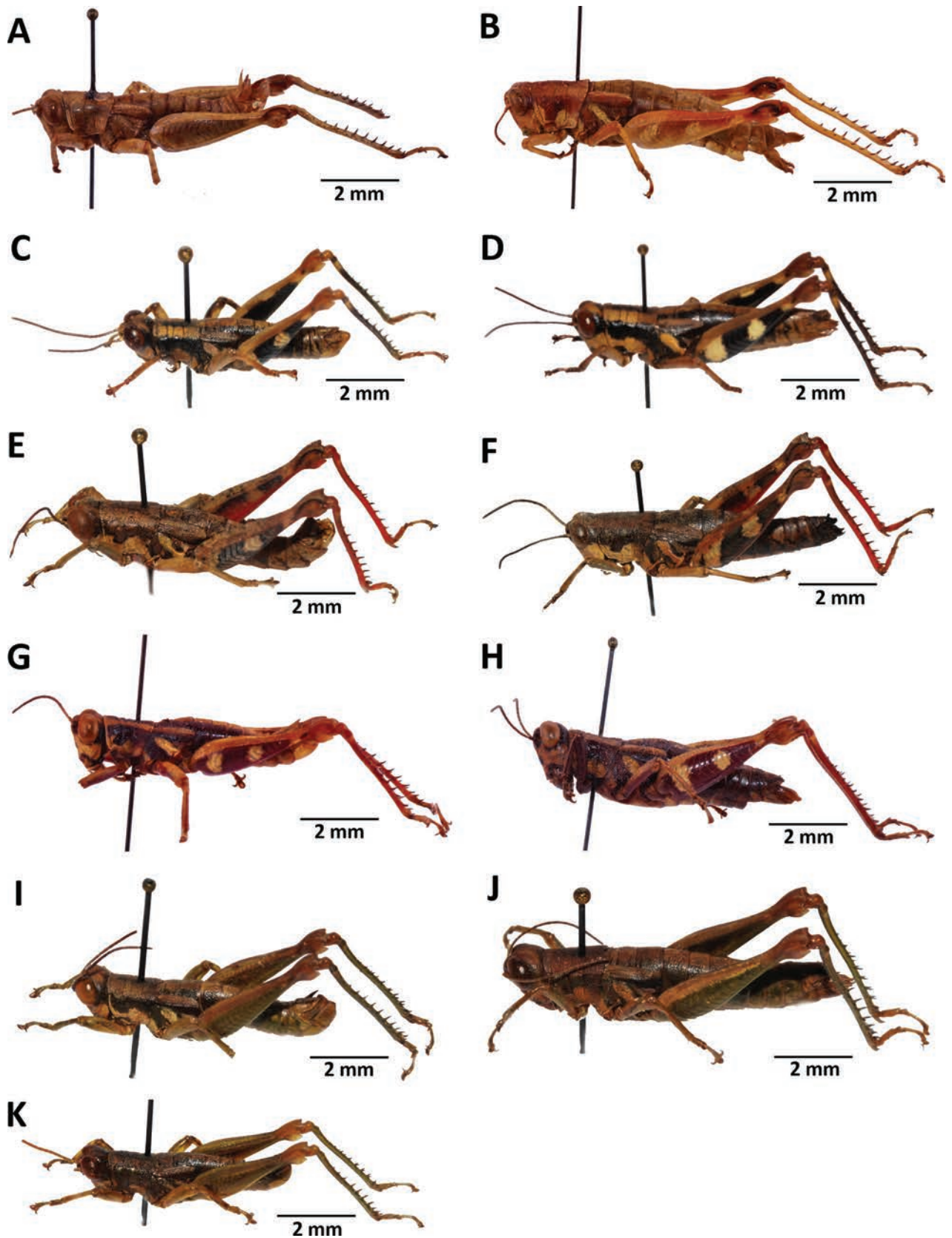


Figure 6. Images of holotypes, allotypes, lectotype and neallotype of *Pteropera* species in lateral view **A** *P. spleniata* (holotype ♂) **B** *P. spleniata* (holotype ♀) **C** *P. teocchii* (holotype ♂) **D** *P. teocchii* (allotype ♀) **E** *P. thibaudi* (holotype ♂) **F** *P. thibaudi* (allotype ♀) **G** *P. verrucigena* (lectotype ♂) **H** *P. verrucigena* (♀) **I** *P. villiersi* (holotype ♂) **J** *P. villiersi* (allotype ♀) **K** *P. uniformis* (neallotype ♂).

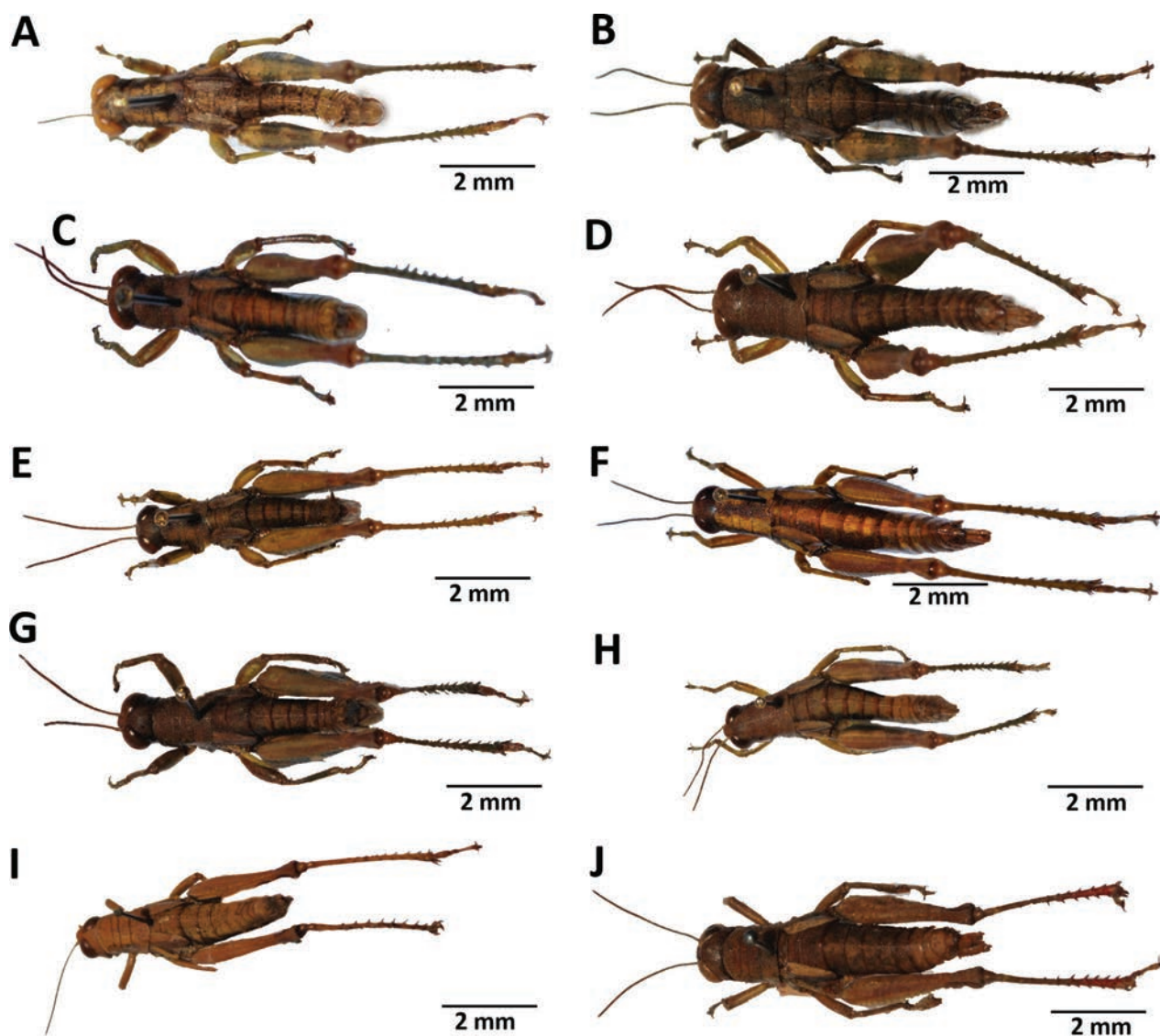


Figure 7. Images of holotypes, allotypes and paratype of *Pteropera* species in dorsal view **A** *P. augustini* (holotype ♂) **B** *P. augustini* (allotype ♀) **C** *P. balachowskyi* (holotype ♂) **D** *P. balachowskyi* (allotype ♀) **E** *P. bertii* (holotype ♂) **F** *P. bertii* (paratype ♀) **G** *P. brosetti* (holotype ♂) **H** *P. brosetti* (allotype ♀) **I** *P. basilewskyi* (paratype ♀) **J** *P. bredoi* (holotype ♀).

Other material examined. CAMEROON • 1 ♂; Ongot; 3°51.517'N, 11°22.367'E; 5 Dec. 2021; J.A. Yetchom Fondjo leg.; SMNK. CAMEROON • 1 ♂; Somalomo, in the Dja Biosphere reserve; 3°22.448'N, 12°43.990'E; 11 Apr. 2022; J.A. Yetchom Fondjo leg.; SMNK.

Redescription. Lower side of the body clear; median dark band on pronotum disc narrow, the two contiguous clear bands faintly marked; posterior basal spot on the lateral lobes of pronotum narrow, not reaching the lower edge; metathoracic episternite with a straight, median stripe limited to the base of the segment; lower half of elytra shiny black, upper half brown; front and middle legs pale green. Inner and outer areas of posterior female hind femora pale, greenish yellow, with small pregenicular black ring; knees pale brown; posterior tibiae green, sometimes very dark; male cerci with small internal preapical lobule. **Epiphallus** (Fig. 15M): bridge thin, narrow; anterior projections lobiform. **Phallic complex** (Fig. 15N–P): dorsal arch of cingulum rounded, almost firm, at the level of the ejaculatory sac, leaving endophallic sclerites almost entirely

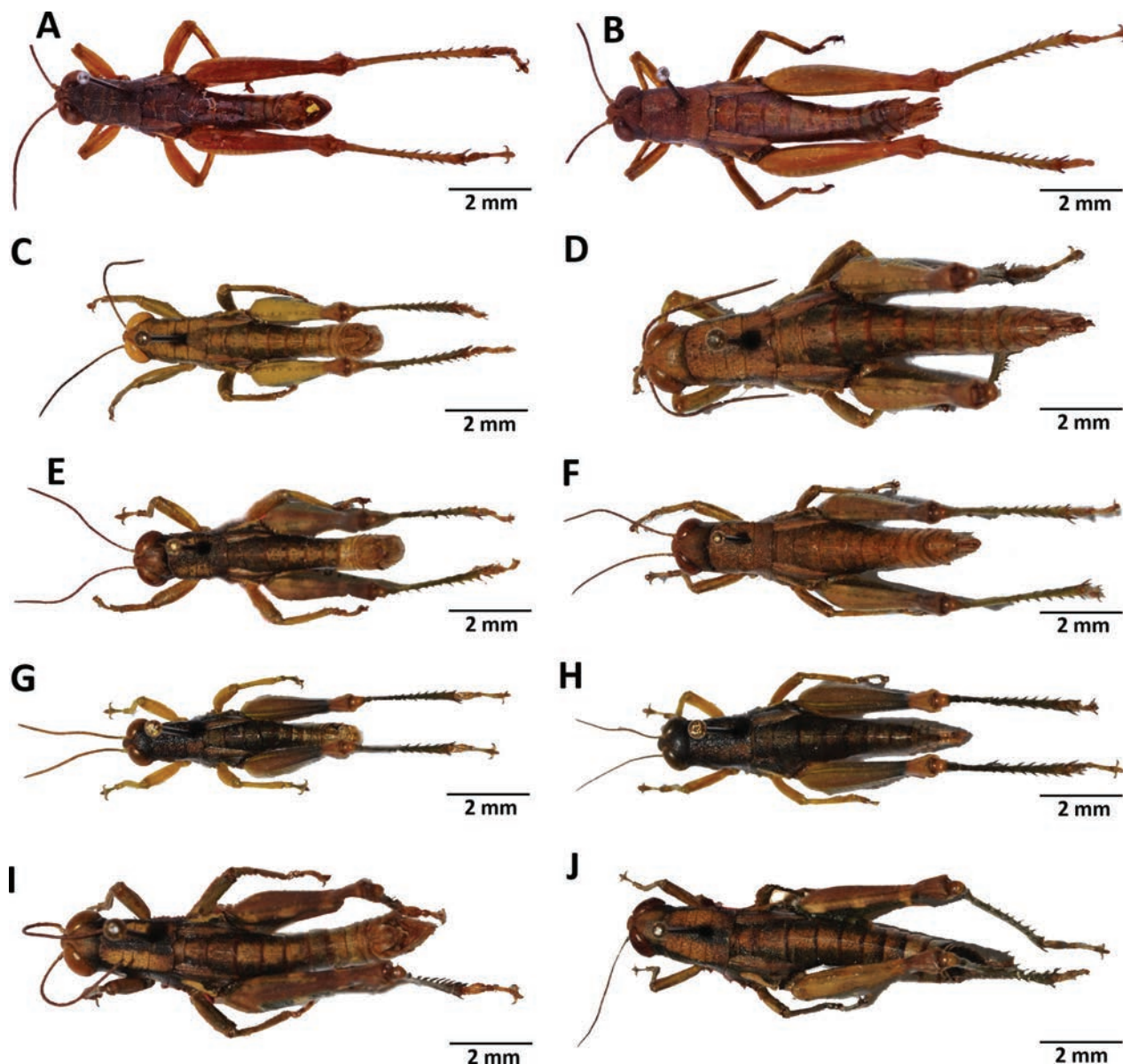


Figure 8. Images of holotypes, allotypes and paratype of *Pteropera* species in dorsal view **A** *P. carnapi* (holotype ♂) **B** *P. carnapi* (paratype ♀) **C** *P. congoensis* (holotype ♂) **D** *P. congoensis* (allotype ♀) **E** *P. cornici* (holotype ♂) **F** *P. cornici* (allotype ♀) **G** *P. descampsi* (holotype ♂) **H** *P. descampsi* (allotype ♀) **I** *P. descarpentriesi* (holotype ♂) **J** *P. descarpentriesi* (allotype ♀).

free, very divergent anteriorly; rami not bent; upper ectophallic sheath long; latero-ventral sclerite in profile, elbowed.

Remarks. The juveniles of this species is unknown.

Distribution. Cameroon (Fig. 18B).

***Pteropera verrucigena* Karsch, 1891**

Figs 6G, H, 11E, F

Type material examined. **Lectotype.** CAMEROON • ♂; Barombi Station; 4°40.016'N, 9°22.999'E; Dr. Paul Preuss leg.; MfN, BA000175S01-DORSA.

Other material examined. CAMEROON • 2 ♂♂, 1 ♀; Sohock; 4°57.250'N, 10°14.833'E; 3 Apr. 2017; J.A. Yetchom Fondjo leg.; SMNK.

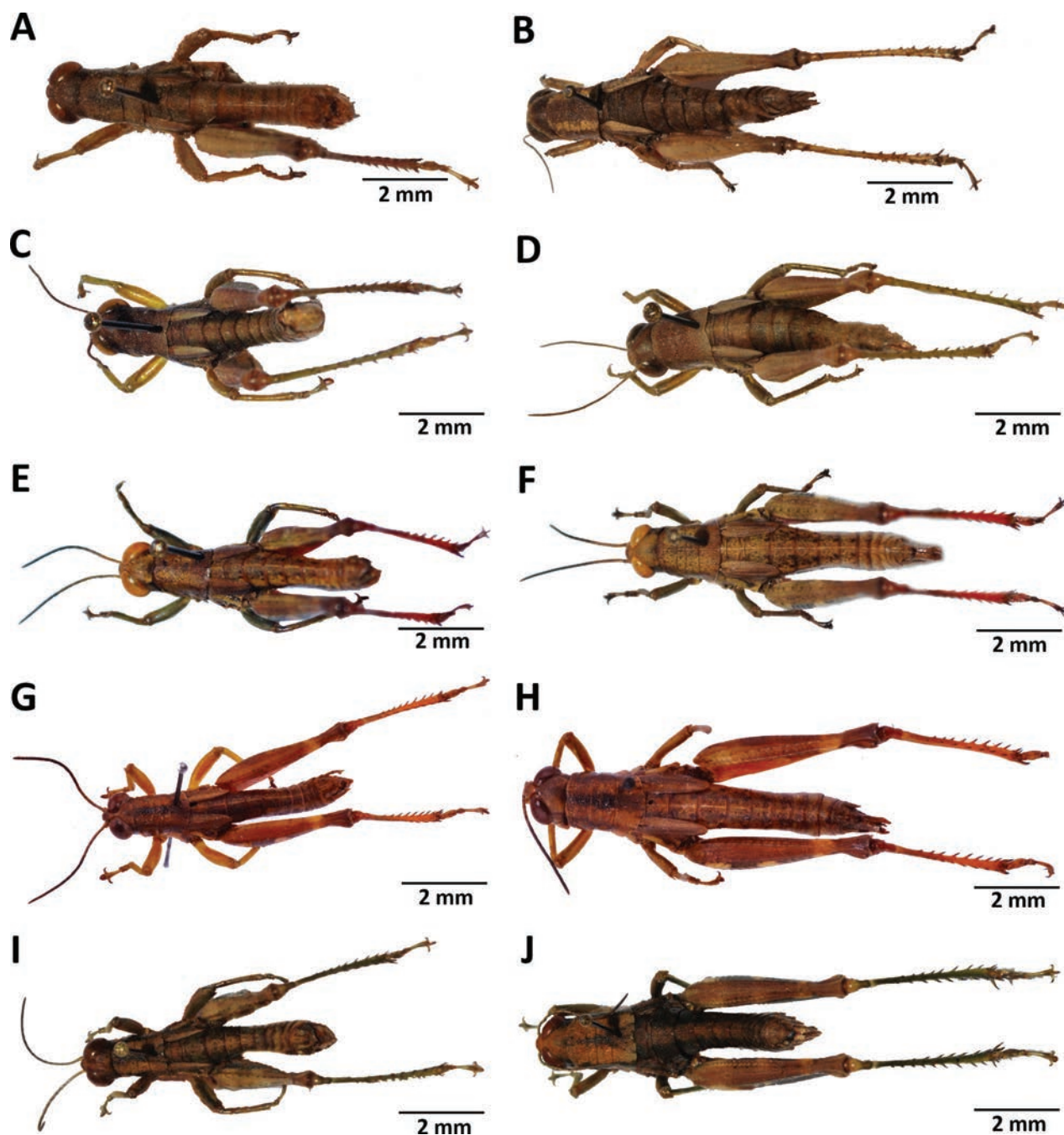


Figure 9. Images of holotypes, allotypes and paratype of *Pteropera* species in dorsal view **A** *P. grilloti* (holotype ♂) **B** *P. meridionalis* (holotype ♀) **C** *P. jeanninae* (holotype ♂) **D** *P. jeanninae* (allotype ♀) **E** *P. karschi karschi* (paratype ♂) **F** *P. karschi karschi* (paratype ♀) **G** *P. karschi zenkeri* (holotype ♂) **H** *P. karschi zenkeri* (allotype ♀) **I** *P. menieri* (holotype ♂) **J** *P. menieri* (allotype ♀).

Redescription. Male: medium size, integument rugous; head conical and oblique; fastigium of vertex short with obtuse apex; eyes prominent and globose; antenna, filiform longer than head and pronotum combined; pronotum without lateral carinae and with straight median carina, crossed by three sulci, its anterior and posterior margins rounded and incised in the middle; pale basal band of lateral lobes of pronotum narrowed in front of second transverse furrow but not interrupted; longitudinal median band of pronotum disc dark and less wider than adjacent clear bands; prozona longer than metazona; prosternal tubercle conical; anterior

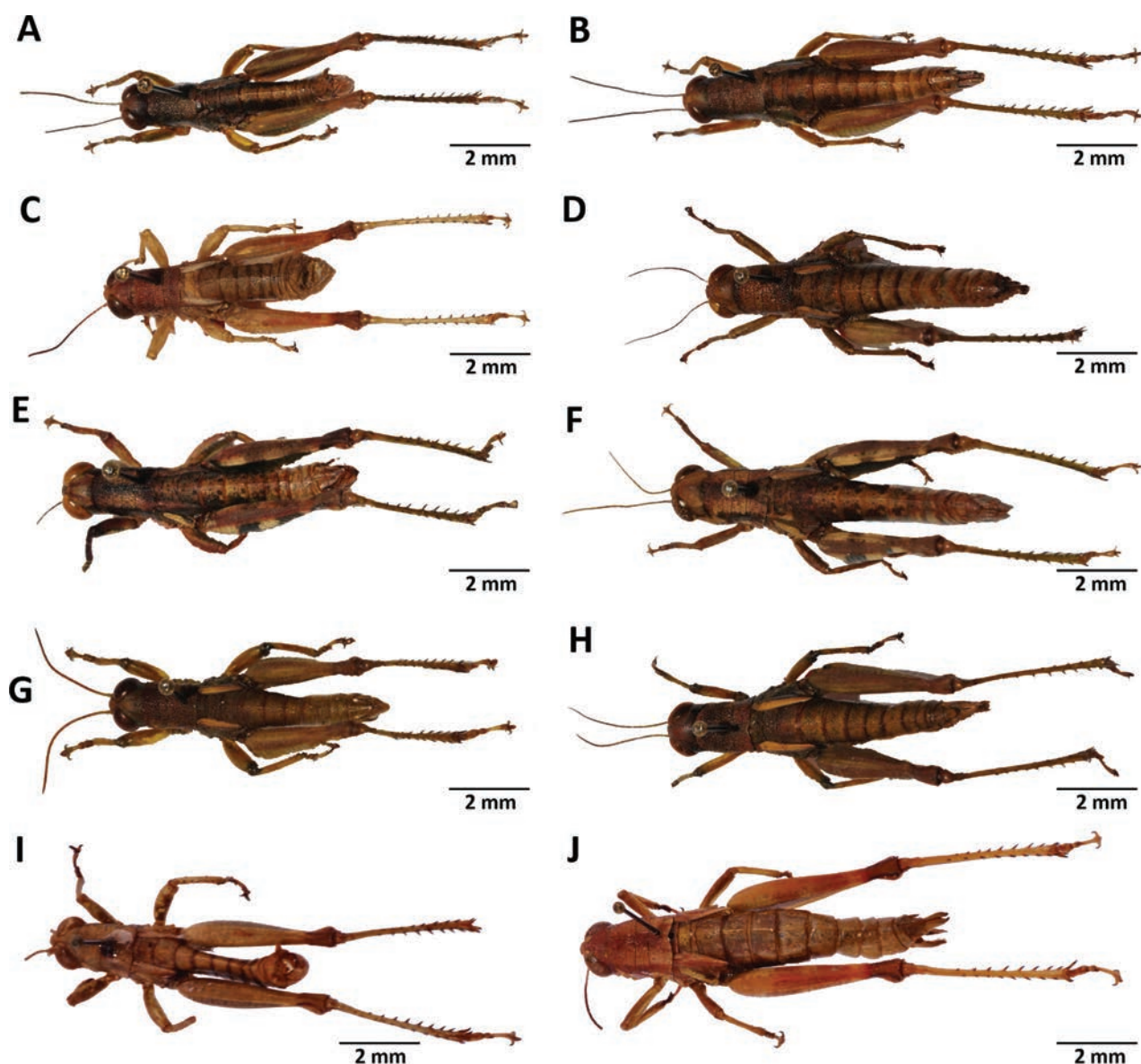


Figure 10. Images of holotypes, allotypes and paratype of *Pteropera* species in dorsal view **A** *P. mirei* (holotype ♂) **B** *P. mirei* (allotype ♀) **C** *P. morini* (holotype ♂) **D** *P. morini* (allotype ♀) **E** *P. pillaulti* (holotype ♂) **F** *P. pillaulti* (allotype ♀) **G** *P. poirieri* (holotype ♂) **H** *P. poirieri* (allotype ♀) **I** *P. spleniata* (holotype ♂) **J** *P. spleniata* (holotype ♀).

margin of mesosternum broadly projected medially; mesosternal space open and longer than it is wide; elytra vestigial or lobiform; median pale spot on inner area of hind femora absent; outer area of hind femora with three pale spots; incipient spots along medio-superior margin at level of outer spots present; dorsal carina of hind femora finely toothed; lower outer areas of hind femora dark, wine-colored; hind tibiae wine-colored; distal half of hind tibiae widened, basal ring present; supra-anal plate subconical, with two digital tubercles near lateral margins; subgenital plate short conical, gradually tapering towards rounded apex; cerci conical, curved inward and without preapical lobule. **Epiphallus** (Fig. 15Q): bridge narrow, short and arched; ancorae small, close together and with acute apex; lophi short, broad and lobiform; lateral plates broad and rounded; anterior and posterior projections short. **Phallic complex** (Fig. 15R–T): dorsal arch of the cingulum V-shaped, strongly open not overlying the endophallic sclerites; latero-ventral sclerite broad,

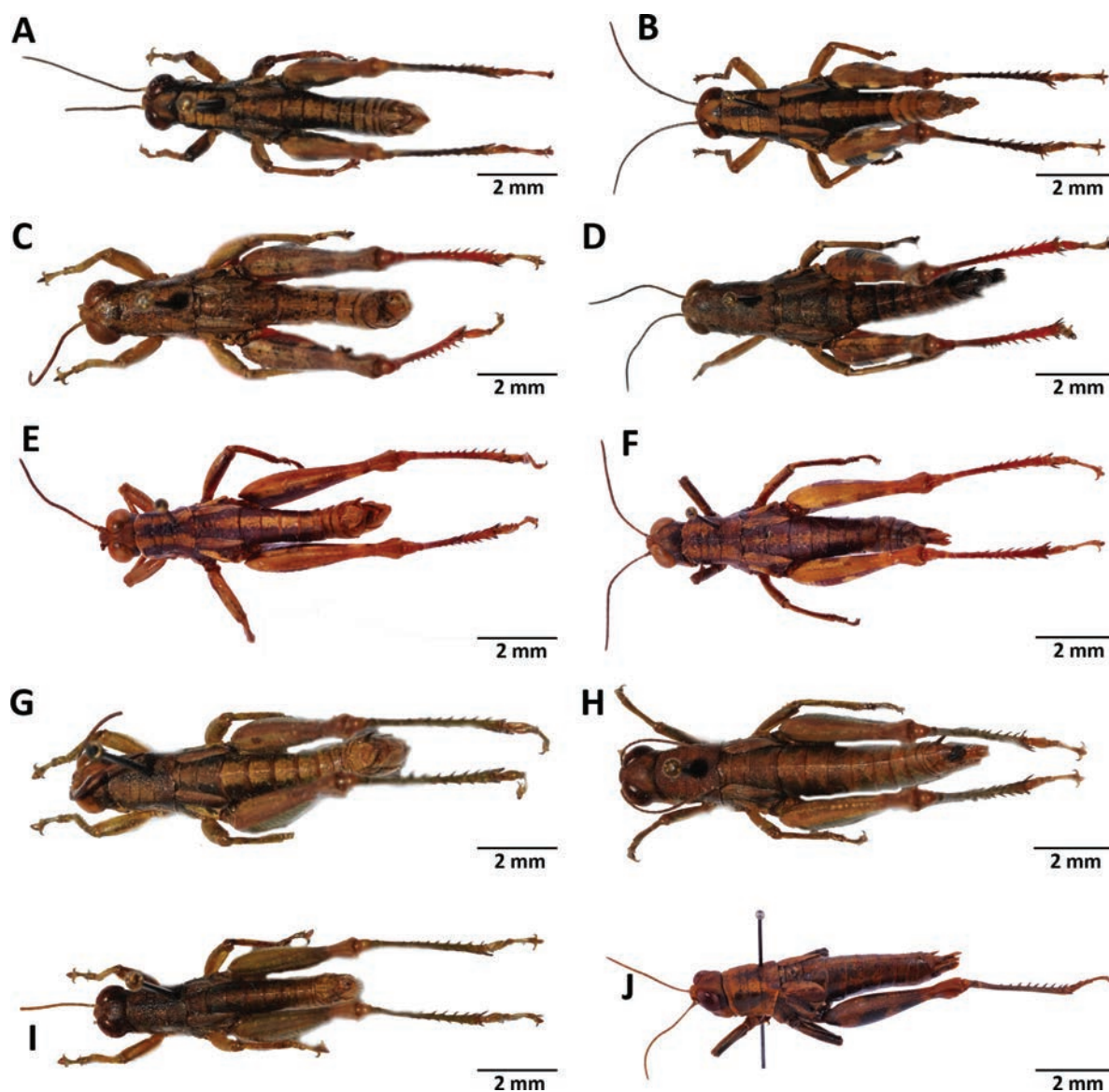


Figure 11. Images of holotypes, allotypes, neallotype and paratype of *Pteropera* species in dorsal view **A** *P. teocchii* (holotype ♂) **B** *P. teocchii* (allotype ♀) **C** *P. thibaudi* (holotype ♂) **D** *P. thibaudi* (allotype ♀) **E** *P. verrucigena* (holotype ♂) **F** *P. verrucigena* (allotype ♀) **G** *P. villiersi* (holotype ♂) **H** *P. villiersi* (allotype ♀) **I** *P. uniformis* (neallotype ♂) **J** *P. femorata* (♀).

subtriangular; zygoma wide; apodemes of the cingulum long, reaching the apex of the endophallic apodemes; lower ectophallic sheath not enveloping the base of the rami; upper ectophallic sheath globular, sloping forward.

Female: Similar to the male but larger; supra-anal plate conical with a transverse groove in the middle field; posterior edge of the subgenital plate projecting; cercus conical with angular apex; dorsal valves of the ovipositor weakly toothed; base of the spermathecal duct widened well before it opened into the copulatory bursa; spermatheca ampulla relatively thin; distal, recurrent trunk of the spermatheca lateral diverticulum > 3× longer than the proximal trunk.

Remarks. *Pteropera verrucigena* was originally described from Barombi station (southwest Cameroon) with some paratypes recorded between Kumba-Mamfé (Southwest Cameroon) by Karsch (1891). We now additionally recorded the species from Sohock (Littoral Cameroon).

Distribution. Cameroon (Fig. 18B).

***Pteropera kennei* Yetchom & Husemann, sp. nov.**

<https://zoobank.org/12D96BC6-86C8-4CA3-A0ED-F5887640A268>

Fig. 12A–M

Type material examined. Holotype. CAMEROON • ♂; Somalomo, in the forest along the Dja River; 3°22.448'N, 12°43.990'E, 606 m a.s.l.; 10 Apr. 2022; J.A. Yetchom Fondjo leg.; SMNK, SMNK-ORTH-0000001. **Paratypes.** CAMEROON • 16 ♂♂, 3 ♀♀; Somalomo, in the forest along the Dja River; 3°22.448'N, 12°43.990'E, 606 m a.s.l.; 10–11 Apr. 2022; J.A. Yetchom Fondjo & A.R. Nzoko-Fiemapong leg.; SMNK, MNHN. CAMEROON • 1 ♂; Deng-Deng National Park; 3°21.364'N, 12°44.615'E, 661 m a.s.l.; 12 Jun. 2022; A.R. Nzoko-Fiemapong leg.; SMNK.

Diagnosis. *Pteropera kennei* sp. nov. is similar to *P. uniformis* Bruner, 1920, from Cameroon in terms of its general coloration, a dark longitudinal band and contiguous pale bands on the pronotum disc and the outer area of hind femora without pale spots. However, the new species can easily be distinguished from *P. uniformis* (Figs 6K, 11I) by its lateral lobes of pronotum without a pale basal band (present in *P. uniformis* as well as in all other *Pteropera* species); its more or less pale green coloration on the hind femora (inner and outer sides of hind femora greenish yellow in *P. uniformis*); male genitalia differ by its closed dorsal arch of cingulum (strongly open in *P. uniformis*); aedeagus horizontal apically, in line with valves (anteriorly sloping in *P. uniformis*); female genitalia differ by egg-guide being slender (broad in *P. uniformis*); and basivalvar sclerites forming an obtuse angle (acute angle in *P. uniformis*).

The new species is also similar to *Pteropera descampsi* Donskoff, 1981, from which it can be distinguished by the following characteristics: a pale basal band on the lateral lobes of the pronotum is absent but present in *P. descampsi*; bilobed male cerci, whereas male cerci are short in *P. descampsi*; the pallium and subgenital plate in males are slightly raised, whereas the apex of the subgenital plate is truncated in *P. descampsi*; the apex of the aedeagus is horizontal, in line with valves, whereas the aedeagus is curved upwards, and the apex is divergent pallets in *P. descampsi*; the dorsal arc of the cingulum is closed, whereas it is strongly open in *P. descampsi*; and the basivalvar sclerites of the female subgenital plate are described as an obtuse angle (acute angle in *P. descampsi*).

Description. Male: General coloration brown with pale green; body and legs with inconspicuous hairs, moderately rugous dorsally, smooth ventrally; eyes prominent; the large subocellar facial spot interrupted at the facial furrow, sometimes extending to the cheeks; antennae thin, filiform, longer than head and pronotum together; pronotum dark brown; dark longitudinal median band on pronotum disc present, wider than adjacent pale bands; basal pale bands on lateral lobes of pronotum absent; two incipient pale spots on the anterior margin of lateral lobes of pronotum; posterior margins of pronotum with or without incipient pale spots; median carina present and crossed dorsally by three sulci; lateral carinae absent; prozona longer than metazona; prosternal process short conical, compressed at its base; tegmina lobiform, only slightly reaching the third abdominal segment, lower half shiny black and upper half pale ochreous; mesosternal interspace open, ~ 1.3× longer than wide; meso- and metathoracic episternites dark brown; front and middle legs, inner and outer sides of hind femora pale green, with

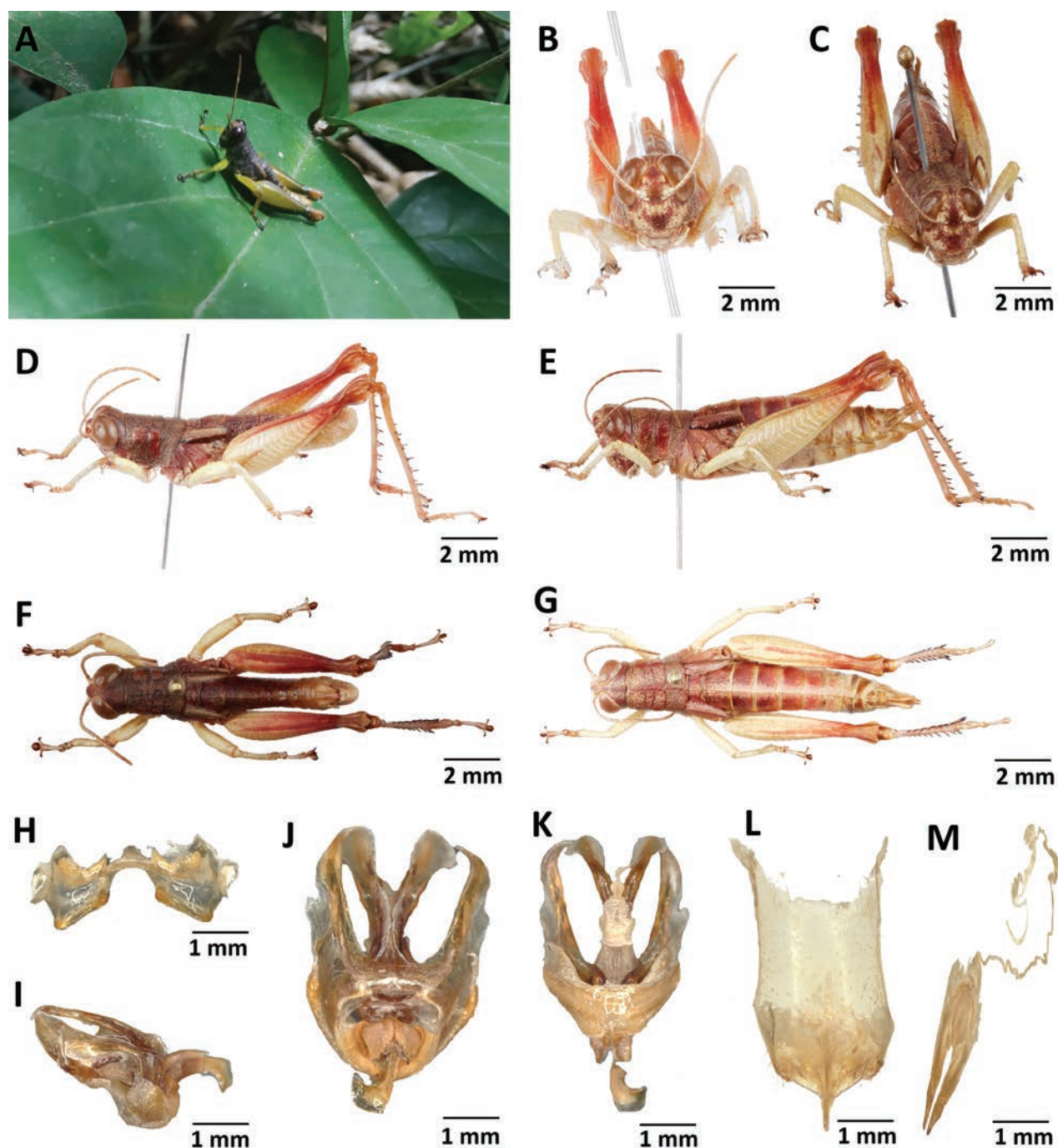


Figure 12. *Pteropera kennei* sp. nov. **A** habitus image of a male under natural conditions **B** male frontal view **C** female frontal view **D** male lateral view **E** female lateral view **F** male dorsal view **G** female dorsal view **H** epiphallus dorsal view **I** phallic complex lateral view **J** phallic complex dorsal view **K** phallic complex ventral view **L** female subgenital plate **M** female spermatheca.

the apical third gradually darkening toward the knee; knee dark orange; dorsal basal lobes of hind femora longer than ventral ones; upper margins of hind femora with fine teeth; hind tibiae dark green, basal ring absent; external apical spines of hind tibiae absent; male cerci bilobed, the inner lobe being twice shorter than the outer; subgenital plate obtuse to rounded in dorsal view; pallium and supra-anal plate of male slightly raised. **Epiphallus** (Fig. 12H): small, bridge narrow, arched; lateral margins parallel; ancorae

small, internally directed; lophi slender. **Phallic complex** (Fig. 12I–K): aedeagus small, short, curved; membranous apex of aedeagus, outside sheaths without sclerites, never filiform, and without ridge-like expansion; membranous apex of aedeagus outside sheaths, without sclerites, enlarged into a broad transverse lamina, never angular, never rolled up on itself; the dorsal arch of cingulum V-shaped, its apex acute, curved inwards; rami not bent, its lower part short; zygoma reduced; latero-ventral sclerites narrow; upper ectophallic sheath tight, short, slightly curved, with acute apex; upper eadeagus valve widened into a transverse blade; lower ectophallic sheath small, not enveloping the base of rami.

Female: As male, but larger; cerci short conical; valves of ovipositor narrow, > 3.5× longer than wide in coalescence position; subgenital plate (Fig. 12L) pentagonal, elongated, with truncated posterior margins; anterior apodemes narrow and short; egg-guide thin and long; ventral pockets of the vaginal floor large; copulatory bursa almost straight, gradually narrowing towards the front; bottom of the copulatory bursa close to the arc of the basivalvar sclerites; copulatory bursa above the basivalvar sclerites with a thick ventral gutter and membranous roof; each basivalvar sclerite barely curved, forming an obtuse angle; internal sclerite of the copulatory bursa short; the recurrent distal trunk of the lateral spermathecal diverticulum 3× longer than the proximal trunk; the base of the spermathecal duct opening at the apex of the bursa; spermathecal ampulla narrowed at the apex; spermathecal duct very long; axial diverticle of the spermatheca almost as long as the lateral diverticulum (Fig. 12M).

Measurements. Males (mm) ($n = 20$): total length of body 11.81–19.83; length of pronotum 3.12–4.32; length of hind femur 11.23–12.53; length of elytra 3.24–4.27. Females (mm) ($n = 5$): total length of body 21.09–25.39; length of pronotum 4.59–5.37; length of hind femur 13.62–15.12; length of elytra 3.65–4.88; length of ovipositor 1.97–3.27. Detailed information is shown in Table 1.

Etymology. The species was named in honor of Professor Martin Kenne in recognition of his work and scientific contribution to the biodiversity of insects in Cameroon.

Habitat. Dense evergreen forest in the Congo Basin, Dja Biosphere Reserve, south Cameroon.

Distribution. Cameroon, Somalomo in the Dja Biosphere Reserve and Deng-Deng National Park (Fig. 17B).

***Pteropera matzkei* Yetchom & Husemann, sp. nov.**

<https://zoobank.org/B6C9D13F-A617-4895-82BB-794E2B5D0708>

Fig. 13A–M

Type material examined. Holotype. CAMEROON • ♂; Somalomo, in the forest along the Dja River; 3°22.448'N, 12°43.990'E, 602 m a.s.l.; 10 Apr. 2022; J.A. Yetchom Fondjo leg.; SMNK, SMNK-ORTH-0000002. **Paratypes.** CAMEROON • 1 ♀; Somalomo, in the forest along the Dja River; 3°22.448'N, 12°43.990'E, 602 m a.s.l.; 10 Apr. 2022; J.A. Yetchom Fondjo leg.; SMNK. CAMEROON • 3 ♂♂, 1 ♀; Somalomo, in the Dja Biosphere reserve; 3°22.448'N, 12°43.990'E, 602 m a.s.l.; 28 Jun. 2022; A.R. Nzoko-Fiemapong leg.; SMNK.

Table 1. Measurements in millimeters (mm) of the examined *Pteropera* species currently known from Cameroon.

Species	<i>Pteropera carnapi</i> Ramme, 1929		<i>Pteropera descampsi</i> Donskoff, 1981		<i>Pteropera karschi zenkeri</i> Ramme, 1929		<i>Pteropera kennei</i> sp. nov.	
	Male	Female	Male	Female	Male	Female	Male	Female
HeadL	1.95 ± 0.15 (n = 7)	2.34 ± 0.18 (n = 6)	2.04 ± 0.20 (n = 8)	2.19 ± 0.13 (n = 8)	4.54 ± 1.04 (n = 4)	4.54 ± 1.04 (n = 4)	2.77 ± 0.24 (n = 20)	3.07 ± 0.11 (n = 5)
HeadW	3.08 ± 0.12 (n = 7)	3.67 ± 0.07 (n = 6)	2.99 ± 0.10 (n = 8)	3.61 ± 0.20 (n = 8)	3.15 ± 0.13 (n = 4)	3.15 ± 0.13 (n = 4)	3.05 ± 0.15 (n = 20)	3.73 ± 0.23 (n = 5)
AntenL	9.57 ± 0.73 (n = 6)	10.34 ± 0.62 (n = 6)	9.64 ± 0.66 (n = 7)	10.22 ± 0.69 (n = 7)	11.62 ± 0.50 (n = 4)	11.62 ± 0.50 (n = 4)	9.73 ± 0.37 (n = 20)	10.36 ± 0.65 (n = 5)
I.O.D.	0.47 ± 0.19 (n = 7)	0.60 ± 0.16 (n = 6)	0.64 ± 0.08 (n = 8)	0.64 ± 0.08 (n = 8)	0.37 ± 0.12 (n = 4)	0.37 ± 0.12 (n = 4)	0.55 ± 0.12 (n = 20)	0.68 ± 0.03 (n = 5)
PronotL	4.32 ± 0.25 (n = 7)	5.02 ± 0.13 (n = 6)	5.06 ± 0.32 (n = 8)	5.06 ± 0.32 (n = 8)	4.27 ± 0.07 (n = 4)	4.27 ± 0.07 (n = 4)	4.01 ± 0.26 (n = 20)	4.94 ± 0.35 (n = 5)
PronotW	3.54 ± 0.38 (n = 7)	4.38 ± 0.24 (n = 6)	4.17 ± 0.26 (n = 8)	4.17 ± 0.26 (n = 8)	3.56 ± 0.26 (n = 4)	3.56 ± 0.26 (n = 4)	3.37 ± 0.28 (n = 20)	4.39 ± 0.28 (n = 5)
TegL	3.58 ± 0.19 (n = 7)	4.43 ± 0.47 (n = 6)	3.73 ± 0.41 (n = 7)	4.31 ± 0.63 (n = 7)	4.17 ± 0.33 (n = 4)	4.17 ± 0.33 (n = 4)	3.80 ± 0.29 (n = 20)	4.26 ± 0.56 (n = 5)
TL	10.45 ± 0.15 (n = 7)	12.42 ± 0.71 (n = 6)	12.11 ± 0.55 (n = 8)	12.11 ± 0.55 (n = 8)	11.59 ± 0.19 (n = 4)	11.59 ± 0.19 (n = 4)	10.27 ± 0.43 (n = 20)	12.49 ± 0.57 (n = 5)
FL	12.07 ± 0.25 (n = 7)	14.39 ± 0.48 (n = 5)	12.17 ± 0.54 (n = 7)	14.03 ± 0.82 (n = 7)	13.52 ± 0.04 (n = 4)	13.52 ± 0.04 (n = 4)	11.91 ± 0.35 (n = 20)	14.32 ± 0.56 (n = 5)
FW	1.61 ± 0.21 (n = 7)	1.91 ± 0.11 (n = 5)	1.64 ± 0.22 (n = 7)	1.75 ± 0.22 (n = 7)	3.10 ± 0.21 (n = 4)	3.10 ± 0.21 (n = 4)	3.10 ± 0.15 (n = 20)	3.67 ± 0.23 (n = 5)
BodyL	19.92 ± 1.26 (n = 7)	25.35 ± 2.20 (n = 6)	24.52 ± 2.41 (n = 8)	24.52 ± 2.41 (n = 8)	21.24 ± 0.58 (n = 4)	21.24 ± 0.58 (n = 4)	18.15 ± 1.71 (n = 20)	23.08 ± 1.69 (n = 5)
Species	<i>Pteropera matzkei</i> sp. nov.		<i>Pteropera missoupi</i> sp. nov.		<i>Pteropera uniformis</i> Bruner, 1920		<i>Pteropera verrucigena</i> Karsch, 1891	
Parameters	Male	Female	Male	Female	Male	Female	Male	Female
HeadL	4.54 ± 1.04 (n = 4)	5.33 ± 1.85 (n = 2)	2.41 ± 0.53 (n = 8)	2.87 ± 0.56 (n = 7)	2.16 ± 0.00 (n = 1)	–	2.04 ± 0.24 (n = 2)	2.24 (n = 1)
HeadW	3.15 ± 0.13 (n = 4)	3.46 ± 0.71 (n = 2)	3.29 ± 0.26 (n = 8)	3.64 ± 0.69 (n = 7)	3.10 ± 0.00 (n = 1)	–	3.43 ± 0.21 (n = 2)	4.48 (n = 1)
AntenL	11.62 ± 0.50 (n = 4)	12.75 ± 0.54 (n = 2)	10.07 ± 0.57 (n = 8)	10.71 ± 0.33 (n = 7)	10.99 ± 0.00 (n = 1)	–	–	–
I.O.D.	0.37 ± 0.12 (n = 4)	0.69 ± 0.68 (n = 2)	0.55 ± 0.08 (n = 8)	0.77 ± 0.19 (n = 7)	0.44 ± 0.00 (n = 1)	–	0.66 ± 0.30 (n = 2)	0.79 (n = 1)
PronotL	4.27 ± 0.07 (n = 4)	5.47 ± 0.11 (n = 2)	4.50 ± 0.26 (n = 8)	5.35 ± 0.16 (n = 7)	4.58 ± 0.00 (n = 1)	–	4.46 ± 0.45 (n = 2)	5.58 (n = 1)
PronotW	3.56 ± 0.26 (n = 4)	4.74 ± 0.01 (n = 2)	3.81 ± 0.40 (n = 8)	4.52 ± 0.56 (n = 7)	3.62 ± 0.00 (n = 1)	–	3.74 ± 0.32 (n = 2)	4.89 (n = 1)
TegL	4.17 ± 0.33 (n = 4)	5.53 ± 0.81 (n = 2)	3.81 ± 0.43 (n = 7)	4.79 ± 0.40 (n = 7)	3.76 ± 0.00 (n = 1)	–	3.70 ± 0.28 (n = 2)	5.91 (n = 1)
TL	11.59 ± 0.19 (n = 4)	14.28 ± 0.33 (n = 2)	11.29 ± 0.28 (n = 8)	13.99 ± 0.46 (n = 6)	10.64 ± 0.00 (n = 1)	–	11.30 ± 0.80 (n = 2)	14.72 (n = 1)
FL	13.52 ± 0.04 (n = 4)	16.40 ± 0.69 (n = 2)	13.20 ± 0.39 (n = 8)	16.32 ± 0.71 (n = 7)	12.83 ± 0.00 (n = 1)	–	12.84 ± 0.78 (n = 2)	17.23 (n = 1)
FW	3.10 ± 0.21 (n = 4)	3.73 ± 0.01 (n = 2)	1.65 ± 0.16 (n = 8)	1.98 ± 0.10 (n = 7)	1.75 ± 0.00 (n = 1)	–	1.74 ± 0.11 (n = 2)	1.69 (n = 1)
BodyL	21.24 ± 0.58 (n = 4)	27.65 ± 0.57 (n = 2)	21.02 ± 1.51 (n = 7)	26.38 ± 1.35 (n = 7)	19.88 ± 0.00 (n = 1)	–	20.37 ± 0.43 (n = 2)	28.86 (n = 1)

The measurements represent the average value of the different body parts plus the standard deviation. **HeadL**: length of head; **HeadW**: width of head; **AntenL**: length of antenna; **I.O.D.**: interocular distance; **FastigL**: length of fastigium of vertex; **PronotL**: Length of the pronotum in the midline; **PronotW**: pronotum width; **TegL**: length of tegmina; **TL**: hind tibia length; **FL**: maximum length of the hind femur; **FW**: width of hind femur, measured as the distance between the two parallel lines running through the dorsal and ventral extremities of the femur, drawn parallel to the long axis of the femur; **BodyL**: body length, measured from the tip of the frons to the hindmost tip of the abdomen; **n**: number of measured individuals; –: not applicable.

Diagnosis. The new species *Pteropera matzkei* sp. nov. is close to *Pteropera bertii* Donskoff, 1981 (Figs 2E, F, 7E, F) from Cameroon, from which it differs by the following characteristics: the entirely yellow coloration of meso- and metathoracic episternites (almost entirely pale in *P. bertii*); the dark brown coloration of hind femora and dark yellow coloration of front and middle legs, and hind tibiae (front and middle legs, hind femora, and hind tibiae are pale green in *P. bertii*); male genitalia differ in shape and size of phallic structures with the dorsal arch of the cingulum closed, long, extending beyond the apex of endophallic valves, and overhanging them apically (slightly open, not reaching apex of endophallic valves nor overhanging them in *P. bertii*); fore apodemes of the female subgenital plate thin, acute (broad, short in *P. bertii*); and the spermathecal ampulla elongate (broad apically in *P. bertii*).

Pteropera matzkei sp. nov. differs from *Pteropera teocchii* Donskoff, 1981 (Figs 6C, D, 11A, B) in that the outer area of its hind femora has only one preapical spot (three spots, beginning of spots along the upper margin at the level of the outer spots in *P. teocchii*); dark yellow coloration of hind tibiae (black in *P. teocchii*); aedeagus slightly curved, describing less than a semicircle (strongly curved, describing an almost complete circle in *P. teocchii*); and female spermathecal ampulla elongated (enlarged at the junction of lateral and axial diverticula in *P. teocchii*).

The new species is also similar to *Pteropera verrucigena* Karsch, 1891 (Figs 6G, H, 11E, F) from which it differs in the following characteristics: a single spot on the outer area of the hind femora, whereas *P. verrucigena* has three spots; dark yellow coloration of the fore and middle legs and hind tibiae, while the fore and middle legs in *P. verrucigena* are dark brown dorsally and wine red-colored ventrally, hind tibiae wine red-colored; membranous apex of aedeagus slightly curved, describing less than one semicircle, the tip short, whereas that of *P. verrucigena* is very curved, describing one semicircle with a long tip; and the dorsal arc of the cingulum is closed, long, extending beyond the apex of endophallic apodemes, whereas in *P. verrucigena*, the dorsal arc of the cingulum is open, not reaching the apex of endophallic apodemes; female spermathecal ampulla is elongated, whereas that of *P. verrucigena* is constricted apically.

Description. Male: Body and legs with inconspicuous hairs; integument moderately rugous dorsally, and smooth ventrally; general coloration dark brown with yellow bands; eyes of medium size; antennae thin, filiform, longer than head and pronotum together, with 21 segments; median subocellar facial spot single or unique; longitudinal median dark band on pronotum disc as wide as adjacent yellow bands, but widened behind the typical groove; basal yellow bands of lateral lobes of pronotum narrowed in front of the second transverse groove, but not interrupted; median carina distinct, crossed dorso-laterally by three sulci; lateral carinae absent; prozona longer than metazona; prosternal process short conical or pyramidal; mesosternal interspace open; meso- and metathoracic episternites entirely yellow; tegmina lobiform, narrow, brown in the lower half and yellow in the upper half, covering the tympanum; wings less developed; fore and middle legs entirely yellow, more or less pale; hind femur almost entirely dark brown, with a pregenicular yellow spot on the external and inner areas; dorsal carinae of hind femora with slight tooth; hind tibiae dark yellow, basal ring absent; external apical spines of the hind tibiae absent; spines on the hind tibiae varying from seven to eight in both external

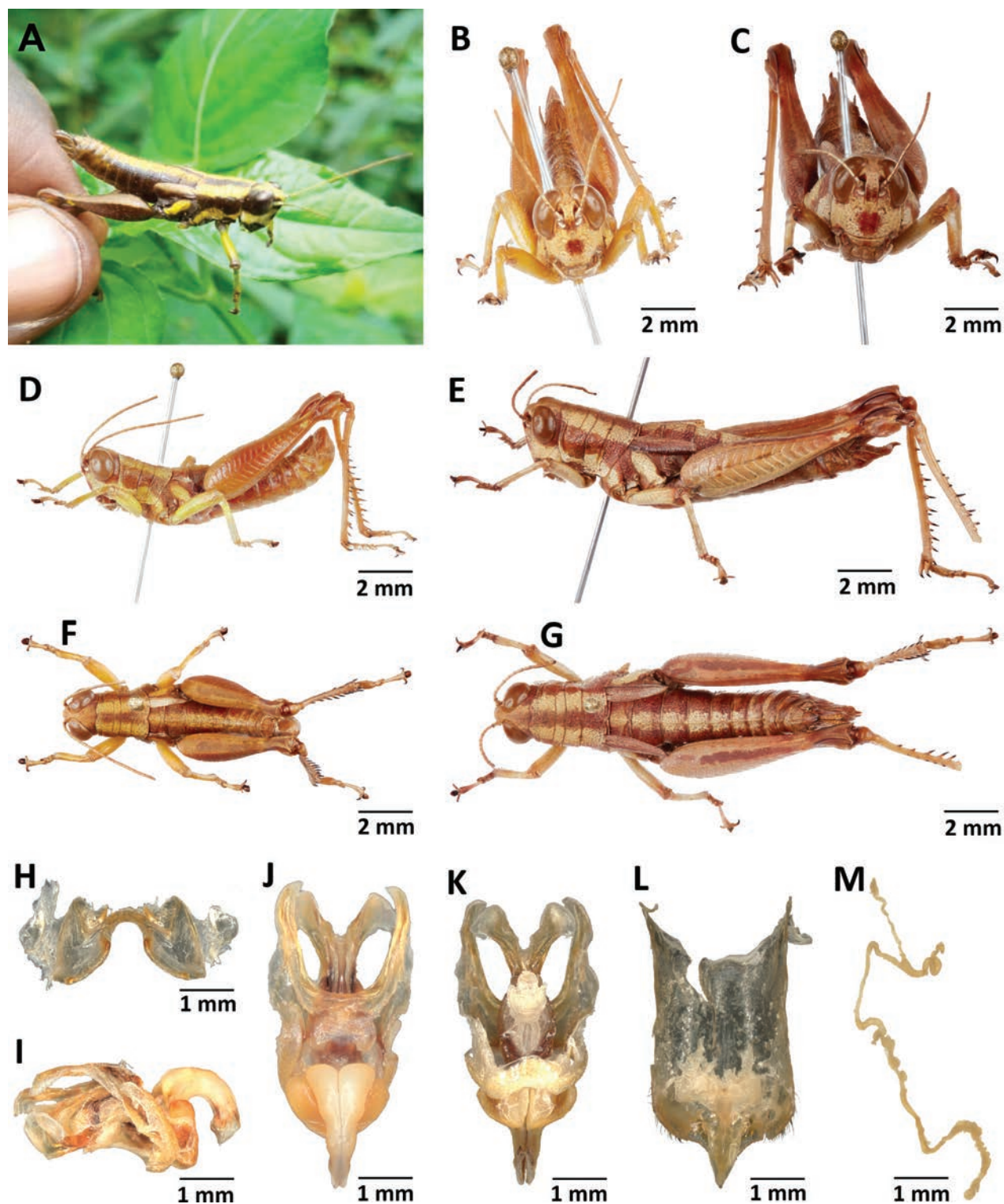


Figure 13. *Pteropera matzkei* sp. nov. **A** image of a female under natural conditions **B** male frontal view **C** female frontal view **D** male lateral view **E** female lateral view **F** male dorsal view **G** female dorsal view **H** epiphallus dorsal view **I** phallic complex lateral view **J** phallic complex dorsal view **K** phallic complex ventral view **L** female subgenital plate **M** female spermatheca.

and internal sides; male subgenital plate acute in dorsal view; the pallium and supra-anal plate of male is not raised; the male cerci long, conical, incurved and exceeding beyond the supra-anal plate. **Epiphallus** (Fig. 13H): large; bridge narrow, arched; ancorae small, strongly curved, interiorly directed; lateral plates domed, extending back from the bridge; anterior projections triangular. **Phallic**

complex (Fig. 13I–K): Dorsal arch of cingulum closed, U-shaped, its apical 2/3 overlapping with endophallic sclerites; apodemes of the cingulum incurved and extending beyond endophallic apodemes; rami slightly bent; lateroventral sclerites narrow, as high as long; aedeagus of larger size, curved, forming a quarter circle; membranous apex of aedeagus, outside endophallic sheaths, supported by a longitudinal division of upper valve, short, broad; apex of aedeagus with a ridge-like expansions; membranous apex of aedeagus subtriangular, down-curved in lateral view; upper ectophallic sheath not enlarged at its base and tightly molding the aedeagus valves; lower ectophallic sheath broad, capping the base of rami.

Female: As male but larger; cerci short conical; subgenital plate (Fig. 13L) pentagonal, broad, with rounded posterior margins; anterior apodemes thin, acute; egg-guide broad with acute apex; distal recurrent trunk of lateral spermathecal diverticulum 3× longer than proximal trunk; spermathecal ampulla elongate; base of spermathecal duct narrow (Fig. 13M).

Measurements. Males (mm) ($n = 4$): total length of body 20.57–21.79; length of pronotum 4.17–4.33; length of hind femur 13.48–13.56; length of elytra 3.90–4.63. Females (mm) ($n = 2$): total length of body 27.25–28.05; length of pronotum 5.39–5.55; length of hind femur 15.91–16.89; length of elytra 4.95–6.10; length of ovipositor 2.96–3.30. Additional measurement information is shown in Table 1.

Etymology. The species was named after Mr. Danilo Matzke, an important taxonomist for Dermaptera in Germany for his dedication and scientific contributions to the taxonomy of earwigs.

Habitat. Dense evergreen forest in the Congo Basin, in the forest along the Dja River.

Distribution. At present, the species is known only from Somalomo in the Dja Biosphere Reserve, Cameroon (Fig. 17B).

***Pteropera missoupi* Yetchom & Husemann, sp. nov.**

<https://zoobank.org/8DD173E3-68BE-40BE-B5A1-54684A435581>

Fig. 14A–M

Materials examined. Holotype. CAMEROON • ♂; Iboti, in the Ebo forest; 4°27.001'N, 10°27.002'E, 731 m a.s.l.; 7 Jan. 2022; J.A. Yetchom Fondjo leg.; SMNK, SMNK-ORTH-0000003. **Paratypes.** CAMEROON • 1 ♂; Ongot; 3°51.517'N, 11°22.367'E; 20 March 2020; J.A. Yetchom Fondjo leg.; SMNK. CAMEROON • 5 ♂♂, 3 ♀♀; Ongot; 3°51.517'N, 11°22.367'E; 15 Jun. 2020; J.A. Yetchom Fondjo & A.R. Nzoko Fiemapong leg.; SMNK). CAMEROON • 1 ♂, 1 ♀; Ongot; 3°51.517'N, 11°22.367'E; 5 Dec. 2021; J.A. Yetchom Fondjo leg.; SMNK. CAMEROON • 2 ♂♂, 3 ♀♀; Iboti, in the Ebo forest; 4°27.001'N, 10°27.002'E, 731 m a.s.l.; 7 Jan. 2022; J.A. Yetchom Fondjo leg.; SMNK.

Diagnosis. *Pteropera missoupi* sp. nov. differs from *Pteropera balachowskyi* Donskoff, 1981 (Figs 3C, D, 8C, D) in the following features: subocellar facial spot fused, single (divided in *P. balachowskyi*); dorsal and ventral areas of abdomen yellowish or greenish (brownish in *P. balachowskyi*); male cerci with a short inner lobe (male cerci simple in *P. balachowskyi*); male genitalia differ in its U-shaped and close dorsal arch of the cingulum (strongly open in *P. balachowskyi*); upper ectophallic sheath short, not bent (bent and globular in *P. balachowskyi*).

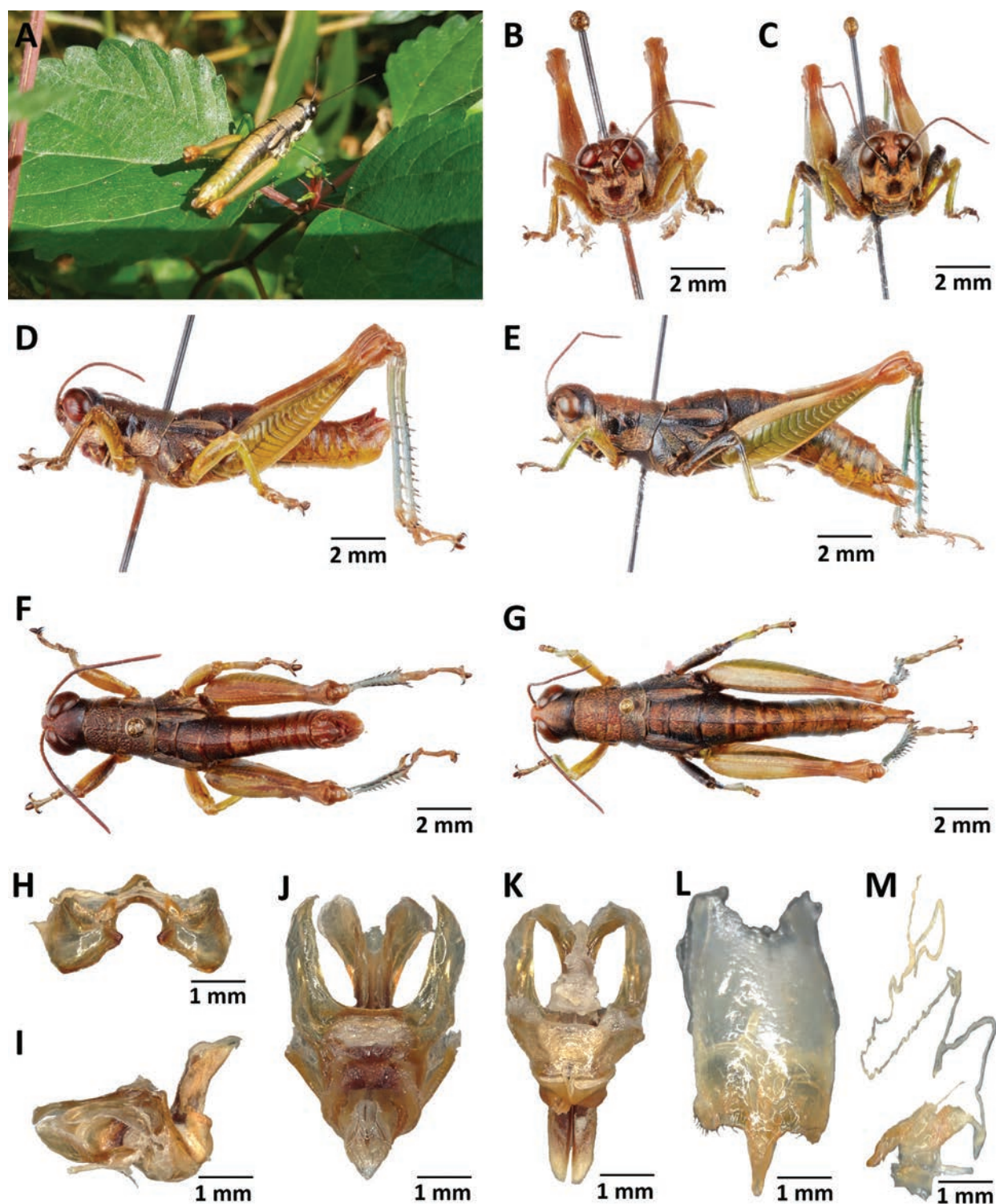


Figure 14. *Pteropera missoupi* sp. nov. A habitus image of a female under natural conditions B male frontal view C female frontal view D male lateral view E female lateral view F male dorsal view G female dorsal view H epiphallus dorsal view I phallic complex lateral view J phallic complex dorsal view K phallic complex ventral view L female subgenital plate M female spermatheca.

The new species is similar to *Pteropera jeanninae* Donskoff, 1981 (Figs 4E, F, 9C, D) from which it differs in that its subocellar facial spot is single (divided into two in *P. jeanninae*); its meso- and metathoracic episternites are pale (yellowish, conspicuous in *P. jeanninae*); its hind femur has a pale green internal area,

with a yellowish median band extending towards the lower margin (uniformly dark green in *P. jeanninae*); male genitalia differ in its U-shaped dorsal arch of the cingulum (V-shaped in *P. jeanninae*); and the upper ectophallic sheath is short, not bent (elongate in *P. jeanninae*).

The new species is also similar to *Pteropera carnapi* Ramme, 1929 (Figs 3A, B, 8A, B), from which it differs in the following characteristics: meso- and metathoracic episternites are pale (yellow in the middle in *P. carnapi*); hind tibia dark green (green bluish in *P. carnapi*); inner lobe of male cerci shorter than the outer one (as long as or longer than the outer lobe in *P. carnapi*); and male genitalia differ in its U-shaped, close dorsal arch of cingulum enveloping, apodemes reaching the apex of endophallic sclerites (open forward, apodemes not exceeding the point of separation of endophallic valves in *P. carnapi*).

The new species *Pteropera missoupi* sp. nov. is similar to *Pteropera mirei* Donskoff, 1981 (Figs 5C, D, 10A, B) from Cameroon in terms of coloration and the shape of the male cercus. However, it can be distinguished from *P. mirei* by the following characteristics: median subocellar facial spot single not divided in both sexes, but divided in males, sometimes confluent in females of *P. mirei*; basal pale bands on the lateral lobes of the pronotum narrowed and not interrupted in front of the second transverse groove, but interrupted in *P. mirei*; and male genitalia differ in the following characteristics: in *Pteropera missoupi* sp. nov., the two membranous tips at the end of the aedeagus belong to the upper valve, whereas in *P. mirei*, each of the two membranous tips at the end of the aedeagus belongs to a separate valve. In addition, in *Pteropera missoupi* sp. nov., the end of the lower tip caps the upper tip, whereas the end of the upper tip caps the lower tip in *P. mirei*.

Description. Male: Body and legs with inconspicuous hairs; integument moderately rugous dorsally and smooth ventrally; eyes prominent; antennae thin, filiform, longer than head and pronotum together; large subocellar facial spot fused in a single spot; vertex, dorsal area of pronotum, external upper area of hind femur pale brown; dark longitudinal median band on pronotum disc absent; basal pale band on lateral lobes of pronotum narrowed in front of the second transverse sulcus but not interrupted; prozona longer than metazona; prosternal process conical in its apical part; meso- and metathoracic episternites pale; tegmina lobiform, only slightly reaching the third abdominal segment; mesosternal interspace open; dorsal and ventral area of abdomen yellowish; fore- and middle legs, external and upper inner areas of hind femur dark green; median and lower inner areas of hind femur yellow; knee brownish; hind tibiae dark blue in fresh specimens; male cerci with a short inner lobe; subgenital plate obtusely rounded in dorsal view; pallium and supra-anal plate of male raised. **Epiphallus** (Fig. 14H): oval sclerites smaller; ancorae smaller, incurved; lateral margins divergent. **Phallic complex** (Fig. 14I–K): dorsal arch of the cingulum U-shaped, close, apodemes only reaching the apex of the endophallic sclerites but not exceeding them; rami bent at an obtuse angle; lateroventral sclerites triangular; zygoma reduced; upper aedeagus valve not bent; upper ectophallic sheath short, not bent; lower ectophallic sheath of smaller size, enveloping the base of the rami; aedeagus short, curved; free end of the aedeagus, outside the ectophallic sheaths, bifid, with broad-sized tips; two membranous tips at the end of the aedeagus belonging to the upper valve; and the end of the lower tip capping the upper tip.

Table 2. Complete list of currently known *Pteropera* species and subspecies considered in the present study.

N°	ID	Species	Type	Sex	Location	Author, year	Coll. date	Depository
1	MNHN-EO-CAELIF11462	<i>Pteropera augustini</i>	Holotype	m	Near Youmbi, Gabon	Donskoff, 1981	11.06.1974	MNHN
	MNHN-EO-CAELIF11463	<i>Pteropera augustini</i>	Allotype	f	Near Youmbi, Gabon	Donskoff, 1981	11.06.1974	MNHN
2	MNHN-EO-CAELIF11013	<i>Pteropera balachowskyi</i>	Holotype	m	Between Mimomgo and Koulamouto, Gabon	Donskoff, 1981	15.06.1974	MNHN
	MNHN-EO-CAELIF11014	<i>Pteropera balachowskyi</i>	Allotype	f	Between Mimomgo and Koulamouto, Gabon	Donskoff, 1981	15.06.1974	MNHN
3	MNHN-EO-CAELIF11461	<i>Pteropera basilewskyi</i>	Paratype	f	Sankuru: Komi, Congo Museum	Donskoff, 1981	12.1913	RMCA
4	MNHN-EO-CAELIF11246	<i>Pteropera bertii</i>	Holotype	m	Nkoemvone, Cameroon	Donskoff, 1981	10–14.11.1975	MNHN
	MNHN-EO-CAELIF11247	<i>Pteropera bertii</i>	Allotype	f	Nkoemvone, Cameroon	Donskoff, 1981	10–14.11.1975	MNHN
5	NA	<i>Pteropera bredoi</i>	Holotype	f	Kalulu	Donskoff, 1981	06.05.1939	RBINS
6	MNHN-EO-CAELIF11197	<i>Pteropera brosseti</i>	Holotype	m	Ipassa Quadrat, Gabon	Donskoff, 1981	3–30.05.1974	MNHN
	MNHN-EO-CAELIF11198	<i>Pteropera brosseti</i>	Allotype	f	Ipassa Quadrat, Gabon	Donskoff, 1981	3–30.05.1974	MNHN
7	BA000180S01 DORSA	<i>Pteropera carnapi</i>	Holotype	m	Yaoundé, Cameroon	Ramme, 1929	11.97	MfN
	BA000180S02 DORSA	<i>Pteropera carnapi</i>	Paratype	f	Yaoundé, Cameroon	Ramme, 1929	11.97	MfN
8	MNHN-EO-CAELIF11162	<i>Pteropera congoensis</i>	Holotype	m	Dimonika, Congo	Donskoff, 1981	01.1964	MNHN
	MNHN-EO-CAELIF11163	<i>Pteropera congoensis</i>	Allotype	f	Dimonika, Congo	Donskoff, 1981	01.1964	MNHN
9	MNHN-EO-CAELIF11249	<i>Pteropera cornici</i>	Holotype	m	N'Go, Congo-Brazzaville	Donskoff, 1981	12.03.1973	MNHN
	MNHN-EO-CAELIF11253	<i>Pteropera cornici</i>	Allotype	f	N'Go, Congo-Brazzaville	Donskoff, 1981	12.03.1973	MNHN
10	MNHN-EO-CAELIF11456	<i>Pteropera descampsi</i>	Holotype	m	Ongot (Yaoundé), Cameroon	Donskoff, 1981	2–4.11.1975	MNHN
	MNHN-EO-CAELIF11457	<i>Pteropera descampsi</i>	Allotype	f	Ongot (Yaoundé), Cameroon	Donskoff, 1981	2–4.11.1975	MNHN
11	MNHN-EO-CAELIF11031	<i>Pteropera descarpentriesi</i>	Holotype	m	Odzala, Congo	Donskoff, 1981	10.1963	MNHN
	MNHN-EO-CAELIF11032	<i>Pteropera descarpentriesi</i>	Allotype	f	Odzala, Congo	Donskoff, 1981	10.1963	MNHN
12	NA	<i>Pteropera femorata</i>	Holotype	f	Boko, Congo-Brazzaville	(Giglio-Tos, 1907)	-	EMT
13	MNHN-EO-CAELIF11493	<i>Pteropera grilloti</i>	Holotype	m	N'Gongo, Congo-Brazzaville	Donskoff, 1981	25.02.1970	MNHN
14	MNHN-EO-CAELIF10990	<i>Pteropera jeanninae</i>	Holotype	m	Between Okondja and Odzala, Gabon	Donskoff, 1981	18.06.1974	MNHN
	MNHN-EO-CAELIF10991	<i>Pteropera jeanninae</i>	Allotype	f	Between Okondja and Odzala, Gabon	Donskoff, 1981	18.06.1974	MNHN
15	MNHN-EO-CAELIF11442	<i>Pteropera karschi karschi</i>	NA	m	Mvoum, Gabon	(I. Bolívar, 1905)	1–15.11.1969	MNHN
	MNHN-EO-CAELIF11443	<i>Pteropera karschi karschi</i>	NA	f	Mont cristal, Gabon	(I. Bolívar, 1905)	3.06.1974	MNHN

N°	ID	Species	Type	Sex	Location	Author, year	Coll. date	Depository
16	BA000178S01 DORSA	<i>Pteropera karschi zenkeri</i>	Holotype	m	Bipindi, Cameroon	Ramme, 1929	02.1904	MfN
	BA000178S06 DORSA	<i>Pteropera karschi zenkeri</i>	Allotype	f	Bipindi, Cameroon	Ramme, 1929	11.04.1897	MfN
17	MNHN-EO-CAELIF11531	<i>Pteropera menieri</i>	Holotype	m	Dimonika, Congo-Brazzaville	Donskoff, 1981	18.02.1978	MNHN
	MNHN-EO-CAELIF11532	<i>Pteropera menieri</i>	Allotype	f	Dimonika, Congo-Brazzaville	Donskoff, 1981	18.02.1978	MNHN
18	NA	<i>Pteropera meridionalis</i>	Holotype	f	Kwango (Popokabak), Coll-Mus-Congo	Donskoff, 1981	1949	Tervuren Museum
19	MNHN-EO-CAELIF11241	<i>Pteropera mirei</i>	Holotype	m	Nkoemvone	Donskoff, 1981	10–14.11.1975	MNHN
	MNHN-EO-CAELIF11242	<i>Pteropera mirei</i>	Allotype	f	Nkoemvone	Donskoff, 1981	10–14.11.1975	MNHN
20	MNHN-EO-CAELIF11238	<i>Pteropera morini</i>	Holotype	m	M'Be, Congo-Brazzaville	Donskoff, 1981	03.1973	MNHN
	MNHN-EO-CAELIF11239	<i>Pteropera morini</i>	Allotype	f	M'Be, Congo-Brazzaville	Donskoff, 1981	5.01.77	MNHN
21	MNHN-EO-CAELIF11232	<i>Pteropera pillaulti</i>	Holotype	m	Djoumouna (Yaka-Yaka), Congo	Donskoff, 1981	4.01.1977	MNHN
	MNHN-EO-CAELIF11233	<i>Pteropera pillaulti</i>	Allotype	f	Djoumouna (Yaka-Yaka), Congo	Donskoff, 1981	4.01.1977	MNHN
22	MNHN-EO-CAELIF11501	<i>Pteropera poirieri</i>	Holotype	m	M'Bomo, Congo	Donskoff, 1981	8.02.1977	MNHN
	MNHN-EO-CAELIF11502	<i>Pteropera poirieri</i>	Allotype	F	M'Bomo, Congo	Donskoff, 1981	8.02.1977	MNHN
23	BA000177S01 DORSA	<i>Pteropera spleniata</i>	Holotype	m	Chinchoxo, Congo	(Karsch, 1896)	NA	MfN
	BA000177S02 DORSA	<i>Pteropera spleniata</i>	Holotype	f	Chinchoxo, Congo	(Karsch, 1896)	NA	MfN
24	MNHN-EO-CAELIF11444	<i>Pteropera teocchii</i>	Holotype	m	La Maboke, RCA	Donskoff, 1981	16.01.1968	MNHN
	MNHN-EO-CAELIF11245	<i>Pteropera teocchii</i>	Allotype	f	La Maboke, RCA	Donskoff, 1981	16.01.1968	MNHN
25	MNHN-EO-CAELIF11509	<i>Pteropera thibaudi</i>	Holotype	m	Vouka (Mossendjo), Congo-Brazzaville	Donskoff, 1981	02.1974	MNHN
	MNHN-EO-CAELIF11510	<i>Pteropera thibaudi</i>	Allotype	f	Vouka (Mossendjo), Congo-Brazzaville	Donskoff, 1981	02.1974	MNHN
26	MNHN-EO-CAELIF11248	<i>Pteropera Uniformis</i>	Neallotype	m	Nkoemvone, Cameroon	Bruner, 1920	10–14.11.1975	MNHN
27	BA000175S01 DORSA	<i>Pteropera verrucigena</i>	Lectotype	H	Barombi Station, Cameroon	Karsch, 1891	NA	MfN
	BA000175S02 DORSA	<i>Pteropera verrucigena</i>	Allotype	f	Barombi Station, Cameroon	Karsch, 1891	NA	MfN
28	MNHN-EO-CAELIF11243	<i>Pteropera villiersi</i>	Holotype	m	Sibiti, Congo	Donskoff, 1981	11.1963	MNHN
	MNHN-EO-CAELIF11244	<i>Pteropera villiersi</i>	Allotype	f	Sibiti, Congo	Donskoff, 1981	11.1963	MNHN
29	SMNK-ORTH-0000001	<i>Pteropera kennei</i> sp. nov.	Holotype	m	Somalomo (Dja), Cameroon	Yetchom & Husemann, 2024	10.04.2022	SMNK
30	SMNK-ORTH-0000002	<i>Pteropera matzkei</i> sp. nov.	Holotype	m	Somalomo (Dja), Cameroon	Yetchom & Husemann, 2024	10.04.2022	SMNK
31	SMNK-ORTH-0000003	<i>Pteropera missoupi</i> sp. nov.	Holotype	m	Iboti (Ebo forest), Cameroon	Yetchom & Husemann, 2024	07.01.2022	SMNK

ID: specimen ID; m: male; f: female; Coll. date: collection date; NA: not applicable.

Table 3. Taxon sampling and GenBank accession numbers for the sequenced markers.

Species	Voucher Codes	Coll. date	Country of origin	GenBank accession number			GenSeq nomenclature
				COI	16S	12S	
<i>P. augustini</i>	CM1205	11.04.2022	Cameroon	PP700650	PP708801	PP737690	Genseq-3 COI, 16S, 12S
<i>P. carnapi</i>	CM1361	12.06.2022	Cameroon	PP707812	PP708833	NA	Genseq-3 Genseq-3 COI, 16S
<i>P. carnapi</i>	CM1363	12.06.2022	Cameroon	PP707813	PP708802	PP737691	Genseq-3 Genseq-3 COI, 16S, 12S
<i>P. carnapi</i>	CM1364	12.06.2022	Cameroon	PP700651	PP708803	PP737728	Genseq-3 Genseq-3 COI, 16S, 12S
<i>P. carnapi</i>	CM1365	12.06.2022	Cameroon	PP700652	PP708804	PP737692	Genseq-3 COI, 16S, 12S
<i>P. carnapi</i>	CM1366	12.06.2022	Cameroon	PP700653	PP708805	PP737729	Genseq-3 COI, 16S, 12S
<i>P. carnapi</i>	CM1371	12.06.2022	Cameroon	NA	PP708806	PP737693	Genseq-3 16S, 12S
<i>P. carnapi</i>	CM1373	12.06.2022	Cameroon	PP700654	PP708834	PP737694	Genseq-3 COI, 16S, 12S
<i>P. descampsi</i>	CM140	20.03.2022	Cameroon	PP707814	PP708835	PP737695	Genseq-3 COI, 16S, 12S
<i>P. descampsi</i>	CM141	20.03.2022	Cameroon	PP700655	PP708807	PP737696	Genseq-3 COI, 16S, 12S
<i>P. descampsi</i>	CM142	20.03.2022	Cameroon	PP700656	PP708808	PP737730	Genseq-3 COI, 16S, 12S
<i>P. descampsi</i>	CM143	20.03.2022	Cameroon	PP707815	PP708809	PP737697	Genseq-3 COI, 16S, 12S
<i>P. descampsi</i>	CM144	20.03.2022	Cameroon	PP707816	PP708836	PP737698	Genseq-3 COI, 16S, 12S
<i>P. karschi zenkeri</i>	CM1425	09.09.2018	Cameroon	NA	NA	PP737731	Genseq-3 12S
<i>P. kennei</i> sp. nov.	CM1131	10.04.2022	Cameroon	PP707817	PP708810	NA	Genseq-2 COI, 16S
<i>P. kennei</i> sp. nov.	CM1135	10.04.2022	Cameroon	PP707818	NA	PP737699	Genseq-2 COI, 12S
<i>P. kennei</i> sp. nov.	CM1136	10.04.2022	Cameroon	PP700657	NA	PP737700	Genseq-2 COI, 12S
<i>P. kennei</i> sp. nov.	CM1138	10.04.2022	Cameroon	PP707819	PP708811	NA	Genseq-2 COI, 16S
<i>P. kennei</i> sp. nov.	CM1183	11.04.2022	Cameroon	NA	PP708815	NA	Genseq-2 16S
<i>P. kennei</i> sp. nov.	CM1139	10.04.2022	Cameroon	NA	NA	PP737732	Genseq-2 12S
<i>P. kennei</i> sp. nov.	CM1141	10.04.2022	Cameroon	PP700658	PP708812	PP737733	Genseq-2 COI, 16S, 12S
<i>P. kennei</i> sp. nov.	CM1142	10.04.2022	Cameroon	PP700659	NA	NA	Genseq-2 COI
<i>P. kennei</i> sp. nov.	CM1143	10.04.2022	Cameroon	NA	PP708813	PP737734	Genseq-2 16S, 12S
<i>P. kennei</i> sp. nov.	CM1182	11.04.2022	Cameroon	PP700660	PP708814	NA	Genseq-2 COI, 16S
<i>P. matzkei</i> sp. nov.	CM1127	10.04.2022	Cameroon	PP700661	PP708816	PP737735	Genseq-2 COI, 16S, 12S
<i>P. matzkei</i> sp. nov.	CM1357	28.06.2022	Cameroon	PP700662	PP708817	NA	Genseq-2 COI, 16S
<i>P. matzkei</i> sp. nov.	CM1358	28.06.2022	Cameroon	PP700663	PP708818	PP737736	Genseq-2 COI, 16S, 12S
<i>P. matzkei</i> sp. nov.	CM1359	28.06.2022	Cameroon	PP700664	PP708819	PP737737	Genseq-2 COI, 16S, 12S
<i>P. missoupi</i> sp. nov.	CM139	20.03.2022	Cameroon	PP700665	PP708837	PP737738	Genseq-2 COI, 16S, 12S
<i>P. missoupi</i> sp. nov.	CM278	15.06.2020	Cameroon	PP700666	PP708820	PP737701	Genseq-2 COI, 16S, 12S
<i>P. missoupi</i> sp. nov.	CM280	15.06.2020	Cameroon	PP700667	PP708838	PP737702	Genseq-2 COI, 16S, 12S
<i>P. missoupi</i> sp. nov.	CM281	15.06.2020	Cameroon	PP700668	PP708821	PP737703	Genseq-2 COI, 16S, 12S
<i>P. missoupi</i> sp. nov.	CM367	05.12.2021	Cameroon	PP707820	PP708839	PP737739	Genseq-2 COI, 16S, 12S
<i>P. missoupi</i> sp. nov.	CM569	07.01.2022	Cameroon	PP700669	PP708822	PP737740	Genseq-2 COI, 16S, 12S
<i>P. missoupi</i> sp. nov.	CM570	07.01.2022	Cameroon	PP700670	PP708823	PP737741	Genseq-2 COI, 16S, 12S
<i>P. missoupi</i> sp. nov.	CM571	07.01.2022	Cameroon	PP700671	PP708824	PP737742	Genseq-2 COI, 16S, 12S
<i>P. missoupi</i> sp. nov.	CM1094	15.06.2020	Cameroon	PP700672	PP708825	PP737704	Genseq-2 COI, 16S, 12S
<i>P. uniformis</i>	CM373	05.12.2021	Cameroon	PP707821	PP708840	PP737705	Genseq-3 COI, 16S, 12S
<i>P. uniformis</i>	CM1187	11.04.2022	Cameroon	PP700673	NA	PP737743	Genseq-3 COI, 12S
<i>P. verrucigena</i>	CM1423	03.04.2017	Cameroon	PP707822	PP708826	PP737706	Genseq-3 COI, 16S, 12S
<i>P. verrucigena</i>	CM1424	04.04.2017	Cameroon	PP707823	PP708841	PP737707	Genseq-3 COI, 16S, 12S
<i>C. stramineus</i>	CM735	06.05.2020	Cameroon	PP700674	NA	NA	Genseq-3 COI
<i>C. stramineus</i>	CM973	09.04.2020	Cameroon	PP707824	NA	PP737744	Genseq-3 COI, 12S
<i>E. modica</i>	CM 342	05.12.2021	Cameroon	PP700675	PP708827	NA	Genseq-3 COI, 16S
<i>E. modica</i>	CM343	05.12.2021	Cameroon	PP700676	PP708842	NA	Genseq-3 COI, 16S
<i>E. modica</i>	CM344	05.12.2021	Cameroon	PP700677	PP708828	PP737745	Genseq-3 COI, 16S, 12S
<i>E. modica</i>	CM345	05.12.2021	Cameroon	PP700678	PP708843	NA	Genseq-3 COI, 16S
<i>P. notatus</i>	CM358	05.12.2021	Cameroon	PP700679	PP708829	NA	Genseq-3 COI, 16S
<i>P. notatus</i>	CM359	05.12.2021	Cameroon	PP707825	PP708830	PP737746	Genseq-3 COI, 16S, 12S
<i>P. notatus</i>	CM360	05.12.2021	Cameroon	PP700680	PP708831	NA	Genseq-3 COI, 16S
<i>P. notatus</i>	CM596	02.03.2021	Cameroon	PP700681	PP708832	NA	Genseq-3 COI, 16S
<i>P. notatus</i>	CM781	17.07.2018	Cameroon	PP700682	NA	NA	Genseq-3 COI

Coll. date: collection date.

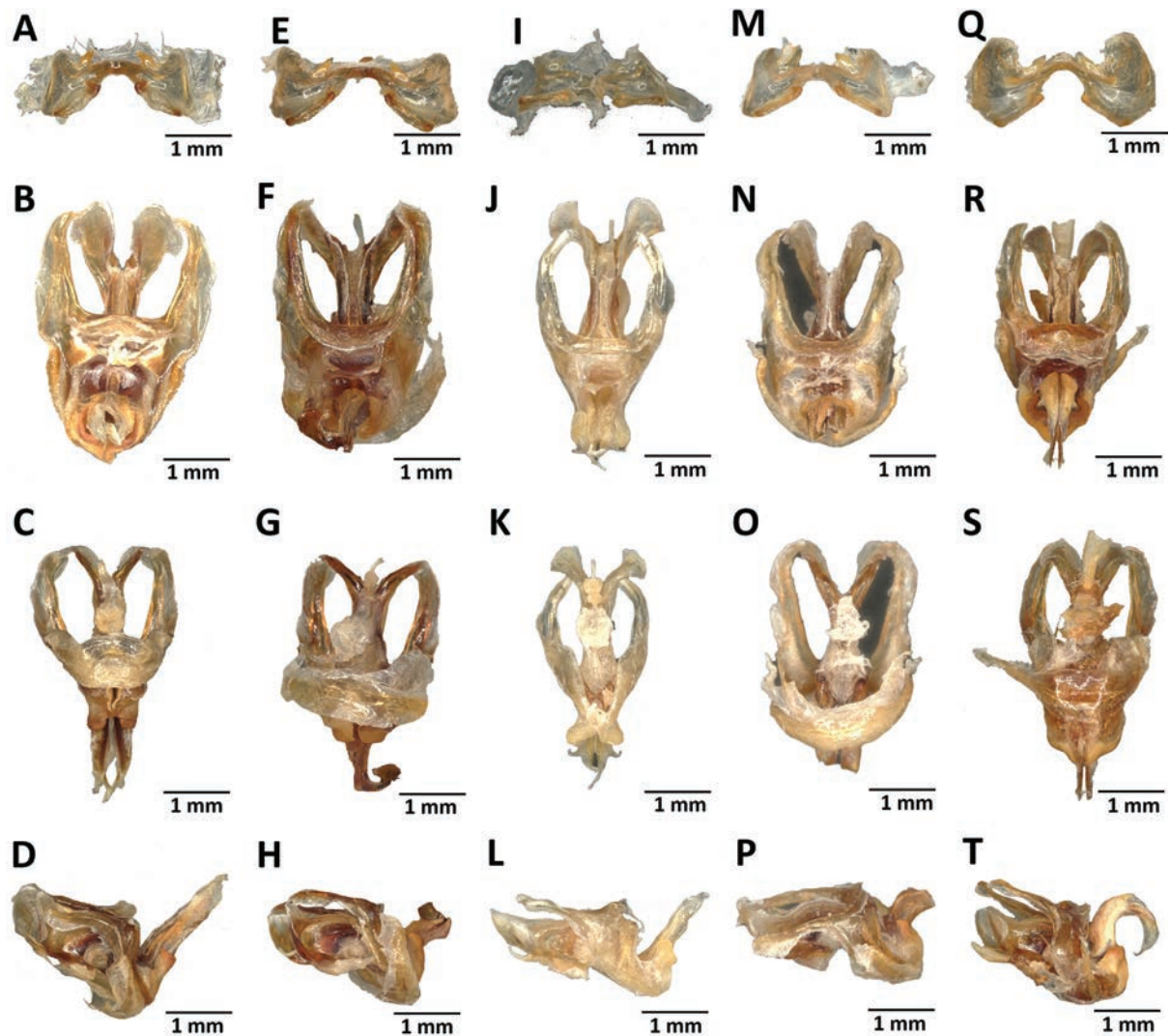


Figure 15. Internal genitalia of *P. carnapi* (A–D), *P. descampsi* (E–H), *P. karschi zenkeri* (I–L), *P. uniformis* (M–P) and *P. verrucigena* (O–T).

Female: As male but larger; cerci short conical; subgenital plate (Fig. 14L) sub-rectangular, with straight anterior margins; anterior apodemes narrow and short; egg-guide thin and long; the recurrent distal trunk of lateral spermathecal diverticulum almost 2.5× longer than the proximal trunk; spermathecal ampulla narrowed at apex; spermathecal duct very long; the base of the copulatory bursa at least as far from the basivalvar sclerites arc as the distance between them; copulatory bursa straight; the base of the spermathecal duct slightly enlarged; copulatory bursa tapering to mid-height; angle formed by the two basivalvar sclerites rounded (Fig. 14M).

Measurements. Males (mm) ($n = 8$): total length of body 18.97–22.91; length of pronotum 3.95–4.74; length of hind femur 12.65–13.77; length of elytra 3.11–4.27. Females (mm) ($n = 7$): total length of body 24.41–28.70; length of pronotum 5.14–5.62; length of hind femur 15.43–17.36; length of elytra 4.32–5.40; length of ovipositor 2.28–3.75. Additional measurement information is shown in Table 1.

Etymology. The species is dedicated to Prof. Alain Didier Missoup in recognition of his work and achievements in the systematic and evolutionary biology of small mammals in Cameroon.

Habitat. Dense evergreen forests in the Ebo forest; degraded forests and along the forest edges.

Distribution. Iboti in the Ebo forest; Ongot in the Centre region, Cameroon (Fig. 18A).

Updated keys to species of *Pteropera*

The keys provided here are derived from those presented by Donskoff (1981) but have been altered to include the newly described species of the genus *Pteropera*.

A. Based on external morphology of males and females

- 1 Three pale spots on the outer area of hind femora (Fig. 2A, B, G–I)..... **2**
 - No pale spots on the outer hind femora **13**
- 2 A dark longitudinal median band on pronotum disc (Fig. 13F, G) **3**
 - No dark longitudinal median band on pronotal disc (Fig. 2G, H, 7G, H)
..... ***P. brosetti* Donskoff, 1981** [Equatorial Guinea, Gabon]
- 3 A pale median spot on the inner side of the hind femora in the upper or central position..... **4**
 - No pale median spot on the inner side of the hind femora; beginning of spots along the upper edge, near the outer spots..... **7**
- 4 Base of the inner area of the hind femora red or orange. Hind tibiae red or orange **5**
 - Base of the inner side of the hind femora dark green or reddish brown. Hind tibiae black or dark green..... **6**
- 5 Male cerci extending beyond the end of the supra-anal plate (Fig. 4G, I).....
..... ***P. karschi***
(I. Bolívar, 1905) [Cameroon, Equatorial Guinea, Gabon, Fernando Poo]
 - Male cerci not extending beyond the end of the supra-anal plate. Hind tibiae always red (Fig. 6E)
..... ***P. thibaudi* Donskoff, 1981** [Congo-Brazzaville, Gabon]
- 6 The pale basal band on the lateral lobes of the pronotum extending from the anterior edge to the posterior edge (Fig. 2A, B)
..... ***P. augustini* Donskoff, 1981** [Cameroon, Gabon]
 - The pale basal band of the lateral lobes of the pronotum limited to the posterior half (Fig. 2I)
..... ***P. basilewskyi* Donskoff, 1981** [Democratic Republic of Congo]
- 7 The pale basal band on the lateral lobes of the pronotum narrows before the second transverse groove but not interrupted **8**
 - The pale basal band of the lateral lobes of the pronotum interrupted in front of the second transverse groove by at least a thin dark line **11**
- 8 Male cerci without inner preapical lobule **9**
 - Male cerci with inner preapical lobule (Fig. 5G)
..... ***P. pillaulti* Donskoff, 1981** [Congo-Brazzaville]
- 9 Hind tibiae black or wine-red; lower-external areas of hind femora darkened..... **10**
 - Hind tibiae green; infero-external areas of hind femora pale (Fig. 3I, J).....
..... ***P. descarpentriesi* Donskoff, 1981** [Gabon]

- 10 Hind tibiae wine-red (Fig. 6G, H)..... ***P. verrucigena* Karsch, 1891** [Cameroon]
- Hind tibiae black (Fig. 6C, D) ***P. teocchii* Donskoff, 1981** [Cameroon, Central African Republic, Congo-Brazzaville]
- 11 Male cerci thickened or very slightly bifid (Fig. 4A) ***P. femorata* (Giglio-tos, 1907)** [Angola, Congo-Brazzaville, Democratic Republic of Congo]
- Male cerci acute **12**
- 12 Male cerci with inner preapical lobule (Fig. 3C) ***P. congoensis* Donskoff, 1981** [Congo-Brazzaville, Democratic Republic of Congo, Gabon]
- Male cerci without inner preapical lobule (Fig. 5A, 9I)..... ***P. menieri* Donskoff, 1981** [Congo-Brazzaville]
- 13 Hind tibiae more or less dark yellow (Fig. 13D–G)..... ***P. matzkei* sp. nov.** [Cameroon]
- Hind tibiae more or less dark green **14**
- 14 A dark longitudinal median band on pronotum disc **15**
- No dark longitudinal median band on the pronotum disc **23**
- 15 A dark longitudinal median band on pronotum disc twice as wide as each of the adjoining pale bands (Fig. 9B) ***P. meridionalis* Donskoff, 1981** [Democratic Republic of Congo]
- A dark longitudinal median band on the pronotum disc as wide as each of the adjoining pale bands **16**
- 16 Inner area of the hind femora almost entirely red without pale spots (Fig. 4C, 9A) ***P. grilloti* Donskoff, 1981** [Congo-Brazzaville]
- Inner side of hind femora more or less dark green **17**
- 17 The pale basal band on the lateral lobe of the pronotum completely absent (Fig. 12A, D, E)..... ***P. kennei* sp. nov.** [Cameroon]
- The pale basal band on the lateral lobes of pronotum present..... **18**
- 18 The pale basal band of the lateral lobes of pronotum interrupted at the level of the second transverse groove by at least a thin dark line **19**
- The pale basal band of the lateral lobes of pronotum not interrupted at the second transverse groove..... **21**
- 19 A large V-shaped facial spot extending from cheek to cheek; male cerci short **20**
- A large subocellar facial spot, dark, median, sometimes divided into two small symmetrical spots centered on the carinae of the frontal side ***P. spleniata* (Karsch, 1896)** [Congo-Brazzaville, Democratic Republic of Congo]
- 20 Male subgenital plate rounded (in dorsal view) (Fig. 11I) ***P. uniformis* Bruner, 1920** [Cameroon]
- Male subgenital plate truncated (in dorsal view) (Fig. 8G)..... ***P. descampsi* Donskoff, 1981** [Cameroon]
- 21 Male cerci acute (Fig. 6I, 7E, 11G)..... **22**
- Male cerci bilobed, subocellar facial patch separated into two (Fig. 3E) ***P. cornici* Donskoff, 1981** [Congo-Brazzaville]
- 22 A large subocellar facial spot single, median ***P. bertii* Donskoff, 1981** [Cameroon]
- A large subocellar facial spot divided into two small symmetrical spots centered on the carinae of the front side..... ***P. villiersi* Donskoff, 1981** [Congo-Brazzaville]

- 23 Basal half of the inner part of hind femora red; hind tibiae red at the base, green at the apex (Fig. 2J)
 ***P. bredoi* Donskoff, 1981** [Democratic Republic of Congo]
 – Inner part of hind femora green.....**24**
- 24 The pale basal band of the lateral lobes of the pronotum always interrupted at the second transverse groove (Fig. 5C, D)
 ***P. mirei* Donskoff, 1981** [Cameroon, Gabon]
 – The pale basal band of the lateral lobes of the pronotum generally not interrupted at the second transverse groove.....**25**
- 25 The pale basal band on the lateral lobes of the pronotum widened in front of the second transverse groove.....**26**
 – The pale basal band of the lateral lobes of the pronotum narrow in front of the second transverse groove**27**
- 26 The pale basal band on the lateral lobes of the pronotum very wide and extends to the lower edge of these lateral lobes. Male cerci with preapical inner lobule (Fig. 5E, F)..... ***P. morini* Donskoff, 1981** [Congo-Brazzaville]
 – Pale basal band on the lateral lobes of pronotum, narrow, with parallel edges. Male cerci tapered (Fig. 5I, J)
 ***P. poirieri* Donskoff, 1981** [Congo-Brazzaville]
- 27 Male cerci simple; pallium and supra-anal plate not raised (Fig. 2C)
 ***P. balachowskyi* Donskoff, 1981** [Cameroon, Gabon]
 – Male cerci bilobed; pallium and supra-anal plate raised.....**28**
- 28 Inner lobe of male cerci as long as or longer than the outer lobe (Fig. 8A)..... ***P. carnapi* Ramme, 1929** [Cameroon, Central African Republic, Congo-Brazzaville, Gabon]
 – Inner lobe of male cerci shorter than the outer lobe (Fig. 4E).....**29**
- 29 A large subocellar facial spot divided into two.....
 ***P. jeanninae* Donskoff, 1981** [Gabon]
 – A large subocellar facial spot fused (Fig. 14B, C)
 ***P. missoupi* sp. nov.** [Cameroon]

B. Based on the male internal genitalia

- 1 End of the aedeagus, outside the ectophallic sheaths, bifid, pointed (Fig. 14I–K)**2**
 – End of aedeagus simple.....**7**
- 2 The two membranous tips at the end of aedeagus belonging to the upper valve**3**
 – Each of the two membranous tips at the end of the aedeagus belonging to a different valve**5**
- 3 The two tips of the end of the aedeagus widened, the end of the lower tip caps the upper tip (Fig. 14I–K)..... ***P. missoupi* sp. nov.** [Cameroon]
 – The two tips at the end of the aedeagus, thin**4**
- 4 The two tips at the end of the aedeagus curved downwards.....
 ***P. balachowskyi* Donskoff, 1981** [Cameroon, Gabon]
 – The lower tip at the end of the aedeagus thin, and the upper tip widened and semicircular, both in line with the valve
 ***P. villiersi* Donskoff, 1981** [Congo-Brazzaville]

- 5 Aedeagus very long, straight, upper tip filiform, lower tip lamellar, lanceolate.....***P. jeanninae* Donskoff, 1981** [Gabon]
- Aedeagus shorter, curved **6**
- 6 The upper ectophallic sheath extended. End of the upper valve of the aedeagus caps the lower valve.....***P. mirei* Donskoff, 1981** [Cameroon, Gabon]
- Upper ectophallic sheath globular. Tips of both valves convergent, plier-like..... ***P. brosetti* Donskoff, 1981** [Equatorial Guinea, Gabon]
- 7 Membranous apex of aedeagus, outside the sheaths, supported by two sclerites, formed by the longitudinal division of the upper valve **8**
- Membranous apex of the aedeagus, outside the sheaths, without sclerites **10**
- 8 Aedeagus strongly curved, upper ectophallic sheath widened dorsally at the base.....***P. descarpentriesi* Donskoff, 1981** [Gabon]
- Aedeagus slightly curved, upper ectophallic sheath not extended at the base (Fig. 13I, J) **9**
- 9 Dorsal arch of cingulum slightly open, not reaching apex of endophallic valves nor overhanging them apically..... ***P. bertii* Donskoff, 1981** [Cameroon]
- Dorsal arch of cingulum closed, long, extending beyond the apex of endophallic valves, and overhanging them apically (Fig. 13J, K) ***P. matzkei* sp. nov.** [Cameroon]
- 10 Aedeagus almost straight..... **11**
- Aedeagus curved..... **15**
- 11 Aedeagus large, upper ectophallic sheath cylindrical, long, membranous apex of upper valve thin, acute (Fig. 15B–D).....***P. carnapi* Ramme, 1929** [Cameroon, Central African Republic, Congo-Brazzaville, Gabon]
- Aedeagus small, Upper ectophallic sheath globular at the apex **12**
- 12 Membranous apex of the upper valve of aedeagus horizontal or oblique **13**
- Membranous apex of the upper valve of aedeagus truncate **14**
- 13 Membranous apex of the upper valve of aedeagus lamellar, horizontal, in the extension of the valve, oval, acute..... ***P. karschi karschi* (I. Bolívar, 1905)** [Equatorial Guinea, Gabon, Fernando Poo]
- Membranous apex of the upper valve of aedeagus lamellar, curved upward, oblique in lateral view (Fig. 15 J–L) ***P. karschi zenkeri* Ramme, 1929** [Cameroon, Equatorial Guinea]
- 14 Lower ectophallic sheath enveloping, lateral ***P. augustini* Donskoff, 1981** [Cameroon, Gabon]
- Lower ectophallic sheath nonenveloping, posterior ***P. thibaudi* Donskoff, 1981** [Congo-Brazzaville, Gabon]
- 15 Aedeagus curved upwards **16**
- Aedeagus curved downwards **17**
- 16 Membranous apex of the aedeagus in diverging pallets (Fig. 15 F–H)..... ***P. descampsi* Donskoff, 1981** [Cameroon]
- Membranous apex of the aedeagus in converging hooks..... ***P. uniformis* Bruner, 1920** [Cameroon]
- 17 Aedeagus small, slightly curved; membranous apex in short triangular blade..... ***P. basilewskyi* Donskoff, 1981** [Democratic Republic of Congo]
- Aedeagus large, well-curved **18**

18	Membranous apex of the aedeagus long, filiform	19
–	Membranous apex of the aedeagus never filiform	23
19	Lower ectophallic sheath, small, nonenveloping.....	20
–	Lower ectophallic sheath, large, enveloping.....	21
20	Upper aedeagus valve thin, regularly curved	<i>P. femorata</i> (Giglio-tos, 1907) [Angola, Congo-Brazzaville, Democratic Republic of Congo]
–	Upper aedeagus valve widened into a transverse blade (Fig. 12I–K).....	<i>P. kennei</i> sp. nov. [Cameroon]
21	Upper ectophallic sheath long, slightly curved; membranous apex of aedeagus recurrent	<i>P. menieri</i> Donskoff, 1981 [Congo-Brazzaville]
–	Upper ectophallic sheath short, strongly curved; membranous apex of aedeagus extending to the curvature of the upper valve.....	22
22	Base of upper ectophallic sheath molding the valves of the aedeagus; membranous apex of the aedeagus long and thin.....	<i>P. spleniata</i> (Karsch, 1896) [Congo-Brazzaville, Democratic Republic of Congo]
–	Base of upper ectophallic sheath swollen dorsally; membranous apex of aedeagus shorter, hook-like.....	<i>P. congoensis</i> Donskoff, 1981 [Congo-Brazzaville, Democratic Republic of Congo, Gabon]
23	Apex of the aedeagus with a ridge-like expansion.....	<i>P. cornici</i> Donskoff, 1981 [Congo-Brazzaville]
–	Apex of aedeagus without ridge-like expansion.....	24
24	Apex of aedeagus short, rounded	<i>P. poirieri</i> Donskoff, 1981 [Congo-Brazzaville]
–	Apex of aedeagus acute or widened.....	25
25	Apex of aedeagus widened.....	26
–	Apex of aedeagus acute	27
26	Apex of aedeagus widened into a rounded spatula.....	<i>P. pillaulti</i> Donskoff, 1981 [Congo-Brazzaville]
–	Apex of aedeagus widened into a transverse angular, self-wrapped blade	<i>P. grilloti</i> Donskoff, 1981 [Congo-Brazzaville]
27	Aedeagus strongly curved, curvature accentuated by the molded ectophallic sheath, long tip.....	28
–	Aedeagus slightly curved, ectophallic sheath widened dorsally at the base, tip short.....	<i>P. morini</i> Donskoff, 1981 [Congo-Brazzaville]
28	Aedeagus forming only a semicircle (Fig. 15T).....	<i>P. verrucigena</i> Karsch, 1891 [Cameroon]
–	Aedeagus forming an almost complete circle	<i>P. teocchii</i> Donskoff, 1981 [Cameroon, Central African Republic, Congo-Brazzaville]

C. Based on female internal genitalia

1	Bottom of the copulatory bursa at least as far from the arc of the basivalvar sclerites as their spacing.....	2
–	Bottom of the copulatory bursa close to the arc of the basivalvar sclerites ...	6
2	The base of spermathecal duct widened to a length equal to the distance between the basivalvar sclerites and parallel to the copulatory bursa.....	3
–	Copulatory bursa curved.....	5

- 3 Copulatory bursa with parallel edges. Angle formed by the two basivalvar sclerites obtuse ***P. jeanninae* Donskoff, 1981** [Gabon]
 - Copulatory bursa tapering to mid-height **4**
- 4 Angle formed by the two basivalvar sclerites right ***P. carnapi* Ramme, 1929** [Cameroon, Central African Republic, Congo-Brazzaville, Gabon]
 - Angle formed by the two basivalvar sclerites rounded (Fig. 14M) ***P. missoupi* sp. nov.** [Cameroon]
- 5 Copulatory bursa above the basivalvar sclerites, formed by a thick ventral gutter and a membranous roof. The base of the spermathecal duct widened, very short, hooked. Basivalvar sclerites bent, obtuse ***P. brosetti* Donskoff, 1981** [Equatorial Guinea, Gabon]
 - Bottom of copulatory bursa thickened, regularly narrowed. The base of the spermathecal duct widened over a large distance and coiled into two inverted spiral arcs. Basivalvar sclerites not bent, almost straight..... ***P. mirei* Donskoff, 1981** [Cameroon, Gabon]
- 6 Copulatory bursa almost straight..... **7**
 - Copulatory bursa arch-shaped **11**
- 7 The base of the spermathecal duct opening laterally into the bursa. Roof of the bursa membranous..... ***P. villiersi* Donskoff, 1981** [Congo-Brazzaville]
 - Base of the spermathecal duct leading to the apex of the copulatory bursa **8**
- 8 Each basivalvar sclerite straight or only slightly curved **9**
 - Each basivalvar sclerite angular ***P. basilewskyi* Donskoff, 1981** [Democratic Republic of Congo]
- 9 Copulatory bursa without internal sclerite..... ***P. karschi* (I. Bolívar, 1905)** [Cameroon, Equatorial Guinea, Gabon, Fernando Poo]
 - Copulatory bursa with two internal sclerites **10**
- 10 The two inner sclerites of the copulatory bursa rounded ***P. augustini* Donskoff, 1981** [Cameroon, Gabon]
 - The two inner sclerites of the copulatory bursa elongate ***P. thibaudi* Donskoff, 1981** [Congo-Brazzaville, Gabon]
- 11 Distal, recurrent section of the lateral spermathecal diverticulum 5× longer than the proximal section **12**
 - Distal, recurrent section of the lateral spermathecal diverticulum < 5× as long as the proximal section..... **13**
- 12 Spermathecal duct fine, widening into a small ampulla at the outlet into the copulatory bursa..... ***P. poirieri* Donskoff, 1981** [Congo-Brazzaville]
 - Spermathecal duct gradually widening at the base ***P. menieri* Donskoff, 1981** [Congo-Brazzaville]
- 13 Arch formed by the copulatory bursa short, medial sclerite, single..... **14**
 - Arch of copulatory bursa long, well-curved or wrapped..... **18**
- 14 Inner sclerite of the copulatory bursa fine **15**
 - Inner sclerite of the copulatory bursa broad and narrow at the apex. Angle formed by the two basivalvar sclerites obtuse..... **16**
- 15 Angle formed by the two basivalvar sclerites acute ***P. uniformis* Bruner, 1920** [Cameroon]
 - Angle formed by the two basivalvar sclerites obtuse (Fig. 12M)..... ***P. kennei* sp. nov.** [Cameroon]

- 16 Inner sclerite of copulatory bursa short. Distal recurrent section of the lateral diverticulum of the spermatheca 4× longer than the proximal section.
..... ***P. descarpentriesi* Donskoff, 1981** [Gabon]
- Inner sclerite of the copulatory bursa long. Distal recurrent section of the lateral diverticulum of the spermatheca 3× as long as the proximal section **17**
- 17 Spermathecal ampulla broad at the apex.....
..... ***P. bertii* Donskoff, 1981** [Cameroon]
- Spermathecal ampulla elongated at the apex (Fig. 13M).....
..... ***P. matzkei* sp. nov.** [Cameroon]
- 18 Arch of copulatory bursa wrapped, forming more than one complete turn. Internal median sclerite of copulatory bursa acute at both ends
..... ***P. cornici* Donskoff, 1981** [Congo-Brazzaville]
- Arch of copulatory bursa less wrapped, forming less than one turn **19**
- 19 Arch of copulatory bursa describing a half-turn..... **20**
- Arch of the copulatory bursa describing only a quarter turn..... **27**
- 20 Copulatory bursa gradually narrow at the apex..... **21**
- Copulatory bursa abruptly narrow at the apex **22**
- 21 Apex of the copulatory bursa descending at the joint of the basivalvar sclerites..... ***P. verrucigena* Karsch, 1891** [Cameroon]
- Apex of the bursa descending below the joint of the basivalvar sclerites ...
..... ***P. teocchii* Donskoff, 1981** [Cameroon, Central African Republic, Congo-Brazzaville]
- 22 Basivalvar sclerites almost straight **23**
- Basivalvar sclerites angular **24**
- 23 Basivalvar sclerites acute ***P. descampsi* Donskoff, 1981** [Cameroon]
- Basivalvar sclerites obtuse.....
..... ***P. meridionalis* Donskoff, 1981** [Democratic Republic of Congo]
- 24 Basivalvar sclerites forming a right angle. Arch of copulatory bursa thin and slender ***P. femorata* (Giglio-tos, 1907)** [Angola, Congo-Brazzaville, Democratic Republic of Congo]
- Basivalvar sclerites obtuse, arch of copulatory bursa short **25**
- 25 Base of the spermathecal duct widened
..... ***P. bredoi* Donskoff, 1981** [Democratic Republic of Congo]
- Base of spermathecal duct narrow **26**
- 26 Anterior apodemes of the subgenital plate short ***P. spleniata* (Karsch, 1896)** [Congo-Brazzaville, Democratic Republic of Congo]
- Anterior apodemes of the subgenital plate long..... ***P. congoensis* Donskoff, 1981** [Congo-Brazzaville, Democratic Republic of Congo, Gabon]
- 27 Roof of the copulatory bursa membranous. The base of the spermathecal duct widened to twice the length of the space between the bases of the two basivalvar sclerites..... ***P. balachowskyi* Donskoff, 1981** [Cameroon, Gabon]
- Bottom of the copulatory bursa thickened. The base of the spermathecal duct widened forming a short arch **28**
- 28 Distal, recurrent section of the lateral spermathecal diverticulum > 4× longer than the proximal section, well-enveloping
..... ***P. pillaulti* Donskoff, 1981** [Congo-Brazzaville]
- Distal, recurrent section of the lateral diverticulum of the spermatheca 3× longer than the proximal section, less enveloping
..... ***P. morini* Donskoff, 1981** [Congo-Brazzaville]

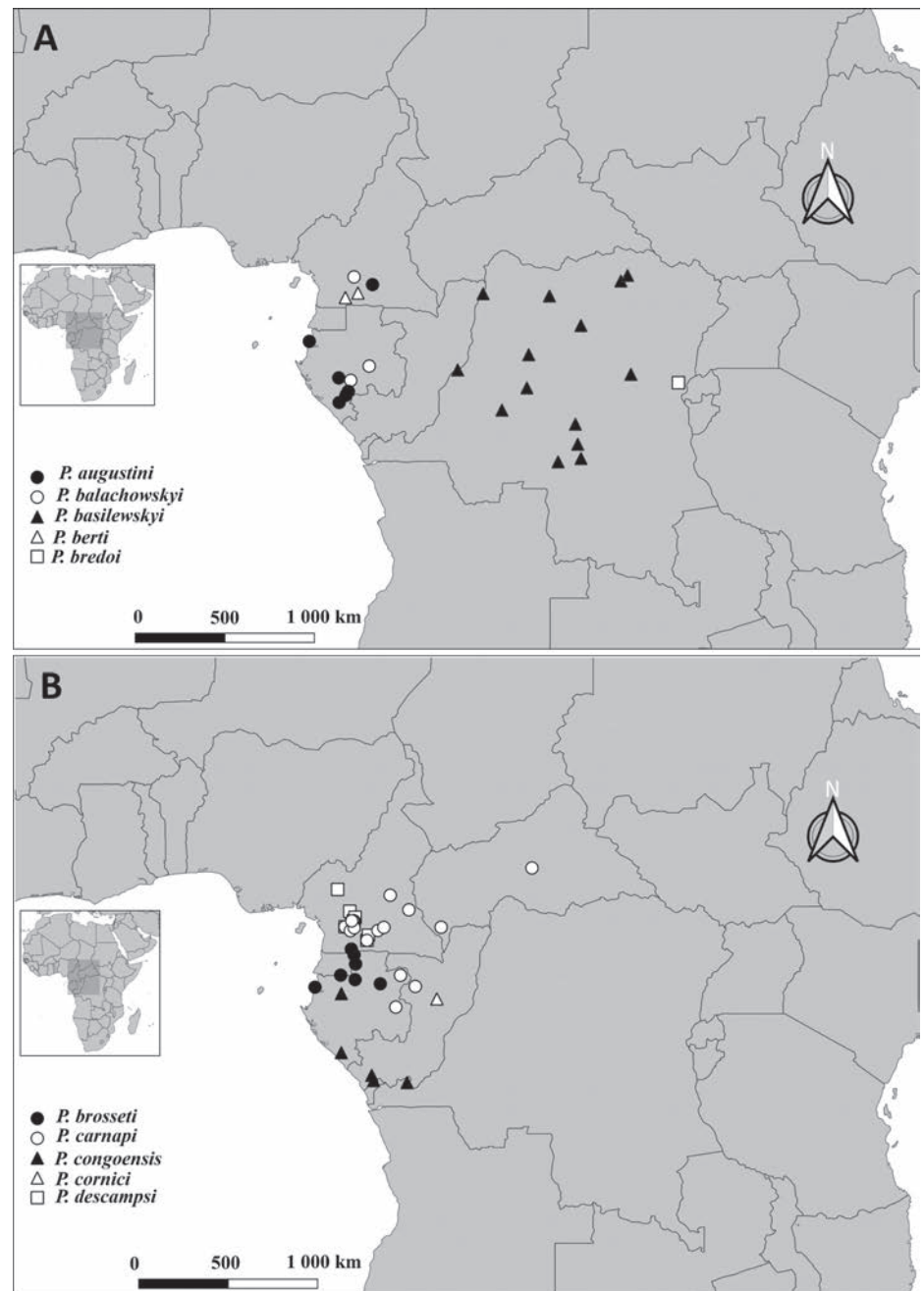


Figure 16. Distribution of *Pteropera* species in African rainforests.

Discussion

Although some attempts have been made to generate the DNA barcode data of orthopterans and mantids from the Central African Republic, Gabon, Ivory Coast, and South Africa (Moulin et al. 2017; Massa et al. 2018; O’Hare et al. 2023), no molecular attempts focusing on Orthoptera have been made in Cameroon thus far. Thus, the present study presents the first barcode data of morphologically identified *Pteropera* species from Cameroon. Many species of this diversified genus are not included in our analyses, as most of them are known only from museum collections of old samples for which it was not possible to extract DNA. We included only Cameroonian species for which we had fresh samples in the trees. Our results revealed that all these *Pteropera* species were

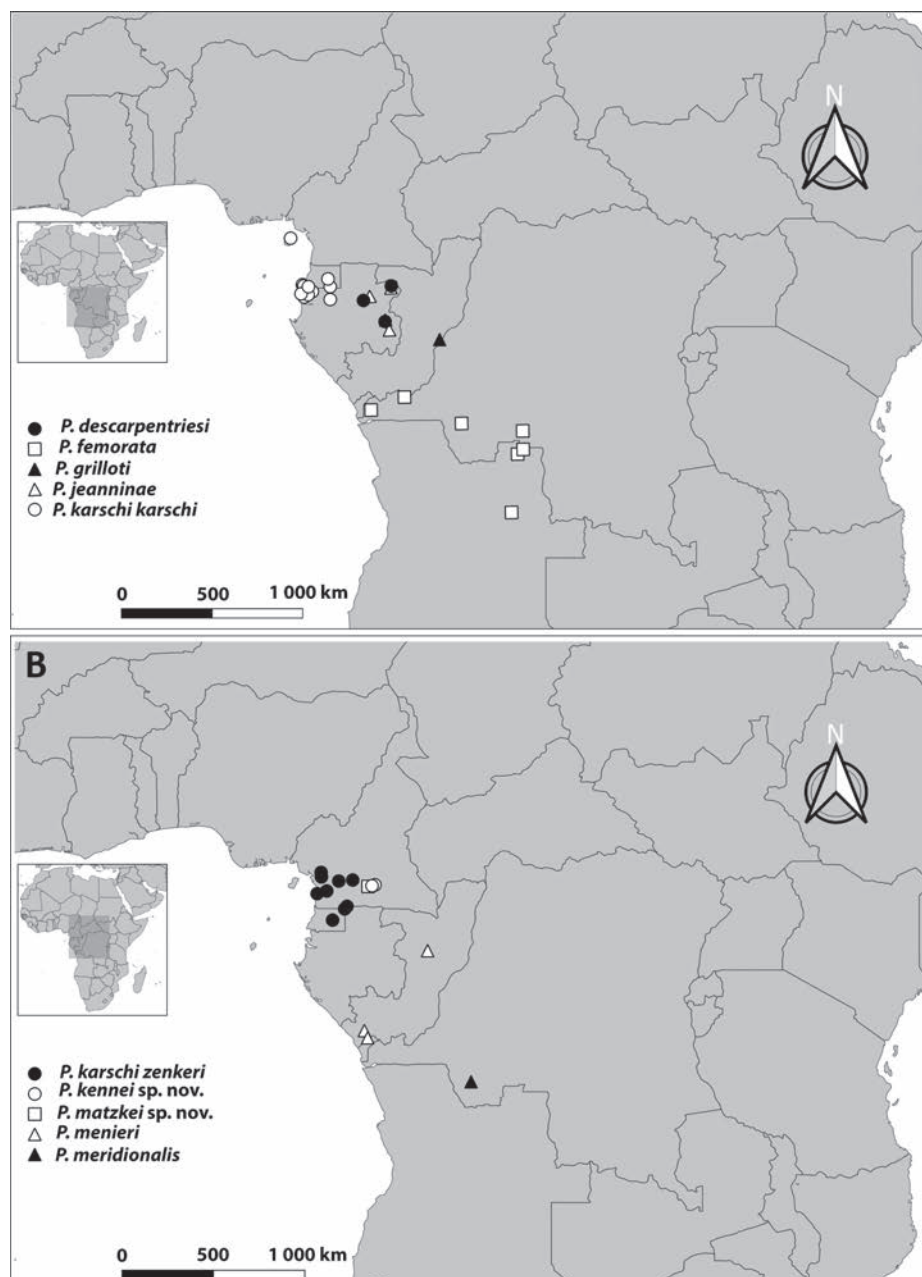


Figure 17. Distribution of *Pteropera* species in African rainforests.

monophyletic, including the newly described taxa. Hence, with the combined data, we are confident that the newly discovered taxa are indeed valid species. Hence, our study demonstrates the potential of using classic DNA barcoding to delimit species and the use of a multilocus dataset to estimate well-supported phylogenetic trees. However, further studies including a larger dataset are needed to obtain a more complete image of the true diversity of the genus.

The works by Ramme (1929) and Donskoff (1981) have thus far been the only contributions to the taxonomy of the genus *Pteropera*. Most species of this genus have restricted distributions; 21 of the 27 previously known species have been recorded only from single localities. In this study, we review the genus through an integrated taxonomic approach and describe three new species. We highlight some morphological differences in some species in comparison

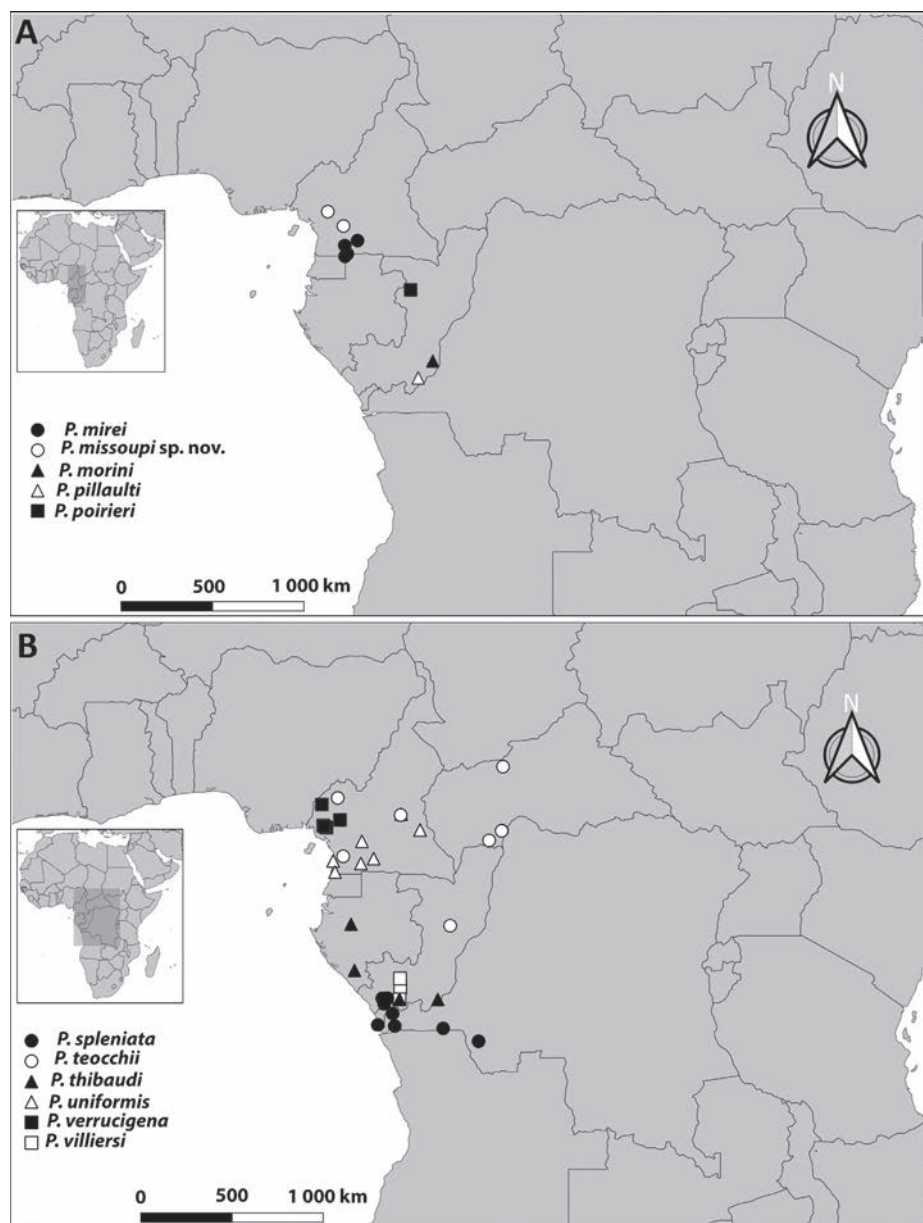


Figure 18. Distribution of *Pteropera* species in African rainforests.

with Donskoff's (1981) descriptions. In *P. carnapi* for example, the apodemes of the cingulum were slender and exceeded the level of separation of endophallic valves, with a strongly incurved apex. In contrast, these structures do not exceed the level of separation of the endophallic valves according to Donskoff (1981). In addition, Donskoff's (1981) descriptions of *P. descampsi* revealed that the apodemes of the cingulum as project at the level of the ejaculatory sac, whereas these structures reach the apex of the endophallic sclerites according to our observations. These differences observed in both studies related to *P. carnapi* and *P. descampsi* could be explained by the intraspecific variation that may have occurred within the genus *Pteropera*.

Moreover, we failed to find three *Pteropera* species previously reported from Cameroon, probably because we did not have the opportunity to sample the localities where they were reported and because most species

are narrow endemics. These species are *P. bertii* and *P. mirei* (both known from Koemvone and Ebolowa in the southern part of Cameroon) and *P. teocchii* (known from Bafut in the western part and Goyoum in the eastern part of Cameroon).

Nevertheless, the distribution range of *P. augustini*, which is known only from Gabon, was extended in this study, as we were able to report the species from Cameroon for the first time. The new record of *P. augustini*, combined with the description of three new species, increases the number of *Pteropera* present in Cameroon from eight to 12 species, and overall to 30 species and subspecies that are currently recorded from Afrotropical regions. Nevertheless, this genus may be more diverse than currently known, given the large number of localities in the African rainforests that have not yet been investigated in general and in Cameroon in particular. Thus, further sampling efforts at different locations and habitat types are needed.

Acknowledgments

The authors thank Cameroon's Ministry of Scientific Research and Innovation for granting the research permit for field collection (N°: 0000010/MINRESI/B00/C00/C10/C13). The authors also thank the Museum of Nature Hamburg for providing the necessary facilities. We are grateful to Prof. Laure Desutter-Grandcolas for permitting us to check the types and paratypes at the Muséum National d'Histoire Naturelle Paris, France. We are also grateful to Dr. Iker Iisari (Manager of Phylogenetic and Phylogenomic section at the ZMH), Dr. Oliver Hawlitschek, Dr. Lara-Sophie Dey, and Dr. Karina Brandao (curator of Lepidoptera at the ZMH) for their support and advice.

Additional information

Conflict of interest

The authors have declared that no competing interests exist.

Ethical statement

No ethical statement was reported.

Funding

This work was financially supported by the Alexander von Humboldt Foundation. The Orthopterists' Society provided additional funding for sequencing genomics through the Theodore J. Cohn research grant 2023. This work also received support from the Linnean Society and the Systematics Association through LineSys: Systematic Research Fund grant 2023.

Author contributions

J.A. Yetchom Fondjo and M. Husemann conceived the study; J.A. Yetchom Fondjo performed the experiments, analyzed the data, and wrote the manuscript; M. Husemann also contributed to the interpretation of the results, provided critical feedback, and contributed to the final manuscript; A. R. Nzoko Fiemapong, M. Tindo, S. Ivković, and T. Fite Duressa provided critical feedback and contributed to the final manuscript.

Author ORCIDs

Jeanne Agrippine Yetchom Fondjo  <https://orcid.org/0000-0003-2192-6366>
Armand Richard Nzoko Fiemapong  <https://orcid.org/0000-0002-8759-8142>
Maurice Tindo  <https://orcid.org/0000-0001-6217-6982>
Tarekegn Fite Duressa  <https://orcid.org/0000-0003-3492-4933>
Slobodan Ivković  <https://orcid.org/0000-0001-5571-8245>
Martin Husemann  <https://orcid.org/0000-0001-5536-6681>

Data availability

All of the data that support the findings of this study are available in the main text or Supplementary Information.

References

- Bruvo-Madarić B, Huber BA, Steinacher A, Pass G (2005) Phylogeny of pholcid spiders (Araneae: Pholcidae): Combined analysis using morphology and molecules. *Molecular Phylogenetics and Evolution* 37: 661–673. <https://doi.org/10.1016/j.ympev.2005.08.016>
- Cigliano MM, Braun H, Eades DC, Otte D (2024) *Pteropera femorata* (Giglio-Tos, 1907). Orthoptera Species File. <http://orthoptera.speciesfile.org/otus/815879/overview>
- Dirsh VM (1965) The African genera of Acridoidea. Anti-Locust Research Centre and Cambridge University Press, London, 579 pp.
- Donskoff M (1981) Les acridiens de la forêt africaine. I. Révision du genre *Pteropera* Karsch, 1891 (Orthoptera, Acrididae). *Annales de la Société entomologique de France* (N.S.) 17 (1): 33–88. [51 figs] <https://doi.org/10.1080/21686351.1981.12278263>
- Edgar RC (2004) MUSCLE: a multiple sequence alignment method with reduced time and space complexity. *BMC Bioinformatics* 5: 113. <https://doi.org/10.1186/1471-2105-5-113>
- Folmer O, Black M, Hoeh W, Lutz R, Vrijenhoek R (1994) DNA primers for amplification of mitochondrial cytochrome c oxidase subunit I from diverse metazoan invertebrates. *Molecular Marine Biology and Biotechnology* 3: 294–299.
- Hall TA (1999) BioEdit: A User-Friendly Biological Sequence Alignment Editor and Analysis Program for Windows 95/98/NT. *Nucleic Acids Symposium Series* 41: 95–98.
- Johnston HB (1956) Annotated catalogue of African grasshoppers. Cambridge University Press, 833 pp.
- Johnston HB (1968) Annotated catalogue of African grasshoppers. Supplement. Cambridge University Press for the Anti-Locust Research Centre, London, xiv + 448 pp.
- Karsch F (1891) Verzeichniss der von Herrn Dr. Paul Preuss in Kamerun erbeuteten Acridiideen. *Berliner Entomologische Zeitschrift* 36(1): 175–196. <https://doi.org/10.1002/mmnd.18910360116>
- Kearse M, Moir R, Wilson A, Stones-Havas S, Cheung M, Sturrock S, Buxton S, Cooper A, Markowitz S, Duran C, Thierer T, Ashton B, Meintjes P, Drummond A (2012) Geneious Basic: an integrated and extendable desktop software platform for the organization and analysis of sequence data. *Bioinformatics* 28(12): 1647–1649. <https://doi.org/10.1093/bioinformatics/bts199>
- Kevan DKM, Akbar SS, Chang YC (1969) The concealed copulatory structures of Pyrgomorphidae (Orthoptera: Acridoidea). Part I. General introduction. *Eos* 44: 165–266.
- Kirby WF (1910) A synonymic catalogue of Orthoptera. Vol. 3. Orthoptera Saltatoria. Part 2. Locustidae vel Acridiidae. Taylor & Francis, London, for the British Museum (Natural History), London, vii + 674 pp.

- Martinelli AB, Waichert C, Barbosa DN, Fagundes V, Azevedo C (2017) The use of Proteinase K to access genitalia morphology, vouchering and DNA extraction in minute wasps. *Annals of the Brazilian Academy of Sciences* 89(3): 1629–1633. <https://doi.org/10.1590/0001-3765201720160825>
- Massa B, Heller KG, Warchałowska-Śliwa E, Moulin N (2018) The tropical African genus *Morgenia* (Orthoptera, Tettigoniidae, Phaneropterinae) with emphasis on the spur at the mid tibia. *Deutsche Entomologische Zeitschrift*. 65 (2): 161–175. <https://doi.org/10.3897/dez.65.26693>
- Moulin N, Decaëns T, Annoyer P (2017) Diversity of mantids (Dictyoptera: Mantodea) of Sangha-Mbaere Region, Central African Republic, with some ecological data and DNA barcoding. *Journal of Orthoptera Research* 26(2): 117–1. <https://doi.org/10.3897/jor.26.19863>
- Nguyen LT, Schmidt HA, von Haeseler A, Quang Minh B (2015) IQ-TREE: A fast and effective stochastic algorithm for estimating maximum likelihood phylogenies. *Molecular Biology and Evolution* 32: 268–274. <https://doi.org/10.1093/molbev/msu300>
- O'Hare M, Sylvain Huguel S, Hendrickse M, Greyling C, Egan B, van Asch B (2023) Documenting the biodiversity of edible grasshoppers in South Africa with traditional knowledge, classic taxonomy and genetic information. *Biodiversity and Conservation* 32:3481–3502. <https://doi.org/10.1007/s10531-023-02676-x>
- Otte D (1995) Orthoptera species file. 4. Grasshoppers [Acridomorpha]. C. Acridoidea. Orthopterists' Society & Academy of Natural Sciences of Philadelphia, vii + 518 pp.
- Palumbi SR, Martin A, Romano S, McMillan WO, Stice L, Garbowski G (1991) The simple fools guide to PCR. A collection of PCR protocols, version 2. University of Hawaii, Honolulu, 45 pp.
- Paxton RJ, Thorén PA, Tengö J, Estoup A, Pamilo P (1996) Mating structure and nest-mate relatedness in a communal bee, *Andrena jacobii* (Hymenoptera, Andrenidae), using microsatellites. *Molecular Ecology* 5: 511–519. <https://doi.org/10.1111/j.1365-294X.1996.tb00343.x>
- Rambaut A (2010) FigTree v1.3.1. Institute of Evolutionary Biology, University of Edinburgh, Edinburgh. <http://tree.bio.ed.ac.uk/software/figtree/>
- Ramme W (1929) Afrikanische Acrididae. Revisionen und Beschreibungen wenig bekannter und neuer Gattungen und Arten. *Mitteilungen aus dem zoologischen Museum in Berlin* 15: 247–492. <https://doi.org/10.1002/mmnz.4830150202>
- Ronquist F, Teslenko M, van der Mark P, Ayres D, Darling A, Hohn S, Larget B, Liu L, Suchard MA, Huelsenbeck JP (2012b) MrBayes 3.2: efficient Bayesian phylogenetic inference and model choice across a large model space. *Systematic Biology* 61: 539–542. <https://doi.org/10.1093/sysbio/sys029>
- Rowell CHF (2013) The Grasshoppers (Caelifera) of Costa Rica and Panama. The Orthopterists' Society publications on Orthopteran diversity, Illinois Natural History Survey, Illinois, USA, 611 pp.
- Rowell CHF, Jago ND, Hemp C (2018) Revision of *Aresceutica* (Orthoptera: Acrididae: Catantopinae) with comments on related genera. *Journal of Orthoptera Research* 27(2): 107–118. <https://doi.org/10.3897/jor.27.23441>
- Sjöstedt Y (1931) Acridoidea aus Kongo und anderen Teilen von Afrika. *Arkiv för Zoologi* (A) 22 (15): 1–64.
- Yetchom Fondjo JA, Kekeunou S, Kenne M, Missoup AD, Huang H, Libin M, Sheng-Quan X (2019) A Checklist of Short-horned Grasshopper Species (Orthoptera: Caelifera) from Littoral Region of Cameroon with description of a new species of the genus *Hemierianthus* Saussure, 1903 (Orthoptera: Chorotypidae). *Zootaxa* 4706 (2): 311–331. <https://doi.org/10.11646/zootaxa.4706.2.6>

Supplementary material 1

Locations and coordinates of all species of *Pteropera*

Authors: Jeanne Agrippine Yetchom Fondjo, Armand Richard Nzoko Fiemapong, Maurice Tindo, Tarekegn Fite Duressa, Slobodan Ivković, Martin Husemann

Data type: csv

Explanation note: Localities and geographical coordinates used to map the distribution of *Pteropera* species (CAR = Central African REPUBLIC; DRC = Democratic Republic of Congo).

Copyright notice: This dataset is made available under the Open Database License (<http://opendatacommons.org/licenses/odbl/1.0/>). The Open Database License (ODbL) is a license agreement intended to allow users to freely share, modify, and use this Dataset while maintaining this same freedom for others, provided that the original source and author(s) are credited.

Link: <https://doi.org/10.3897/zookeys.1216.130270.suppl1>

Nine new spider species of *Belisana* Thorell, 1898 (Araneae, Pholcidae) from karst caves, with a list of species of the genus from Guizhou, southwestern China

Bing Wang¹, Jinglin Li¹, Shuqiang Li², Zhiyuan Yao¹

¹ College of Life Science, Shenyang Normal University, Shenyang 110034, Liaoning, China

² Institute of Zoology, Chinese Academy of Sciences, Beijing 100101, China

Corresponding authors: Zhiyuan Yao (yaozy@synu.edu.cn); Shuqiang Li (lisq@ioz.ac.cn)

Abstract

Species of the spider genus *Belisana* Thorell, 1898 exhibit high diversity in Guizhou, southwestern China. Previously, only eight species of *Belisana* were recorded in Guizhou. In this study, nine new species are described from karst caves: *Belisana bijie* Wang, S. Li & Yao, **sp. nov.**, *B. liupanshui* Wang, S. Li & Yao, **sp. nov.**, *B. majiang* Wang, S. Li & Yao, **sp. nov.**, *B. nayong* Wang, S. Li & Yao, **sp. nov.**, *B. qixingguan* Wang, S. Li & Yao, **sp. nov.**, *B. xiuwen* Wang, S. Li & Yao, **sp. nov.**, *B. yongcong* Wang, S. Li & Yao, **sp. nov.**, *B. zhouxi* Wang, S. Li & Yao, **sp. nov.**, and *B. zunyi* Wang, S. Li & Yao, **sp. nov.** *Belisana zhangji* Tong & Li, 2007 is reported from Guizhou for the first time. In addition, a list of all species of *Belisana* from Guizhou is provided.

Key words: Biodiversity, cellar spiders, daddy-long-legs, invertebrate, morphology, taxonomy



Academic editor: Alireza Zamani

Received: 20 July 2024

Accepted: 3 October 2024

Published: 25 October 2024

ZooBank: <https://zoobank.org/0E173F72-36D3-4B97-BC43-F096067A3D1E>

Citation: Wang B, Li J, Li S, Yao Z (2024) Nine new spider species of *Belisana* Thorell, 1898 (Araneae, Pholcidae) from karst caves, with a list of species of the genus from Guizhou, southwestern China. ZooKeys 1216: 265–302. <https://doi.org/10.3897/zookeys.1216.132561>

Copyright: © Bing Wang et al.
This is an open access article distributed under terms of the Creative Commons Attribution License (Attribution 4.0 International – CC BY 4.0).

Introduction

Belisana Thorell, 1898, the second largest genus in the Pholcidae C.L. Koch, 1850, comprises 160 species (WSC 2024). These species inhabit diverse micro-habitats, e.g., beneath rocks, in caves, on the underside of leaves, among leaf litter, and amidst foliage in the canopy (Huber 2005; Yao et al. 2015; Zhao et al. 2023a). They are primarily distributed in southern China, as well as in the Indo-Malayan and Australasian regions (Huber 2005; Yao and Li 2013; Yao et al. 2018; Zhu et al. 2020; Zhu and Li 2021). Currently, 46% of the species (74 spp.) have been documented from southern China (WSC 2024), of which Yunnan boasts the highest concentration of species, accounting for 42% (31 spp.; Zhang et al. 2024b). Guangxi and Hainan, which have the second and third highest species diversity of *Belisana*, respectively, have recorded only 11 and ten species. Recently, numerous surveys targeting pholcid spiders have been conducted in China, resulting in the discovery and reporting of a large number of new species (e.g., Yao et al. 2021; Lu et al. 2022; Zhao et al. 2023b; Yang et al. 2024a, b). Nevertheless, these efforts have primarily focused on *Pholcus* Walckenaer, 1805, found in epigeal environments in northern and central

China, with relatively few reports on *Belisana* from hypogean environments in southern China (10 spp.; Wang et al. 2024; Zhang et al. 2024a, b).

Guizhou, located in the southwest of China, is renowned for its abundant karst caves. The extreme cave environmental conditions have been regarded as the primary factors of maintaining species endemism within caves (Lefébure et al. 2006; Yao et al. 2016). Nevertheless, only eight endemic species of *Belisana* have been recorded from Guizhou (Chen et al. 2009; Zhang and Peng 2011; Chen et al. 2016; Yang et al. 2023a; Wang et al. 2024). Among these, seven species are collected from caves. This work aims to report the nine new species, a new record found in karst caves (Fig. 1), and to provide an updated list of species of *Belisana* from Guizhou (Table 1).

Materials and methods

Specimens were examined and measured with a Leica M205 C stereomicroscope. Left male palps were photographed. Epigynes were photographed before dissection. Vulvae were photographed after treating them in a 10% warm solution of potassium hydroxide (KOH) to dissolve soft tissues. Images were captured with a Canon EOS 750D wide zoom digital camera (24.2 megapixels) mounted on the stereomicroscope mentioned above and assembled using Helicon Focus v. 3.10.3 image stacking software (Khmelik et al. 2005). Drawings were done with Procreate 5.0.2 (Savage Interactive Pty. Ltd.). All measurements are given in millimeters (mm). Leg measurements are shown as: total length (femur, patella, tibia, metatarsus, tarsus). Leg segments were measured on their dorsal sides. The distribution map was generated with ArcGIS v. 10.2 (ESRI Inc.). The specimens studied are preserved in 75% ethanol and deposited in the Institute of Zoology, Chinese Academy of Sciences (**IZCAS**) in Beijing, China.

Table 1. A list of species of *Belisana* from Guizhou, China.

No.	Species	Habitat	Reference
1	<i>B. bijie</i> sp. nov.	karst cave	this paper
2	<i>B. daji</i> Chen, Zhang & Zhu, 2009	karst cave	Chen et al. (2009)
3	<i>B. douqing</i> Chen, Zhang & Zhu, 2009	karst cave	Chen et al. (2009)
4	<i>B. galeiformis</i> Zhang & Peng, 2011	/	Zhang and Peng (2011)
5	<i>B. lii</i> Chen, Yu & Guo, 2016	karst cave	Chen et al. (2016)
6	<i>B. liupanshui</i> sp. nov.	karst cave	this paper
7	<i>B. majiang</i> sp. nov.	karst cave	this paper
8	<i>B. nayong</i> sp. nov.	karst cave	this paper
9	<i>B. qixingguan</i> sp. nov.	karst cave	this paper
10	<i>B. wangchengi</i> Wang, Yao & Zhang, 2024	karst cave	Wang et al. (2024)
11	<i>B. xishui</i> Chen, Zhang & Zhu, 2009	karst cave	Chen et al. (2009)
12	<i>B. xiuwen</i> sp. nov.	karst cave	this paper
13	<i>B. yanhe</i> Chen, Zhang & Zhu, 2009	karst cave	Chen et al. (2009)
14	<i>B. yongcong</i> sp. nov.	karst cave	this paper
15	<i>B. yuhaoi</i> Yang & Yao, 2023	karst cave	Yang et al. (2023a)
16	<i>B. zhangji</i> Tong & Li, 2007	karst cave	this paper; Tong and Li (2007)
17	<i>B. zhouxi</i> sp. nov.	karst cave	this paper
18	<i>B. zunyi</i> sp. nov.	karst cave	this paper

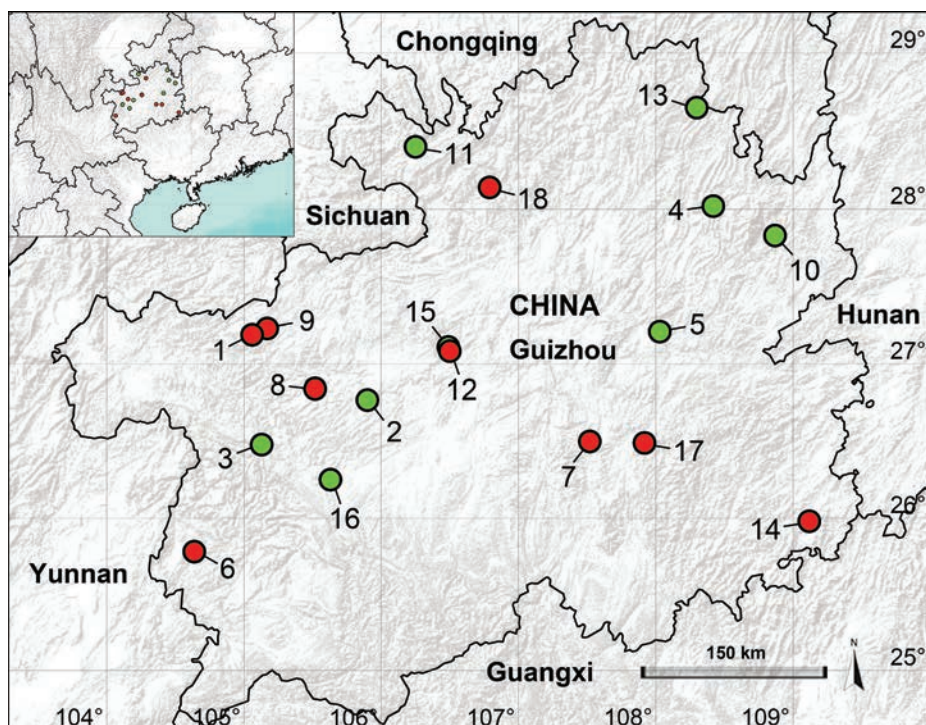


Figure 1. Distribution records of the *Belisana* species from Guizhou, China **1** *Belisana bijie* sp. nov. **2** *B. daji* Chen, Zhang & Zhu, 2009 **3** *B. douqing* Chen, Zhang & Zhu, 2009 **4** *B. galeiformis* Zhang & Peng, 2011 **5** *B. lii* Chen, Yu & Guo, 2016 **6** *B. liupanshui* sp. nov. **7** *B. majiang* sp. nov. **8** *B. nayong* sp. nov. **9** *B. qixingguan* sp. nov. **10** *B. wangchengi* Wang, Yao & Zhang, 2024 **11** *B. xishui* Chen, Zhang & Zhu, 2009 **12** *B. xiuwen* sp. nov. **13** *B. yanhe* Chen, Zhang & Zhu, 2009 **14** *B. yongcong* sp. nov. **15** *B. yuhai* Yang & Yao, 2023 **16** *B. zhangji* Tong & Li, 2007 **17** *B. zhouxi* sp. nov. **18** *B. zunyi* sp. nov.

Terminology and taxonomic descriptions follow Huber (2005) and Yao et al. (2015). The following abbreviations are used: **aa** = anterior arch, **ALE** = anterior lateral eye, **b** = bulb, **ba** = bulbal apophysis, **da** = distal apophysis, **e** = embolus, **ep** = epigynal pocket, **f** = flap, **L/d** = length/diameter, **pa** = proximo-lateral apophysis, **PME** = posterior median eye, **pp** = pore plate, **pr** = procurus.

Taxonomy

Family Pholcidae C.L. Koch, 1850

Subfamily Pholcinae C.L. Koch, 1850

Genus *Belisana* Thorell, 1898

Type species. *Belisana tauricornis* Thorell, 1898.

***Belisana bijie* Wang, S. Li & Yao, sp. nov.**

<https://zoobank.org/938091C8-867C-4607-9EB1-9B4BE301F78F>

Figs 2, 3, 22A, B, 24A, B

Type material. Holotype: CHINA • ♂; Guizhou, Bijie, Qixingguan District, Salaxi Town, Shuanglongdao Cave; 27°11.493'N, 105°03.850'E; alt. 1920 m; 18 Nov. 2011; Z. Chen & Z. Zha leg.; IZCAS-Ar45175. **Paratype:** CHINA • 1 ♀; same data as for holotype; IZCAS-Ar45176.

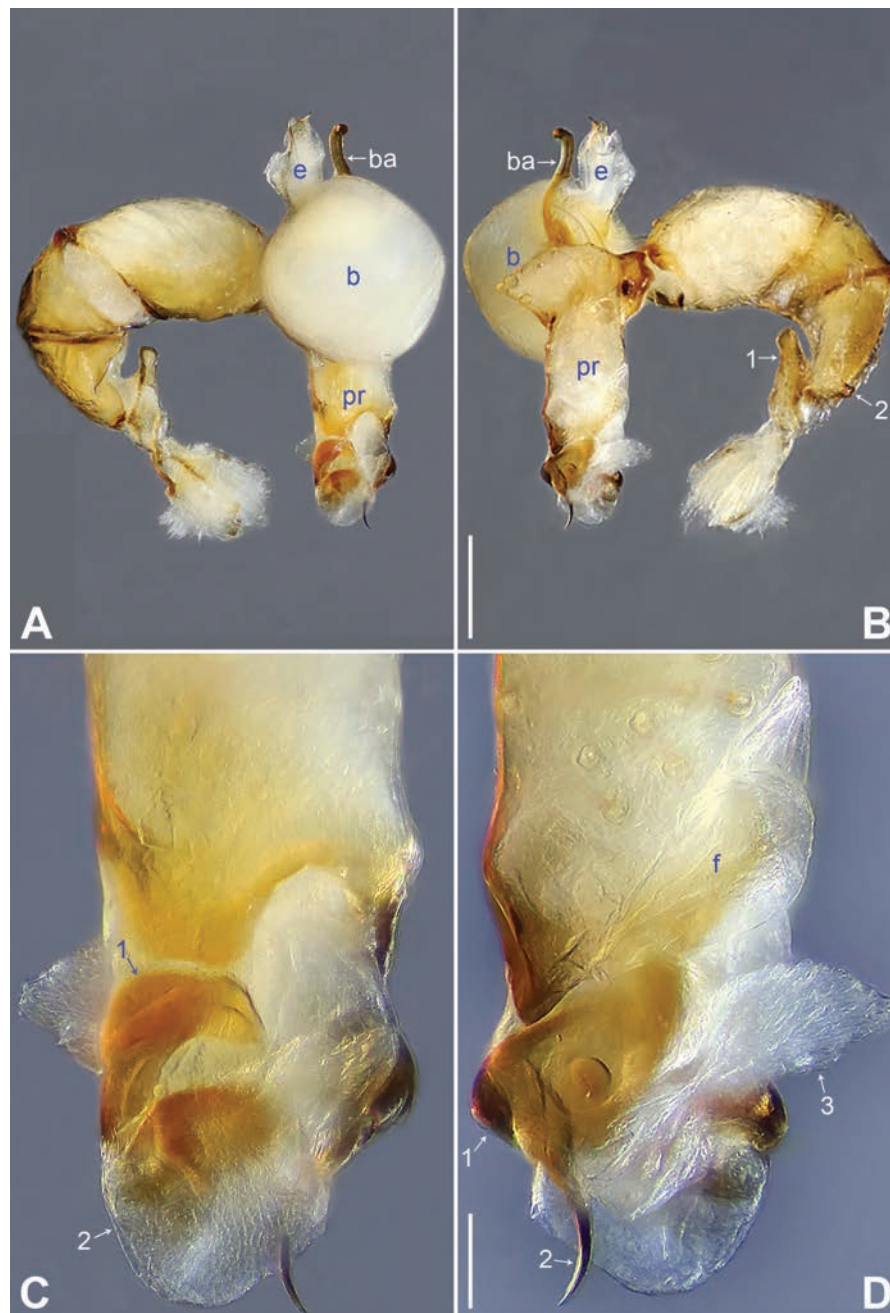


Figure 2. *Belisana bijie* sp. nov., holotype male **A, B** palp (**A** prolateral view **B** retrolateral view, arrow 1 points at ventral apophysis, arrow 2 points at retrolatero-proximal protrusion) **C, D** distal part of procurus (**C** prolateral view, arrow 1 points at prolatero-subdistal sclerite, arrow 2 points at prolatero-distal membranous lamella **D** retrolateral view, arrow 1 points at sclerotized dorso-subdistal apophysis, arrow 2 points at retrolatero-distal spine, arrow 3 points at retrolatero-subdistal membranous process). Abbreviations: b = bulb, ba = bulbal apophysis, e = embolus, f = flap, pr = procurus. Scale bars: 0.20 (**A, B**); 0.05 (**C, D**).

Diagnosis. The new species resembles *B. wangchengi* Wang, Yao & Zhang, 2024 (Wang et al. 2024: 2, figs 1A–D, 2A–H, 3A–D) by having similar male chelicerae (tips of distal apophyses widely separated and pointing inwards; Fig. 3D), bulbal apophysis (hooked; Fig. 3C), and epigyne (epigynal pockets on lateral part of epigynal plate; Figs 3A, 24A), but can be distinguished by procurus with retrolatero-subdistal membranous process (arrow 3 in Figs 2D, 22B vs absent), by vulval pore plates with nearly angular sclerites (arrow in Figs 3B, 24B vs

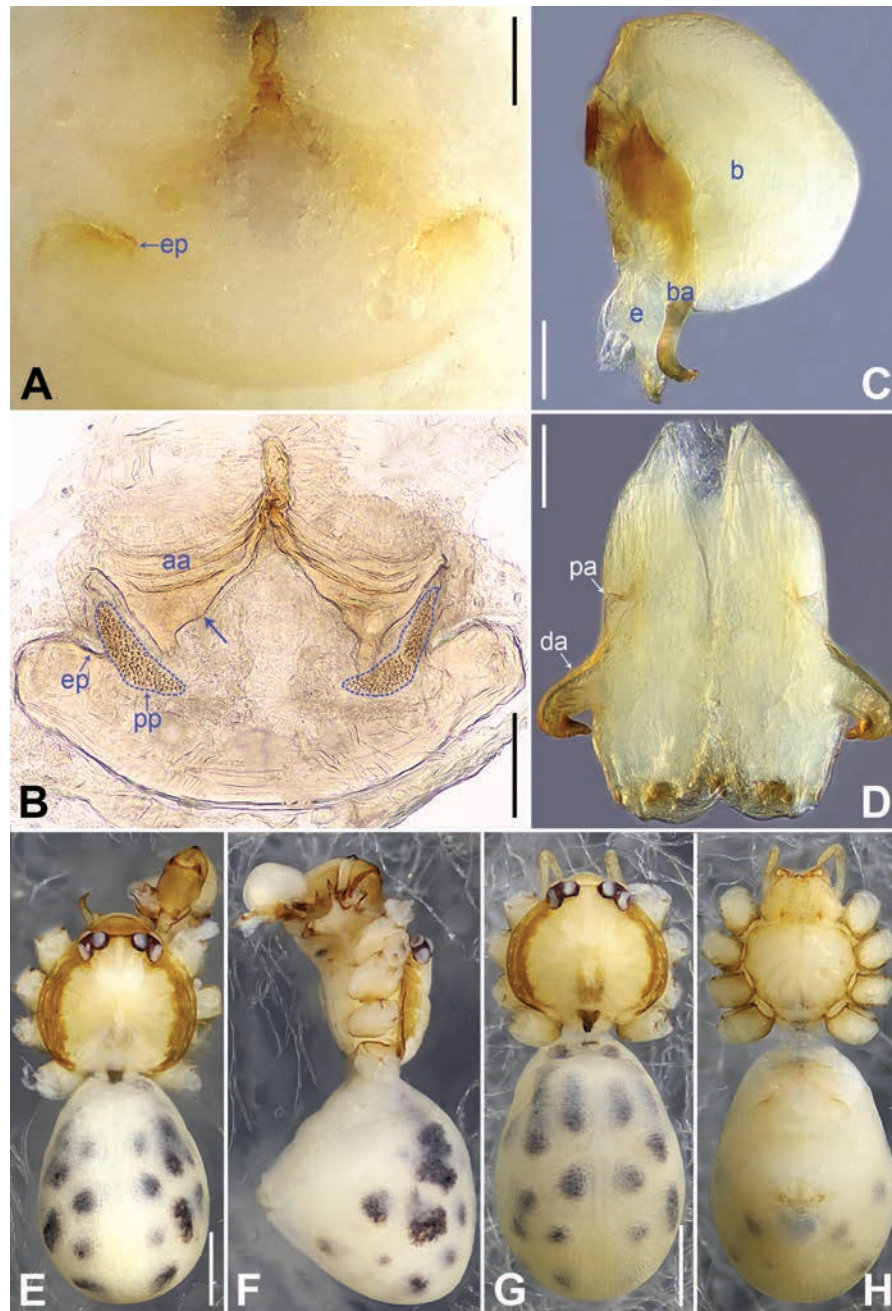


Figure 3. *Belisana bijie* sp. nov., holotype male (C–F) and paratype female (A, B, G, H) A epigyne, ventral view B vulva, dorsal view, arrow points at lateral sclerite C bulb, prolateral view D chelicerae, frontal view E–H habitus (E, G dorsal view F lateral view H ventral view). Abbreviations: aa = anterior arch, b = bulb, ba = bulbal apophysis, da = distal apophysis, e = embolus, ep = epigynal pocket, pa = proximo-lateral apophysis, pp = pore plate. Scale bars: 0.10 (A–D); 0.40 (E–H).

blunt), and by dorsal shield of prosoma with lateral brown bands (Fig. 3E, G vs absent, but with median radiating marks).

Description. Male (holotype): Total length 1.95 (2.08 with clypeus), prosoma 0.70 long, 0.82 wide, opisthosoma 1.25 long, 0.90 wide. Leg I: 19.96 (5.13, 0.38, 5.05, 7.52, 1.88), leg II: 13.25 (3.52, 0.37, 3.32, 4.70, 1.34), leg III: 7.81 (2.25, 0.30, 1.90, 2.59, 0.77), leg IV: 9.83 (3.09, 0.30, 2.45, 3.16, 0.83); tibia I L/d: 73. Eye interdistances and diameters: PME–PME 0.11, PME 0.10, PME–ALE 0.02. Sternum width/length: 0.63/0.56. Habitus as in Fig. 3E, F. Dorsal shield of prosoma yellowish, with brown lateral bands; clypeus brown; sternum yellowish.

Legs whitish, without darker rings. Opisthosoma yellowish, with black spots. Thoracic furrow absent. Clypeus unmodified. Chelicerae with pair of proximo-lateral apophyses (pa in Fig. 3D) and pair of curved distal apophyses (distance between tips: 0.31; da in Fig. 3D). Palp as in Fig. 2A, B; trochanter with ventral apophysis (2× longer than wide, arrow 1 in Fig. 2B); femur with retrolatero-proximal protrusion (arrow 2 in Fig. 2B); procurus simple proximally but complex distally, with prolatero-subdistal sclerite (arrow 1 in Figs 2C, 22A), prolatero-distal membranous lamella (arrow 2 in Figs 2C, 22A) bearing proximally sclerotized part, sclerotized dorso-subdistal apophysis (arrow 1 in Figs 2D, 22B), retrolatero-distal spine (arrow 2 in Figs 2D, 22B), retrolatero-subdistal membranous process (arrow 3 in Figs 2D, 22B), and retrolateral membranous flap (f in Figs 2D, 22B); bulb with hooked apophysis (ba in Fig. 3C) and simple embolus (e in Fig. 3C). Retrolateral trichobothria on tibia I at 9% proximally; legs with short vertical setae on metatarsi; tarsus I with 17 distinct pseudosegments.

Female (paratype, IZCAS-Ar45176): Similar to male, habitus as in Fig. 3G, H. Total length 1.96 (2.09 with clypeus), prosoma 0.66 long, 0.83 wide, opisthosoma 1.30 long, 1.01 wide; tibia I: 3.40; tibia I L/d: 49. Eye interdistances and diameters: PME–PME 0.10, PME 0.10, PME–ALE 0.02. Sternum width/length: 0.60/0.53. Dorsal shield of prosoma with distinct postero-median marks; clypeus yellowish. Epigyne simple and flat, posteriorly curved, with pair of lateral pockets 0.31 apart (ep in Figs 3A, 24A). Vulva with ridge-shaped anterior arch bearing pair of nearly angular sclerites (arrow in Figs 3B, 24B), and pair of nearly triangular pore plates (4× longer than wide, pp in Figs 3B, 24B).

Habitat. The species was found in the dark zone inside the cave.

Distribution. China (Guizhou, type locality; Fig. 1).

Etymology. The specific name refers to the type locality; noun in apposition.

***Belisana liupanshui* Wang, S. Li & Yao, sp. nov.**

<https://zoobank.org/4C5D21CD-86E7-43FA-B974-0235DB601B2B>

Figs 4, 5, 22C, D, 24C, D

Type material. Holotype: CHINA • ♂; Guizhou, Liupanshui, Pan County, Biyun Cave; 25°46.527'N, 104°38.278'E; alt. 1468 m; 13 Apr. 2007; J. Liu & Y. Lin leg.; IZCAS-Ar45181. **Paratypes:** CHINA • 5♂; same data as for holotype; IZCAS-Ar45182–86 • 7♀; same data as for holotype; IZCAS-Ar45187–93.

Diagnosis. The new species resembles *B. jiuxiang* Zhang, Li & Yao, 2024 (Zhang et al. 2024b: 261, figs 4A–D, 5A–H, 18C, D, 20C, D) by having similar male chelicerae (distal apophyses directed towards frontally, but tips pointing inwards; Fig. 5D) and epigyne (epigynal pockets on median part of epigynal plate, epigynal plate posteriorly straight; Figs 5A, 24C), but can be distinguished by procurus with prolatero-subdistal and subdistal membranous processes (arrows 1, 3 in Figs 4C, 22C vs absent) and nearly rectangle dorso-subdistal membranous process (arrow 4 in Figs 4C, 22C vs angular), by bulbal apophysis with angular subdistal apophysis (arrow in Fig. 5C vs absent), and by vulval pore plates anteriorly narrow and posteriorly wide (pp in Figs 5B, 24D vs nearly quadrilateral).

Description. Male (holotype): Total length 1.71 (1.79 with clypeus), prosoma 0.63 long, 0.67 wide, opisthosoma 1.08 long, 0.81 wide. Leg I: – (4.04, 0.29, 4.50, 5.96, –), leg II: 11.08 (2.80, 0.30, 2.97, 3.92, 1.09), leg III: 7.98 (2.22, 0.25,

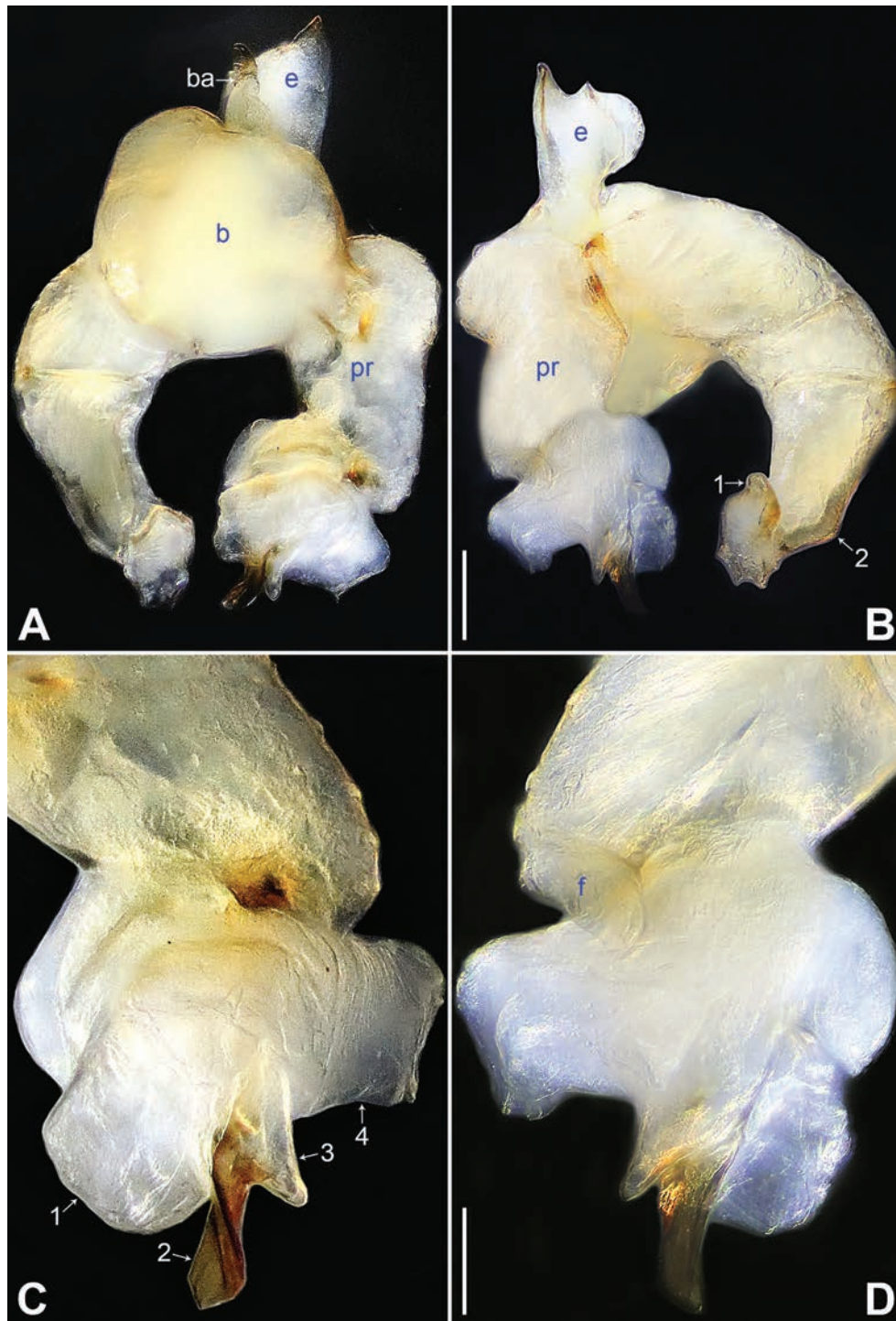


Figure 4. *Belisana liupanshui* sp. nov., holotype male **A, B** palp (**A** prolateral view **B** retrolateral view, arrow 1 points at ventral apophysis, arrow 2 points at retrolatero-proximal protrusion) **C, D** distal part of procurus (**C** prolateral view, arrow 1 points at prolatero-subdistal membranous process, arrow 2 points at sclerotized distal apophysis, arrow 3 points at subdistal membranous process, arrow 4 points at dorso-subdistal membranous process **D** retrolateral view). Abbreviations: b = bulb, ba = bulbal apophysis, e = embolus, f = flap, pr = procurus. Scale bars: 0.10 (**A, B**); 0.05 (**C, D**).

1.98, 2.72, 0.81), leg IV: 10.20 (3.00, 0.26, 2.63, 3.45, 0.86); tibia I L/d: 63. Eye interdistances and diameters: PME–PME 0.09, PME 0.08, PME–ALE 0.02. Sternum width/length: 0.51/0.44. Habitus as in Fig. 5E, F. Dorsal shield of prosoma yellowish, with brownish radiating marks; clypeus brownish; sternum yellowish.

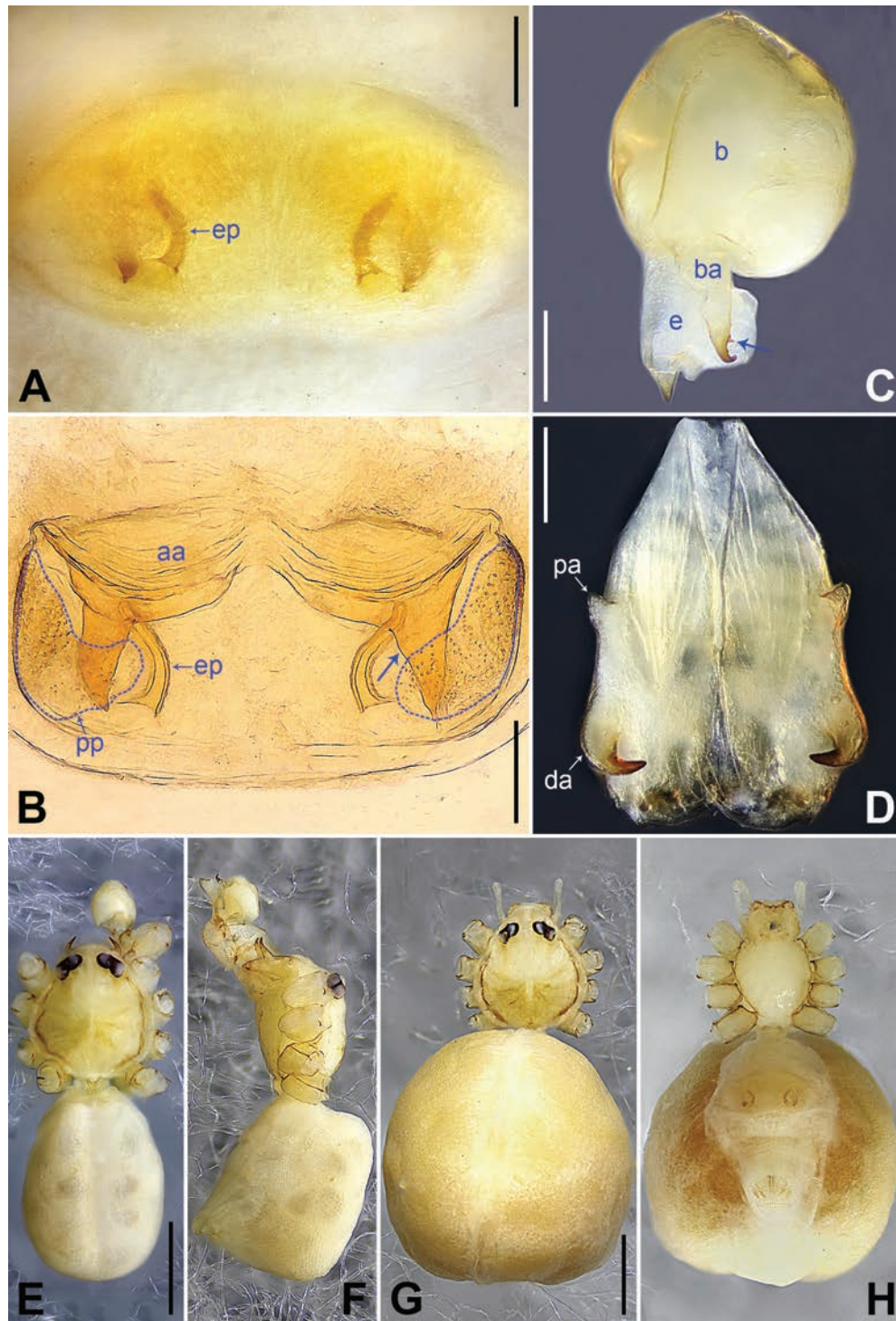


Figure 5. *Belisana liupanshui* sp. nov., holotype male (C–F) and paratype female (A, B, G, H) **A** epigyne, ventral view **B** vulva, dorsal view, arrow points at lateral sclerite **C** bulb, prolateral view, arrow points at subdistal apophysis **D** chelicerae, frontal view **E–H** habitus (**E, G** dorsal view **F** lateral view **H** ventral view). Abbreviations: aa = anterior arch, b = bulb, ba = bulbal apophysis, da = distal apophysis, e = embolus, ep = epigynal pocket, pa = proximo-lateral apophysis, pp = pore plate. Scale bars: 0.10 (A–D); 0.50 (E–H).

Legs whitish, without darker rings. Opisthosoma yellowish, without spots. Thoracic furrow absent. Clypeus unmodified. Chelicerae with pair of proximo-lateral apophyses (pa in Fig. 5D) and pair of curved distal apophyses (distance between tips: 0.17; da in Fig. 5D). Palp as in Fig. 4A, B; trochanter with ventral

apophysis (as long as wide, arrow 1 in Fig. 4B); femur with retrolatero-proximal protrusion (arrow 2 in Fig. 4B); procurus simple proximally but complex distally, with prolatero-subdistal membranous process (arrow 1 in Figs 4C, 22C), sclerotized distal apophysis (arrow 2 in Figs 4C, 22C), subdistal membranous process (arrow 3 in Figs 4C, 22C), dorso-subdistal membranous process (arrow 4 in Figs 4C, 22C), and retrolateral membranous flap (f in Figs 4D, 22D); bulb with hooked apophysis bearing angular subdistal apophysis (arrow in Fig. 5C) and simple embolus (e in Fig. 5C). Retrolateral trichobothria on tibia I at 4% proximally; legs with short vertical setae on metatarsi.

Female (paratype, IZCAS-Ar45187): Similar to male, habitus as in Fig. 5G, H. Total length 2.53 (2.65 with clypeus), prosoma 0.67 long, 0.75 wide, opisthosoma 1.86 long, 1.80 wide; tibia I: 4.05; tibia I L/d: 51. Eye interdistances and diameters: PME–PME 0.11, PME 0.07, PME–ALE 0.02. Sternum width/length: 0.52/0.46. Epigyne simple and flat, posteriorly straight, with pair of median pockets 0.20 apart (ep in Figs 5A, 24C). Vulva with ridge-shaped anterior arch bearing pair of angular lateral sclerites (arrow in Figs 5B, 24D), and pair of anteriorly narrow and posteriorly wide pore plates (3× longer than wide, pp in Figs 5B, 24D).

Variation. Tibia I in five male paratypes (IZCAS-Ar45182–86): 4.50, 4.55, 4.62, 4.65, 4.70. Tibia I in the other six female paratypes (IZCAS-Ar45188–93): 3.56–3.85.

Habitat. The species was found in the dark zone inside the cave.

Distribution. China (Guizhou, type locality; Fig. 1).

Etymology. The specific name refers to the type locality; noun in apposition.

***Belisana majiang* Wang, S. Li & Yao, sp. nov.**

<https://zoobank.org/75C0DB39-2F6A-40D1-93A0-3C85CD956A53>

Figs 6, 7, 22E, F, 24E, F

Type material. Holotype: CHINA • ♂; Guizhou, Kaili, Majiang County, Xingshan Town, Gubin Village, Guazhutou Cave; 26°30.257'N, 107°30.943'E; alt. 1056 m; 28 Nov. 2011; Z. Chen & Z. Zha leg.; IZCAS-Ar45194. **Paratypes:** CHINA • 1♂; same data as for holotype; IZCAS-Ar45195 • 2♀; same data as for holotype; IZCAS-Ar45196–97.

Diagnosis. The new species resembles *B. zhouxu* sp. nov. (Figs 18, 19, 23E, F, 25G, H) by having similar male chelicerae (tips of distal apophyses pointing downwards; Fig. 7D), bulbal apophysis (hooked; Fig. 7C), and epigyne (epigynal pockets on antero-lateral part of epigynal plate, epigynal plate posteriorly curved; Figs 7A, 24E), but can be distinguished by procurus with distinct ventro-subdistal membranous process and dorso-distal spine (arrows 1, 3 in Figs 6C, 22E vs absent) and by vulval pore plates long elliptic (3× longer than wide, pp in Figs 7B, 24F vs 2×); also distinguished from *B. tongle* Zhang, Chen & Zhu, 2008 (Zhang et al. 2008: 654, figs 1–5) by procurus with dorso-subdistal membranous process (arrow 4 in Figs 6C, 22E vs absent), by prolatero-distal membranous lamella of procurus without rectangular sclerite (arrow 2 in Figs 6C, 22E vs present), by ventro-subdistal membranous process of procurus 3× longer than wide (arrow 1 in Figs 6C, 22E vs 8×), and by dorso-distal spine of procurus 6× longer than wide (arrow 3 in Figs 6C, 22E vs 12×).

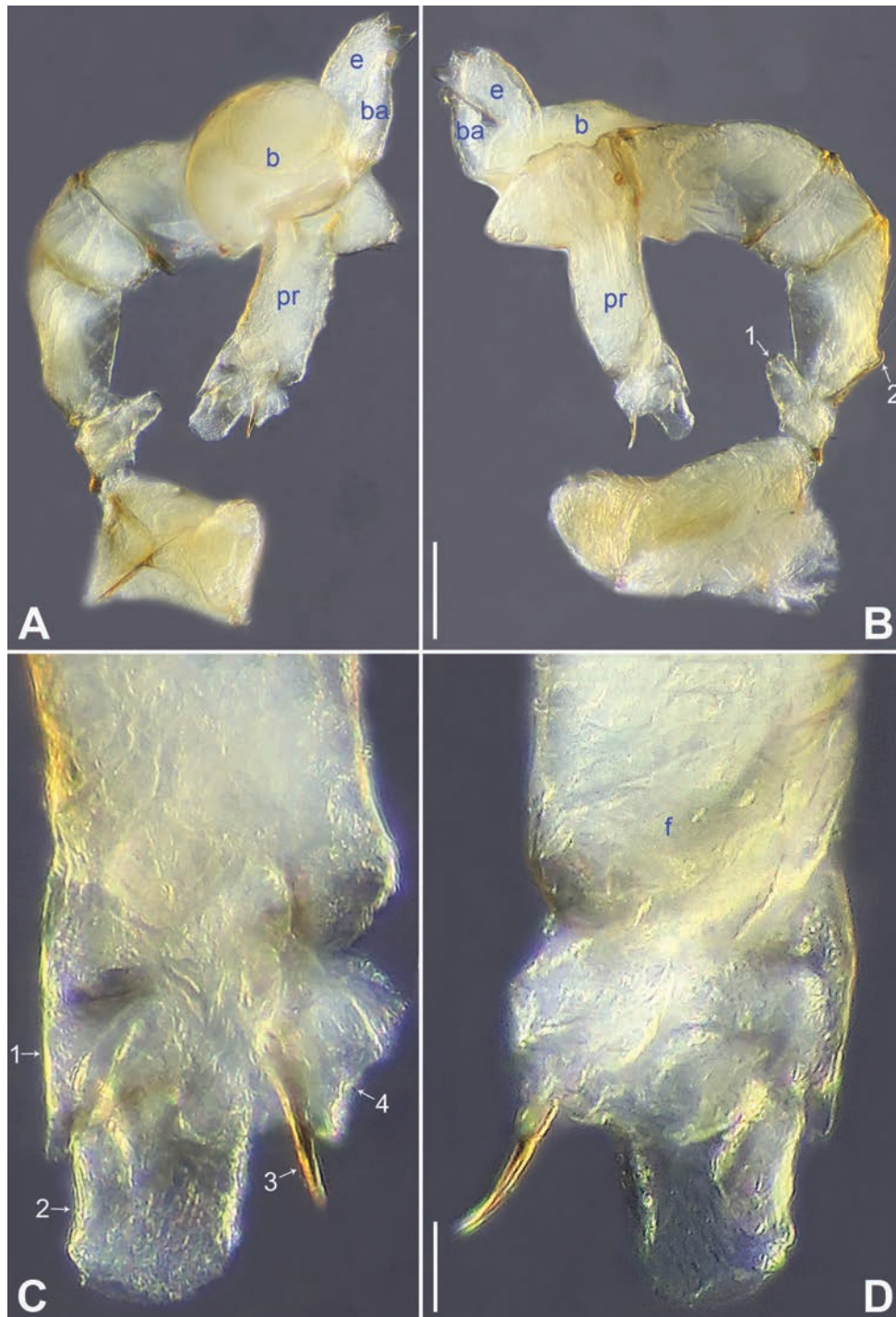


Figure 6. *Belisana majiang* sp. nov., holotype male **A, B** palp (**A** prolateral view **B** retrolateral view, arrow 1 points at ventral apophysis, arrow 2 points at retrolatero-proximal protrusion) **C, D** distal part of procurus (**C** prolateral view, arrow 1 points at ventro-subdistal membranous process, arrow 2 points at prolatero-distal membranous lamella, arrow 3 points at dorso-distal spine, arrow 4 points at dorso-subdistal membranous process **D** retrolateral view). Abbreviations: b = bulb, ba = bulbal apophysis, e = embolus, f = flap, pr = procurus. Scale bars: 0.10 (**A, B**); 0.02 (**C, D**).

Description. Male (holotype): Total length 1.35 (1.43 with clypeus), prosoma 0.52 long, 0.59 wide, opisthosoma 0.83 long, 0.64 wide. Leg I missing, leg II: 6.13 (1.78, 0.22, 1.50, 1.90, 0.73), leg III: 4.19 (1.28, 0.20, 0.95, 1.33, 0.43), leg IV: 5.87 (1.72, 0.22, 1.48, 1.80, 0.65). Eye interdistances and diameters: PME–PME 0.08, PME 0.06, PME–ALE 0.02. Sternum width/length: 0.44/0.38. Habitus

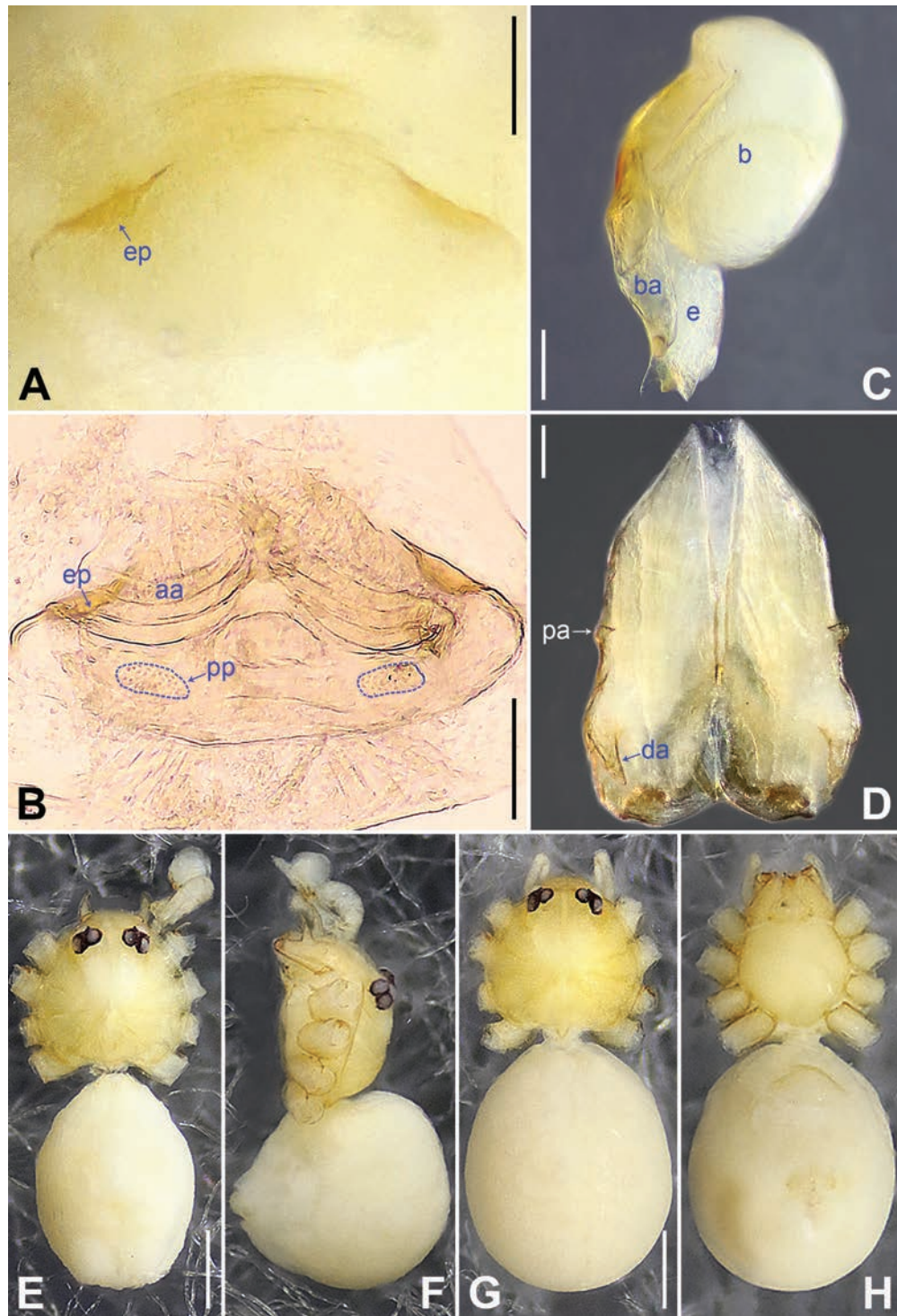


Figure 7. *Belisana majiang* sp. nov., holotype male (**C–F**) and paratype female (**A, B, G, H**) **A** epigyne, ventral view **B** vulva, dorsal view **C** bulb, prolateral view **D** chelicerae, frontal view **E–H** habitus (**E, G** dorsal view **F** lateral view **H** ventral view). Abbreviations: aa = anterior arch, b = bulb, ba = bulbal apophysis, da = distal apophysis, e = embolus, ep = epigynal pocket, pa = proximo-lateral apophysis, pp = pore plate. Scale bars: 0.05 (**A–D**); 0.30 (**E–H**).

as in Fig. 7E, F. Dorsal shield of prosoma yellowish, without marks; clypeus and sternum yellowish. Legs whitish, without darker rings. Opisthosoma yellowish, without spots. Thoracic furrow absent. Clypeus unmodified. Chelicerae with pair of proximo-lateral apophyses (pa in Fig. 7D) and pair of curved distal apophyses (distance between tips: 0.19; da in Fig. 7D). Palp as in Fig. 6A, B;

trochanter with ventral apophysis (1.5× longer than wide, arrow 1 in Fig. 6B); femur with retrolatero-proximal protrusion (arrow 2 in Fig. 6B); procurrus simple proximally but complex distally, with ventro-subdistal membranous process (arrow 1 in Figs 6C, 22E), prolatero-distal membranous lamella (arrow 2 in Figs 6C, 22E) bearing proximally slightly sclerotized part, dorso-distal spine (arrow 3 in Figs 6C, 22E), dorso-subdistal membranous process (arrow 4 in Figs 6C, 22E), and retrolateral membranous flap (f in Figs 6D, 22F); bulb with hooked apophysis (ba in Fig. 7C) and simple embolus (e in Fig. 7C).

Female (paratype, IZCAS-Ar45196): Similar to male, habitus as in Fig. 7G, H. Total length 1.48 (1.58 with clypeus), prosoma 0.48 long, 0.56 wide, opisthosoma 1.00 long, 0.84 wide. Eye interdistances and diameters: PME–PME 0.08, PME 0.06, PME–ALE 0.02. Sternum width/length: 0.43/0.39. Epigyne simple and flat, posteriorly curved, with pair of antero-lateral pockets 0.14 apart (ep in Figs 7A, 24E). Vulva with ridge-shaped anterior arch (aa in Figs 7B, 24F) and pair of long elliptic pore plates (3× longer than wide, pp in Figs 7B, 24F).

Variation. Unknown. Legs I missing in male paratype (IZCAS-Ar45195) and another female paratype (IZCAS-Ar45197).

Habitat. The species was found in the dark zone inside the cave.

Distribution. China (Guizhou, type locality; Fig. 1).

Etymology. The specific name refers to the type locality; noun in apposition.

***Belisana nayong* Wang, S. Li & Yao, sp. nov.**

<https://zoobank.org/2374804C-1CDB-4013-885E-336618ED0D2B>

Figs 8, 9, 22G, H, 24G, H

Type material. Holotype: CHINA • ♂; Guizhou, Bijie, Nayong County, Laosiba Town, Bailong Cave; 26°50.166'N, 105°31.222'E; alt. 1468 m; 27 Apr. 2007; J. Liu & Y. Lin leg.; IZCAS-Ar45198. **Paratypes:** CHINA • 3♂; same data as for holotype; IZCAS-Ar45199–201 • 4♀; same data as for holotype; IZCAS-Ar45202–05.

Diagnosis. The new species resembles *B. yongcong* sp. nov. (Figs 14, 15, 23A, B, 25C, D) by having similar bulbal apophysis (hooked; Fig. 9C) and vulva (anterior arch ridge-shaped, pore plates curved, long elliptic and 8× longer than wide; Figs 9B, 24H), but can be distinguished by procurrus with pointed ventro-subdistal membranous process (arrow 1 in Figs 8C, 22G vs blunt), by male cheliceral distal apophyses pointing inwards (da in Fig. 9D vs outwards), and by epigyne with postero-median pockets (ep in Figs 9A, 24G vs lateral).

Description. Male (holotype): Total length 2.33 (2.50 with clypeus), prosoma 0.86 long, 0.89 wide, opisthosoma 1.47 long, 1.15 wide. Leg I: 31.51 (8.33, 0.42, 7.82, 13.08, 1.86), leg II missing, leg III: 19.77 (5.08, 0.39, 5.04, 7.88, 1.38), leg IV missing; tibia I L/d: 89. Eye interdistances and diameters: PME–PME 0.10, PME 0.10, PME–ALE 0.02. Sternum width/length: 0.68/0.64. Habitus as in Fig. 9E, F. Dorsal shield of prosoma yellowish, with brown radiating marks; clypeus brown; sternum yellowish. Legs whitish, without darker rings. Opisthosoma yellowish, without spots. Thoracic furrow absent. Clypeus unmodified. Chelicerae with pair of proximo-lateral apophyses (pa in Fig. 9D) and pair of curved distal apophyses (distance between tips: 0.02; da in Fig. 9D). Palp as in Fig. 8A, B; trochanter with ventral apophysis (as long as wide, arrow 1 in Fig. 8B); femur with retrolatero-proximal protrusion (arrow 2 in Fig. 8B); procurrus simple

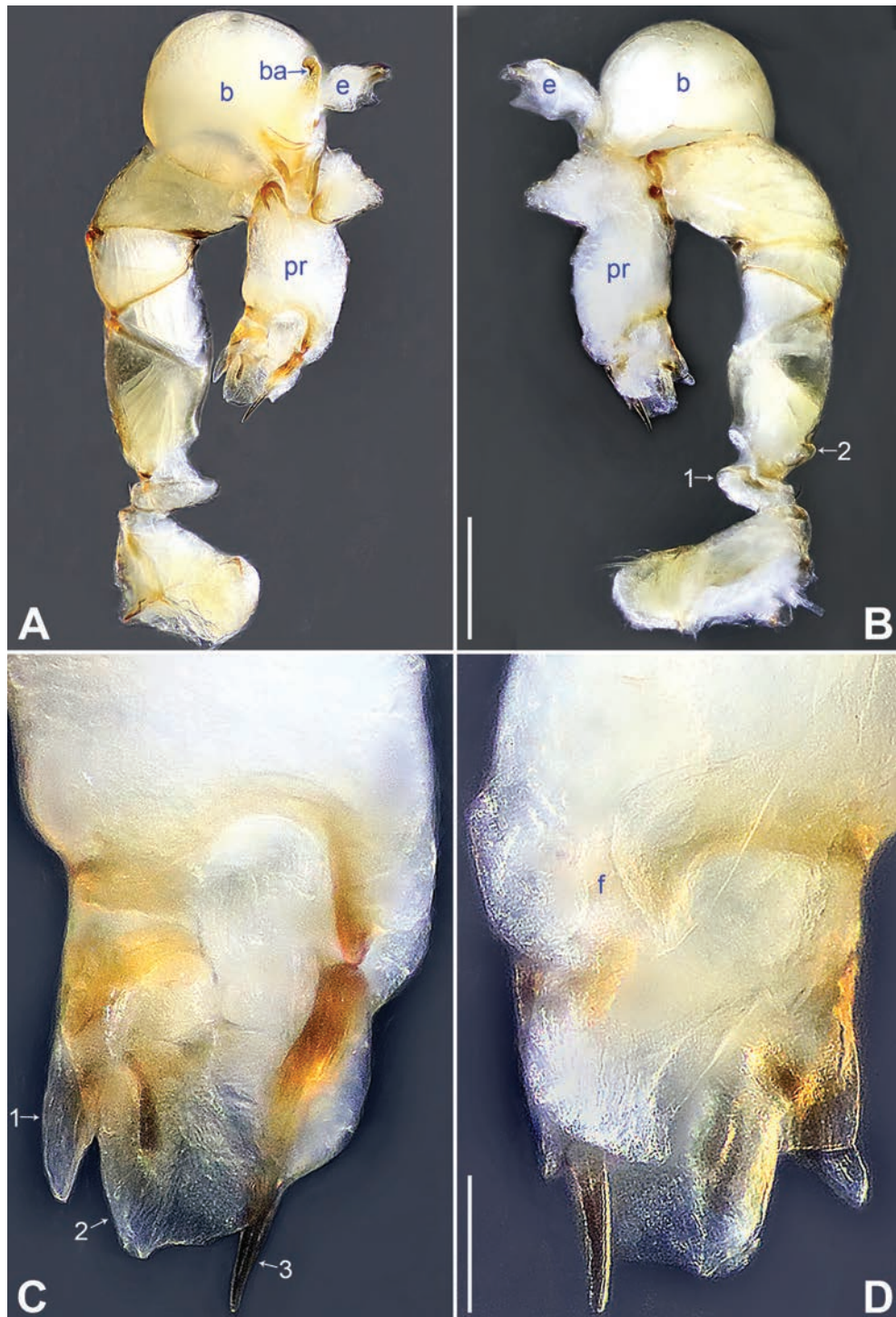


Figure 8. *Belisana nayong* sp. nov., holotype male **A, B** palp (**A** prolateral view **B** retrolateral view, arrow 1 points at ventral apophysis, arrow 2 points at retrolatero-proximal protrusion) **C, D** distal part of procurus (**C** prolateral view, arrow 1 points at ventro-subdistal membranous process, arrow 2 points at prolatero-distal membranous lamella, arrow 3 points at dorso-distal spine **D** retrolateral view). Abbreviations: b = bulb, ba = bulbal apophysis, e = embolus, f = flap, pr = procurus. Scale bars: 0.20 (**A, B**); 0.05 (**C, D**).

proximally but complex distally, with ventro-subdistal membranous process (arrow 1 in Figs 8C, 22G), prolatero-distal membranous lamella (arrow 2 in Figs 8C, 22G) bearing proximally sclerotized part, dorso-distal spine (arrow 3 in Figs 8C, 22G), and retrolateral membranous flap (f in Figs 8D, 22H); bulb with

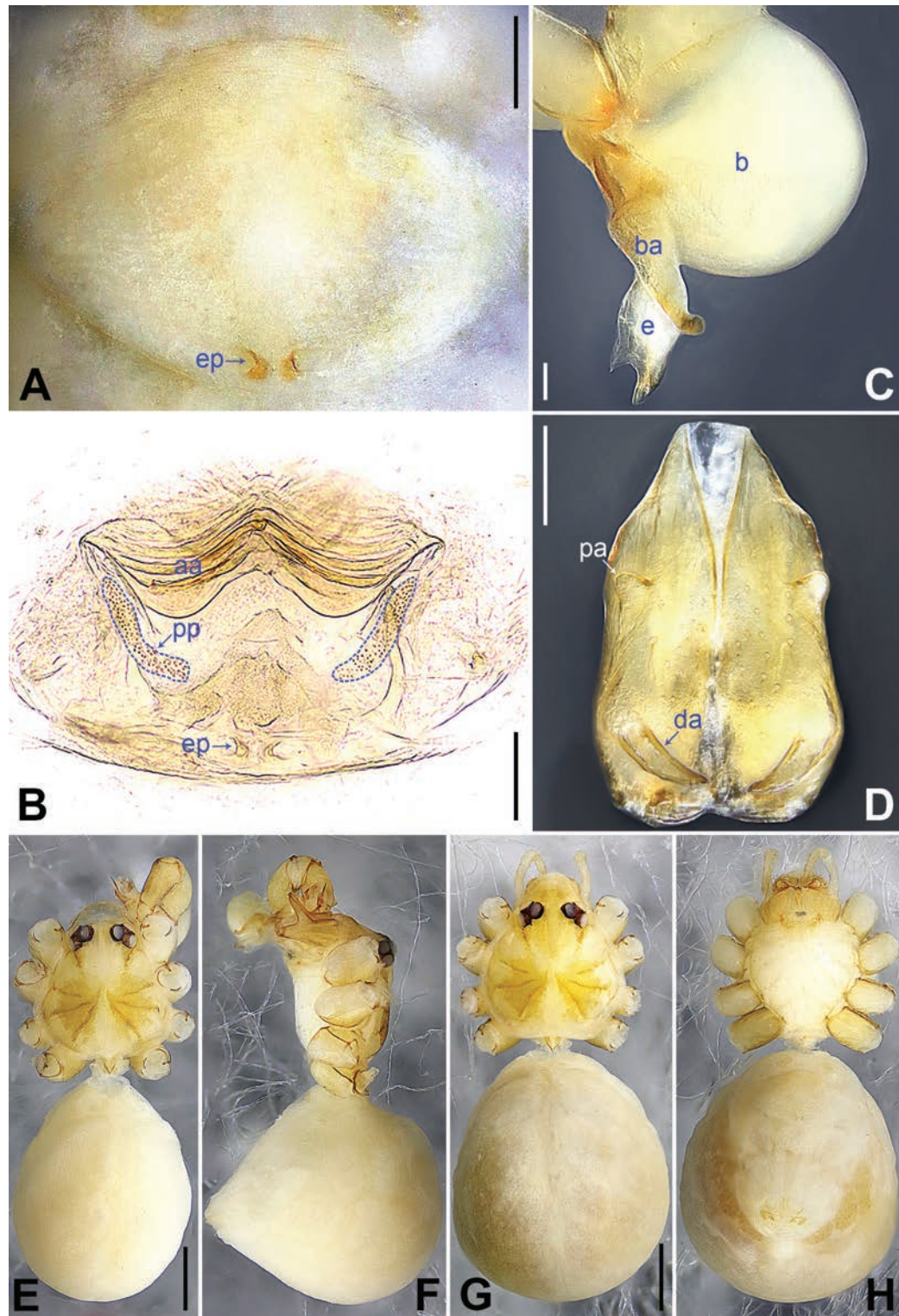


Figure 9. *Belisana nayong* sp. nov., holotype male (C–F) and paratype female (A, B, G, H) **A** epigyne, ventral view **B** vulva, dorsal view **C** bulb, prolateral view **D** chelicerae, frontal view **E–H** habitus (**E, G** dorsal view **F** lateral view **H** ventral view). Abbreviations: aa = anterior arch, b = bulb, ba = bulbal apophysis, da = distal apophysis, e = embolus, ep = epigynal pocket, pa = proximo-lateral apophysis, pp = pore plate. Scale bars: 0.05 (A–D); 0.40 (E–H).

hooked apophysis (ba in Fig. 9C) and simple embolus (e in Fig. 9C). Retrolateral trichobothria on tibia I at 4% proximally; legs with short vertical setae on metatarsi; tarsus I with 18 distinct pseudosegments.

Female (paratype, IZCAS-Ar45202): Similar to male, habitus as in Fig. 9G, H. Total length 2.47 (2.67 with clypeus), prosoma 0.81 long, 0.88 wide, opisthosoma 1.66 long, 1.40 wide; tibia I: 4.65; tibia I L/d: 58. Eye interdistances and diameters: PME–PME 0.11, PME 0.10, PME–ALE 0.02. Sternum width/length: 0.68/0.64. Epigyne simple and flat, posteriorly curved, with pair of postero-medial pockets 0.02 apart (ep in Figs 9A, 24G). Vulva with ridge-shaped anterior arch (aa in Figs 9B, 24H) and pair of curved, long elliptic pore plates (8× longer than wide, pp in Figs 9B, 24H).

Variation. Tibia I in three male paratypes (IZCAS-Ar45199–201): 6.15, 6.35, 6.50. Tibia I in the other three female paratypes (IZCAS-Ar45203–05): 4.45, 4.50, 4.74.

Habitat. The species was found in the dark zone inside the cave.

Distribution. China (Guizhou, type locality; Fig. 1).

Etymology. The specific name refers to the type locality; noun in apposition.

***Belisana qixingguan* Wang, S. Li & Yao, sp. nov.**

<https://zoobank.org/36AE89A6-13DA-416B-9C06-C86DD3300EC4>

Figs 10, 11, 22I, J, 24I, J

Type material. Holotype: CHINA • ♂; Guizhou, Bijie, Qixingguan District, Changchun Town, Changchun Village, Changchun Cave; 27°13.904'N, 105°10.397'E; alt. 1580 m; 29 Apr. 2007; J. Liu & Y. Lin leg.; IZCAS-Ar45206. **Paratypes:** CHINA • 7♀; same data as for holotype; IZCAS-Ar45207–13.

Diagnosis. The new species resembles *B. tongi* Zhang, Li & Yao, 2024 (Zhang et al. 2024b: 273, figs 12A–D, 13A–H, 18K, L, 21C, D) by having similar distal part of procurus (distal membranous process nearly half-round; arrow 1 in Figs 10C, 22I), bulbal apophysis (hooked; Fig. 11C), and epigyne (epigynal pockets on postero-lateral part of epigynal plate, epigynal plate posteriorly curved; Figs 11A, 24I), but can be distinguished by procurus without distal membranous lamella (Figs 10C, 22I vs present), by male cheliceral distal apophyses pointing downwards (da in Fig. 11D vs outwards), by vulva without teeth (Figs 11B, 24J vs present), and by vulval pore plates medially narrow and posteriorly strongly widened (pp in Figs 11B, 24J vs nearly triangular).

Description. Male (holotype): Total length 1.78 (1.89 with clypeus), prosoma 0.68 long, 0.75 wide, opisthosoma 1.10 long, 0.77 wide. Leg I: 14.43 (3.80, 0.31, 3.72, 5.00, 1.60), leg II: – (3.00, 0.31, 2.66, 3.75, –), leg III missing, leg IV: 7.17 (2.13, 0.27, 1.66, 2.41, 0.70); tibia I L/d: 50. Eye interdistances and diameters: PME–PME 0.14, PME 0.08, PME–ALE 0.02. Sternum width/length: 0.55/0.48. Habitus as in Fig. 11E, F. Dorsal shield of prosoma yellowish, with brown radiating marks; ocular area with brown median stripe; clypeus brown; sternum yellowish. Legs whitish, without darker rings. Opisthosoma yellowish, with black spots. Thoracic furrow absent. Clypeus unmodified. Chelicerae with pair of proximo-lateral apophyses (pa in Fig. 11D) and pair of curved distal apophyses (distance between tips: 0.29; da in Fig. 11D). Palp as in Fig. 10A, B; trochanter with ventral apophysis (as long as wide, arrow 1 in Fig. 10B); femur with retro-latero-proximal protrusion (arrow 2 in Fig. 10B); procurus simple, with distal membranous process (arrow 1 in Figs 10C, 22I) and subdistal spine (arrow 2 in Figs 10C, 22I); bulb with hooked apophysis (ba in Fig. 11C) and simple embolus

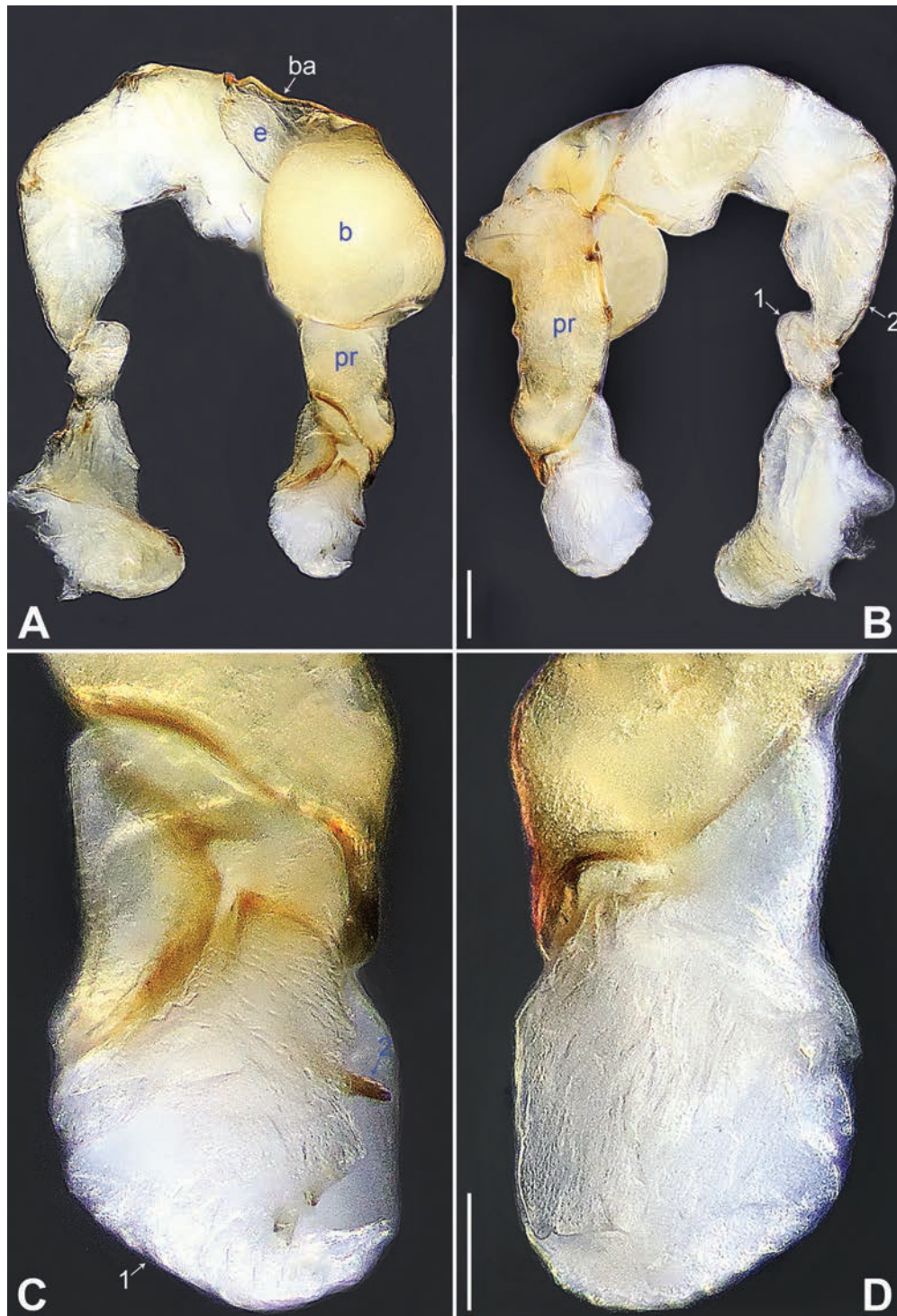


Figure 10. *Belisana qixingguan* sp. nov., holotype male **A, B** palp (**A** prolateral view **B** retrolateral view, arrow 1 points at ventral apophysis, arrow 2 points at retrolatero-proximal protrusion) **C, D** distal part of procurus (**C** prolateral view, arrow 1 points at distal membranous process, arrow 2 points at subdistal spine **D** retrolateral view). Abbreviations: b = bulb, ba = bulbal apophysis, e = embolus, pr = procurus. Scale bars: 0.10 (**A, B**); 0.05 (**C, D**).

(e in Fig. 11C). Retrolateral trichobothria on tibia I at 10% proximally; legs with short vertical setae on metatarsi; tarsus I with 15 distinct pseudosegments.

Female (paratype, IZCAS-Ar45207): Similar to male, habitus as in Fig. 11G, H. Total length 2.04 (2.15 with clypeus), prosoma 0.78 long, 0.81 wide, opisthosoma 1.26 long, 1.00 wide; tibia I: 3.08; tibia I L/d: 39. Eye interdistances

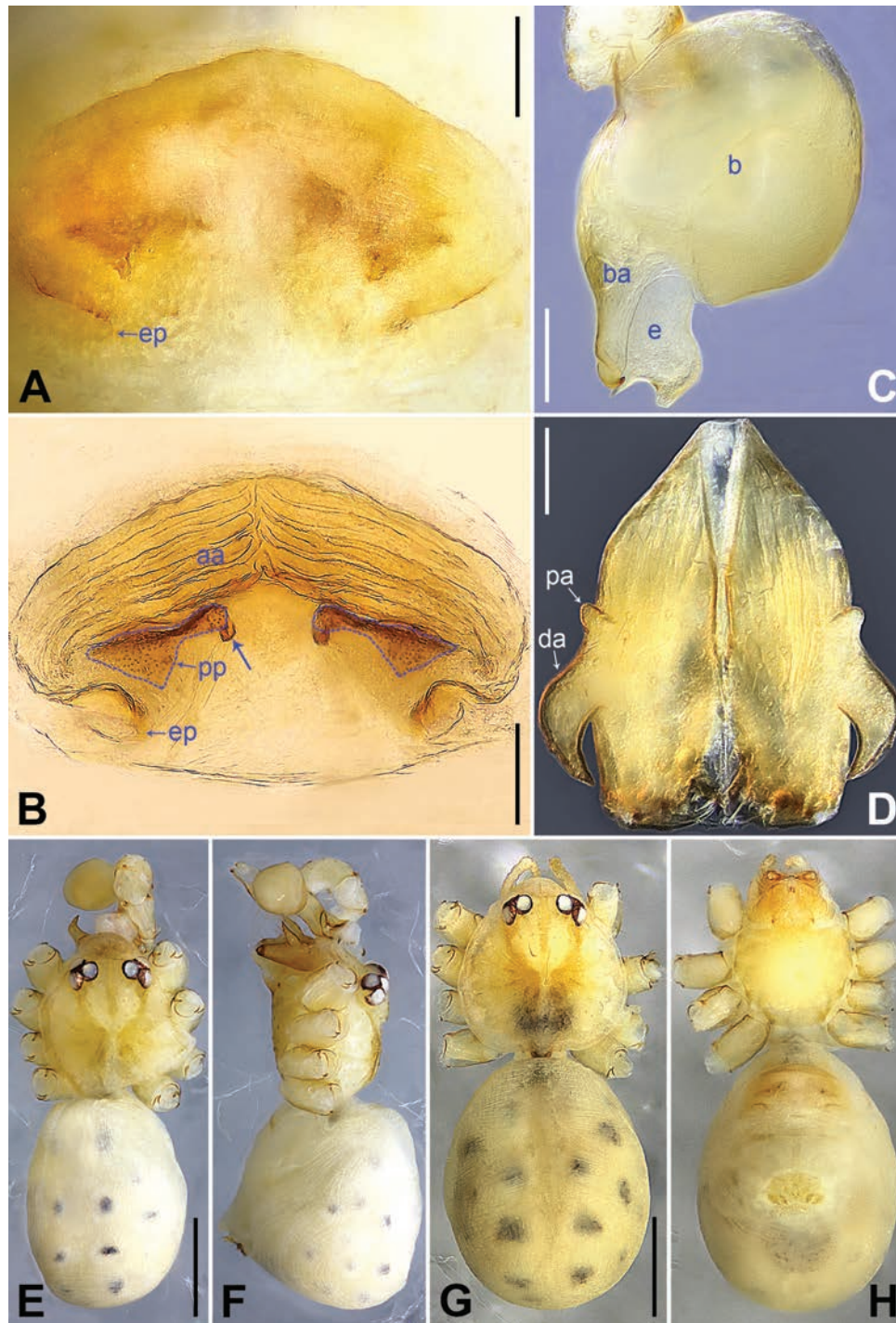


Figure 11. *Belisana qixingguan* sp. nov., holotype male (C–F) and paratype female (A, B, G, H) **A** epigyne, ventral view **B** vulva, dorsal view, arrow points at sclerotized protrusion **C** bulb, prolateral view **D** chelicerae, frontal view **E–H** habitus (**E**, **G** dorsal view **F** lateral view **H** ventral view). Abbreviations: aa = anterior arch, b = bulb, ba = bulbal apophysis, da = distal apophysis, e = embolus, ep = epigynal pocket, pa = proximo-lateral apophysis, pp = pore plate. Scale bars: 0.10 (A–D); 0.50 (E–H).

and diameters: PME–PME 0.12, PME 0.08, PME–ALE 0.02. Sternum width/length: 0.55/0.46. Epigyne simple and flat, posteriorly curved, with pair of postero-lateral pockets 0.28 apart (ep in Figs 11A, 24I). Vulva with curved anterior arch (aa in Figs 11B, 24J), pair of medially narrow and posteriorly strongly widened pore plates (pp in Figs 11B, 24J), and pair of sclerotized protrusions (arrow in Figs 11B, 24J).

Variation. Tibia I in the other six female paratypes (IZCAS-Ar45208–13): 2.89–3.09.

Habitat. The species was found in the dark zone inside the cave.

Distribution. China (Guizhou, type locality; Fig. 1).

Etymology. The specific name refers to the type locality; noun in apposition.

***Belisana xiuwen* Wang, S. Li & Yao, sp. nov.**

<https://zoobank.org/92A64C94-8BCB-4211-9EDE-4930EEC2467A>

Figs 12, 13, 22K, L, 25A, B

Type material. Holotype: CHINA • ♂; Guizhou, Guiyang, Xiuwen County, Liutong Town, Daxing Village, Duobing Cave; 27°06.552'N, 106°29.675'E; alt. 1035 m; 20 Apr. 2007; J. Liu & Y. Lin leg.; IZCAS-Ar45214. **Paratypes:** CHINA • 3♀; same data as for holotype; IZCAS-Ar45215–17.

Diagnosis. The new species resembles *B. yongcong* sp. nov. (Figs 14, 15, 23A, B, 25C, D) by having similar male chelicerae (tips of distal apophyses widely separated and pointing inwards; Fig. 13D), bulbal apophysis (hooked; Fig. 13C), and epigyne (epigynal pockets on lateral part of epigynal plate, epigynal plate posteriorly curved; Figs 13A, 25A), but can be distinguished by procurus with distal spine (arrow 1 in Figs 12C, 22K vs absent) and without ventro-subdistal membranous lamella, prolatero-distal membranous lamella, and sclerotized dorso-subdistal apophysis (Figs 12C, 22K vs present), and by vulval pore plates long elliptic (3× longer than wide, pp in Figs 13B, 25B vs curved and 9×).

Description. Male (holotype): Total length 1.35 (1.48 with clypeus), prosoma 0.57 long, 0.59 wide, opisthosoma 0.78 long, 0.60 wide. Leg I: 10.06 (2.48, 0.21, 2.73, 3.36, 1.28), leg II: 6.94 (2.00, 0.22, 1.74, 2.18, 0.80), leg III: 5.08 (1.50, 0.20, 1.14, 1.64, 0.60), leg IV: 6.72 (1.94, 0.20, 1.72, 2.15, 0.71); tibia I L/d: 46. Eye interdistances and diameters: PME–PME 0.09, PME 0.05, PME–ALE 0.02. Sternum width/length: 0.45/0.40. Habitus as in Fig. 13E, F. Dorsal shield of prosoma yellowish, without marks; clypeus and sternum yellowish. Legs whitish, without darker rings. Opisthosoma yellowish, without spots. Thoracic furrow absent. Clypeus unmodified. Eye pigments indistinct. Chelicerae with pair of proximo-lateral apophyses (pa in Fig. 13D) and pair of curved distal apophyses (distance between tips: 0.30; da in Fig. 13D). Palp as in Fig. 12A, B; trochanter with ventral apophysis (as long as wide, arrow 1 in Fig. 12B); femur with retro-latero-proximal protrusion (arrow 2 in Fig. 12B); procurus simple, with distal spine (arrow 1 in Figs 12C, 22K) and retrolateral membranous flap (f in Figs 12D, 22L); bulb with hooked apophysis (ba in Fig. 13C) and simple embolus (e in Fig. 13C). Retrolateral trichobothria on tibia I at 6% proximally; legs with short vertical setae on metatarsi; tarsus I with 15 distinct pseudosegments.

Female (paratype, IZCAS-Ar45215): Similar to male, habitus as in Fig. 13G, H. Total length 1.75 (1.85 with clypeus), prosoma 0.56 long, 0.59 wide, opisthosoma 1.19 long, 0.80 wide; tibia I: 2.19; tibia I L/d: 44. Eye interdistances and diameters: PME–PME 0.09, PME 0.05, PME–ALE 0.02. Sternum width/length: 0.44/0.38. Epigyne simple and flat, posteriorly curved, with pair of lateral pockets 0.33 apart (ep in Figs 13A, 25A). Vulva with ridge-shaped anterior arch (aa in Figs 13B, 25B) and pair of long elliptic pore plates (3× longer than wide, pp in Figs 13B, 25B).

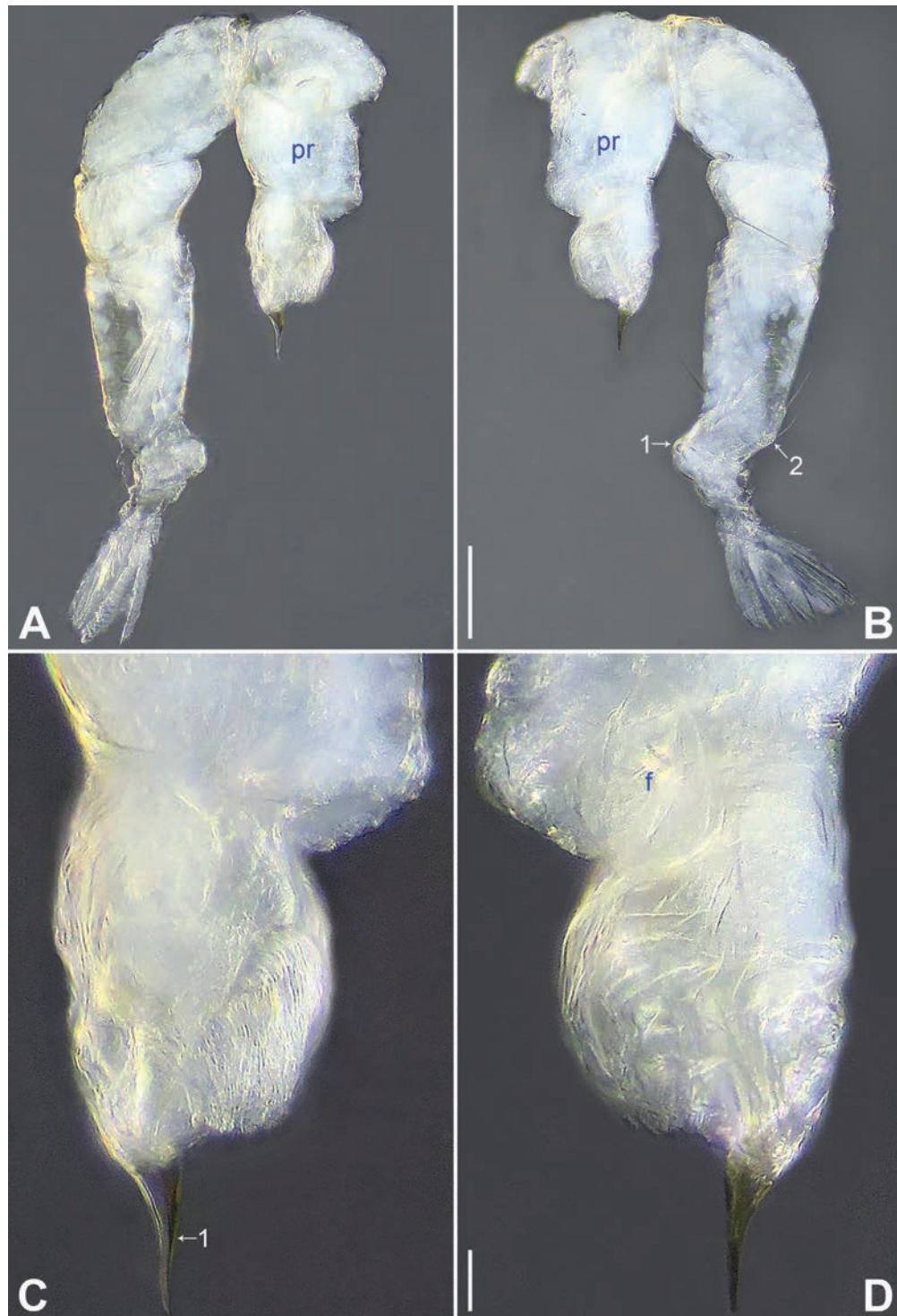


Figure 12. *Belisana xiuwen* sp. nov., holotype male **A, B** palp (**A** prolateral view **B** retrolateral view, arrow 1 points at ventral apophysis, arrow 2 points at retrolatero-proximal protrusion) **C, D** distal part of procurus (**C** prolateral view, arrow 1 points at distal spine **D** retrolateral view). Abbreviations: f = flap, pr = procurus. Scale bars: 0.10 (**A, B**); 0.02 (**C, D**).

Variation. Tibia I in the other two female paratypes (IZCAS-Ar45216–17): 2.10, 2.18.

Habitat. The species was found in the dark zone inside the cave.

Distribution. China (Guizhou, type locality; Fig. 1).

Etymology. The specific name refers to the type locality; noun in apposition.

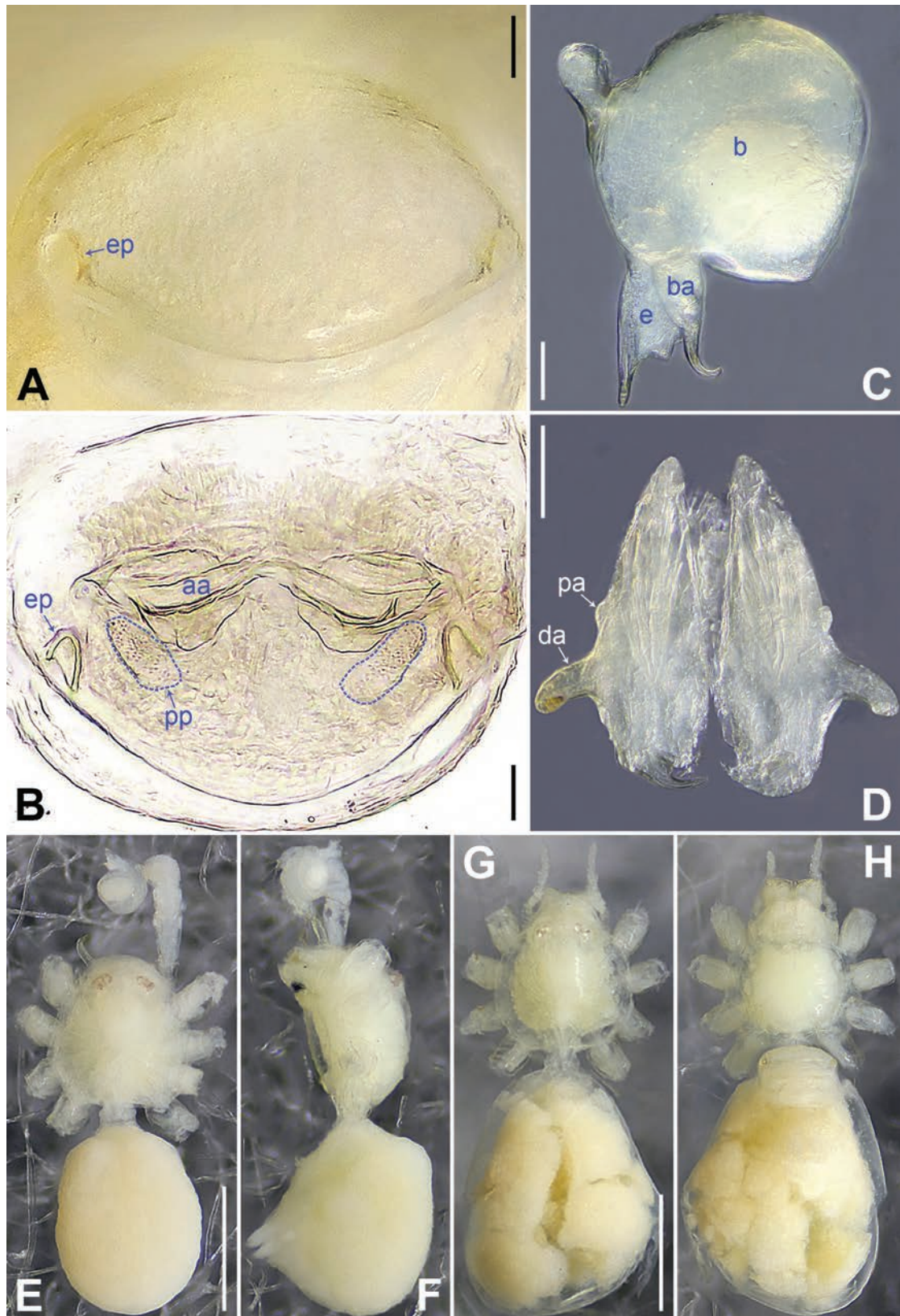


Figure 13. *Belisana xiuwen* sp. nov., holotype male (C–F) and paratype female (A, B, G, H) A epigyne, ventral view B vulva, dorsal view C bulb, prolateral view D chelicerae, frontal view E–H habitus (E, G dorsal view F lateral view H ventral view). Abbreviations: aa = anterior arch, b = bulb, ba = bulbal apophysis, da = distal apophysis, e = embolus, ep = epigynal pocket, pa = proximo-lateral apophysis, pp = pore plate. Scale bars: 0.05 (A–D); 0.50 (E–H).

***Belisana yongcong* Wang, S. Li & Yao, sp. nov.**

<https://zoobank.org/1E1B4058-113E-48F6-9734-39D486FF0FB9>

Figs 14, 15, 23A, B, 25C, D

Type material. Holotype: CHINA • ♂; Guizhou, Qiandongnan, Liping County, Yongcong Town, Guantuan Village, Guantuan Cave; 25°59.028'N, 109°06.979'E; alt. 544 m; 23 May 2007; J. Liu & Y. Lin leg.; IZCAS-Ar45218. **Paratypes:** CHINA • 2♂; same data as for holotype; IZCAS-Ar45219–20 • 5♀; same data as for holotype; IZCAS-Ar45221–25.

Diagnosis. The new species resembles *B. nayong* sp. nov. (Figs 8, 9, 22G, H, 24G, H) by having similar bulbal apophysis (hooked; Fig. 15C) and vulva (anterior arch ridge-shaped, pore plates curved, long elliptic and 8× longer than wide; Figs 15B, 25D), but can be distinguished by procurus with blunt ventro-subdistal membranous process (arrow 1 in Figs 14C, 23A vs pointed), by male cheliceral distal apophyses pointing outwards (da in Fig. 15D vs inwards), and by epigyne with lateral pockets (ep in Figs 15A, 25C vs postero-median).

Description. Male (holotype): Total length 1.73 (1.82 with clypeus), prosoma 0.83 long, 0.67 wide, opisthosoma 0.90 long, 0.66 wide. Leg I: 14.76 (3.60, 0.34, 4.05, 5.58, 1.56), leg II: 12.45 (3.36, 0.32, 3.08, 4.60, 1.09), leg III: 8.21 (2.38, 0.26, 1.98, 2.84, 0.75), leg IV: 10.64 (3.20, 0.26, 2.66, 3.72, 0.80); tibia I L/d: 46. Eye interdistances and diameters: PME–PME 0.06, PME 0.09, PME–ALE 0.02. Sternum width/length: 0.54/0.49. Habitus as in Fig. 15E, F. Dorsal shield of prosoma yellowish, with brownish radiating marks; clypeus and sternum yellowish. Legs whitish, without darker rings. Opisthosoma yellowish, without spots. Thoracic furrow absent. Clypeus unmodified. Chelicerae with pair of proximo-lateral apophyses (pa in Fig. 15D) and pair of curved distal apophyses (distance between tips: 0.32; da in Fig. 15D). Palp as in Fig. 14A, B; trochanter with ventral apophysis (as long as wide, arrow 1 in Fig. 14B); femur with retrolatero-proximal protrusion (arrow 2 in Fig. 14B); procurus simple proximally but complex distally, with ventro-subdistal membranous lamella (arrow 1 in Figs 14C, 23A) bearing proximally sclerotized part, prolatero-distal membranous lamella (arrow 2 in Figs 14C, 23A) bearing proximally sclerotized part, sclerotized dorso-subdistal apophysis (arrow 3 in Figs 14C, 23A), and retrolateral membranous flap (f in Figs 14D, 23B); bulb with hooked apophysis (ba in Fig. 15C) and simple embolus (e in Fig. 15C). Retrolateral trichobothria on tibia I at 10% proximally; legs with short vertical setae on metatarsi; tarsus I with 20 distinct pseudosegments.

Female (paratype, IZCAS-Ar45221): Similar to male, habitus as in Fig. 15G, H. Total length 2.17 (2.29 with clypeus), prosoma 0.87 long, 0.76 wide, opisthosoma 1.30 long, 1.08 wide; tibia I: 3.65; tibia I L/d: 47. Eye interdistances and diameters: PME–PME 0.09, PME 0.08, PME–ALE 0.02. Sternum width/length: 0.59/0.45. Epigyne simple and flat, posteriorly curved, with pair of lateral pockets 0.35 apart (ep in Figs 15A, 25C). Vulva with ridge-shaped anterior arch (aa in Figs 15B, 25D) and pair of curved, long elliptic pore plates (9× longer than wide, pp in Figs 15B, 25D).

Variation. Tibia I in one male paratype (IZCAS-Ar45219): 5.32 (leg I missing in IZCAS-Ar45220). Tibia I in the other four female paratypes (IZCAS-Ar45222–25): 3.76, 3.85, 3.96, 4.16.

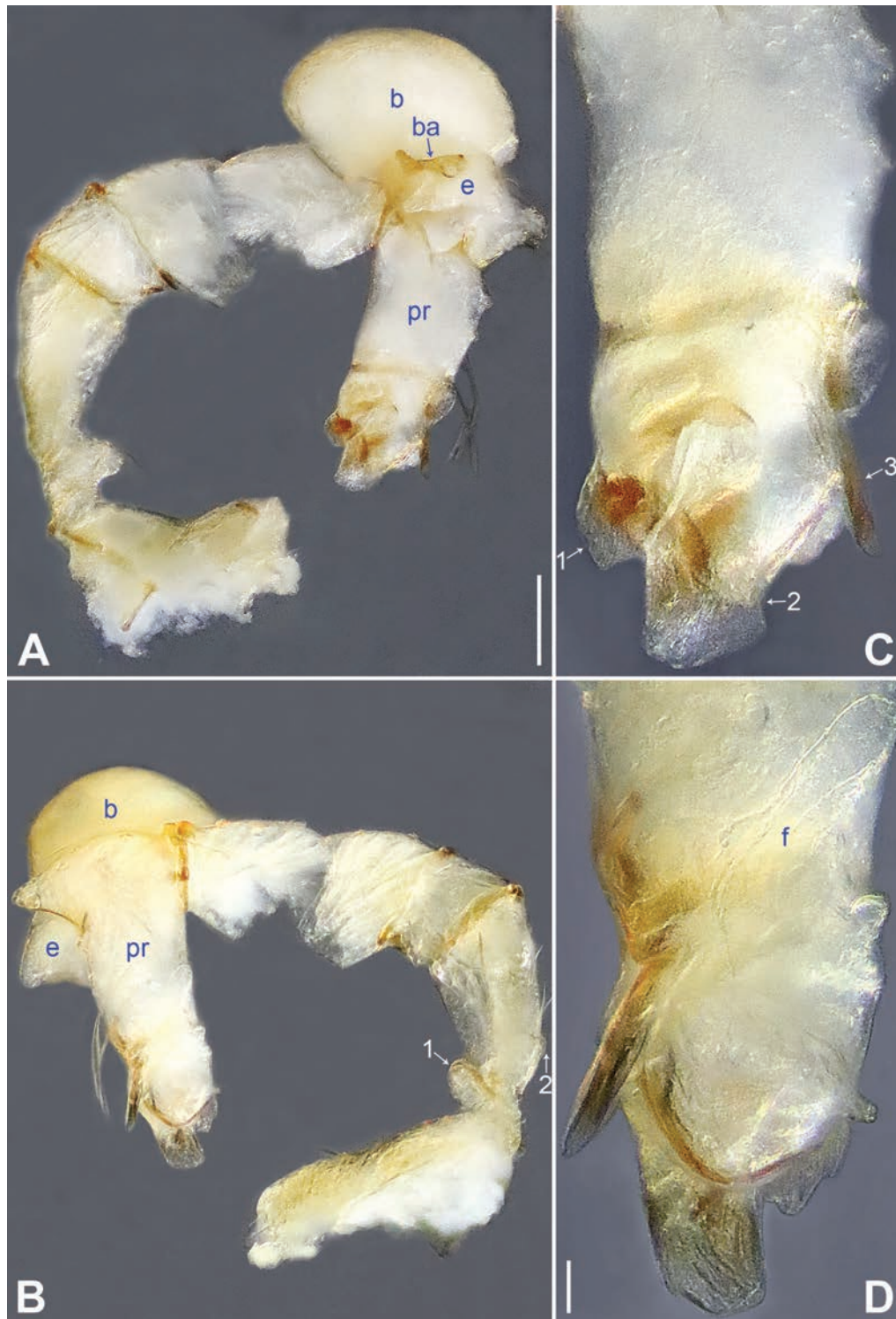


Figure 14. *Belisana yongcong* sp. nov., holotype male **A, B** palp (**A** prolateral view **B** retrolateral view, arrow 1 points at ventral apophysis, arrow 2 points at retrolatero-proximal protrusion) **C, D** distal part of procurus (**C** prolateral view, arrow 1 points at ventro-subdistal membranous lamella, arrow 2 points at prolatero-distal membranous lamella, arrow 3 points at sclerotized dorso-subdistal apophysis **D** retrolateral view). Abbreviations: b = bulb, ba = bulbal apophysis, e = embolus, f = flap, pr = procurus. Scale bars: 0.10 (**A, B**); 0.02 (**C, D**).

Habitat. The species was found in the dark zone inside the cave.

Distribution. China (Guizhou, type locality; Fig. 1).

Etymology. The specific name refers to the type locality; noun in apposition.

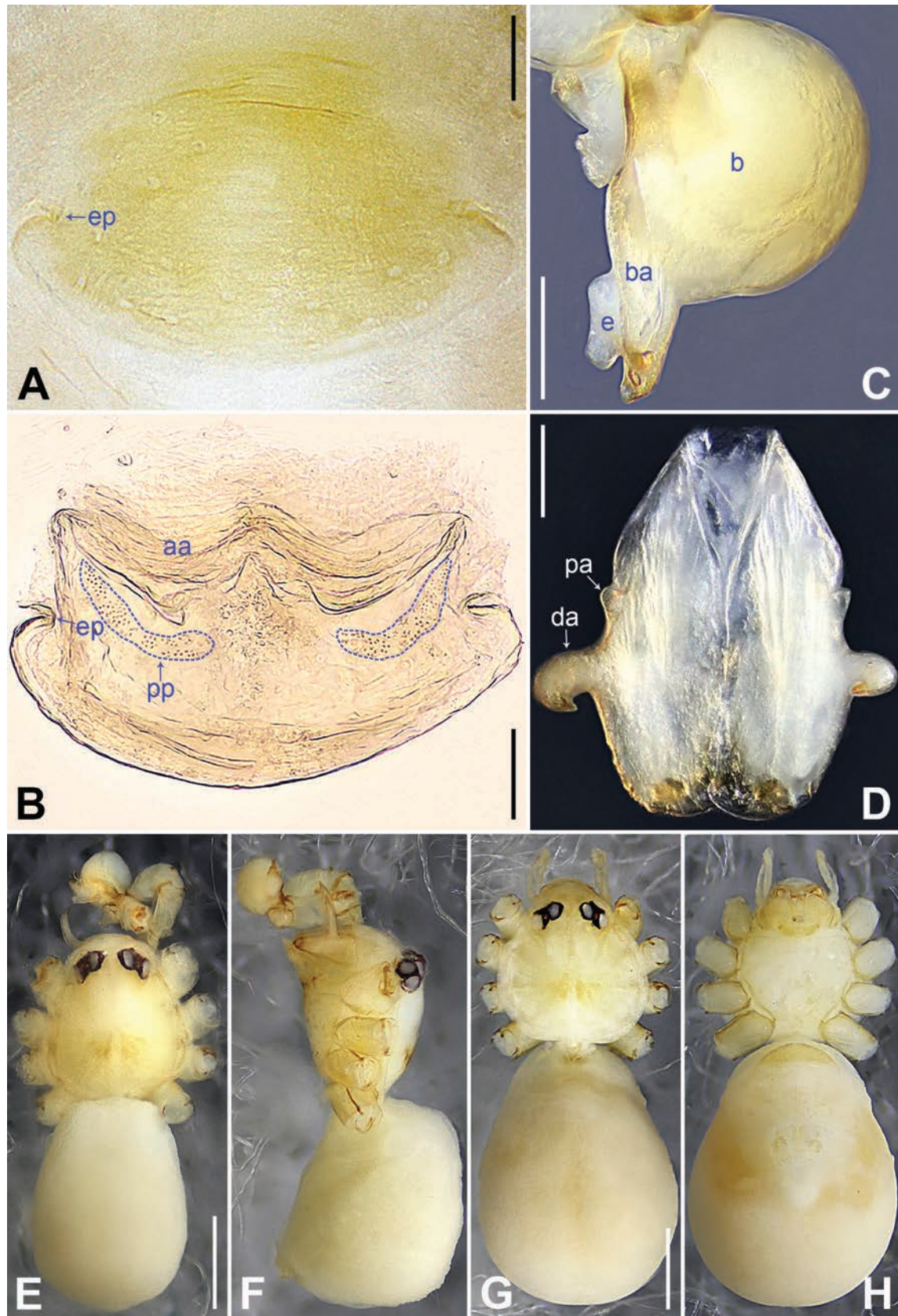


Figure 15. *Belisana yongcong* sp. nov., holotype male (C–F) and paratype female (A, B, G, H) **A** epigyne, ventral view **B** vulva, dorsal view **C** bulb, prolateral view **D** chelicerae, frontal view **E–H** habitus (**E, G** dorsal view **F** lateral view **H** ventral view). Abbreviations: aa = anterior arch, b = bulb, ba = bulbal apophysis, da = distal apophysis, e = embolus, ep = epigynal pocket, pa = proximo-lateral apophysis, pp = pore plate. Scale bars: 0.10 (A–D); 0.40 (E–H).

***Belisana zhangji* Tong & Li, 2007**

Figs 16, 17, 23C, D, 25E, F

Belisana zhangji Tong and Li 2007: 505, figs 1–6.

Material examined. CHINA • 1♂; Guizhou, Anshun, Puding County, Huachu Town, Jinqian Cave; 26°14.835'N, 105°37.521'E; 3 May 2005; collector unknown; IZCAS-Ar45177 • 3♀; same data as for preceding; IZCAS-Ar45178–80.

Diagnosis. The species resembles *B. yuhaoi* Yang & Yao, 2023 (Yang et al. 2023a: 178, figs 2A, B, 3A–D, 4A–H) by having similar bulbal apophysis (hooked; Fig. 17C) and epigyne (epigynal pockets on posterior part of epigynal plate, epigynal plate posteriorly curved; Figs 17A, 25E), but can be distinguished by procurus with nearly angular ventro-subdistal membranous lamella (arrow 1 in Figs 16C, 23C vs nearly round) and curved retrolateral membranous flap (f in Figs 16D, 23D vs angular), by male cheliceral distal apophyses pointing inwards (da in Fig. 17D vs downwards), and by vulval pore plates long elliptic (pp in Figs 17B, 25F vs nearly triangular).

Habitat. The species was found in the dark zone inside the cave.

Distribution. China (Guangxi, type locality; Guizhou, Fig. 1).

***Belisana zhouxi* Wang, S. Li & Yao, sp. nov.**

<https://zoobank.org/D2E3F0DB-7736-46DA-ADC9-9F1FC1CF3ACD>

Figs 18, 19, 23E, F, 25G, H

Type material. **Holotype:** CHINA • ♂; Guizhou, Kaili, Zhouxi Town, Hebian Cave; 26°29.280'N, 107°55.442'E; alt. 665 m; 25 May 2007; J. Liu & Y. Lin leg.; IZCAS-Ar45226. **Paratypes:** CHINA • 2♀; same data as for holotype; IZCAS-Ar45227–28.

Diagnosis. The new species resembles *B. majiang* sp. nov. (Figs 6, 7, 22E, F, 24E, F) by having similar male chelicerae (tips of distal apophyses pointing downwards; Fig. 19D), bulbal apophysis (hooked; Fig. 19C), and epigyne (epigynal pockets on antero-lateral part of epigynal plate, epigynal plate posteriorly curved; Figs 19A, 25G), but can be distinguished by procurus without ventro-subdistal membranous process and dorso-distal spine (Figs 18C, 23E vs present) and by vulval pore plates elliptic (2× longer than wide, pp in Figs 19B, 25H vs 3×).

Description. Male (holotype): Total length 1.17 (1.27 with clypeus), prosoma 0.46 long, 0.50 wide, opisthosoma 0.71 long, 0.61 wide. Leg I: 6.72 (1.84, 0.21, 1.66, 2.13, 0.88), leg II: 4.56 (1.36, 0.19, 1.06, 1.36, 0.59), leg III: 3.29 (0.96, 0.19, 0.66, 1.01, 0.47), leg IV: 4.69 (1.44, 0.18, 1.16, 1.42, 0.49); tibia I L/d: 27. Eye interdistances and diameters: PME–PME 0.08, PME 0.06, PME–ALE 0.02. Sternum width/length: 0.41/0.33. Habitus as in Fig. 19E, F. Dorsal shield of prosoma yellowish, without marks; clypeus and sternum yellowish. Legs whitish, without darker rings. Opisthosoma yellowish, without spots. Thoracic furrow absent. Clypeus unmodified. Chelicerae with pair of proximo-lateral apophyses (pa in Fig. 19D) and pair of curved distal apophyses (distance between tips: 0.19; da in Fig. 19D). Palp as in Fig. 18A, B; trochanter with ventral apophysis (as long as wide, arrow 1 in Fig. 18B); femur with retrolatero-proximal protrusion (arrow

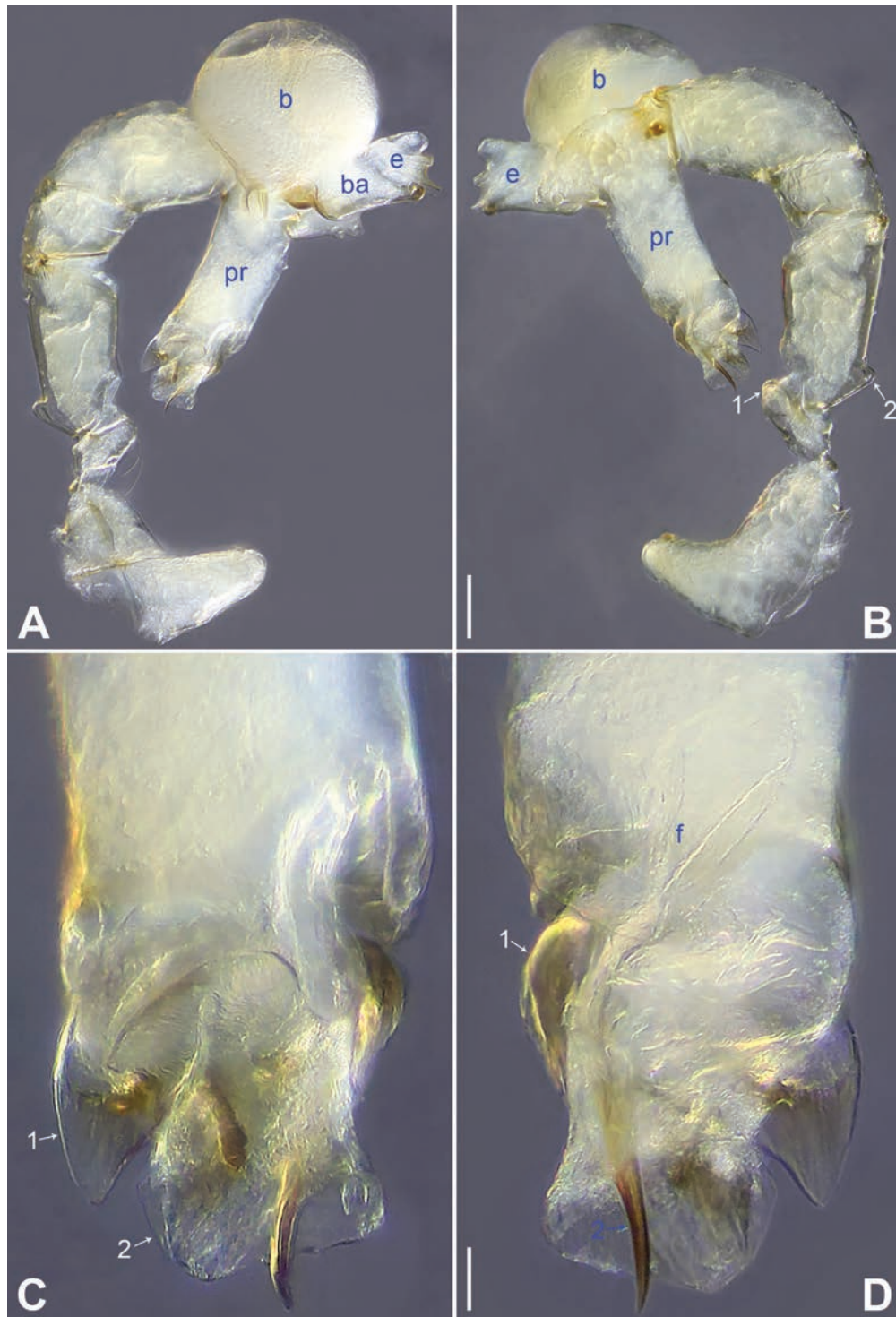


Figure 16. *Belisana zhangi* Tong & Li, 2007, male **A, B** palp (**A** prolateral view **B** retrolateral view, arrow 1 points at ventral apophysis, arrow 2 points at retrolatero-proximal protrusion) **C, D** distal part of procurus (**C** prolateral view, arrow 1 points at ventro-subdistal membranous lamella, arrow 2 points at prolatero-distal membranous lamella **D** retrolateral view, arrow 1 points at sclerotized dorso-subdistal apophysis, arrow 2 points at retrolatero-distal spine). Abbreviations: b = bulb, ba = bulbal apophysis, e = embolus, f = flap, pr = procurus. Scale bars: 0.10 (**A, B**); 0.02 (**C, D**).

2 in Fig. 18B); procurus simple proximally but complex distally, with prolatero-distal membranous lamella (arrow 1 in Figs 18C, 23E) bearing proximally slightly sclerotized part, dorso-subdistal membranous process (arrow 2 in Figs 18C, 23E), and retrolateral membranous flap (f in Figs 18D, 23F); bulb with

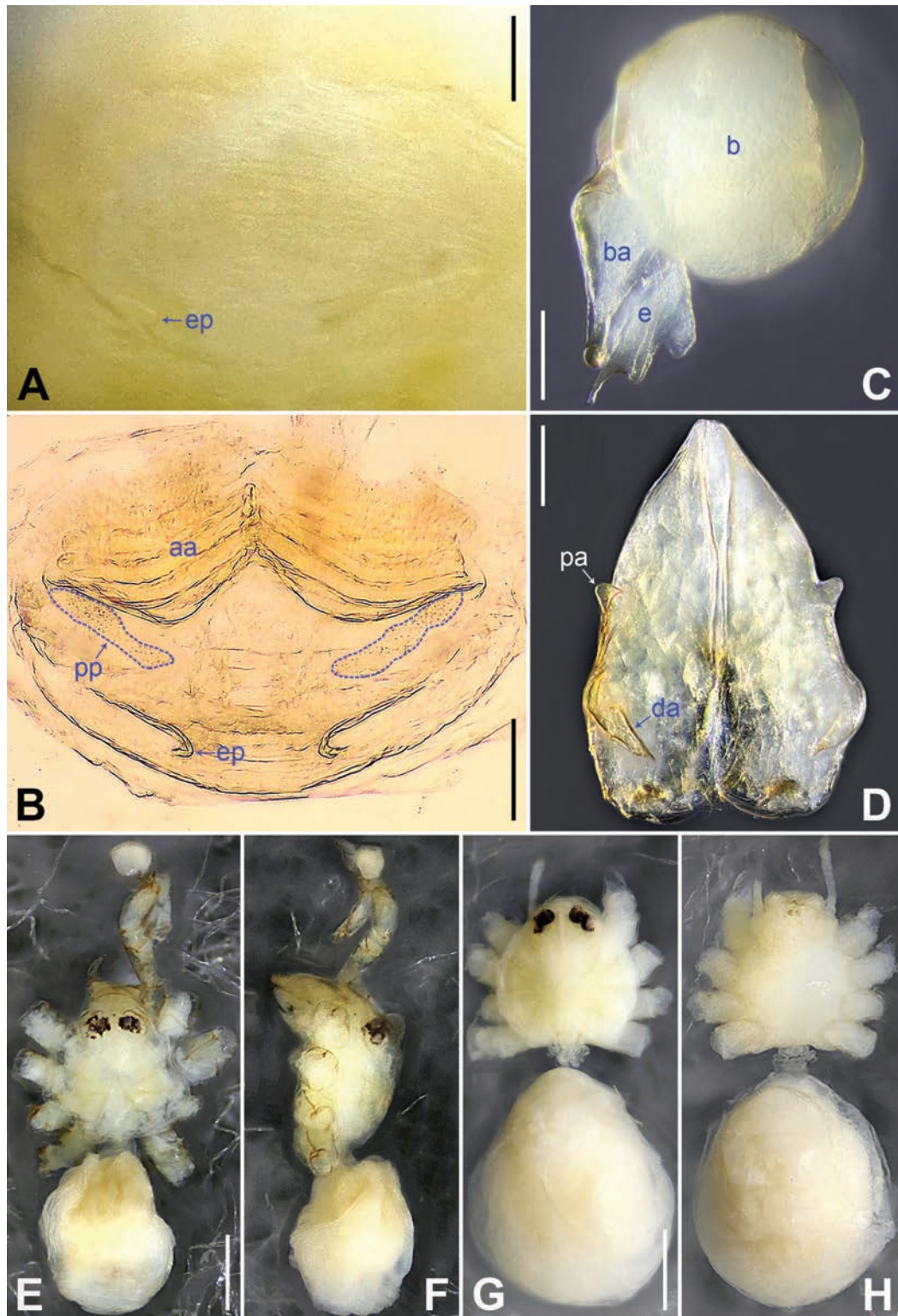


Figure 17. *Belisana zhangji* Tong & Li, 2007, male (**C–F**) and female (**A, B, G, H**) **A** epigyne, ventral view **B** vulva, dorsal view **C** bulb, prolateral view **D** chelicerae, frontal view **E–H** habitus (**E, G** dorsal view **F** lateral view **H** ventral view). Abbreviations: aa = anterior arch, b = bulb, ba = bulbal apophysis, da = distal apophysis, e = embolus, ep = epigynal pocket, pa = proximo-lateral apophysis, pp = pore plate. Scale bars: 0.10 (**A–D**); 0.40 (**E–H**).

hooked apophysis (ba in Fig. 19C) and simple embolus (e in Fig. 19C). Retro-lateral trichobothria on tibia I at 7% proximally; legs with short vertical setae on metatarsi; tarsus I with 14 distinct pseudosegments.

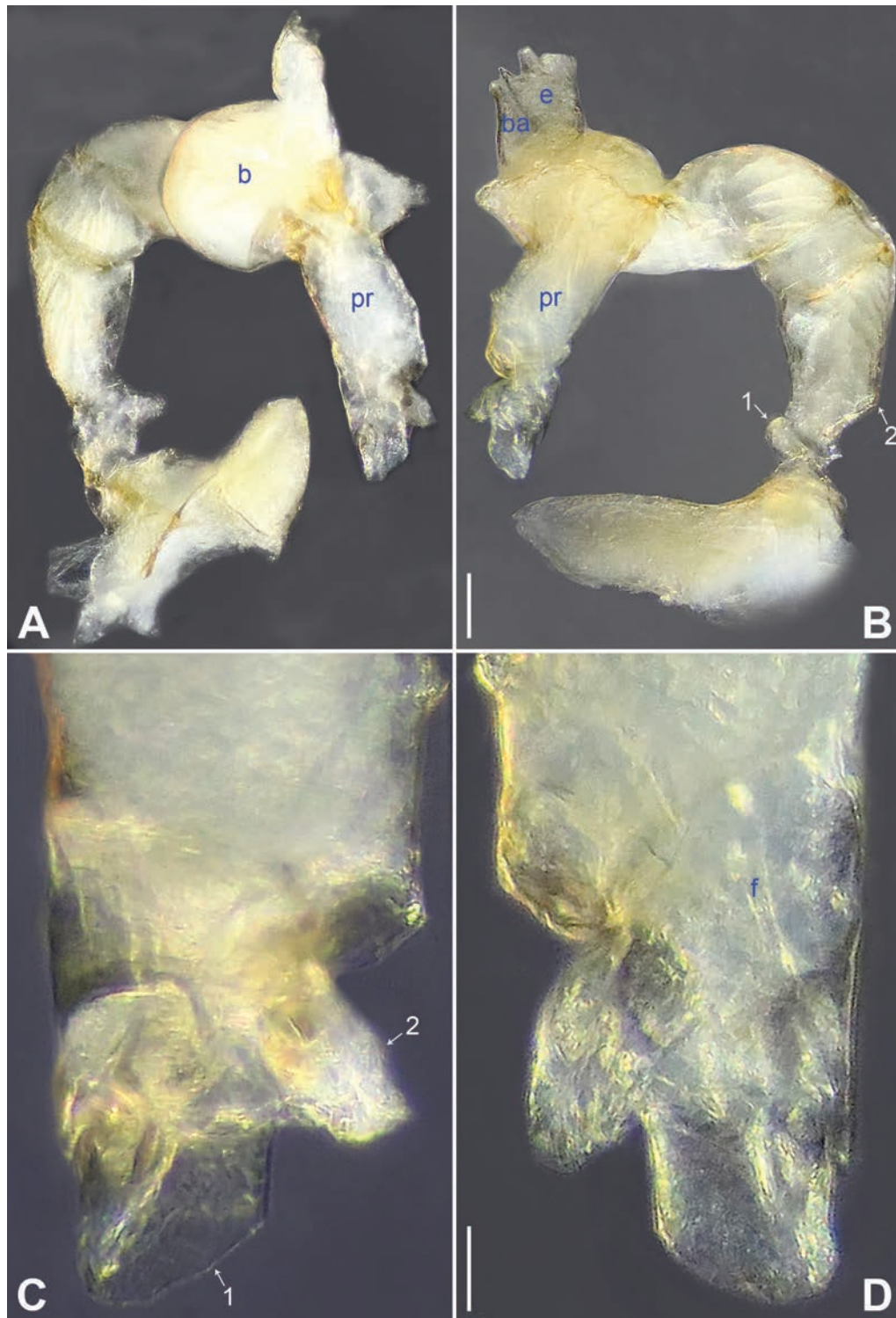


Figure 18. *Belisana zhouxii* sp. nov., holotype male **A, B** palp (**A** prolateral view **B** retrolateral view, arrow 1 points at ventral apophysis, arrow 2 points at retrolatero-proximal protrusion) **C, D** distal part of procurus (**C** prolateral view, arrow 1 points at prolatero-distal membranous lamella, arrow 2 points at dorso-subdistal membranous process **D** retrolateral view). Abbreviations: b = bulb, ba = bulbal apophysis, e = embolus, f = flap, pr = procurus. Scale bars: 0.05 (**A, B**); 0.02 (**C, D**).

Female (paratype, IZCAS-Ar45227): Similar to male, habitus as in Fig. 19G, H. Total length 1.21 (1.31 with clypeus), prosoma 0.49 long, 0.57 wide, opisthosoma 0.72 long, 0.63 wide; tibia I: 1.22; tibia I L/d: 22. Eye interdistances and diameters: PME–PME 0.07, PME 0.06, PME–ALE 0.01. Sternum width/

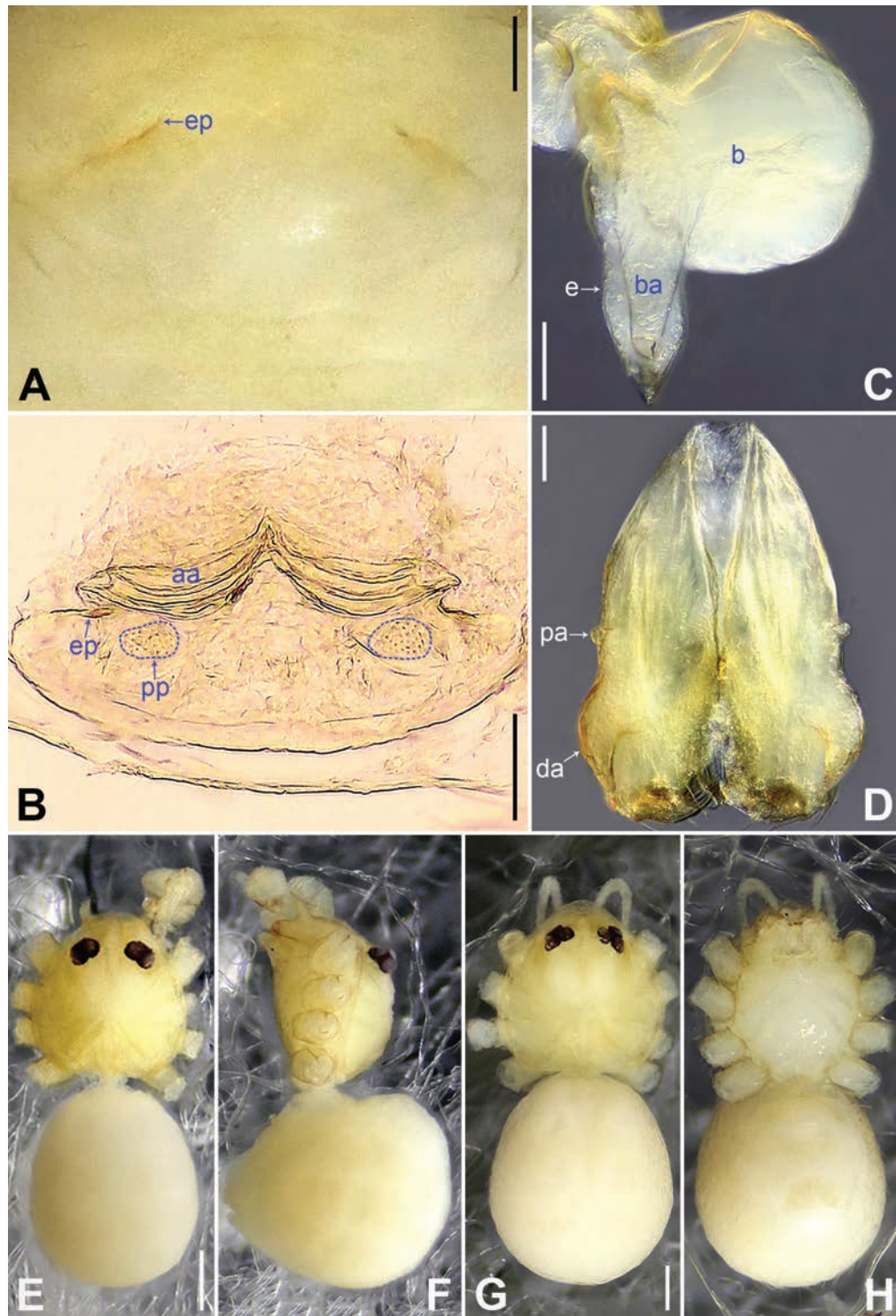


Figure 19. *Belisana zhouxi* sp. nov., holotype male (C–F) and paratype female (A, B, G, H) A epigyne, ventral view B vulva, dorsal view C bulb, prolateral view D chelicerae, frontal view E–H habitus (E, G dorsal view F lateral view H ventral view). Abbreviations: aa = anterior arch, b = bulb, ba = bulbal apophysis, da = distal apophysis, e = embolus, ep = epigynal pocket, pa = proximo-lateral apophysis, pp = pore plate. Scale bars: 0.05 (A–D); 0.20 (E–H).

length: 0.43/0.32. Epigyne simple and flat, posteriorly curved, with pair of antero-lateral pockets 0.16 apart (ep in Figs 19A, 25G). Vulva with ridge-shaped anterior arch (aa in Figs 19B, 25H) and pair of elliptic pore plates (2× longer than wide, pp in Figs 19B, 25H).

Variation. Unknown. Leg I missing in another female paratype (IZCAS-Ar45228).

Habitat. The species was found in the dark zone inside the cave.

Distribution. China (Guizhou, type locality; Fig. 1).

Etymology. The specific name refers to the type locality; noun in apposition.

***Belisana zunyi* Wang, S. Li & Yao, sp. nov.**

<https://zoobank.org/7A299DDB-C11D-4D42-8354-65D16BC50C90>

Figs 20, 21, 23G, H, 25I, J

Type material. **Holotype:** CHINA • ♂; Guizhou, Zunyi, Tongzi County, Leishanguan Town, Yangliuping Village; 28°08.692'N, 106°47.378'E; alt. 1008 m; 11 May 2007; J. Liu & Y. Lin leg.; IZCAS-Ar45229. **Paratypes:** CHINA • 4♂; same data as for holotype; IZCAS-Ar45230–33 • 13♀; same data as for holotype; IZCAS-Ar45234–46.

Diagnosis. The new species resembles *B. zhangji* Tong & Li, 2007 (Tong and Li 2007: 505, figs 1–6) by having similar bulbal apophysis (hooked; Fig. 21C) and vulva (anterior arch ridge-shaped, pore plates long elliptic and 6× longer than wide; Figs 21B, 25J), but can be distinguished by procurus with dorso-subdistal membranous process (arrow 3 in Figs 20C, 23G vs sclerotized apophysis) and without ventro-subdistal membranous lamella (Figs 20C, 23G vs present), by tips of male cheliceral distal apophyses close to each other (da in Fig. 21D vs widely separated), and by epigyne with median pockets (ep in Figs 21A, 25I vs postero-median).

Description. Male (holotype): Total length 1.62 (1.72 with clypeus), prosoma 0.60 long, 0.66 wide, opisthosoma 1.02 long, 0.78 wide. Leg I: 13.53 (3.60, 0.29, 3.50, 4.60, 1.54), leg II: 8.40 (2.25, 0.30, 2.08, 2.81, 0.96), leg III: 5.69 (1.64, 0.25, 1.34, 1.86, 0.60), leg IV: 7.72 (2.12, 0.24, 2.00, 2.56, 0.80); tibia I L/d: 43. Eye interdistances and diameters: PME–PME 0.09, PME 0.08, PME–ALE 0.02. Sternum width/length: 0.53/0.47. Habitus as in Fig. 21E, F. Dorsal shield of prosoma yellowish, without marks; clypeus and sternum yellowish. Legs whitish, without darker rings. Opisthosoma yellowish, without spots. Thoracic furrow absent. Clypeus unmodified. Chelicerae with pair of proximo-lateral apophyses (pa in Fig. 21D) and pair of curved distal apophyses (distance between tips: 0.04; da in Fig. 21D). Palp as in Fig. 20A, B; trochanter with ventral apophysis (as long as wide, arrow 1 in Fig. 20B); femur with retrolatero-proximal protrusion (arrow 2 in Fig. 20B); procurus simple proximally but complex distally, with prolatero-distal membranous lamella (arrow 1 in Figs 20C, 23G) bearing proximally sclerotized part, dorso-distal spine (arrow 2 in Figs 20C, 23G), dorso-subdistal membranous process (arrow 3 in Figs 20C, 23G), and retrolateral membranous flap (f in Figs 20D, 23H); bulb with hooked apophysis (ba in Fig. 21C) and simple embolus (e in Fig. 21C). Retrolateral trichobothria on tibia I at 10% proximally; legs with short vertical setae on metatarsi; tarsus I with 15 distinct pseudosegments.

Female (paratype, IZCAS-Ar45234): Similar to male, habitus as in Fig. 21G, H. Total length 1.57 (1.66 with clypeus), prosoma 0.60 long, 0.68 wide, opisthosoma 0.97 long, 0.78 wide; tibia I: 2.33; tibia I L/d: 35. Eye interdistances and diameters: PME–PME 0.08, PME 0.06, PME–ALE 0.02. Sternum width/length:

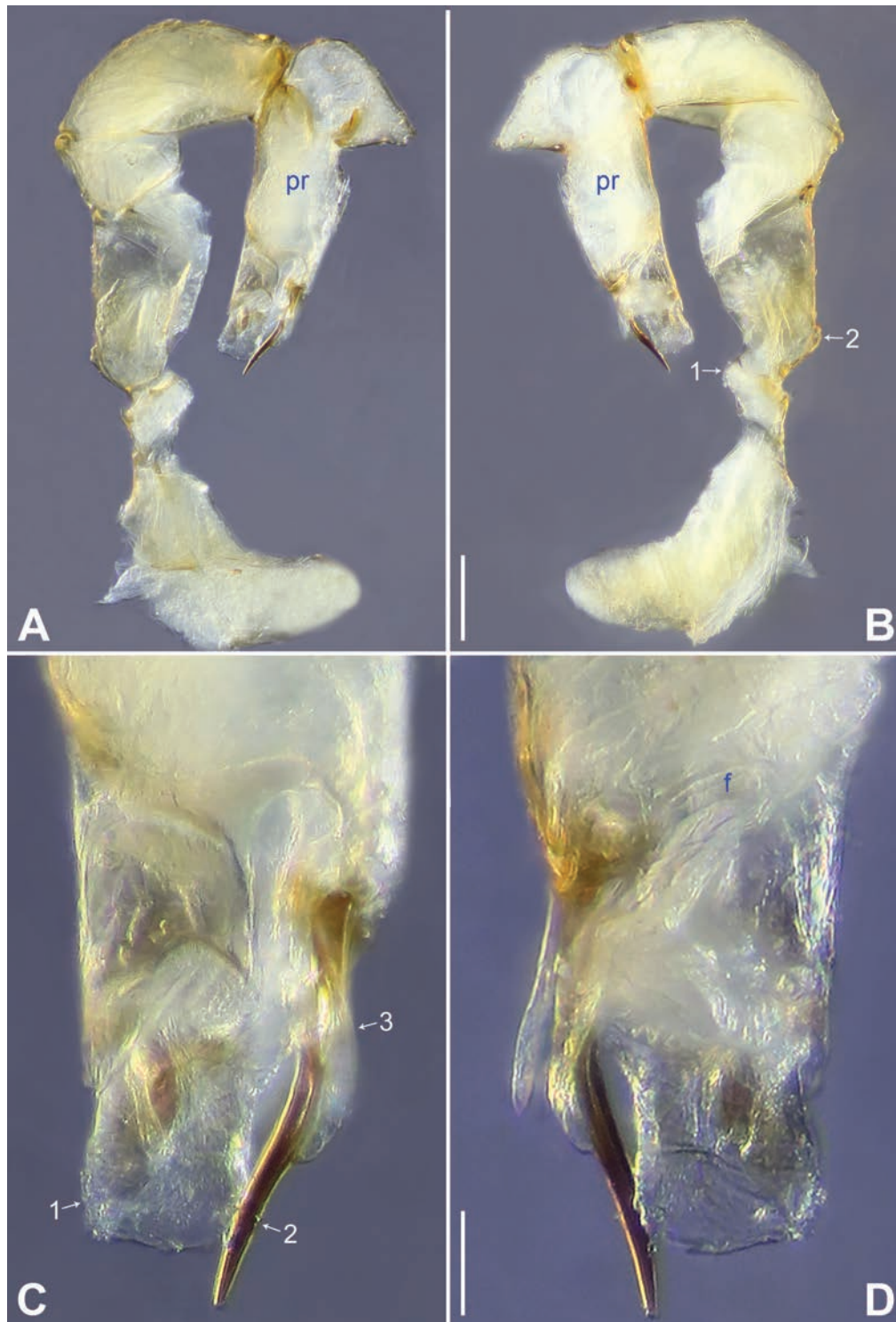


Figure 20. *Belisana zunyi* sp. nov., holotype male **A, B** palp (**A** prolateral view **B** retrolateral view, arrow 1 points at ventral apophysis, arrow 2 points at retrolatero-proximal protrusion) **C, D** distal part of procurus (**C** prolateral view, arrow 1 points at prolatero-distal membranous lamella, arrow 2 points at dorso-distal spine, arrow 3 points at dorso-subdistal membranous process **D** retrolateral view). Abbreviations: f = flap, pr = procurus. Scale bars: 0.10 (**A, B**); 0.03 (**C, D**).

0.50/0.46. Epigyne simple and flat, posteriorly straight, with pair of median pockets 0.06 apart (ep in Figs 21A, 25I). Vulva with ridge-shaped anterior arch (aa in Figs 21B, 25J) and pair of long elliptic pore plates (6× longer than wide, pp in Figs 21B, 25J).

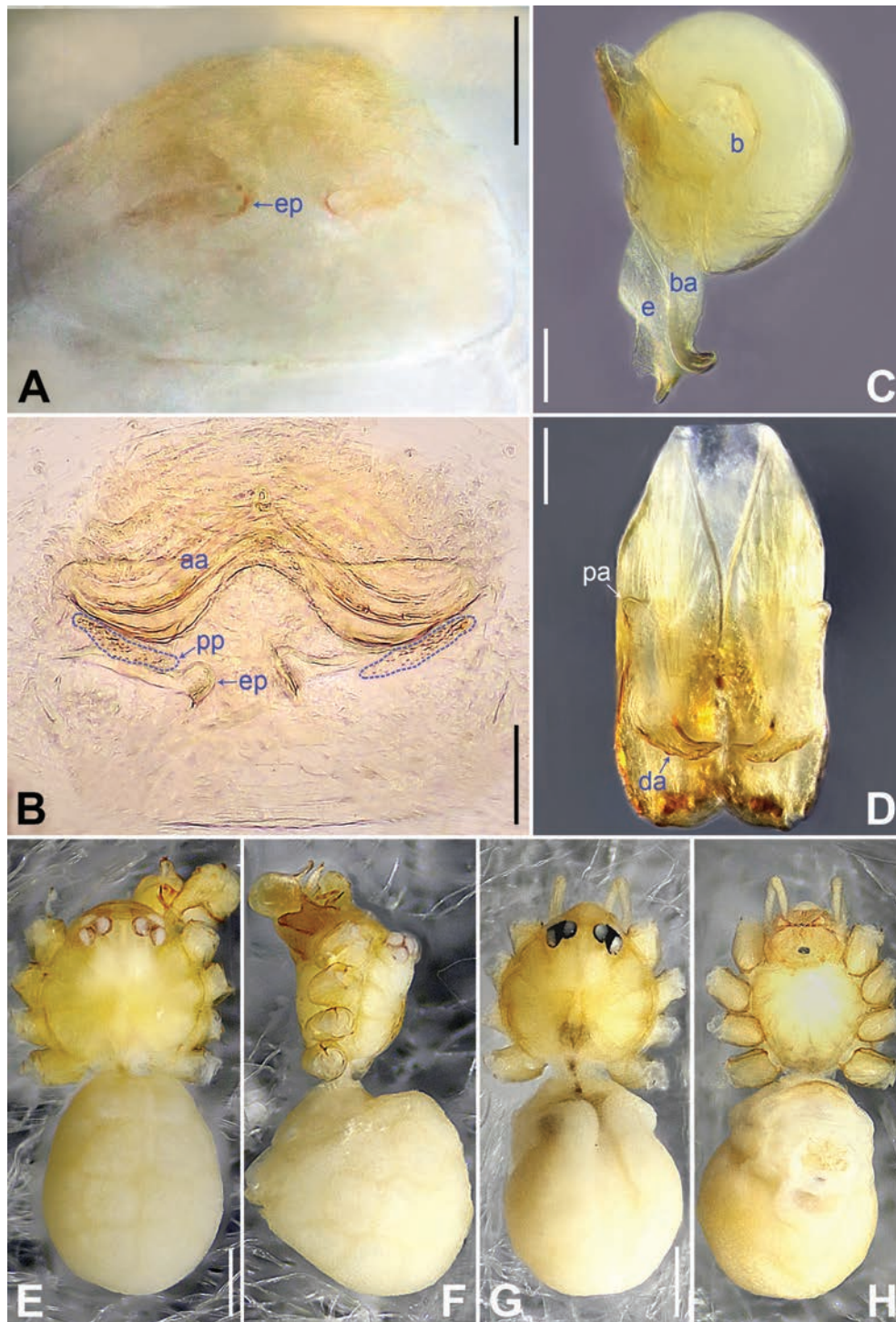


Figure 21. *Belisana zunyi* sp. nov., holotype male (C–F) and paratype female (A, B, G, H) **A** epigyne, ventral view **B** vulva, dorsal view **C** bulb, prolateral view **D** chelicerae, frontal view **E–H** habitus (**E, G** dorsal view **F** lateral view **H** ventral view). Abbreviations: aa = anterior arch, b = bulb, ba = bulbal apophysis, da = distal apophysis, e = embolus, ep = epigynal pocket, pa = proximo-lateral apophysis, pp = pore plate. Scale bars: 0.10 (A–D); 0.30 (E–H).

Variation. Tibia I in four male paratypes (IZCAS-Ar45230–45233): 3.12, 3.20, 3.28, 3.70. Tibia I in the other 12 female paratypes (IZCAS-Ar45235–46): 2.31–2.50.

Habitat. The species was found in the dark zone inside the cave.

Distribution. China (Guizhou, type locality; Fig. 1).

Etymology. The specific name refers to the type locality; noun in apposition.

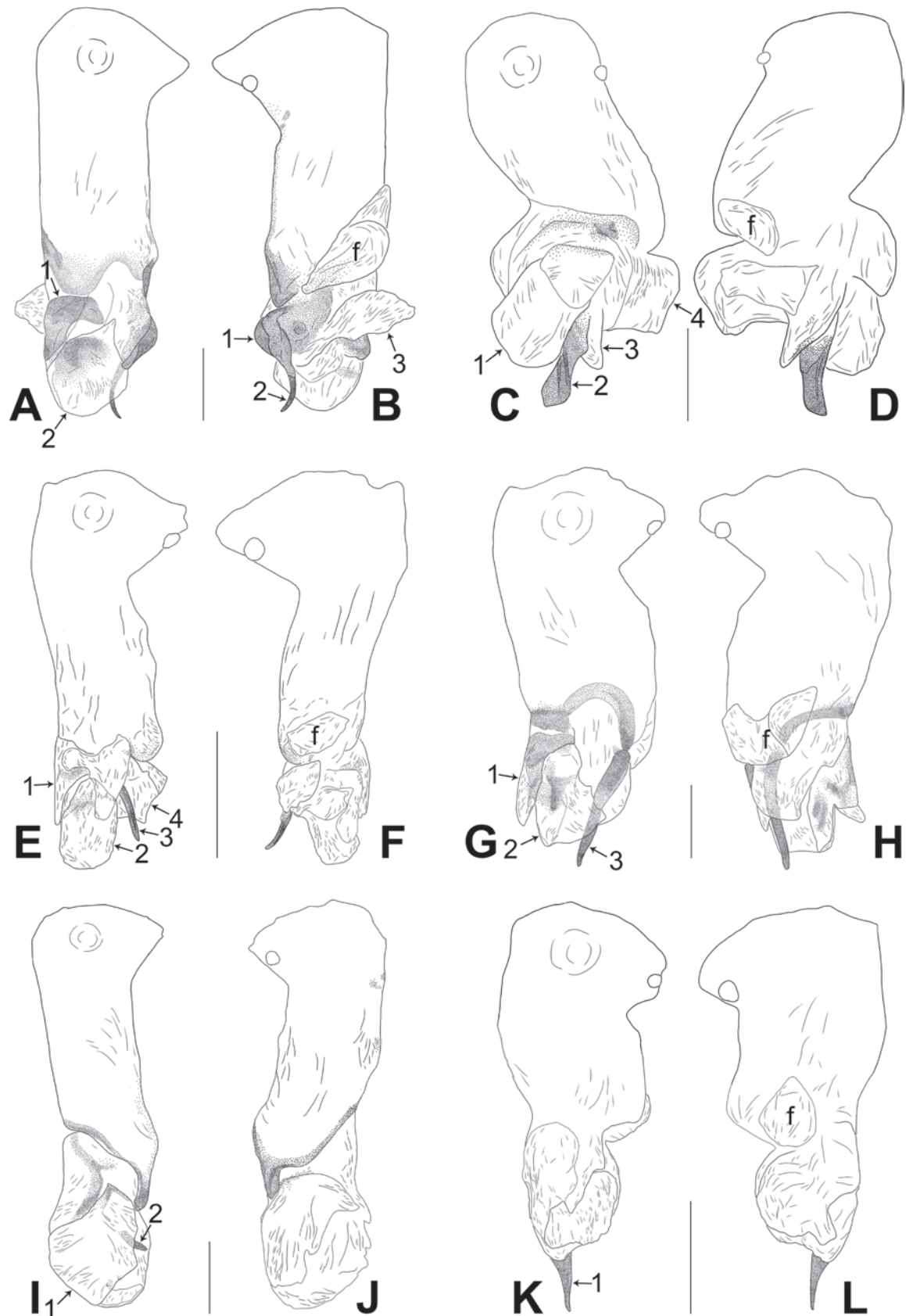


Figure 22. Procurus in prolateral and retrolateral views (The arrows point at the same structures as those shown in the photos of each species) **A, B** *Belisana bijie* sp. nov. **C, D** *B. liupanshui* sp. nov. **E, F** *B. majiang* sp. nov. **G, H** *B. nayong* sp. nov. **I, J** *B. qixinguan* sp. nov. **K, L** *B. xiuwen* sp. nov. Abbreviation: f = flap. Scale bars: 0.10.

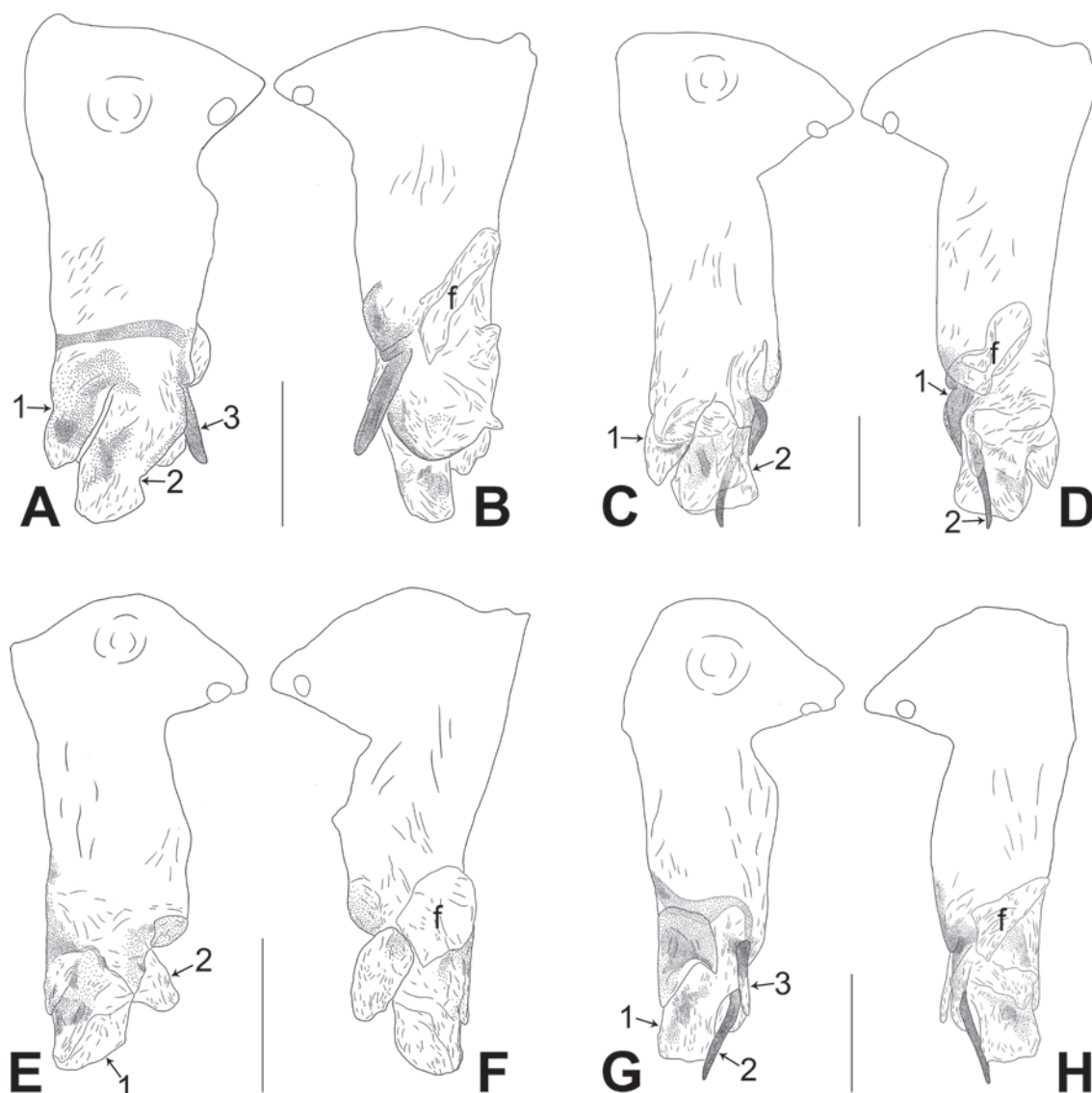


Figure 23. Procurus in prolateral and retrolateral views (The arrows point at the same structures as those shown in the photos of each species) **A, B** *Belisana yongcong* sp. nov. **C, D** *B. zhangji* Tong & Li, 2007 **E, F** *B. zhouxi* sp. nov. **G, H** *B. zunyi* sp. nov. Abbreviation: f = flap. Scale bars: 0.10.

Discussion

Belisana is highly diverse in southern China. Including the nine species described in this paper, there are now 83 species of *Belisana* in southern China, representing 49% of the global total of the genus. Thailand, Indonesia, and Vietnam rank second, third, and fourth, respectively, in species diversity of *Belisana*; however, these countries have recorded only 19, 18, and 17 species, respectively. Other countries, such as Laos (8 spp.), Malaysia (8 spp.), and Sri Lanka (6 spp.), have recorded fewer than ten species (WSC 2024). This high level of activity in China contrasts with the sporadic coverage of Southeast Asia, where most research has been conducted by foreign arachnologists, and several countries lack native expertise in this field (Yao and Li 2021; Zhang et al. 2022; Yang et al. 2023b). Given that Southeast Asia encompasses the Indo-Burma and Sundaland biodiversity hotspots, we anticipate that further exploration will reveal additional, as-yet-undiscovered species diversity of *Belisana*.

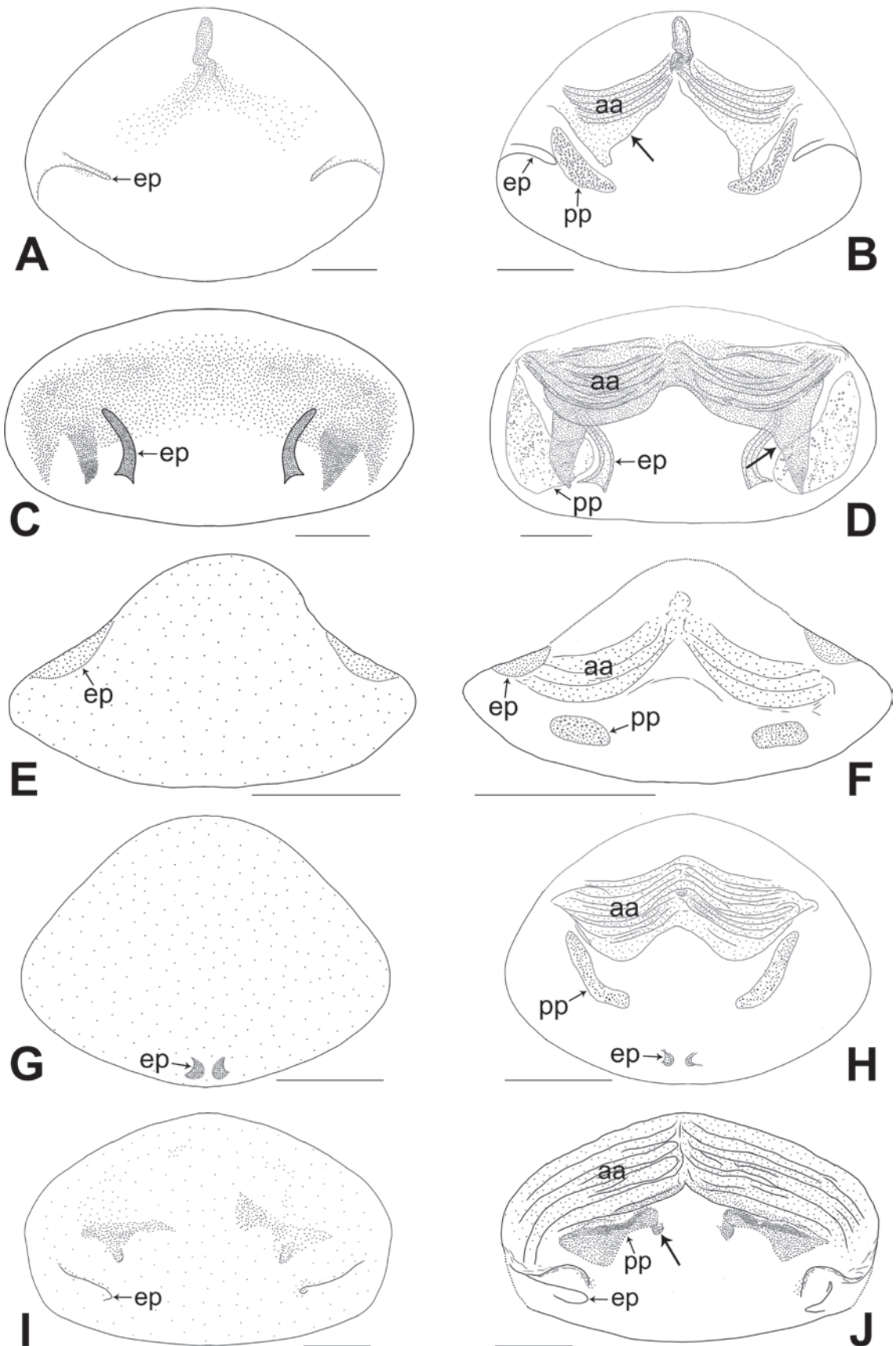


Figure 24. Female genitalia in ventral and dorsal views **A, B** *Belisana bijie* sp. nov., arrow points at lateral sclerite **C, D** *liupanshui* sp. nov., arrow points at lateral sclerite **E, F** *majiang* sp. nov. **G, H** *nayong* sp. nov. **I, J** *qixingguan* sp. nov., arrow points at sclerotized protrusion. Abbreviations: aa = anterior arch, ep = epigynal pocket, pp = pore plate. Scale bars: 0.10.

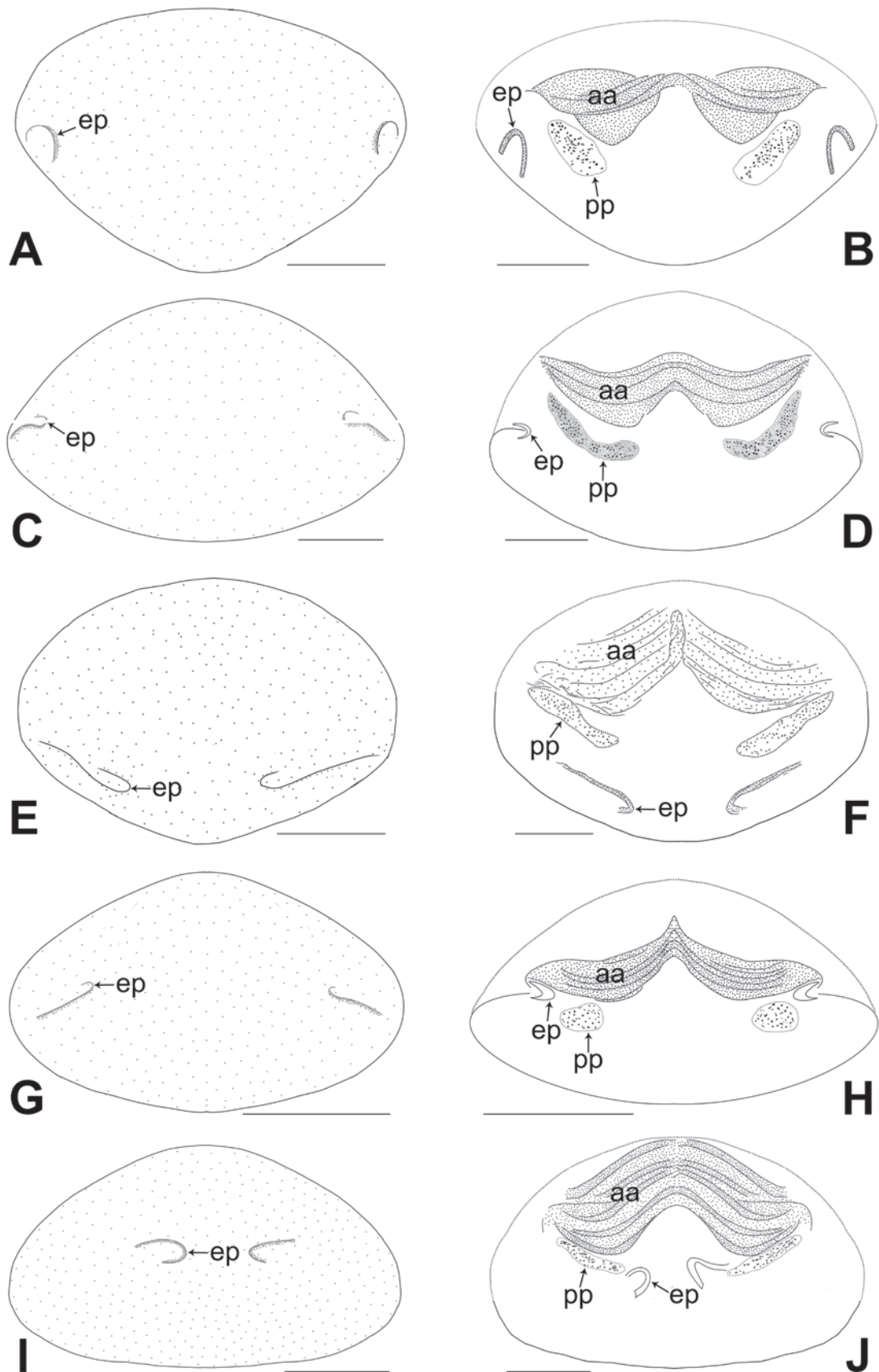


Figure 25. Female genitalia in ventral and dorsal views **A, B** *Belisana xiuwen* sp. nov. **C, D** *B. yongcong* sp. nov. **E, F** *B. zhangji* Tong & Li, 2007 **G, H** *B. zhoxui* sp. nov. **I, J** *B. zunyi* sp. nov. Abbreviations: aa = anterior arch, ep = epigynal pocket, pp = pore plate. Scale bars: 0.10.

Acknowledgements

The manuscript benefited greatly from comments by Alireza Zamani, Yanfeng Tong, and Bernhard Huber.

Additional information

Conflict of interest

The authors have declared that no competing interests exist.

Ethical statement

No ethical statement was reported.

Funding

This study was supported by the National Natural Science Foundation of China (NSFC-32170461, 31872193).

Author contributions

ZY and SL designed the study. BW, SL, and ZY performed morphological species identification. BW and JL finished the descriptions and took the photos and drawings. ZY, BW, and SL drafted and revised the manuscript.

Author ORCIDs

Bing Wang  <https://orcid.org/0009-0009-7047-4395>

Jinglin Li  <https://orcid.org/0009-0008-3932-309X>

Shuqiang Li  <https://orcid.org/0000-0002-3290-5416>

Zhiyuan Yao  <https://orcid.org/0000-0002-1631-0949>

Data availability

All of the data that support the findings of this study are available in the main text.

References

- Chen H, Zhang F, Zhu M (2009) Four new troglophilous species of the genus *Belisana* Thorell, 1898 (Araneae, Pholcidae) from Guizhou Province, China. *Zootaxa* 2092: 58–68. <https://doi.org/10.11646/zootaxa.2092.1.5>
- Chen H, Yu Z, Guo X (2016) One new spider species of genus *Belisana* (Araneae: Pholcidae) from Guizhou, China. *Sichuan Journal of Zoology* 35(2): 227–230.
- Huber BA (2005) High species diversity, male-female coevolution, and metaphyly in Southeast Asian pholcid spiders: The case of *Belisana* Thorell 1898 (Araneae, Pholcidae). *Zoologica* 155: 1–126.
- Khmelik VV, Kozub D, Glazunov A (2005) *Helicon Focus* 3.10.3. <https://www.heliconsoft.com/heliconsoft-products/helicon-focus/> [Accessed 6 July 2024]
- Lefébure T, Douady CJ, Gouy M, Trontelj P, Briolay J, Gibert J (2006) Phylogeography of a subterranean amphipod reveals cryptic diversity and dynamic evolution in extreme environments. *Molecular Ecology* 15: 1797–1806. <https://doi.org/10.1111/j.1365-294X.2006.02888.x>
- Lu Y, Chu C, Zhang X, Li S, Yao Z (2022) Europe vs China: *Pholcus* (Araneae, Pholcidae) from Yanshan-Taihang Mountains confirms uneven distribution of spiders in Eurasia.

- Zoological Research 43(4): 532–534 [& Suppl. 1–78]. <https://doi.org/10.24272/j.issn.2095-8137.2022.103>
- Tong Y, Li S (2007) A new six-eyed pholcid spider (Araneae, Pholcidae) from Karst Tiankeng of Leye County, Guangxi, China. *Acta Zootaxonomica Sinica* 32: 505–507.
- Wang B, Yao Z, Zhang X (2024) A new spider species of *Belisana* Thorell, 1898 (Araneae, Pholcidae) from Guizhou Province, south-western China. *Biodiversity Data Journal* 12: e125111 [1–7]. <https://doi.org/10.3897/BDJ.12.e125111>
- WSC (2024) World Spider Catalog, Version 25.5. Natural History Museum Bern. <https://wsc.nmbe.ch> [Accessed 19 September 2024]
- Yang L, Zhao F, He Q, Yao Z (2023a) A survey of pholcid spiders (Araneae, Pholcidae) from Guiyang, Guizhou Province, China. *ZooKeys* 1186: 175–184. <https://doi.org/10.3897/zookeys.1186.105736>
- Yang R, Yan M, Zhang L, Liu H, Koh JKH, He Q, Yao Z (2023b) New taxa of spiders (Araneae) from the world in 2022. *Biodiversity Science* 31(10): 23175 [1–7]. <https://doi.org/10.17520/biods.2023175>
- Yang L, Fu C, Zhang Y, He Q, Yao Z (2024a) A survey of *Pholcus* spiders (Araneae, Pholcidae) from the Qinling Mountains of central China, with descriptions of seven new species. *Zoosystematics and Evolution* 100(1): 199–221. <https://doi.org/10.3897/zse.100.116759>
- Yang L, He Q, Yao Z (2024b) Taxonomic study of four closely-related species of the *Pholcus yichengicus* species group (Araneae, Pholcidae) from China's Qinling Mountains: An integrated morphological and molecular approach. *Zoosystematics and Evolution* 100(1): 279–289. <https://doi.org/10.3897/zse.100.115633>
- Yao Z, Li S (2013) New and little known pholcid spiders (Araneae: Pholcidae) from Laos. *Zootaxa* 3709(1): 1–51. <https://doi.org/10.11646/zootaxa.3709.1.1>
- Yao Z, Li S (2021) Annual report of Chinese spider taxonomy in 2020. *Biodiversity Science* 29(8): 1058–1063. <https://doi.org/10.17520/biods.2021140>
- Yao Z, Pham DS, Li S (2015) Pholcid spiders (Araneae: Pholcidae) from northern Vietnam, with descriptions of nineteen new species. *Zootaxa* 3909(1): 1–82. <https://doi.org/10.11646/zootaxa.3909.1.1>
- Yao Z, Dong T, Zheng G, Fu J, Li S (2016) High endemism at cave entrances: a case study of spiders of the genus *Uthina*. *Scientific Reports* 6: 35757 [1–9 & Suppl. 1–LII]. <https://doi.org/10.1038/srep35757>
- Yao Z, Zhu K, Du Z, Li S (2018) The *Belisana* spiders (Araneae: Pholcidae) from Xishuangbanna Tropical Botanical Garden, Yunnan, China. *Zootaxa* 4425(2): 243–262. <https://doi.org/10.11646/zootaxa.4425.2.3>
- Yao Z, Wang X, Li S (2021) Tip of the iceberg: species diversity of *Pholcus* spiders (Araneae, Pholcidae) in the Changbai Mountains, northeast China. *Zoological Research* 42(3): 267–271 [& Suppl. 1–60]. <https://doi.org/10.24272/j.issn.2095-8137.2021.037>
- Zhang F, Peng Y (2011) Eleven new species of the genus *Belisana* Thorell (Araneae: Pholcidae) from south China. *Zootaxa* 2989: 51–68. <https://doi.org/10.11646/zootaxa.2989.1.2>
- Zhang Y, Chen H, Zhu M (2008) A new troglophilous *Belisana* spider from Guangxi, China (Araneae, Pholcidae). *Acta Zootaxonomica Sinica* 33: 654–656.
- Zhang L, Lu Y, Chu C, He Q, Yao Z (2022) New spider taxa of the world in 2021. *Biodiversity Science* 30(8): 22163 [1–8]. <https://doi.org/10.17520/biods.2022163>
- Zhang L, Wang Y, Li S, Zhang X, Yao Z (2024a) Three new spider species of *Belisana* Thorell, 1898 (Araneae, Pholcidae) from karst caves, with a list of *Belisana* species

- from Guangxi, China. *ZooKeys* 1209: 315–330. <https://doi.org/10.3897/zookeys.1209.127951>
- Zhang L, Wu Z, Li S, Yao Z (2024b) Eight new spider species of *Belisana* Thorell, 1898 (Araneae, Pholcidae), with an updated overview of *Belisana* species from Yunnan, China. *ZooKeys* 1202: 255–286. <https://doi.org/10.3897/zookeys.1202.121633>
- Zhao F, Yang L, Li S, Zheng G, Yao Z (2023a) A further study on the *Belisana* spiders (Araneae: Pholcidae) from Xishuangbanna, Yunnan, China. *Zootaxa* 5351(5): 543–558. <https://doi.org/10.11646/zootaxa.5351.5.3>
- Zhao F, Yang L, Zou Q, Ali A, Li S, Yao Z (2023b) Diversity of *Pholcus* spiders (Araneae: Pholcidae) in China's Lüliang Mountains: an integrated morphological and molecular approach. *Insects* 14(4): 364 [1–34]. <https://doi.org/10.3390/insects14040364>
- Zhu W, Li S (2021) Six new species of the spider genus *Belisana* (Araneae: Pholcidae) from Southeast Asia. *Zootaxa* 4963(1): 115–137. <https://doi.org/10.11646/zootaxa.4963.1.5>
- Zhu W, Yao Z, Zheng G, Li S (2020) Six new species of the spider genus *Belisana* Thorell, 1898 (Araneae: Pholcidae) from southern China. *Zootaxa* 4810(1): 175–197. <https://doi.org/10.11646/zootaxa.4810.1.12>